

# Approaches to the Efficient Synthesis of *N*-Glycosyl Amides and Triazoles

David P. Temelkoff

By

David P. Temelkoff

Submitted in Partial Fulfillment of the Requirements

For the Degree of

Master of Science

In the Chemistry Program

YOUNGSTOWN STATE UNIVERSITY

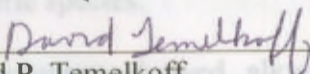
August, 2005

## Approaches to the Efficient Synthesis of *N*-Glycosyl Amides and Triazoles

David P. Temelkoff

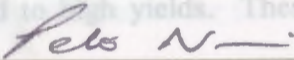
I hereby release this thesis to the public. I understand that this thesis will be made available from the OhioLINK ETD Center and the Maag Library Circulation Desk for public access. I also authorize the University or other individuals to make copies of this thesis as needed for scholarly research.

Signature:

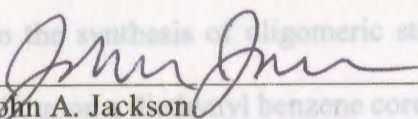
  
David P. Temelkoff

8/4/05

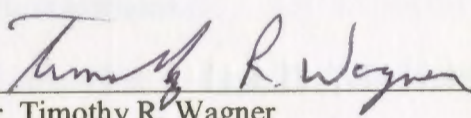
Approvals:

  
Dr. Peter Norris  
Thesis Advisor

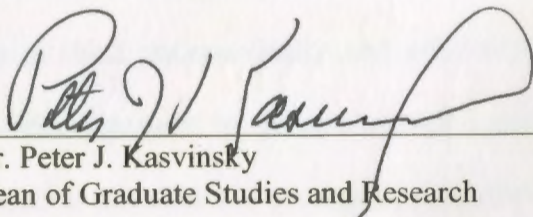
8/4/05  
Date

  
Dr. John A. Jackson  
Committee Member

8/4/05  
Date

  
Dr. Timothy R. Wagner  
Committee Member

8/4/05  
Date

  
Dr. Peter J. Kasvinsky  
Dean of Graduate Studies and Research

8/9/05  
Date



## Thesis Abstract

The stereoselective and regiospecific synthesis of *N*-glycosides was accomplished using two powerful sets of reaction conditions. Modified Staudinger chemistry using bis(diphenylphosphino)ethane as a phosphine in reaction with a  $\beta$ -glycosyl azide and acylating agent afforded  $\beta$ -glycosyl amides in good yields. A glucuronic acid-derived acyl chloride was prepared and the Staudinger conditions were used to investigate the synthesis of oligomeric species.

Several carbohydrate-derived alkynes were also prepared and reacted with glycosyl azides using Cu(I)-catalysis in order to form only 1,4-disubstituted- $\beta$ -glycosyl-1,2,3-triazoles in good to high yields. These reaction conditions furnish *N*-glycosidic products that also maintain the stereochemistry of the  $\beta$ -glycosyl azide precursor. X-Ray crystallography was used to verify regiochemistry and stereochemistry. These conditions were also applied to the synthesis of oligomeric structures, as well as several divalent species that were built upon a diethynyl benzene core.

Finally, I would like to thank Dr. Peter Norris for the interesting project and his continuous support towards my scientific development. Dr. Norris is a great teacher and has inspired me to think independently and critically about chemistry problems. I appreciate his encouragement in presenting my research at national and regional conferences, as well as his efforts in publishing research results. Under his advisement I have been able to develop numerous valuable skills and a knowledge base necessary for a successful career in chemistry, and for this I am extremely grateful.

## Acknowledgements

I would like to thank the Youngstown State University Chemistry Department as well as the School of Graduate Studies for permitting me to pursue and obtain the M.S. degree in Chemistry. I would like to express my appreciation to Dr. John Jackson and Dr. Timothy Wagner, my thesis committee members, for reviewing this thesis and offering helpful advice towards its revision. Many thanks go to Dr. Matthias Zeller who has worked very hard at solving a number of X-Ray crystal structures for this research, as well as Ray Hoff who has been "instrumental" in the collection of analytical data.

My special thanks go to my parents, Paul and Sonja, and my brother and sisters, Dan, Tanja, Christina, and Suzanne for their support throughout my academic career. A special thank you goes to Katy Dobozy for her lasting support over the past several years and also to my little girl, Ruby, who has brightened my life in many ways during the completion of the M.S. program. Thank you to all of my colleagues in the Norris research group, especially Travis for keeping a lively atmosphere and Mat for many inspiring scientific discussions.

Finally, I would like to thank Dr. Peter Norris for the interesting project and his continuous support towards my scientific development. Dr. Norris is a great teacher and has inspired me to think independently and critically about chemistry problems. I appreciate his encouragement in presenting my research at national and regional conferences, as well as his efforts in publishing research results. Under his advisement I have been able to develop numerous valuable skills and a knowledge base necessary for a successful career in chemistry, and for this I am extremely grateful.

**Table of Contents**

Title Page	i
Signature Page	ii
Abstract	iii
Acknowledgements	iv
Table of Contents	v
List of Tables	vi
List of Schemes	vi
List of Equations	vi
List of Figures	viii
Introduction	1
Statement of Problem	14
Results and Discussion	15
1. Synthesis of <i>N</i> -glycosyl amides using modified Staudinger chemistry	
2. Evidence for the imidoyl chloride intermediate	
3. Application to amide-linked oligosaccharides	
4. Cu(I)-catalyzed cycloadditions to form 1,4-disubstituted 1,2,3-triazoles	
5. Synthesis of divalent species	
Experimental Procedures	71
References	131
Appendix A	135
Appendix B	280



## List of Tables

<b>Table 1.</b>	Number of structural isomers possible.....	6
<b>Table 2.</b>	Small library of $\beta$ -glycosyl amides.....	24
<b>Table 3.</b>	1,4-Disubstituted- $\beta$ -glycosyl 1,2,3-triazoles.....	53

## List of Schemes

<b>Scheme 1.</b>	“Traceless” Staudinger ligation, X = cleavable linkage.....	9
<b>Scheme 2.</b>	Synthesis of 2,3,4,6-Tetra- <i>O</i> -acetyl- $\beta$ -D-glucopyranosyl azide ( <b>3</b> ).....	15
<b>Scheme 3.</b>	Pathway for modified Staudinger chemistry.....	18
<b>Scheme 4.</b>	Synthesis of 1,2,3,4-Tetra- <i>O</i> -acetyl- $\beta$ -D-glucopyranosyl chloride ( <b>23</b> ).....	37
<b>Scheme 5.</b>	Synthesis of 2,3,4,6-tetra- <i>O</i> -acetyl- $\beta$ -D-glucopyranosyl azide ( <b>36</b> ).....	52
<b>Scheme 6.</b>	Route to alkynyl ketone <b>33</b> .....	55
<b>Scheme 7.</b>	Proposed method for functionalization of acetate-protected carbohydrate dimers.....	61
<b>Scheme 8.</b>	Synthetic route to azide <b>47</b> .....	67

## List of Equations

<b>Equation 1.</b>	Regioisomeric products of thermal cycloaddition.....	11
<b>Equation 2.</b>	Cu(I)-Catalyzed 1,2,3-triazole formation on solid-phase.....	11
<b>Equation 3.</b>	Cu(I)-Catalyzed 1,2,3-triazole formation in aqueous medium.....	12
<b>Equation 4.</b>	<i>p</i> -Nitrobenzoic acid-(2,3,4,6-tetra- <i>O</i> -acetyl- $\beta$ -D-glucopyranosyl) -amide ( <b>4</b> ).....	22

<b>Equation 5.</b>	Furan-2-carboxylic acid-(2,3,4,6-tetra- <i>O</i> -acetyl- $\beta$ -D-glucopyranosyl)- amide and unknown compound.....	31
<b>Equation 6.</b>	Attempted synthesis of imidoyl azide.....	33
<b>Equation 7.</b>	Preparation of glucuronic acid-derived anhydride <b>21</b> .....	35
<b>Equation 8.</b>	Synthesis of amide-linked carbohydrate dimer <b>24</b> .....	38
<b>Equation 9.</b>	Lewis acid-catalyzed azidation of <b>24</b> .....	40
<b>Equation 10.</b>	Formation of amide-linked carbohydrate trimer <b>26</b> .....	41
<b>Equation 11.</b>	1,2:3,4-di- <i>O</i> -isopropylidene-6-(prop-2-ynyloxy)-D- galactopyranose ( <b>28</b> ).....	43
<b>Equation 12.</b>	Formation of triazole <b>37</b> using Cu(PPh <sub>3</sub> ) <sub>3</sub> Br catalyst.....	45
<b>Equation 13.</b>	Formation of <b>37</b> by Cu(I)-catalysis in aqueous medium.....	47
<b>Equation 14.</b>	Prop-2-ynyl 1,2,3,4-tetra- <i>O</i> -acetyl- $\beta$ -D-glucopyranuronate ( <b>29</b> ).....	48
<b>Equation 15.</b>	Preparation of alkyne <b>30</b> .....	49
<b>Equation 16.</b>	Formation of triazole <b>39</b> by Cu(I)-catalysis in aqueous medium.....	50
<b>Equation 17.</b>	1,2:3,4-Di- <i>O</i> -isopropylidene- $\alpha$ -D-galacto-hexodialdo-1,5- pyranose ( <b>31</b> ).....	56
<b>Equation 18.</b>	Addition of ethynyl magnesium bromide to aldehyde ( <b>31</b> ) to form mixture of propargyl alcohols ( <b>32a/32b</b> ).....	57
<b>Equation 19.</b>	Moffatt oxidation of mixture ( <b>32a/32b</b> ) to give alkynyl ketone <b>33</b> .....	59
<b>Equation 20.</b>	Formation of triazole <b>43</b> by Cu(I)-catalysis in aqueous medium.....	59
<b>Equation 21.</b>	Acidic bromination of <b>40</b> to give bromide <b>44</b> .....	61
<b>Equation 22.</b>	Formation of azide <b>45</b> .....	63

<b>Equation 23.</b>	Formation of triazole-linked carbohydrate trimer <b>48</b> .....	65
<b>Equation 24.</b>	Formation of divalent triazole <b>49</b> by Cu(I)-catalysis in aqueous medium.....	68
<b>Equation 25.</b>	Formation of divalent triazole <b>50</b> by Cu(I)-catalysis in aqueous medium.....	69
<b>Equation 26.</b>	Formation of divalent triazole <b>51</b> by Cu(I)-catalysis in aqueous medium.....	70
<b>List of Figures</b>		
<b>Figure 1.</b>	$\beta$ -D-glucose.....	1
<b>Figure 2.</b>	Example of carbohydrate as multifunctional scaffold.....	2
<b>Figure 3.</b>	Examples of <i>O</i> - and <i>N</i> -glycosides.....	3
<b>Figure 4.</b>	<i>N</i> -linked glycopeptide.....	4
<b>Figure 5.</b>	Example of a cerebroside.....	4
<b>Figure 6.</b>	Stereoselectivity in <i>O</i> -glycoside synthesis.....	7
<b>Figure 7.</b>	Isomerization of glycosylamine.....	8
<b>Figure 8.</b>	Triazole as an amide isostere.....	13
<b>Figure 9.</b>	X-ray crystal structure of glucosyl azide <b>3</b> .....	17
<b>Figure 10.</b>	<sup>1</sup> H NMR spectrum of aza-ylide intermediate (2.2-5.4 ppm).....	20
<b>Figure 11.</b>	X-ray crystal structure of amides <b>4</b> , <b>6</b> , <b>13</b> , and <b>16</b> .....	25
<b>Figure 12.</b>	Cosy spectrum of amide <b>16</b> .....	29
<b>Figure 13.</b>	Nuclear overhauser effect spectrum of amide <b>16</b> .....	30
<b>Figure 14.</b>	Proposed mechanistic depiction of intramolecular cyclization to	



	form 1,5-disubstituted tetrazole <b>19</b> .....	34
<b>Figure 15.</b>	Two places for aza-ylide intermediate to attack.....	36
<b>Figure 16.</b>	Glucuronic acid and its amide derivative promote 1,2- <i>cis</i> -glucosides..	39
<b>Figure 17.</b>	Proposed mechanism for Cu(I)-catalyzed triazole formation.....	42
<b>Figure 18.</b>	X-ray crystal structure of alkyne <b>29</b> .....	48
<b>Figure 19.</b>	X-ray crystal structure of alkyne <b>30</b> .....	50
<b>Figure 20.</b>	X-ray crystal structure of azide <b>45</b> .....	64
<b>Figure 21.</b>	400 MHz $^1\text{H}$ NMR spectrum of bromide <b>2</b> .....	136
<b>Figure 22.</b>	100 MHz $^{13}\text{C}$ NMR spectrum of bromide <b>2</b> .....	137
<b>Figure 23.</b>	400 MHz $^1\text{H}$ NMR spectrum of azide <b>3</b> .....	138
<b>Figure 24.</b>	100 MHz $^{13}\text{C}$ NMR spectrum of azide <b>3</b> .....	139
<b>Figure 25.</b>	Low resolution mass spectrum of azide <b>3</b> .....	140
<b>Figure 26.</b>	400 MHz $^1\text{H}$ NMR spectrum of amide <b>4</b> .....	141
<b>Figure 27.</b>	100 MHz $^{13}\text{C}$ NMR spectrum of amide <b>4</b> .....	142
<b>Figure 28.</b>	Low resolution mass spectrum of amide <b>4</b> .....	143
<b>Figure 29.</b>	High resolution mass spectrum of amide <b>4</b> .....	144
<b>Figure 30.</b>	400 MHz $^1\text{H}$ NMR spectrum of amide <b>5</b> .....	145
<b>Figure 31.</b>	100 MHz $^{13}\text{C}$ NMR spectrum of amide <b>5</b> .....	146
<b>Figure 32.</b>	Low resolution mass spectrum of amide <b>5</b> .....	147
<b>Figure 33.</b>	High resolution mass spectrum of amide <b>5</b> .....	148
<b>Figure 34.</b>	400 MHz $^1\text{H}$ NMR spectrum of amide <b>6</b> .....	149
<b>Figure 35.</b>	100 MHz $^{13}\text{C}$ NMR spectrum of amide <b>6</b> .....	150
<b>Figure 36.</b>	Low resolution mass spectrum of amide <b>6</b> .....	151

<b>Figure 37.</b>	High resolution mass spectrum of amide 6.....	152
<b>Figure 38.</b>	400 MHz $^1\text{H}$ NMR spectrum of amide 7.....	153
<b>Figure 39.</b>	100 MHz $^{13}\text{C}$ NMR spectrum of amide 7.....	154
<b>Figure 40.</b>	Low resolution mass spectrum of amide 7.....	155
<b>Figure 41.</b>	400 MHz $^1\text{H}$ NMR spectrum of amide 8.....	156
<b>Figure 42.</b>	100 MHz $^{13}\text{C}$ NMR spectrum of amide 8.....	157
<b>Figure 43.</b>	Low resolution mass spectrum of amide 8.....	158
<b>Figure 44.</b>	400 MHz $^1\text{H}$ NMR spectrum of amide 9.....	159
<b>Figure 45.</b>	100 MHz $^{13}\text{C}$ NMR spectrum of amide 9.....	160
<b>Figure 46.</b>	Low resolution mass spectrum of amide 9.....	161
<b>Figure 47.</b>	400 MHz $^1\text{H}$ NMR spectrum of amide 10.....	162
<b>Figure 48.</b>	Low resolution mass spectrum of amide 10.....	163
<b>Figure 49.</b>	400 MHz $^1\text{H}$ NMR spectrum of amide 11.....	164
<b>Figure 50.</b>	100 MHz $^{13}\text{C}$ NMR spectrum of amide 11.....	165
<b>Figure 51.</b>	Low resolution mass spectrum of amide 11.....	166
<b>Figure 52.</b>	High resolution mass spectrum of amide 11.....	167
<b>Figure 53.</b>	400 MHz $^1\text{H}$ NMR spectrum of amide 12.....	168
<b>Figure 54.</b>	100 MHz $^{13}\text{C}$ NMR spectrum of amide 12.....	169
<b>Figure 55.</b>	Low resolution mass spectrum of amide 12.....	170
<b>Figure 56.</b>	400 MHz $^1\text{H}$ NMR spectrum of amide 13.....	171
<b>Figure 57.</b>	100 MHz $^{13}\text{C}$ NMR spectrum of amide 13.....	172
<b>Figure 58.</b>	Low resolution mass spectrum of amide 13.....	173
<b>Figure 59.</b>	High resolution mass spectrum of amide 13.....	174

<b>Figure 60.</b>	400 MHz $^1\text{H}$ NMR spectrum of amide <b>14</b> .....	175
<b>Figure 61.</b>	100 MHz $^{13}\text{C}$ NMR spectrum of amide <b>14</b> .....	176
<b>Figure 62.</b>	Low resolution mass spectrum of amide <b>14</b> .....	177
<b>Figure 63.</b>	High resolution mass spectrum of amide <b>14</b> .....	178
<b>Figure 64.</b>	400 MHz $^1\text{H}$ NMR spectrum of amide <b>15</b> .....	179
<b>Figure 65.</b>	100 MHz $^{13}\text{C}$ NMR spectrum of amide <b>15</b> .....	180
<b>Figure 66.</b>	Low resolution mass spectrum of amide <b>15</b> .....	181
<b>Figure 67.</b>	High resolution mass spectrum of amide <b>15</b> .....	182
<b>Figure 68.</b>	400 MHz $^1\text{H}$ NMR spectrum of amide <b>16</b> .....	183
<b>Figure 69.</b>	100 MHz $^{13}\text{C}$ NMR spectrum of amide <b>16</b> .....	184
<b>Figure 70.</b>	COSY spectrum of amide <b>16</b> .....	185
<b>Figure 71.</b>	nOe spectrum of amide <b>16</b> .....	186
<b>Figure 72.</b>	Low resolution mass spectrum of amide <b>16</b> .....	187
<b>Figure 73.</b>	High resolution mass spectrum of amide <b>16</b> .....	188
<b>Figure 74.</b>	400 MHz $^1\text{H}$ NMR spectrum of amide <b>17</b> .....	189
<b>Figure 75.</b>	100 MHz $^{13}\text{C}$ NMR spectrum of amide <b>17</b> .....	190
<b>Figure 76.</b>	Low resolution mass spectrum of amide <b>17</b> .....	191
<b>Figure 77.</b>	400 MHz $^1\text{H}$ NMR spectrum of imidoyl chloride <b>18</b> .....	192
<b>Figure 78.</b>	100 MHz $^{13}\text{C}$ NMR spectrum of imidoyl chloride <b>18</b> .....	193
<b>Figure 79.</b>	Low resolution mass spectrum of imidoyl chloride <b>18</b> .....	194
<b>Figure 80.</b>	High resolution mass spectrum of imidoyl chloride <b>18</b> .....	195
<b>Figure 81.</b>	400 MHz $^1\text{H}$ NMR spectrum of 1,5-disubstituted tetrazole <b>19</b> .....	196
<b>Figure 82.</b>	100 MHz $^{13}\text{C}$ NMR spectrum of 1,5-disubstituted tetrazole <b>19</b> .....	197



<b>Figure 83.</b>	Low resolution mass spectrum of 1,5-disubstituted tetrazole <b>19</b> .....	198
<b>Figure 84.</b>	High resolution mass spectrum of 1,5-disubstituted tetrazole <b>19</b> .....	199
<b>Figure 85.</b>	400 MHz $^1\text{H}$ NMR spectrum of anhydride <b>21</b> .....	200
<b>Figure 86.</b>	100 MHz $^{13}\text{C}$ NMR spectrum of anhydride <b>21</b> .....	201
<b>Figure 87.</b>	400 MHz $^1\text{H}$ NMR spectrum of carboxylic acid <b>22</b> .....	202
<b>Figure 88.</b>	100 MHz $^{13}\text{C}$ NMR spectrum of carboxylic acid <b>22</b> .....	203
<b>Figure 89.</b>	400 MHz $^1\text{H}$ NMR spectrum of acid chloride <b>23</b> .....	204
<b>Figure 90.</b>	100 MHz $^{13}\text{C}$ NMR spectrum of acid chloride <b>23</b> .....	205
<b>Figure 91.</b>	400 MHz $^1\text{H}$ NMR spectrum of amide-linked carbohydrate dimer <b>24</b> .....	206
<b>Figure 92.</b>	100 MHz $^{13}\text{C}$ NMR spectrum of amide-linked carbohydrate dimer <b>24</b> .....	207
<b>Figure 93.</b>	Cosy spectrum of dimer <b>24</b> .....	208
<b>Figure 94.</b>	Low resolution mass spectrum of dimer <b>24</b> .....	209
<b>Figure 95.</b>	High resolution mass spectrum of dimer <b>24</b> .....	210
<b>Figure 96.</b>	400 MHz $^1\text{H}$ NMR spectrum of azide <b>25</b> .....	211
<b>Figure 97.</b>	400 MHz $^1\text{H}$ NMR spectrum of amide linked trimer <b>26</b> .....	212
<b>Figure 98.</b>	Low resolution mass spectrum of amide linked trimer <b>26</b> .....	213
<b>Figure 99.</b>	High resolution mass spectrum of amide linked trimer <b>26</b> .....	214
<b>Figure 100.</b>	400 MHz $^1\text{H}$ NMR spectrum of alkyne <b>28</b> .....	215
<b>Figure 101.</b>	100 MHz $^{13}\text{C}$ NMR spectrum of alkyne <b>28</b> .....	216
<b>Figure 102.</b>	Low resolution mass spectrum alkyne <b>28</b> .....	217

<b>Figure 103.</b>	High resolution mass spectrum alkyne <b>28</b> .....	218
<b>Figure 104.</b>	400 MHz $^1\text{H}$ NMR spectrum of alkyne <b>29</b> .....	219
<b>Figure 105.</b>	100 MHz $^{13}\text{C}$ NMR spectrum of alkyne <b>29</b> .....	220
<b>Figure 106.</b>	Low resolution mass spectrum alkyne <b>29</b> .....	221
<b>Figure 107.</b>	High resolution mass spectrum alkyne <b>29</b> .....	222
<b>Figure 108.</b>	400 MHz $^1\text{H}$ NMR spectrum of alkyne <b>30</b> .....	223
<b>Figure 109.</b>	100 MHz $^{13}\text{C}$ NMR spectrum of alkyne <b>30</b> .....	224
<b>Figure 110.</b>	Low resolution mass spectrum alkyne <b>30</b> .....	225
<b>Figure 111.</b>	400 MHz $^1\text{H}$ NMR spectrum of aldehyde <b>31</b> .....	226
<b>Figure 112.</b>	100 MHz $^{13}\text{C}$ NMR spectrum of aldehyde <b>31</b> .....	227
<b>Figure 113.</b>	400 MHz $^1\text{H}$ NMR spectrum of propargyl alcohol <b>32</b> .....	228
<b>Figure 114.</b>	100 MHz $^{13}\text{C}$ NMR spectrum of propargyl alcohol <b>32</b> .....	229
<b>Figure 115.</b>	Low resolution mass spectrum propargyl alcohol <b>32</b> .....	230
<b>Figure 116.</b>	400 MHz $^1\text{H}$ NMR spectrum of alkynyl ketone <b>33</b> .....	231
<b>Figure 117.</b>	Low resolution mass spectrum alkynyl ketone <b>33</b> .....	232
<b>Figure 118.</b>	400 MHz $^1\text{H}$ NMR spectrum of galactosyl bromide <b>35</b> .....	233
<b>Figure 119.</b>	100 MHz $^{13}\text{C}$ NMR spectrum of galactosyl bromide <b>35</b> .....	234
<b>Figure 120.</b>	400 MHz $^1\text{H}$ NMR spectrum of galactosyl azide <b>36</b> .....	235
<b>Figure 121.</b>	100 MHz $^{13}\text{C}$ NMR spectrum of galactosyl azide <b>36</b> .....	236
<b>Figure 122.</b>	Low resolution mass spectrum galactosyl azide <b>36</b> .....	237
<b>Figure 123.</b>	400 MHz $^1\text{H}$ NMR spectrum of triazole <b>37</b> .....	238
<b>Figure 124.</b>	100 MHz $^{13}\text{C}$ NMR spectrum of triazole <b>37</b> .....	239
<b>Figure 125.</b>	Low resolution mass spectrum of triazole <b>37</b> .....	240

<b>Figure 126.</b>	High resolution mass spectrum of triazole <b>37</b> .....	241
<b>Figure 127.</b>	400 MHz $^1\text{H}$ NMR spectrum of triazole <b>38</b> .....	242
<b>Figure 128.</b>	Low resolution mass spectrum of triazole <b>38</b> .....	243
<b>Figure 129.</b>	400 MHz $^1\text{H}$ NMR spectrum of triazole <b>39</b> .....	244
<b>Figure 130.</b>	100 MHz $^{13}\text{C}$ NMR spectrum of triazole <b>39</b> .....	245
<b>Figure 131.</b>	Low resolution mass spectrum of triazole <b>39</b> .....	246
<b>Figure 132.</b>	High resolution mass spectrum of triazole <b>39</b> .....	247
<b>Figure 133.</b>	400 MHz $^1\text{H}$ NMR spectrum of triazole <b>40</b> .....	248
<b>Figure 134.</b>	100 MHz $^{13}\text{C}$ NMR spectrum of triazole <b>40</b> .....	249
<b>Figure 135.</b>	Cosy spectrum of triazole <b>40</b> .....	250
<b>Figure 136.</b>	Low resolution mass spectrum of triazole <b>40</b> .....	251
<b>Figure 137.</b>	400 MHz $^1\text{H}$ NMR spectrum of triazole <b>41</b> .....	252
<b>Figure 138.</b>	100 MHz $^{13}\text{C}$ NMR spectrum of triazole <b>41</b> .....	253
<b>Figure 139.</b>	Low resolution mass spectrum of triazole <b>41</b> .....	254
<b>Figure 140.</b>	400 MHz $^1\text{H}$ NMR spectrum of triazole <b>42</b> .....	255
<b>Figure 141.</b>	100 MHz $^{13}\text{C}$ NMR spectrum of triazole <b>42</b> .....	256
<b>Figure 142.</b>	Low resolution mass spectrum of triazole <b>42</b> .....	257
<b>Figure 143.</b>	400 MHz $^1\text{H}$ NMR spectrum of triazole <b>43</b> .....	258
<b>Figure 144.</b>	Low resolution mass spectrum of triazole <b>43</b> .....	259
<b>Figure 145.</b>	400 MHz $^1\text{H}$ NMR spectrum of bromide <b>44</b> .....	260
<b>Figure 146.</b>	100 MHz $^{13}\text{C}$ NMR spectrum of bromide <b>44</b> .....	261
<b>Figure 147.</b>	400 MHz $^1\text{H}$ NMR spectrum of azide <b>45</b> .....	262
<b>Figure 148.</b>	100 MHz $^{13}\text{C}$ NMR spectrum of azide <b>45</b> .....	263



<b>Figure 149.</b>	Low resolution mass spectrum of azide <b>45</b> .....	264
<b>Figure 150.</b>	400 MHz $^1\text{H}$ NMR spectrum of bromide <b>46</b> .....	265
<b>Figure 151.</b>	100 MHz $^{13}\text{C}$ NMR spectrum of bromide <b>46</b> .....	266
<b>Figure 152.</b>	400 MHz $^1\text{H}$ NMR spectrum of azide <b>47</b> .....	267
<b>Figure 153.</b>	100 MHz $^{13}\text{C}$ NMR spectrum of azide <b>47</b> .....	268
<b>Figure 154.</b>	Low resolution mass spectrum of azide <b>47</b> .....	269
<b>Figure 155.</b>	400 MHz $^1\text{H}$ NMR spectrum of triazole-linked trimer <b>48</b> .....	270
<b>Figure 156.</b>	Low resolution mass spectrum of triazole-linked trimer <b>48</b> .....	271
<b>Figure 157.</b>	400 MHz $^1\text{H}$ NMR spectrum of divalent triazole <b>49</b> .....	272
<b>Figure 158.</b>	Low resolution mass spectrum of divalent triazole <b>49</b> .....	273
<b>Figure 159.</b>	400 MHz $^1\text{H}$ NMR spectrum of divalent triazole <b>50</b> .....	274
<b>Figure 160.</b>	100 MHz $^{13}\text{C}$ NMR spectrum of divalent triazole <b>50</b> .....	275
<b>Figure 161.</b>	Low resolution mass spectrum of divalent triazole <b>50</b> .....	276
<b>Figure 162.</b>	400 MHz $^1\text{H}$ NMR spectrum of divalent triazole <b>51</b> .....	277
<b>Figure 163.</b>	100 MHz $^{13}\text{C}$ NMR spectrum of divalent triazole <b>51</b> .....	278
<b>Figure 164.</b>	Low resolution mass spectrum of divalent triazole <b>51</b> .....	279
<b>Figure 165.</b>	X-ray crystal structure of azide <b>3</b> .....	281
<b>Figure 166.</b>	X-ray crystal structure of amide <b>4</b> .....	290
<b>Figure 167.</b>	X-ray crystal structure of amide <b>6</b> .....	297
<b>Figure 168.</b>	X-ray crystal structure of amide <b>13</b> .....	307
<b>Figure 169.</b>	X-ray crystal structure of amide <b>16</b> .....	314
<b>Figure 170.</b>	X-ray crystal structure of alkyne <b>29</b> .....	321
<b>Figure 171.</b>	X-ray crystal structure of alkyne <b>30</b> .....	327

**Figure 172.** X-ray crystal structure of azide 45.....334

"What role do carbohydrates play in biological systems?" Twenty years ago, this question may have been answered by referring to carbohydrates as sources of energy or as good structural building blocks for polymers such as starch and cellulose. Research efforts over the past several decades in such areas as biochemistry and physiology have revealed that carbohydrates are often involved in biological communication events controlling such processes as egg fertilization, microbial infection, inflammation, and cancer metastasis.<sup>1</sup>

Carbohydrates are the most abundant class of organic compounds that are found in living organisms. The simplest examples have the empirical formula  $CH_2O$  and are considered to be hydrates of carbon. Carbohydrates, or saccharides, are also referred to as sugars when the molecules are small. In solution, carbohydrates exist either as open chain structures, or in a five- or six-membered ring form referred to as the furanose and pyranose forms, respectively. The pyranose form of carbohydrates have been shown to be studied for the present research. The smallest individual carbohydrate unit is called a monosaccharide, and a simple monosaccharide known as  $\beta$ -D-glucose, the most abundant sugar on the planet, is shown below (Figure 1).

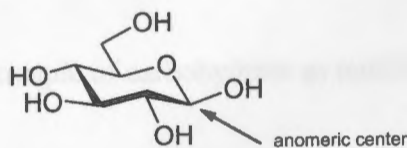


Figure 1.  $\beta$ -D-glucopyranose

**Introduction:**

“What role do carbohydrates play in biological systems?” Twenty years ago, this question may have been answered by referring to carbohydrates as sources of energy or as good structural building blocks for polymers such as starch and cellulose. Research efforts over the past several decades in such areas as biochemistry and glycobiology have revealed that carbohydrates are often involved in biological communication events controlling such processes as egg fertilization, microbial infection, inflammation, and cancer metastasis.<sup>1</sup>

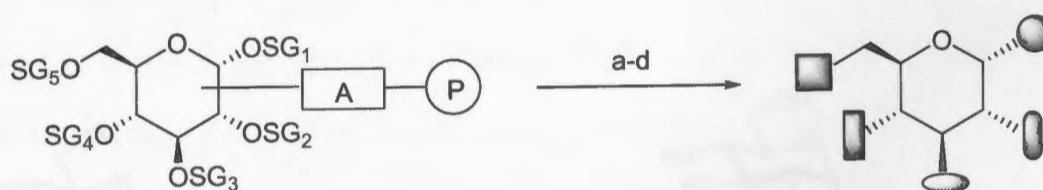
Carbohydrates are the most abundant class of organic compounds that are found in living organisms. The simplest examples have the empirical formula  $\text{CH}_2\text{O}$  and are considered to be hydrates of carbon. Carbohydrates, or saccharides, are also referred to as sugars when the molecules are small. In solution, carbohydrates exist either as open chain structures, or in a five- or six-membered ring form referred to as the furanose and pyranose forms, respectively. The pyranose forms of carbohydrates have been chosen to be studied for the present research. The smallest individual carbohydrate unit is called a monosaccharide, and a simple monosaccharide known as  $\beta$ -D-glucose, the most abundant sugar on the planet, is shown below (Figure 1).



**Figure 1.**  $\beta$ -D-glucose

A molecule consisting of just two carbohydrate monomers is called a disaccharide. Oligosaccharides are typically composed of 2-10 monosaccharide units, while polysaccharides generally contain ten or more sugar units.

A few things should be noted about carbohydrates in general. First, each carbon in a carbohydrate is attached to oxygen making these molecules highly functionalized. Secondly, the orientation of the hydroxyl groups is actually what differentiates the various monosaccharides in Nature and is what gives carbohydrates their unique potential for diversity. The hydroxyl groups in  $\beta$ -D-glucose are all situated equatorially in relation to the ring making this particular configuration extremely stable. The fact that carbohydrates have multiple stereocenters makes them ideal starting materials that can be built upon, in other words, serving as multifunctional chiral scaffolds. These transformations can be accomplished in solution, as well as in a solid phase combinatorial approach as demonstrated by Wunberg *et al* (Figure 2).<sup>2</sup>



Strategy of combinatorial synthesis with carbohydrate scaffold: SG = protecting group, A = anchor, P = polymer (carrier); a) selective deprotection; b) functionalization; c) washing; d) cleavage of the anchor.

**Figure 2.** Example of carbohydrate as multifunctional scaffold

Lastly, the anomeric center, pointed out in Figure 1, is subject to a unique electronic feature known as the anomeric effect. The anomeric effect, not limited to just carbohydrates, is the phenomenon where an electronegative substituent at the anomeric

position prefers to occupy an axial position. This is due to the partial donation of the ring-oxygen electrons into the antibonding  $\sigma^*$  orbital of the electronegative atom or group. Particular attention is often paid to this phenomenon since it can determine the stereochemical outcome of the reactions involving carbohydrates.<sup>1</sup>

When the hydroxyl group at the anomeric position is replaced with an alcohol, or any other non-hydroxyl group, the result is a glycoside. The atom directly attached to the anomeric carbon designates the type of glycoside. Attachment of the anomeric carbon to oxygen, nitrogen, carbon, or sulfur gives *O*-, *N*-, *C*-, and *S*-glycosides. Glycosides are plentiful in biological systems. Many various enzymes, such as glycosidases and glycosyl transferases, are responsible for attaching and removing sugars to and from biomolecules in the body. These enzymes have evolved over long periods of time and are extremely efficient and selective at glycosylation and oligoasaccharide construction, attributes that are often times difficult to mimic using modern synthetic methods. Some examples of *N*- and *O*-glycosides are shown in Figure 3.

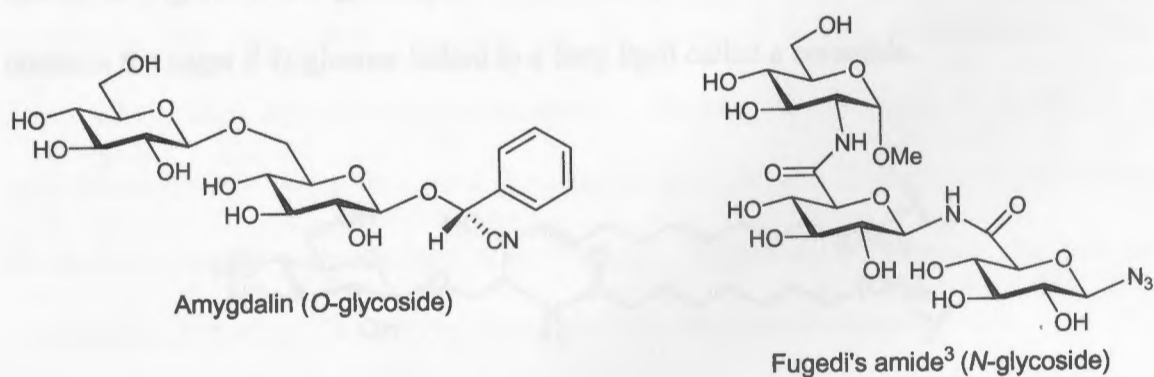


**Figure 3:** Examples of *O*- and *N*-glycosides



Oligosaccharides can be found dissolved in the aqueous media surrounding all cells of the body or attached to other biomolecules to form glycoconjugates, such as glycopeptides or glycolipids. The two main types of glycopeptides are the N-linked peptides (Figure 4), linked through the side chain amide of asparagine, and the O-linked peptides, linked through the side chain hydroxyl of serine or threonine.

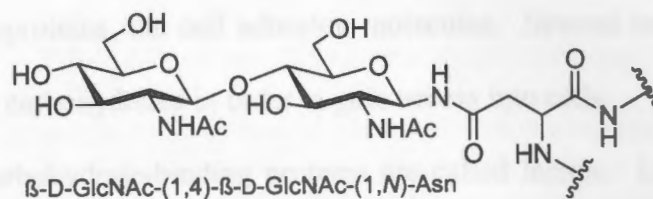


**Figure 4.** N-linked glycopeptide

Glycolipids possess both a polar carbohydrate and a nonpolar lipid portion. The lipid portion of these biomolecules is buried into the outer lipid portion of the cell, while the carbohydrate end extends outward and away from the cell. Cerebrosides, an example shown in Figure 4, are glycolipids found in high levels in the brain. The example contains the sugar  $\beta$ -D-glucose linked to a fatty lipid called a ceramide.

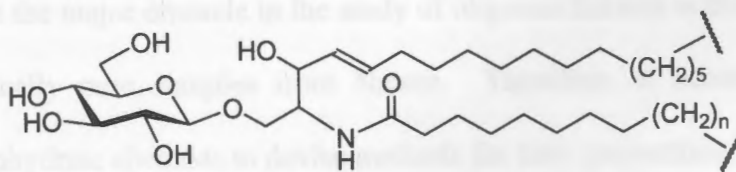


**Figure 5.** Example of a cerebroside

Due to their hydrophilic nature, carbohydrates are generally found outside of the cell wall. Therefore, it is argued that the first contact that cells have with each other is between the carbohydrates that adorn the surface of the cell. This implicates the carbohydrates at these locations to be involved in many complex roles such as cell recognition and cell differentiation. In a very simplistic view, the carbohydrates can act as points of attachment for other cells, bacteria, toxins, and hormones, in events that are mediated by glycoproteins, the cell adhesion molecules. Several bacteria and parasites utilize cell surface carbohydrates in order to gain access into cells.

Specific carbohydrate-binding proteins are called lectins. Lectins are found on the surface of all cell membranes and interact with nearby oligosaccharides contributing to their role in molecular recognition. They bind only weakly to monosaccharides, so in order to be effective for molecular recognition, other selective factors need to be involved. A popular view is that the selectivity is promoted through multiple binding, also referred to as multivalent interactions. Multivalency can enhance the weak binding of monovalent carbohydrates significantly. Binding events, whether enzymatic or non-enzymatic, are very often dependent on the presence of the carbohydrates, their accessibility, and their spatial presentation. Keeping these issues in mind, it is unfortunate that the major obstacle in the study of oligosaccharides is the low availability of stereochemically pure samples from Nature. Therefore, it becomes the task of motivated carbohydrate chemists to devise methods for their preparation.<sup>4</sup>

Table 1 illustrates the diversity that can be achieved through linking individual carbohydrate monomers in their pyranose forms. This potential stems from the various attachment points possible between carbohydrate monomers. The great diversity of

structure explains why carbohydrates can code or store a great deal of biological information.

Combination of Individual Monomer Units	Number of Carbohydrates
Two Identical Units, A-A dimer	11
Three Identical Units, A-A-A trimer	176
Three Different Units, A-B-C trimer	1,056
Five Different Units, A-B-C-D-E pentamer	2,144,640

**Table 1.** Number of structural isomers possible

The chemical synthesis of carbohydrates is often a time-consuming and laborious process. The hydroxyl groups of carbohydrates possess similar reactivity requiring them to be protected, sometimes selectively. After protection, the necessary linkages can be made, and then the carbohydrate can be deprotected. Following deprotection it is still not uncommon to end up with a mixture of isomers. This introduces one of the classical problems in carbohydrate chemistry, selectivity around the anomeric center.

Figure 6 illustrates the selectivity issues involved with *O*-glycoside synthesis. Departure of the leaving group at the anomeric results in the formation of the oxycarbonium ion. This leaves an exposed  $sp^2$  anomeric carbon that can be attacked on either face by a suitable nucleophile to give either an alpha or beta product. The stereochemical outcome can often depend upon the protecting group at C-2. For example, when C-2 is acetate protected, the beta product is expected through anchimeric assistance.

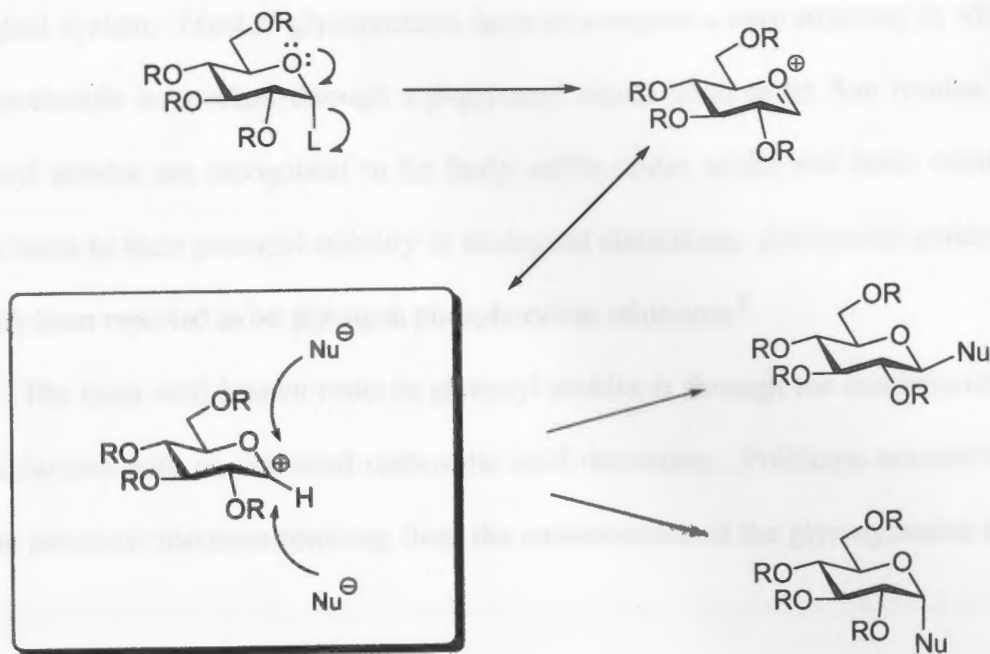


**Figure 6.** Stereoselectivity in *O*-glycoside synthesis

In biological systems, *N*-glycosylation is an important post-translational modification of proteins.<sup>5</sup> One important consequence of *N*-glycosidic linking events and the presence of *N*-glycans is proper folding of proteins.<sup>6</sup> Some proteins require the presence of the glycans, but it is not always a prerequisite for a protein to fold. While their presence may not necessarily induce permanent secondary structure, the glycans help keep a compact order around the glycosylation sites. It is also interesting to note that cleavage of the glycan does not affect the folded protein.

Since the carbohydrates on glycoproteins and other biomolecules vary in their stereochemical presentation, it is important to be able to control the stereochemistry of the glycosidic linkage in the chemical synthesis of molecules that will be used as potential biomimetics or tools to probe biological processes. The glycosyl amide linkage is one such linkage in which the stereochemical orientation can affect the activity in a

biological system. Most *N*-glycoproteins have in common a core structure in which an oligosaccharide is attached through a  $\beta$ -glycosyl amide bond to an Asn residue.<sup>7</sup> *N*-Glycosyl amides are recognized to be fairly stable under acidic and basic conditions, which lends to their potential stability in biological conditions.  $\beta$ -Glycosyl amides have recently been reported to be glycogen phosphorylase inhibitors.<sup>8</sup>

The most well known route to glycosyl amides is through the condensation of a glycosylamine with an activated carboxylic acid derivative. Problems associated with this are anomeric mixtures resulting from the isomerization of the glycosylamine (Figure 7).<sup>9</sup>

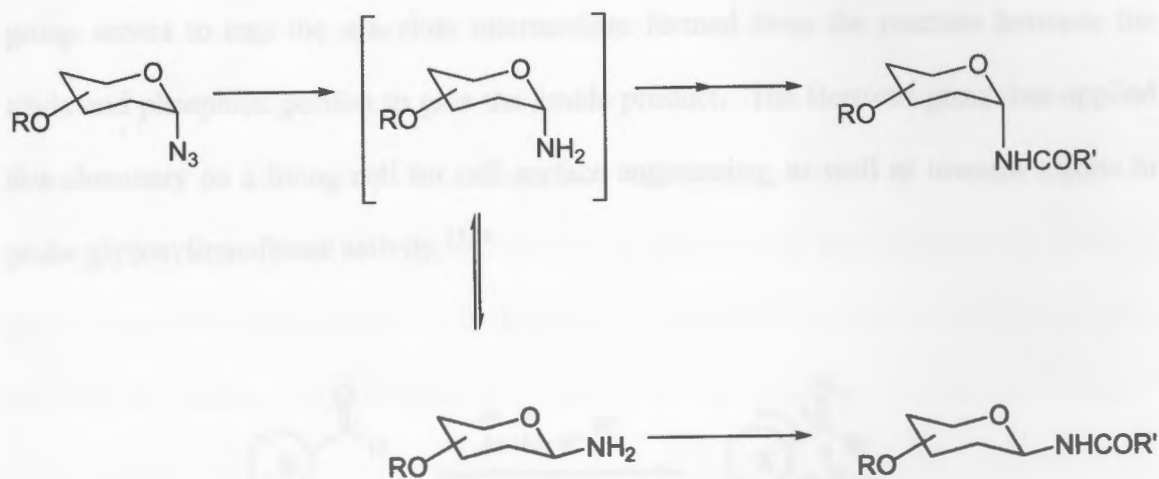
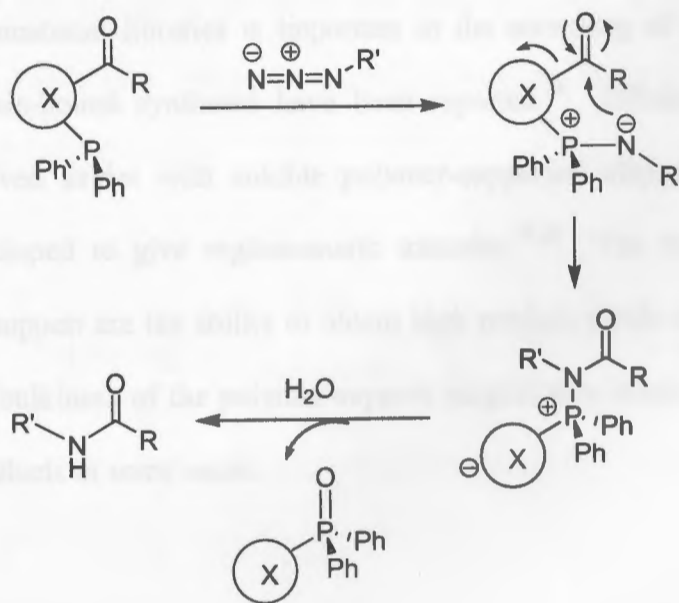


**Figure 7.** Isomerization of glycosylamine

Another inconvenience is the fact that the glycosyl amines are usually prepared from the glycosyl azide requiring reduction of the azide group. Alternatives to using glycosylamines as precursors have been investigated, such as glycosyl isothiocyanates and pentenyl glycosides.<sup>10</sup>



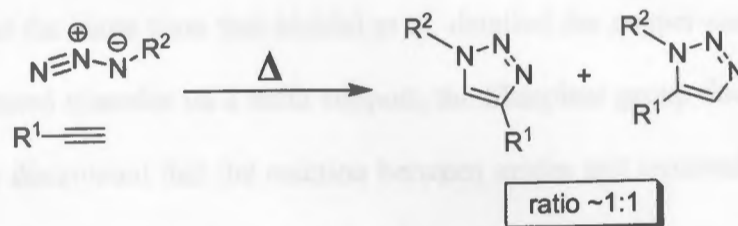
Methods of acquiring the glycosyl amides directly from glycosyl azides have been developed, although selectivity remains a major issue.<sup>11</sup> One of the more popular methods investigated has been a Staudinger modification employing an azide, carboxylic acid (or derivative), and a phosphine.<sup>12,13</sup> In this type of reaction, an azide and phosphine react to give an aza-ylide intermediate which is allowed to react with the carboxylic acid derivative. One of the most recent developments in this type of chemistry has been the “traceless” Staudinger ligation (Scheme 1).<sup>14</sup> This is a modified Staudinger reaction involving only two components, an azide and a specialized triaryl phosphine that has a methoxycarbonyl group attached to one of the aromatic rings. The methoxycarbonyl group serves to trap the aza-ylide intermediate formed from the reaction between the azide and phosphine portion to give the amide product. The Bertozzi group has applied this chemistry on a living cell for cell surface engineering, as well as towards efforts to probe glycosyltransferase activity.<sup>15,16</sup>



**Scheme 1.** “Traceless” Staudinger ligation, X = cleavable linkage

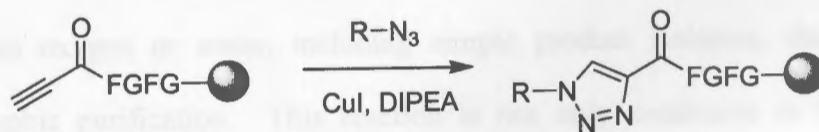
Another class of compounds receiving much attention in the past several years has been 1,2,3-triazoles. The study of 1,2,3-triazoles has proven to be useful in medicinal chemistry. 1,2,3-Triazole derivatives have been used as synthetic intermediates in the synthesis of nucleosides,<sup>17</sup> antibiotics,<sup>18</sup> rotaxanes,<sup>19</sup> and glycosidase inhibitors<sup>20</sup> in addition to having microbial, analgesic, anti-inflammatory, local anaesthetic,<sup>21</sup> and antiallergenic activities,<sup>22</sup> to name a few. Some glucosylated 1,2,3-triazole derivatives have shown antitumor and antiviral activities<sup>23</sup> indicating that carbohydrate-derived triazoles are of pharmaceutical importance.

Synthesis of triazoles is predominantly accomplished using a 1,3-dipolar cycloaddition, the most popular and useful reagents arguably being azides and terminal alkynes.<sup>24</sup> According to Equation 1, the heating of an azide and a terminal alkyne results in a mixture of regioisomeric products. While the synthesis of triazoles can be successfully carried out in solution, solid-phase synthesis of triazoles also has been an area of recent development since the need for reaction environments that allow for quick building of combinatorial libraries is important in the screening of drug candidates.<sup>25</sup> Solid support resin-bound syntheses have been reported.<sup>26</sup> Efficient methods using carbohydrate-derived azides with soluble polymer-supported alkynes also have been successfully developed to give regioisomeric triazoles.<sup>27,28</sup> The benefits of using a soluble polymer support are the ability to obtain high product yields and convenience of use although the bulkiness of the polymer-support reagent may inhibit the formation of regioisomeric products in some cases.



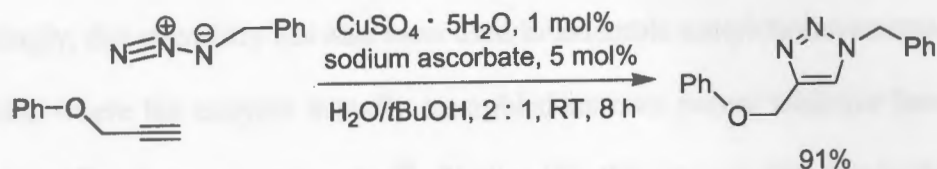
**Equation 1.** Regioisomeric products of thermal cycloaddition

Recent research by Meldal and coworkers has resulted in a novel regioselective solid phase synthesis of 1,2,3-triazoles using a copper(I)-catalyzed 1,3-dipolar cycloaddition of azides with terminal alkynes (Equation 2).<sup>29</sup> This method allows the syntheses of a variety of 1,4-disubstituted 1,2,3-triazoles in peptide backbones and side chains. Additional research has resulted in the identification of novel 1,2,3-triazoles as protease inhibitors.<sup>30</sup> Another recent example is a traceless solid-phase synthesis of 1,2,3-triazoles using 2-methoxy-substituted resin as well as the bromo-Wang resin to give a wide variety of 4- and 5-mono-substituted and disubstituted triazole products.<sup>31</sup> The ability to control the formation of one isomer over the other is important because it allows for the creation of a wider variety of compounds, increasing the potential of finding biologically active species.



**Equation 2.** Cu(I)-Catalyzed 1,2,3-triazole formation on solid-phase

At about the same time that Meldal et al. detailed the copper-catalyzed synthesis of 1,4-disubstituted triazoles on a solid support, the Sharpless group documented similar findings. They discovered that the reaction between azides and terminal alkynes to form triazoles could be performed using Cu(II) salts in aqueous media at room temperature. The Cu(I) is formed in situ with use of a reductant, such as ascorbic acid or sodium ascorbate (Equation 3). The reactions are reportedly high yielding, affording pure product in 6-36 hours, and requiring no chromatography, but rather the products are collected by mere filtration.<sup>32</sup>



**Equation 3.** Cu(I)-Catalyzed 1,2,3-triazole formation in aqueous medium

The Huisgen 1,3-dipolar cycloaddition of azides and alkynes, in light of the rate acceleration and regioselectivity afforded by Cu(I)-catalysis, has been referred to as a “click” reaction. These are reactions that are broad in scope and generally high yielding over a variety of starting materials. A click reaction should be easy to perform, insensitive to oxygen or water, including simple product isolation, that is, without chromatographic purification. This reaction is not only conducive to the expedient preparation of molecules for drug discovery, but also reliably produces an inflexible linking functionality that shares useful topological and electronic features with amides (Figure 8). Triazoles, however, withstand hydrolytic cleavage and are near impossible to

reduce or oxidize. They also possess a large dipole moment, and the nitrogen atoms at the two and three position function as weak hydrogen bond acceptors.<sup>33</sup>

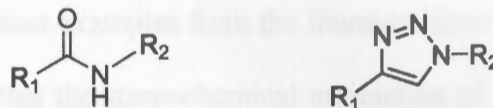


**Figure 8.** Triazole as an amide isostere

Applications of this click chemistry are broad and far reaching, from use in herbicides and fungicides<sup>34</sup> to use in compounds displaying anti-HIV activity.<sup>35</sup> Quite interestingly, this chemistry has also been used to assemble acetylcholinesterase (AChE) inhibitors, where the enzyme actually assembled its own potent inhibitor based on the constraints of the enzyme active site.<sup>36</sup> Studies like this are possible due to the discrete unreactivity of the alkyne and azide functional groups in biological systems.



## Statement of Problem

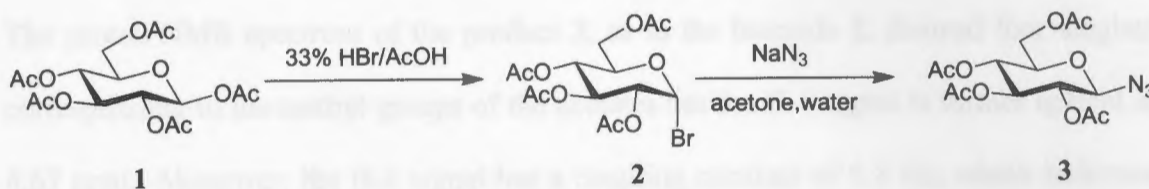
Carbohydrates, oligosaccharides in particular, play important roles in many biological processes. Some carbohydrate-derived oligomers have been investigated for their use as mimetics, with most examples from the literature involving sugar/amino acid research. It is well known that the stereochemical orientation of the glycosidic linkage can significantly affect the activity in biological systems. The shape and structural nuances of biomolecules are also important. Therefore, the need to develop approaches to achieve these requirements is increasingly important. The modified Staudinger and Cu(I)-catalyzed cycloaddition chemistries will be used to synthesize molecules that not only may serve as potential glycomimetics, but also serve as useful intermediates towards the synthesis of oligosaccharides. Stereochemical and regiochemical control will be a central focus of the research.

### Scheme 2: Synthesis of 2,3,4,6-Tetra-O-acetyl- $\beta$ -D-glucopyranosyl azide (1)

The preparation of  $\beta$ -glucosyl azide 1 was achieved in two simple steps starting from  $\beta$ -D-glucose peracetonate. In the first step, the peracetonate 1 is dissolved in 10% HCl in acetic acid and stirred for at least one hour after which thin layer chromatography (TLC) analysis showed complete consumption of the starting material 1 and the appearance of a new low polar compound with an  $R_f$  value of 0.33 (1:1 hexane:ethyl acetate). The only product from this reaction is the  $\alpha$ -glucosyl bromide 2. The bromination occurs in an  $S_N1$  process affording the  $\alpha$ -bromide solely quantitatively due to the anomeric effect. Proton nuclear magnetic resonance ( $^1H$  NMR) spectroscopy analysis of the product 2 showed four singlets ranging from 1.93 to 2.02 ppm, which

## Results and Discussion:

The main goal of the research was the synthesis of novel *N*-glycosides whereby the construction of related oligomers could be investigated. A major premise of the research was to maintain stereochemical control around the anomeric position of the resulting glycosides in an efficient and predictable manner. A valuable means to achieve this stereocontrol was realized through the introduction of the azide moiety at the anomeric position of a pyranose sugar according to Scheme 2. The azide group is introduced stereospecifically and serves as a chemical handle with which, as will be illustrated shortly, powerful transformations may be conducted with ease.



**Scheme 2:** Synthesis of 2,3,4,6-Tetra-O-acetyl- $\beta$ -D-glucopyranosyl azide (**3**)

The preparation of  $\beta$ -glucosyl azide **3** was achieved in two simple steps starting from  $\beta$ -D-glucose pentaacetate. In the first step, the pentaacetate **1** is dissolved in 33% HBr in acetic acid and stirred for at least one hour after which thin layer chromatography (TLC) analysis showed complete consumption of the starting material **1** and the appearance of a new less polar compound with an  $R_f$  value of 0.37 (1:1 hexanes:ethyl acetate). The only product from this reaction is the  $\alpha$ -glucosyl bromide **2**. The bromination occurs in an  $S_N1$  process affording the  $\alpha$ -bromide nearly quantitatively due to the anomeric effect. Proton nuclear magnetic resonance (<sup>1</sup>H NMR) spectroscopy analysis of the product **2** showed four singlets ranging from 1.95 to 2.02 ppm, which

correspond to the methyl groups of the acetate protecting groups, indicating the presence of only four such groups. A deshielded doublet at 6.54 ppm with a coupling constant of 4.0 Hz corresponds to H-1 and suggests the expected alpha configuration around the anomeric position.

The bromine of  $\alpha$ -glucosyl bromide **2** is easily displaced in an  $S_N2$  process using an excess of sodium azide in acetone and water. The reaction progress was monitored by TLC and showed disappearance of the starting material (**2**), in addition to the appearance of a slightly more polar spot with an  $R_f$  value of 0.35 (1:1 hexanes:ethyl acetate). Several hours is all that is needed to reveal our stereochemically pure  $\beta$ -glucosyl azide **3**, which after recrystallization from methanol is isolated as a highly crystalline solid in 82% yield. The proton NMR spectrum of the product **3**, as in the bromide **2**, showed four singlets corresponding to the methyl groups of the acetates but the H-1 signal is further upfield at 4.67 ppm. Moreover, the H-1 signal has a coupling constant of 8.8 Hz, which indicates inversion to the beta azide. Another key feature of the proton spectrum is a very well-resolved doublet of doublet of doublets at 3.81 ppm corresponding to H-5. This splitting pattern is due to the diastereotopic nature of the two protons at C-6, which also lends itself to explain the two sets of doublets of doublets at 4.17 and 4.28 ppm corresponding to H-6 and H-6'. The ease of purification and the amenability to scale-up makes access to large quantities of this starting material a trivial matter. The X-ray crystal structure of the  $\beta$ -glucosyl azide was obtained and supports the structural assignment, as does NMR evidence.

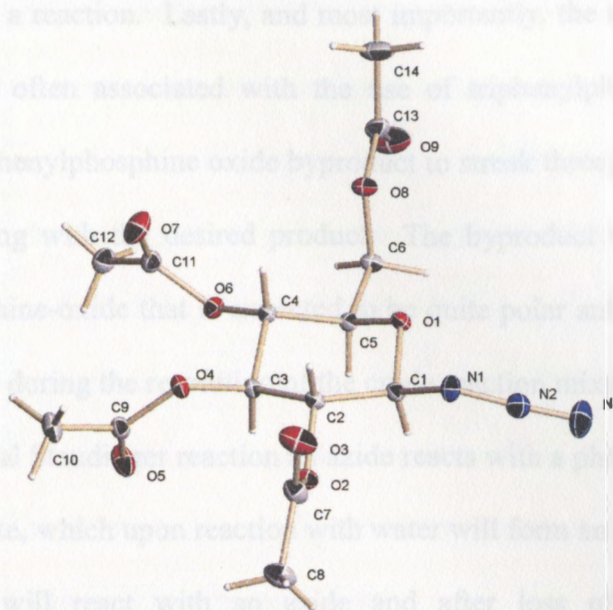


**Figure 9:** X-ray crystal structure of glucosyl azide 3

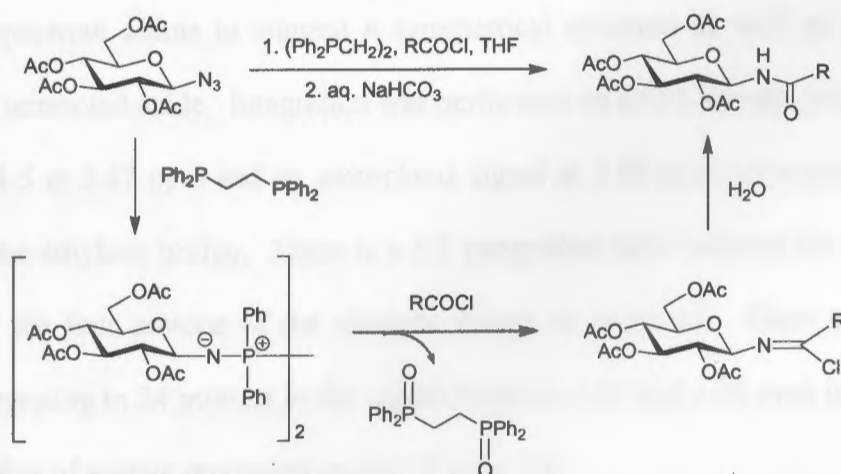
### Synthesis of *N*-glycosyl amides using modified Staudinger chemistry

With the pure  $\beta$ -glucosyl azide in hand, the task of employing and refining a method for the synthesis of *N*-glycosyl amides could be undertaken. Previous researchers within the Norris group had utilized polymer-supported triphenylphosphine,<sup>37</sup> as well as bis(diphenylphosphino)ethane as a phosphine,<sup>38</sup> in reaction with azides and acyl chlorides to produce *N*-glycosyl amides with an appreciable degree of success. Since polymer-supported reagents are expensive and require long reaction times, the solution phase method using bis(diphenylphosphino)ethane was explored in order to probe the nature of the modified Staudinger reaction, make any necessary refinements, and finally to apply it to the synthesis of oligomeric carbohydrate-derived amides.

There are several advantages to using bis(diphenylphosphino)ethane, herein referred to as DPPE. First, it is a stable solid that is easy to work with. Secondly, in theory, since there are two phosphines per molecule, little more than half an equivalent

should be needed in a reaction. Lastly, and most importantly, the use of DPPE helps to avoid the problems often associated with the use of triphenylphosphine, namely the tendency for the triphenylphosphine oxide byproduct to streak through a column of silica, often times co-eluting with the desired product. The byproduct of the reaction using DPPE is a bisphosphine-oxide that is expected to be quite polar and therefore less likely to cause interference during the resolution of the crude reaction mixtures.

In the classical Staudinger reaction an azide reacts with a phosphine to produce an aza-ylide intermediate, which upon reaction with water will form an amine. For example, triphenylphosphine will react with an azide and after loss of nitrogen forms an iminophosphorane. The iminophosphorane will react with water to give rise to an amine as well as the well-favored triphenylphosphine oxide. In light of the inevitable reactive nature of the aza-ylide intermediate, care would have to be taken to exclude water from the reaction mixture. Scheme 3 illustrates the expected reaction pathway for the modified Staudinger reaction as well as the conditions used to achieve good results with this chemistry.



**Scheme 3:** Pathway for modified Staudinger chemistry



The pathway begins with reaction between the glucosyl azide and DPPE to generate an aza-ylide intermediate, often referred to as a phosphazene, after loss of nitrogen. In the presence of an acylating agent, the nucleophilic nitrogen of the ylide will attack the carbonyl carbon, and proceed to lose bisphosphine-oxide through a tetrahedral intermediate. The formation of the bisphosphine-oxide is a driving force in this reaction since it is a stable byproduct. The result is an imidoyl chloride, which undergoes hydrolysis to give the  $\beta$ -glucosyl amide as the major reaction product. In most cases within this research, the imidoyl chloride intermediate was short-lived, but an example where this was not the case will be presented shortly.

In order to get an appreciation for the solution structure of the aza-ylide intermediate, the reaction of glucosyl azide with DPPE was performed in  $\text{CDCl}_3$ . Immediate evolution of gas, assumedly nitrogen, was observed. Total consumption of the glucosyl azide after 30 minutes was revealed by TLC with disappearance of the azide and the appearance of a UV spot on the baseline (1:1 hexanes:ethyl acetate) that burned on the TLC plate when treated with a 5% sulfuric acid in ethanol solution and heated. At this time the reaction mixture could be observed by proton NMR spectroscopy (Figure 10). The spectrum seems to suggest a symmetrical structure as well as showing no evidence of unreacted azide. Integration was performed on select signals, particularly the signal for H-5 at 3.47 ppm and an amorphous signal at 2.50 ppm corresponding to the protons of the ethylene bridge. There is a 1:2 integration ratio between the two protons of H-5 and the four protons of the ethylene bridge as expected. There are also four singlets integrating to 24 protons in the region between 1.87 and 1.99 ppm indicating the correct number of acetate protecting groups (Figure 10).

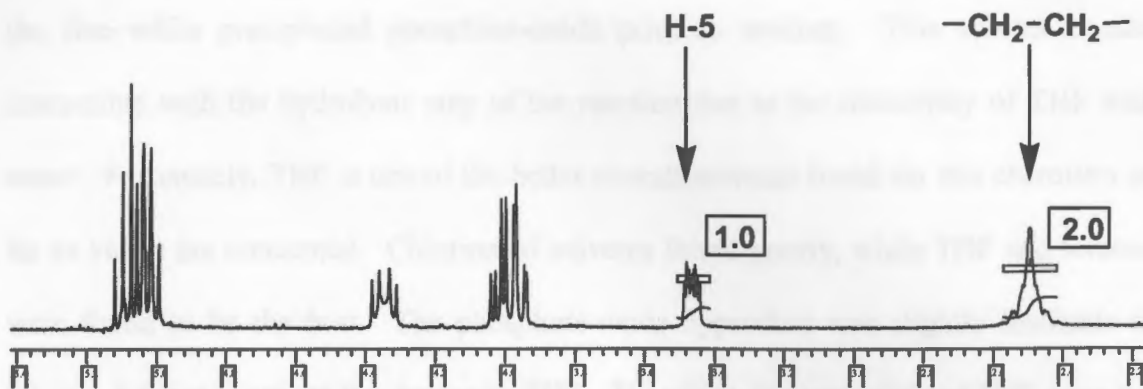


**Figure 10:**  $^1\text{H}$  NMR spectrum of aza-ylide intermediate (2.2-5.4 ppm)

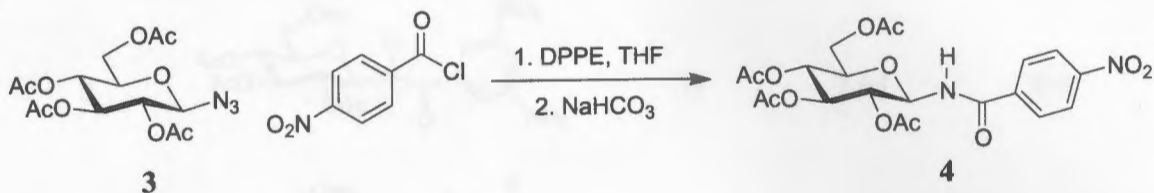
While considering past work with this chemistry within the group, as well as consulting the literature for guidance, some decisions had to be made regarding the order of addition of the reagents in the modified Staudinger chemistry to be employed. Investigations by Boullanger et al. were made utilizing an analogous system using triphenylphosphine with acyl chlorides.<sup>12</sup> These researchers discovered it to be beneficial to have the acylating reagent in the presence of the azide during addition of the phosphine. It has been reasoned that, in addition to better yields, having the acylating agent readily available minimized the anomerization of the  $\beta$ -phosphazene to the  $\alpha$ -phosphazene. These findings were consistent with our initial experimental results in that the yields were better when the reagents occurred in this order rather than first forming the phosphazene and then adding the acyl chloride.

The use of THF as the solvent for this chemistry proved to be useful. It was previously discovered<sup>38</sup> that the bis-oxide byproduct that would result from this chemistry has a low solubility in cold THF. It was reasonable to use this physical

consequence to our advantage in the purification process having the option to filter off the fine white precipitated phosphine-oxide prior to workup. This solvent is also compatible with the hydrolysis step of the reaction due to the miscibility of THF with water. Fortunately, THF is one of the better overall solvents found for this chemistry as far as yields are concerned. Chlorinated solvents fared poorly, while THF and toluene were found to be the best. The phosphine-oxide byproduct was slightly insoluble in toluene, but not nearly to the degree as THF. Therefore, the versatility of THF gave the use of this solvent preference in the Staudinger chemistry performed for this research.

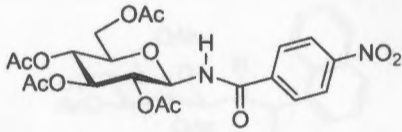
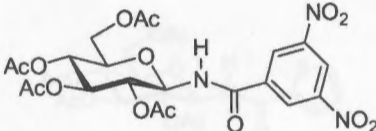
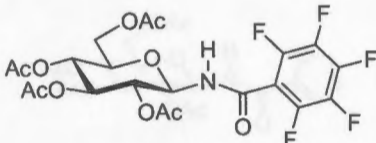
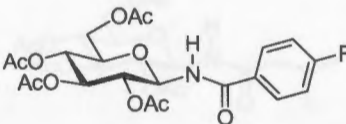
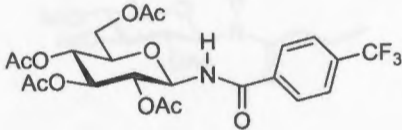
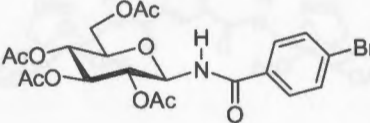
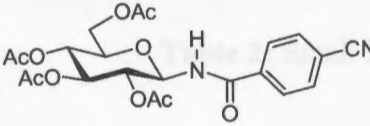
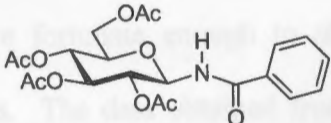
The typical protocol followed for the construction of  $\beta$ -glucosyl amides began with the glucosyl azide **3** and an acyl chloride, *p*-nitrobenzoyl chloride for example, dissolved in THF in a flame-dried vessel under nitrogen (Equation 4). It was felt that attempts should be made to exclude water from the reaction at this point in time to avoid possible hydrolysis of the phosphazene. The DPPE (0.65 equivalents) in a solution of THF was added slowly dropwise and immediate evolution of gas was observed. The reaction mixture was monitored by TLC, usually about 20 minutes after the evolution of nitrogen stopped. In the case of the reaction with *p*-nitrobenzoyl chloride, TLC analysis at this time would show disappearance of the azide, appearance of a new more polar UV active spot with an  $R_f$  value of 0.24 (1:1, hexanes:ethyl acetate) that burns as a carbohydrate, presumably the desired amide product, and the occasional appearance of a separate UV active spot that was less polar than both the glucosyl azide and amide product, speculated to be the imidoyl chloride intermediate. Usually within one hour, a fine white precipitate could be observed in the reaction mixture, which was expected to be the bis-oxide byproduct. The precipitate could be filtered off, and then saturated

sodium bicarbonate added to ensure hydrolysis of any imidoyl chloride intermediate still present at this time. After removing the THF, the crude mixture was taken up in chloroform, washed with water, reduced, and the crude product purified by elution over a short column of silica to give the desired amide product **4** in 82% yield.



**Equation 4:** *p*-Nitrobenzoic acid-(2,3,4,6-tetra-*O*-acetyl- $\beta$ -D-glucopyranosyl)-amide (**4**)

Using the protocol just described, a small library of  $\beta$ -glucosyl amides was produced using a variety of acyl chlorides (Table 2). The reaction conditions are suitable for use with both aromatic and aliphatic acyl chlorides. It was observed that the amide products resulting from reaction with benzoyl derivatives containing electron-withdrawing groups were formed more quickly than in the absence of electron-withdrawing groups. Analysis using TLC usually showed the presence of two carbohydrate compounds in the reaction mixture, one corresponding to the amide product, the other to the expected imidoyl chloride intermediate. After the addition of water the top spot would, in most circumstances, slowly fade indicating conversion to the desired species, namely the amide product. Ambiguities confronted in this hydrolysis step will be discussed shortly.

entry	$\beta$ -glycosyl amide	% yield	N-H signal $\delta$ , in ppm	N-H - H-1 <i>J</i> value, in Hz
4		82	7.29	8.8
5		58	7.64	8.6
6		77	6.95	9.2
7		71	7.03	9.0
8		70	7.29	8.8
9		67	7.04	9.0
10		74	7.27	8.4
11		60	7.14	9.2

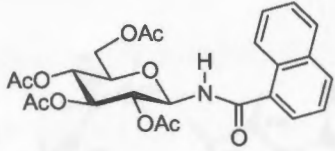
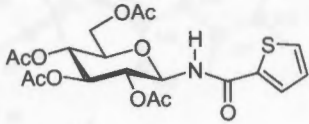
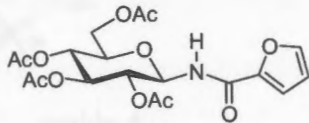
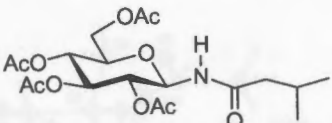
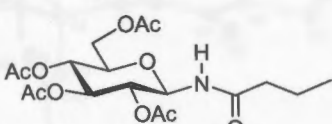
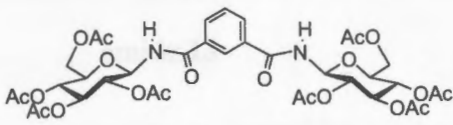
entry	$\beta$ -glycosyl amide	% yield	N-H signal $\delta$ , in ppm	N-H - H-1 <i>J</i> value, in Hz
12		50	6.83	9.7
13		75	6.94	9.0
14		59	7.16	9.3
15		71	6.22	9.3
16		64	6.44	9.3
17		24	7.37	7.8

Figure 11: X-ray crystal structure of amide 12 (30% yield)

**Table 2:** Small library of  $\beta$ -glycosyl amides

We were fortunate enough to obtain the X-ray crystal structures for four  $\beta$ -glycosyl amides. The data obtained from these analyses confirms the stereoselectivity afforded by the present chemistry. This data divulges the *trans* relationship between the H-1 and H-2 protons of the glucose ring indicating retention of stereochemistry around



the anomeric center. The data from the solid state structures agrees with the spectral data from the solution state discussed below.

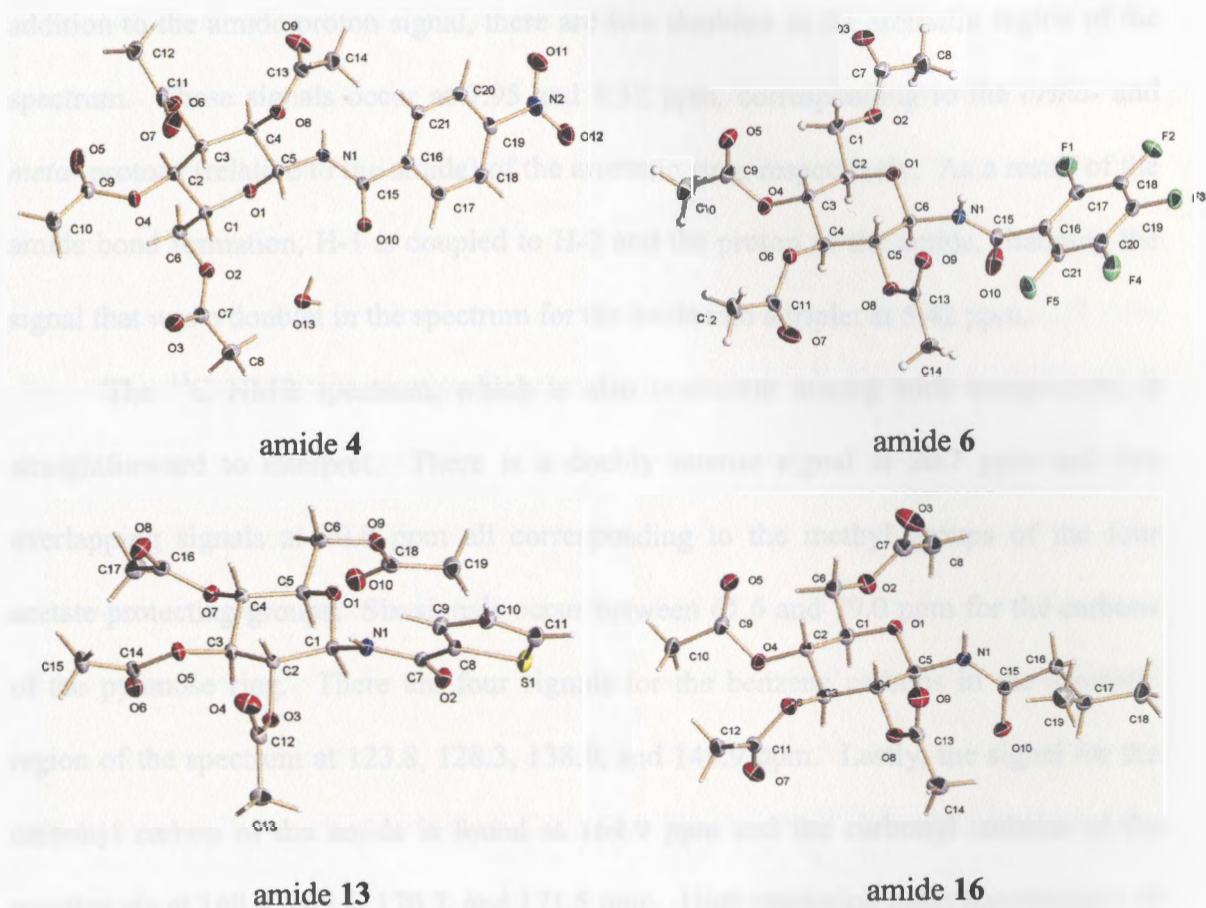


**Figure 11:** X-ray crystal structure of amides 4, 6, 13, and 16

The proton NMR spectrum for the  $\beta$ -glucosyl amide 4, derived from *p*-nitrobenzoyl chloride, exemplifies the typical proton spectrum obtained for the amide products. There are three singlets integrating to twelve protons between 2.06 and 2.09 ppm corresponding to the methyl groups of the acetates. The doublet of doublet of doublets for H-5 and the two doublet of doublets for H-6 and H-6' are all present with

similar chemical shifts to the azide precursor. The real defining signal is the doublet at 7.29 ppm that corresponds to the amide proton. This signal has a coupling constant of 8.8 Hz, which suggests a beta orientation of the aglycone (non-carbohydrate portion). In addition to the amide proton signal, there are two doublets in the aromatic region of the spectrum. These signals occur at 7.95 and 8.32 ppm, corresponding to the *ortho*- and *meta*- protons (relative to the amide) of the aromatic ring, respectively. As a result of the amide bond formation, H-1 is coupled to H-2 and the proton of the amide, changing the signal that was a doublet in the spectrum for the azide into a triplet at 5.42 ppm.

The  $^{13}\text{C}$  NMR spectrum, which is also consistent among such compounds, is straightforward to interpret. There is a doubly intense signal at 20.7 ppm and two overlapping signals at 20.8 ppm all corresponding to the methyl groups of the four acetate protecting groups. Six signals occur between 61.6 and 79.0 ppm for the carbons of the pyranose ring. There are four signals for the benzene carbons in the aromatic region of the spectrum at 123.8, 128.3, 138.0, and 149.9 ppm. Lastly, the signal for the carbonyl carbon of the amide is found at 164.9 ppm and the carbonyl carbons of the acetates are at 169.4, 169.6, 170.3, and 171.5 ppm. High resolution mass spectrometry of the product indicated the measured  $M(+\text{Na})$  at 519.1227 resulting in zero deviation from the calculated  $M(+\text{Na})$  of 519.1227.

The reaction of the aza-ylide with pentafluorobenzoyl chloride produced the  $\beta$ -glucosyl amide **6** in 77% yield after flash column chromatography. The observance of the bisphosphine-oxide byproduct within 45 minutes from the start of the reaction suggested that the reaction proceeded quite quickly. The proton NMR spectrum of the product showed all of the typical signals corresponding to the protons of the sugar

between 2.04 and 5.43 ppm. The only other signal was a doublet corresponding to the amide proton at 6.95 ppm with a coupling constant of 9.2 Hz.

The reaction of the aza-ylide with butyryl chloride produced the  $\beta$ -glucosyl amide **16** in 64% yield. The bisphosphine-oxide in the reaction mixture was not observed as quickly as in other derivatives, usually appearing between 4-8 hours, suggesting that the reaction was slower than with aromatic acyl chlorides with electron-withdrawing groups. Perhaps aromatic acyl chlorides with electron-withdrawing groups can be viewed as being "more activated" due to the possibility that electron density will be pulled away from the carbonyl carbon, making it more electrophilic. In contrast, in reactions with aromatic acyl chlorides where the aromatic ring is devoid of electron withdrawing-groups, as in benzoyl chloride, the electron delocalization is expected to decrease the electrophilicity of the carbonyl. Still, the proton NMR for product **16** is similar to the above examples with the addition of signals at 0.92, 1.58, and 2.10 ppm, which correspond to the alkyl protons of the aglycone. The doublet for the amide proton shows at 6.44 ppm with a coupling constant of 9.3 Hz. The shielding of this proton is expected compared with the amide protons in the aromatic derivatives with electron withdrawing-groups, which are expected to deshield the amide proton through electron withdrawal.

It has been demonstrated that the proton NMR of the  $\beta$ -glucosyl amides derived from various acyl chlorides share key similarities. The signals for the protons of the carbohydrate portion of the molecules stay consistent with that of the azide precursor except for the proton at the anomeric carbon, no longer a doublet, but rather a triplet due to coupling between the amide proton and H-2. The signal for the amide shows in the appropriate region of the spectrum with a large coupling constant indicating the

stereoselective nature of the reaction. The shape of the signals that relate to H-1, H-2, H-3, and H-4 are consistently triplets. One would expect these signals to be doublets of doublets so it is evident that  $J_1$  and  $J_2$  are equivalent in these cases. All of the groups on the glucose portion are equatorial and the protons axial. Therefore, the protons are all in similar environments relative to their coupling companions and have closely matching coupling constants.

Another similarity seen in the proton NMR spectra of several amides is the overlap of the above-mentioned triplets corresponding to the protons of the sugar ring, especially the signals occurring further downfield. One dimensional NMR spectroscopy is not enough to actually distinguish between these signals, which all have coupling constants of about 9.0 Hz. Correlation spectroscopy (Figure 12) was performed on the butyric acid derivative **16** in order to further elucidate the structural nuances of the compound. A correlation is observed between the H-5 signal and the triplet at 5.07 ppm implicating this signal as the H-4 proton signal. The middle portion of the spectrum gets a little crowded but with careful analysis reveals the H-2 proton signal at 4.94 ppm and the H-3 proton at 5.32 ppm. Finally, it is discovered that the slightly upfield portion of the overlapping signals, at 5.30 ppm, belongs to the H-1 signal through correlation with the amide proton signal.

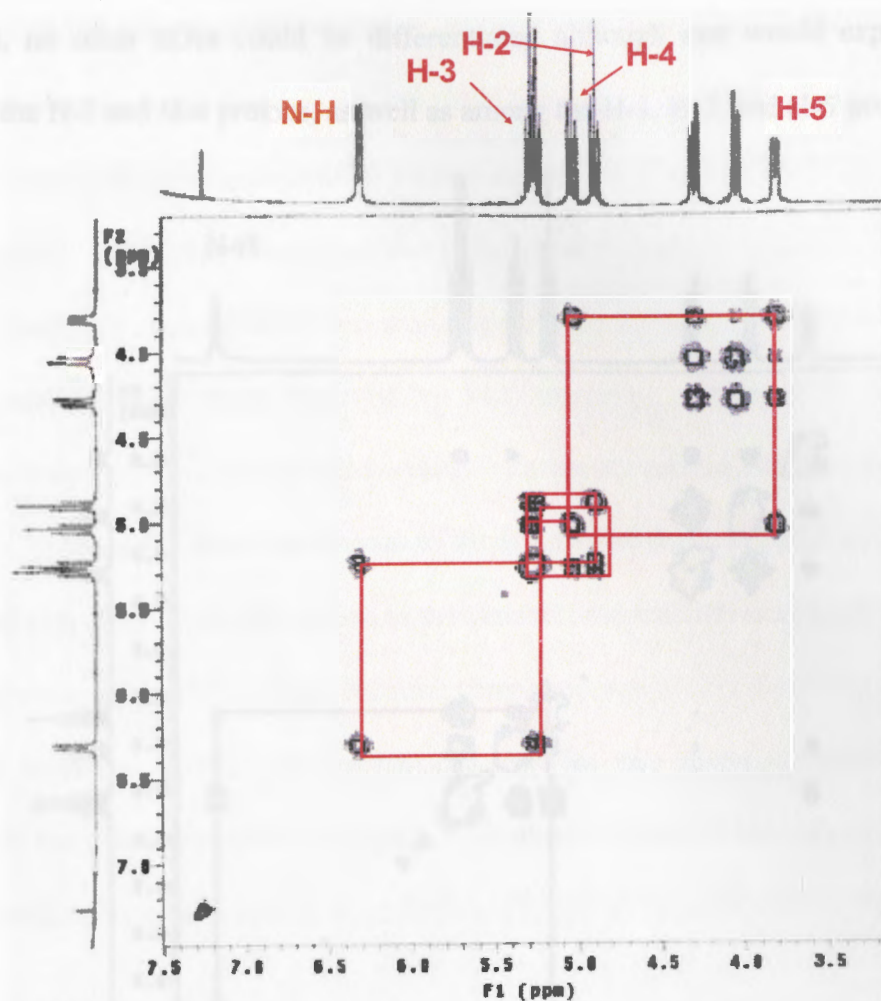


Figure 12: Cosy spectrum of amide 16

Nuclear overhauser effect spectroscopy was also conducted on amide 16 in order to investigate the axial orientation of the protons of the carbohydrate and their relationship to the amide proton (Figure 13). A small nOe is observed between the amide proton signal and the H-2 signal. This observance is expected since the amide proton in an energy minimized 3D structure will be above the plane of the ring as well as the H-2 proton creating a nOe between the protons. Due to the crowded nature of the rest of the



spectrum, no other nOes could be differentiated although one would expect an nOe between the H-2 and H-4 protons, as well as among the H-1, H-3, and H-5 protons.

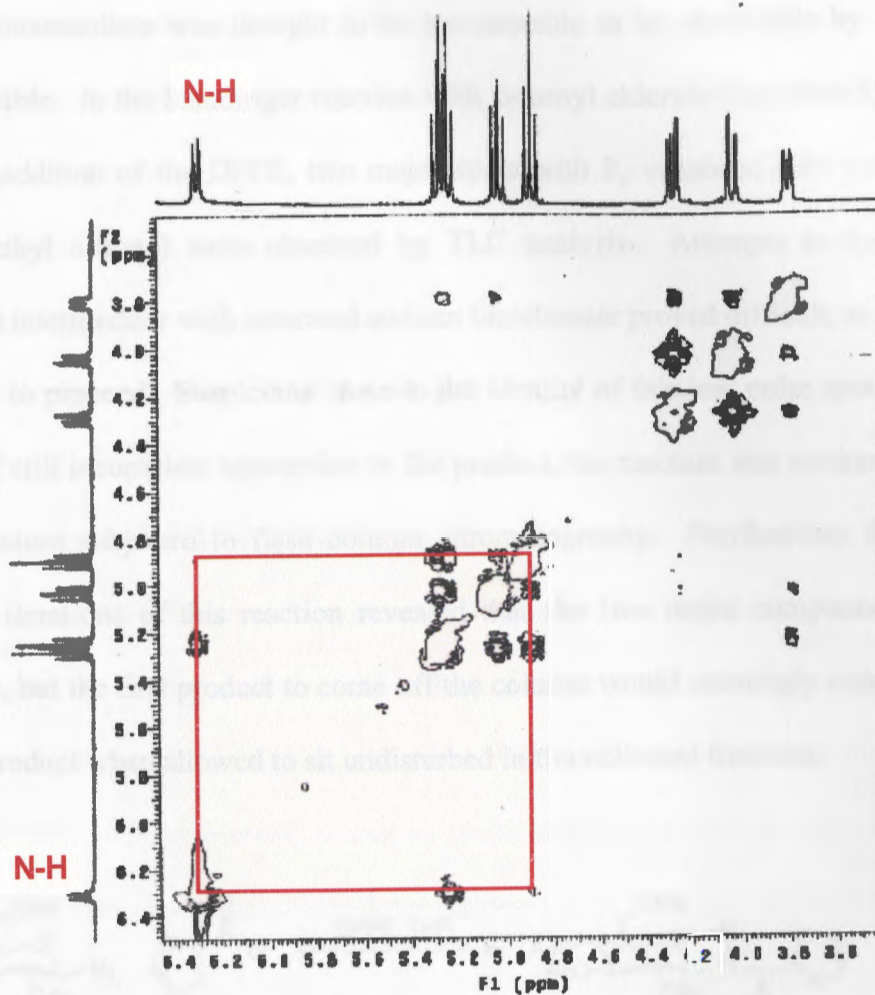


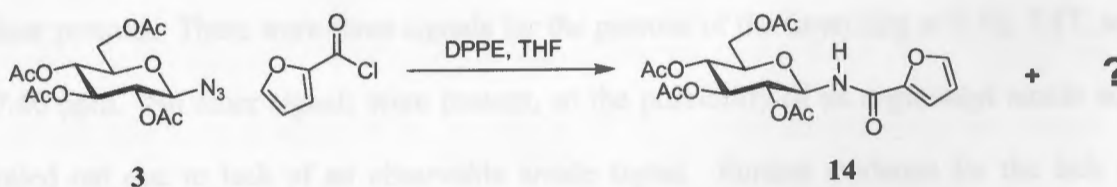
Figure 13: Nuclear overhauser effect spectrum of amide 16

### Evidence for the imidoyl chloride intermediate

The formation of the imidoyl chloride intermediate was confirmed as a result of the difficulty confronted in the reaction of the aza-ylide with 2-furoyl chloride. The reaction pathway of the modified Staudinger chemistry described thus far has been a result of all the data collected in the research. It was not until the investigation into the



identity of the species from reaction with this particular acyl chloride that we confirmed the expected pathway of the reaction. It should be mentioned that, initially, the imidoyl chloride intermediate was thought to be too unstable to be observable by TLC, never mind isolable. In the Staudinger reaction with 2-furoyl chloride (Equation 5), two hours after the addition of the DPPE, two major spots with  $R_f$  values of 0.19 and 0.38 (1:1, hexanes:ethyl acetate) were observed by TLC analysis. Attempts to hydrolyze the suspected intermediate with saturated sodium bicarbonate proved difficult, as the reaction was slow to proceed. Suspicions arose to the identity of this less polar spot. After two days, and still incomplete conversion to the product, the reaction was worked up and the crude mixture subjected to flash column chromatography. Purifications from several different iterations of this reaction revealed that the two major compounds could be separated, but the first product to come off the column would seemingly convert into the desired product when allowed to sit undisturbed in the collected fractions.



**Equation 5:** Furan-2-carboxylic acid-(2,3,4,6-tetra-*O*-acetyl- $\beta$ -D-glucopyranosyl)-amide and unknown compound

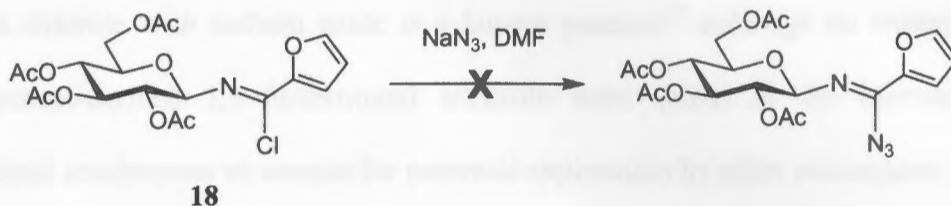
Since the imidoyl chloride intermediate was not expected to be stable enough to be isolated, the compound was thought to possibly be the  $\alpha$ -glucosyl amide. If this were the case, then it would suggest that in order to convert to the product, the  $\alpha$ -glucosyl amide would have to go through some kind of ring-opening equilibration to the more

stable  $\beta$ -glucosyl amide. This would be feasible under conditions that may promote solution phase acid catalysis, perhaps the slightly acidic nature of the silica used during the purification. On the other hand, if this was indeed an equilibration process, then the  $\beta$ -glucosyl amide should equilibrate to the  $\alpha$ -glucosyl amide, albeit in small quantities. TLC experiments were performed in order to test this hypothesis by allowing the  $\beta$ -glucosyl amide to sit in solution for up to two weeks. TLC analysis showed no observable equilibration back to the  $\alpha$ -glucosyl amide.

Attention was turned back to the isolation of this unknown compound. Quick isolation from a flash column, meaning as soon as detected the compound was removed from solution, provided a white solid that was a homogenous spot by TLC. Proton NMR unveiled a unique spectrum that contained signals for a furan ring as well as the carbohydrate. Four singlets from 1.97-2.09 ppm were assigned to the methyl groups of the acetates. The signals for H-5, H-6, and H-6' were consistent with the unaffected glucose portion of the molecule as well as multiplets from 5.18-5.40 ppm integrating to four protons. There were three signals for the protons of the furan ring at 6.52, 7.17, and 7.60 ppm. No other signals were present, so the possibility of an  $\alpha$ -glucosyl amide was ruled out due to lack of an observable amide signal. Further evidence for the lack of amide formation was found in the  $^{13}\text{C}$  NMR spectrum of the compound. No signal was found in the region normally associated with an amide carbonyl carbon, rather a peak was found at 136.5 ppm suggesting that the corresponding carbon was still  $\text{sp}^2$  hybridized as it would be in the imidoyl chloride, but certainly not an amide carbonyl carbon.

While awaiting the high resolution mass spectrometry data, an experiment was run to try to confirm the isolation of the imidoyl chloride. Putative imidoyl chloride **18**

was dissolved in anhydrous DMF and treated with 4 equivalents of sodium azide in efforts to form the imidoyl azide through nucleophilic acyl substitution (Equation 6).



**Equation 6:** Attempted synthesis of imidoyl azide

TLC showed complete consumption of the starting material and formation of a new more polar spot with an  $R_f$  value of 0.22 (1:2, hexanes:ethyl acetate). After extraction and isolation of the product, proton NMR showed an unexpected distribution of signals. For the most part the spectrum was similar to the spectrum for the imidoyl chloride predecessor except there were now three well-resolved triplets at 5.31, 5.45, and 6.01 ppm and more intriguingly a doublet at 6.22 ppm with a coupling constant measuring 9.3 Hz. This result did not agree with the expectations of an imidoyl azide product, but instead suggests the presence of an electron-withdrawing substituent or aromatic group at the anomeric position based on the chemical shift of this signal. The large coupling constant indicated that the group was in the beta orientation.

Working through a reaction mechanism of an azide nucleophile attacking the imidoyl chloride carbonyl carbon exposes an intermediate which may go through an intramolecular cyclization to give the 1,5-disubstituted tetrazole **19** (Figure 14). High resolution mass spectrometry confirmed the imidoyl chloride intermediate with the  $M(+Na)$  found at 482.0835 and the calculated  $(M+Na)$  at 482.0830. The tetrazole was

also confirmed by high resolution mass spectrometry measuring the  $M(+Na)$  at 489.1245, which was calculated at 489.1234. The literature was consulted to try to find incidents of tetrazole formation that resembled this pathway. It turned out that the reaction of an imidoyl chloride with sodium azide is a known reaction<sup>39</sup> although no examples of a carbohydrate-derived 1,5-disubstituted tetrazole were found in the literature. This unexpected result opens an avenue for potential exploration by other researchers.

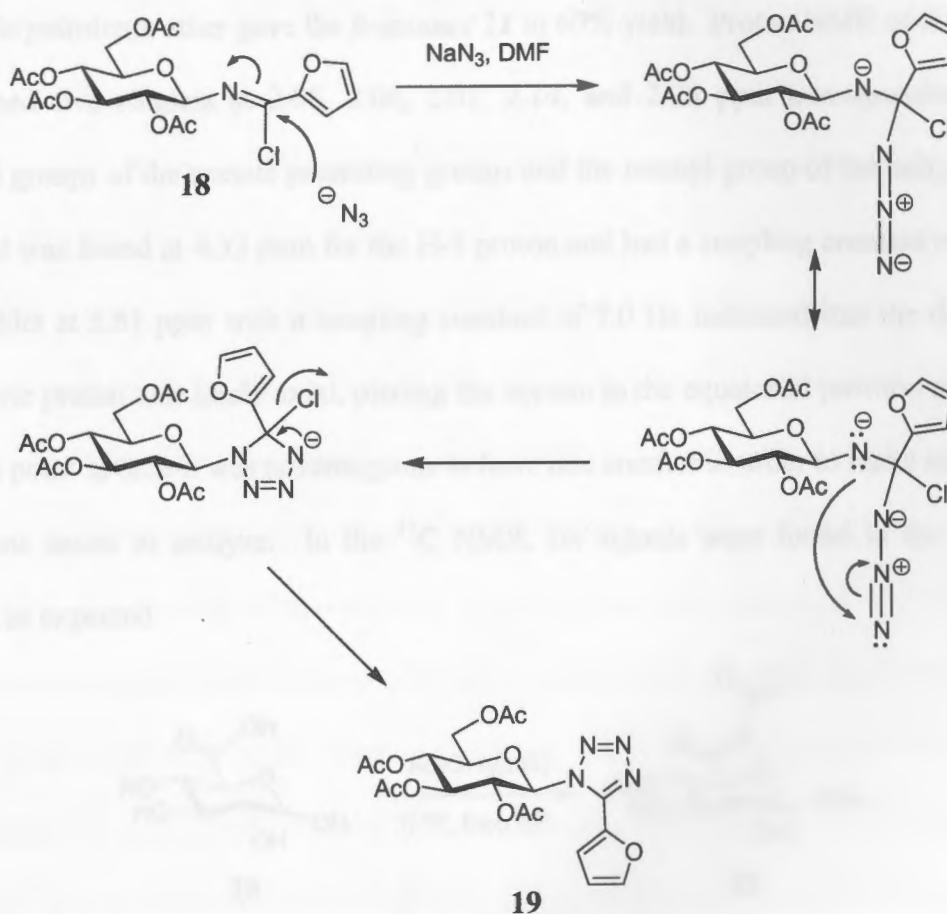
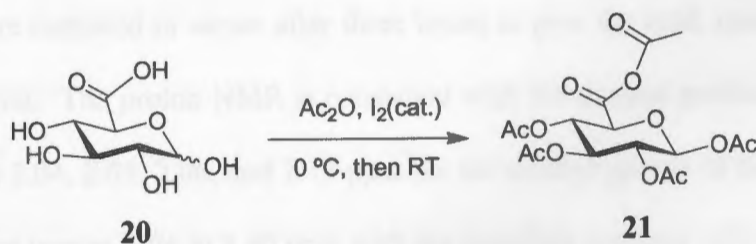


**Figure 14:** Proposed mechanistic depiction of intramolecular cyclization to form 1,5-disubstituted tetrazole 19

### Application to amide-linked oligosaccharides.

In order to apply the modified Staudinger chemistry to the synthesis of oligosaccharides, a carbohydrate-derived acylating agent needed to be prepared. We chose to prepare an anhydride as described by Murphy et al., according to Equation 7.<sup>40</sup> Treatment of D-glucuronic acid (**20**) with an iodine catalyst in acetic anhydride at 0 °C for two hours, then at room temperature for an additional three hours, yielded a mixture of the  $\alpha/\beta$  products after workup. Recrystallization of the mixture using methylene chloride/petroleum ether gave the  $\beta$ -anomer **21** in 60% yield. Proton NMR of the product contained five singlets at 2.05, 2.06, 2.07, 2.14, and 2.28 ppm corresponding to the methyl groups of the acetate protecting groups and the methyl group of the anhydride. A doublet was found at 4.33 ppm for the H-5 proton and had a coupling constant of 9.0 Hz. A doublet at 5.81 ppm with a coupling constant of 7.0 Hz indicated that the deshielded anomeric proton was likely axial, placing the acetate in the equatorial position as desired. At this point in time it was advantageous to have one anomer in order to make subsequent reactions easier to analyze. In the <sup>13</sup>C NMR, six signals were found in the carbonyl region as expected.



**Equation 7:** Preparation of glucuronic acid-derived anhydride **21**

The Staudinger chemistry previously described was attempted using the  $\beta$ -glucosyl azide and the carbohydrate-derived anhydride as the acylating agent. The

reaction mixtures appeared very complicated by TLC analysis and when purification did not give satisfactory results, the anhydride was abandoned as a suitable acylating candidate. It was thought that problems with this approach arose from the presence of two possible points of attack for the aza-ylide as depicted in Figure 15.

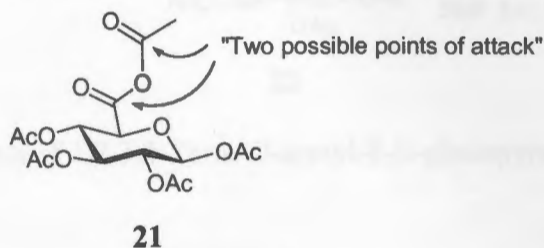
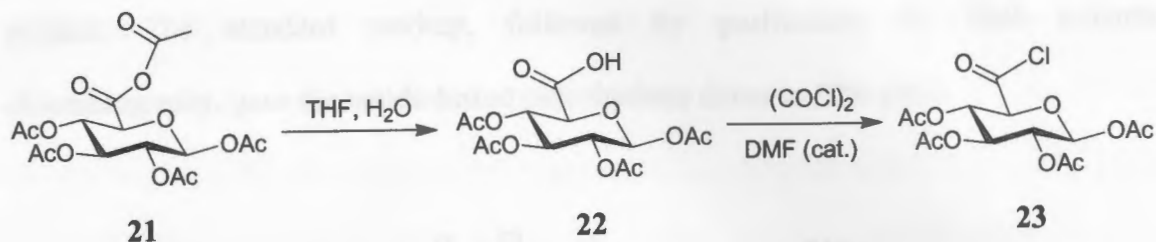


**Figure 15:** Two places for aza-ylide intermediate to attack

To remedy this problem it became apparent to prepare the acyl chloride, a compound reportedly made *in situ* by Murphy et al., from the anhydride, to see if it would fair any better in the Staudinger reaction. This conversion is easily accomplished in two steps, forming carboxylic acid **22**, and then the acyl chloride **23** (Scheme 4). The conversion of anhydride **21** to carboxylic acid **22** occurs in a mixture of THF and water. The solvents are removed *in vacuo* after three hours to give the acid, quantitatively, as a fluffy white solid. The proton NMR is consistent with the desired product showing only four singlets at 2.04, 2.05, 2.06, and 2.13 ppm for the methyl groups of the acetates. The anomeric proton moves little to 5.80 ppm with the coupling constant still reflecting the  $\beta$ -configuration at 7.5 Hz. A broad singlet is documented at 9.17 ppm in the experimental section of this work. This signal corresponds to the carboxylic acid proton and actually will show at varying chemical shift values in the proton NMR spectrum. The  $^{13}\text{C}$  NMR



shows loss of one carbonyl carbon from the starting material, while all other signals changed little.

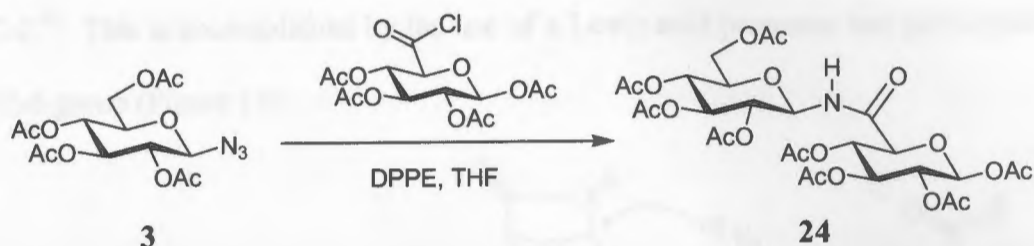


**Scheme 4:** Synthesis of 1,2,3,4-Tetra-*O*-acetyl- $\beta$ -D-glucopyranosyl chloride (**23**)

The acid (**22**) was converted to the acyl chloride (**23**) in dry methylene chloride in the presence of two equivalents of oxalyl chloride and a catalytic amount of DMF (Scheme 4). The use of two equivalents of oxalyl chloride was employed to ensure full conversion of starting material. Removal of the volatiles after two and a half hours revealed the acyl chloride (**23**) as a purple solid with a chalky consistency in near quantitative yield. The proton NMR of the product differed from that of the precursor in the absence of the broad carboxylic acid signal. The signals for the protons of the pyranose ring also separated from their previous presentation as overlapping multiplet signals. The signals were now two well-resolved doublets of doublets at 5.12 and 5.28 ppm and a triplet at 5.41 ppm correlating to H-2, H-3, and H-4 respectively. The signal for the anomeric proton remained a doublet at 5.89 ppm and had a coupling constant of 6.4 Hz.

The Staudinger chemistry could now be attempted with the carbohydrate-derived acyl chloride (Equation 8). The reaction was performed using the typical modified Staudinger conditions discussed above, but only 1.6 equivalents of the acyl chloride was

discovered to be needed to ensure acceptable results with this chemistry. After 5 hours, consumption of the aza-ylide was observed by TLC with the appearance of a new spot with an  $R_f$  value of 0.19 (4:5, hexanes:ethyl acetate), assumed to be the desired amide product. The standard workup, followed by purification by flash column chromatography, gave the amide-linked carbohydrate dimer in 72% yield.



**Equation 8:** Synthesis of amide-linked carbohydrate dimer 24

Analysis of the proton NMR spectrum indicated seven singlets integrating to 24 protons, which correspond to the eight acetate protecting groups of the dimer. The signals for H-5, H-6, and H-6' of the glucose portion of the dimer are well-resolved. The signals for H-5 and H-1 of the glucuronic acid portion of the dimer are doublets at 4.04 and 5.75 ppm. The telltale sign of amide bond formation is the appearance of a doublet at 7.13 ppm with a coupling constant of 9.2 Hz. This value confirms that the amide bond had been formed stereoselectively. High resolution mass spectrometry found the mass to be  $M(+Na)$  714.1808.

The idea to be investigated after successful formation of the amide-linked disaccharide 24 was to see whether the acetate-protected anomeric position of the glucuronic acid portion of the dimer could be functionalized again. The sequence of reactions was hoped to be as simple as bromination to the  $\alpha$ -bromide followed by

azidation in an  $S_N2$  process. Unfortunately, the acidic conditions of the bromination appeared too drastic as TLC analysis of the reaction mixture showed a complicated mixture of compounds that would be too troublesome to isolate in an efficient manner. Therefore, another method had to be found to achieve functionalization of the dimer.

Murphy et al. reported that glucuronic acid and its amide derivatives promote 1,2-*cis*-glycosides even in the presence of an equatorially positioned acetate protecting group at C-2.<sup>40</sup> This is accomplished by the use of a Lewis acid promoter and participation of the C-6 group (Figure 16).

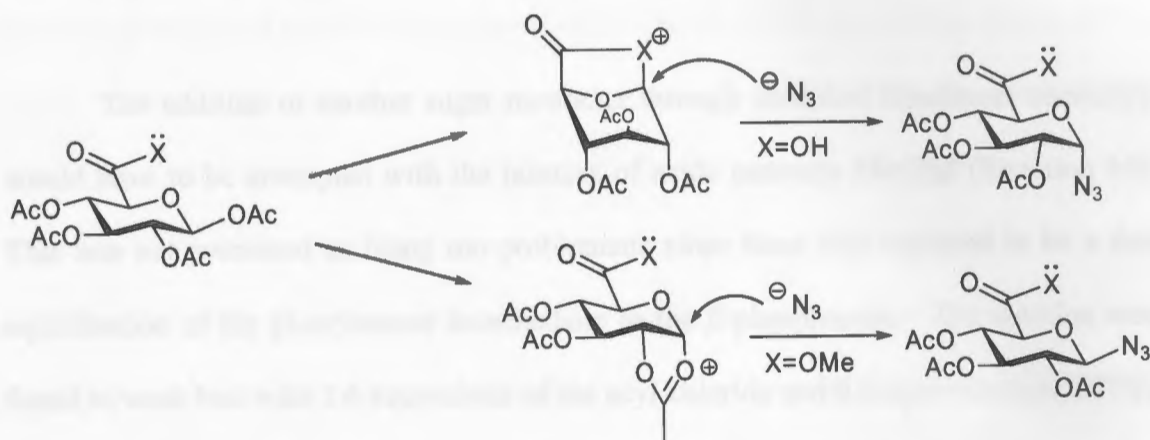
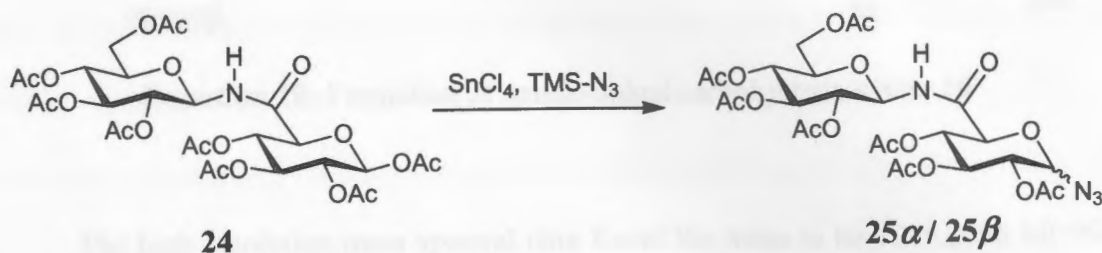


**Figure 16:** Glucuronic acid and its amide derivative promote 1,2-*cis*-glycosides

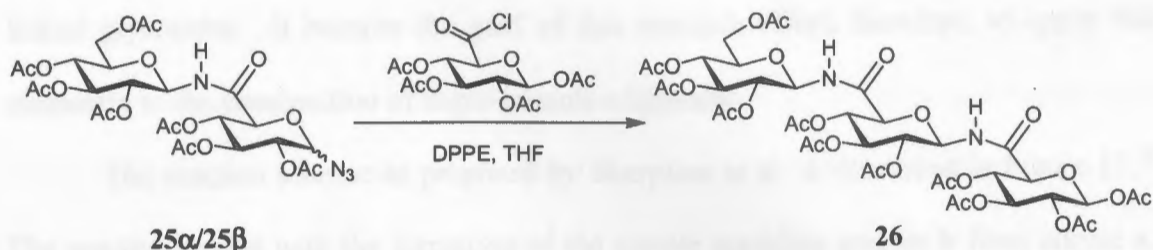
Attack by the nucleophile occurs from underneath the carbohydrate ring to give primarily the  $\alpha$ -glycoside. Our attempt at this method employed treatment of **24** with  $\text{SnCl}_4$  (0.5 equiv.) and  $\text{TMS-N}_3$  (2.5 equiv.) and gave mixed results (Equation 9). The reaction was performed in dry methylene chloride and run for 15 hours after which TLC showed consumption of starting material and formation of a new less polar spot. While formation of the  $\alpha$ -azide was accomplished, the  $\beta$ -azide was also detected in the proton NMR spectrum of the reaction mixtures in ratios that varied. Isolation of only the  $\alpha$ -

azide was not accomplished and the best  $\alpha/\beta$  ratio obtained was 5:1. Silica flash column chromatography was not practical enough to separate the anomers consistently.



**Equation 9:** Lewis acid-catalyzed azidation of **24**

The addition of another sugar monomer through modified Staudinger chemistry would have to be attempted with the mixture of azide anomers **25 $\alpha$ /25 $\beta$**  (Equation 10). This was not perceived as being too problematic since there was expected to be a fast equilibration of the phosphazene intermediate to the  $\beta$ -phosphazene. The reaction was found to work best with 1.6 equivalents of the acyl chloride and 0.6 equivalents of DPPE, which was added in the typical manner. The reaction was allowed to stir for 6 hours by which time consumption of the azide mixture was observed and a new more polar spot appeared on a TLC plate. The reaction was subjected to the standard workup. Flash column chromatography provided the desired product in 53% yield. Some of the product was collected as a mixture with another compound thought to be the  $\alpha$ -anomer.



**Equation 10: Formation of amide-linked carbohydrate trimer 26**

The high resolution mass spectral data found the mass to be 1015.2618 M(+Na). The proton NMR spectrum of the major product **26** contained nine signals from 2.03-2.21 ppm integrating to 33 protons corresponding to the 11 acetate protecting groups of the trimer. Two doublets appear at 3.97 and 4.09 ppm each with coupling constants of 10.1 Hz. These are the signals that correlate with the H-5 protons of the glucuronic acid portions of the molecule. Lastly, two doublets were observed at 7.14 and 7.32 ppm indicating the presence of two amide bonds. The coupling constants were 9.5 and 9.3 Hz respectively confirming the beta configuration of C-1 of each ring. It has been concluded that the modified Staudinger chemistry can be effectively applied to carbohydrate amide oligomer synthesis. The major problem confronted was the separation of diastereomeric mixtures of products.

**Cu(I)-catalyzed cycloadditions to form 1,4-disubstituted 1,2,3-triazoles.**

There has been much interest in the so-called “click chemistry” reactions in the past several years. The Cu(I)-catalyzed reaction of terminal alkynes with an azide to form exclusively 1,4-disubstituted 1,2,3-triazoles is one such reaction that has received much attention. Past and present research within the Norris research group has demonstrated this set of reaction conditions to be quite useful for constructing triazole-

linked glycosides. It became the goal of this research effort, therefore, to apply this chemistry to the construction of sugar-triazole oligomers.

The reaction scheme as proposed by Sharpless et al. is illustrated in Figure 17.<sup>32</sup> The reaction begins with the formation of the copper acetylide species **b** from alkyne **a**. The internal nitrogen then coordinates to the copper of the acetylide to form **c** with subsequent attack on C-2 of the acetylide by the azide terminus to form the metallocycle **d**. Collapse of the metallocycle into the copper triazole species **e** is followed by proteolysis to give the 1,4-disubstituted 1,2,3-triazole **f** exclusively.

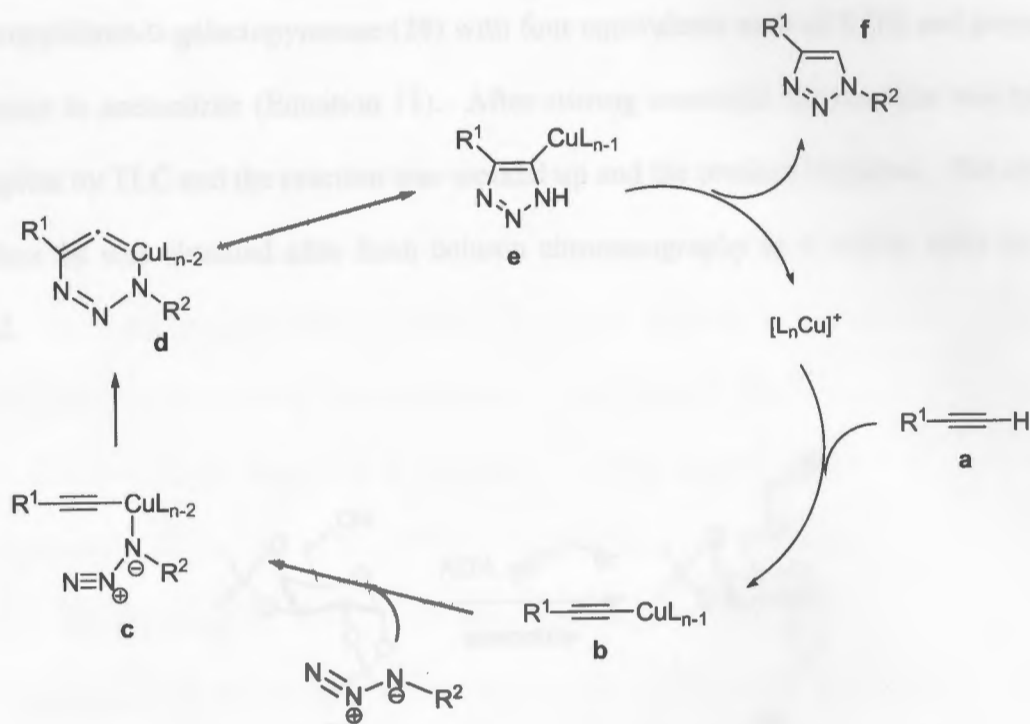


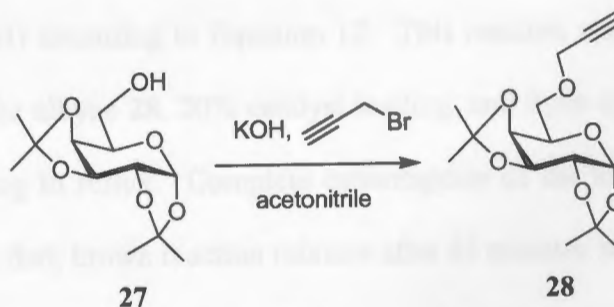
**Figure 17:** Proposed mechanism for Cu(I)-catalyzed triazole formation

There are several features of this chemistry that make it particularly appealing to use for the construction of oligomeric structures. First, the stereochemical outcome of the reaction can easily be controlled through use of a stereochemically pure azide. Since



we can easily prepare a  $\beta$ -glycosyl azide, we expect to retain the stereochemistry giving primarily the  $\beta$ -glycoside. Secondly, by using the Cu(I)-catalyzed conditions we can control the regiochemistry of the reaction product. The uncatalyzed thermal cycloaddition yields a mixture of 1,4- and 1,5-disubstituted triazoles, a mixture of regioisomers. Lastly, the reactions are generally high yielding and provide triazole-linked products that usually do not need further purification.

Before the construction of oligomers could be attempted, carbohydrate-derived alkynes had to be prepared. Alkyne **28** was made by treating 1,2:3,4-di-*O*-isopropylidene-D-galactopyranose (**29**) with four equivalents each of KOH and propargyl bromide in acetonitrile (Equation 11). After stirring overnight the reaction was judged complete by TLC and the reaction was worked up and the product extracted. The desired product **28** was obtained after flash column chromatography as a yellow solid in 80% yield.



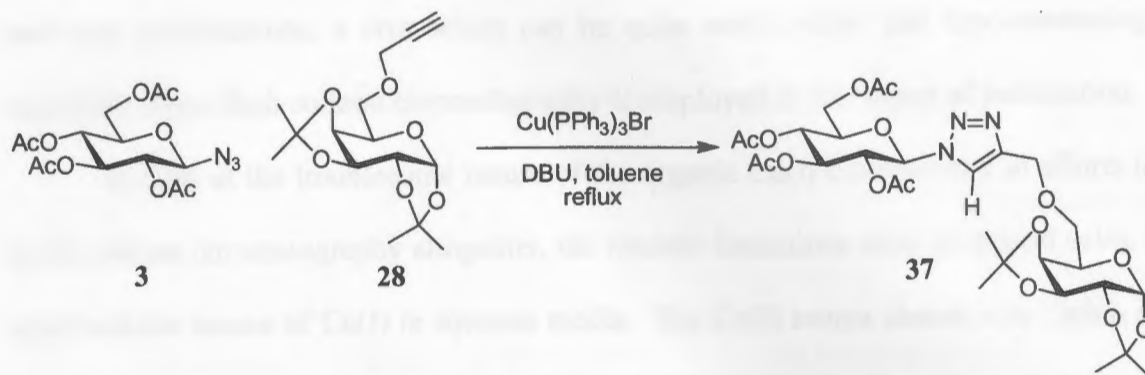
**Equation 11:** 1,2:3,4-di-*O*-isopropylidene-6-(prop-2-ynoxy)-D-galactopyranose (**28**)

The  $^1\text{H}$  NMR spectrum of alkyne **28** contained four singlets, integrating to three protons each, belonging to the methyl groups of the two isopropylidene protecting groups. The proton of the alkyne could be found at 2.44 ppm as a triplet. The coupling

constant was found to be 2.0 Hz, a small value indicating coupling to the remote methylene protons between the ether oxygen and the alkyne. High resolution mass spectrometry found the  $M(+Na)$  to be 694.2433.

To see if the glucosyl azide **3** and carbohydrate-derived alkyne **28** would be compatible in the cycloaddition chemistry, the reaction was tested thermally and without catalysis. The setup simply required the azide and alkyne to be dissolved in toluene and refluxed. Several attempts were made to bring the reaction to completion, but there would remain starting material, as evidenced by TLC even after 8 days. Regardless, the TLC showed formation of two major spots that burned lower on a TLC plate, as well as unreacted starting material. A mixture of the regioisomers (0.39 g, 58%) was isolated after column chromatography with a 1:1 ratio of regioisomers, which is typical for the Huisgen 1,3-dipolar cycloaddition.<sup>1</sup>

Since the reaction between glucosyl azide **3** and alkyne **28** was successful, the Cu(I)-catalyzed version was explored using a  $Cu(PPh_3)_3Br$  catalyst, an organic and air-stable source of Cu(I) according to Equation 12. This reaction was first attempted with 1.1 equivalents of the alkyne **28**, 20% catalyst loading, and three equivalents of DBU in toluene while heating to reflux. Complete consumption of the azide was observed by TLC analysis of the dark brown reaction mixture after 45 minutes with appearance of one new more polar spot that matched, by TLC, one of the compounds from the thermal cycloaddition. The reaction was allowed to stir for an additional 16 hours to observe any possible changes by which time several new spots appeared, which were even more polar than the alleged product. The triazole (**37**) was obtained after evaporation of the reaction mixture and flash column chromatography (1:2, hexanes:ethyl acetate).



**Equation 12:** Formation of triazole **37** using  $\text{Cu(PPh}_3)_3\text{Br}$  catalyst

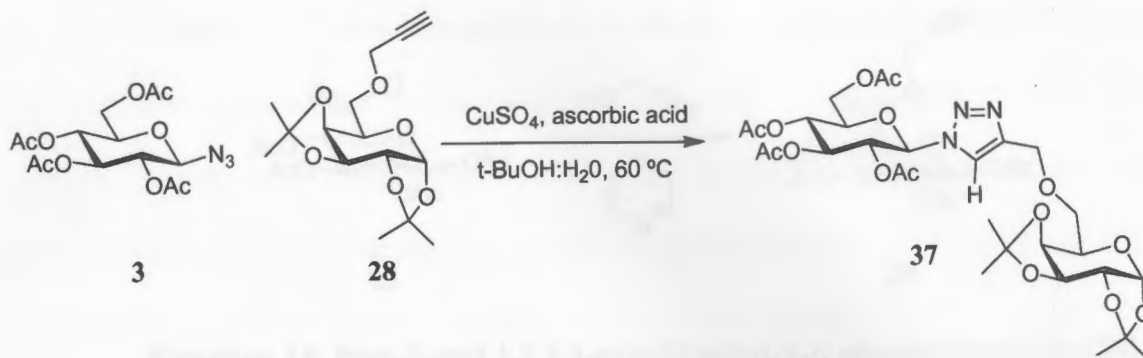
The  $^1\text{H}$  NMR spectrum of triazole **37** showed one singlet at 7.84 ppm corresponding to the triazole proton. The protons from the protecting groups of the different carbohydrates are easily discernible. Four singlets are found from 1.34-1.54 ppm for the methyl protons of the isopropylidene groups while four singlets from 1.88-2.09 ppm belong to the methyl protons of the acetate protecting groups. Other noteworthy signals include the doublet at 5.56 ppm with a  $J$  value of 4.9 Hz indicating the H-1 proton of the galactopyranose sugar and a doublet at 5.89 ppm,  $J = 8.8$  Hz, for the H-1 proton of the glucose portion. The coupling constants of these doublets reflect the stereochemistry around the anomeric centers of the parent sugars, alpha and beta, respectively.

The best yield obtained for the system just discussed was 38.7% of **37** obtained as a yellow syrup. When the base was switched to DIPEA and the reaction time shortened to 1.5 hours, the yield was increased to 85% following flash column chromatography. It was observed by Santoyo-Gonzalez et al. using similar chemistry that the best source of Cu(I) varied among distinct carbohydrate systems with seemingly no observable trend.<sup>41</sup>

The success of coupling sugars through this method required screening various catalyst and base combinations, a task which can be quite cumbersome and time-consuming, especially when flash column chromatography is employed as the means of purification.

In light of the troublesome nature of the organic Cu(I) catalysts and in efforts to avoid column chromatography altogether, the triazole formations were attempted using a water-soluble source of Cu(I) in aqueous media. The Cu(I) source chosen was CuSO<sub>4</sub> in the presence of ascorbic acid which will reduce Cu(II) to Cu(I). These "green" reaction conditions, as mentioned by the groups who presented this remarkable finding, would require stoichiometric amounts of the reactants and minimal amounts of the catalyst.<sup>32</sup> They report extreme efficiency usually within 24 hours when the reaction is conducted in water at room temperature, with the occasional use of a co-solvent such as *t*-BuOH to help dissolve non-polar molecules. The products were isolated by mere filtration and the yields were often times near quantitative. This seemed to be a very promising path to explore due to its many practical benefits.

The formation of triazole **37** was achieved in 90 minutes using 12.5% ascorbic acid and 1.3% CuSO<sub>4</sub> in water and *t*-BuOH with heating to 60 °C (Equation 13). The reaction began as a heterogeneous mixture and upon heating became a homogenous solution. TLC showed disappearance of both starting materials and formation of a new more polar spot, which matched the R<sub>f</sub> of the desired compound. The reaction mixture was cooled, the excess alcohol removed by reduced-pressure evaporation to a suspension, and upon addition of water the product precipitated. The precipitate was collected on a glass frit to give 84% of the product as a colorless solid.

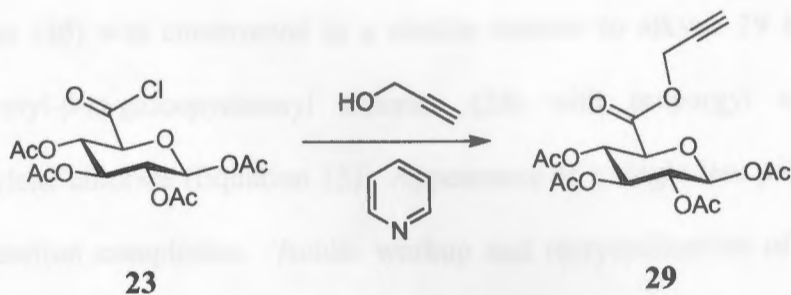


**Equation 13:** Formation of **37** by Cu(I)-catalysis in aqueous medium

Attempts were made to remove the isopropylidene protecting groups of **37** with various concentrations and strengths of acids in hopes that the anomeric position of the galactopyranose portion of the molecule could be functionalized again. Results were ambiguous, as the crude reaction mixtures were difficult to interpret by NMR, with the integrity of the ether moiety under question. The deprotection attempts were aborted at this time to follow alternate routes to functionalizable compounds.

It was decided that alkynes with acetate protecting groups were obvious candidates for providing quicker access to molecules with substituents at the anomeric position that could be manipulated further. The precursor for the first peracetylated alkyne was already routinely synthesized for use in the modified Staudinger chemistry. Treatment of 1,2:3,4-tetra-*O*-acetyl- $\beta$ -D-glucopyranosyl chloride (**23**) with propargyl alcohol and pyridine in methylene chloride gave quick access to the desired ester alkyne **29** through nucleophilic acyl substitution (Equation 14).





**Equation 14:** Prop-2-ynyl 1,2,3,4-tetra-*O*-acetyl- $\beta$ -D-glucopyranuronate (**29**)

The reaction was monitored by TLC and judged complete with the appearance of one new spot that differed from the streak that the chloride starting material would leave at the baseline. After acidic workup the essentially pure solid material could be recrystallized from hot methanol to give the alkyne **29** as clear crystals. The X-ray crystal structure was obtained and the resulting solid state data was published (Figure 18).<sup>42</sup> In the <sup>1</sup>H NMR spectrum, the signal for the alkyne may be found at 2.53 ppm as a triplet. It is coupled to the methylene protons and has a small coupling constant of 2.5 Hz.

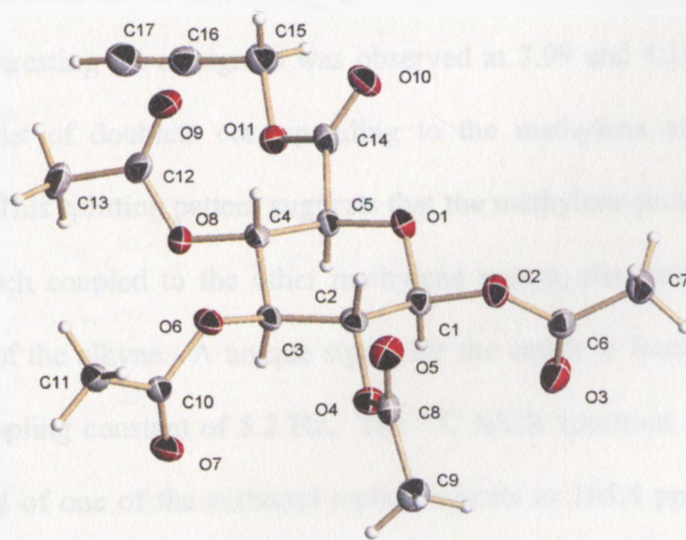
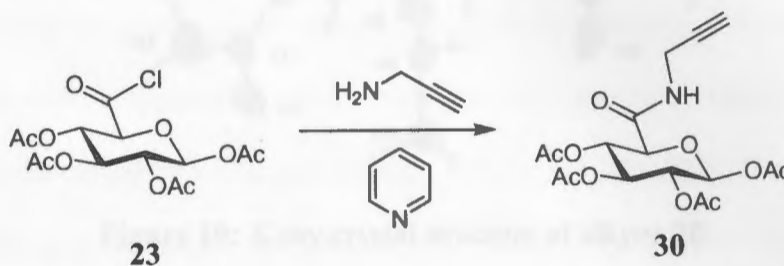


**Figure 18:** X-ray crystal structure of alkyne **29**



The alkyne (**30**) was constructed in a similar manner to alkyne **29** by treating 1,2,3,4-tetra-*O*-acetyl- $\beta$ -D-glucopyranosyl chloride (**23**) with propargyl amine and pyridine in methylene chloride (Equation 15). Appearance of a single less polar spot by TLC indicated reaction completion. Acidic workup and recrystallization of the crude solid material gave the desired compound as thin white crystals which were analyzed by X-ray crystallography (Figure 19).



**Equation 15:** Preparation of alkyne **30**

The alkynyl proton signal, observed at 2.27 ppm ( $J = 2.6$  Hz), is slightly upfield compared with the signal for the ester alkyne proton in the proton NMR spectrum. This shift likely results from the more electronegative character of an oxygen compared with nitrogen. An interesting set of signals was observed at 3.99 and 4.16 ppm, that of two doublet of doublet of doublets corresponding to the methylene protons next to the nitrogen group. This splitting pattern suggests that the methylene protons are in different environments, each coupled to the other methylene proton, the amide proton, and the terminal proton of the alkyne. A unique signal for the amide is found at 6.50 ppm as a triplet with a coupling constant of 5.2 Hz. The  $^{13}\text{C}$  NMR spectrum indicates about a 3 ppm shift upfield of one of the carbonyl carbon signals to 165.4 ppm representing the carbonyl carbon of the amide.

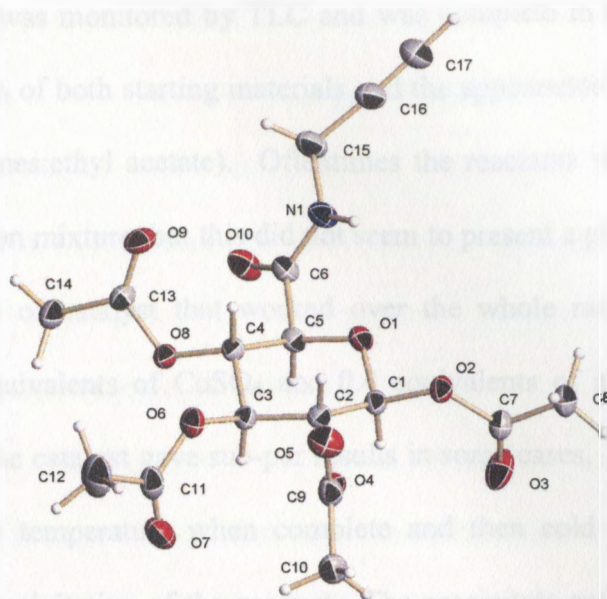
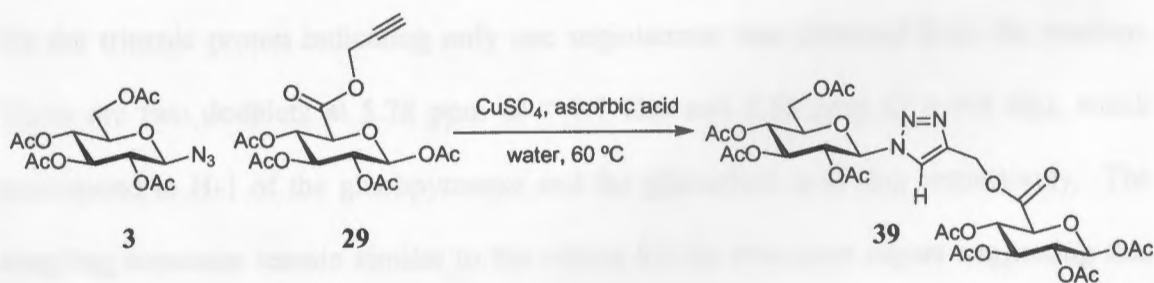


**Figure 19:** X-ray crystal structure of alkyne **30**

The Cu(I)-catalyzed cycloadditions could now be attempted using the carbohydrate-derived alkynes with the glucosyl azide. Since the azide and alkyne were both protected with acetate groups, it was thought that the reaction could be conducted in only water. A typical reaction was run with stoichiometric amounts of the azide **3** and alkyne **29**, CuSO<sub>4</sub> (0.2 equiv.), ascorbic acid (0.4 equiv.) in water (0.1 g/mL) and heated to 60 °C (Equation 16).



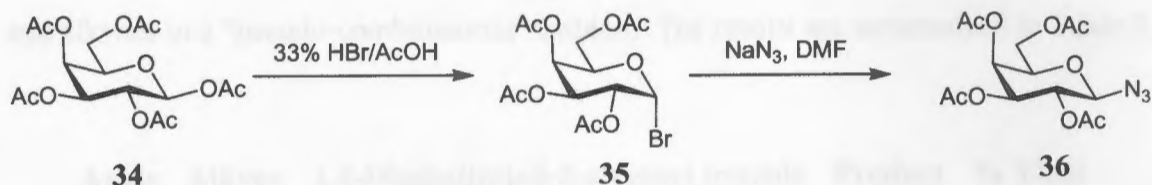
**Equation 16:** Formation of triazole **39** by Cu(I)-catalysis in aqueous medium

The reaction was monitored by TLC and was complete in about 6 hours. TLC revealed consumption of both starting materials and the appearance of a more polar spot ( $R_f = 0.32$ , 1:2 hexanes:ethyl acetate). Oftentimes the reactants would not completely dissolve in the reaction mixture, but this did not seem to present a problem in most cases. The optimal amount of catalyst that worked over the whole range of carbohydrates explored was 0.2 equivalents of  $\text{CuSO}_4$  and 0.4 equivalents of ascorbic acid. Using smaller amounts of the catalyst gave sub-par results in some cases. The reaction mixture was cooled to room temperature when complete and then cold water was added to facilitate adequate precipitation of the product. The precipitate could simply be filtered over a glass frit to give the product **39** as a white solid in 71% yield. The best results were obtained when the crude reaction mixture was extracted into methylene chloride instead of filtering the precipitate, and then reduced to the same white solid in 95.5% yield. A possible explanation for the difference in yield is that during filtration there exists the propensity for a portion of the product to pass through the filter and escape collection thereby lowering the yield. The important note here is that no column chromatography is needed after the synthesis of any of the acetate-protected dimers.

Analysis of the  $^1\text{H}$  NMR spectrum for triazole **39** showed a singlet at 7.89 ppm for the triazole proton indicating only one regioisomer was obtained from the reaction. There are two doublets at 5.78 ppm ( $J = 7.7$  Hz) and 5.88 ppm ( $J = 9.0$  Hz), which correspond to H-1 of the glucopyranose and the glucuronic acid ring respectively. The coupling constants remain similar to the values for the precursor sugars suggesting that the stereochemistry was retained and there is no epimerization around the anomeric carbon of the glucopyranose ring. The signals for the methyl groups of the acetates are

observed as seven singlets from 1.89-2.12 ppm that integrate to 24 protons. In the  $^{13}\text{C}$  NMR there are eleven signals from 62.6-92.3 ppm that correspond to the carbons of the sugar rings. Two signals resonate at 124.0 and 143.0 ppm for the carbon of the heterocycle, while nine signals from 167.2-171.4 ppm signify the carbons from the carbonyls of the eight acetates and the ester group at C-6 of the glucuronic acid. High resolution mass spectrometry found 796.2031 M(+Na).

With access to several carbohydrate-derived alkynes and only one sugar azide, it seemed plausible to prepare a different sugar azide in order to introduce structural diversity into the triazole products and to see if the chemistry was equally applicable. A galactosyl azide was prepared as shown in Scheme 5.



**Scheme 5:** Synthesis of 2,3,4,6-tetra-*O*-acetyl- $\beta$ -D-glucopyranosyl azide (36)

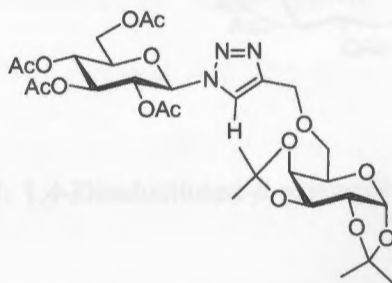
The galactosyl bromide 35 was prepared through reaction of the pentaacetate 34 with 33% HBr in acetic acid. After one hour TLC analysis showed disappearance of the starting material (34) and appearance of a new less polar spot with an  $R_f$  value of 0.47 (1:1 hexanes:ethyl acetate). After a basic workup the bromide 35 was obtained as a clear syrup (98%). The proton NMR spectrum for 35 showed a doublet at 6.69 ppm with a coupling constant of 3.8 Hz corresponding to H-1 and indicating the isolation of the  $\alpha$ -bromide.

Treatment of the bromide **35** with 4.0 equivalents of sodium azide in DMF at room temperature gave access to the  $\beta$ -galactosyl azide **36**. The reaction was judged complete using TLC when the starting material spot disappeared and a new spot, slightly more polar, appeared with an  $R_f$  value of 0.44 (1:1 hexanes:ethyl acetate). The DMF was removed and the crude reaction mixture was partitioned between methylene chloride and water. After reducing to a clear syrup the product was recrystallized by slow evaporation from methanol or by seeding a saturated methanolic solution to obtain large crystals (73%). The  $^1\text{H}$  NMR spectrum of **36** showed a shift upfield of the H-1 signal from 6.59 to 4.62 ppm. The coupling constant for this doublet is 8.8 Hz indicating the change of orientation to the  $\beta$ -galactosyl azide. The Cu(I)-catalyzed cycloadditions could now be attempted to produce 1,4-disubstituted 1,2,3-triazoles from carbohydrate-derived azides and alkynes in a "pseudo-combinatorial" fashion. The results are summarized in Table 3.

**Azide**   **Alkyne**   **1,4-Disubstituted- $\beta$ -glycosyl triazole**   **Product**   **% Yield**

3

28

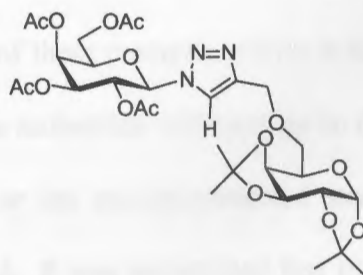


37

84

36

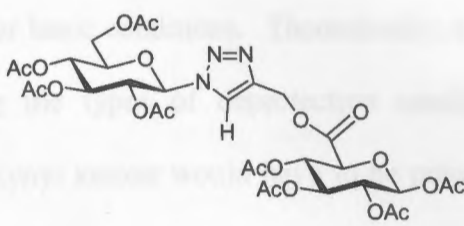
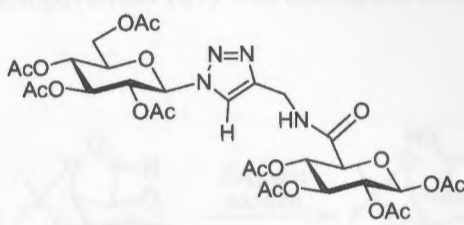
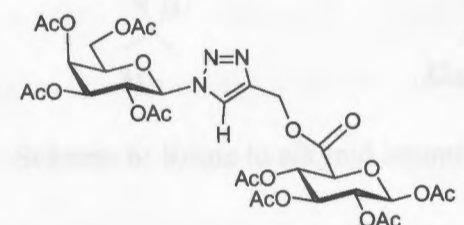
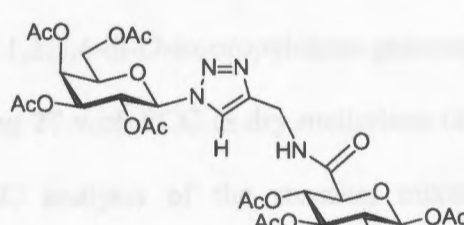
28



38

75

**Azide Alkyne 1,4-Disubstituted- $\beta$ -glycosyl triazole Product % Yield**

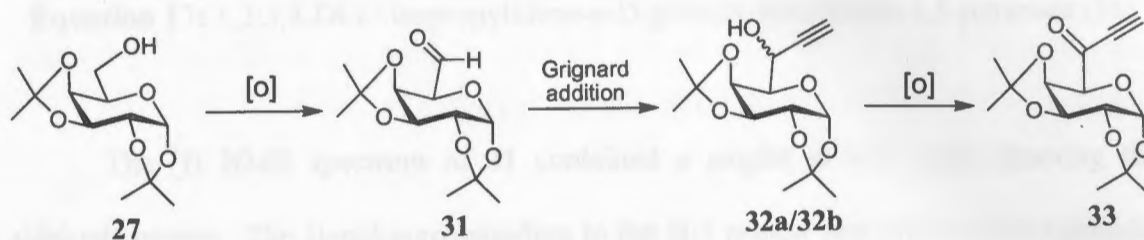
3	29		39	95
3	30		40	91
36	29		41	90
36	30		42	92

**Table 3:** 1,4-Disubstituted- $\beta$ -glycosyl 1,2,3-triazoles

Since one of the goals of these research efforts is the construction of *N*-glycosides to serve as glycomimetics, the molecules will have to be deprotected in order to make them biologically accessible. For the acetate-protected analogues, basic reaction conditions would have to be employed. It was recognized that the ester linkage in triazoles 39 and



**41** would be severed under these conditions. This foresight led to the preparation of the alkyne **30** and subsequent triazoles **40** and **42**. The amide group is expected to stay intact during deprotection under basic conditions. Theoretically, a ketone would have the best chance of withstanding the types of deprotection conditions required, therefore a carbohydrate-derived alkynyl ketone would have to be prepared. A route from 1,2:3,4-di-*O*-isopropylidene galactopyranose (**27**) was attempted according to Scheme 6.

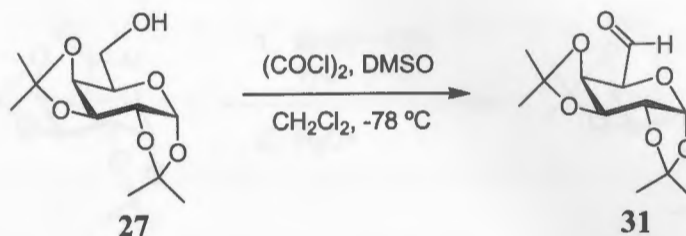


**Scheme 6:** Route to alkynyl ketone **33**

The oxidation of 1,2:3,4-di-*O*-isopropylidene galactopyranose (**27**) to aldehyde **31** was attempted by treating **27** with PCC in dry methylene chloride in the presence of 4Å molecular sieves. TLC analysis of the reaction mixture after 24 hours showed disappearance of the starting material and appearance of a new less polar spot that streaked. Inconsistent results were obtained after passing the crude reaction mixture through a short column of silica, possibly leading to the acid-catalyzed formation of the hydrate.

The aldehyde **31** was obtained by subjecting **27** to Swern conditions (Equation 17). Three hours after addition of triethylamine, TLC showed complete disappearance of the starting material and the appearance of a new less polar spot ( $R_f = 0.36$ , 1:1

hexanes:ethyl acetate). Following acidic workup and extraction, the product was obtained in 83 % yield as a yellow syrup that was used without further purification.

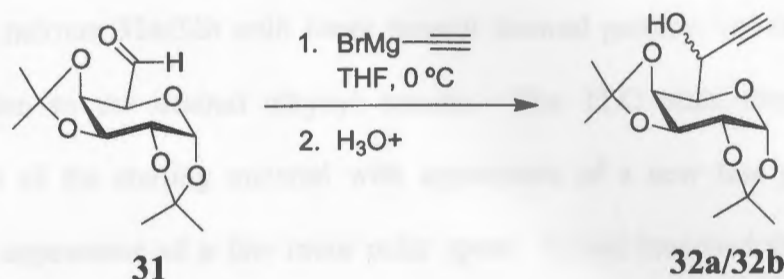


**Equation 17:** 1,2:3,4-Di-*O*-isopropylidene- $\alpha$ -D-galacto-hexodialdo-1,5-pyranose (**31**)

The  $^1\text{H}$  NMR spectrum of **31** contained a singlet at 9.63 ppm denoting the aldehyde proton. The signal corresponding to the H-1 proton was observed as a doublet at 5.68 ppm ( $J = 4.8$  Hz) and the H-5 proton signal, also a doublet, was found at 4.20 ppm ( $J = 2.2$  Hz). Four singlets at 1.32, 1.36, 1.45, and 1.52 ppm, integrating to three protons apiece, designate the methyl groups of the two isopropylidene protecting groups. In the  $^{13}\text{C}$  NMR spectrum the signal corresponding to the carbonyl of the aldehyde was found at 199.9 ppm.

Treatment of aldehyde **31** with 1.5 equivalents of ethynylmagnesium bromide in THF at 0 °C was used to obtain a mixture of propargyl alcohols **32a/32b** (Equation 18). The TLC changed only in the respect that the slight streaking of the starting material resolved, appearing as two overlapping spots as expected since the Grignard reagent may add to either prochiral face of the carbonyl. After quenching the reaction mixture with ammonium chloride, the product was extracted into methylene chloride, dried, and reduced to a yellow syrup that was flash chromatographed using 2:1 hexanes:ethyl acetate to give the product as a mixture of diastereomers. One diastereomer was partially

isolated, but the remaining material was a mixture with an overall yield of 74.2%. NMR analysis of the crude mixture showed a 2:1 ratio of the diastereomers.



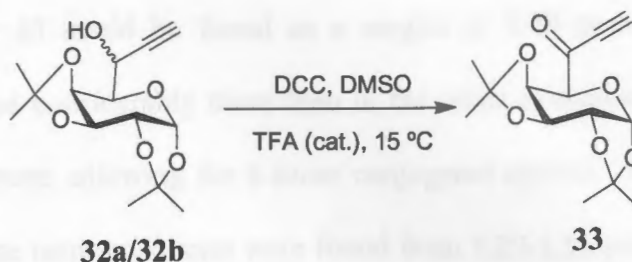
**Equation 18:** Addition of ethynyl magnesium bromide to aldehyde (**31**) to form mixture of propargyl alcohols (**32a/32b**)

The  $^1\text{H}$  NMR spectrum of the single diastereomer was devoid of the aldehyde proton signal. The addition of the alkynyl group was confirmed by the appearance of a doublet at 2.57 ppm with a small coupling constant value of 2.2 Hz. This signal shape and  $J$  value can be attributed to the distant coupling of the terminal proton of the alkyne with the methine proton. In the  $^{13}\text{C}$  NMR, the signal for the aldehyde carbonyl carbon was not present. In the  $^{13}\text{C}$  NMR spectrum for aldehyde **31**, there were five signals from 70.3-96.1 ppm for the carbons of the pyranose ring, but in the spectrum for the propargyl alcohol **32** there were now eight signals in the region from 62.5-96.4 ppm. This accounts for the addition of two carbons from the ethynyl magnesium bromide and the changing of the  $\text{sp}^2$  carbon in aldehyde **31** to  $\text{sp}^3$  in propargyl alcohol **32**.

The propargyl alcohol **32** proved to be challenging to oxidize as several sets of reaction conditions failed to convert the mixture to the corresponding alkynyl ketone. Oxidations attempted with PCC and  $\text{MnO}_2$  showed no change in the starting material by TLC analysis. Swern conditions were found to be unfavorable. The TLC from the

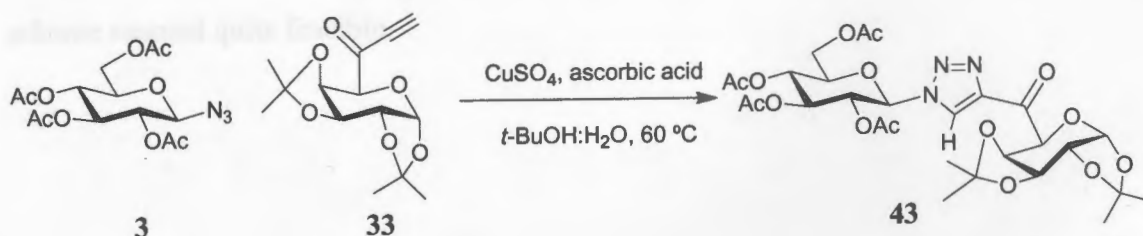
Swern showed disappearance of the starting material and the appearance of a new spot at the baseline assumed to be a decomposition product. A reaction with bleach provided multiple products by TLC and a complicated  $^1\text{H}$  NMR of the crude reaction mixture. Treatment of mixture **32a/32b** with Jones reagent showed promise but resulted in only half conversion to the desired alkynyl ketone. The TLC plate showed complete disappearance of the starting material with appearance of a new less polar spot, the product, and appearance of a few more polar spots. It was reasoned that these fairly harsh conditions were possibly cleaving the isopropylidene protecting groups.

Success was found with the neutral oxidative conditions afforded by performing a Moffatt oxidation (Equation 19). The mixture **32a/32b**, in excess DCC and DMSO, was treated with a catalytic amount of TFA and reacted for six hours after which TLC showed complete consumption of the starting material and the appearance of a new less polar spot ( $R_f = 0.32$ , 1:1 hexanes:ethyl acetate). A white precipitate, dicyclohexylurea, was formed during the reaction, most of which could be removed through filtration after diluting the reaction mixture with ether. After reduction of the filtrate, the residue was flash chromatographed and the alkynyl ketone **33** was obtained as a yellow solid in 74% yield. The  $^1\text{H}$  NMR of the pure alkynyl ketone showed disappearance of the doublets at 2.54 and 2.56 ppm, which were the alkyne proton signals from **32a/32b**. The appearance of a tall, sharp singlet at 3.42 ppm designated the presence of the proton of the alkynyl ketone since it would not display any coupling as in the previously prepared alkynes. The chemical shift is also consistent with several literature examples of non-carbohydrate alkynyl ketones.



**Equation 19:** Moffatt oxidation of mixture (**32a/32b**) to give alkynyl ketone **33**

The Cu(I)-catalyzed reaction of glucosyl azide **3** and alkynyl ketone **33** (Equation 20) was performed using stoichiometric amounts of the reactants, 0.2 equivalents of  $\text{CuSO}_4$ , and 0.4 equivalents of ascorbic acid. The reaction required addition of *t*-BuOH to the water and the reaction mixture was heated to 60 °C for 1.5 hours after which TLC showed consumption of both starting materials and the formation of a new more polar UV active spot that burned ( $R_f = 0.15$ ). The product was most easily acquired through extraction with methylene chloride with column chromatography necessary to remove an unidentified impurity. Triazole **43** was obtained in 78% yield.



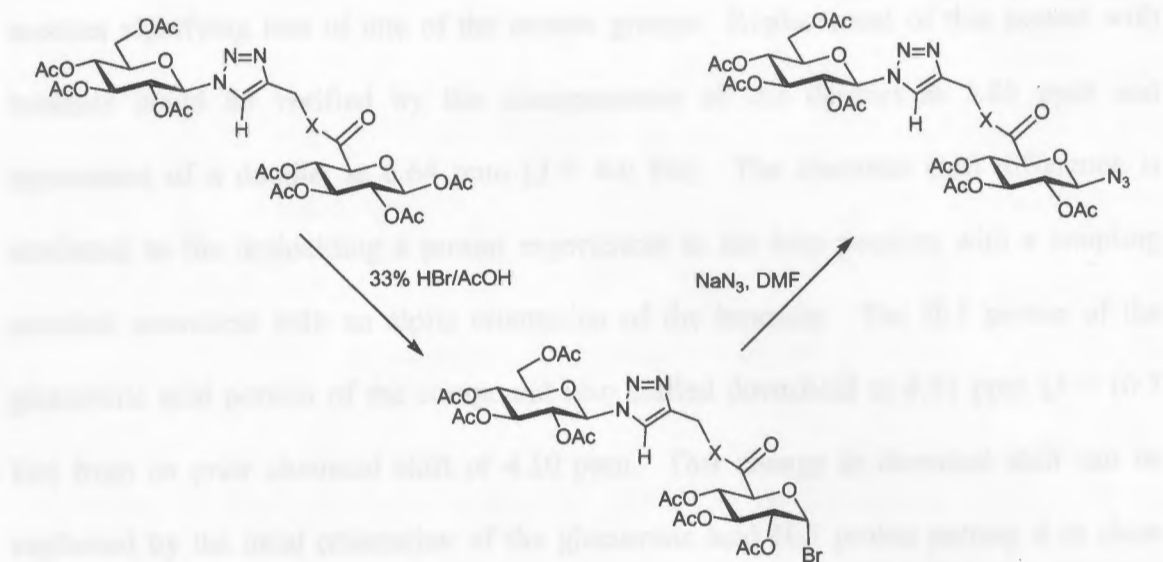
**Equation 20:** Formation of triazole **43** by Cu(I)-catalysis in aqueous medium

The  $^1\text{H}$  NMR spectrum for **43** showed substantial differentiation between the signals of the respective sugars. Absent were the alkynyl singlet at 3.42 ppm from alkyne **33** and the doublet at 4.67 ppm for the H-1 proton of azide **3**. Most importantly, the

triazole proton for **43** could be found as a singlet at 8.49 ppm. This was shifted downfield somewhat considerably more than in the other examples possibly due to the presence of the ketone, allowing for a more conjugated system. Four singlets for the methyl groups of the isopropylidenes were found from 1.27-1.58 ppm, while four singlets for the methyl groups of the acetates were found from 1.90-2.10 ppm. Two doublets were found at 5.78 ppm ( $J = 5.1$  Hz) and 5.95 ppm ( $J = 9.2$  Hz) for the H-1 protons of galactose and glucose respectively. The coupling constants are consistent with the stereochemical configurations of their parent sugars.

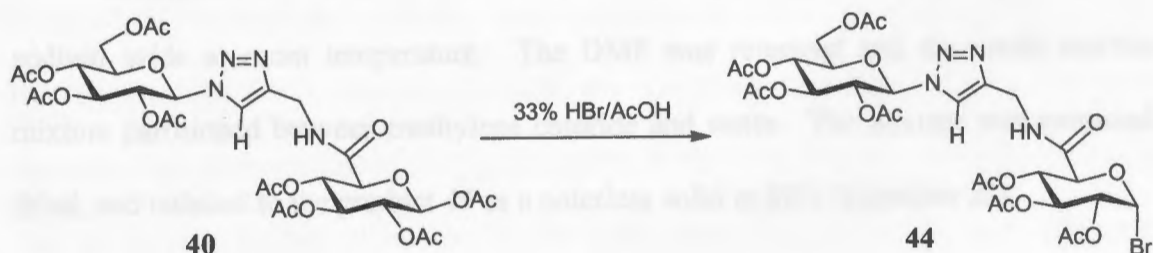
It has been shown that the Cu(I)-catalyzed cycloaddition chemistry is applicable in the presence of a variety of functional groups and using a number of different starting sugars. The next focus would be attempting the synthesis of a triazole-linked carbohydrate trimer. The acetate-protected triazole-linked dimers provided the most direct means of further functionalization because the acetate-protected anomeric position is subject to manipulation using the established chemistry according to Scheme 7. Since the triazole moiety itself stands up well to acidic and basic conditions, the proposed scheme seemed quite feasible.





**Scheme 7:** Proposed method for functionalization of acetate-protected carbohydrate dimers, (X = -O, -NH)

Triazole **40** was treated with 33% HBr in acetic acid for two hours (Equation 21). TLC showed consumption of starting material and appearance of a new less polar spot. The reaction mixture was extracted with chloroform after a basic workup, dried, and reduced to give bromide **44** as a tan foam in 92% yield.

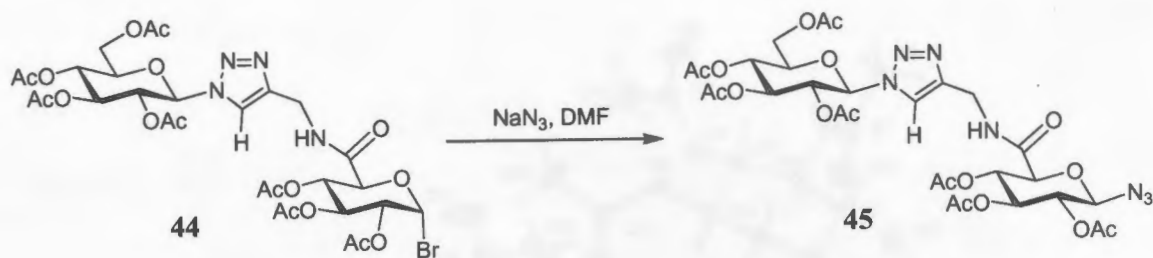


**Equation 21:** Acidic bromination of **40** to give bromide **44**

The <sup>1</sup>H NMR spectrum of **44** appropriately showed seven singlets, integrating to three protons each, from 1.88-2.10 ppm corresponding to the methyl groups of the

acetates signifying loss of one of the acetate groups. Replacement of this acetate with bromine could be verified by the disappearance of the doublet at 5.85 ppm and appearance of a doublet at 6.64 ppm ( $J = 4.0$  Hz). The chemical shift difference is attributed to the deshielding a proton experiences in the beta position with a coupling constant consistent with an alpha orientation of the bromide. The H-5 proton of the glucuronic acid portion of the compound also shifted downfield to 4.51 ppm ( $J = 10.3$  Hz) from its prior chemical shift of 4.10 ppm. This change in chemical shift can be explained by the axial orientation of the glucuronic acid H-5 proton putting it in close proximity to the axially positioned bromine atom thus pulling the signal further downfield. The triazole proton signal was found as a singlet at 7.82 ppm. The  $^{13}\text{C}$  NMR spectrum contained all of the signals as the spectrum for the octaacetate precursor minus one signal in the ester carbonyl region of the spectrum, indicating loss of the acetate at C-1. The only other difference was the shift of the signal from 91.1 ppm in the octaacetate to 85.4 ppm in the bromide. The upfield shift can be expected since the carbon is now attached to a less electronegative atom.

Bromide **44** was dissolved in dry DMF and treated with four equivalents of sodium azide at room temperature. The DMF was removed and the crude reaction mixture partitioned between methylene chloride and water. The mixture was extracted, dried, and reduced to the product **45** as a colorless solid in 82% (Equation 22).



**Equation 22: Formation of azide 45**

The <sup>1</sup>H NMR spectrum proved the formation of the desired product 45 by disappearance of the doublet at 6.64 ppm from the α-bromide and appearance of a new doublet at 4.77 ppm (*J* = 8.8 Hz). The glucuronic acid H-5 proton shifted back upfield to 4.09 ppm (*J* = 9.9 Hz), which reveals now a noticeable trend in the chemical shift of the H-5 proton of a pyranose sugar as influenced by the orientation of the anomeric substituent. The triazole proton showed as a singlet at 7.87 ppm. The <sup>13</sup>C NMR spectrum did not differ much from that of bromide 44.

The X-ray crystal structure of triazole 45 was obtained from crystals grown using vapor diffusion (acetonitrile:ether). This solid state structure (Figure 20) illustrates success in achieving some of the key goals of the project. First, the regiochemistry of the triazole product 45 is confirmed to be the 1,4-disubstituted product as expected. Secondly, the stereochemistry during formation of the triazole was conserved indicating that the stereochemical orientation of the azide precursor dictates the stereochemical outcome of the reaction. Lastly, the additional functionalization of the triazole-linked dimer may be controlled using the predictability of the anomeric effect to dictate the stereochemical outcome, thereby introducing an addition handle to be built upon.

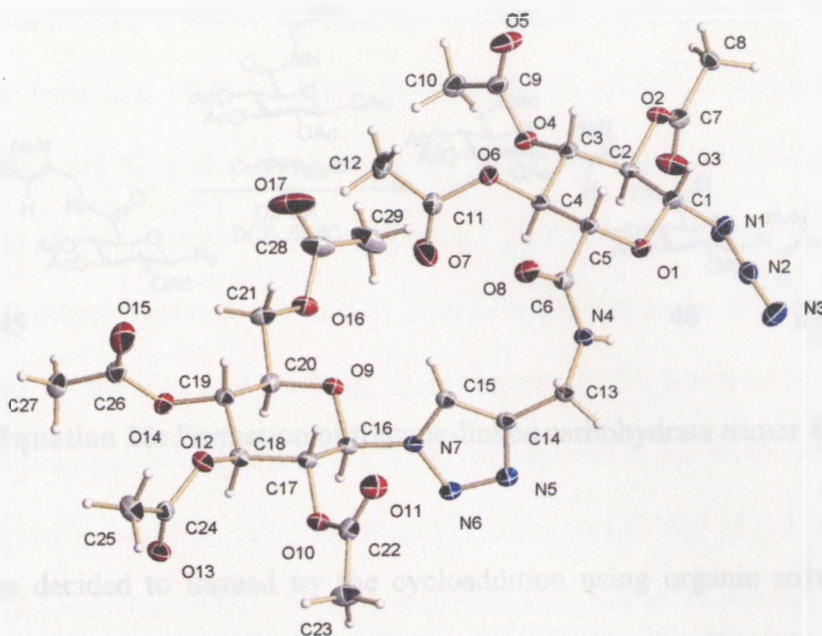
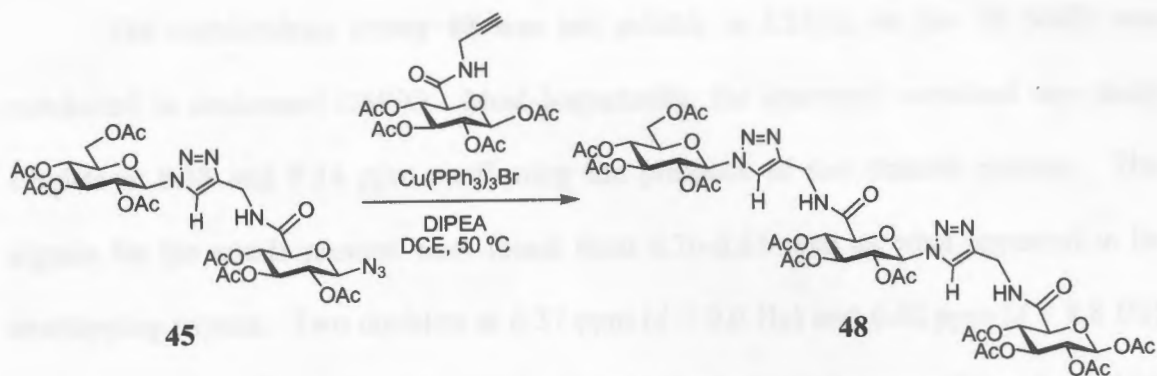


**Figure 20:** X-ray crystal structure of azide **45**

An additional monomer unit could now be potentially added to triazole **45** using the Cu(I)-catalyzed conditions set forth thus far. The reaction was first attempted using stoichiometric amounts of the azide **45** and alkyne **30** in water using the CuSO<sub>4</sub>/ascorbic acid protocol. The reaction mixture was heated to 60 °C and followed by TLC with the reactants failing to show any signs of dissolution. After five days, with TLC evidence of the formation of a new more polar spot, but still unreacted starting material, the reaction was stopped. The <sup>1</sup>H NMR spectrum showed the appearance of new singlets in the region where triazole protons normally show. Assuming these signals corresponded with the desired product, integration revealed that the reaction went to about half completion. Subsequent attempts using the same catalytic conditions with the addition of co-solvents like *t*-BuOH and ethanol proved inefficient as well. It was concluded that solubility was the main issue prohibiting the reaction from occurring at an appreciable rate.



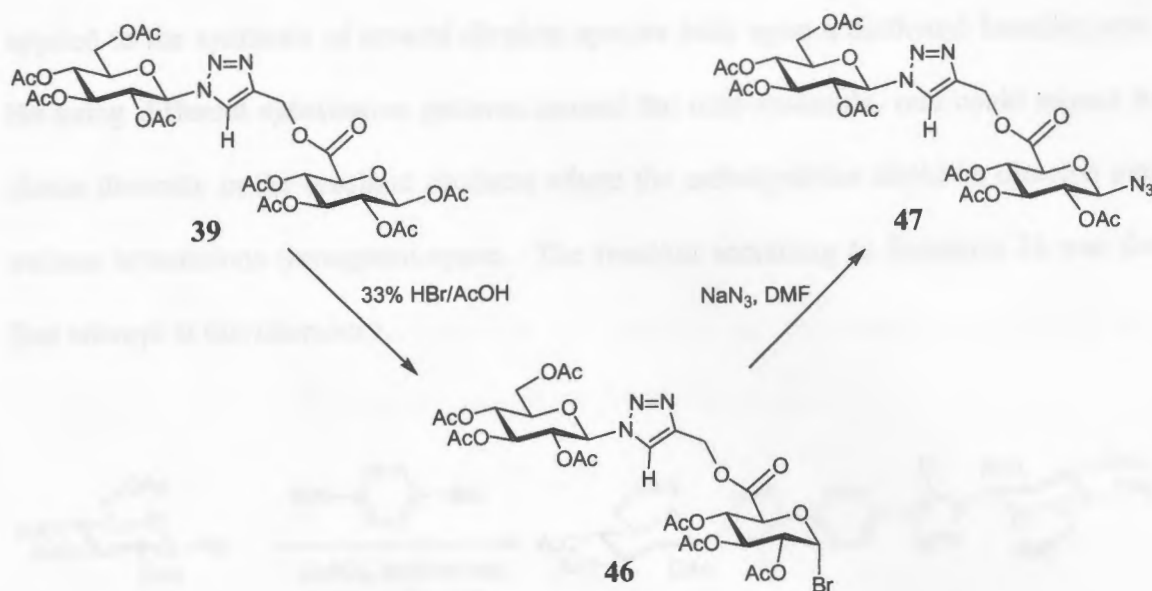
**Equation 23:** Formation of triazole-linked carbohydrate trimer **48**

It was decided to instead try the cycloaddition using organic solvents and the  $\text{Cu}(\text{PPh}_3)_3\text{Br}$  catalyst (Equation 23). The conditions chosen were using one equivalent of azide **45**, 1.1 equivalents of alkyne **30**, 20% of the catalyst, and three equivalents of DIPEA in toluene. Even with heating to reflux, the reactants did not appear to dissolve and the reaction did not proceed. Switching the solvent to DMF and heating to  $50\text{ }^\circ\text{C}$  allowed for the reactants to dissolve, but the reaction did not proceed to completion. The best results were obtained when dichloroethane was used as the solvent. Simply heating the reaction mixture to  $50\text{ }^\circ\text{C}$  promoted reaction progress. TLC analysis after one hour showed complete consumption of the starting azide **45** and the appearance of a new more polar spot. After removal of the solvent, methanol was added to the crude mixture and the contents were heated in hopes of recrystallizing the product. Surprisingly, the product remained insoluble in even large volumes of methanol. After cooling the contents of the flask the solution was decanted and the process repeated twice to leave the product as a white solid in 55% yield. Low resolution mass spectrometry found a mass of  $1177.7\text{ M}(+\text{Na})$ .

The carbohydrate trimer **48** was not soluble in  $\text{CDCl}_3$ , so the  $^1\text{H}$  NMR was conducted in deuterated DMSO. Most importantly, the spectrum contained two sharp singlets at 8.18 and 8.24 ppm confirming the presence of two triazole protons. The signals for the amide protons were found from 8.76-8.81 ppm as what appeared to be overlapping triplets. Two doublets at 6.37 ppm ( $J = 9.0$  Hz) and 6.42 ppm ( $J = 8.8$  Hz) were assigned as the anomeric protons situated next to the heterocycles. A doublet slightly further upfield at 6.02 ppm ( $J = 8.2$  Hz) corresponds to the proton at the anomeric center of the newly added sugar. This signal is not as deshielded as the signals for the protons next to the heterocycles. Nine singlets that integrate to 33 protons can be found from 1.83-2.12 ppm. This indicated the correct number of acetate protecting groups. The area from 4.10-5.68 ppm integrates to 18 protons accounting for the rest of the protons not already mentioned. This region consists mostly of overlapping triplets. Unfortunately, the identification of these signals would require extensive spectroscopic studies which were beyond the scope of instrumentation available.

Similar to the preparation of azide **45**, the acetate **39** was treated with 33% HBr in acetic acid to give bromide **46** in 98% yield, and subsequently treated with excess sodium azide in DMF to give azide **47** in 77% yield after flash column chromatography (Scheme 8).





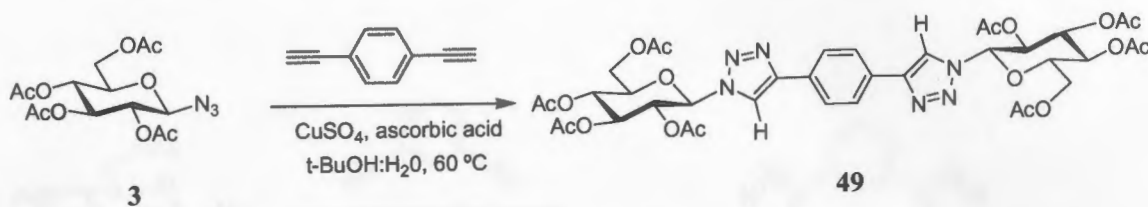
**Scheme 8: Synthetic route to azide 47**

Attempts were made to add an additional carbohydrate monomer, alkyne **29**, to azide **47**. The same conditions were applied to this system as in the synthesis of trimer **48**. Multiple washings of the crude product gave mostly the desired product although residual amounts of what was believed to be the copper catalyst were detected in the <sup>1</sup>H NMR spectrum. A sufficient chromatography system could not be found for this compound due to its poor solubility in many solvents. Perhaps removal of the protecting groups would result in a molecule that could be chromatographed.

### Synthesis of divalent species

Multivalency is an important occurrence in Nature functioning as a way to increase binding activities to biologically significant levels. This phenomenon can be incorporated into synthetic strategies to develop compounds that have higher affinities for their desired target. The Cu(I)-catalyzed cycloaddition chemistry was successfully

applied to the synthesis of several divalent species built upon a diethynyl benzene core. By using different substitution patterns around the core molecule, one could expect to obtain diversity in the resultant products where the carbohydrates could be directed into various orientations throughout space. The reaction according to Equation 24 was the first attempt at this chemistry.

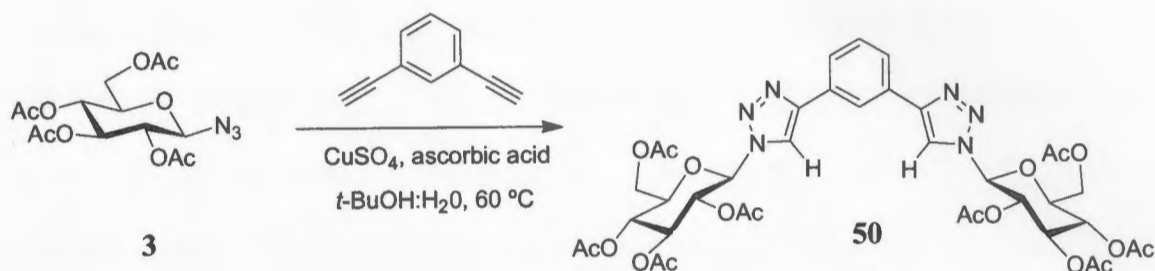


**Equation 24:** Formation of divalent triazole **49** by Cu(I)-catalysis in aqueous medium

Two equivalents of the azide **3** would be needed for every one equivalent of 1,4-diethynyl benzene. Catalyst loading was based upon the amount of azide used, 0.2 and 0.4 equivalents of the  $\text{CuSO}_4$  and ascorbic acid, respectively. A 50% *t*-BuOH in water mixture was used and the reaction mixture was heated to 60 °C and monitored by TLC. After stirring overnight, TLC showed complete consumption of the starting materials and appearance of a new, more polar, UV-active spot. The mixture was cooled, cold water added, and the resulting precipitate was collected by filtration over a glass frit. The precipitate was washed with several portions of cold water and the divalent triazole **49** was isolated as an orange solid in 79% yield. The  $^1\text{H}$  NMR spectrum of **49** revealed the molecule to be symmetrical. A singlet was found at 8.09 ppm for the triazole protons. A singlet with twice the intensity as the triazole signal was found at 7.93 ppm corresponding to the four protons of the aromatic ring, all in an equivalent environment.

The signal for the H-1 protons occurred as a doublet at 5.97 ppm ( $J = 9.3$  Hz), the coupling constant indicative of the retention of  $\beta$ -stereochemistry. The rest of the signals held the shapes and approximate chemical shifts as in the azide starting material.

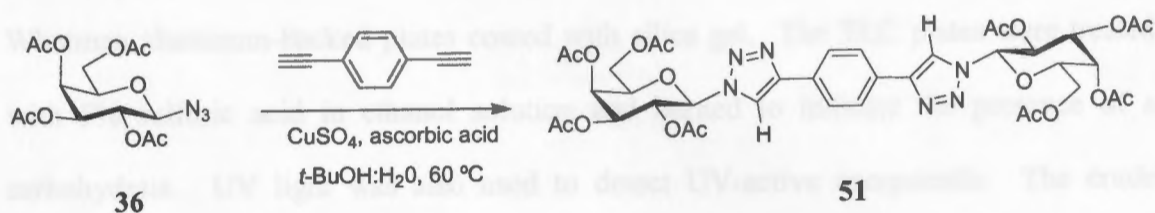
A reaction was run using 1,3-diethynyl benzene under identical conditions (Equation 25). After completion and the addition of cold water the product was successfully filtered off as a yellow solid in 87% yield.



**Equation 25:** Formation of divalent triazole **50** by Cu(I)-catalysis in aqueous medium

The  $^1\text{H}$  NMR for **50** similarly showed the product to be symmetrical. The spectrum for this analogue was almost identical to that of compound **49**. The proton for the triazole showed as a sharp singlet at 8.18 ppm and integrated to two protons. The signals for the protons of the aromatic ring were found at 7.49, 7.84, and 8.29 ppm integrating to one, two, and one proton, respectively. These integration values reflect the substitution pattern on the aromatic ring. The  $^{13}\text{C}$  NMR spectrum also reflects the symmetry of the product. Six signals from 118.1-147.7 ppm account for the carbons of the aromatic and heterocyclic rings. Low resolution mass spectrometry found the mass to be 873.4 ( $M + 1$ ). A reaction between azide **36** and 1,4-diethynyl benzene under similar

conditions led to the isolation of divalent species **51** in 87% yield as a pale yellow solid (Equation 26).

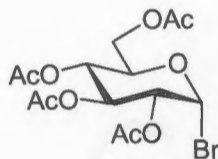


**Equation 26:** Formation of divalent triazole **51** by Cu(I)-catalysis in aqueous medium

**Experimental Procedures:**

Reaction progress was monitored by thin layer chromatography (TLC) on Whatman aluminum-backed plates coated with silica gel. The TLC plates were treated with 5% sulfuric acid in ethanol solution and burned to indicate the presence of a carbohydrate. UV light was also used to detect UV-active compounds. The crude reaction products were purified either by recrystallization or flash column chromatography (60-Å silica gel). Pure products were identified using Nuclear Magnetic Resonance spectroscopy on a Varian Gemini 2000 system at frequencies of 400 MHz and 100 MHz for  $^1\text{H}$  spectra and  $^{13}\text{C}$  spectra, respectively. The chemical shifts were recorded in parts per million (ppm). Splitting patterns of the signals were labeled as follows: s (singlet), d (doublet), dd (doublet of doublets), ddd (doublet of doublet of doublets), t (triplet), q (quartet), m (multiplet), dm (doublet of multiplets) and the coupling constants ( $J$ ) were measured in Hertz. A Bruker Esquire-HP 1100 mass spectrometer was used for low-resolution MS. High resolution MS was obtained from The Ohio State University. A Perkin-Elmer 343 polarimeter was used to measure the optical rotation of all homogenous compounds. X-Ray diffraction was also used in order to establish connectivity in a number of the compounds.

## Preparation of 2,3,4,6-Tetra-*O*-acetyl- $\alpha$ -D-glucopyranosyl bromide (2)



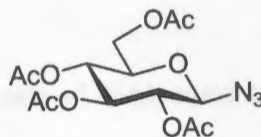
$\beta$ -D-glucopyranosyl pentaacetate (5.0 g, 12.81 mmol) was dissolved in 33% HBr/AcOH (20 mL) in an oven-dried 100 mL round bottom flask fitted with a rubber septum and magnetic stir bar. The brown solution was allowed to stir for three hours or until TLC (1:1, hexanes:ethyl acetate, product  $R_f = 0.37$ ) showed consumption of starting material. The solvents were removed *in vacuo* and the resulting brown syrup was diluted with 100 mL each cold of water and saturated sodium bicarbonate. The mixture was extracted with chloroform (3 x 50 mL) after which the combined extracts were dried over anhydrous magnesium sulfate, filtered, and reduced to a clear syrup (5.24 g, 99%).

$^1\text{H NMR}$  ( $\text{CDCl}_3$ ):  $\delta$  1.95 (s, 3H,  $\text{COCH}_3$ ), 1.97 (s, 3H,  $\text{COCH}_3$ ), 2.01 (s, 3H,  $\text{COCH}_3$ ), 2.02 (s, 3H,  $\text{COCH}_3$ ), 4.04 (dd, 1H, H-6,  $J = 1.6, 12.4$  Hz), 4.19-4.28 (m, 2H, H-5, H-6'), 4.76 (dd, 1H, H-2,  $J = 4.0, 10.1$  Hz), 5.08 (t, 1H, H-3,  $J = 9.7$  Hz), 5.47 (t, 1H, H-4,  $J = 9.7$  Hz), 6.54 (d, 1H, H-1,  $J = 4.0$  Hz).

$^{13}\text{C NMR}$  ( $\text{CDCl}_3$ ):  $\delta$  20.6, 20.7, 20.7 (double intensity), 60.9, 67.0, 70.0, 70.5, 72.0, 86.5, 169.1, 169.4, 169.5, 170.2.



**Preparation of 2,3,4,6-Tetra-*O*-acetyl- $\beta$ -D-glucopyranosyl azide (3) from  $\alpha$ -glucosyl bromide (2) via  $S_N2$  reaction.**



In a 100 mL round bottom flask equipped with a rubber septum and magnetic stir bar was dissolved the  $\alpha$ -glucosyl bromide (5.20 g, 12.64 mmol) in a 5:1 acetone and water mixture (70 mL). Sodium azide (3.92 g, 50.58 mmol) was added and the solution was allowed to stir overnight or until TLC (1:1, hexanes:ethyl acetate) showed complete consumption of starting material. The acetone was removed *in vacuo* and the remaining slurry was partitioned between water and methylene chloride (50 mL each). The organic layer was removed and the aqueous layer extracted with methylene chloride (2 x 50 mL). The combined extracts were dried over anhydrous magnesium sulfate, filtered, and reduced to a white solid which was recrystallized from hot methanol to give 3.97 g of a clear crystalline solid (83 %).

$^1\text{H NMR}$  ( $\text{CDCl}_3$ ):  $\delta$  2.02 (s, 3H,  $\text{COCH}_3$ ), 2.04 (s, 3H,  $\text{COCH}_3$ ), 2.08 (s, 3H,  $\text{COCH}_3$ ), 2.11 (s, 3H,  $\text{COCH}_3$ ), 3.81 (ddd, 1H, H-5,  $J = 2.4, 4.8, 10.1$  Hz), 4.17 (dd, 1H, H-6,  $J = 2.3, 12.5$  Hz), 4.28 (dd, 1H, H-6',  $J = 4.8, 12.5$  Hz), 4.67 (d, 1H, H-1,  $J = 8.8$  Hz), 4.96 (dd, 1H, H-2,  $J = 8.8, 9.5$  Hz), 5.11 (t, 1H, H-3,  $J = 9.8$  Hz), 5.23 (t, 1H, H-4,  $J = 9.5$  Hz).

$^{13}\text{C NMR}$  ( $\text{CDCl}_3$ ):  $\delta$  61.6, 67.8, 70.5, 72.5, 73.9, 87.8, 168.9, 169.0, 169.8, 170.3.

Low resolution MS:  $m/z$  calculated 396.102 (+Na)  $m/z$  found 396.1 (+Na)

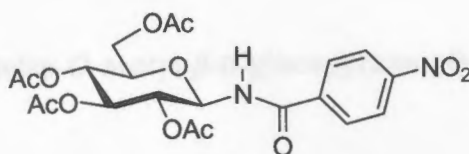
Melting Point: 124-126 °C

$[\alpha]_D -29.6^\circ$  (c. 1.0, CH<sub>2</sub>Cl<sub>2</sub>)

**Typical procedure for the synthesis of *N*-glycosyl amides using modified Staudinger chemistry.**

To a mixture of glucosyl azide (1.0 mmol) and acylating agent (2.0 mmol), dissolved in dry THF (0.1 g/mL), was added dropwise a solution of ethylenebis(diphenylphosphine) (0.65 mmol) in dry THF (0.1 g/mL) at room temperature. The mixture was allowed to stir for at least 1 hour and monitored by TLC. When disappearance of the intermediate ylid was observed, saturated NaHCO<sub>3</sub> was added and the mixture was allowed to stir vigorously overnight. The THF was removed under vacuum, the crude product extracted into chloroform (3 x 20 mL), and the combined extracts were washed with water (20 mL). After drying over anhydrous magnesium sulfate, the solution was filtered, evaporated to dryness and the crude product purified over silica gel using flash column chromatography.

***p*-Nitrobenzoic acid-(2,3,4,6-tetra-*O*-acetyl- $\beta$ -D-glucopyranosyl)-amide (4).**



Prepared from 2,3,4,6-tetra-*O*-acetyl- $\beta$ -D-glucopyranosyl azide (0.373 g, 1.0 mmol), *p*-nitrobenzoyl chloride (0.371 g, 2.0 mmol), and DPPE (0.259 g, 0.65 mmol) according to the typical procedure. Purification by flash column chromatography (1:1, hexanes:ethyl acetate) yielded a highly crystalline solid (0.405g, 81.6%).

$^1\text{H NMR}$  ( $\text{CDCl}_3$ ):  $\delta$  2.06 (s, 6H, 2 x  $\text{COCH}_3$ ), 2.07 (s, 3H,  $\text{COCH}_3$ ), 2.09 (s, 3H,  $\text{COCH}_3$ ), 3.93 (ddd, 1H, H-5,  $J = 2.1, 4.2, 10.1$  Hz), 4.12 (dd, 1H, H-6,  $J = 2.1, 12.5$  Hz), 4.33 (dd, 1H, H-6',  $J = 4.3, 12.5$  Hz), 5.05 (t, 1H, H-3,  $J = 9.6$  Hz), 5.12 (t, 1H, H-4,  $J = 9.8$  Hz), 5.42 (2t, overlapping, 2H, H-1, H-2,  $J = 9.5, 9.2$  Hz), 7.29 (d, 1H, N-H,  $J = 8.8$  Hz), 7.95 (d, 2H, *o*-Ar-H,  $J = 9.2$  Hz), 8.32 (d, 2H, *m*-Ar-H,  $J = 8.8$  Hz).

$^{13}\text{C NMR}$  ( $\text{CDCl}_3$ ):  $\delta$  20.7 (double intensity), 20.81, 20.84, 61.6, 68.1, 70.9, 72.3, 73.7, 79.0, 123.8 (double intensity), 128.4 (double intensity), 138.0, 149.9, 164.9, 169.3, 169.6, 170.3, 171.5.

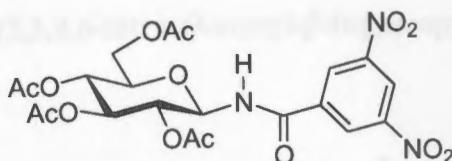
Low resolution MS:  $m/z$  calculated 519.123 (+Na)  $m/z$  found 519.1 (+Na)

HRMS:  $m/z$  calculated 519.1227 (+Na)  $m/z$  found 519.1227 (+Na)

Melting Point: 199-201 °C

$[\alpha]_D -29.6^\circ$  (c. 1.0, CH<sub>2</sub>Cl<sub>2</sub>)

**3,5-Dinitrobenzoic-(2,3,4,6-tetra-*O*-acetyl- $\beta$ -D-glucopyranosyl)-amide (5).**



Prepared from 2,3,4,6-tetra-*O*-acetyl- $\beta$ -D-glucopyranosyl azide (0.746 g, 2.0 mmol), 3,5-dinitrobenzoyl chloride (0.922 g, 4.0 mmol), and DPPE (0.478 g, 1.2 mmol) according to the typical procedure. Purification by flash column chromatography (5:4, hexanes:ethyl acetate) yielded a white crystalline solid (0.565 g, 58.2%).

<sup>1</sup>H NMR (CDCl<sub>3</sub>):  $\delta$  2.072 (s, 3H, COCH<sub>3</sub>), 2.074 (s, 3H, COCH<sub>3</sub>), 2.08 (s, 3H, COCH<sub>3</sub>), 2.09 (s, 3H, COCH<sub>3</sub>), 3.94 (ddd, 1H, H-5,  $J = 2.2, 4.5, 10.2$  Hz), 4.14 (dd, 1H, H-6,  $J = 2.1, 12.5$  Hz), 4.34 (dd, 1H, H-6',  $J = 4.4, 12.6$  Hz), 5.07 (t, 1H, H-2,  $J = 9.6$  Hz), 5.14 (t, 1H, H-3,  $J = 9.8$  Hz), 5.43 (t, 1H, H-4,  $J = 9.6$  Hz), 5.45 (t, 1H, H-1,  $J = 9.52$  Hz), 7.64 (d, 1H, N-H,  $J = 8.6$  Hz), 8.98 (d, 2H, *m*-Ar-H,  $J = 2.2$  Hz), 9.21 (t, 1H, *p*-Ar-H,  $J = 2.0$  Hz).

<sup>13</sup>C NMR (CDCl<sub>3</sub>):  $\delta$  20.6, 20.7, 20.8 (double intensity), 61.9, 68.2, 70.9, 72.5, 73.8, 78.8, 121.6, 127.5, 136.1, 148.5, 162.6, 169.6 (double intensity), 170.5, 171.1.

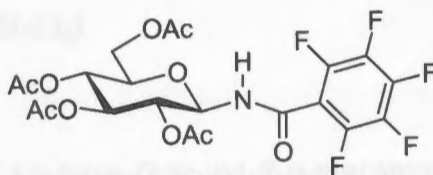
Low resolution MS:  $m/z$  calculated 564.108 (+Na)  $m/z$  found 564.1 (+Na)

HRMS:  $m/z$  calculated 564.1078 (+Na)  $m/z$  found 564.1074 (+Na)

Melting Point: 149-152 °C

$[\alpha]_D -36.8^\circ$  (c. 1.0, CH<sub>2</sub>Cl<sub>2</sub>)

**Pentafluorobenzoic acid-(2,3,4,6-tetra-*O*-acetyl- $\beta$ -D-glucopyranosyl)-amide (6).**



Prepared from 2,3,4,6-tetra-*O*-acetyl- $\beta$ -D-glucopyranosyl azide (0.373 g, 1.0 mmol), pentafluorobenzoyl chloride (0.29 mL, 2.0 mmol), and DPPE (0.259 g, 0.65 mmol) according to the typical procedure. Purification by flash column chromatography (7:4, hexanes:ethyl acetate) yielded a crystalline solid, which was recrystallized from MeOH to give crystals suitable for X-ray diffraction (0.418 g, 77.2%).

<sup>1</sup>H NMR (CDCl<sub>3</sub>):  $\delta$  2.04 (s, 3H, COCH<sub>3</sub>), 2.05 (s, 3H, COCH<sub>3</sub>), 2.09 (s, 3H, COCH<sub>3</sub>), 2.10 (s, 3H, COCH<sub>3</sub>), 3.90 (ddd, 1H, H-5,  $J = 2.1, 4.3, 10.2$  Hz), 4.12 (dd, 1H, H-6,  $J = 2.2, 12.5$  Hz), 4.36 (dd, 1H, H-6',  $J = 4.5, 12.5$  Hz), 5.02 (t, 1H, H-3,  $J = 9.6$  Hz), 5.10 (t, 1H, H-4,  $J = 9.7$  Hz), 5.36 (t, 1H, H-2,  $J = 9.5$  Hz), 5.39 (t, 1H, H-1,  $J = 9.3$  Hz), 6.95 (d, 1H, N-H,  $J = 9.2$  Hz).

$^{13}\text{C}$  NMR ( $\text{CDCl}_3$ ):  $\delta$  20.6, 20.7 (double intensity), 20.8, 61.5, 68.0, 70.2, 72.4, 73.9, 78.4, 110.2, 137.4 (2C, dm,  $J = 256.4$  Hz), 142.5 (dm,  $J = 258.6$  Hz), 143.9 (2C, dm,  $J = 248.7$  Hz), 157.6, 169.3, 169.6, 170.4, 170.8.

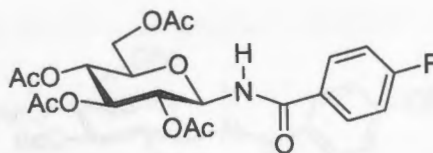
Low resolution MS:  $m/z$  calculated 564.091 (+Na)  $m/z$  found 564.0 (+Na)

HRMS:  $m/z$  calculated 564.0905 (+Na)  $m/z$  found 564.0915 (+Na)

Melting Point: 129-132 °C

$[\alpha]_{\text{D}} +4.7^\circ$  (c. 1.0,  $\text{CH}_2\text{Cl}_2$ )

#### 4-Fluorobenzoic acid-(2,3,4,6-tetra-*O*-acetyl- $\beta$ -D-glucopyranosyl)-amide (7).



Prepared from 2,3,4,6-tetra-*O*-acetyl- $\beta$ -D-glucopyranosyl azide (0.373 g, 1.0 mmol), 4-fluorobenzoyl chloride (0.236 mL, 2.0 mmol), and DPPE (0.259 g, 0.65 mmol) according to the typical procedure. Purification by flash column chromatography (1:1, hexanes:ethyl acetate) yielded a white solid (0.331 g, 70.6 %).

$^1\text{H}$  NMR ( $\text{CDCl}_3$ ):  $\delta$  2.05 (s, 9H, 3 x  $\text{COCH}_3$ ), 2.08 (s, 3H,  $\text{COCH}_3$ ), 3.91 (ddd, 1H, H-5,  $J = 2.1, 4.2, 10.2$  Hz), 4.11 (dd, 1H, H-6,  $J = 2.0, 12.6$  Hz), 4.36 (dd, 1H, H-6',  $J = 4.2, 12.6$  Hz), 5.05 (t, 1H, H-2,  $J = 9.7$  Hz), 5.12 (t, 1H, H-3,  $J = 9.7$  Hz), 5.40 (t, 1H, H-4,  $J = 9.6$  Hz), 5.41 (t, 1H, H-1,  $J = 9.3$  Hz), 7.03 (d, 1H, N-H,  $J = 9.0$  Hz), 7.11-7.15 (m, 2H, *o*-Ar-H), 7.76-7.80 (m, 2H, *p*-Ar-H).



$^{13}\text{C}$  NMR ( $\text{CDCl}_3$ ):  $\delta$  20.6 (double intensity), 20.8 (double intensity), 61.6, 68.1, 70.8, 72.5, 73.5, 78.8, 115.7 (2C, d,  $J = 22.1$  Hz), 128.7 (d,  $J = 3.1$  Hz), 129.54 (2C, d,  $J = 9.2$  Hz), 164.9 (d,  $J = 252.5$  Hz), 165.8, 169.3, 169.5, 170.3, 171.2.

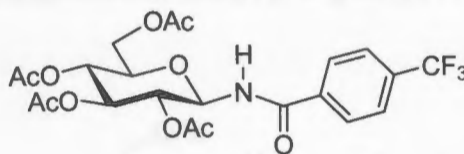
Low resolution MS:  $m/z$  calculated 492.128 (+Na)  $m/z$  found 492.2 (+Na)

Melting Point: 149-152 °C

$[\alpha]_{\text{D}} -17.8^\circ$  (c. 1.0,  $\text{CH}_2\text{Cl}_2$ )

***p*-Trifluoromethylbenzoic acid-(2,3,4,6-tetra-*O*-acetyl- $\beta$ -D-glucopyranosyl)-amide**

(8).



Prepared from 2,3,4,6-tetra-*O*-acetyl- $\beta$ -D-glucopyranosyl azide (0.373 g, 1.0 mmol), *p*-trifluoromethylbenzoyl chloride (0.30 mL, 2.0 mmol), and DPPE (0.259 g, 0.65 mmol) according to the typical procedure. Purification by flash column chromatography (1:1, hexanes:ethyl acetate) yielded a white solid (0.364 g, 70 %).

$^1\text{H}$  NMR ( $\text{CDCl}_3$ ):  $\delta$  2.06 (s, 9H, 3 x  $\text{COCH}_3$ ), 2.08 (s, 3H,  $\text{COCH}_3$ ), 3.93 (ddd, 1H, H-5,  $J = 2.1, 4.2, 10.2$  Hz), 4.12 (dd, 1H, H-6,  $J = 2.0, 12.6$  Hz), 4.36 (dd, 1H, H-6',  $J = 4.3, 12.5$  Hz), 5.07 (t, 1H, H-2,  $J = 9.6$  Hz), 5.12 (t, 1H, H-3,  $J = 9.8$

H<sub>z</sub>), 5.42 (t, 1H, H-4,  $J = 9.5$  Hz), 5.45 (t, 1H, H-1,  $J = 9.3$  Hz), 7.29 (d, 1H, N-H,  $J = 8.8$  Hz), 7.72 (d, 2H, *o*-Ar-H,  $J = 8.4$  Hz), 7.89 (d, 2H, *m*-Ar-H,  $J = 8.1$  Hz).

Ar-H,  $J = 8.1$  Hz).

<sup>13</sup>C NMR (CDCl<sub>3</sub>):  $\delta$  20.6 (double intensity), 20.8 (double intensity), 61.6, 68.1, 70.8, 72.4, 73.6, 78.9, 123.3 (q,  $J = 271.9$  Hz), 125.6 (2C, q,  $J = 3.1$  Hz), 127.6, 133.9 (q,  $J = 32.8$  Hz), 135.8, 165.6, 169.3, 169.5, 170.3, 171.3.

77.7

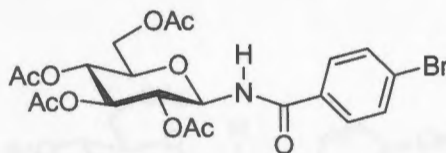
Low resolution MS:  $m/z$  calculated 542.125 (+Na)  $m/z$  found 542.2 (+Na)

Melting Point: 189-190 °C

$[\alpha]_D -15.7^\circ$  (c. 1.0, CH<sub>2</sub>Cl<sub>2</sub>)

(10% CH<sub>2</sub>Cl<sub>2</sub> in CHCl<sub>3</sub>)

***p*-Bromobenzoic acid-(2,3,4,6-tetra-*O*-acetyl- $\beta$ -D-glucopyranosyl)-amide (9).**



Prepared from 2,3,4,6-tetra-*O*-acetyl- $\beta$ -D-glucopyranosyl azide (0.373 g, 1.0 mmol), *p*-bromobenzoyl chloride (0.439 g, 2.0 mmol), and DPPE (0.259 g, 0.65 mmol) according to the typical procedure. Purification by flash column chromatography (1:1, hexanes:ethyl acetate) yielded a white solid (0.360 g, 67 %).

<sup>1</sup>H NMR (CDCl<sub>3</sub>):  $\delta$  2.05 (s, 3H, COCH<sub>3</sub>), 2.06 (s, 6H, 2 x COCH<sub>3</sub>), 2.08 (s, 3H, COCH<sub>3</sub>), 3.91 (ddd, 1H, H-5,  $J = 2.0, 4.1, 10.1$  Hz), 4.11 (dd, 1H, H-6,  $J = 2.1, 12.5$  Hz), 4.36 (dd, 1H, H-6',  $J = 4.2, 12.6$  Hz), 5.04 (t, 1H, H-2,  $J = 9.6$  Hz), 5.12

(dd, 1H, H-3,  $J = 9.7$  Hz), 5.40 (t, 1H, H-4,  $J = 9.6$  Hz), 5.41 (t, 1H, H-1,  $J = 9.3$  Hz), 7.04 (d, 1H, N-H,  $J = 9.0$  Hz), 7.59 (d, 2H, Ar-H,  $J = 8.8$  Hz), 7.63 (d, 2H, Ar-H,  $J = 8.8$  Hz).

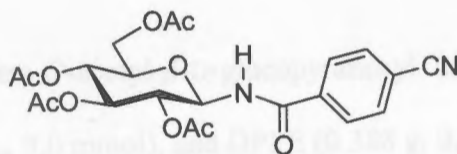
$^{13}\text{C}$  NMR ( $\text{CDCl}_3$ ):  $\delta$  20.6 (double intensity), 20.7 (double intensity), 61.5, 68.1, 70.7, 72.4, 73.5, 78.8, 127.1, 128.6, 131.4, 131.7, 165.9, 169.3, 169.5, 170.2, 171.1.

Low resolution MS:  $m/z$  calculated 552.048 (+Na)  $m/z$  found 552.2 (+Na)

Melting Point: 179-180 °C

$[\alpha]_{\text{D}} -2.6^\circ$  (c. 1.0,  $\text{CH}_2\text{Cl}_2$ )

#### 4-Cyanobenzoic acid-(2,3,4,6-tetra-*O*-acetyl- $\beta$ -D-glucopyranosyl)-amide (10).



Prepared from 2,3,4,6-tetra-*O*-acetyl- $\beta$ -D-glucopyranosyl azide (0.373 g, 1.0 mmol), 4-cyanobenzoyl chloride (0.331 g, 2.0 mmol), and DPPE (0.259 g, 0.65 mmol) according to the typical procedure. Purification by flash column chromatography (1:1, hexanes:ethyl acetate) yielded a white solid (0.352 g, 73.9%).

$^1\text{H}$  NMR ( $\text{CDCl}_3$ ):  $\delta$  2.058 (s, 6H, 2 x  $\text{COCH}_3$ ), 2.063 (s, 3H,  $\text{COCH}_3$ ), 2.08 (s, 3H,  $\text{COCH}_3$ ), 3.92 (ddd, 1H, H-5,  $J = 2.1, 4.3, 10.1$  Hz), 4.12 (dd, 1H, H-6,  $J =$

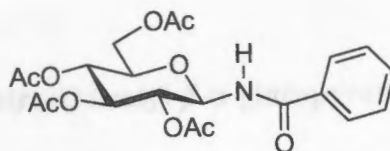
4.3, 12.5 Hz), 4.35 (dd, 1H, H-6',  $J = 2.1, 12.5$  Hz), 5.04 (t, 1H, H-2,  $J = 9.6$  Hz), 5.12 (t, 1H, H-3,  $J = 9.8$  Hz), 5.405, 5.413 (2t overlapping, 2H, H-1, H-4,  $J = 9.2, 9.5$  Hz), 7.27 (d, 1H, N-H,  $J = 8.4$  Hz), 7.77 (d, 2H, *o*-Ar-H,  $J = 8.6$  Hz), 7.88 (d, 2H, *m*-Ar-H,  $J = 8.8$  Hz).

Low resolution MS:  $m/z$  calculated 499.133 (+Na)  $m/z$  found 499.2 (+Na)

Melting Point: 105-107 °C

$[\alpha]_D -22.3^\circ$  (c. 1.0, CH<sub>2</sub>Cl<sub>2</sub>)

**Benzoic acid-(2,3,4,6-tetra-*O*-acetyl- $\beta$ -D-glucopyranosyl)-amide (11).**



Prepared from 2,3,4,6-tetra-*O*-acetyl- $\beta$ -D-glucopyranosyl azide (0.560 g, 1.5 mmol), benzoyl chloride (0.35 mL, 3.0 mmol), and DPPE (0.388 g, 0.975 mmol) according to the typical procedure. Purification by flash column chromatography (1:1, hexanes:ethyl acetate) yielded a fluffy crystalline solid (0.406 g, 60%).

<sup>1</sup>H NMR (CDCl<sub>3</sub>):  $\delta$  2.05 (s, 3H, COCH<sub>3</sub>), 2.06 (s, 6H, 2 x COCH<sub>3</sub>), 2.08 (s, 3H, COCH<sub>3</sub>), 3.92 (ddd, 1H, H-5,  $J = 2.1, 4.2, 10.2$  Hz), 4.10 (dd, 1H, H-6,  $J = 2.1, 12.5$  Hz), 4.36 (dd, 1H, H-6',  $J = 4.2, 12.6$  Hz), 5.08 (t, 1H, H-3,  $J = 9.6$  Hz), 5.12 (t, 1H, H-4,  $J = 9.7$  Hz), 5.40 (t, 1H, H-2,  $J = 9.5$  Hz), 5.46 (t, 1H, H-1,  $J = 9.3$

Hz), 7.14 (d, 1H, N-H,  $J = 9.2$  Hz), 7.43-7.47 (m, 2H, Ar-H), 7.53 (m, 1H, Ar-H), 7.76-7.78 (m, 2H, Ar-H).

$^{13}\text{C}$  NMR ( $\text{CDCl}_3$ ):  $\delta$  20.7 (double intensity), 20.8 (double intensity), 61.6, 68.1, 70.7, 72.5, 73.5, 78.8, 127.0, 128.6, 132.2, 132.5, 166.8, 169.3, 169.6, 170.4, 171.2.

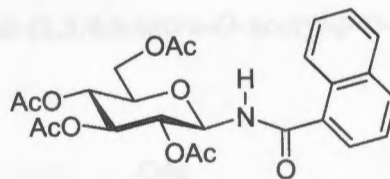
Low resolution MS:  $m/z$  calculated 474.138 (+Na)  $m/z$  found 474.2 (+Na)

HRMS:  $m/z$  calculated 474.1376 (+Na)  $m/z$  found 474.1337 (+Na)

Melting Point: 190-192 °C

$[\alpha]_{\text{D}} -14.5^\circ$  (c. 1.0,  $\text{CH}_2\text{Cl}_2$ )

### 1-Naphthoic acid-(2,3,4,6-tetra-*O*-acetyl- $\beta$ -D-glucopyranosyl)-amide (12).



Prepared from 2,3,4,6-tetra-*O*-acetyl- $\beta$ -D-glucopyranosyl azide (0.373 g, 1.0 mmol), 1-naphthoyl chloride (0.30 mL, 2.0 mmol), and DPPE (0.259 g, 0.65 mmol) according to the typical procedure. Purification by flash column chromatography (1:1, hexanes:ethyl acetate) yielded a white solid (0.250 g, 50%).

$^1\text{H}$  NMR ( $\text{CDCl}_3$ ):  $\delta$  2.05 (s, 3H,  $\text{COCH}_3$ ), 2.06 (s, 3H,  $\text{COCH}_3$ ), 2.09 (s, 3H,  $\text{COCH}_3$ ), 2.10 (s, 3H,  $\text{COCH}_3$ ), 3.95 (ddd, 1H, H-5,  $J = 2.1, 4.2, 10.1$  Hz), 4.16

(dd, 1H, H-6,  $J = 2.1, 12.5$  Hz), 4.37 (dd, 1H, H-6',  $J = 4.3, 12.5$  Hz), 5.06 (t, 1H, H-2,  $J = 9.6$  Hz), 5.13 (t, 1H, H-3,  $J = 9.7$  Hz), 5.41 (t, 1H, H-4,  $J = 9.5$  Hz), 5.58 (t, 1H, H-1,  $J = 9.4$  Hz), 6.83 (d, 1H, N-H,  $J = 9.7$  Hz), 7.45 (dd, 1H, Ar-H,  $J = 7.1, 8.1$  Hz), 7.51-7.58 (m, 2H, Ar-H), 7.86-7.89 (m, 1H, Ar-H), 7.95 (d, 1H, Ar-H,  $J = 8.2$  Hz), 8.32-8.35 (m, 1H, Ar-H).

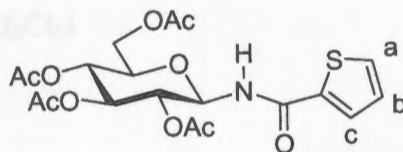
$^{13}\text{C}$  NMR ( $\text{CDCl}_3$ ):  $\delta$  20.7 (double intensity), 20.78, 20.83, 61.7, 68.2, 70.7, 72.8, 73.7, 78.4, 124.4, 125.0, 125.1, 126.4, 127.2, 128.2, 129.9, 131.5, 132.1, 133.5, 169.0, 169.3, 169.6, 170.4, 170.7.

Low resolution MS:  $m/z$  calculated 524.153 (+Na)  $m/z$  found 524.2 (+Na)

Melting Point: 165-168 °C

$[\alpha]_{\text{D}} +16.5^\circ$  (c. 1.0,  $\text{CH}_2\text{Cl}_2$ )

**Thiophene-2-carboxylic acid-(2,3,4,6-tetra-*O*-acetyl- $\beta$ -D-glucopyranosyl)-amide(13).**



Prepared from 2,3,4,6-tetra-*O*-acetyl- $\beta$ -D-glucopyranosyl azide (0.560 g, 1.5 mmol), 2-thiophenecarbonyl chloride (0.32 mL, 3.0 mmol), and DPPE (0.388 g, 0.975 mmol) according to the typical procedure. Purification by flash column chromatography (3:2,



hexanes:ethyl acetate) yielded a crystalline solid which was recrystallized from MeOH to give crystals suitable for X-ray diffraction (0.513 g, 74.8%).

$^1\text{H NMR}$  ( $\text{CDCl}_3$ ):  $\delta$  2.04 (s, 3H,  $\text{COCH}_3$ ), 2.048 (s, 3H,  $\text{COCH}_3$ ), 2.050 (s, 3H,  $\text{COCH}_3$ ), 2.09 (s, 3H,  $\text{COCH}_3$ ), 3.90 (ddd, 1H, H-5,  $J = 2.1, 4.3, 10.2$  Hz), 4.11 (dd, 1H, H-6,  $J = 2.1, 12.5$  Hz), 4.36 (dd, 1H, H-6',  $J = 4.3, 12.5$  Hz), 5.04 (t, 1H, H-3,  $J = 9.6$  Hz), 5.11 (t, 1H, H-4,  $J = 9.8$  Hz), 5.38 (t, 1H, H-2,  $J = 9.3$  Hz), 5.39 (t, 1H, H-1,  $J = 9.5$  Hz), 6.94 (d, 1H, N-H,  $J = 9.0$  Hz), 7.09 (dd, 1H, H<sub>b</sub>,  $J = 3.8, 5.0$  Hz), 7.49 (dd, 1H, H<sub>c</sub>,  $J = 1.1, 3.9$  Hz), 7.55 (dd, 1H, H<sub>a</sub>,  $J = 1.10, 5.1$  Hz).

$^{13}\text{C NMR}$  ( $\text{CDCl}_3$ ):  $\delta$  20.7 (double intensity), 20.8 (double intensity), 61.6, 68.1, 70.6, 72.5, 73.5, 78.8, 127.2, 129.0, 131.5, 137.3, 161.4, 169.3, 169.6, 170.4, 171.3.

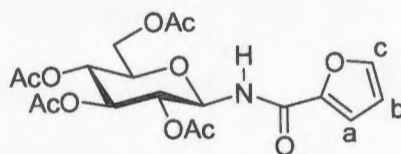
Low resolution MS:  $m/z$  calculated 480.094 (+Na)  $m/z$  found 480.1 (+Na)

HRMS:  $m/z$  calculated 480.0940 (+Na)  $m/z$  found 480.0936 (+Na)

Melting Point: 170-171 °C

$[\alpha]_{\text{D}} -32.2^\circ$  (c. 1.0,  $\text{CH}_2\text{Cl}_2$ )

**Furan-2-carboxylic acid-(2,3,4,6-tetra-*O*-acetyl- $\beta$ -D-glucopyranosyl)-amide (14).**



Prepared from 2,3,4,6-tetra-*O*-acetyl- $\beta$ -D-glucopyranosyl azide (0.373 g, 1 mmol), 2-furoyl chloride (0.197 mL, 2 mmol), and DPPE (0.259 g, 0.65 mmol) according to the typical procedure except the hydrolysis was performed using 3.0 mL of a pH 6.8 sodium acetate buffer. Purification by flash column chromatography (4:5, hexanes:ethyl acetate) yielded a crystalline solid (0.260 g, 59.0 %).

$^1\text{H}$  NMR ( $\text{CDCl}_3$ ):  $\delta$  2.03 (s, 3H,  $\text{COCH}_3$ ), 2.04 (s, 3H,  $\text{COCH}_3$ ), 2.05 (s, 3H,  $\text{COCH}_3$ ), 2.08 (s, 3H,  $\text{COCH}_3$ ), 3.90 (ddd, 1H, H-5,  $J = 2.1, 4.3, 10.2$  Hz), 4.10 (dd, 1H, H-6,  $J = 2.1, 12.5$  Hz), 4.38 (dd, 1H, H-6',  $J = 4.3, 12.5$  Hz), 5.08 (t, 1H, H-3,  $J = 9.6$  Hz), 5.12 (t, 1H, H-4,  $J = 9.7$  Hz), 5.38, 5.43 (2t overlapping, 2H, H-1, H-2,  $J = 9.9, 9.5$  Hz), 6.52 (dd, 1H, H<sub>b</sub>,  $J = 1.8, 3.5$  Hz), 7.16 (d, 1H, N-H,  $J = 9.3$  Hz), 7.18 (d, 1H, H<sub>a</sub>,  $J = 3.5$  Hz), 7.50 (d, 1H, H<sub>c</sub>,  $J = 1.8$  Hz).

$^{13}\text{C}$  NMR ( $\text{CDCl}_3$ ):  $\delta$  20.6 (double intensity), 20.7, 20.8, 61.5, 68.0, 70.3, 72.6, 73.4, 77.9, 112.2, 115.8, 144.7, 146.3, 157.8, 169.3, 169.6, 170.3, 170.6.

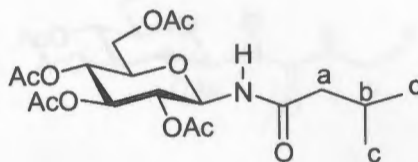
Low resolution MS:  $m/z$  calculated 464.117 (+Na)  $m/z$  found 464.1 (+Na)

HRMS:  $m/z$  calculated 464.1169 (+Na)  $m/z$  found 464.1169 (+Na)

Melting Point: 160-163 °C

$[\alpha]_{\text{D}} -17.7^\circ$  (c. 1.0,  $\text{CH}_2\text{Cl}_2$ )

**Isovaleric acid-(2,3,4,6-tetra-*O*-acetyl- $\beta$ -D-glucopyranosyl)-amide (15).**



Prepared from 2,3,4,6-tetra-*O*-acetyl- $\beta$ -D-glucopyranosyl azide (1.120g, 3.0 mmol), isovaleryl chloride (0.74 mL, 6.0 mmol), and DPPE (0.777 g, 1.95 mmol) according to the typical procedure. Purification by flash column chromatography (1:2, hexanes:ethyl acetate) yielded a crystalline solid (0.91 g, 70.5%).

$^1\text{H NMR}$  ( $\text{CDCl}_3$ ):  $\delta$  0.91 (d, 3H,  $\text{H}_c$ ,  $J = 6.2$  Hz), 0.94 (d, 3H,  $\text{H}_c$ ,  $J = 6.2$  Hz), 1.96-2.15, (m, 3H,  $\text{H}_a$ ,  $\text{H}_b$ ), 2.03 (s, 3H,  $\text{COCH}_3$ ), 2.04 (s, 6H, 2 x  $\text{COCH}_3$ ), 2.08 (s, 3H,  $\text{COCH}_3$ ), 3.83 (ddd, 1H, H-5,  $J = 2.1, 4.4, 10.1$  Hz), 4.07 (dd, 1H, H-6,  $J = 2.1, 12.5$  Hz), 4.33 (dd, 1H, H-6',  $J = 4.4, 12.5$  Hz), 4.93 (t, 1H, H-3,  $J = 9.6$  Hz), 5.07 (t, 1H, H-4,  $J = 9.8$  Hz), 5.28 (t, 1H, H-2,  $J = 9.5$  Hz), 5.31 (t, 1H, H-1,  $J = 9.5$  Hz), 6.22 (d, 1H, N-H,  $J = 9.3$  Hz).

$^{13}\text{C NMR}$  ( $\text{CDCl}_3$ ):  $\delta$  20.6 (double intensity), 20.7, 20.8, 22.2, 22.3, 26.0, 45.9, 61.6, 68.1, 70.4, 72.6, 73.4, 77.9, 169.2, 169.5, 170.3, 170.6, 172.5.

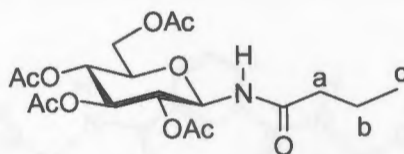
Low resolution MS:  $m/z$  calculated 454.169 (+Na)  $m/z$  found 454.1 (+Na)

HRMS:  $m/z$  calculated 454.1689 (+Na)  $m/z$  found 454.1691 (+Na)

Melting Point: 137-139 °C

$[\alpha]_D +11.8^\circ$  (c. 1.0,  $\text{CH}_2\text{Cl}_2$ )

**Butyric acid-(2,3,4,6-tetra-*O*-acetyl- $\beta$ -D-glucopyranosyl)-amide (16).**



Prepared from 2,3,4,6-tetra-*O*-acetyl- $\beta$ -D-glucopyranosyl azide (1.120 g, 3.0 mmol), butyryl chloride (0.63 mL, 6.0 mmol), and DPPE (0.777 g, 1.95 mmol) according to the typical procedure. Purification by flash column chromatography (1:2, hexanes:ethyl acetate) yielded a crystalline solid (0.82 g, 63.6%).

$^1\text{H NMR}$  ( $\text{CDCl}_3$ ):  $\delta$  0.92 (t, 3H,  $\text{H}_c$ ,  $J = 7.42$  Hz), 1.58 (m, 2H,  $\text{H}_b$ ), 2.10 (m, 2H,  $\text{H}_a$ ) 2.03 (s, 3H,  $\text{COCH}_3$ ), 2.04 (s, 3H,  $\text{COCH}_3$ ), 2.05 (s, 3H,  $\text{COCH}_3$ ), 2.09 (s, 3H,  $\text{COCH}_3$ ), 3.85 (ddd, 1H, H-5,  $J = 2.1, 4.3, 10.2$  Hz), 4.08 (dd, 1H, H-6,  $J = 2.1, 12.5$  Hz), 4.33 (dd, 1H, H-6',  $J = 4.3, 12.5$  Hz), 4.94 (t, 1H, H-2,  $J = 9.6$  Hz), 5.07 (t, 1H, H-4,  $J = 9.7$  Hz), 5.30 (t, 1H, H-1,  $J = 9.7$  Hz), 5.32 (t, 1H, H-3,  $J = 9.6$  Hz), 6.44 (d, 1H, N-H,  $J = 9.3$  Hz).

$^{13}\text{C NMR}$  ( $\text{CDCl}_3$ ):  $\delta$  13.6, 18.6, 20.59 (double intensity), 20.64, 20.7, 38.4, 61.6, 68.0, 70.4, 72.6, 73.4, 77.9, 169.2, 169.5, 170.3, 170.5, 172.9.

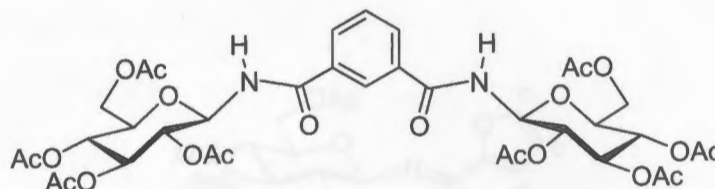
Low resolution MS:  $m/z$  calculated 440.153 (+Na)  $m/z$  found 440.2 (+Na)

HRMS:  $m/z$  calculated 440.1533 (+Na)  $m/z$  found 440.1541 (+Na)

Melting Point: 114-117 °C

$[\alpha]_D +12.9^\circ$  (c. 1.0,  $\text{CH}_2\text{Cl}_2$ )

### Amide dimer derived from isophthaloyl dichloride 17.



Prepared from 2,3,4,6-tetra-*O*-acetyl- $\beta$ -D-glucopyranosyl azide (0.747 g, 2.0 mmol), isophthaloyl dichloride (0.203 g, 1.0 mmol), and DPPE (0.398 g, 1.0 mmol) according to the typical procedure. Purification by flash column chromatography (1:2, hexanes:ethyl acetate) yielded a crystalline solid (0.20 g, 24.3%).

$^1\text{H NMR}$  ( $\text{CDCl}_3$ ):  $\delta$  2.06 (s, 18H, 6 x  $\text{COCH}_3$ ), 2.08 (s, 6H, 2 x  $\text{COCH}_3$ ), 3.93 (ddd, 2H, H-5,  $J = 2.1, 4.2, 10.1$  Hz), 4.11 (dd, 2H, H-6,  $J = 2.2, 13.2$  Hz), 4.34 (dd, 2H, H-6',  $J = 4.4, 12.6$  Hz), 5.10 (t, 2H, H-2,  $J = 9.5$  Hz), 5.13 (t, 2H, H-3,  $J = 9.7$  Hz), 5.41 (t, 2H, H-4,  $J = 9.5$  Hz), 5.48 (t, 2H, H-1,  $J = 9.3$  Hz), 7.37 (d, 2H, N-H,  $J = 9.0$  Hz), 7.59 (t, 1H, Ar-H,  $J = 7.8$  Hz), 7.96 (dd, 2H, Ar-H,  $J = 1.7, 7.9$  Hz), 8.23 (s, 1H, Ar-H).

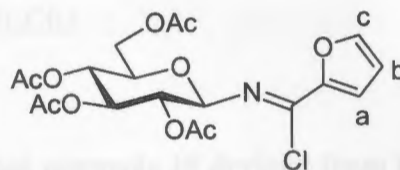
$^{13}\text{C NMR}$  ( $\text{CDCl}_3$ ):  $\delta$  20.64, 20.74, 20.79, 61.61, 68.04, 70.77, 72.70, 73.51, 78.67, 125.97, 129.09, 131.00, 133.11, 166.01, 169.34, 169.62, 170.34, 170.98.

Low resolution MS:  $m/z$  calculated 824.249  $m/z$  found 825.5 ( $M + 1$ )

Melting Point: 131-135  $^\circ\text{C}$

$[\alpha]_{\text{D}} -33.7^\circ$  (c. 1.0,  $\text{CH}_2\text{Cl}_2$ )

**Isolation of imidoyl chloride intermediate 18 derived from 2-furoyl chloride, glycosyl azide, and DPPE in modified Staudinger reaction.**



To a mixture of glucosyl azide (0.747 g, 2.0 mmol) and 2-furoyl chloride (0.396 mL, 4.0 mmol), dissolved in dry THF (0.1 g/mL), was added dropwise a solution of ethylenebis(diphenylphosphine) (0.518 g, 1.3 mmol), in dry THF (0.1 g/mL) at room temperature. The mixture was allowed to stir for 1 hour and monitored by TLC. The THF was removed under vacuum and the crude product was dissolved in chloroform (70 mL), washed with saturated NaHCO<sub>3</sub> (20 mL), and then water (20 mL). The organic layer was dried with MgSO<sub>4</sub>, filtered, and reduced to a yellow slurry. The imidoyl chloride was obtained after flash column chromatography (1:1, hexanes:ethyl acetate) as a colorless solid (0.626 g, 68.1%).

<sup>1</sup>H NMR (CDCl<sub>3</sub>): δ 1.97 (s, 3H, COCH<sub>3</sub>), 2.03 (s, 3H, COCH<sub>3</sub>), 2.06 (s, 3H, COCH<sub>3</sub>), 2.09 (s, 3H, COCH<sub>3</sub>), 3.91 (ddd, 1H, H-5, *J* = 2.4, 4.8, 10.0 Hz), 4.19 (dd, 1H, H-6, *J* = 2.3, 12.4 Hz), 4.28 (dd, 1H, H-6', *J* = 4.9, 12.4 Hz), 5.18-5.29 (m, 3H, H-2, H-3, H-4), 5.38 (m, 1H, H-1), 6.53 (dd, 1H, H<sub>b</sub>, *J* = 1.7, 3.6 Hz), 7.18 (d, 1H, H<sub>a</sub>, *J* = 3.6 Hz), 7.61 (d, 1H, H<sub>c</sub>, *J* = 1.7 Hz).

<sup>13</sup>C NMR (CDCl<sub>3</sub>): δ 20.6, 20.7 (double intensity), 20.8, 62.0, 68.2, 71.8, 73.1, 73.6, 89.1, 112.2, 118.8, 136.5, 147.0, 147.2, 168.8, 169.1, 170.0, 170.4.



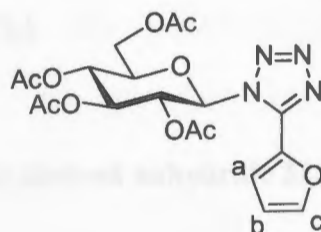
Low resolution MS:  $m/z$  calculated 482.083 (+Na)  $m/z$  found 482.1 (+Na)

HRMS:  $m/z$  calculated 482.0830 (+Na)  $m/z$  found 482.0835 (+Na)

Melting Point: 120-122 °C

$[\alpha]_D -36.4^\circ$  (c. 1.0, CH<sub>2</sub>Cl<sub>2</sub>)

### Synthesis of 1,5-disubstituted tetrazole 19 derived from furan imidoyl chloride 18.



Imidoyl chloride (0.53 g, 1.15 mmol) was dissolved in dry DMF (3 mL) to which NaN<sub>3</sub> (0.30 g, 4.61 mmol) was added and the solution allowed to stir for 5 hours at room temperature. Most of the DMF was removed under vacuum and the resulting slurry was partitioned between CH<sub>2</sub>Cl<sub>2</sub> and water and extracted into CH<sub>2</sub>Cl<sub>2</sub> (3 x 20 mL). The combined extracts were dried over MgSO<sub>4</sub>, filtered, and the remaining crude product purified by flash column chromatography (1:2, hexanes:ethyl acetate) to give a white foam (0.51 g, 95.1%).

<sup>1</sup>H NMR (CDCl<sub>3</sub>):  $\delta$  1.86 (s, 3H, COCH<sub>3</sub>), 2.04 (s, 3H, COCH<sub>3</sub>), 2.06 (s, 3H, COCH<sub>3</sub>), 2.08 (s, 3H, COCH<sub>3</sub>), 4.08 (ddd, 1H, H-5,  $J = 2.5, 5.1, 10.1$  Hz), 4.17 (dd, 1H, H-6,  $J = 2.4, 12.6$  Hz), 4.26 (dd, 1H, H-6',  $J = 5.1, 12.6$  Hz), 5.31 (t, 1H, H-3,  $J = 9.8$  Hz), 5.45 (t, 1H, H-4,  $J = 9.4$  Hz), 6.01 (t, 1H, H-2,  $J = 9.4$  Hz), 6.22 (d, 1H, H-1,  $J = 9.3$  Hz), 6.70-6.72 (m, 1H, H<sub>b</sub>), 7.40-7.41 (m, 1H, H<sub>a</sub>), 7.75-7.76

(m, 1H, H<sub>c</sub>).

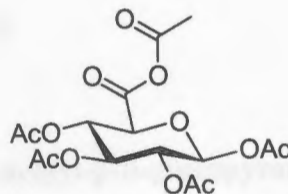
<sup>13</sup>C NMR (CDCl<sub>3</sub>): δ 20.3, 20.6 (double intensity), 20.7, 61.5, 67.5, 69.4, 73.1, 74.9, 83.6, 112.5, 116.1, 138.8, 145.9, 146.9, 168.1, 168.9, 170.0, 170.1.

Low resolution MS: *m/z* calculated 489.123 (+Na) *m/z* found 489.1 (+Na)

HRMS: *m/z* calculated 489.1234 (+Na) *m/z* found 489.1245 (+Na)

[α]<sub>D</sub> -15.1° (c. 1.0, CH<sub>2</sub>Cl<sub>2</sub>)

### Preparation of glucuronic acid-derived anhydride 21.



In a flame-dried 250 mL round bottom flask, D-glucuronic acid (5.0 g, 25.75 mmol) was suspended in acetic anhydride (70 mL) and cooled to 0 °C. Iodine (0.350 g) was slowly added and the dark reddish-brown suspension was allowed to stir for 2 hours at 0 °C and then 3 hours longer at room temperature after which the solution became homogenous. The solvents were removed *in vacuo* to remove most of the acetic anhydride and the remaining solid was taken up in methylene chloride (70 mL). The organic layer was washed with 1M Na<sub>2</sub>SO<sub>3</sub> (2 x 40 mL), then water (40 mL), dried with anhydrous magnesium sulfate, filtered, then reduced to give a mostly white solid (9.99 g, 96%). The

$\beta$ -anomer may be separated from the mixture by recrystallization from methylene chloride/petroleum ether to give a clear crystalline solid (6.22 g, 60%).

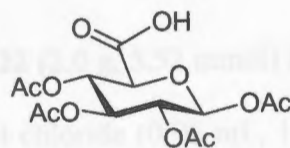
$^1\text{H NMR}$  ( $\text{CDCl}_3$ ):  $\delta$  2.05 (s, 3H,  $\text{COCH}_3$ ), 2.06 (s, 3H,  $\text{COCH}_3$ ), 2.07 (s, 3H,  $\text{COCH}_3$ ), 2.14 (s, 3H,  $\text{COCH}_3$ ), 2.28 (s, 3H,  $\text{C}(\text{O})\text{OC}(\text{O})\text{CH}_3$ ), 4.33 (d, 1H, H-5,  $J = 9.0$  Hz), 5.13 (dd, 1H, H-2,  $J = 7.0, 8.4$  Hz), 5.30 (t, 1H, H-3,  $J = 8.9$  Hz), 5.38 (t, 1H, H-4,  $J = 9.1$  Hz), 5.81 (d, 1H, H-1,  $J = 9.1$  Hz).

$^{13}\text{C NMR}$  ( $\text{CDCl}_3$ ):  $\delta$  20.5, 20.6 (double intensity), 20.7, 22.1, 68.0, 69.9, 71.1, 72.8, 91.1, 162.2, 164.5, 168.4, 168.9, 169.1, 169.5.

Melting Point: 130-132  $^\circ\text{C}$

$[\alpha]_{\text{D}}^{+4.9^\circ}$  (c. 1.0,  $\text{CH}_2\text{Cl}_2$ )

#### Preparation of 1,2,3,4-Tetra-*O*-acetyl- $\beta$ -D-glucopyranuronic acid (**22**).



The anhydride **21** (5.13 g, 12.69 mmol) was dissolved in 90 mL water and THF (1:2 mixture) and allowed to stir for 3 hours at room temperature. The solvents were removed *in vacuo* to give a fluffy white solid (4.45 g, 97%).

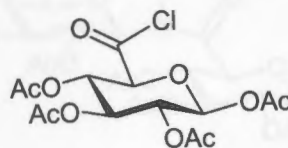
$^1\text{H}$  NMR ( $\text{CDCl}_3$ ):  $\delta$  2.04 (s, 3H,  $\text{COCH}_3$ ), 2.05 (s, 3H,  $\text{COCH}_3$ ), 2.06 (s, 3H,  $\text{COCH}_3$ ), 2.13 (s, 3H,  $\text{COCH}_3$ ), 4.24 (m, 1H, H-5), 5.13 (m, 1H, H-2), 5.27-5.35 (m, 2H, H-3, H-4), 5.80 (d, 1H, H-1,  $J = 7.5$  Hz), 9.17 (broad s, 1H,  $\text{COOH}$ ).

$^{13}\text{C}$  NMR ( $\text{CDCl}_3$ ):  $\delta$  20.6 (triple intensity), 20.8, 68.6, 70.0, 71.7, 72.2, 91.1, 168.8, 169.16, 169.19, 169.7, 169.9.

Melting Point: 80-83  $^\circ\text{C}$

$[\alpha]_D +12.3^\circ$  (c. 1.0,  $\text{CH}_2\text{Cl}_2$ )

### Preparation of 1,2,3,4-Tetra-*O*-acetyl- $\beta$ -D-glucopyranosyl chloride (23).



To a solution of carboxylic acid **22** (2.0 g, 5.52 mmol) in methylene chloride (0.02 g/mL) cooled to 0  $^\circ\text{C}$  was added oxalyl chloride (0.96 mL, 11.04 mmol). With stirring, DMF (2.5 mL) was slowly added and evolution of gases was observed. The pale yellow solution was allowed to stir for 30 minutes at 0  $^\circ\text{C}$  and then 2 hours at room temperature. The solvents were removed *in vacuo* to leave a purple chalky solid (2.04 g, 97%), which was stored under vacuum.

$^1\text{H}$  NMR ( $\text{CDCl}_3$ ):  $\delta$  2.05 (s, 3H,  $\text{COCH}_3$ ), 2.07 (s, 3H,  $\text{COCH}_3$ ), 2.08 (s, 3H,  $\text{COCH}_3$ ), 2.15 (s, 3H,  $\text{COCH}_3$ ), 4.46 (d, 1H, H-5,  $J = 8.6$  Hz), 5.12 (dd, 1H, H-2,

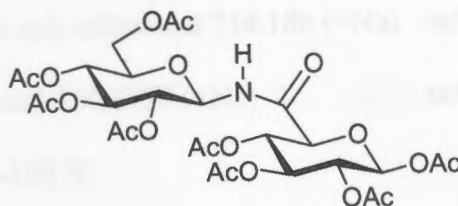
$J = 6.3, 8.1$  Hz), 5.28 (dd, 1H, H-3,  $J = 8.2, 8.8$  Hz), 5.41 (t, 1H, H-4,  $J = 8.7$  Hz), 5.89 (d, 1H, H-1,  $J = 6.4$  Hz).

$^{13}\text{C}$  NMR ( $\text{CDCl}_3$ ):  $\delta$  20.5, 20.6 (double intensity), 20.8, 67.6, 69.7, 70.7, 78.7, 90.9, 168.2, 168.8 (double intensity), 169.4, 169.5.

Melting Point: 120-123 °C

$[\alpha]_{\text{D}} +6.4^\circ$  (c. 1.0,  $\text{CH}_2\text{Cl}_2$ )

#### Amide-linked carbohydrate dimer 24.



Prepared from 2,3,4,6-tetra-*O*-acetyl- $\beta$ -D-glucopyranosyl azide (0.747 g, 2.0 mmol), 1,2,3,4-tetra-*O*-acetyl- $\beta$ -D-glucopyranosyl chloride (1.218 g, 3.2 mmol), and DPPE (0.518 g, 1.3 mmol) according to the typical modified Staudinger procedure. Purification by flash column chromatography (1:2 Hexanes-EtOAc) yielded a white crystalline solid (0.99 g, 71.7%).

$^1\text{H}$  NMR ( $\text{CDCl}_3$ ):  $\delta$  2.026 (s, 6H, 2 x  $\text{COCH}_3$ ), 2.029 (s, 3H,  $\text{COCH}_3$ ), 2.050 (s, 3H,  $\text{COCH}_3$ ), 2.052 (s, 3H,  $\text{COCH}_3$ ), 2.09 (s, 3H,  $\text{COCH}_3$ ), 2.15 (s, 3H,  $\text{COCH}_3$ ), 2.19 (s, 3H,  $\text{COCH}_3$ ), 3.79 (ddd, 1H, H-5<sub>glucose</sub>,  $J = 2.1, 4.4, 10.1$  Hz), 4.04 (d, 1H,

$^1\text{H}$  NMR ( $\text{CDCl}_3$ ):  $\delta$  4.31 (dd, 1H, H-5<sub>glucuronic acid</sub>,  $J = 10.1$  Hz), 4.05 (dd, 1H, H-6<sub>glucose</sub>,  $J = 1.9, 12.5$  Hz), 4.31 (dd, 1H, H-6<sub>glucose</sub>,  $J = 4.5, 12.5$  Hz), 4.95 (t, 1H,  $J = 9.61$  Hz), 5.00 (dd, 1H, H-4<sub>glucuronic acid</sub>,  $J = 9.6, 10.0$  Hz), 5.06 (t, 1H,  $J = 9.8$  Hz), 5.10-5.16 (m, 2H), 5.29 (t, 1H,  $J = 9.4$  Hz), 5.31 (t, 1H, H-2<sub>glucose</sub>,  $J = 9.5$  Hz), 5.75 (d, 1H, H-1<sub>glucuronic acid</sub>,  $J = 8.2$  Hz), 7.13 (d, 1H, N-H,  $J = 9.3$  Hz).

$^{13}\text{C}$  NMR ( $\text{CDCl}_3$ ):  $\delta$  20.56 (double intensity), 20.59 (triple intensity), 20.66, 20.73, 20.81, 61.48, 67.83, 68.54, 69.90, 70.10, 71.78, 72.45, 72.53, 73.56, 77.63, 90.85, 166.28, 168.50, 168.90, 169.20 (double intensity), 169.42, 169.49, 170.28, 170.95.

Low resolution MS:  $m/z$  calculated 714.186 (+Na)  $m/z$  found 714.2 (+Na)

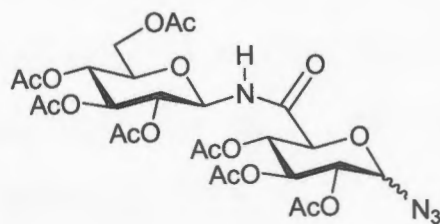
HRMS:  $m/z$  calculated 714.1857 (+Na)  $m/z$  found 714.1808 (+Na)

Melting Point: 185-188 °C

$[\alpha]_D +4.7^\circ$  (c. 1.0,  $\text{CH}_2\text{Cl}_2$ )

### Lewis acid-catalyzed azidation of amide-linked carbohydrate dimer 24 to form azide 25.

25.

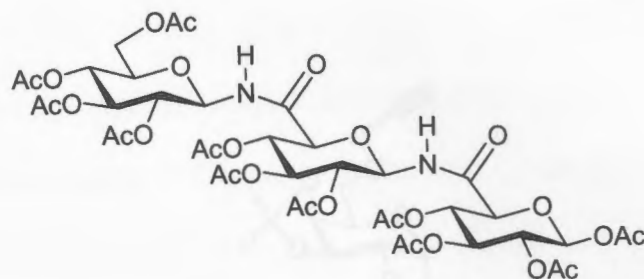


Dimer **24** (0.368 g, 0.53 mmol) was dissolved in dry methylene chloride (4 mL) in a flame-dried 50 mL round bottom flask equipped with a magnetic stir bar under an inert atmosphere of nitrogen gas. Trimethylsilyl azide (0.174 mL, 1.33 mmol) and SnCl<sub>4</sub> (0.03 mL, 0.265 mmol) were added successively *via* syringe and the mixture was allowed to stir for 15 hours. The reaction mixture was diluted with methylene chloride (25 mL) and saturated sodium bicarbonate (25 mL), and the suspension stirred vigorously for 30 minutes. The mixture was transferred to a separatory funnel, the organic layer drained, and the aqueous layer extracted with methylene chloride (2 x 25 mL). The combined extracts were washed with water (2 x 50 mL), dried over anhydrous magnesium sulfate, filtered and reduced to an off-white foam. Flash column chromatography (4:5, hexanes ethyl acetate) gave the product as a white foam (0.23 g, 64.4%), which was a mixture of  $\alpha/\beta$  isomers (5:1).

<sup>1</sup>H NMR (CDCl<sub>3</sub>):  $\delta$  2.02 (s, 3H, COCH<sub>3</sub>), 2.04 (s, 6H, 2 x COCH<sub>3</sub>), 2.05 (s, 3H, COCH<sub>3</sub>), 2.08 (s, 3H, COCH<sub>3</sub>), 2.12 (s, 3H, COCH<sub>3</sub>), 2.15 (s, 3H, COCH<sub>3</sub>), 3.80 (ddd, 1H, H-5<sub>glucose</sub>,  $J = 2.1, 4.3, 10.2$  Hz), 4.08 (dd, 1H, H-6<sub>glucose</sub>,  $J = 2.0, 12.4$  Hz), 4.30 (dd, 1H, H-6'<sub>glucose</sub>,  $J = 4.4, 12.6$  Hz), 4.37 (d, 1H, H-5<sub>glucuronic acids</sub>,  $J = 10.3$  Hz), 4.86-4.95 (m, 2H), 5.06 (t, 1H,  $J = 9.8$  Hz), 5.17 (t, 1H,  $J = 9.4$  Hz), 5.33 (t, 1H,  $J = 9.6$  Hz), 5.42 (t, 1H,  $J = 9.9$  Hz), 5.70 (d, 1H, H-1<sub>glucuronic acids</sub>,  $J = 4.4$  Hz), 7.12 (d, 1H, N-H,  $J = 9.3$  Hz).



### Formation of amide-linked carbohydrate trimer 26.



Prepared from azide **25** (0.690 g, 1.023 mmol), acid chloride **23** (0.623 g, 1.637 mmol), and DPPE (0.245 g, 0.614 mmol) according to the typical modified Staudinger procedure. Flash column chromatography (1:3, hexanes:ethyl acetate) yielded the title compound as a white solid (0.546 g, 52.6%).

$^1\text{H NMR}$  ( $\text{CDCl}_3$ ):  $\delta$  2.03 (s, 9H, 3 x  $\text{COCH}_3$ ), 2.04 (s, 3H,  $\text{COCH}_3$ ), 2.05 (s, 3H,  $\text{COCH}_3$ ), 2.06 (s, 6H, 2 x  $\text{COCH}_3$ ), 2.09 (s, 3H,  $\text{COCH}_3$ ), 2.14 (s, 3H,  $\text{COCH}_3$ ), 2.15 (s, 3H,  $\text{COCH}_3$ ), 2.21 (s, 3H,  $\text{COCH}_3$ ), 3.76 (m, 1H, H-5<sub>glucose</sub>), 3.97 (d, 1H, H-5<sub>glucuronic acid</sub>,  $J = 10.1$  Hz), 4.05 (dd, 1H, H-6<sub>glucose</sub>,  $J = 1.7, 12.5$  Hz), 4.09 (d, 1H, H-5<sub>glucuronic acid</sub>,  $J = 10.1$  Hz), 4.29 (dd, 1H, H-6'<sub>glucose</sub>,  $J = 4.6, 12.4$  Hz), 4.88-5.08 (m, 5H), 5.12-5.18 (m, 3H), 5.28-5.37 (m, 3H), 5.79 (d, 1H, H-1<sub>glucuronic acid</sub>,  $J = 8.1$  Hz), 7.14 (d, 1H, N-H,  $J = 9.5$  Hz), 7.32 (d, 1H, N-H,  $J = 9.3$  Hz).

Low resolution MS:  $m/z$  calculated 1015.266 (+Na)  $m/z$  found 1015.7 (+Na)

HRMS:  $m/z$  calculated 1015.2655 (+Na)  $m/z$  found 1015.2618 (+Na)

Melting Point: 178-180 °C

$[\alpha]_{\text{D}}^{\circ} +5.2^{\circ}$  (c. 1.0,  $\text{CH}_2\text{Cl}_2$ )

## Synthesis of carbohydrate-derived alkynes:

### Preparation of 1,2:3,4-di-*O*-isopropylidene-6-(prop-2-ynyloxy)-D-galactopyranose

(28).



In a 200 mL oven-dried round bottom flask, 1,2:3,4-di-*O*-isopropylidene-D-galactopyranose (4.02 g, 15.37 mmol) was dissolved in 40 mL of acetonitrile. Crushed KOH (3.60 g, 62.34 mmol) was added and after 15 minutes of stirring an 80% propargyl bromide solution in toluene (5.38 mL, 62.39 mmol) was slowly added *via* syringe. The mixture was allowed to stir overnight and until TLC analysis revealed the reaction to be complete. The reaction mixture was reduced to a brown wet solid to which 150 mL of ice water was added and subsequently extracted with methylene chloride (3 x 75 mL). The combined extracts were washed with water, dried over anhydrous magnesium sulfate, filtered, and reduced to a brown syrup. Flash column chromatography using 5:1 hexanes and ethyl acetate yielded 3.66 g (80%) of a pale yellow solid.

$^1\text{H NMR}$  ( $\text{CDCl}_3$ ):  $\delta$  1.33 (s, 3H,  $\text{CH}_3$ ), 1.35 (s, 3H,  $\text{CH}_3$ ), 1.46 (s, 3H,  $\text{CH}_3$ ), 1.55 (s, 3H,  $\text{CH}_3$ ), 2.44 (t, 1H, alkyne-H,  $J = 2.0$  Hz), 3.67 (dd, 1H, H-6,  $J = 7.1, 10.1$  Hz), 3.78 (dd, 1H, H-6',  $J = 5.2, 10.2$  Hz), 4.00 (m, 1H, H-5), 4.17-4.33 (m, 4H, H-2, H-4, - $\text{CH}_2$ ), 4.61 (dd, 1H, H-3,  $J = 2.3, 8.0$  Hz), 5.55 (d, 1H, H-1,  $J = 5.1$  Hz).

$^{13}\text{C}$  NMR ( $\text{CDCl}_3$ ):  $\delta$  25.7, 26.1, 27.2, 27.3, 59.6, 67.8, 69.8, 71.5, 71.7, 72.2, 75.8, 80.7, 97.4, 109.6, 110.3.

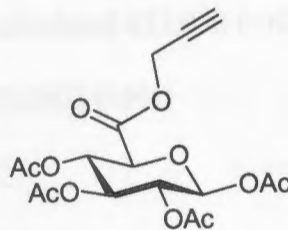
Low resolution MS:  $m/z$  calculated 321.131 (+Na)  $m/z$  found 321.1 (+Na)

HRMS:  $m/z$  calculated 321.1314 (+Na)  $m/z$  found 321.1297 (+Na)

Melting Point: 50-54 °C

$[\alpha]_{\text{D}} -3.2^\circ$  (c. 1.0,  $\text{CH}_2\text{Cl}_2$ )

### Preparation of Prop-2-ynyl 1,2,3,4-tetra-*O*-acetyl- $\beta$ -D-glucopyranuronate (29).



To a solution of carboxylic acid **22** (1.609 g, 4.44 mmol) in methylene chloride (0.02 g/mL) cooled to 0 °C was added oxalyl chloride (0.387 mL, 4.44 mmol). With stirring, DMF (1.8 mL) was slowly added and evolution of gases was observed. The pale yellow solution was allowed to stir for 30 minutes at 0 °C and then 2 hours at room temperature. A solution of propargyl alcohol (0.388 mL, 6.66 mmol) and pyridine (2.5 mL) in 5 mL of methylene chloride was slowly added *via* syringe and the mixture was allowed to stir overnight. The reaction mixture was poured over 100 mL of ice water and extracted with methylene chloride (3 x 50 mL). The extracts were washed with 5%  $\text{H}_2\text{SO}_4$  (3 x 50 mL), then water (50 mL), dried with anhydrous magnesium sulfate, filtered and reduced to a

cream colored solid (1.77 g, 100%). The crude product was recrystallized from hot methanol to give clear crystals (1.68 g, 95%).

$^1\text{H}$  NMR ( $\text{CDCl}_3$ ):  $\delta$  2.04 (s, 3H,  $\text{COCH}_3$ ), 2.05 (s, 3H,  $\text{COCH}_3$ ), 2.07 (s, 3H,  $\text{COCH}_3$ ), 2.13 (s, 3H,  $\text{COCH}_3$ ), 2.53 (t, 1H, alkyne-H,  $J = 2.5$  Hz), 4.24 (d, 1H, H-5,  $J = 9.5$  Hz), 4.71 (m, 2H,  $\text{CH}_2$ ), 5.15 (dd, 1H, H-2,  $J = 7.7, 9.0$  Hz), 5.25 (t, 1H, H-4,  $J = 9.5$  Hz), 5.33 (t, 1H, H-3,  $J = 9.0$  Hz), 5.78 (d, 1H, H-1,  $J = 7.7$  Hz).

$^{13}\text{C}$  NMR ( $\text{CDCl}_3$ ):  $\delta$  21.8 (triple intensity), 22.0, 54.8, 69.9, 71.2, 72.8, 73.8, 77.2, 77.5, 92.3, 166.7, 169.7, 170.1, 170.4, 170.8.

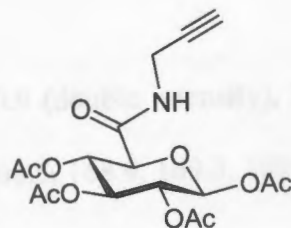
Low resolution MS:  $m/z$  calculated 423.090 (+Na)  $m/z$  found 423.1 (+Na)

HRMS:  $m/z$  calculated 423.0903 (+Na)  $m/z$  found 423.0907 (+Na)

Melting Point: 138-141 °C

$[\alpha]_{\text{D}} +10.8^\circ$  (c. 1.0,  $\text{CH}_2\text{Cl}_2$ )

### Preparation of amide alkyne 30.



To a solution of carboxylic acid **22** (1.0 g, 2.76 mmol) in dry methylene chloride (0.02 g/mL) cooled to 0 °C was added oxalyl chloride (0.48 mL, 5.52 mmol). With stirring,

DMF (1.2 mL) was slowly added and evolution of gases was observed. The pale yellow solution was allowed to stir for 30 minutes at 0 °C and then 2 hours at room temperature. The solvents were removed *in vacuo* to leave a purple solid which was dissolved in dry methylene chloride (20 mL). To this was added a solution of propargyl amine (0.19 mL, 3.04 mmol) and pyridine (0.67 mL, 8.28 mmol) in methylene chloride (5 mL) after which immediate precipitation of an off-white solid was observed and the mixture was allowed to stir overnight. The reaction mixture was poured into 50 mL of ice water and extracted with methylene chloride (3 x 25 mL). The combined extracts were washed with 5% H<sub>2</sub>SO<sub>4</sub> (3 x 15 mL), then water (15 mL), dried with anhydrous magnesium sulfate, filtered and reduced to a cream colored solid which was recrystallized upon slow evaporation from methanol to give fine white crystals (0.91 g, 82.7%).

<sup>1</sup>H NMR (CDCl<sub>3</sub>): δ 2.03 (s, 3H, COCH<sub>3</sub>), 2.05 (s, 3H, COCH<sub>3</sub>), 2.08 (s, 3H, COCH<sub>3</sub>), 2.16 (s, 3H, COCH<sub>3</sub>), 2.27 (t, 1H, alkyne-H, *J* = 2.6 Hz), 4.11 (d, 1H, H-5, *J* = 9.7 Hz), 3.99, (ddd, 1H, CH<sub>2</sub>, *J* = 2.6, 5.3, 17.6 Hz), 4.06 (ddd, 1H, CH<sub>2</sub>, *J* = 2.7, 5.5, 17.6 Hz), 5.12 (dd, 1H, H-2, *J* = 8.0, 8.9 Hz), 5.22 (t, 1H, H-3, *J* = 9.5 Hz), 5.31 (t, 1H, H-4, *J* = 9.2 Hz), 5.77 (d, 1H, H-1, *J* = 7.9 Hz), 6.50 (t, 1H, N-H, *J* = 5.2 Hz).

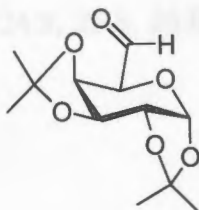
<sup>13</sup>C NMR (CDCl<sub>3</sub>): δ 20.6 (double intensity), 20.7, 20.8, 28.9, 68.6, 70.0, 71.7, 72.0, 72.7, 91.1, 165.4, 168.5, 168.9, 169.3, 169.5.

Low resolution MS: *m/z* calculated 422.106 (+Na) *m/z* found 422.1 (+Na)

Melting Point: 166-167 °C

$[\alpha]_D +3.7^\circ$  (c. 1.0,  $\text{CH}_2\text{Cl}_2$ )

**Preparation of 1,2:3,4-Di-*O*-isopropylidene- $\alpha$ -D-galacto-hexodialdo-1,5-pyranose (31).**

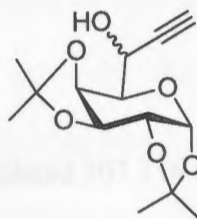


A flame-dried 100 mL 3-neck round bottom flask fitted with two addition funnels, a magnetic stir bar, and a rubber septum was charged with  $(\text{COCl})_2$  (0.47 mL, 5.34 mmol) in dry methylene chloride (10 mL) and cooled to  $-78^\circ\text{C}$  under an atmosphere of  $\text{N}_2$ . DMSO (0.83 mL, 11.65 mmol) in dry methylene chloride (2 mL) was added dropwise and the mixture was stirred for 10 minutes. A solution of 1,2:3,4-di-*O*-isopropylidene-D-galactopyranose (1.26 g, 4.86 mmol) in dry methylene chloride (12 mL) was added dropwise and the mixture was allowed to stir for 15 minutes. Triethylamine (3.41 mL, 24.28 mmol) was added slowly *via* syringe and the solution was allowed to warm to room temperature. After 3 hours the mixture was poured over ice water (50 mL) and extracted with methylene chloride (3 x 25 mL). The combined extracts were washed with 5%  $\text{H}_2\text{SO}_4$  (2 x 30 mL), then water (30 mL), dried over anhydrous magnesium sulfate, filtered, then reduced to a pale yellow syrup (1.04 g, 82.9%) which could be used without further purification.

$^1\text{H}$  NMR ( $\text{CDCl}_3$ ):  $\delta$  1.32 (s, 3H,  $\text{CH}_3$ ), 1.36 (s, 3H,  $\text{CH}_3$ ), 1.45 (s, 3H,  $\text{CH}_3$ ), 1.52 (s, 3H,  $\text{CH}_3$ ), 4.20 (d, 1H, H-5,  $J = 2.2$  Hz), 4.39 (dd, 1H, H-2,  $J = 2.4, 4.9$  Hz), 4.61 (dd, 1H, H-4,  $J = 2.2, 7.9$  Hz), 4.66 (dd, 1H, H-3,  $J = 2.4, 7.9$  Hz), 5.68 (d, 1H, H-1,  $J = 4.8$  Hz), 9.63 (s, 1H, aldehyde-H).

$^{13}\text{C}$  NMR ( $\text{CDCl}_3$ ):  $\delta$  24.3, 24.8, 25.8, 26.0, 70.3, 70.4, 71.6, 73.1, 96.1, 108.9, 109.8, 199.9.

#### Addition of ethynyl magnesium bromide to aldehyde (31) to form 32a/32b.



In a flame-dried 100 mL round bottom flask fitted with an addition funnel and magnetic stir bar, aldehyde **31** (0.94 g, 3.64 mmol) was dissolved in dry methylene chloride (10 mL) and the solution was cooled to 0 °C. A 0.5 M solution of ethynyl magnesium bromide in THF (10.8 mL, 5.42 mmol) was added slowly dropwise and the mixture was allowed to stir at 0 °C for three hours or until judged complete by TLC. The reaction was quenched with saturated  $\text{NH}_4\text{Cl}$  (30 mL) and extracted with ethyl acetate (3 x 30 mL). The combined extracts were washed with brine, dried with anhydrous magnesium sulfate, filtered and reduced to a yellow solid. Flash column chromatography (2:1, hexanes:ethyl



acetate) gave 0.258 g (24.9%) of one diastereomer and 0.52 g (49.3%) of a mixture of diastereomers.

**Diastereomer.**

$^1\text{H}$  NMR ( $\text{CDCl}_3$ ):  $\delta$  1.35 (s, 3H,  $\text{CH}_3$ ), 1.38 (s, 3H,  $\text{CH}_3$ ), 1.50 (s, 3H,  $\text{CH}_3$ ), 1.55 (s, 3H,  $\text{CH}_3$ ), 2.57 (d, 1H, alkyne-H,  $J = 2.2$  Hz), 3.43 (d, 1H, -OH,  $J = 8.1$  Hz), 3.83 (d, 1H, H-5,  $J = 6.2$  Hz), 4.35-4.36 (m, 1H, -CH), 4.62 (dd, 1H, H-4,  $J = 2.2, 6.2$  Hz), 4.64 (dd, 1H, H-3,  $J = 2.0, 6.0$  Hz), 4.67 (m, 1H, H-2), 5.62 (d, 1H, H-1,  $J = 4.9$  Hz).

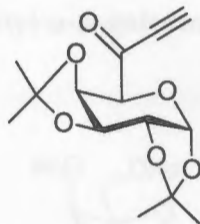
$^{13}\text{C}$  NMR ( $\text{CDCl}_3$ ):  $\delta$  24.3, 24.9, 25.8, 26.0, 62.49, 68.6, 70.3, 70.6, 71.1, 74.2, 82.23, 96.4, 108.7, 109.6.

Low resolution MS:  $m/z$  calculated 307.116 (+Na)  $m/z$  found 307.1 (+Na)

Melting Point: 118-122 °C

$[\alpha]_D^{+69.2^\circ}$  (c. 1.0,  $\text{CH}_2\text{Cl}_2$ )

**Moffatt oxidation of mixture 32a/32b to give alkynyl ketone 33.**



The alcohol (0.284 g, 1.0 mmol), DCC (3 mL of 1.0 M solution in hexanes, 3 mmol), and DMSO (1.42 mL) were combined in a flame-dried 50 mL round bottom flask equipped with a septum and magnetic stir bar. After cooling to 15 °C, trifluoroacetic acid (0.04 mL, 0.5 mmol) was slowly added dropwise and the reaction mixture, which develops a precipitate, was stirred for 6 hours at room temperature. The reaction mixture was diluted with ether (30 mL) and filtered to remove the fine white solid byproduct. The filtrate was washed with water, then brine (20 mL each), dried with anhydrous magnesium sulfate, filtered, and reduced to a brown syrup. Flash column chromatography (3:1, hexanes:ethyl acetate) yielded the alkynyl ketone as a yellow solid (0.21 g, 74%).

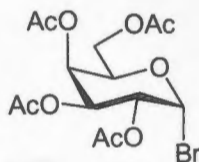
$^1\text{H NMR}$  ( $\text{CDCl}_3$ ):  $\delta$  1.34 (s, 3H,  $\text{CH}_3$ ), 1.35 (s, 3H,  $\text{CH}_3$ ), 1.45 (s, 3H,  $\text{CH}_3$ ), 1.53 (s, 3H,  $\text{CH}_3$ ), 3.42 (s, 1H, alkyne-H), 4.40-4.42 (m, 2H, H-2 and H-5 overlapping), 4.69 (dd, 1H, H-4,  $J = 2.6, 7.7$  Hz), 4.75 (dd, 1H, H-3,  $J = 2.3, 7.6$  Hz), 5.69 (d, 1H, H-1,  $J = 4.9$  Hz).

Low resolution MS:  $m/z$  calculated 305.279 (+Na)  $m/z$  found 305.0 (+Na)

Melting Point: 115-118 °C

$[\alpha]_D -104.2^\circ$  (c. 1.0,  $\text{CH}_2\text{Cl}_2$ )

### Preparation of 2,3,4,6-Tetra-*O*-acetyl- $\alpha$ -D-galactopyranosyl bromide (35).

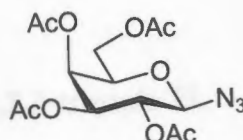


$\beta$ -D-galactose pentaacetate (5.0 g, 12.81 mmol) was dissolved in 33% HBr/AcOH (20 mL) in an oven-dried 100 mL round bottom flask fitted with a rubber septum and magnetic stir bar. The brown solution was allowed to stir for one hour or until TLC (1:1, hexanes:ethyl acetate, product  $R_f = 0.47$  (1:1, hexanes:ethyl acetate), showed consumption of starting material. The solvents were removed *in vacuo* and the resulting brown syrup was diluted with 100 mL each of cold water and saturated sodium bicarbonate. The mixture was extracted with chloroform (3 x 50 mL) after which the combined extracts were dried over anhydrous magnesium sulfate, filtered, and reduced to a clear syrupy solid (5.18 g, 98%).

$^1\text{H NMR}$  ( $\text{CDCl}_3$ ):  $\delta$  2.00 (s, 3H,  $\text{COCH}_3$ ), 2.05 (s, 3H,  $\text{COCH}_3$ ), 2.11 (s, 3H,  $\text{COCH}_3$ ), 2.14 (s, 3H,  $\text{COCH}_3$ ), 4.10 (dd, 1H, H-6,  $J = 6.8, 11.4$  Hz), 4.18 (dd, 1H, H-6',  $J = 6.3, 11.4$  Hz), 4.48 (m, 1H, H-5), 5.04 (dd, 1H, H-2,  $J = 3.9, 10.6$  Hz), 5.39 (dd, 1H, H-3,  $J = 3.3, 10.6$  Hz), 5.51 (d, 1H, H-4,  $J = 3.3$  Hz), 6.69 (d, 1H, H-1,  $J = 3.8$  Hz).

$^{13}\text{C}$  NMR ( $\text{CDCl}_3$ ):  $\delta$  21.8 (double intensity), 21.9, 22.0, 60.7, 66.8, 67.6, 67.8, 70.9, 88.0, 169.4, 169.5, 169.7, 169.9.

**Preparation of 2,3,4,6-Tetra-*O*-acetyl- $\beta$ -D-glucopyranosyl azide (36) from  $\alpha$ -glucosyl bromide (35) via  $\text{S}_{\text{N}}2$  reaction.**



Bromide **35** (5.18 g, 12.60 mmol) was dissolved in 25 mL dry DMF in a 100 mL flame-dried round bottom flask equipped with a rubber septum and magnetic stir bar. The pale yellow solution was stirred for 3 hours until TLC showed complete consumption of the starting material and the appearance of a new more polar spot. The DMF was removed *in vacuo* and the resulting slurry partitioned between water and methylene chloride (50 mL each). The organic layer was removed and the aqueous layer extracted with methylene chloride (2 x 50 mL). The combined extracts were dried over anhydrous magnesium sulfate, filtered, and reduced to a pale yellow syrup which was recrystallized from hot methanol to give 3.509 g (74.6%) of a clear crystalline solid.

$^1\text{H}$  NMR ( $\text{CDCl}_3$ ):  $\delta$  2.00 (s, 3H,  $\text{COCH}_3$ ), 2.07 (s, 3H,  $\text{COCH}_3$ ), 2.10 (s, 3H,  $\text{COCH}_3$ ), 2.18 (s, 3H,  $\text{COCH}_3$ ), 4.02 (m, 1H, H-5), 4.13-4.22 (m, 2H, H-6, H-6'), 4.62 (d, 1H, H-1,  $J = 8.8$  Hz), 5.05 (dd, 1H, H-2,  $J = 3.3, 10.4$  Hz), 5.17 (dd, 1H, H-3,  $J = 8.7, 10.5$  Hz), 5.43 (dd, 1H, H-4,  $J = 1.1, 3.3$  Hz).

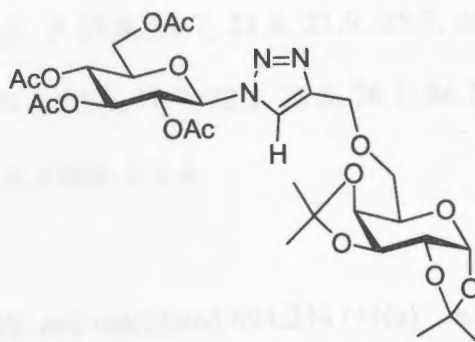
$^{13}\text{C}$  NMR ( $\text{CDCl}_3$ ):  $\delta$  20.56, 20.65, 20.71 (double intensity), 61.2, 66.8, 67.9, 70.6, 72.7, 88.1, 169.1, 169.7, 169.8, 170.0.

Low resolution MS:  $m/z$  calculated 396.305 (+Na)  $m/z$  found 396.1 (+Na)

Melting Point: 90-91  $^\circ\text{C}$

$[\alpha]_{\text{D}} -4.1^\circ$  (c. 1.0,  $\text{CH}_2\text{Cl}_2$ )

### Formation of 1,4-disubstituted 1,2,3-triazole 37.



In a 100 mL 2-neck round bottom flask equipped with a reflux condenser, thermometer, and magnetic stir bar, azide **3** (2.62 g, 7.0 mmol) and ether alkyne **28** (2.09 g, 7.0 mmol) were suspended in 40 mL *t*-BuOH and water (1:1). Ascorbic acid (3.5 mL of 1 M solution, 3.5 mmol) and  $\text{CuSO}_4$  (0.35 mL of 1M solution, 0.35 mmol) were added and after heating the suspension to 60  $^\circ\text{C}$  the light yellow solution became clear. TLC showed consumption of both starting materials after 1.5 hours. The mixture was allowed to cool to room temperature and most of the *t*-BuOH was removed *in vacuo*. Ice water (25 mL) was added and the product was filtered off through a glass frit funnel and washed with cold water (2 x 25 mL) to afford a white solid (3.97 g, 84.4%).

$^1\text{H}$  NMR ( $\text{CDCl}_3$ ):  $\delta$  1.34 (s, 3H,  $\text{CH}_3$ ), 1.35 (s, 3H,  $\text{CH}_3$ ), 1.45 (s, 3H,  $\text{CH}_3$ ), 1.54 (s, 3H,  $\text{CH}_3$ ), 1.88 (s, 3H,  $\text{COCH}_3$ ), 2.04 (s, 3H,  $\text{COCH}_3$ ), 2.08 (s, 3H,  $\text{COCH}_3$ ), 2.09 (s, 3H,  $\text{COCH}_3$ ), 3.68 (dd, 1H, H-6<sub>galactose</sub>,  $J = 7.0, 10.1$  Hz), 3.74 (dd, 1H, H-6' galactose,  $J = 5.6, 10.2$  Hz), 4.00 (m, 2H, H-5<sub>glucose</sub>, H-5<sub>galactose</sub>), 4.12 (dd, 1H, H-6<sub>glucose</sub>,  $J = 1.5, 12.5$  Hz), 4.25-4.33 (m, 3H, H-6' glucose, H-2<sub>galactose</sub>, H-3<sub>galactose</sub>), 4.61 (dd, 1H, H-4<sub>galactose</sub>,  $J = 2.2, 7.9$  Hz), 4.68 (m, 2H,  $\text{CH}_2$ ), 5.24 (t, 1H, H-4<sub>glucose</sub>,  $J = 9.4$  Hz), 5.40 (m, 2H, H-2<sub>glucose</sub>, H-3<sub>glucose</sub>), 5.56 (d, 1H, H-1<sub>galactose</sub>,  $J = 4.9$  Hz), 5.89 (d, 1H, H-1<sub>glucose</sub>,  $J = 8.8$  Hz), 7.84 (s, 1H, triazole-H).

$^{13}\text{C}$  NMR ( $\text{CDCl}_3$ ):  $\delta$  21.4, 21.7, 21.8, 21.9, 25.7, 26.1, 27.2, 27.3, 62.7, 65.8, 67.9, 68.8, 70.5, 71.4, 71.6, 71.7, 72.2, 73.8, 76.1, 86.7, 97.4, 109.6, 110.3, 122.0, 146.9, 169.8, 170.3, 170.8, 171.4.

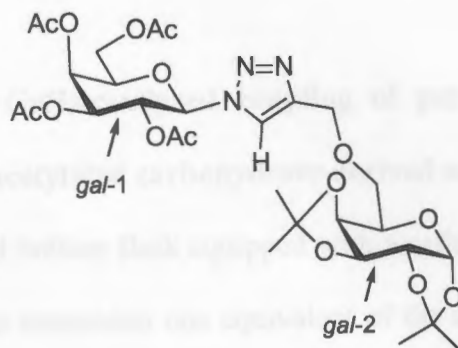
Low resolution MS:  $m/z$  calculated 694.244 (+Na)  $m/z$  found 694.2 (+Na)

HRMS:  $m/z$  calculated 694.2435 (+Na)  $m/z$  found 694.2433 (+Na)

Melting Point: 160-163 °C

$[\alpha]_{\text{D}} -44.3^\circ$  (c. 1.0,  $\text{CH}_2\text{Cl}_2$ )

### Formation of 1,4-disubstituted 1,2,3-triazole 38



In a 50 mL two-neck round bottom flask equipped with a reflux condenser, thermometer, and magnetic stir bar, azide **36** (0.373 g, 1 mmol) and ether alkyne **28** (0.298.3 g, 1 mmol) were suspended in 10 mL *t*-BuOH and water (1:1). Ascorbic acid (0.070 g, 0.4 mmol) and CuSO<sub>4</sub> (0.050 g, 0.2 mmol), each in 1 mL of water, were added and after heating the suspension to 60 °C the light yellow solution became clear. TLC analysis showed consumption of both starting materials after 1.5 hours. The reaction mixture was cooled and then extracted with methylene chloride (3 x 30 ml). The solvent was removed *in vacuo* and the crude yellow syrup was subjected to flash column chromatography (1:1, hexanes:ethyl acetate) to give the product as a white solid (0.506 g, 75%).

<sup>1</sup>H NMR (CDCl<sub>3</sub>): δ 1.34 (s, 3H, CH<sub>3</sub>), 1.36 (s, 3H, CH<sub>3</sub>), 1.45 (s, 3H, CH<sub>3</sub>), 1.55 (s, 3H, CH<sub>3</sub>), 1.90 (s, 3H, COCH<sub>3</sub>), 2.02 (s, 3H, COCH<sub>3</sub>), 2.06 (s, 3H, COCH<sub>3</sub>), 2.23 (s, 3H, COCH<sub>3</sub>), 3.68 (dd, 1H, H-6<sub>gal-2</sub>, *J* = 7.0, 10.1 Hz), 3.73 (dd, 1H, H-6' <sub>gal-2</sub>, *J* = 5.6, 10.2 Hz), 3.99 (m, 1H), 4.11-4.29 (m, 5H), 4.33 (dd, 1H, *J* = 2.4, 4.9 Hz), 4.62 (dd, 1H, *J* = 2.4, 7.9 Hz), 4.69 (m, 2H), 5.26 (dd, 1H, *J* = 3.3, 13.2 Hz), 5.54- 5.59 (m, 3H), 5.86 (d, 1H, H-1<sub>gal-1</sub>, *J* = 9.4 Hz), 7.89 (s, 1H, triazole-H).



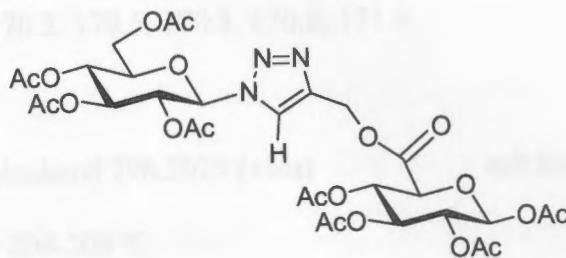
Melting Point: 204-208 °C

$[\alpha]_D -5.8^\circ$  (c. 1.0,  $\text{CH}_2\text{Cl}_2$ )

**General procedure for Cu(I)-catalyzed coupling of peracetylated carbohydrate-derived alkynes and peracetylated carbohydrate-derived azides.**

In a 100 mL 2-neck round bottom flask equipped with a reflux condenser, thermometer, and magnetic stir bar, was suspended one equivalent of the azide and one equivalent of the alkyne in water (0.1 g/mL). Ascorbic acid (0.4 equivalents) and  $\text{CuSO}_4$  (0.2 equivalents) were added and, while heating to 60 °C, the contents stirred vigorously until the reaction was determined complete by TLC (6-18 hours). After cooling to room temperature, water was added and the resulting precipitate could be collected over a glass frit. To obtain the best yield, the reaction mixture was extracted with methylene chloride. The extracts were dried over anhydrous magnesium sulfate, filtered and reduced to give the product as a solid which in most cases required no further purification.

### Formation of 1,4-disubstituted 1,2,3-triazole 39.



Prepared from glucosyl azide **3** (0.747 g, 2.0 mmol), alkyne **29** (0.801 g, 2 mmol), ascorbic acid (0.141 g, 0.8 mmol), and CuSO<sub>4</sub> (0.100 g, 0.4 mmol) in 20 mL of water according to the general procedure. The product was isolated on a glass frit as a white solid (1.101 g, 71.2 %).

Alternatively, prepared from glucosyl azide **3** (0.668 g, 1.79 mmol), alkyne **29** (0.716 g, 1.79 mmol), ascorbic acid (0.126g, 0.72 mmol), and CuSO<sub>4</sub> (0.090 g, 0.358 mmol) in 15 mL water according to general procedure. After extraction, the product was obtained as a white solid (1.29 g, 95.5%).

<sup>1</sup>H NMR (CDCl<sub>3</sub>): δ 1.89 (s, 3H, COCH<sub>3</sub>), 1.99 (s, 3H, COCH<sub>3</sub>), 2.01 (s, 3H, COCH<sub>3</sub>), 2.04 (s, 6H, 2 x COCH<sub>3</sub>), 2.08 (s, 3H, COCH<sub>3</sub>), 2.10 (s, 3H, COCH<sub>3</sub>), 2.12 (s, 3H, COCH<sub>3</sub>), 4.01 (ddd, 1H, H-5<sub>glucose</sub>, *J* = 2.3, 4.9, 10.1 Hz), 4.14 (dd, 1H, H-6<sub>glucose</sub>, *J* = 2.2, 12.9 Hz), 4.20 (d, 1H, H-5<sub>glucuronic acid</sub>, *J* = 9.7 Hz), 4.29 (dd, 1H, H-6<sub>glucose</sub>, *J* = 4.9, 12.6 Hz), 5.11 (m, 8H, H-2<sub>glucose</sub>, H-2<sub>glucuronic acid</sub>, H-3<sub>glucose</sub>, H-3<sub>glucuronic acid</sub>, H-4<sub>glucose</sub>, H-4<sub>glucuronic acid</sub>, OCH<sub>2</sub>), 5.76 (d, 1H, H-1<sub>glucuronic acid</sub>, *J* = 7.7 Hz), 5.88 (d, 1H, H-1<sub>glucose</sub>, *J* = 9.0 Hz), 7.89 (s, 1H, H-triazole).

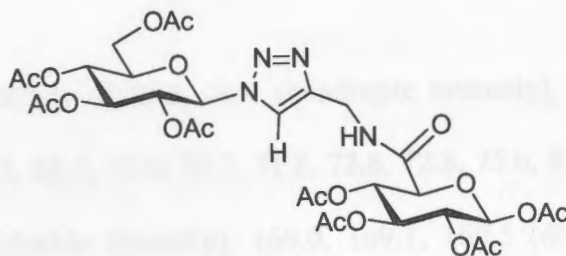
$^{13}\text{C}$  NMR ( $\text{CDCl}_3$ ):  $\delta$  21.4, 21.7, 21.8 (quadruple intensity), 21.9, 22.0, 59.9, 62.6, 68.7, 69.8, 71.2, 71.3, 72.9, 73.7, 73.8, 76.2, 86.8, 92.3, 124.0, 143.0, 167.2, 169.8, 170.1, 170.2, 170.5, 170.7, 170.8, 171.4.

HRMS:  $m/z$  calculated 796.2025 (+Na)  $m/z$  found 796.2031 (+Na)

Melting Point: 204-208 °C

$[\alpha]_D -5.8^\circ$  (c. 1.0,  $\text{CH}_2\text{Cl}_2$ )

### Formation of 1,4-disubstituted 1,2,3-triazole 40.



Prepared from glucosyl azide **3** (0.747 g, 2 mmol), alkyne **30** (0.798 g, 2 mmol), ascorbic acid (0.141 g, 0.8 mmol), and  $\text{CuSO}_4$  (0.100 g, 0.4 mmol) in 20 mL of water according to the general procedure. The product was isolated on a glass frit as an off-white solid (1.250 g, 80.9%).

Alternatively, prepared from glucosyl azide (0.844 g, 2.26 mmol), alkyne (0.900 g, 2.26 mmol), ascorbic acid (0.159 g, 0.90 mmol), and  $\text{CuSO}_4$  (0.113 g, 0.45 mmol) in 20 mL water according to general procedure. After extraction, the product was obtained as a white solid (1.59 g, 91.4%).

$^1\text{H}$  NMR ( $\text{CDCl}_3$ ):  $\delta$  1.88 (s, 3H,  $\text{COCH}_3$ ), 2.02 (s, 3H,  $\text{COCH}_3$ ), 2.03 (s, 3H,  $\text{COCH}_3$ ), 2.04 (s, 3H,  $\text{COCH}_3$ ), 2.07 (s, 3H,  $\text{COCH}_3$ ), 2.10 (s, 3H,  $\text{COCH}_3$ ), 2.13 (s, 3H,  $\text{COCH}_3$ ), 3.98 (m, 1H, H-5<sub>glucose</sub>), 4.10 (d, 1H, H-5<sub>glucuronic acid</sub>,  $J = 9.7$  Hz), 4.16 (m, 1H, H-6<sub>glucose</sub>), 4.30 (dd, 1H, H-6'<sub>glucose</sub>,  $J = 4.9, 12.5$  Hz), 4.46 (dd, 1H,  $\text{CH}_2$ ,  $J = 5.7, 15.2$  Hz), 4.59 (dd, 1H,  $\text{CH}_2$ ,  $J = 6.2, 15.6$  Hz), 5.10 (t, 1H, H-2<sub>glucuronic acid</sub>,  $J = 8.7$  Hz), 5.19 (t, 1H, H-4<sub>glucuronic acid</sub>,  $J = 9.6$  Hz), 5.26 (t, 1H, H-4<sub>glucose</sub>,  $J = 9.5$  Hz), 5.31 (t, 1H, H-3<sub>glucuronic acid</sub>,  $J = 9.3$  Hz), 5.41 (t, 1H, H-3<sub>glucose</sub>,  $J = 9.3$  Hz), 5.47 (t, 1H, H-2<sub>glucose</sub>,  $J = 9.3$  Hz), 5.75 (d, 1H, H-1<sub>glucuronic acid</sub>,  $J = 8.1$  Hz), 5.85 (d, 1H, H-1<sub>glucose</sub>,  $J = 9.0$  Hz), 6.89 (t, 1H, N-H,  $J = 6.0$  Hz), 7.82 (s, 1H, triazole-H).

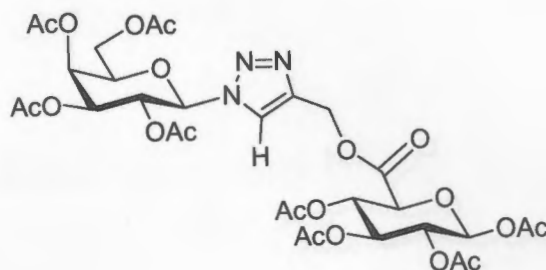
$^{13}\text{C}$  NMR ( $\text{CDCl}_3$ ):  $\delta$  20.3, 20.6 (quadruple intensity), 20.8 (triple intensity), 34.6, 61.5, 67.5, 68.7, 70.0, 70.2, 71.8, 72.6, 72.8, 75.0, 85.6, 91.1, 121.1, 144.7, 165.8, 168.5 (double intensity), 169.0, 169.1, 169.5 (double intensity), 169.7, 170.27.

Low resolution MS:  $m/z$  calculated 772.229  $m/z$  found 773.4 ( $M + 1$ )

Melting Point: 221-224 °C

$[\alpha]_{\text{D}} -9.4^\circ$  (c. 1.0,  $\text{CH}_2\text{Cl}_2$ )

### Formation of 1,4-disubstituted 1,2,3-triazole 41.



Prepared from galactosyl azide **36** (0.373 g, 1 mmol) and alkyne **29** (0.400 g, 1 mmol) in 10 mL of water according to general procedure. After extraction, the product was obtained as a white solid (0.696 g, 90 %).

$^1\text{H NMR}$  ( $\text{CDCl}_3$ ):  $\delta$  1.90 (s, 3H,  $\text{COCH}_3$ ), 2.005 (s, 3H,  $\text{COCH}_3$ ), 2.011 (s, 3H,  $\text{COCH}_3$ ), 2.02 (s, 3H,  $\text{COCH}_3$ ), 2.04 (s, 3H,  $\text{COCH}_3$ ), 2.05 (s, 3H,  $\text{COCH}_3$ ), 2.12 (s, 3H,  $\text{COCH}_3$ ), 2.24 (s, 3H,  $\text{COCH}_3$ ), 4.13-4.24 (m, 4H), 5.12-5.33 (m, 6H), 5.53-5.58 (m, 2H), 5.77 (d, 1H, H-1<sub>glucuronic acid</sub>,  $J = 7.7$  Hz), 5.86 (d, 1H, H-1<sub>galactose</sub>,  $J = 9.3$  Hz), 7.95 (s, 1H, triazole-H).

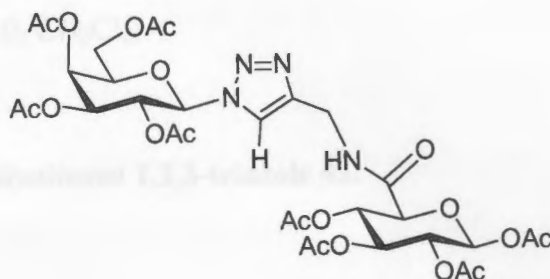
$^{13}\text{C NMR}$  ( $\text{CDCl}_3$ ):  $\delta$  20.3, 20.49, 20.54, 20.6 (double intensity), 20.69, 20.72, 20.8, 58.7, 61.2, 66.8, 67.7, 68.6, 70.0, 70.7, 71.7, 72.5, 73.9, 86.1, 91.1, 123.0, 141.8, 166.1, 168.5, 168.7, 168.9, 169.1, 169.49, 169.52, 169.7, 170.0.

Low resolution MS:  $m/z$  calculated 773.213 (+Na)  $m/z$  found 774.3 (+Na)

Melting Point: 171-172 °C

$[\alpha]_{\text{D}} +3.2^\circ$  (c. 1.0,  $\text{CH}_2\text{Cl}_2$ )

### Formation of 1,4-disubstituted 1,2,3-triazole 42.



Prepared from galactosyl azide **36** (0.373 g, 1 mmol) and alkyne **30** (0.400 g, 1 mmol) in 10 mL of water according to general procedure. After extraction, the product was obtained as a white solid (0.71 g, 92%).

$^1\text{H}$  NMR ( $\text{CDCl}_3$ ):  $\delta$  1.89 (s, 3H,  $\text{COCH}_3$ ), 2.007 (s, 3H,  $\text{COCH}_3$ ), 2.013 (s, 3H,  $\text{COCH}_3$ ), 2.04 (s, 3H,  $\text{COCH}_3$ ), 2.05 (s, 3H,  $\text{COCH}_3$ ), 2.10 (s, 3H,  $\text{COCH}_3$ ), 2.12 (s, 3H,  $\text{COCH}_3$ ), 2.23 (s, 3H,  $\text{COCH}_3$ ), 4.12 (d, 1H, H-5<sub>glucuronic acid</sub>,  $J = 7.3$  Hz), 4.13-4.25 (m, 3H), 4.48 (dd, 1H,  $\text{CH}_2$ ,  $J = 5.7, 15.4$  Hz), 4.57 (dd, 1H,  $\text{CH}_2$ ,  $J = 6.0, 15.4$  Hz), 5.11 (dd, 1H,  $J = 8.1, 9.2$  Hz), 5.20 (t, 1H,  $J = 9.5$  Hz), 5.25 (dd, 1H,  $J = 3.3, 10.3$  Hz), 5.29 (t, 1H,  $J = 8.6$  Hz), 5.31 (t, 1H,  $J = 9.2$  Hz), 5.54-5.59, (m, 2H), 5.76 (d, 1H, H-1<sub>glucuronic acid</sub>,  $J = 8.1$  Hz), 5.83 (d, 1H, H-1<sub>galactose</sub>,  $J = 9.3$  Hz), 6.98 (t, 1H, N-H,  $J = 5.9$  Hz), 7.86 (s, 1H, triazole-H).

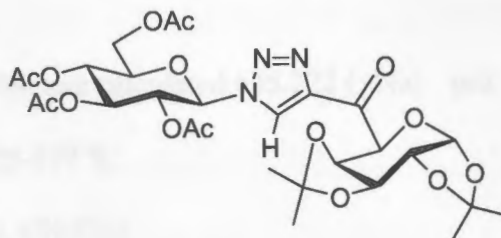
$^{13}\text{C}$  NMR ( $\text{CDCl}_3$ ):  $\delta$  20.2, 20.52 (double intensity), 20.54, 20.6, 20.65, 20.69, 20.74, 34.5, 61.2, 66.8, 67.8, 68.7, 70.0, 70.7, 71.8, 72.8, 73.8, 86.0, 91.1, 121.1, 144.4, 165.8, 168.5, 168.6, 168.9, 169.3, 169.46, 169.52, 169.7, 170.0.

Low resolution MS:  $m/z$  calculated 772.229 (+Na)  $m/z$  found 773.3 (+Na)

Melting Point: 220-222 °C

$[\alpha]_D^{+2.1^\circ}$  (c. 1.0, CH<sub>2</sub>Cl<sub>2</sub>)

### Formation of 1,4-disubstituted 1,2,3-triazole 43.



In a 50 mL two-neck round bottom flask equipped with a reflux condenser, thermometer, and magnetic stir bar, glucosyl azide (0.373 g, 1.0 mmol) and alkynyl ketone (0.282 g, 1.0 mmol) were suspended in 8 mL of *t*-BuOH and water (1:1). Ascorbic acid (0.070 g, 0.4 mmol) and CuSO<sub>4</sub> (0.050 g, 0.2 mmol), each in 1 mL water, were added and the suspension was heated to 60 °C. The reaction mixture clears after 30 minutes and the reaction was stirred for one and a half hours after which time TLC showed complete consumption of the starting materials. After cooling to room temperature, water (50 mL) was added and the mixture was extracted with methylene chloride (3 x 30 mL). The combined extracts were dried over anhydrous magnesium sulfate, filtered, then reduced to a yellow syrup. Flash column chromatography (1:1, hexanes:ethyl acetate) gave the title compound as a white solid (0.51 g, 77.9 %).

<sup>1</sup>H NMR (CDCl<sub>3</sub>):  $\delta$  1.27 (s, 3H, CH<sub>3</sub>), 1.37 (s, 3H, CH<sub>3</sub>), 1.43 (s, 3H, CH<sub>3</sub>), 1.58 (s, 3H, CH<sub>3</sub>), 1.90 (s, 3H, COCH<sub>3</sub>), 2.04 (s, 3H, COCH<sub>3</sub>), 2.08 (s, 3H, COCH<sub>3</sub>),



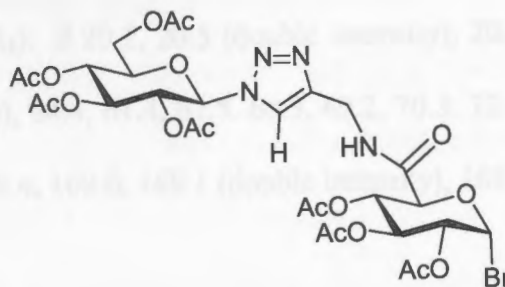
2.10 (s, 3H, COCH<sub>3</sub>), 4.05 (ddd, 1H, H-5<sub>glucose</sub>,  $J = 2.3, 4.9, 10.2$  Hz), 4.15 (m, 1H, H-6<sub>glucose</sub>), 4.31 (dd, 1H, H-6'<sub>glucose</sub>,  $J = 4.9, 12.6$  Hz), 4.45 (dd, 1H, H-galactose,  $J = 2.6, 5.1$  Hz), 4.72 (dd, 1H,  $J = 2.6, 7.7$  Hz), 5.01 (dd, 1H,  $J = 2.3, 7.8$  Hz), 5.24 (d, 1H, H-5<sub>galactose</sub>,  $J = 2.4$  Hz), 5.27 (t, 1H, H-2<sub>glucose</sub>,  $J = 9.8$  Hz), 5.44 (t, 1H, H-3<sub>glucose</sub>,  $J = 9.4$  Hz), 5.55 (t, 1H, H-4<sub>glucose</sub>,  $J = 9.4$  Hz), 5.78 (d, 1H, H-1<sub>galactose</sub>,  $J = 5.1$  Hz), 5.95 (d, 1H, H-1<sub>glucose</sub>,  $J = 9.2$  Hz), 8.49 (s, 1H, triazole-H).

Low resolution MS:  $m/z$  calculated 655.222 (+Na)  $m/z$  found 656.3 (+Na)

Melting Point: 175-177 °C

$[\alpha]_D -63.3^\circ$  (c. 1.0, CH<sub>2</sub>Cl<sub>2</sub>)

#### Bromination of triazole 40 to form bromide 44.



In a 100 mL flame-dried round bottom flask equipped with a magnetic stir bar and rubber septum, triazole-linked dimer **40** (0.750 g, 0.97 mmol) was dissolved in 8 mL of 33% HBr/AcOH. The brown solution was allowed to stir for two hours when TLC (5% MeOH in toluene) showed consumption of starting material. The reaction mixture was transferred to a larger vessel, diluted with chloroform (50 mL) and neutralized by slow

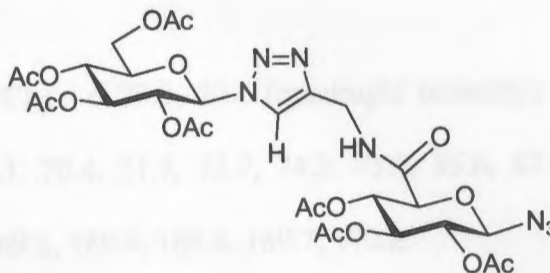
addition of saturated sodium bicarbonate. The mixture was extracted with chloroform (3 x 30 mL), the extracts washed with water (100 mL), dried over magnesium sulfate, filtered, and reduced to a tan foam (0.71 g, 92.2%).

$^1\text{H}$  NMR ( $\text{CDCl}_3$ ):  $\delta$  1.88 (s, 3H,  $\text{COCH}_3$ ), 2.03 (s, 3H,  $\text{COCH}_3$ ), 2.04 (s, 3H,  $\text{COCH}_3$ ), 2.07 (s, 3H,  $\text{COCH}_3$ ), 2.08 (s, 3H,  $\text{COCH}_3$ ), 2.09 (s, 3H,  $\text{COCH}_3$ ), 2.10 (s, 3H,  $\text{COCH}_3$ ), 4.02 (ddd, 1H, H-5<sub>glucose</sub>,  $J = 2.4, 4.9, 10.2$  Hz), 4.16 (dd, 1H, H-6<sub>glucose</sub>,  $J = 2.0, 12.6$  Hz), 4.31 (dd, 1H, H-6'<sub>glucose</sub>,  $J = 4.9, 12.6$  Hz), 4.47 (dd, 1H,  $\text{CH}_2$ ,  $J = 5.6, 15.3$  Hz), 4.51 (d, 1H, H-5<sub>glucuronic acid</sub>,  $J = 10.3$  Hz), 4.59 (dd, 1H,  $\text{CH}_2$ ,  $J = 6.0, 15.4$  Hz), 4.83 (dd, 1H, H-2<sub>glucuronic acid</sub>,  $J = 4.1, 10.0$  Hz), 5.21 (dd, 1H,  $J = 9.5, 10.3$  Hz), 5.26 (m, 1H), 5.40 (m, 2H), 5.61 (t, 1H,  $J = 9.8$  Hz), 5.89 (m, 1H, H-1<sub>glucose</sub>), 6.64 (d, 1H, H-1<sub>glucuronic acid</sub>,  $J = 4.0$  Hz), 7.16 (t, 1H, N-H,  $J = 5.7$  Hz), 7.82 (s, 1H, triazole-H).

$^{13}\text{C}$  NMR ( $\text{CDCl}_3$ ):  $\delta$  20.2, 20.5 (double intensity), 20.6 (double intensity), 20.7 (double intensity), 34.4, 61.4, 67.5, 68.3, 69.2, 70.3, 72.4, 72.5, 84.9, 85.4, 121.4, 144.4, 165.8, 168.4, 169.0, 169.1 (double intensity), 169.5, 169.6, 170.2.

$[\alpha]_{\text{D}} +71.2^\circ$  (c. 1.0,  $\text{CH}_2\text{Cl}_2$ )

**Azidation of bromide 44 to form azide 45 via S<sub>N</sub>2 reaction.**



Bromide 44 (0.68 g, 0.86 mmol) was dissolved in dry DMF (8 mL) in a 100 mL flame-dried round bottom flask equipped with a magnetic stir bar and rubber septum. Sodium azide (0.250, 3.85 mmol) was added and the orange solution was allowed to stir for 6 hours. The DMF was removed *in vacuo* and the crude mixture was partitioned between water and methylene chloride (50 mL each). The organic layer was drained and the aqueous layer was extracted with methylene chloride (2 x 50 mL). The combined extracts were washed with large volumes of water (3 x 150 mL), dried over anhydrous magnesium sulfate, filtered, and reduced to a white foamy solid (0.53 g, 81.5%).

<sup>1</sup>H NMR (CDCl<sub>3</sub>): δ 1.87 (s, 3H, COCH<sub>3</sub>), 2.02 (s, 3H, COCH<sub>3</sub>), 2.03 (s, 3H, COCH<sub>3</sub>), 2.07 (s, 3H, COCH<sub>3</sub>), 2.08 (s, 3H, COCH<sub>3</sub>), 2.09 (s, 6H, 2 x COCH<sub>3</sub>), 4.04 (ddd, 1H, H-5<sub>glucose</sub>, *J* = 2.4, 4.9, 10.1 Hz), 4.09 (d, 1H, H-5<sub>glucuronic acid</sub>, *J* = 9.9 Hz), 4.17 (dd, 1H, H-6<sub>glucose</sub>, *J* = 2.1, 12.5 Hz), 4.31 (dd, 1H, H-6'<sub>glucose</sub>, *J* = 4.9, 12.6 Hz), 4.50 (dd, 1H, CH<sub>2</sub>, *J* = 5.9, 15.4 Hz), 4.61 (dd, 1H, CH<sub>2</sub>, *J* = 6.0, 15.5 Hz), 4.77 (d, 1H, H-1<sub>glucuronic acid</sub>, *J* = 8.8 Hz), 4.94 (t, 1H, *J* = 9.2 Hz), 5.17 (t, 1H, *J* = 9.7 Hz), 5.25 (m, 2H), 5.43 (t, 1H, *J* = 9.4 Hz), 5.48 (t, 1H, *J* = 9.3 Hz),

5.90 (d, 1H, H-1,  $J = 9.0$  Hz), 7.23 (t, 1H, N-H,  $J = 6.0$  Hz), 7.87 (s, 1H, triazole-H).

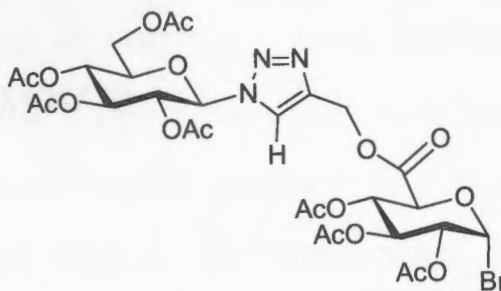
$^{13}\text{C}$  NMR ( $\text{CDCl}_3$ ):  $\delta$  20.3, 20.6 (quadruple intensity), 20.7, 20.8, 34.7, 61.6, 67.6, 68.9, 70.3, 70.4, 71.7, 72.7, 74.2, 75.0, 85.6, 87.9, 121.1, 144.7, 165.8, 168.5, 168.9, 169.1, 169.4, 169.6, 169.7, 170.2.

Low resolution MS:  $m/z$  calculated 778.214 (+Na)  $m/z$  found 778.4 (+Na)

Melting Point: 193 °C decomposition

$[\alpha]_{\text{D}} -19.7^\circ$  (c. 1.0,  $\text{CH}_2\text{Cl}_2$ )

### Bromination of triazole 39 to form bromide 46.



In a 100 mL flame-dried round bottom flask equipped with a magnetic stir bar and rubber septum, triazole-linked dimer **39** (1.81 g, 2.34 mmol) was dissolved in 10 mL of 33% HBr/AcOH. The brown solution was allowed to stir for two hours when TLC (5% MeOH in toluene) showed consumption of starting material. The reaction mixture was transferred to a larger vessel, diluted with chloroform (50 mL), and neutralized by slow addition of saturated sodium bicarbonate. The mixture was extracted with chloroform (3

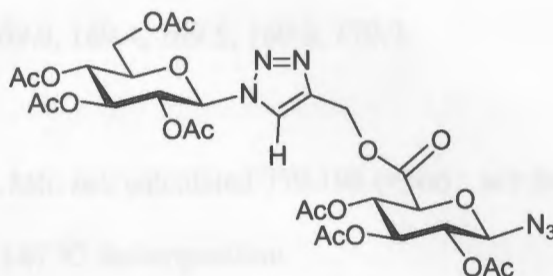
x 30 mL), the extracts washed with water (100 mL), dried over magnesium sulfate, filtered, and reduced to a tan foam (1.83 g, 98 %).

$^1\text{H}$  NMR ( $\text{CDCl}_3$ ):  $\delta$  1.89 (s, 3H,  $\text{COCH}_3$ ), 2.00 (s, 3H,  $\text{COCH}_3$ ), 2.03 (s, 3H,  $\text{COCH}_3$ ), 2.04 (s, 3H,  $\text{COCH}_3$ ), 2.07 (s, 3H,  $\text{COCH}_3$ ), 2.09 (s, 6H, 2 x  $\text{COCH}_3$ ), 4.01 (ddd, 1H, H-1<sub>glucose</sub>,  $J = 2.3, 5.0, 10.0$  Hz), 4.16 (dd, 1H, H-6<sub>glucose</sub>,  $J = 2.2, 12.6$  Hz), 4.31 (dd, 1H, H-6'<sub>glucose</sub>,  $J = 4.9, 12.6$  Hz), 4.60 (d, 1H, H-5<sub>glucuronic acid</sub>,  $J = 10.3$  Hz), 4.85 (dd, 1H, H-2<sub>glucuronic acid</sub>,  $J = 4.0, 10.1$  Hz), 5.19-5.27 (m, 4H), 5.40 (m, 2H), 5.60 (m, 1H), 5.88 (m, 1H), 6.63 (d, 1H, 1H<sub>glucuronic acid</sub>,  $J = 4.0$  Hz), 7.89 (s, 1H, triazole-H).

$^{13}\text{C}$  NMR ( $\text{CDCl}_3$ ):  $\delta$  20.2, 20.4, 20.5, 20.6 (triple intensity), 20.7, 58.8, 61.4, 67.5, 68.2, 69.2, 70.1 (double intensity), 71.8, 72.5, 75.0, 85.2, 85.6, 122.7, 141.8, 165.8, 168.6, 169.00, 169.2 (double intensity), 169.3, 169.6, 170.1.

$[\alpha]_{\text{D}}^{+72.0^\circ}$  (c. 1.0,  $\text{CH}_2\text{Cl}_2$ )

**Azidation of bromide 46 to form azide 47 via S<sub>N</sub>2 reaction.**



Bromide **46** (1.00 g, 1.26 mmol) was dissolved in dry DMF (10 mL) in a 100 mL flame-dried round bottom flask equipped with a magnetic stir bar and rubber septum. Sodium azide (0.400, 6.15 mmol) was added and the purple solution was allowed to stir for 2 hours after which TLC (6% MeOH in toluene) showed consumption of starting material. The DMF was removed *in vacuo* and the crude mixture was partitioned between water and methylene chloride (50 mL each). The organic layer was drained and the aqueous layer was extracted with methylene chloride (2 x 50 mL). The combined extracts were washed with large volumes of water (3 x 150 mL), dried over anhydrous magnesium sulfate, filtered, and reduced to a white foamy solid. Flash column chromatography (2% MeOH in chloroform) yielded the azide as a glassy solid (0.73 g, 76.7 %).

<sup>1</sup>H NMR (CDCl<sub>3</sub>): δ 1.89 (s, 3H, COCH<sub>3</sub>), 1.98 (s, 3H, COCH<sub>3</sub>), 2.01 (s, 3H, COCH<sub>3</sub>), 2.04 (s, 3H, COCH<sub>3</sub>), 2.08 (s, 6H, 2 x COCH<sub>3</sub>), 2.09 (s, 3H, COCH<sub>3</sub>), 4.02 (ddd, 1H, H-5<sub>glucose</sub>, *J* = 2.3, 4.8, 10.1 Hz), 4.15-4.18 (m, 2H, H-5<sub>glucuronic acid</sub>, H-6<sub>glucose</sub>), 4.31 (dd, 1H, H-6' <sub>glucose</sub>, *J* = 5.0, 12.7 Hz), 4.72 (d, 1H, H-1<sub>glucuronic acid</sub>, *J* = 8.6 Hz), 4.96 (t, 1H, *J* = 9.0 Hz), 5.20 (t, 1H, *J* = 9.5 Hz), 5.23-5.34 (m, 4H), 5.41-5.46 (m, 3H), 5.90 (d, 1H, H-1<sub>glucose</sub>, *J* = 9.0 Hz), 7.92 (s, 1H, triazole-H).

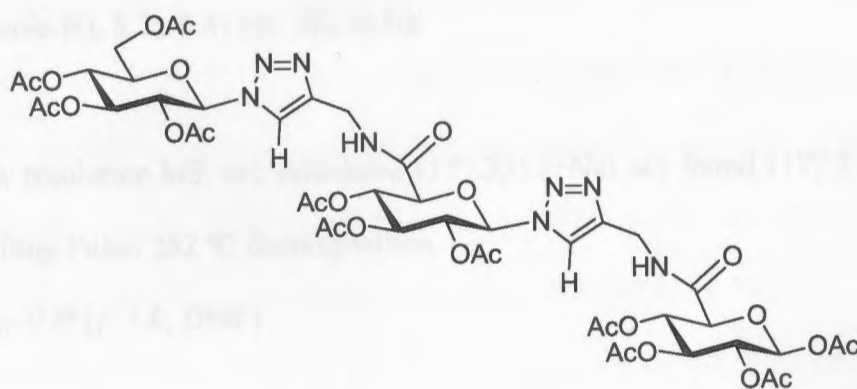
$^{13}\text{C}$  NMR ( $\text{CDCl}_3$ ):  $\delta$  20.2, 20.46, 20.6 (quadruple intensity), 20.7, 58.7, 61.4, 67.5, 68.7, 70.1, 70.2, 71.7, 72.5, 73.7, 75.0, 85.5, 87.8, 122.8, 141.9, 165.7, 168.5, 168.8, 169.0, 169.4, 169.5, 169.6, 170.2.

Low resolution MS:  $m/z$  calculated 779.198 (+Na)  $m/z$  found 778.4 (+Na)

Melting Point: 147 °C decomposition

$[\alpha]_D^{20}$  -25.5 (c. 1.0,  $\text{CH}_2\text{Cl}_2$ )

### Formation of triazole-linked carbohydrate trimer from azide **45** and alkyne **30**.



Azide **45** (0.200 g, 0.265 mmol), alkyne **30** (0.116 g, 0.292 mmol),  $\text{Cu}(\text{PPh}_3)_3\text{Br}$  (0.049 g, 0.53 mmol), and diisopropylethylamine (0.138 mL, 0.795 mmol) were dissolved in 5 mL dry dichloroethane in a two-neck 50 mL roundbottom flask equipped with a thermometer and magnetic stir bar. The orange solution was heated to 60 °C and stirred for one hour after which time TLC analysis showed consumption of the azide starting material. The solution was cooled and the solvent was removed *in vacuo*. Methanol was added (50 mL) and the resulting suspension was heated to boiling. After cooling to room



temperature, the methanol was decanted. The addition of methanol followed by decantation was repeated (2 x 50 mL). The residual methanol was removed *in vacuo* to give the product as a white solid (0.165 g, 54%).

$^1\text{H NMR}$  (DMSO- $d_6$ ):  $\delta$  1.83 (s, 3H, COCH<sub>3</sub>), 1.85 (s, 3H, COCH<sub>3</sub>), 1.95 (s, 3H, COCH<sub>3</sub>), 2.00 (s, 6H, 2 x COCH<sub>3</sub>), 2.02 (s, 6H, 2 x COCH<sub>3</sub>), 2.057 (s, 3H, COCH<sub>3</sub>), 2.062 (s, 3H, COCH<sub>3</sub>), 2.08 (s, 3H, COCH<sub>3</sub>), 2.12 (s, 3H, COCH<sub>3</sub>), 4.10 (m, 1H), 4.18 (m, 1H), 4.26-4.43 (m, 6H), 4.55 (d, 1H,  $J = 9.89$  Hz), 5.03 (dd, 1H,  $J = 8.5, 9.6$  Hz), 5.16 (t, 1H,  $J = 9.7$ ), 5.21 (t, 1H,  $J = 9.7$ ), 5.37 (t, 1H,  $J = 9.5$  Hz), 5.50 (t, 1H,  $J = 9.6$  Hz), 5.57-5.68 (m, 4H), 6.02 (d, 1H,  $J = 8.2$  Hz), 6.37 (d, 1H,  $J = 9.0$  Hz), 6.42 (d, 1H,  $J = 8.8$  Hz), 8.18 (s, 1H, triazole-H), 8.24 (s, 1H, triazole-H), 8.76-8.81 (m, 2H, N-H).

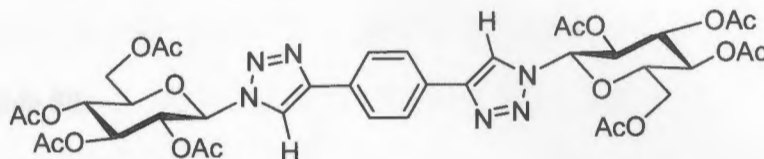
Low resolution MS:  $m/z$  calculated 1177.331 (+Na)  $m/z$  found 1177.7 (+Na)

Melting Point: 252 °C decomposition

$[\alpha]_D -9.8^\circ$  (c. 1.0, DMF)

## Formation of triazole-linked carbohydrate dimers around diethynyl benzene core.

### Divalent triazole 49.



In a 100 mL two-neck round bottom flask equipped with a reflux condenser, thermometer, and magnetic stir bar, glucosyl azide (0.747 g, 2.0 mmol), 1,4-diethynyl benzene (0.126 g, 1.0 mmol), ascorbic acid (0.141, 0.8 mmol), and  $\text{CuSO}_4$  (0.100g, 0.4 mmol) were suspended in 10 mL of *t*-BuOH and water (1:1). The orange suspension was stirred vigorously at 60 °C for three hours after which time TLC analysis showed consumption of starting material. The mixture was cooled to room temperature and the *t*-BuOH removed *in vacuo*. Cold water (50 mL) was added and the precipitate was filtered over a glass frit to yield the product as an orange solid (0.692 g, 79.3%).

$^1\text{H}$  NMR ( $\text{CDCl}_3$ ):  $\delta$  1.91 (s, 6H, 2 x  $\text{COCH}_3$ ), 2.06 (s, 6H, 2 x  $\text{COCH}_3$ ), 2.09 (s, 6H, 2 x  $\text{COCH}_3$ ), 2.10 (s, 6H, 2 x  $\text{COCH}_3$ ), 4.06 (ddd, 2H, H-5,  $J = 2.3, 4.9, 10.1$  Hz), 4.17 (dd, 2H, H-6,  $J = 2.0, 12.6$  Hz), 4.35 (dd, 2H, H-6',  $J = 5.0, 12.7$  Hz), 5.30 (t, 2H, H-2,  $J = 9.8$  Hz), 5.47 (t, 2H, H-3,  $J = 9.4$  Hz), 5.56 (t, 2H, H-4,  $J = 9.4$  Hz), 5.97 (d, 2H, H-1,  $J = 9.3$  Hz), 7.93 (s, 4H, Ar-H), 8.09 (s, 2H, triazole-H).

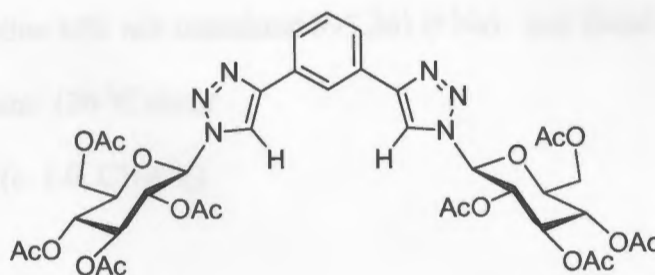
$^{13}\text{C}$  NMR ( $\text{CDCl}_3$ ):  $\delta$  20.4, 20.6, 20.7, 20.8, 61.2, 66.9, 67.7, 70.7, 74.0, 86.2, 117.9, 126.1 (double intensity), 129.8, 147.6, 168.9, 169.5, 169.7, 170.1.

Low resolution MS:  $m/z$  calculated 895.261(+Na)  $m/z$  found 895.6 (M + 1)

Melting Point: 310 °C decomposition

$[\alpha]_D -74.3^\circ$  (c. 1.0, CH<sub>2</sub>Cl<sub>2</sub>)

### Divalent triazole 50.



In a 100 mL two-neck round bottom flask equipped with a reflux condenser, thermometer, and magnetic stir bar, glucosyl azide **3** (1.493 g, 4.0 mmol), 1,3-diethynyl benzene (0.266 mL, 2.0 mmol), ascorbic acid (0.282 g, 1.6 mmol), and CuSO<sub>4</sub> (0.200 g, 0.8 mmol) were suspended in 25 mL of *t*-BuOH and water (1:1). The yellow suspension was stirred vigorously at 60 °C overnight after which the mixture was cooled to room temperature and the *t*-BuOH removed *in vacuo*. Cold water (50 mL) was added and the precipitate was filtered over a glass frit to yield the product as a yellow solid (1.52 g, 87.1%).

<sup>1</sup>H NMR (CDCl<sub>3</sub>):  $\delta$  1.91 (s, 6H, 2 x COCH<sub>3</sub>), 2.06 (s, 6H, 2 x COCH<sub>3</sub>), 2.09 (s, 6H, 2 x COCH<sub>3</sub>), 2.11 (s, 6H, 2 x COCH<sub>3</sub>), 4.11 (ddd, 2H, H-5,  $J = 2.3, 4.9, 10.1$  Hz), 4.19 (dd, 2H, H-6,  $J = 2.0, 12.6$  Hz), 4.37 (dd, 2H, H-6',  $J = 4.9, 12.7$  Hz), 5.33 (t, 2H, H-2,  $J = 9.7$  Hz), 5.49 (t, 2H, H-3,  $J = 9.3$  Hz), 5.57 (t, 2H, H-4,  $J =$

9.4 Hz), 6.01 (d, 2H, H-1,  $J = 9.2$  Hz), 7.49 (t, 1H, Ar-H,  $J = 7.78$  Hz), 7.84 (dd, 2H, Ar-H,  $J = 1.7, 7.9$  Hz), 8.29 (t, 1H, Ar-H,  $J = 1.6$  Hz).

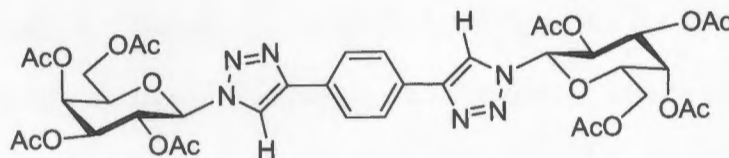
$^{13}\text{C}$  NMR ( $\text{CDCl}_3$ ):  $\delta$  20.3, 20.6 (double intensity), 20.3, 61.5, 67.6, 70.2, 72.6, 75.0, 85.7, 118.1, 122.9, 125.7, 129.3, 130.3, 147.7, 168.7, 169.1, 169.6, 170.3.

Low resolution MS:  $m/z$  calculated 895.261 (+Na)  $m/z$  found 895.5 (+Na)

Melting Point: 130 °C sinter

$[\alpha]_{\text{D}} -70.0^\circ$  (c. 1.0,  $\text{CH}_2\text{Cl}_2$ )

### Divalent triazole 51.



In a 50 mL two-neck round bottom flask equipped with a reflux condenser, thermometer, and magnetic stir bar, glucosyl azide **36** (0.747 g, 2.0 mmol), 1,4-diethynyl benzene (0.126 g, 1.0 mmol), ascorbic acid (0.141 g, 0.8 mmol), and  $\text{CuSO}_4$  (0.100 g, 0.4 mmol) were suspended in 10 mL of *t*-BuOH and water (1:1). The orange suspension was stirred vigorously at 60 °C overnight after which the mixture was cooled to room temperature and the *t*-BuOH removed *in vacuo*. Cold water (50 mL) was added and the precipitate was filtered over a glass frit to yield the product as a pale yellow solid (0.873 g, 87.1%).

<sup>1</sup>H NMR (CDCl<sub>3</sub>): δ 1.93 (s, 6H, 2 x COCH<sub>3</sub>), 2.04 (s, 6H, 2 x COCH<sub>3</sub>), 2.06 (s, 6H, 2 x COCH<sub>3</sub>), 2.27 (s, 6H, 2 x COCH<sub>3</sub>), 4.17-4.33 (m, 6H, H-5, H-6, H-6'), 5.32 (m, 2H), 5.59 (m, 2H), 5.66 (t, 2H, *J* = 9.8 Hz), 5.95 (d, 2H, H-1, *J* = 9.3 Hz), 7.95 (s, 4H, Ar-H), 8.13 (s, 2H, triazole-H).

*Chem. Ind. Ed.* 1996, 37, 2503-2505.

Low resolution MS: *m/z* calculated 895.261 (+Na) *m/z* found 895.5 (+Na)

Melting Point: 232 °C decomposition

[α]<sub>D</sub> -66.4° (c. 1.0, CH<sub>2</sub>Cl<sub>2</sub>)

Oxford University Press: New York, 2001.

5. Bertozzi, C. R.; Klasing, L. L. *Science* 1991, 257, 2207-2210.

6. Imperiali, B.; O'Connor, B. E. *Carb. Opin. Chem. Biol.* 1999, 3, 613.

7. He, Y.; Hsieh, R. J.; Cheng, J.; Klasing, L. L. *Org. Lett.* 2004, 6, 6479-6482.

8. Györgyósk, Z.; Hódy, Z.; Földes, K.; Károlyi, A.; Nagy, V.; Tóth, M.; Bencsik, A.; Dóczi, T.; Gergely, P.; Székely, L. *Europ. Med. Chem.* 2004, 39, 4861-4870.

9. Bianchi, A.; Rossi, A.; Bernardi, A. *Tetrahedron - Asymmetry* 2005, 16, 383-386.

10. Taylor, C. M. *Tetrahedron* 1998, 54, 11317-11362.

11. Kovács, L.; Ott, E.; Domokos, V.; Holzer, W.; Györgyósk, Z. *Tetrahedron* 2001, 57, 4609-4621.

12. Bollinger, F.; Maudet, V.; Laffont, D. *Carbohydr. Res.* 2000, 324, 99-106.

13. Danko, F.; Dellweg, P. *J. Am. Chem. Soc.* 2003, 125, 4426-4429.

14. Giese, B.; Armstrong, J. L.; Bertozzi, C. R. *Org. Lett.* 2000, 3, 2141-2143.

## References

1. Davis, B.; Fairbanks, A. *Carbohydrate Chemistry*, Oxford University Press: New York, 2002.
2. Wunberg, T.; Kallus, C.; Opatz, T.; Henke, S.; Schmidt, W. Kunz, H. *Angew. Chem. Int. Ed.* **1998**, *37*, 2503-2505.
3. Fügedi, P.; Pető, C. J.; Wang, L. *9th European Carbohydrate Symposium*, Utrecht, Netherlands, **1997**, pp. A113-A114.
4. Osborn, H.; Khan, T. *Oligosaccharides: Their synthesis and biological roles*, Oxford University Press: New York, 2000.
5. Bertozzi, C. R.; Kiessling, L. L. *Science* **2001**, *291*, 2357-2364.
6. Imperiali, B.; O'Connor, S. E. *Curr. Opin. Chem. Biol.* **1999**, *3*, 643.
7. He, Y.; Hinklin, R. J.; Chang, J.; Kiessling, L. L. *Org. Lett.* **2004**, *6*, 4479-4482.
8. Györgydeák, Z.; Hadady, Z.; Felföldi, Krakomperger, A.; Nagy, V.; Tóth, M.; Brunyánszki, A.; Dosca, T.; Gergely, P.; Somsák, L. *Bioorg. Med. Chem.* **2004**, *12*, 4861-4870.
9. Bianchi, A.; Russo, A.; Bernardi, A. *Tetrahedron: Assymetry* **2005**, *16*, 381-386.
10. Taylor, C. M. *Tetrahedron* **1998**, *54*, 11317-11362.
11. Kovács, L.; Osz, E.; Domokos, V.; Holzer, W.; Györgydeák, Z. *Tetrahedron* **2001**, *57*, 4609-4621.
12. Boullanger, P.; Maunier, V.; Lafont, D. *Carbohydr. Res.* **2000**, *324*, 97-106.
13. Damkaci, F.; DeShong, P. *J. Am. Chem. Soc.* **2003**, *125*, 4408-4409.
14. Saxon, E.; Armstrong, J. I.; Bertozzi, C. R. *Org. Lett.* **2000**, *2*, 2141-2143.

15. Yarema, K. J.; Mahal, L. K.; Bruehl, R. E.; Rodriguez, C. R.; Bertozzi, C. R. *J. Biol. Chem.* **1998**, *273*, 31168.
16. Hang, H. C.; Yu, C.; Pratt, M. R.; Bertozzi, C. R. *J. Am. Chem. Soc.* **2004**, *126*, 6-7.
17. Norris, P.; Horton, D.; Levine, B. R.; *Heterocycles* **1996**, *43*, 2643-2655.
18. Peto, C.; Batta, G.; Györgydeák, Z.; Sztaricskai, F. *J. Carbohydr. Chem.* **1996**, *15*, 465.
19. Ashton, P. R.; Glink, P. T.; Stoddart, J. F.; Tasker, P. A.; White, A. J. P.; Williams, D. J. *Chemistry* **1996**, *2*, 729-736.
20. Marco-Contelles, J.; Rodríguez-Fernández, M. *J. Org. Chem.* **2001**, *66*, 3717-3725.
21. Banu, K. M.; Dinakar, A.; Anathanarayanan, C. *Indian J. Pharm. Sci.* **1999**, *61*, 202-205.
22. Buckle, D. R.; Rockell, C. J. M.; Smith, H.; Spicer, B. A. *J. Med. Chem.* **1983**, *27*, 223-227.
23. Xiao-Min, C.; Zhan-Jiang, L.; Zhong-Xu, R.; Zhi-Tang, H. *Carbohydr. Res.* **1999**, *315*, 262-267.
24. Padwa, A. *1,3-Dipolar Cycloaddition Chemistry*, Wiley & Sons: New York, 1984.
25. Terrett, N. K.; Gardner, M.; Gordon, D. W.; Kobylecki, R. J., Steele, J. *Tetrahedron* **1995**, *51*, 8135-8173.
26. Zaragoza, F.; Peterson, S. V. *Tetrahedron* **1996**, *52*, 10823-10826.
27. Moore, M.; Norris, P. *Tetrahedron Lett.* **1998**, *39*, 7027-7030.



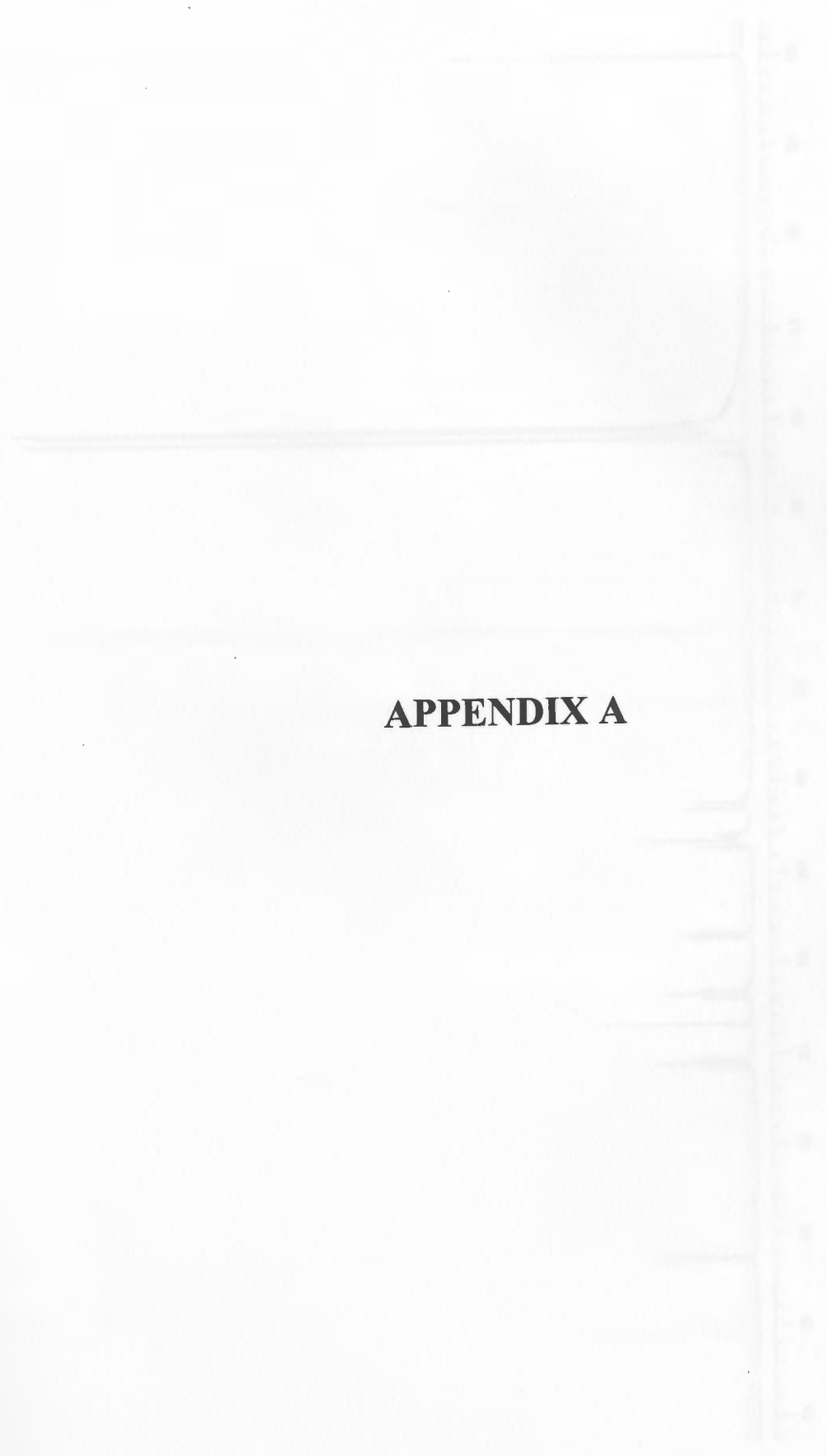
28. Freeze, S.; Norris, P. *Heterocycles* **1999**, *51*, 1807-1817.
29. Tornøe, C. W.; Christensen, C.; Meldal, M. *J. Org. Chem.* **2002**, *67*, 3057-3064.
30. Tornøe, C. W.; Sanderson, S. J.; Mottram, J. C.; Coombs, G. H., Meldal, M. J. *Comb. Chem.* **2003**, in Press.
31. Blass, B. E.; Coburn, K. R.; Faulkner, A. L.; Hunn, C. L.; Natchus, M. G.; Parker, M. S.; Portlock, D. E.; Tullis, J. S.; Wood, R. *Tetrahedron Lett.* **2002**, *43*, 4059-4061.
32. Rostovtsev, V. V.; Green, L. G.; Fokin, V. V.; Sharpless, K. B. *Angew. Chem. Int. Ed.* **2002**, *41*, 2596-2599.
33. Kolb, H. C.; Sharpless, K. B. *Drug Discovery Today* **2003**, *8*, 1128-1137.
34. Wamhoff, H. *Comprehensive Heterocyclic Chemistry*, Vol. 5, Pergamon: Oxford, 1984.
35. Alvarez, R.; Velazquez, S.; San-Felix. A.; Aquaro, S.; De Clercq, E.; Perno, C.-F.; Karlsson, A.; Balzarini, J.; Camarasa, M. J. *J. Med. Chem.* **1994**, *37*, 4185-4194.
36. Menetsch, R.; Krasinski, A.; Radić, Z.; Raushel, J.; Taylor, P.; Sharpless, B.; Kolb, H. C. *J. Am. Chem. Soc.* **2004**, *126*, 12809-12818.
37. Root, Y. Y., M.S. Thesis, Youngstown State University, **2003**.
38. Kibler, D. A., M. S. Thesis, Youngstown State University, **2003**.
39. Artamonova, T. V.; Zhivich, A. B.; Dubinskii, M. Y.; Koldobskii, G. I. *Synthesis* **1996**, 1428-1430.
40. Tosin, M.; Murphy, P. *Org. Lett.* **2002**, *4*, 3675-3678.

41. Pérez-Balderas, F.; Ortega-Muñoz, M.; Morales-Sanfrutos, J.; Hernández-Mateo, F.; Calvo-Flores, F. G.; Calvo-Asín, J. A.; Isac-García, J.; Santoyo-González, F. *Org. Lett.* **2003**, *5*, 1951-1954.
42. Temelkoff, D. T.; Norris, P.; Zeller, M. *Acta Cryst. E Structure Reports Online* **2004**, *E60*, 2273-2274.

APPENDIX A

**APPENDIX A**

Figure 21-111: IR spectrum of benzoin 2



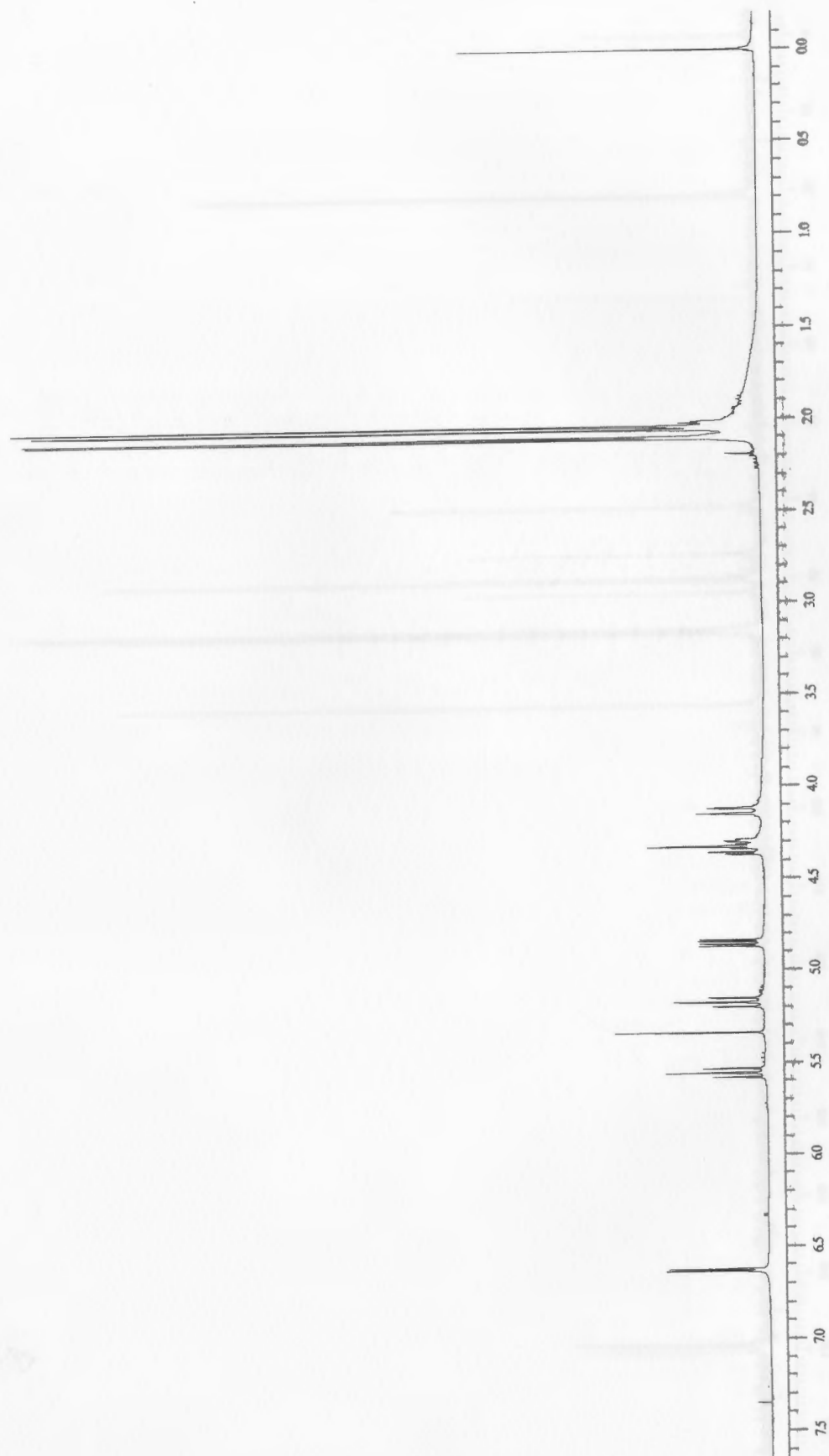


**Figure 21:** 400 MHz  $^1\text{H}$  NMR spectrum of bromide 2

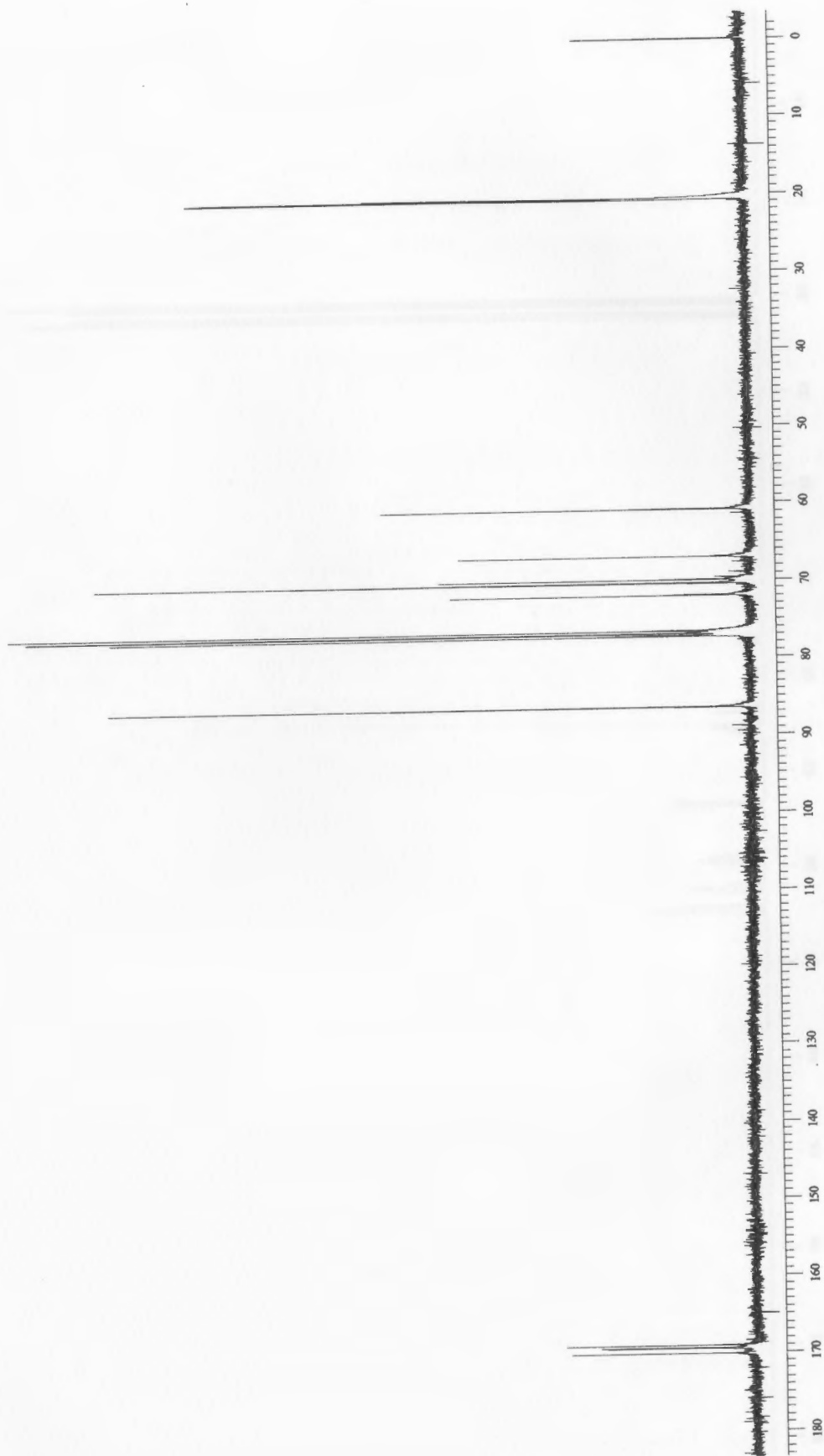
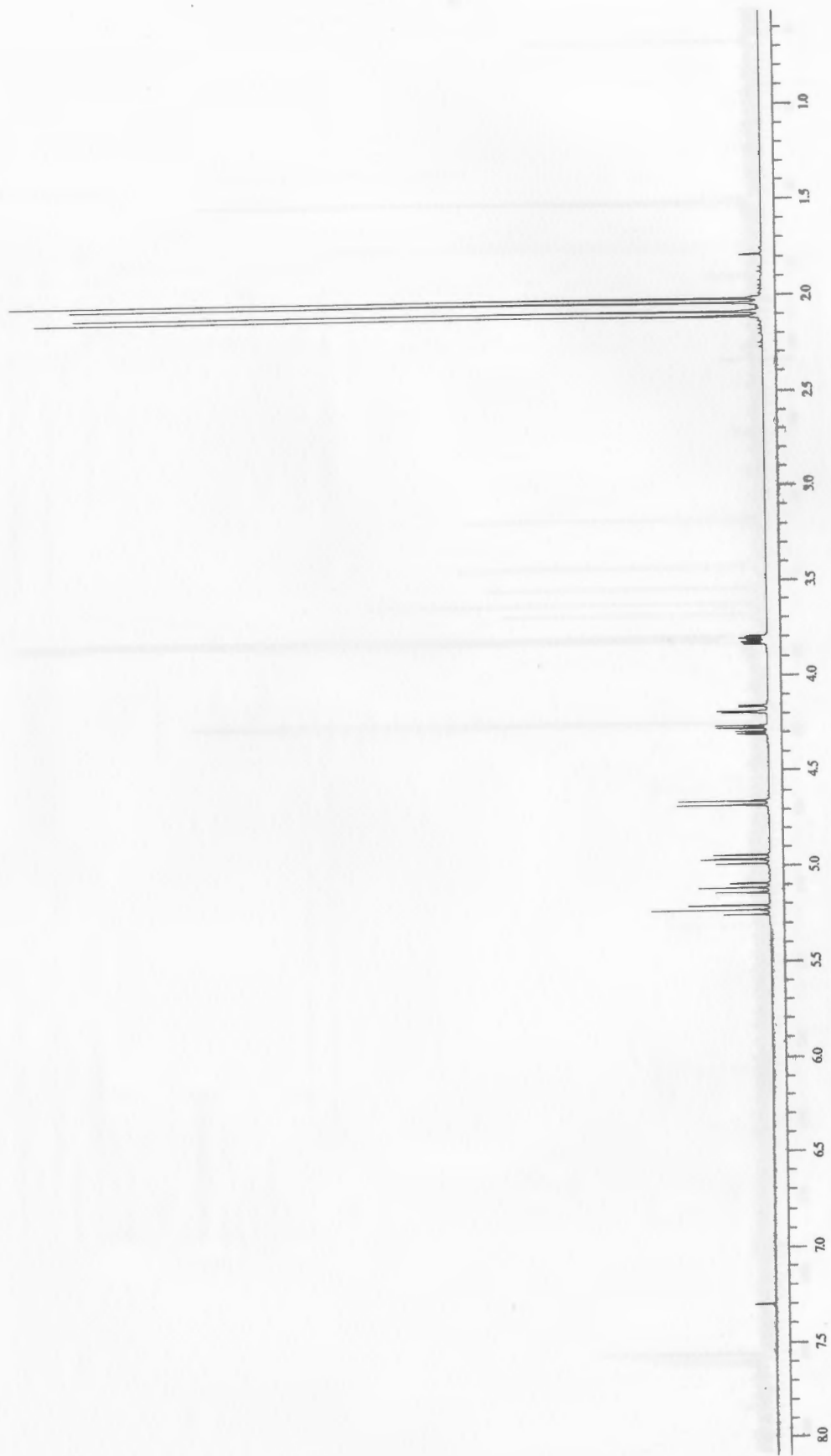


Figure 22: 100 MHz  $^{13}\text{C}$  NMR spectrum of bromide 2



**Figure 23:** 400 MHz <sup>1</sup>H NMR spectrum of azide 3

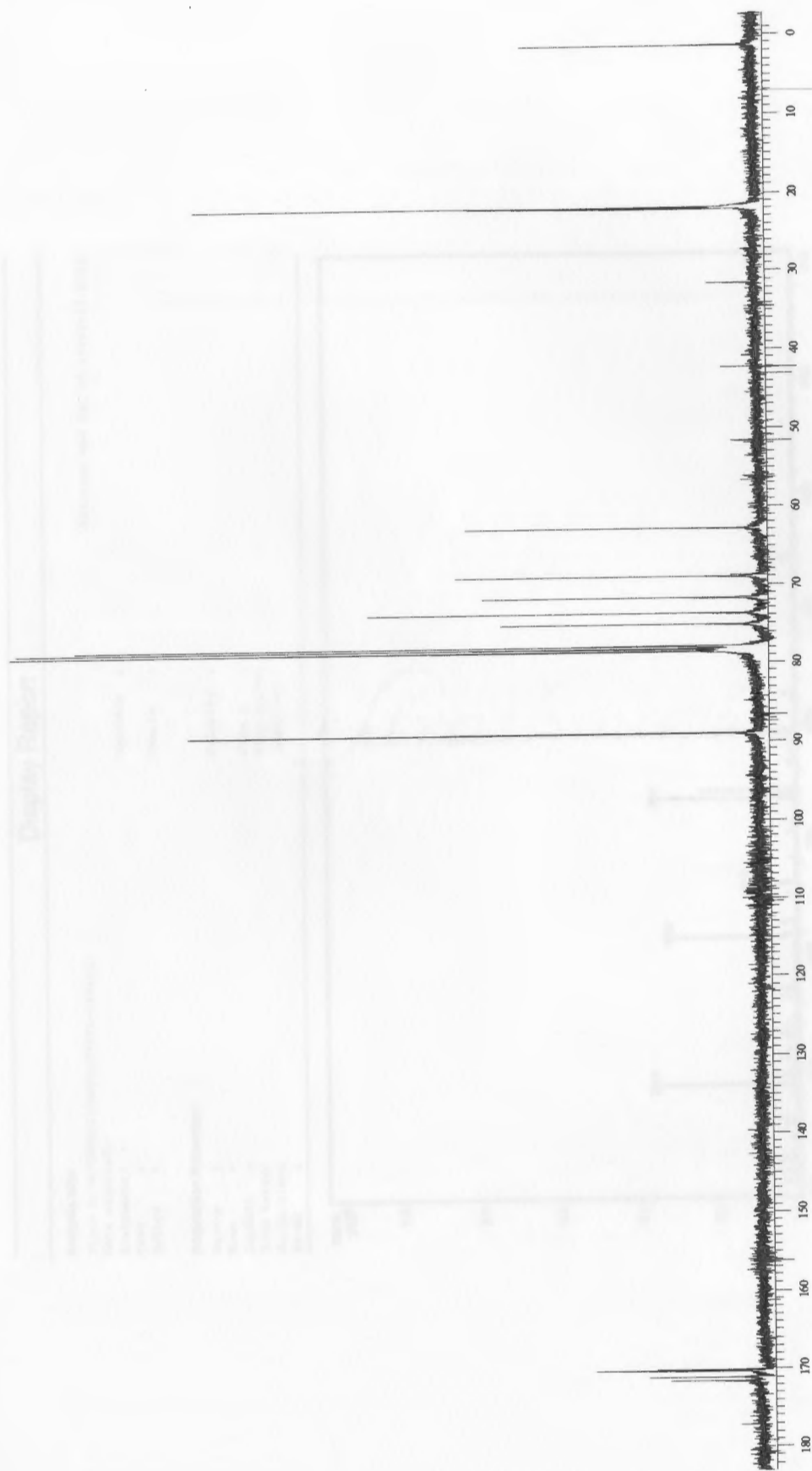


Figure 24: 100 MHz  $^{13}\text{C}$  NMR spectrum of azide 3



## Display Report

**Analysis Info:**

File: D:\HPCHEM\1\DATA\DT\DT1-2101.D  
 Date acquired:  
 Instrument:  
 Task :  
 Method :

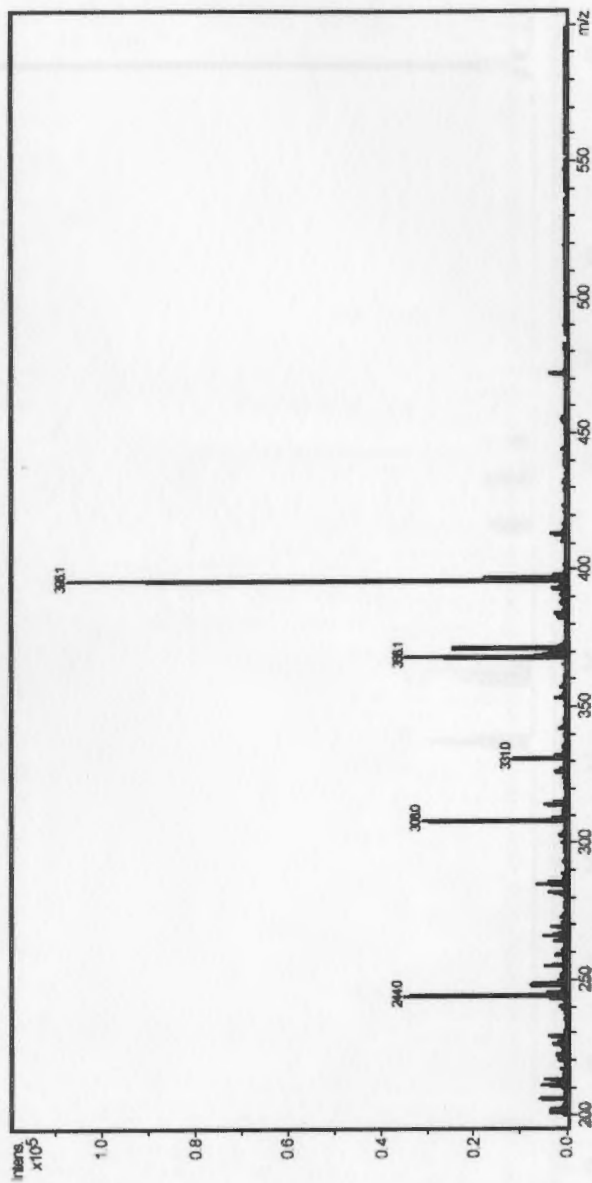
Printed: Wed Jul 27 15:41:14 2005

Operator :  
 Sample :

**Acquisition Parameter:**

Source :  
 Mode :  
 CapExit :  
 Scan Range:  
 Accum.time:  
 MS/MS I

Polarity :  
 Skim 1 :  
 Trap Drive:  
 Summation :



Brucker DataAnalysis Sequiza-LC 1.6m, © Bruker Daltonik GmbH  
 Licensed to EQ\_135, Uni. of Ohio

**Figure 25: Low resolution mass spectrum of azide 3**

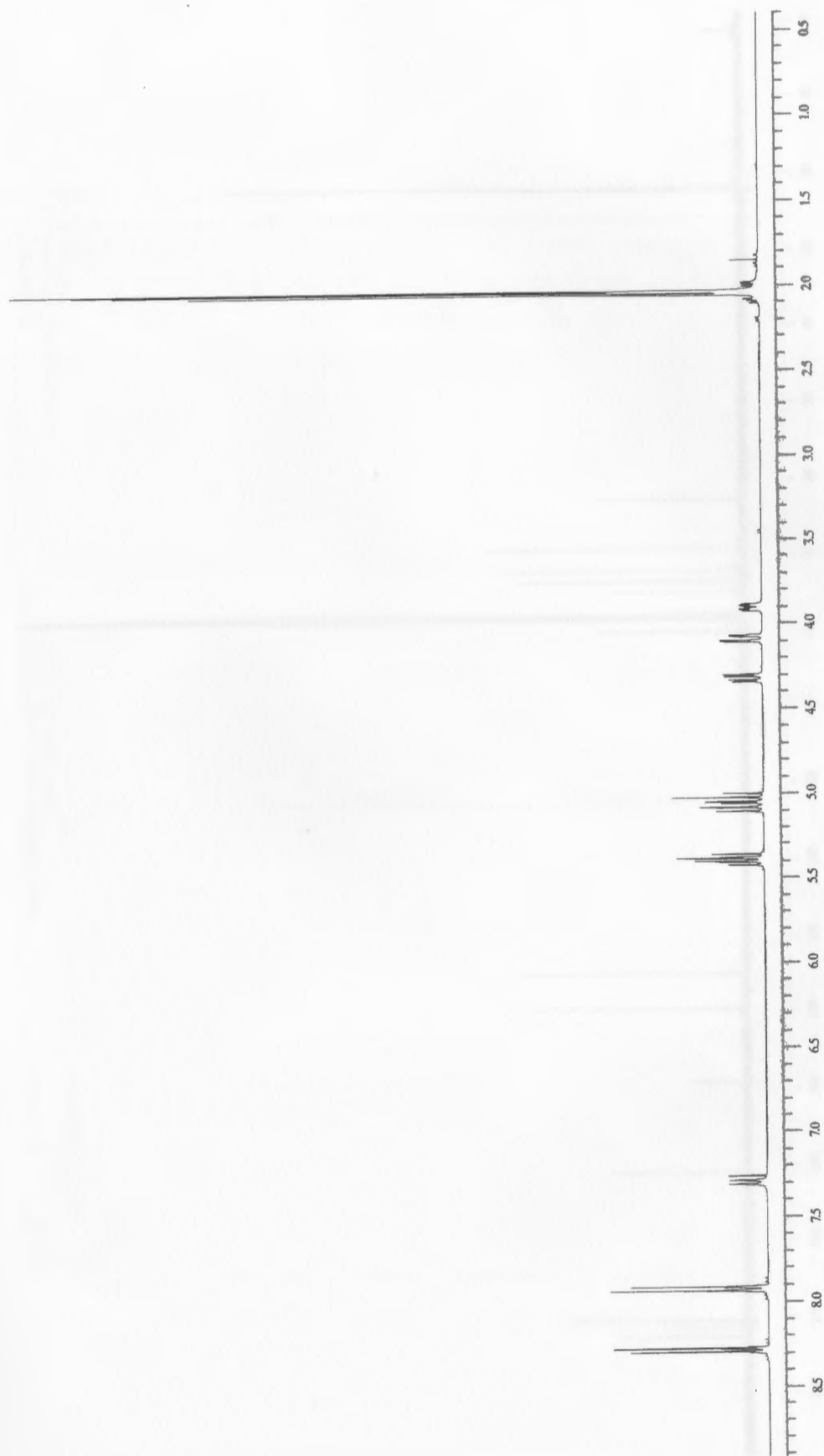


**Figure 26:** 400 MHz  $^1\text{H}$  NMR spectrum of amide 4

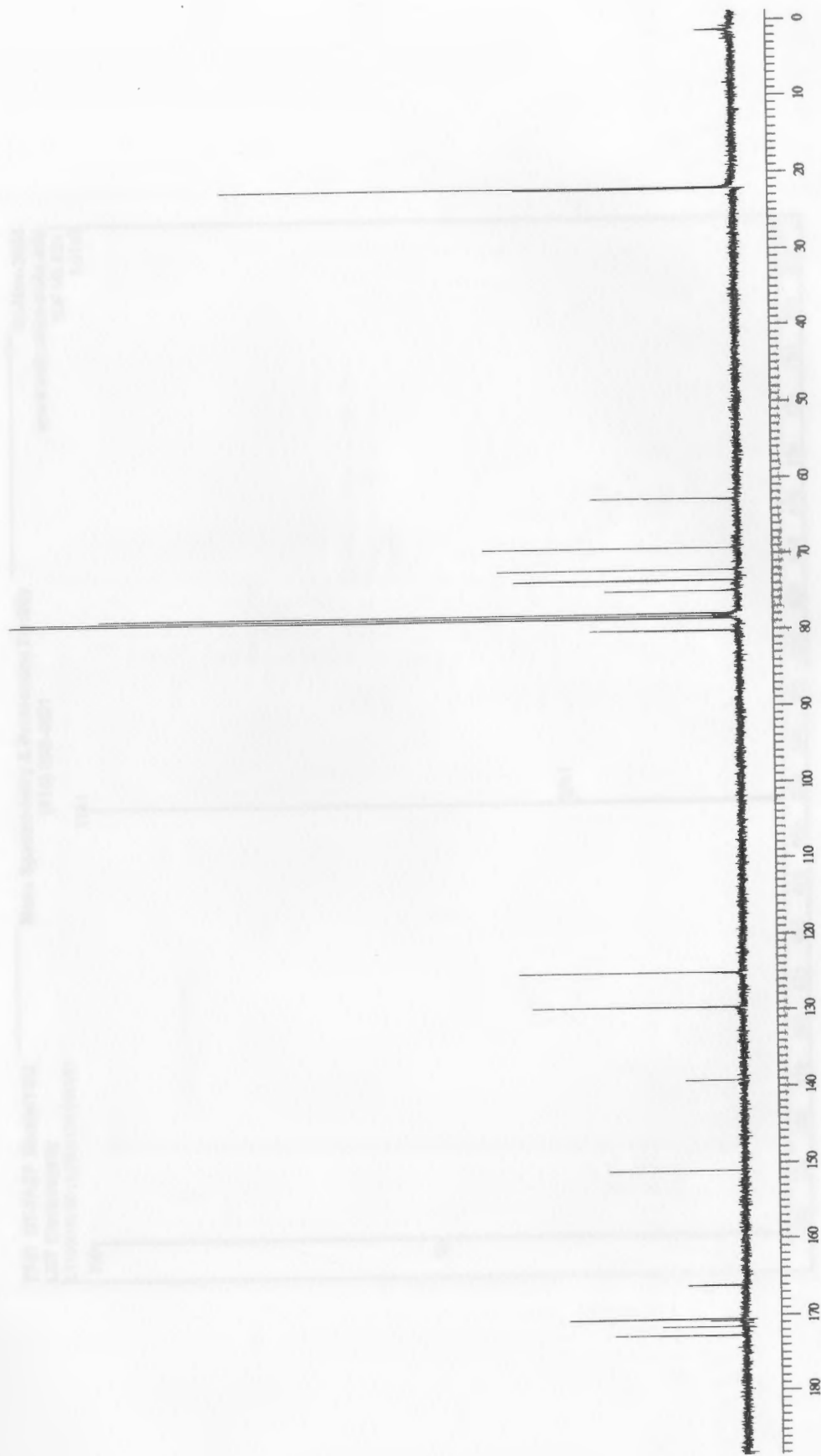


Figure 27: 100 MHz  $^{13}\text{C}$  NMR spectrum of amide 4

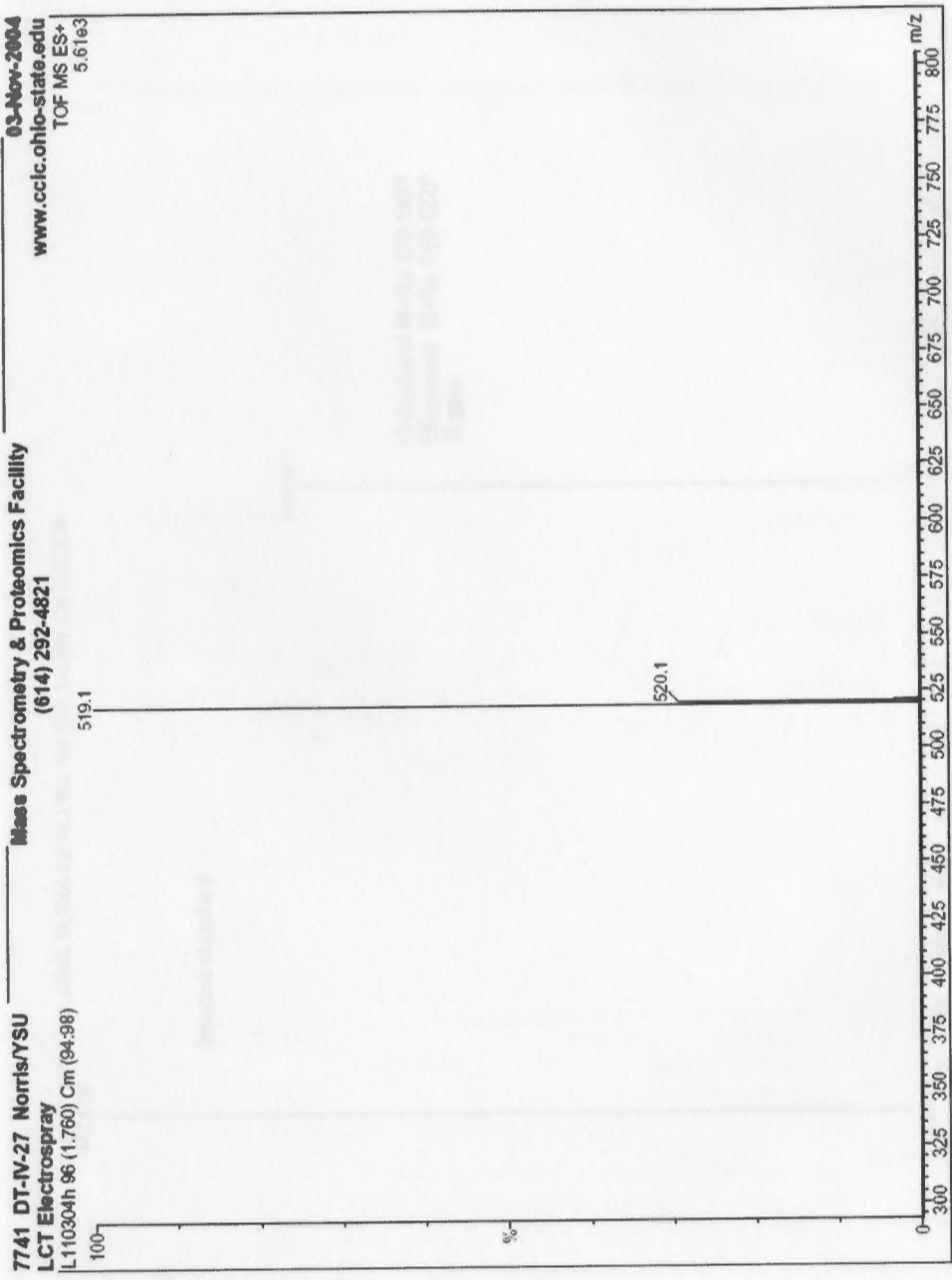
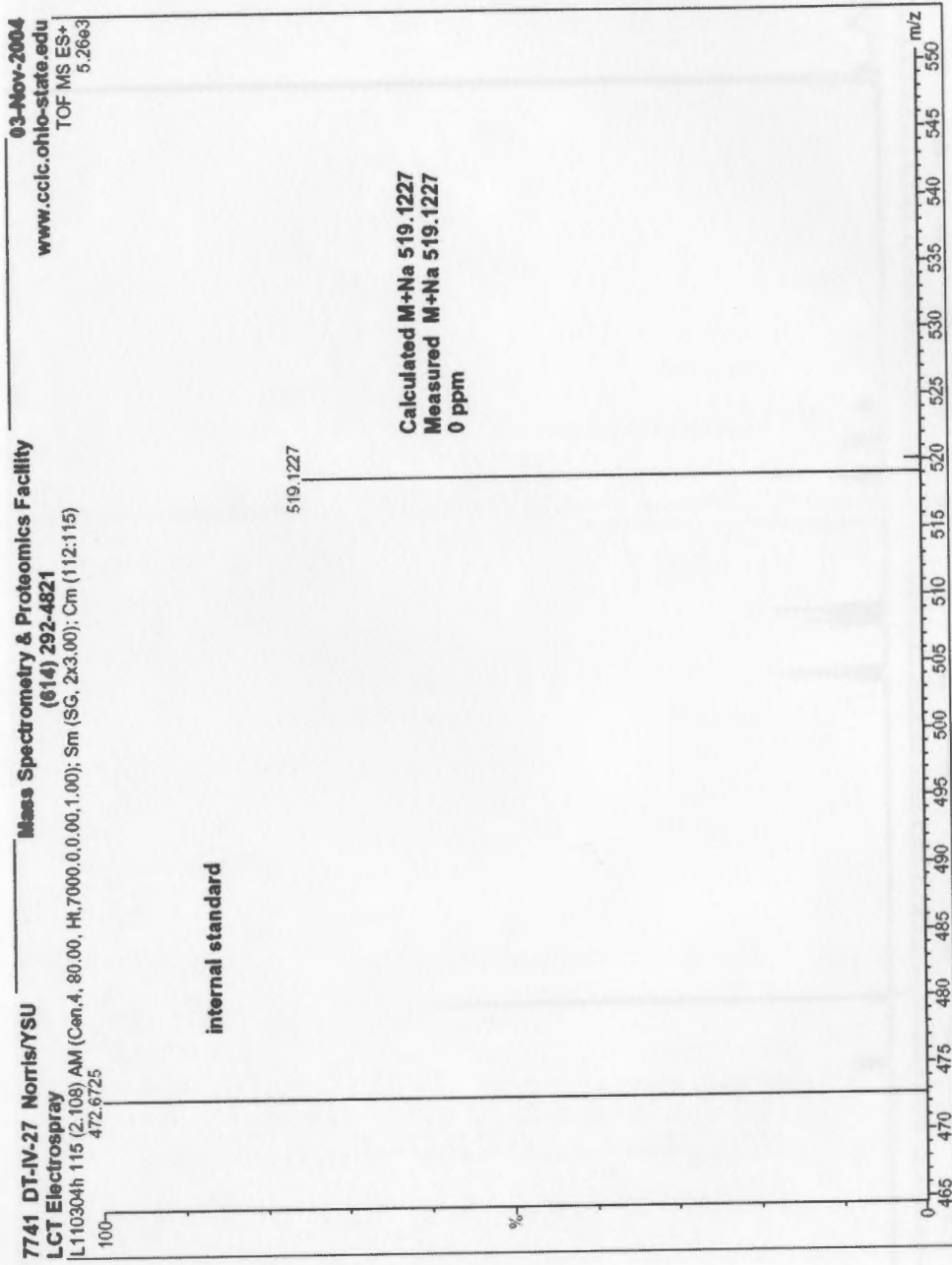
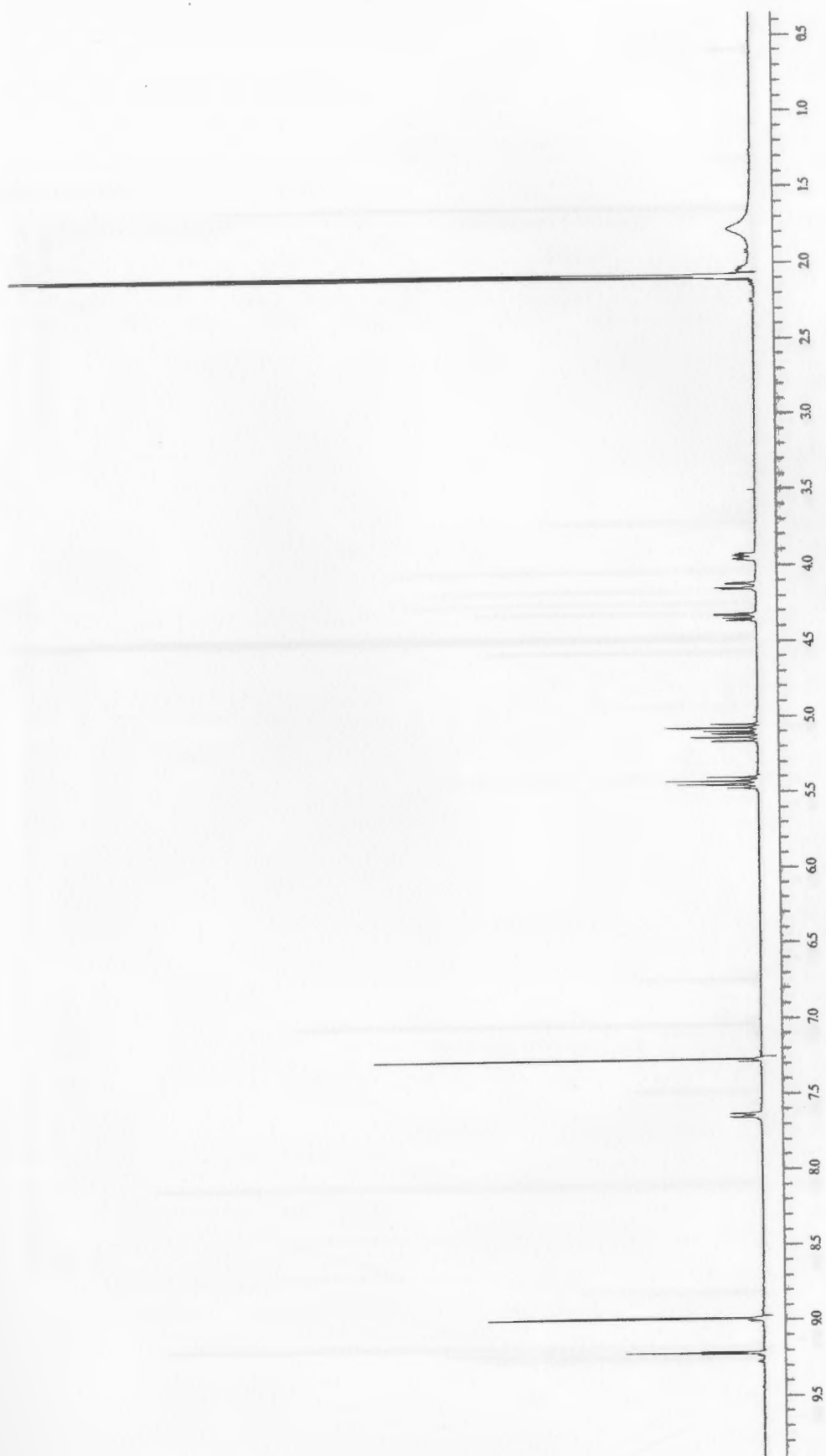


Figure 28: Low resolution mass spectrum of amide 4



**Figure 29: High resolution mass spectrum of amide 4**



**Figure 30:** 400 MHz  $^1\text{H}$  NMR spectrum of amide 5

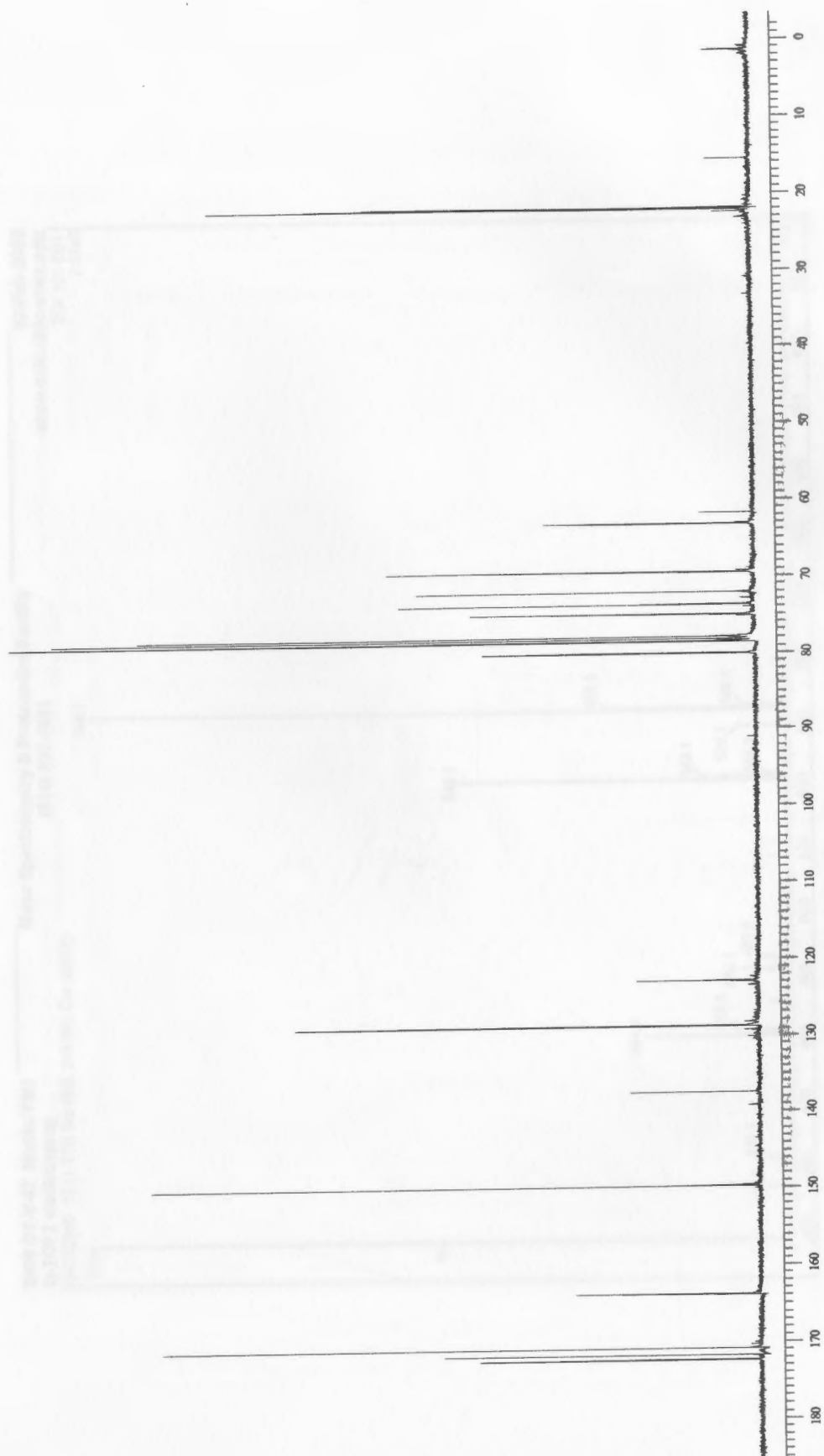


**Figure 31:** 100 MHz  $^{13}\text{C}$  NMR spectrum of amide 5



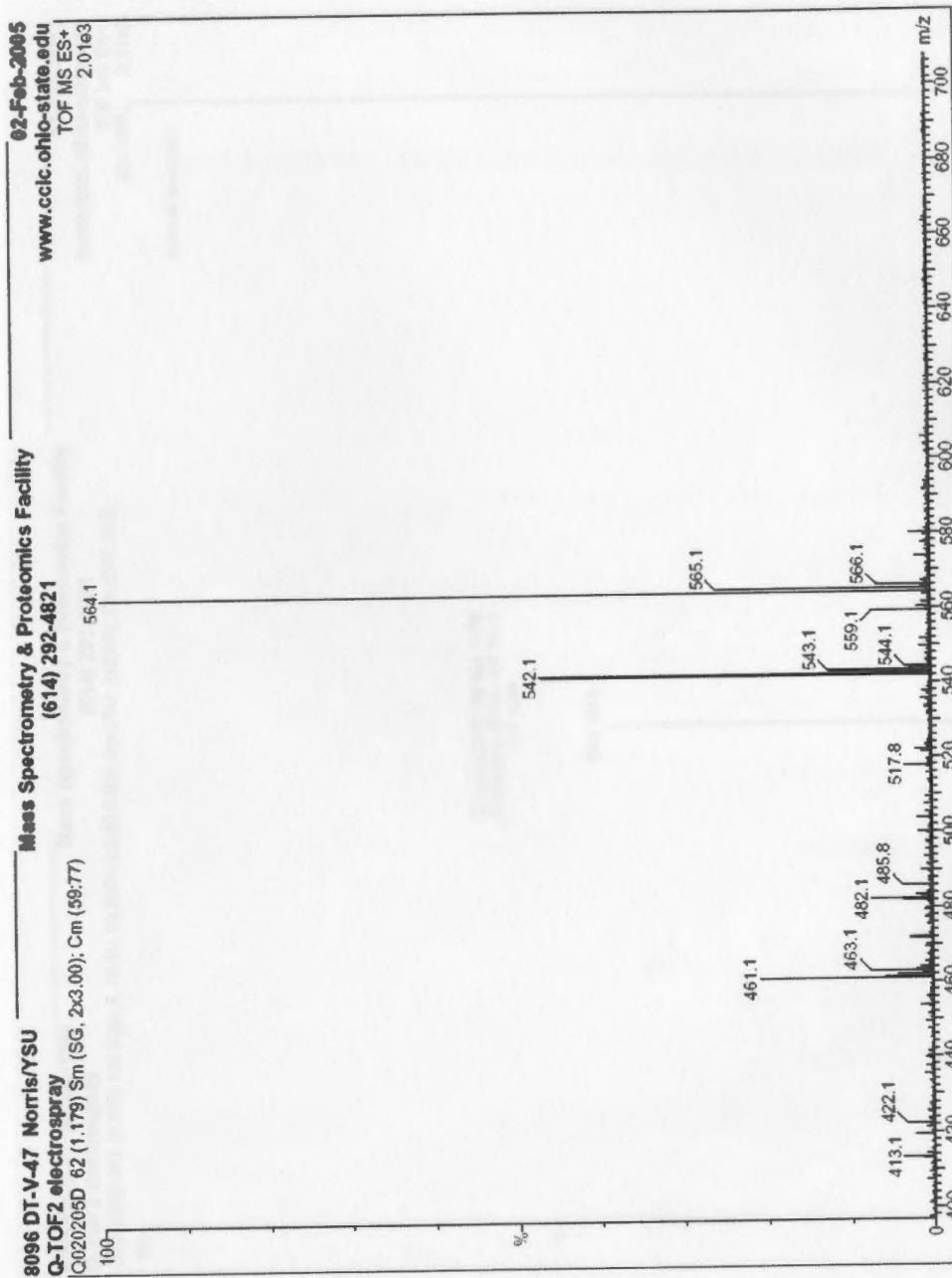


Figure 32: Low resolution mass spectrum of amide 5

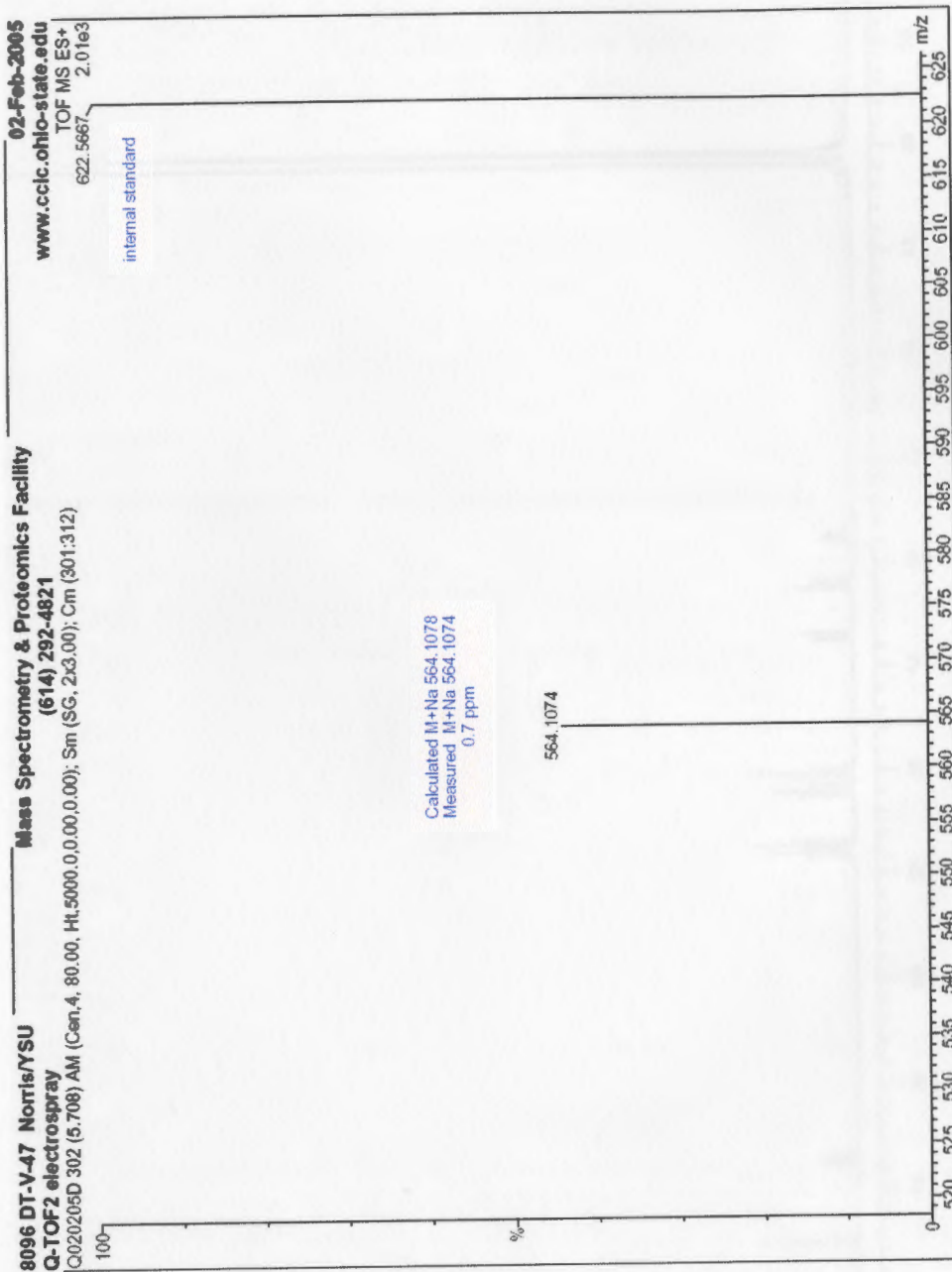
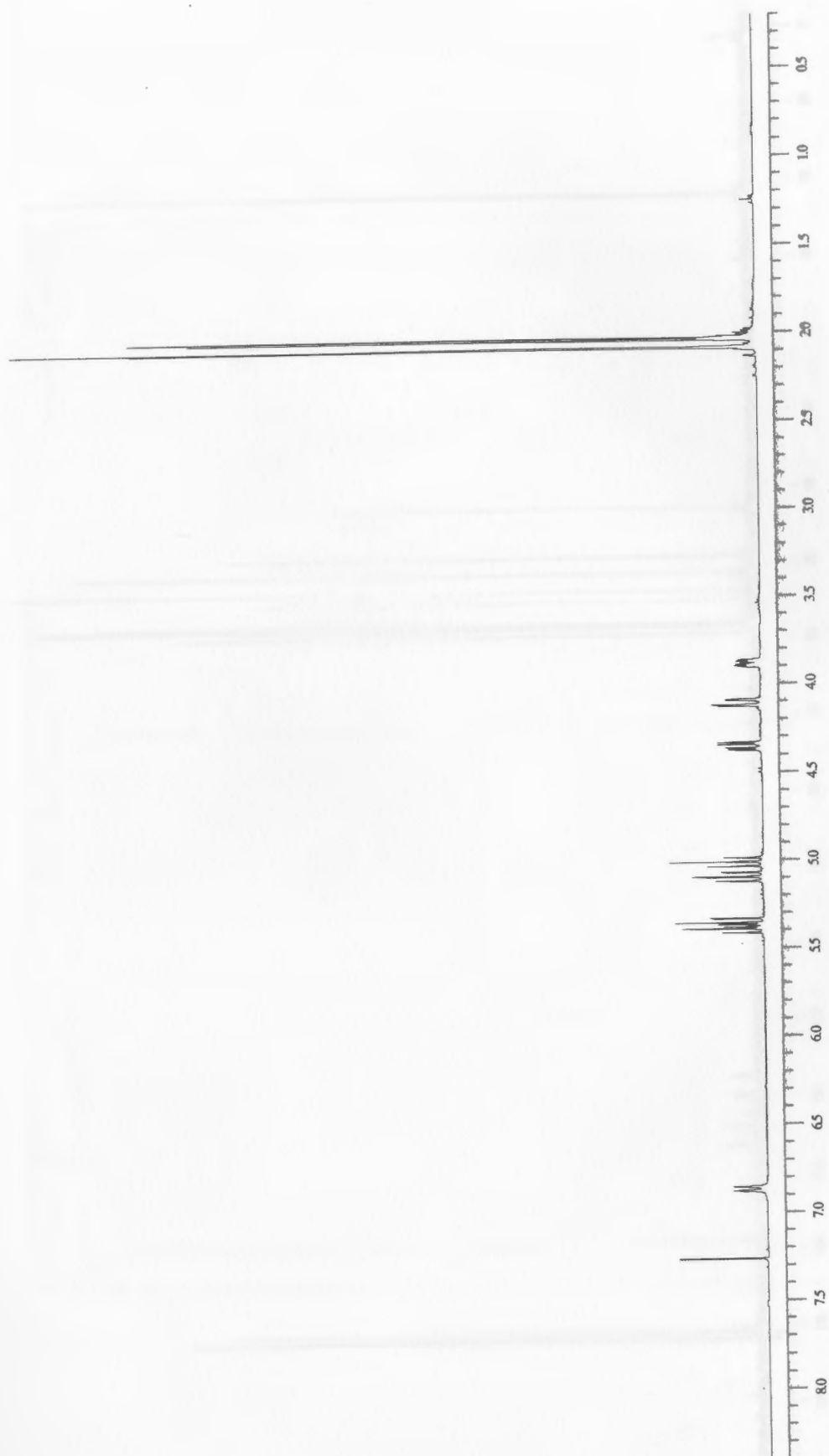
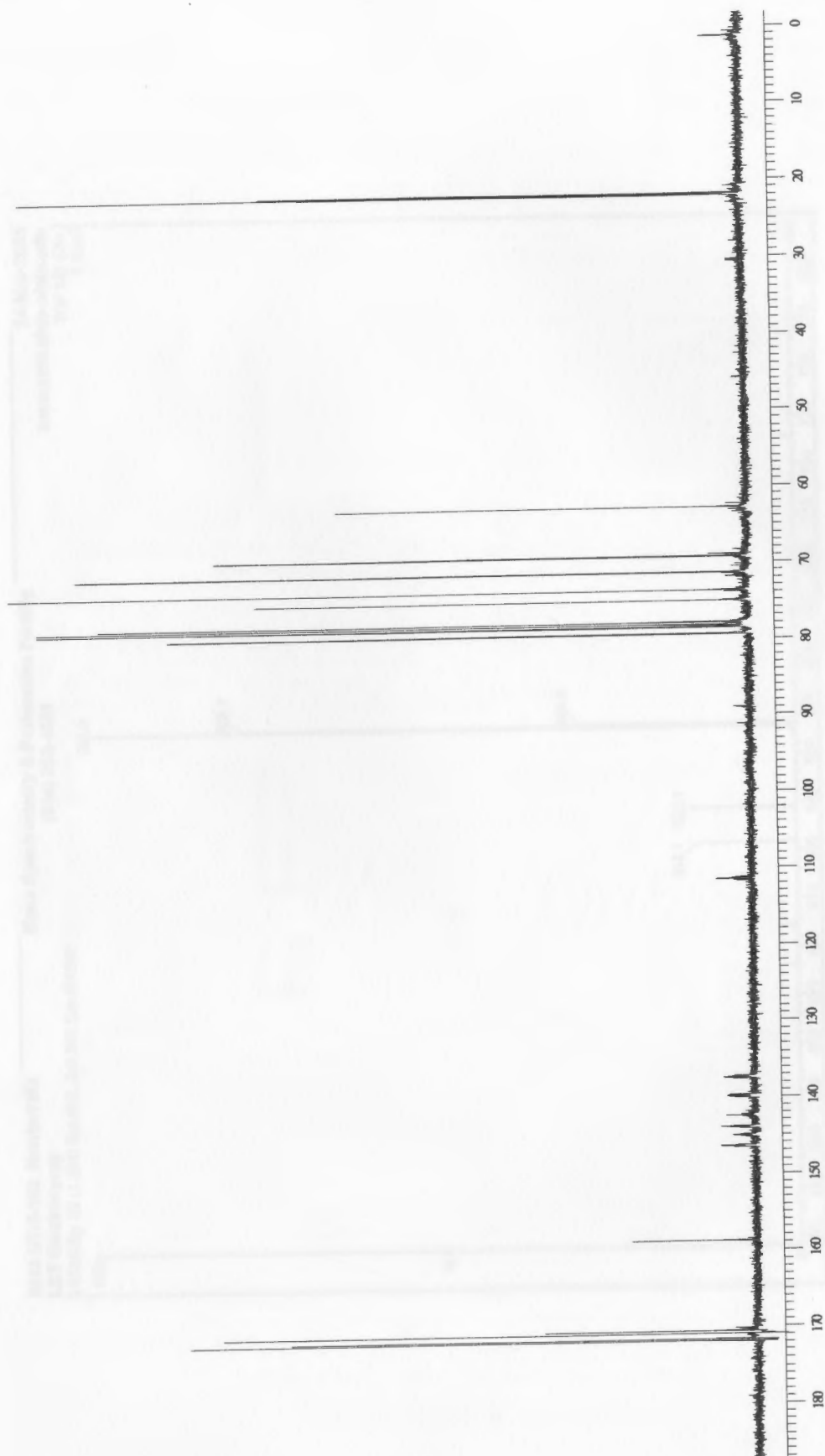


Figure 33: High resolution mass spectrum of amide 5



**Figure 34:** 400 MHz  $^1\text{H}$  NMR spectrum of amide 6



**Figure 35:** 100 MHz  $^{13}\text{C}$  NMR spectrum of amide 6

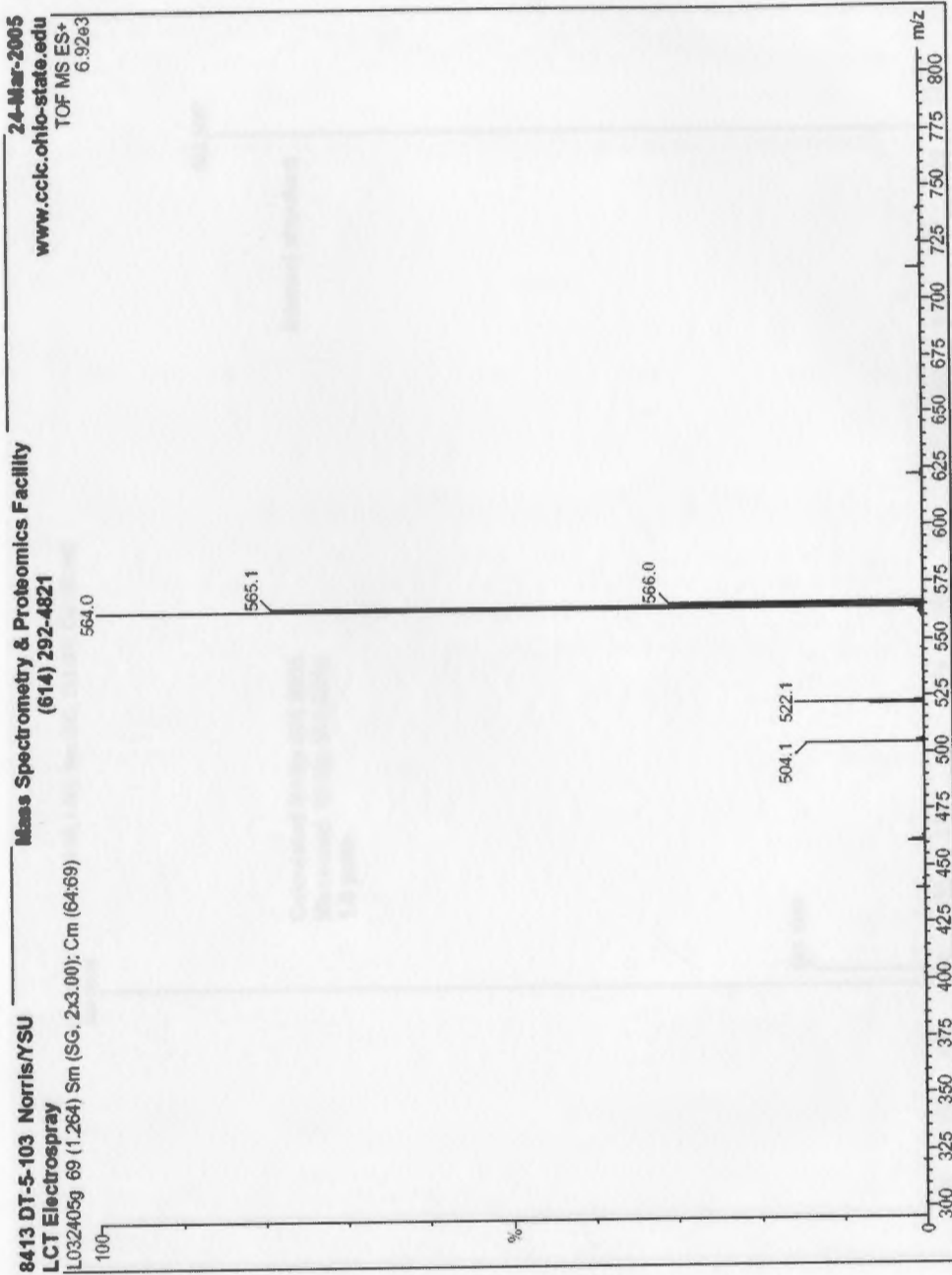


Figure 36: Low resolution mass spectrum of amide 6

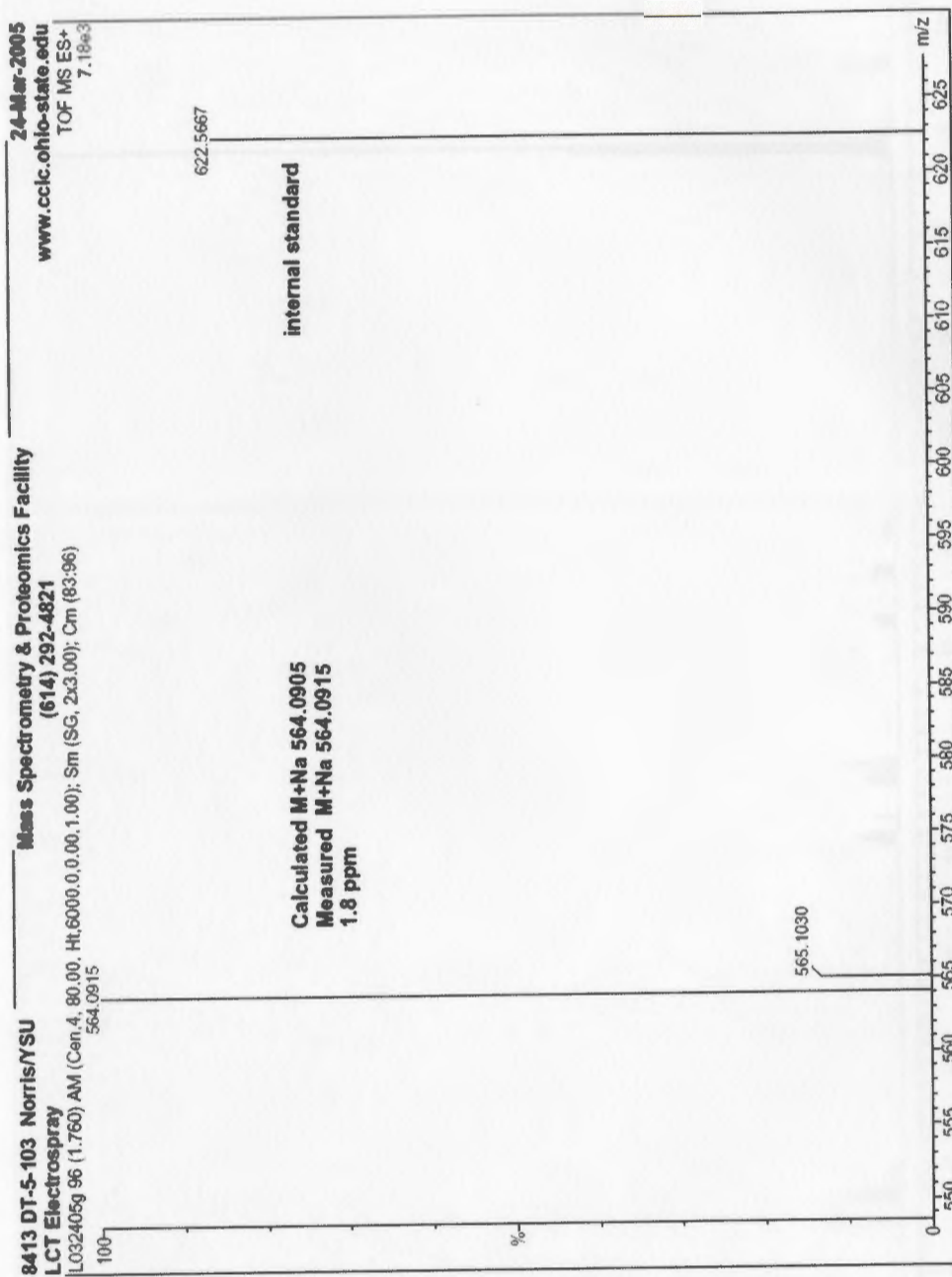
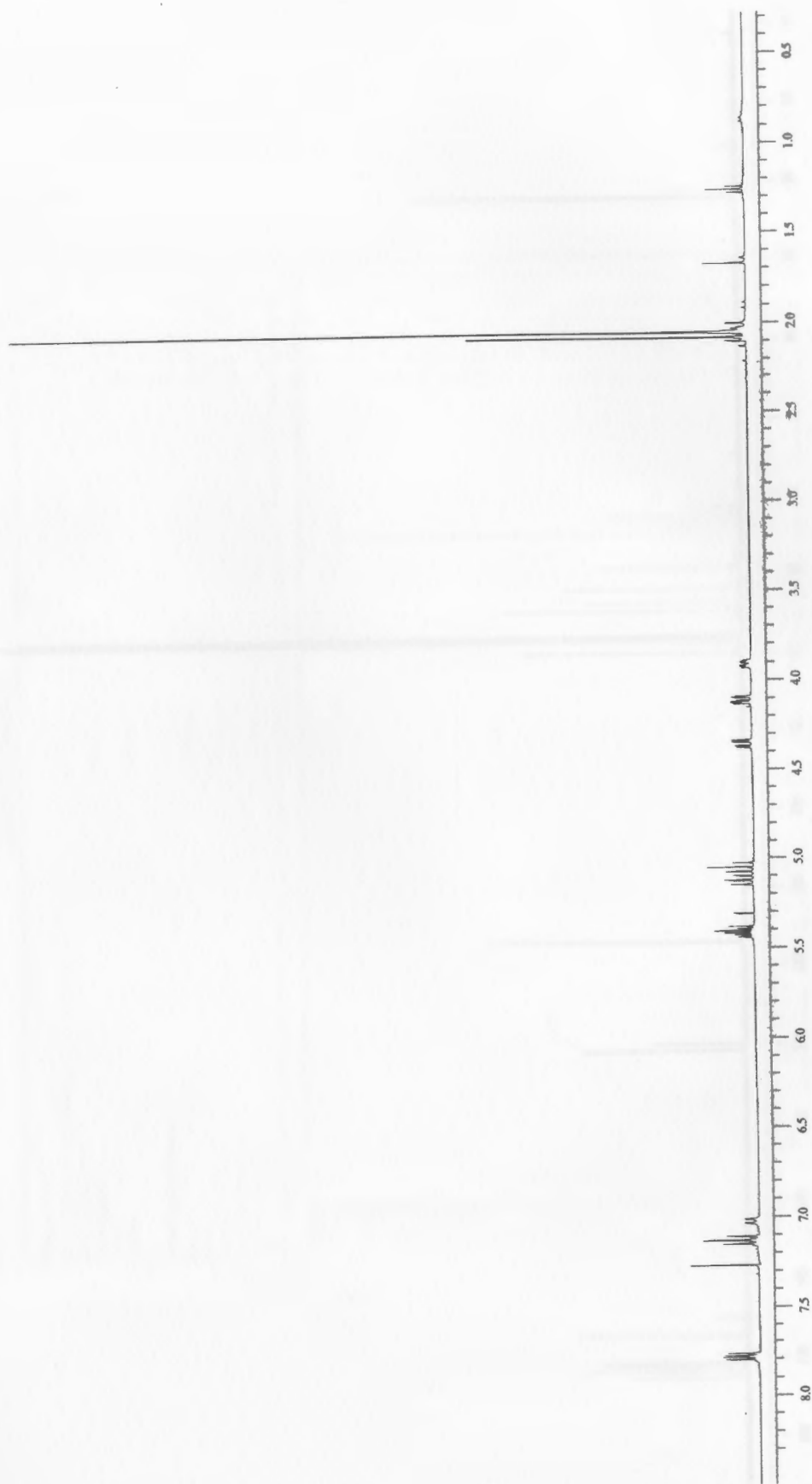


Figure 37: High resolution mass spectrum of amide 6



**Figure 38:** 400 MHz  $^1\text{H}$  NMR spectrum of amide 7

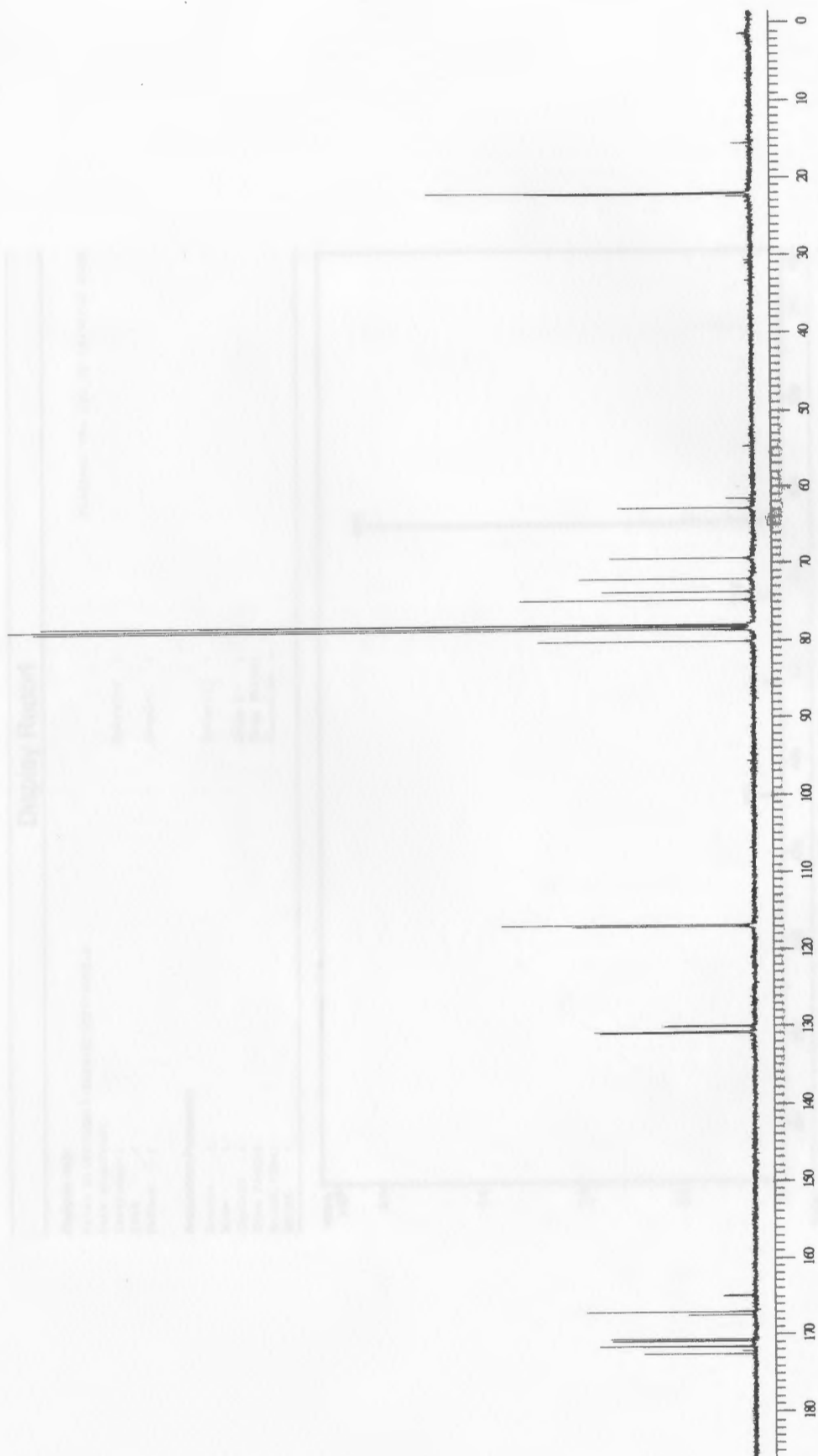


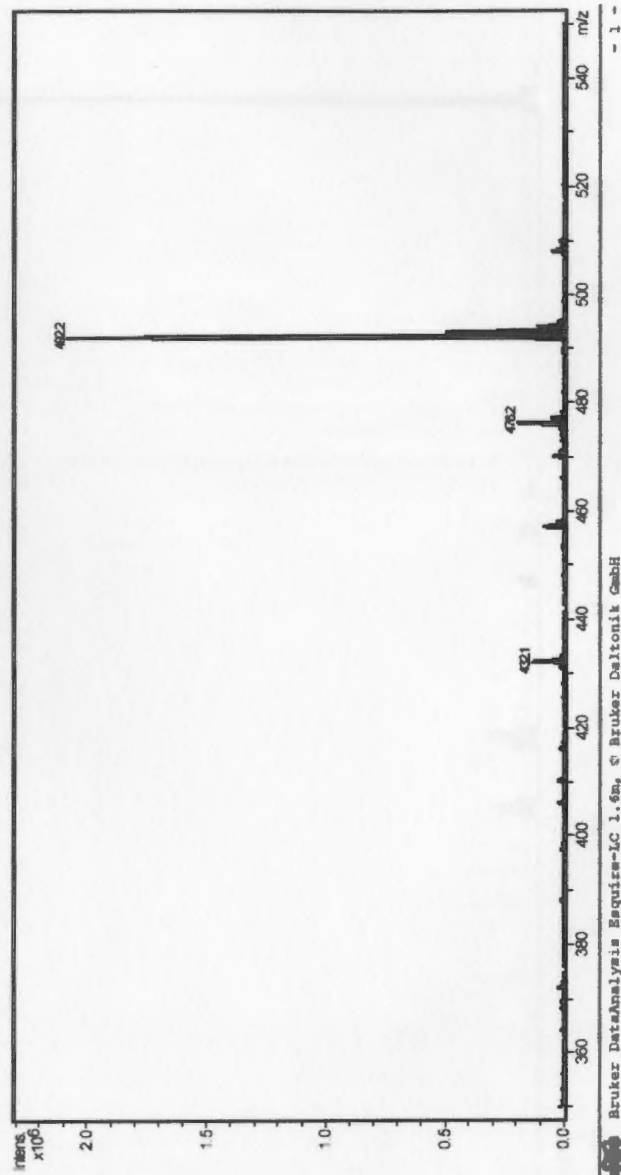
Figure 39: 100 MHz  $^{13}\text{C}$  NMR spectrum of amide 7



## Display Report

**Analysis Info:**  
File: D:\HECHEM\1\DATA\DT\DT7-0902.D  
Date acquired: Thu Jul 28 12:30:33 2005  
Instrument:  
Task :  
Method :  
Operator :  
Sample :  
Polarity :  
Skim 1 :  
Trap Drive:  
Summation :

**Acquisition Parameter:**  
Source :  
Mode :  
CapExit :  
Scan Range:  
Accum.time:  
MS/MS :



Brucker DataAnalysis Esquire-LC 1.6m, © Brucker Daltonik GmbH  
Licensed to EQ\_135, Uni. of Ohio

Figure 40: Low resolution mass spectrum of amide 7

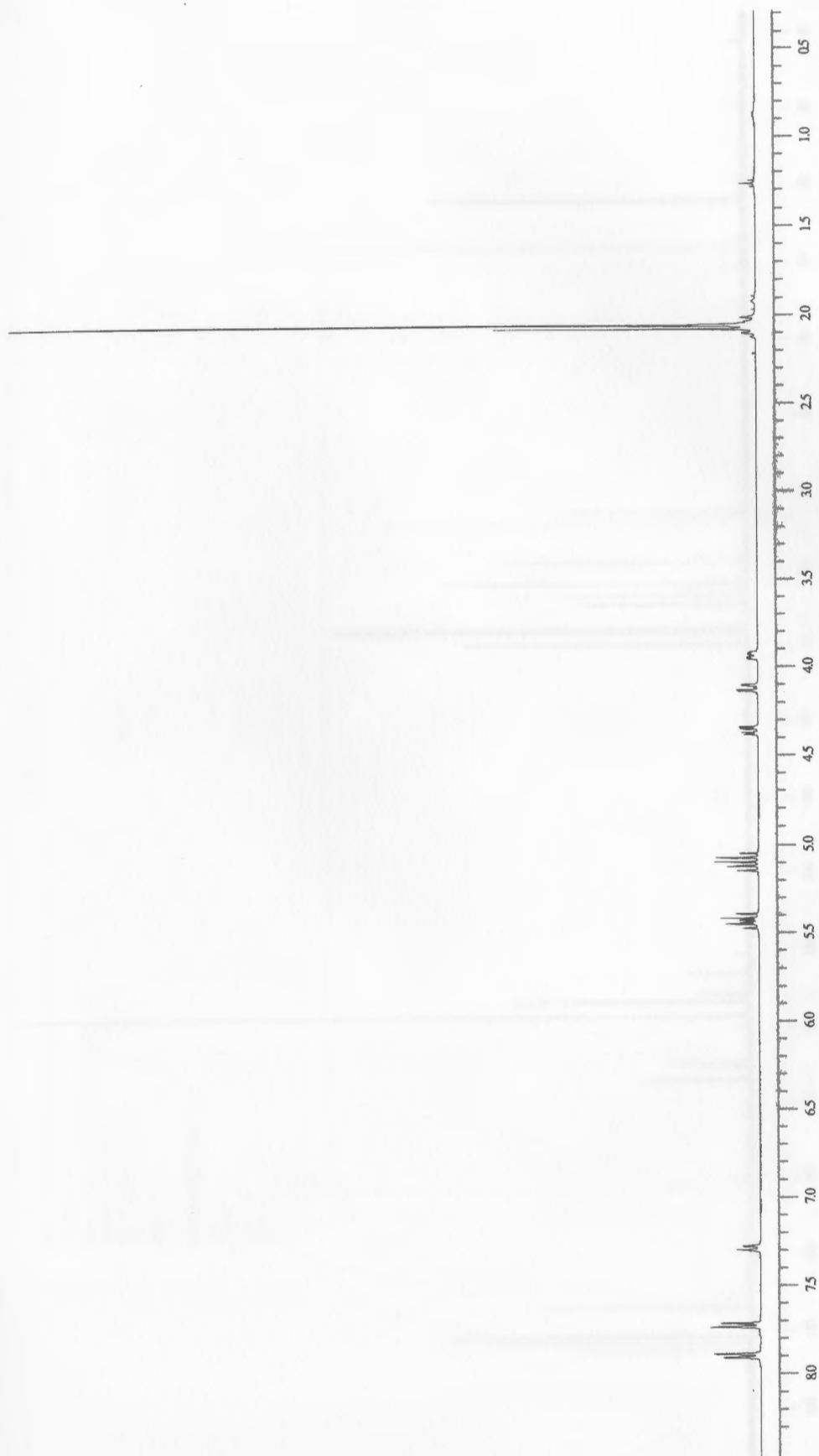


**Figure 41:** 400 MHz  $^1\text{H}$  NMR spectrum of amide 8

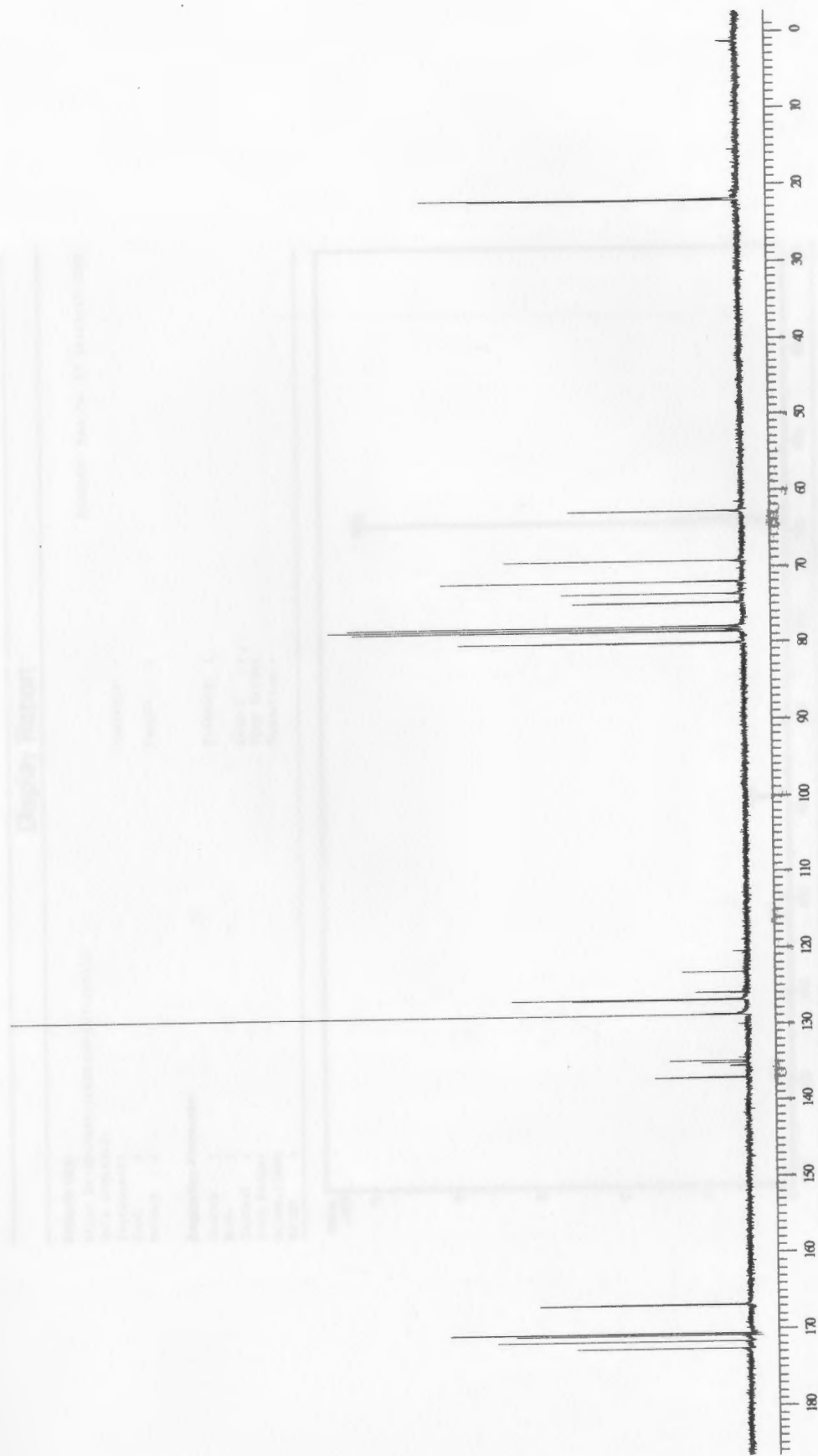


Figure 42: 100 MHz  $^{13}\text{C}$  NMR spectrum of amide 8

## Display Report

**Analysis Info:**

File: D:\BPCHEM\1\DATA\DF\DF7-1102.D

Date acquired:

Instrument:

Task :

Method :

Operator :

Sample :

**Acquisition Parameter:**

Source :

Mode :

CapExit :

Scan Range:

Accum.Time:

MS/MS :

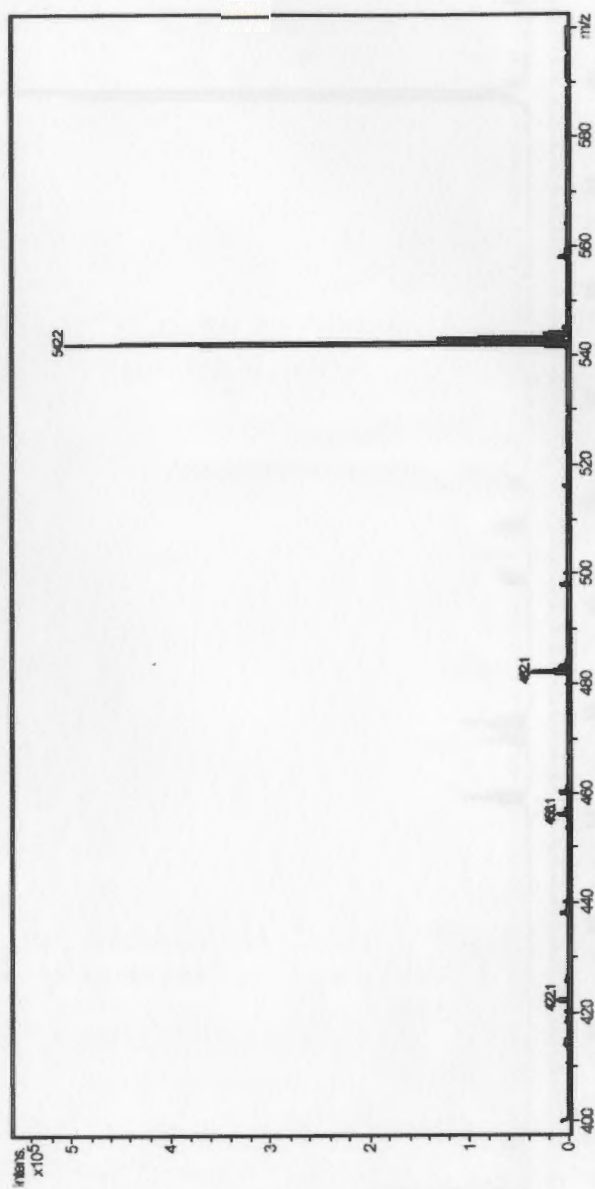
Polarity :

Skim 1 :

Trap Drive:

Summation :

Printed: Wed Jul 27 15:43:15 2005


 Bruker DataAnalysis Esquire-LC 1.6m, © Bruker Daltonik GmbH  
 Licensed to EQ 135, Uni. of Ohio

-- 1 --

**Figure 43: Low resolution mass spectrum of amide 8**

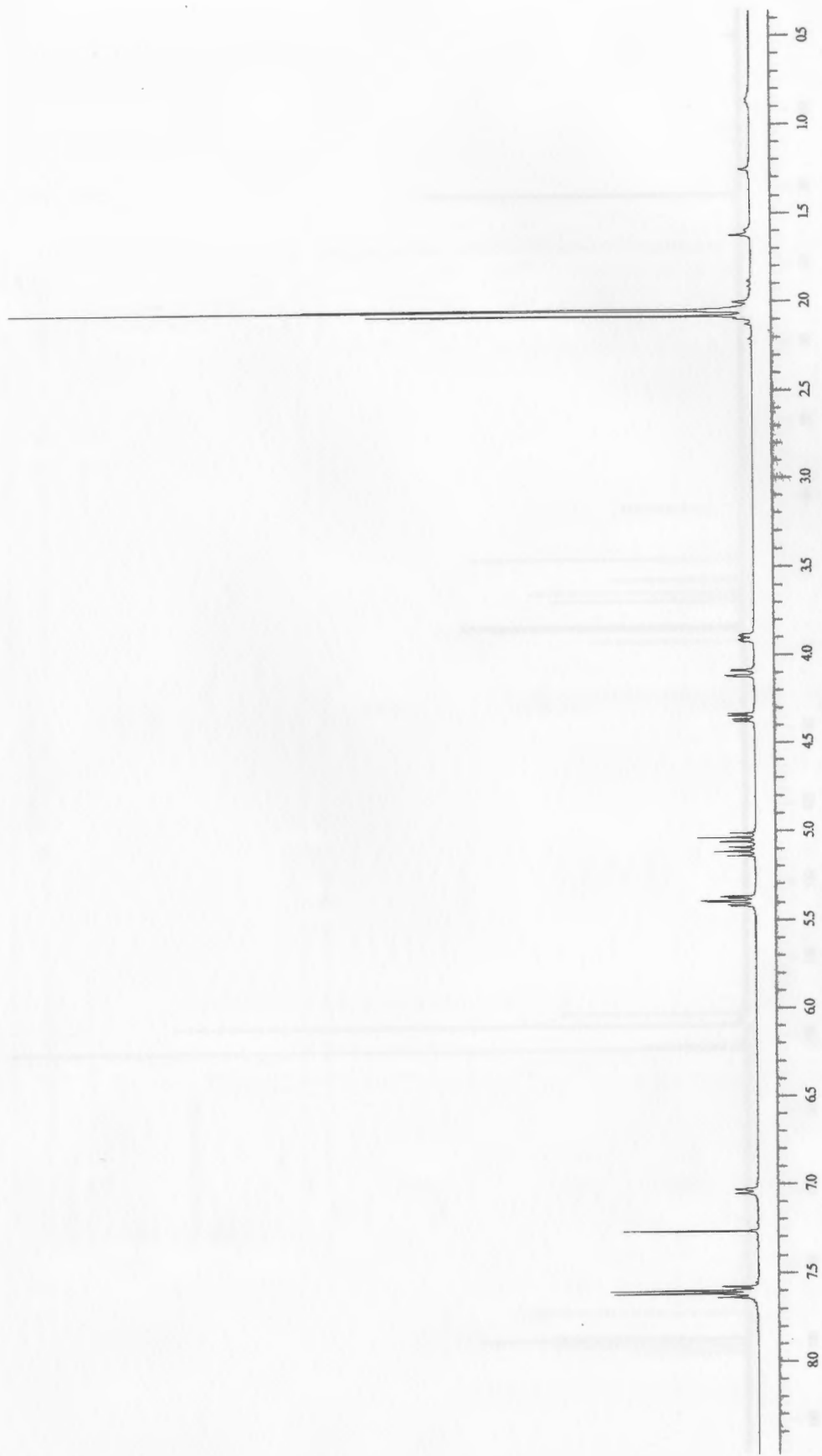


**Figure 44:** 400 MHz  $^1\text{H}$  NMR spectrum of amide 9

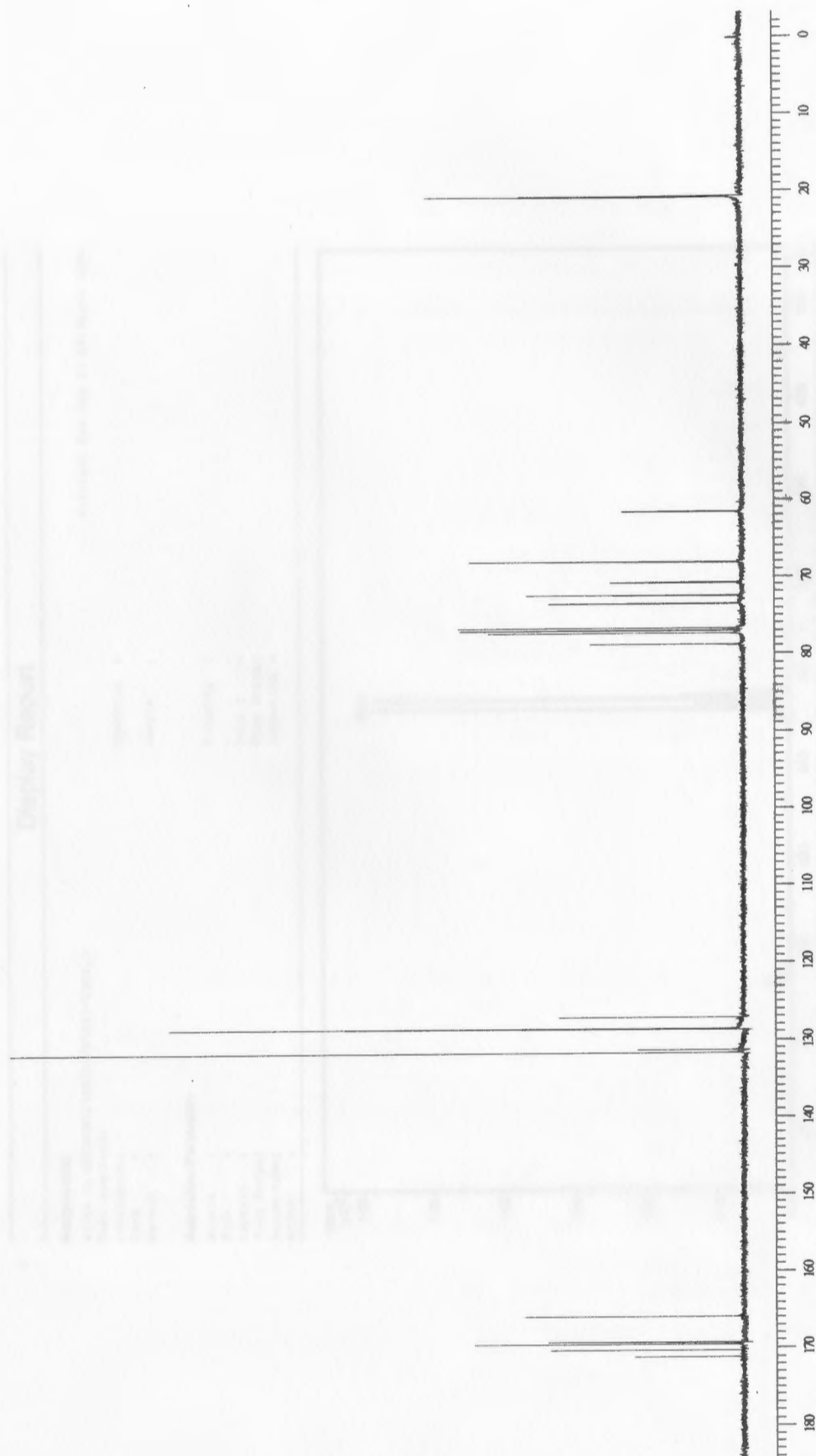
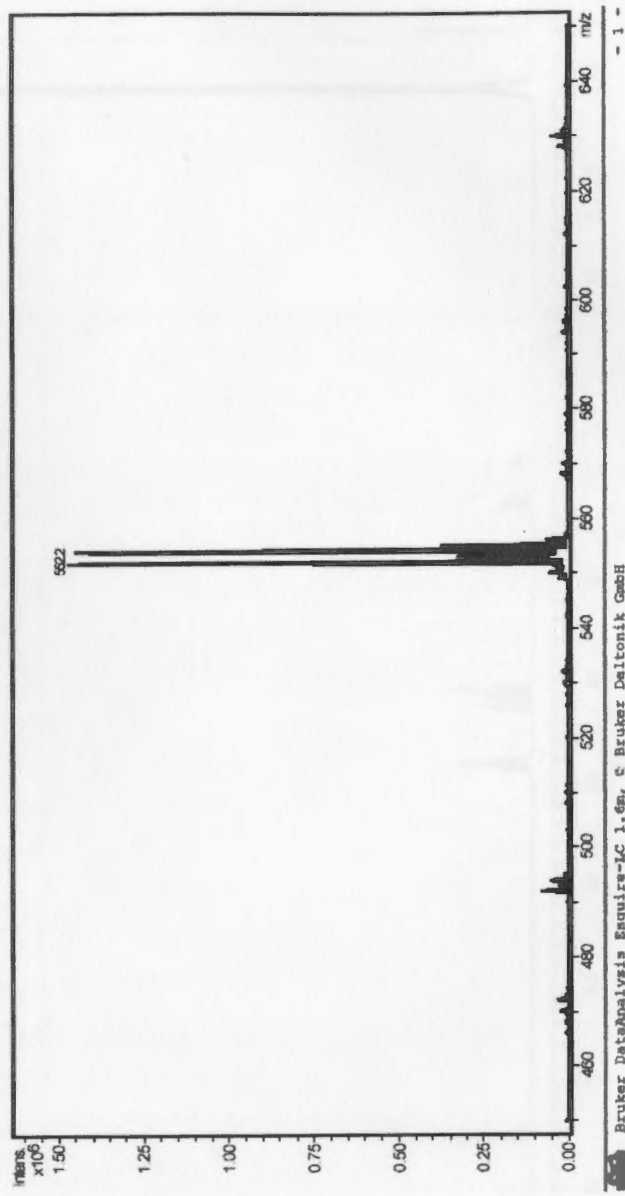


**Figure 45:** 100 MHz  $^{13}\text{C}$  NMR spectrum of amide 9

# Display Report

**Analysis Info:**  
File: D:\BPCKEM\1\DATA\DT\DT7-1302.D  
Date acquired:   
Instrument:   
Task :   
Method :   
Operator :   
Sample :   
Polarity :   
Skim 1 :   
Trap Drive:   
Summation:   
  
**Acquisition Parameter:**  
Source :   
Mode :   
CapExit :   
Scan Range:   
Accum.time:   
MS/MS :

Printed: Wed Jul 27 18:38:50 2005



Brucker DataAnalysis Esquire-IC 1.6m, © Brucker Daltonik GmbH  
Licensed to EQ\_135, Uni. of Ohio

Figure 46: Low resolution mass spectrum of amide 9

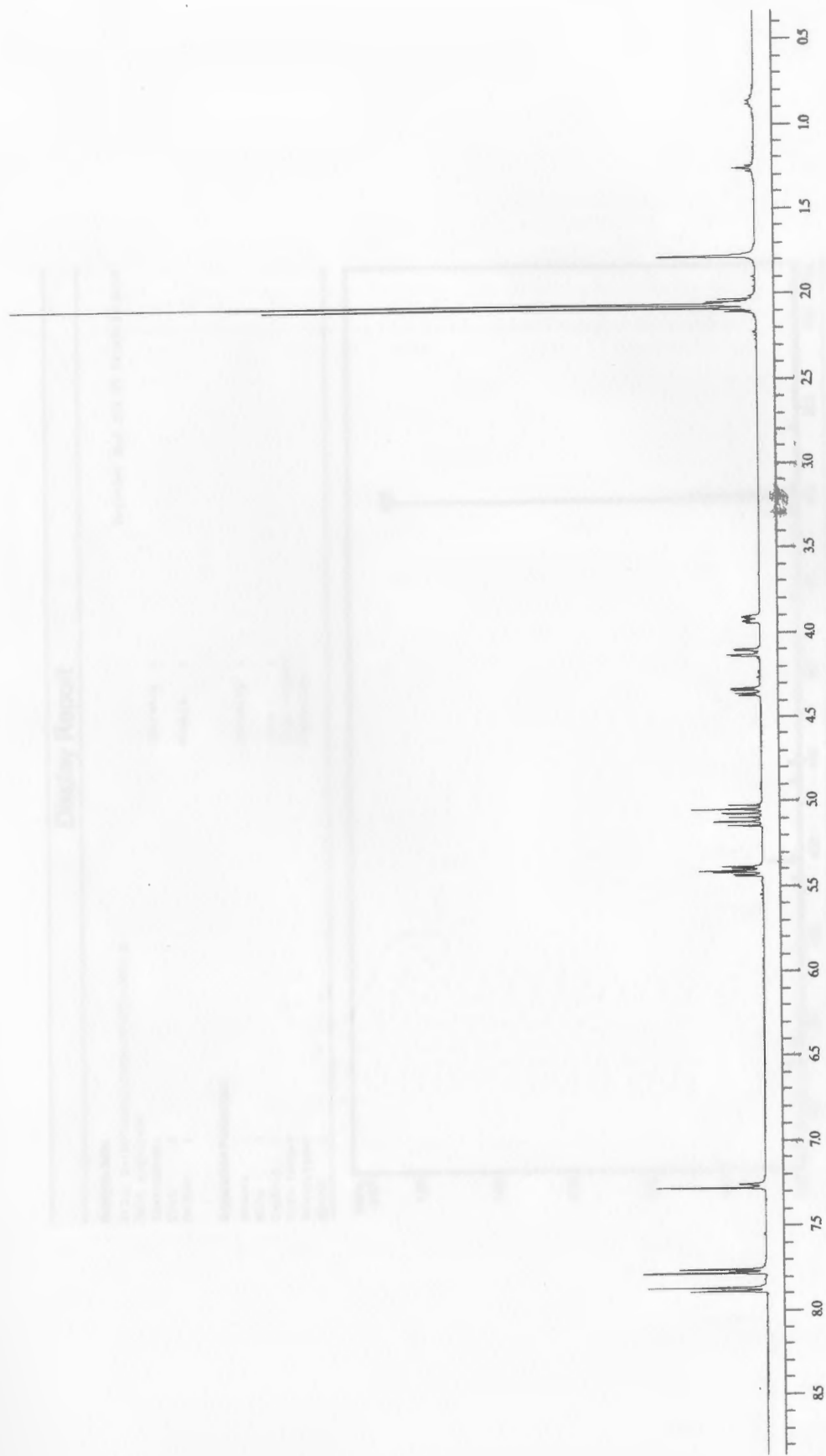


**Figure 47:** 400 MHz  $^1\text{H}$  NMR spectrum of amide 10



## Display Report

**Analysis Info:**  
 File: D:\HPCHEM\1\DATA\DT\DT7-CN01.D  
 Date acquired: Printed: Wed Jul 27 18:22:03 2005  
 Instrument:  
 Task :  
 Method :  
**Acquisition Parameter:**  
 Source :  
 Mode :  
 CapExit :  
 Scan Range:  
 Accum.time:  
 MS/MS :  
 Operator :  
 Sample :  
 Polarity :  
 Skim 1 :  
 Trap Drive:  
 Summation :

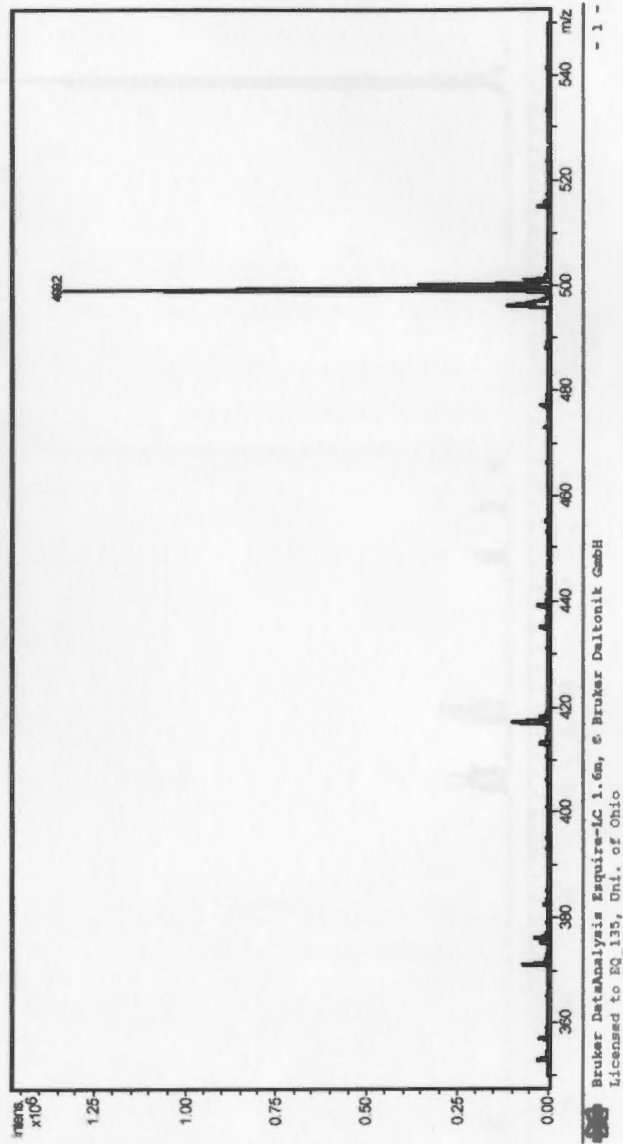


**Figure 48:** Low resolution mass spectrum of amide 10

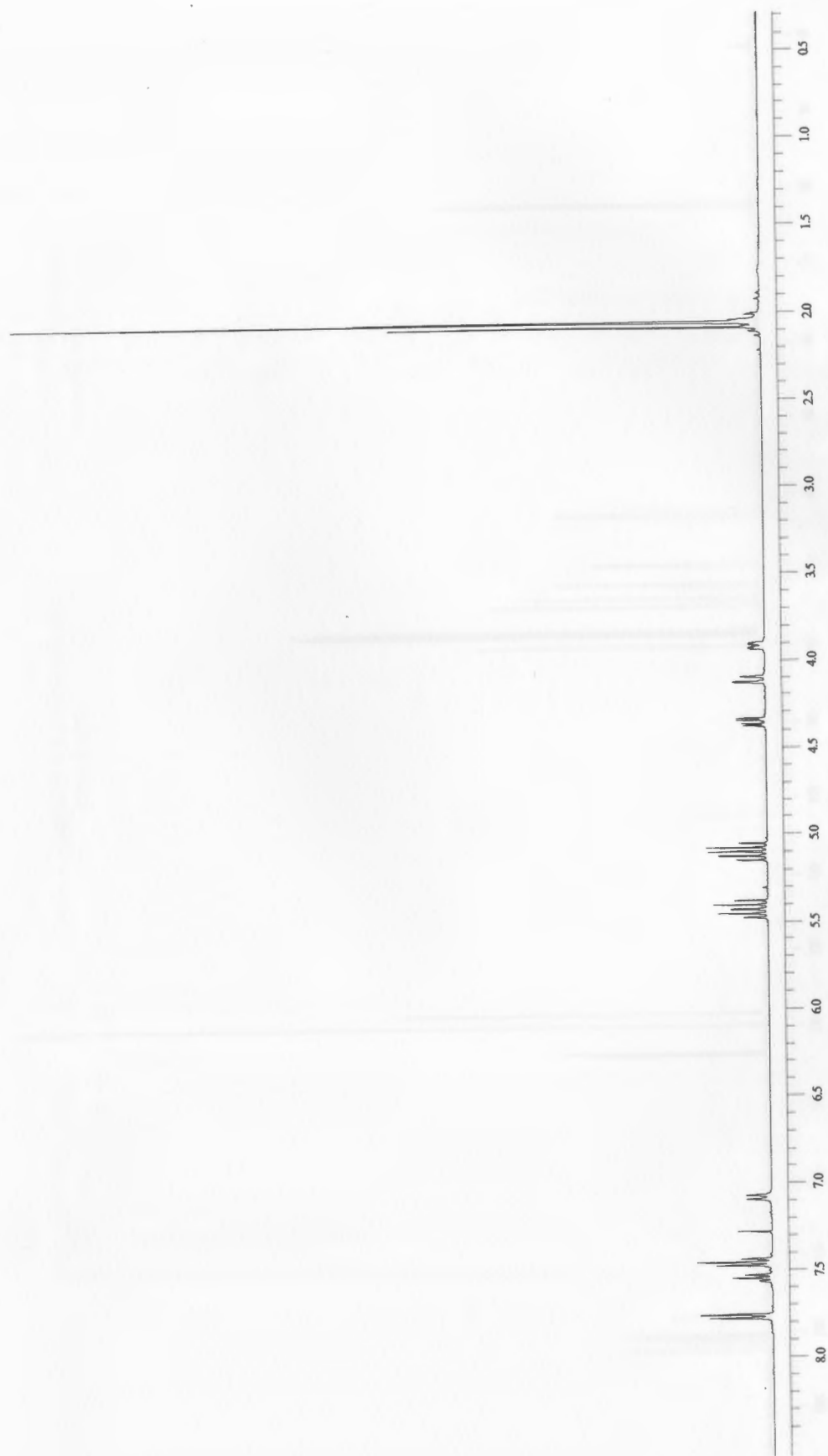


**Figure 49:** 400 MHz  $^1\text{H}$  NMR spectrum of amide 11

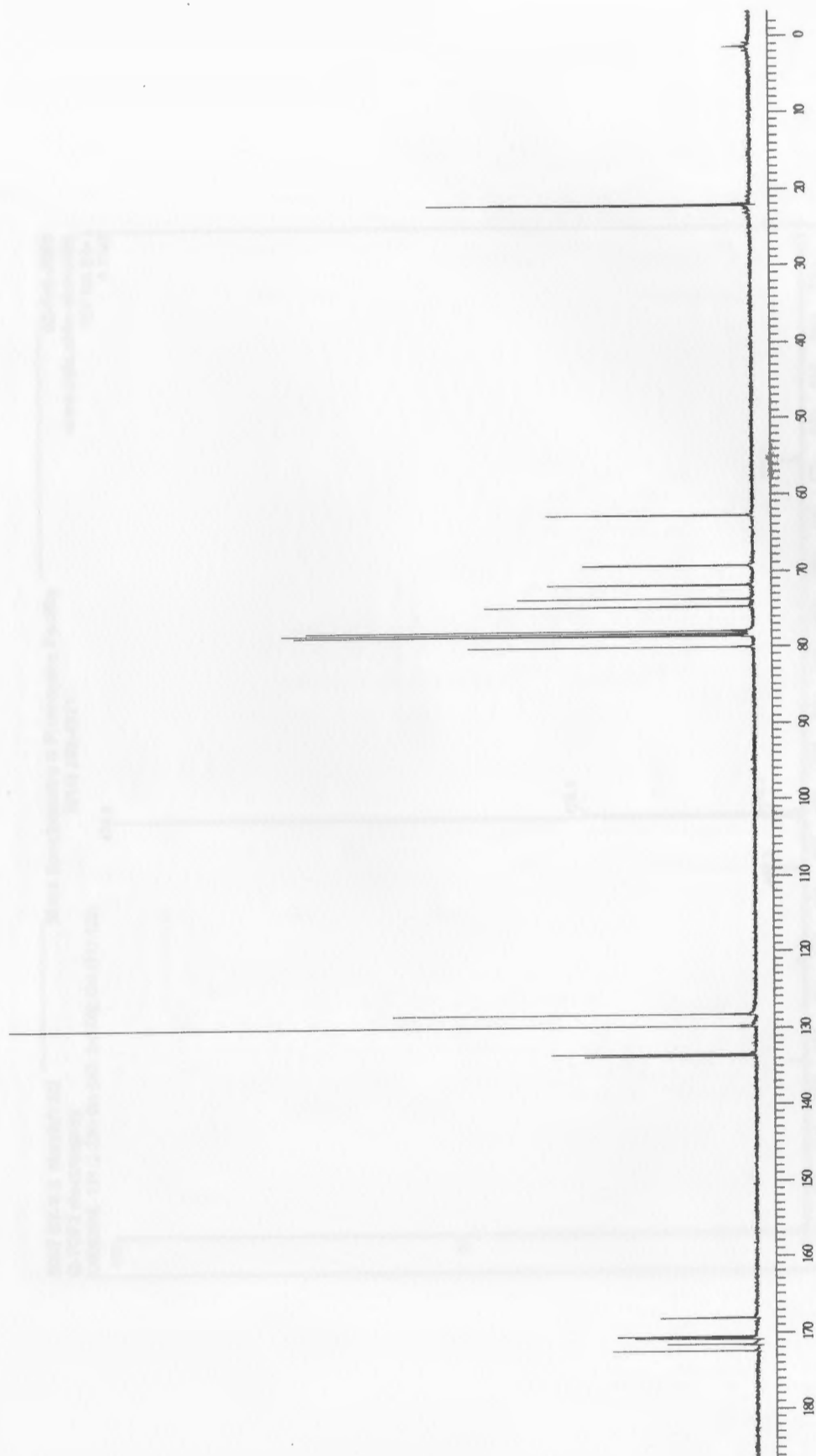


**Figure 50:** 100 MHz  $^{13}\text{C}$  NMR spectrum of amide 11

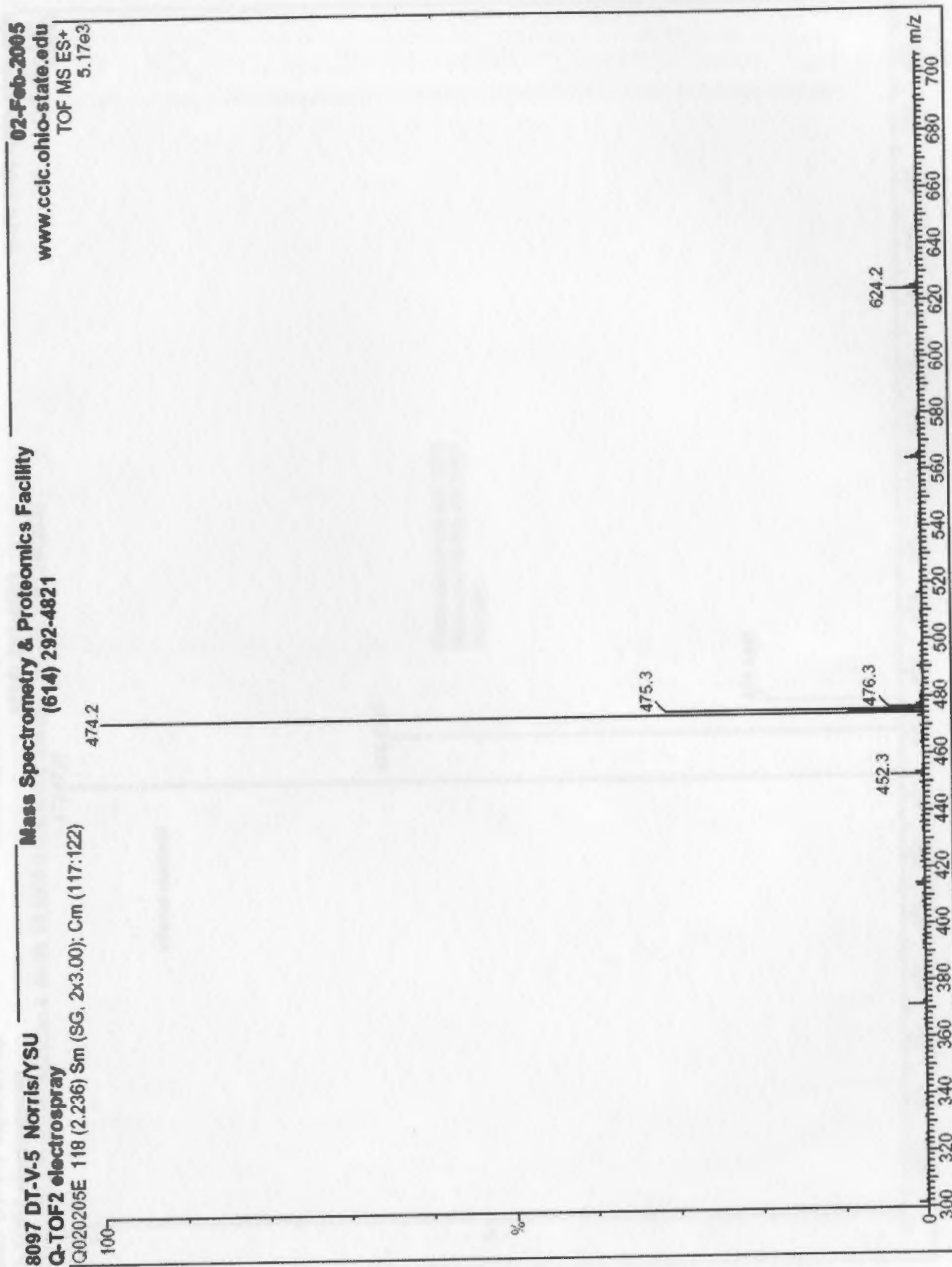


Figure 51: Low resolution mass spectrum of amide 11

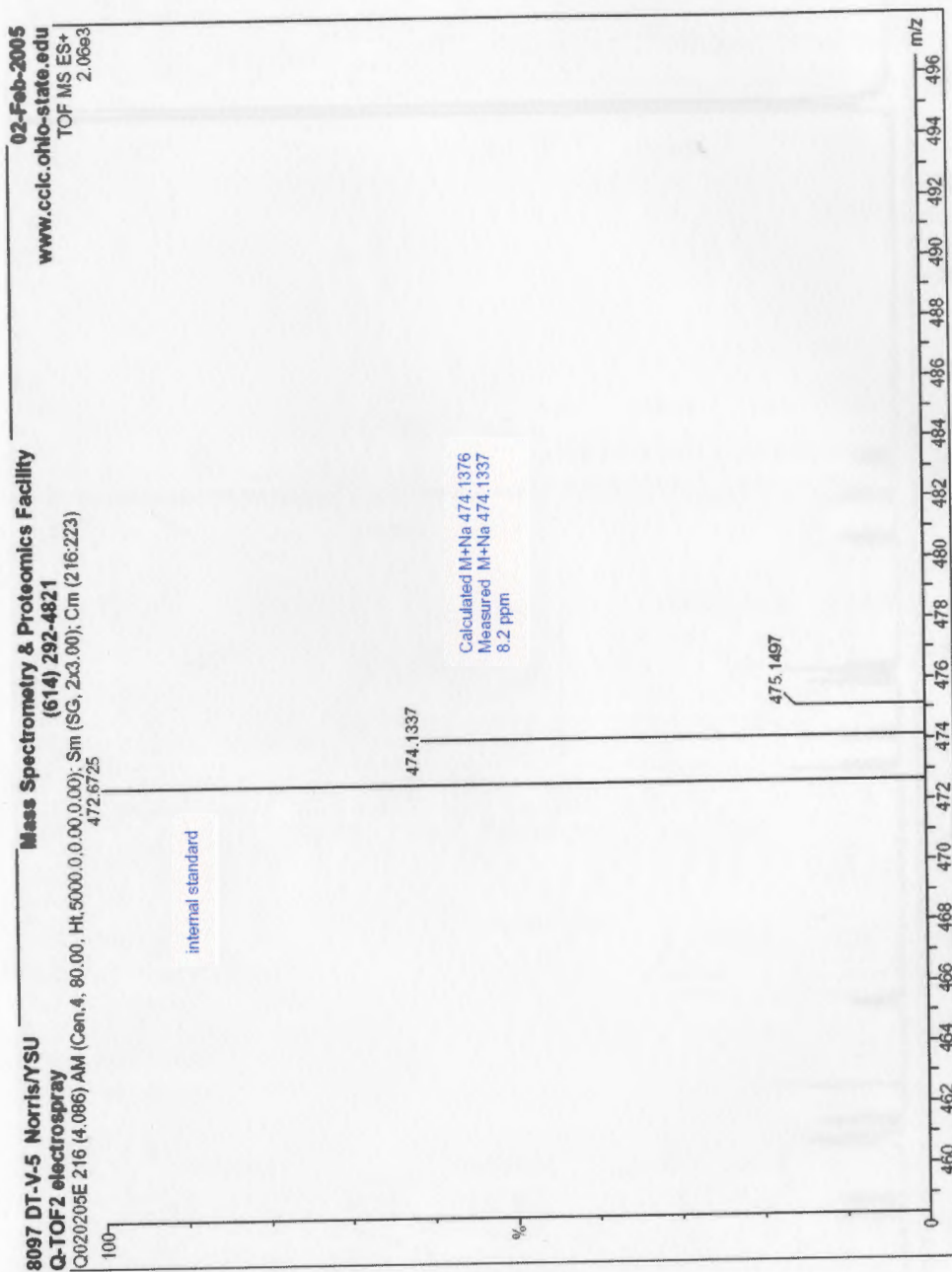
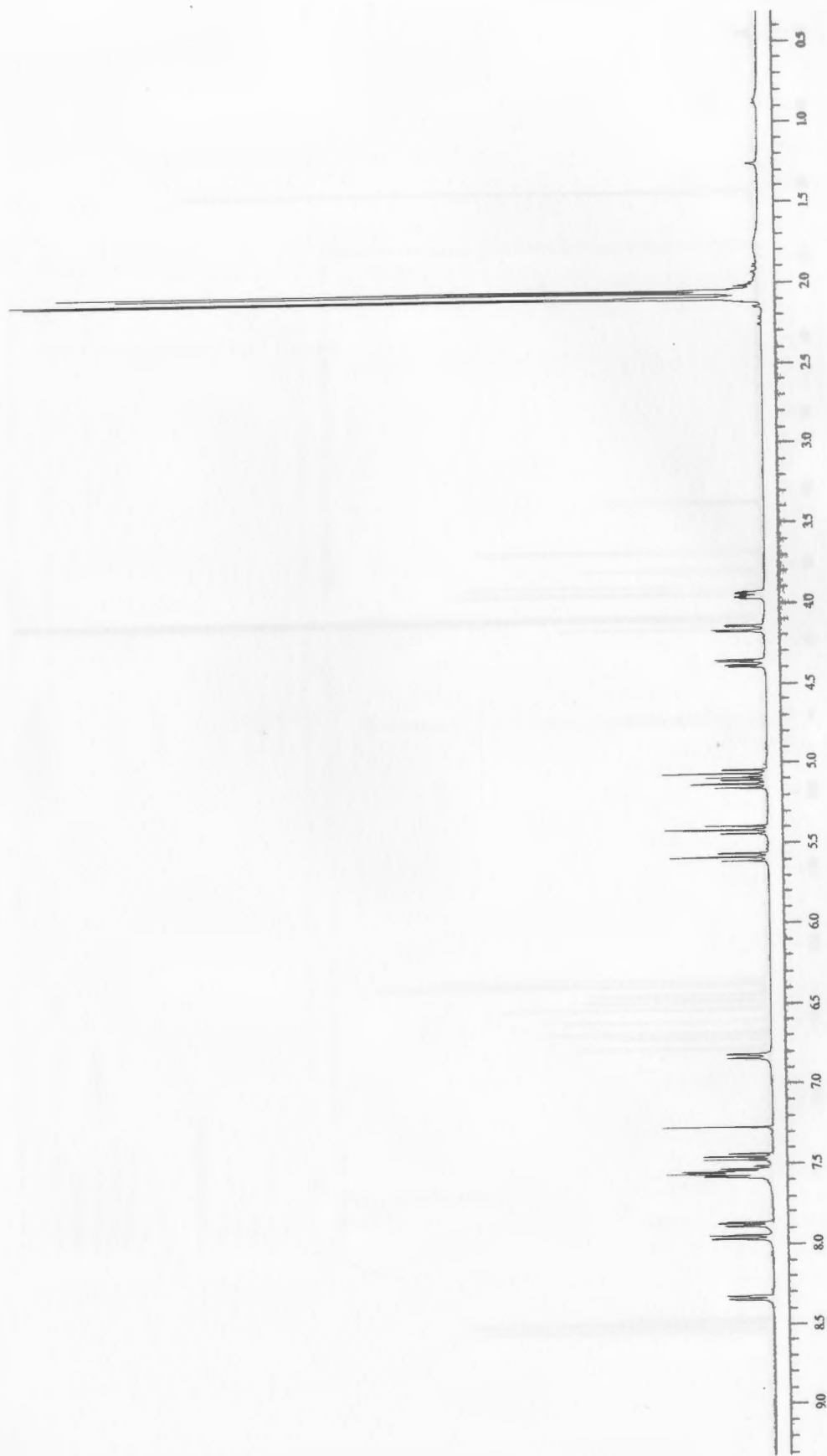
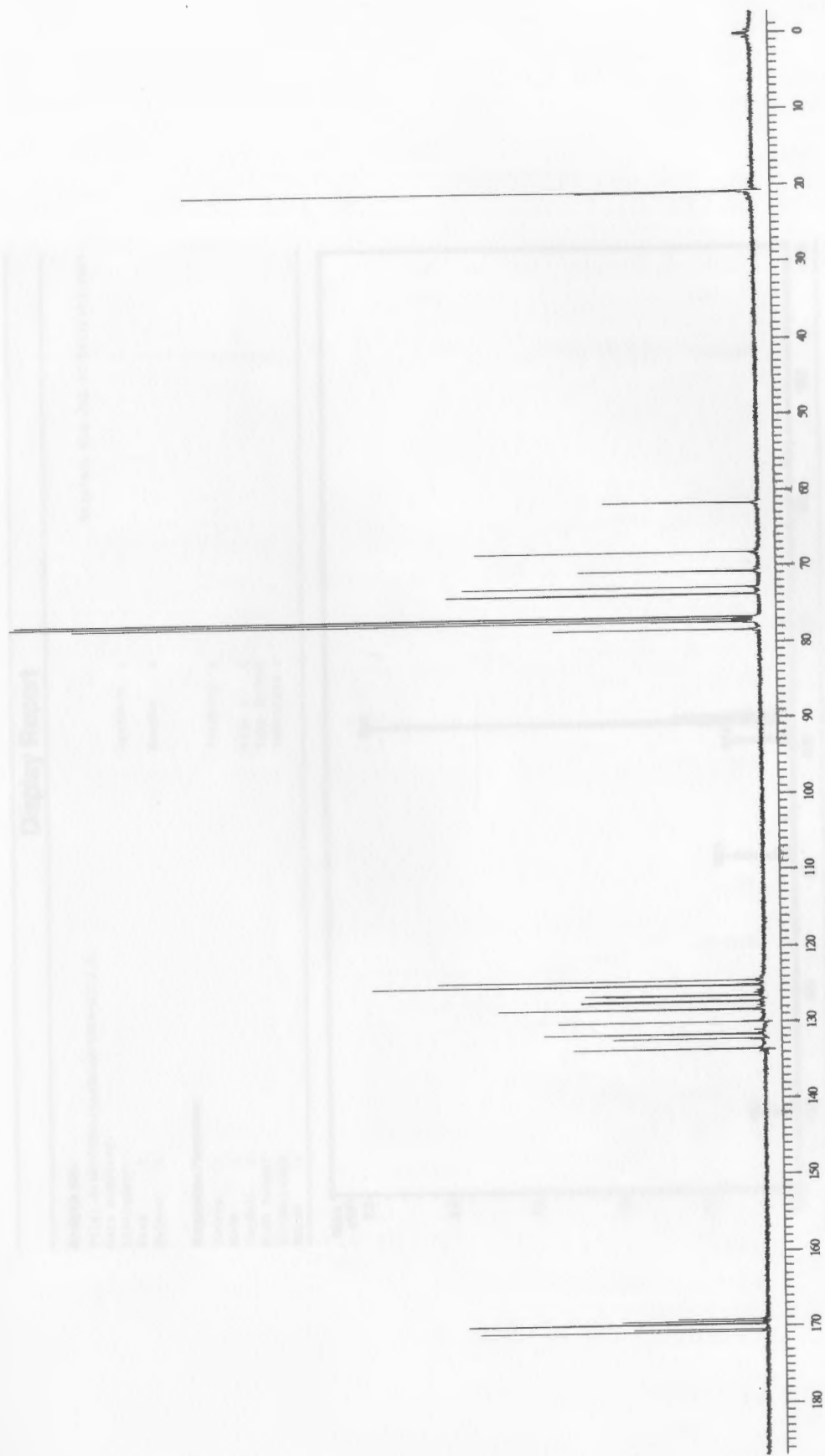


Figure S2: High resolution mass spectrum of amide 11



**Figure 53:** 400 MHz  $^1\text{H}$  NMR spectrum of amide 12



**Figure 54:** 100 MHz  $^{13}\text{C}$  NMR spectrum of amide 12

## Display Report

**Analysis Info:**  
 File: D:\HECHEM\1\DATA\DT6-1013.D  
 Date acquired: Wed Jul 27 18:22:50 2005  
 Instrument:  
 Task :  
 Method :  
 Operator :  
 Sample :  
 Polarity :  
 Skim 1 :  
 Trap Drive:  
 Summation :

**Acquisition Parameter:**  
 Source :  
 Mode :  
 CapExit :  
 Scan Range:  
 Accum.time:  
 MS/MS :

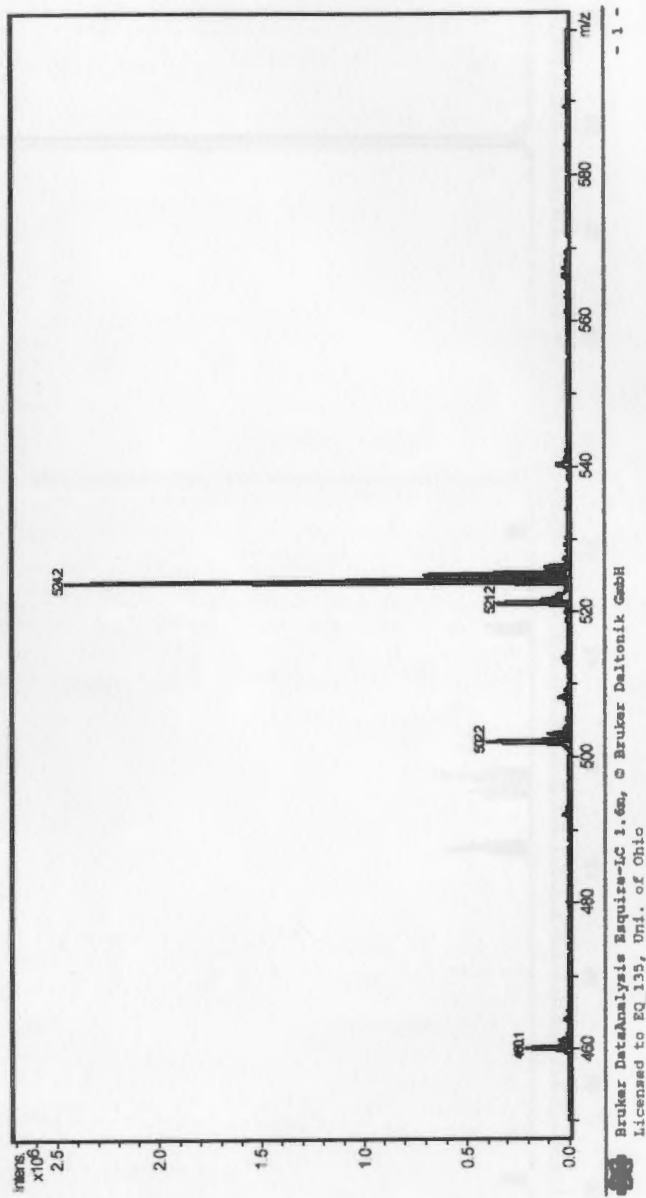
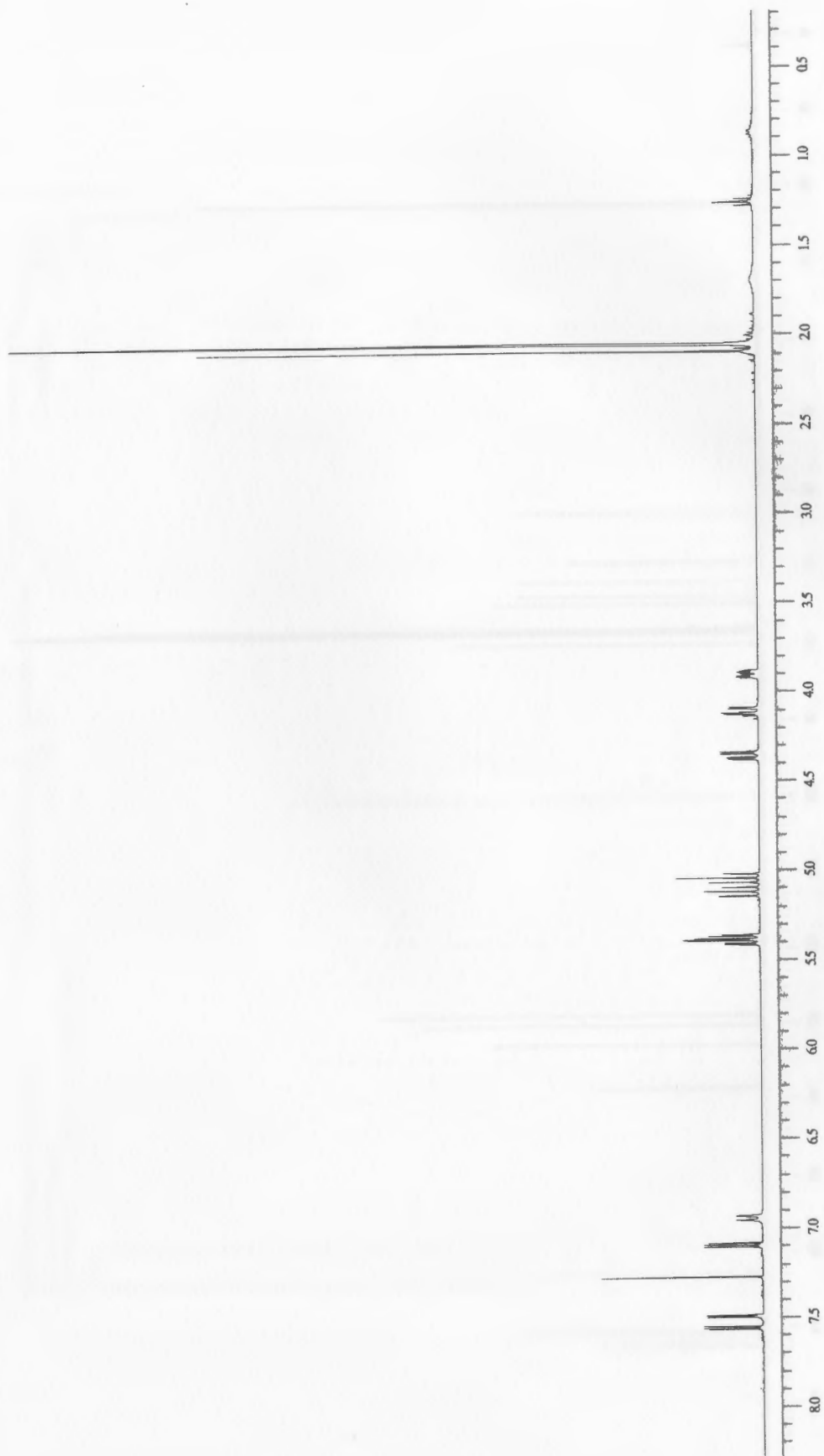


Figure 55: Low resolution mass spectrum of amide 12





**Figure 56:** 400 MHz  $^1\text{H}$  NMR spectrum of amide 13

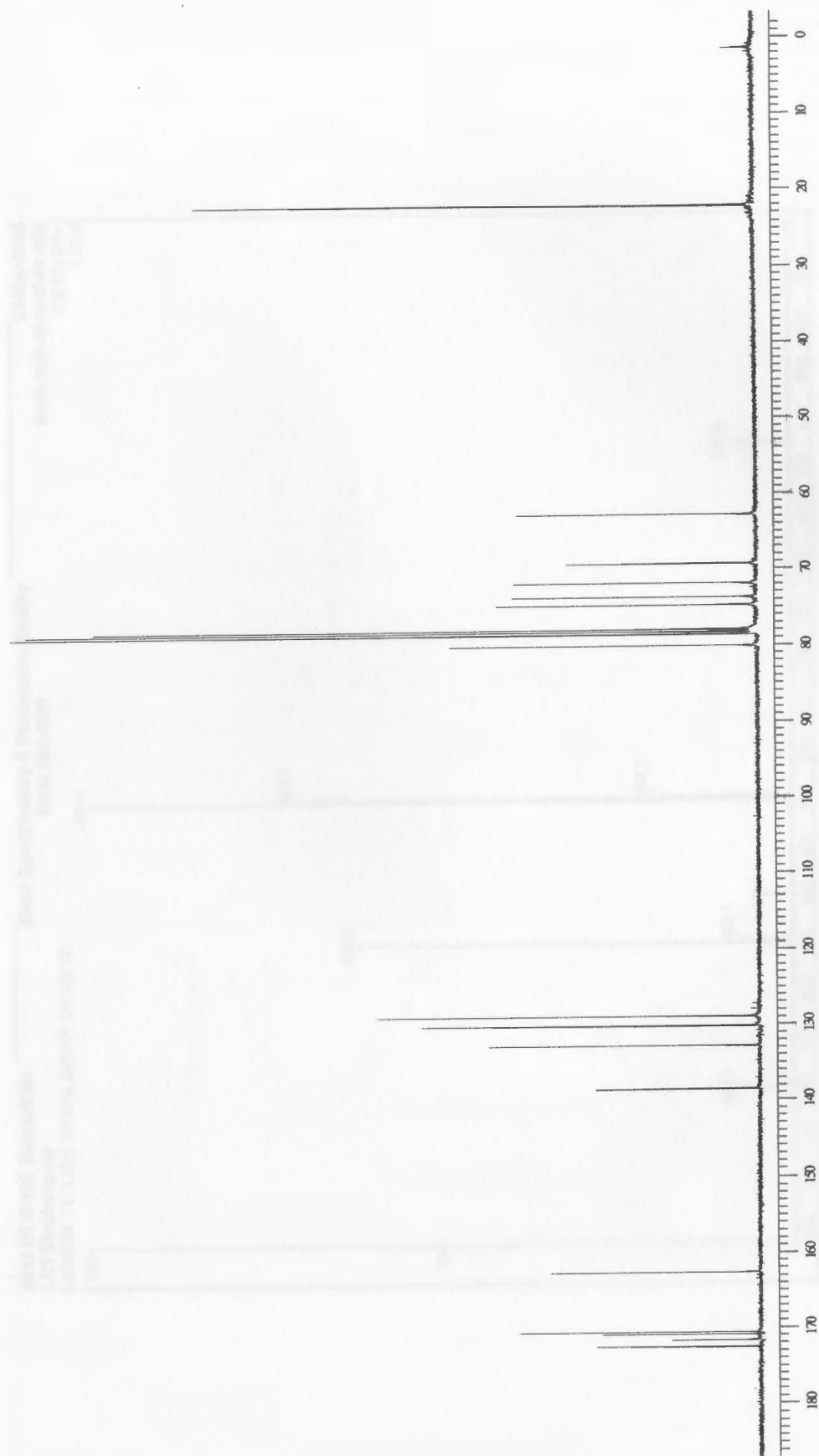


Figure 57: 100 MHz  $^{13}\text{C}$  NMR spectrum of amide 13

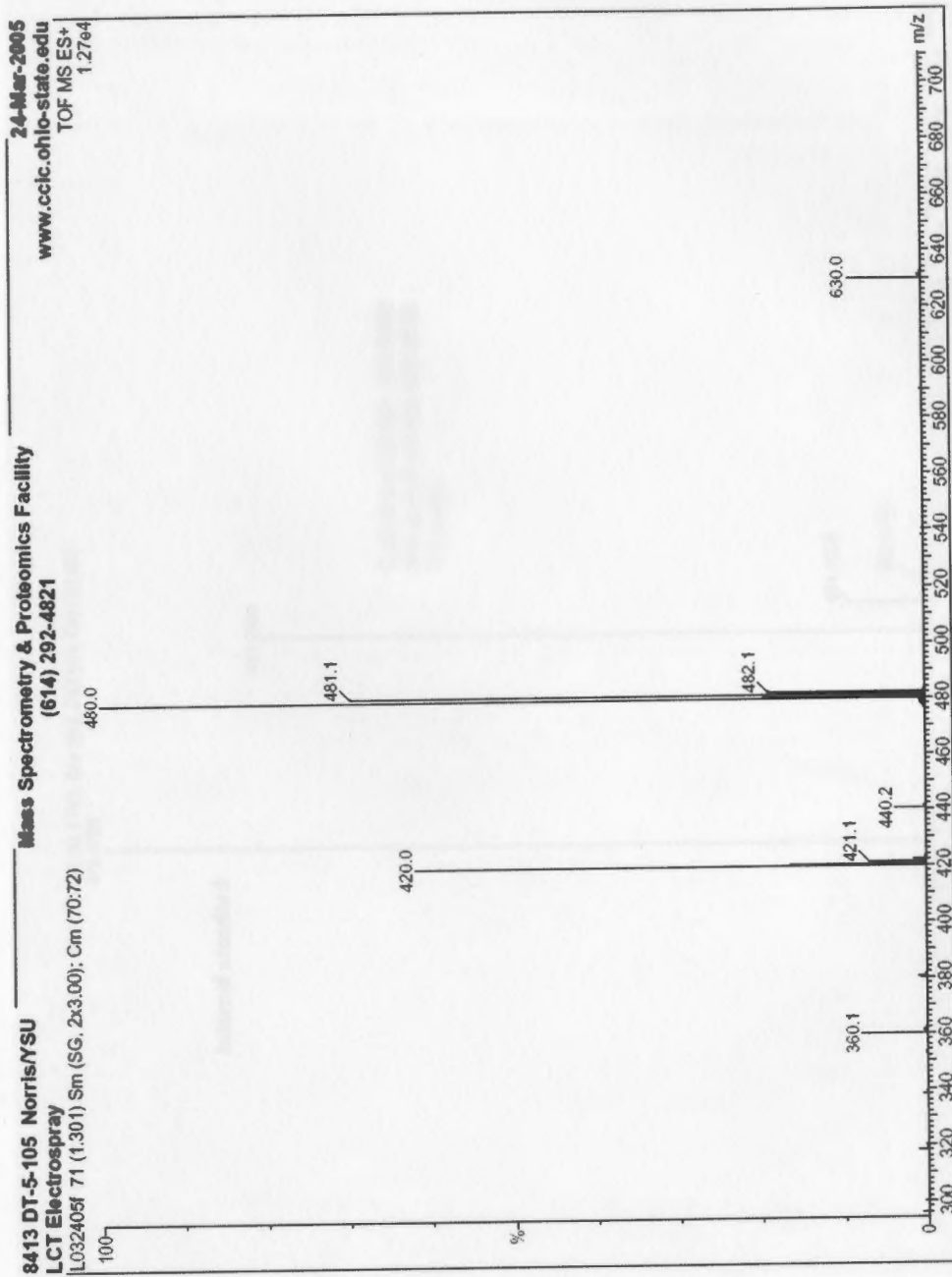


Figure 58: Low resolution mass spectrum of amide 13

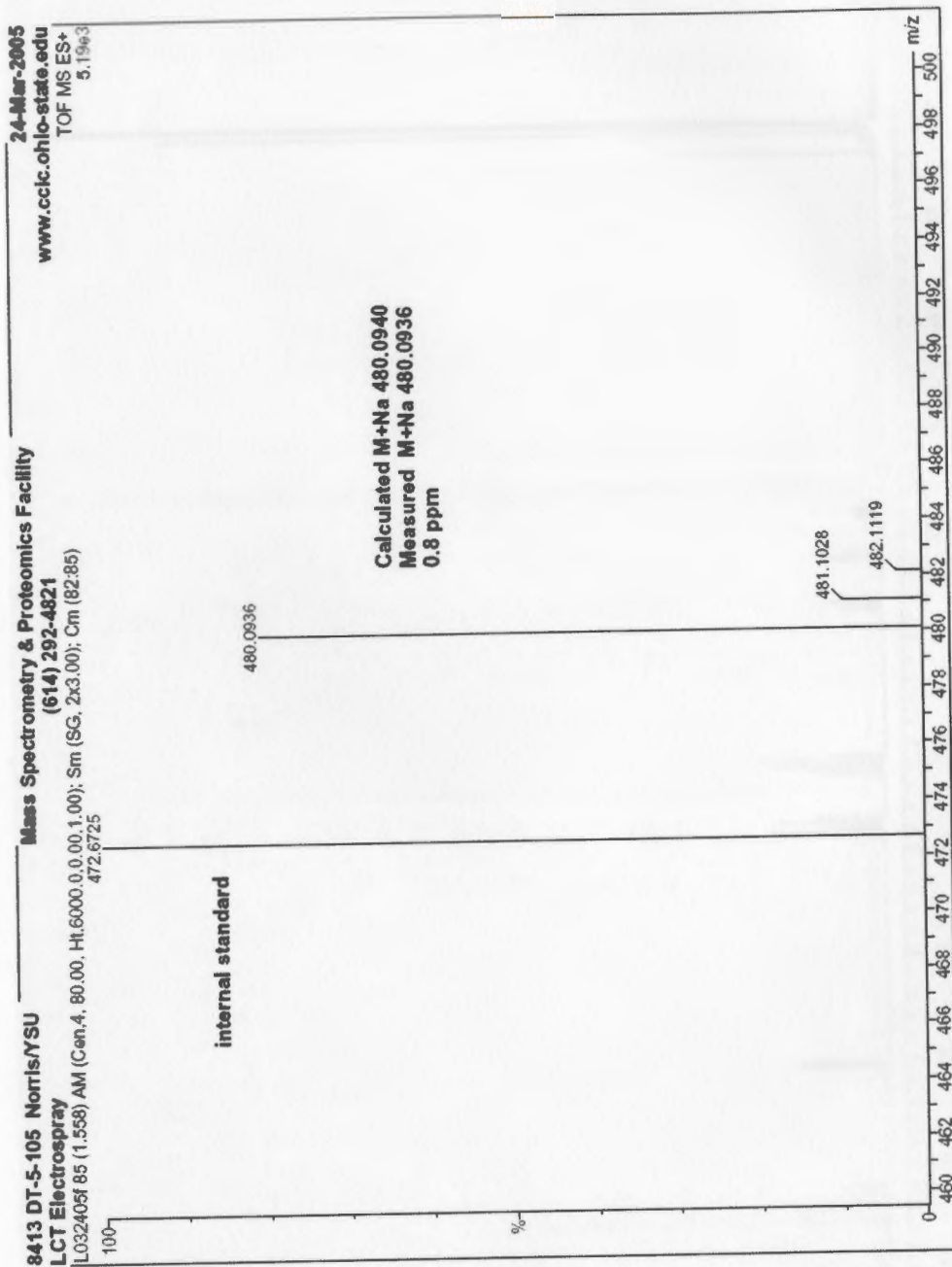
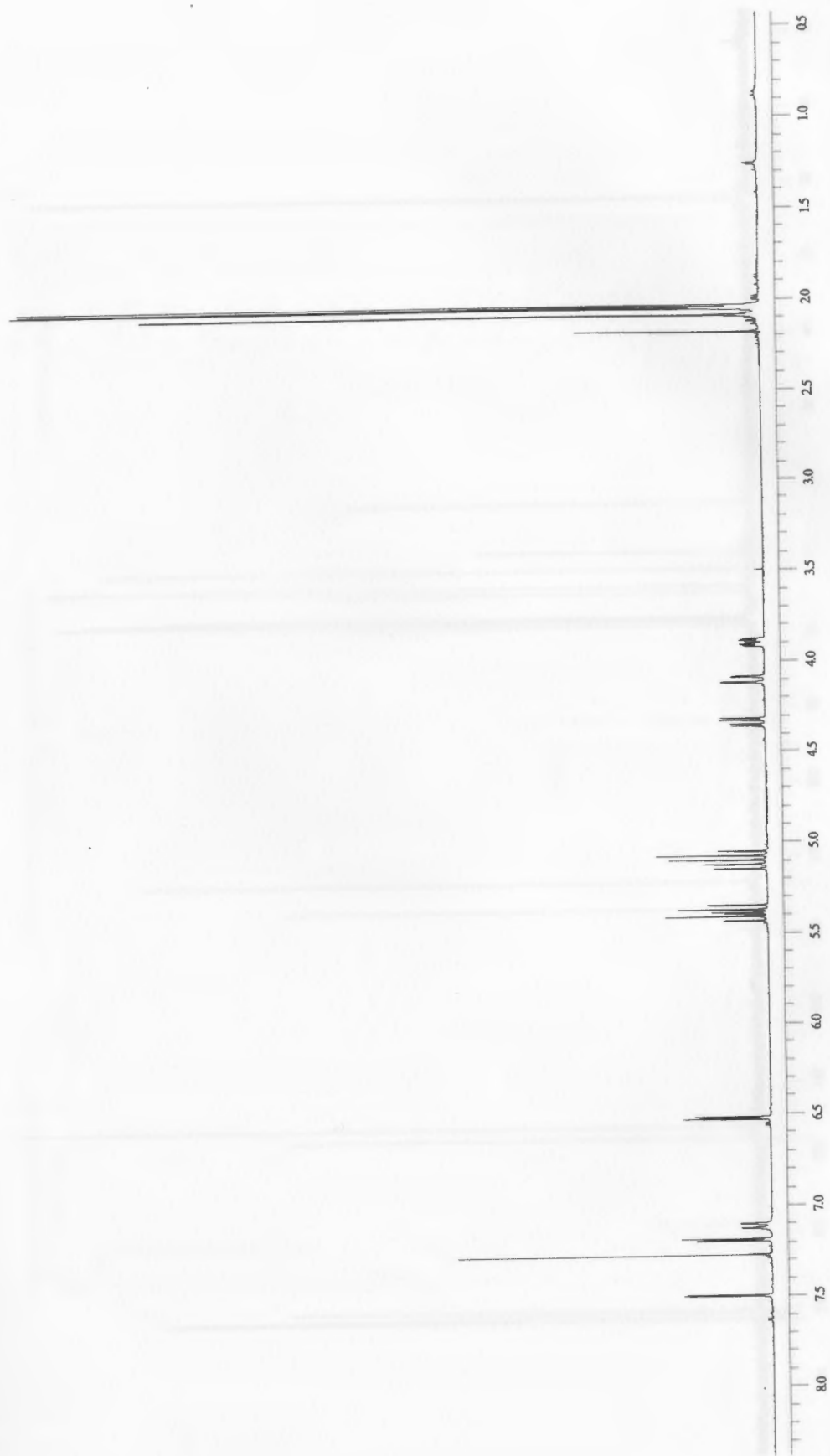
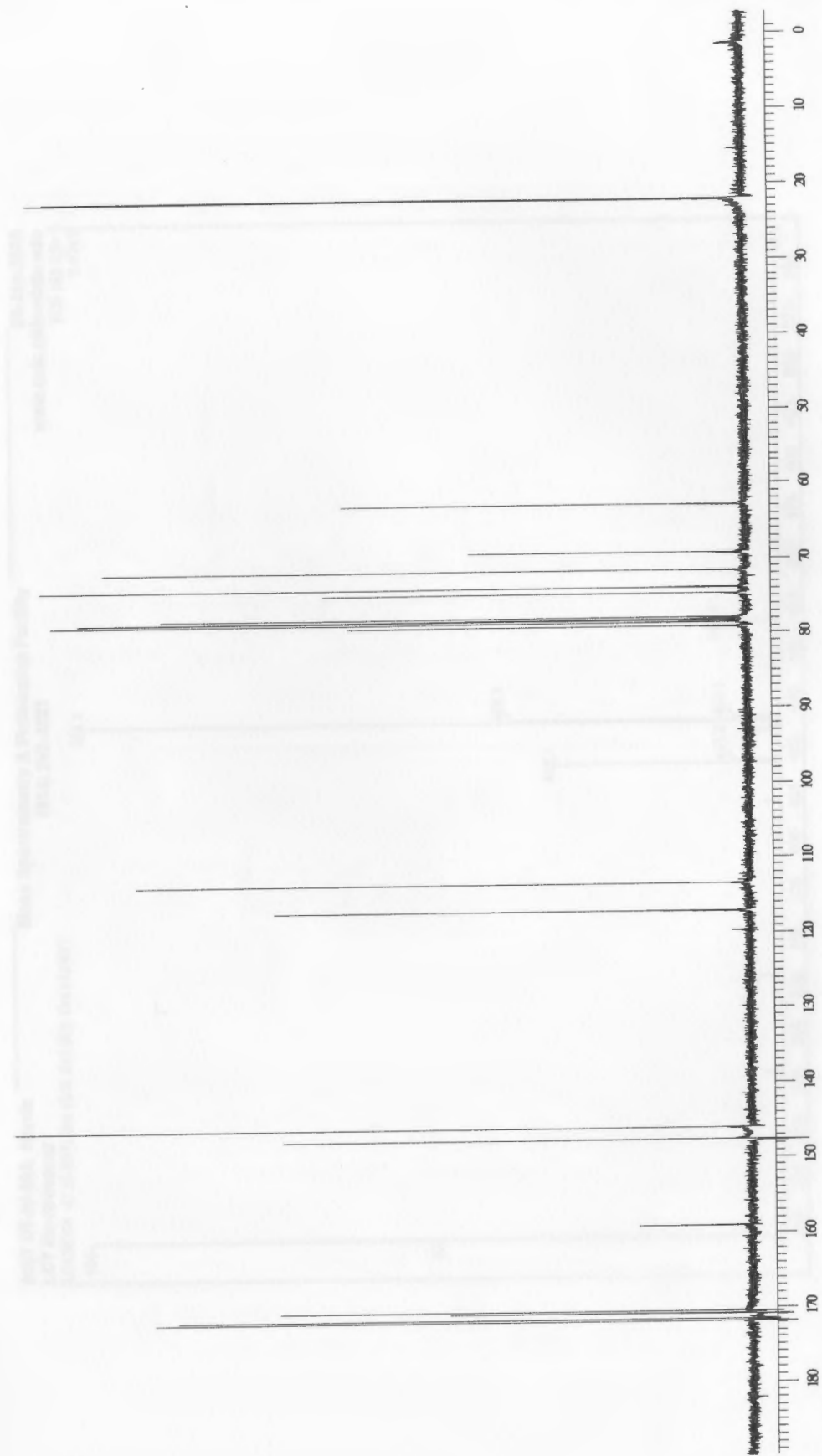


Figure 59: High resolution mass spectrum of amide 13



**Figure 60:** 400 MHz  $^1\text{H}$  NMR spectrum of amide 14



**Figure 61:** 100 MHz  $^{13}\text{C}$  NMR spectrum of amide 14

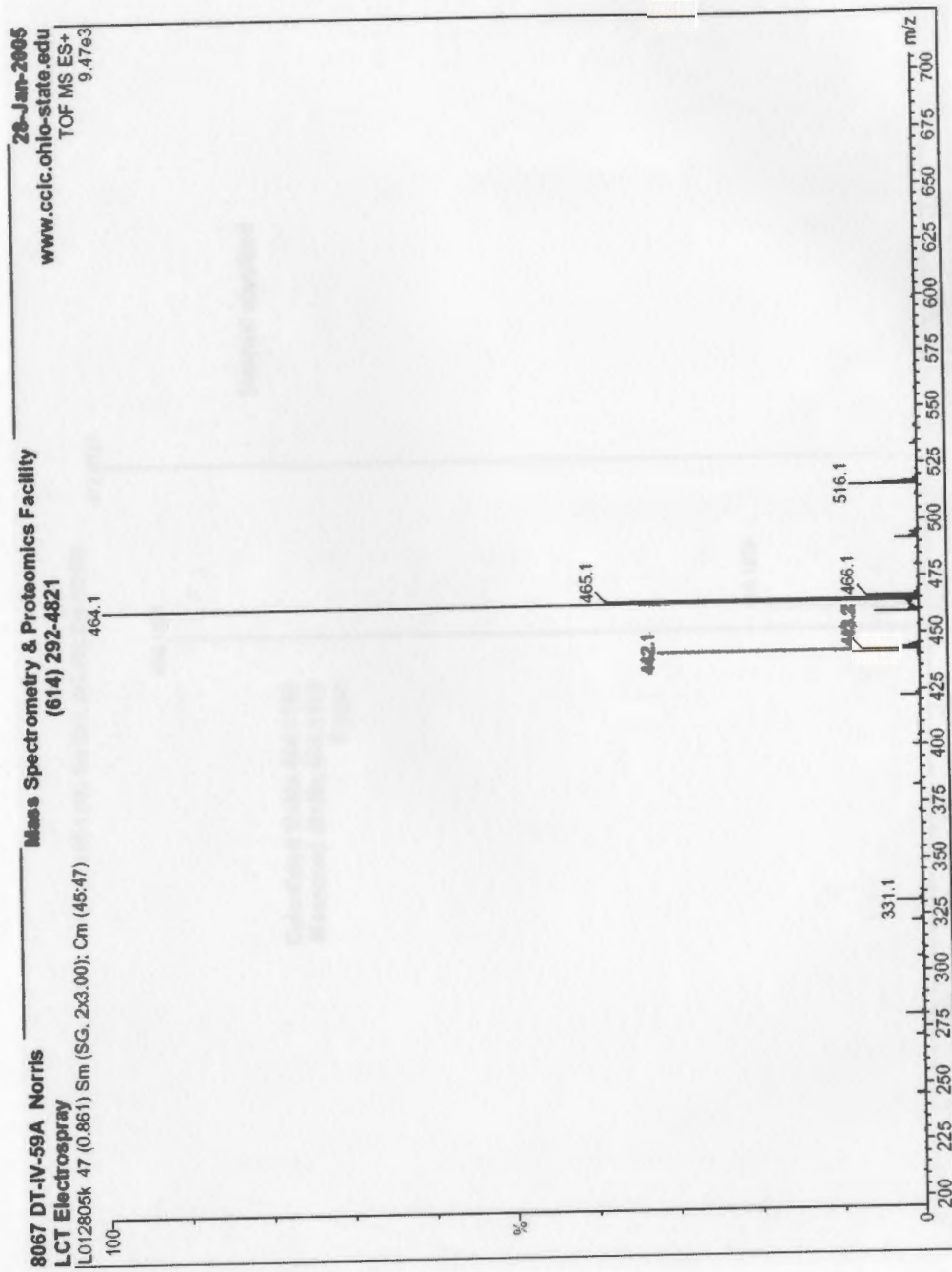


**Figure 62:** Low resolution mass spectrum of amide 14

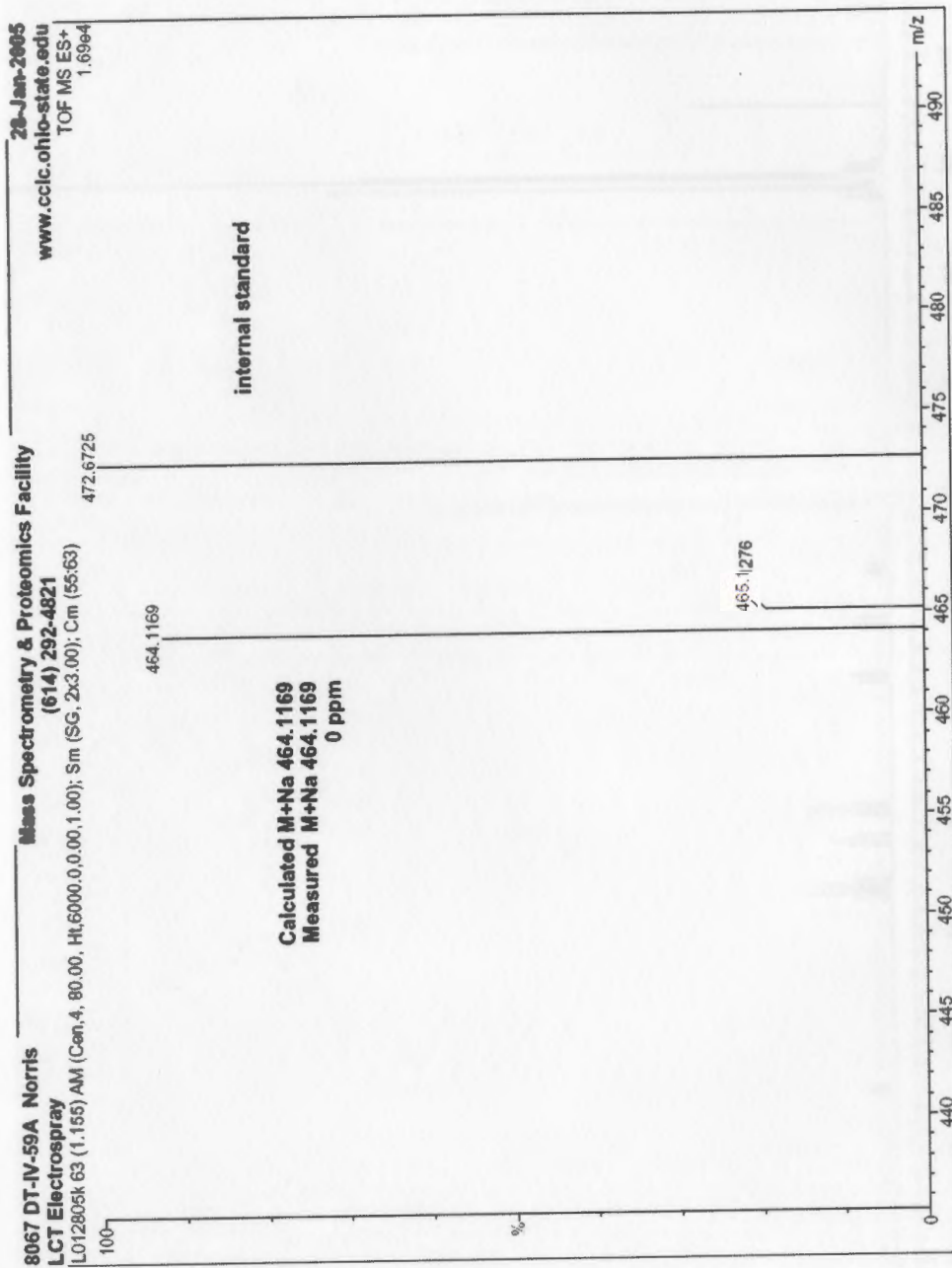


Figure 63: High resolution mass spectrum of amide 14





**Figure 64:** 400 MHz  $^1\text{H}$  NMR spectrum of amide 15

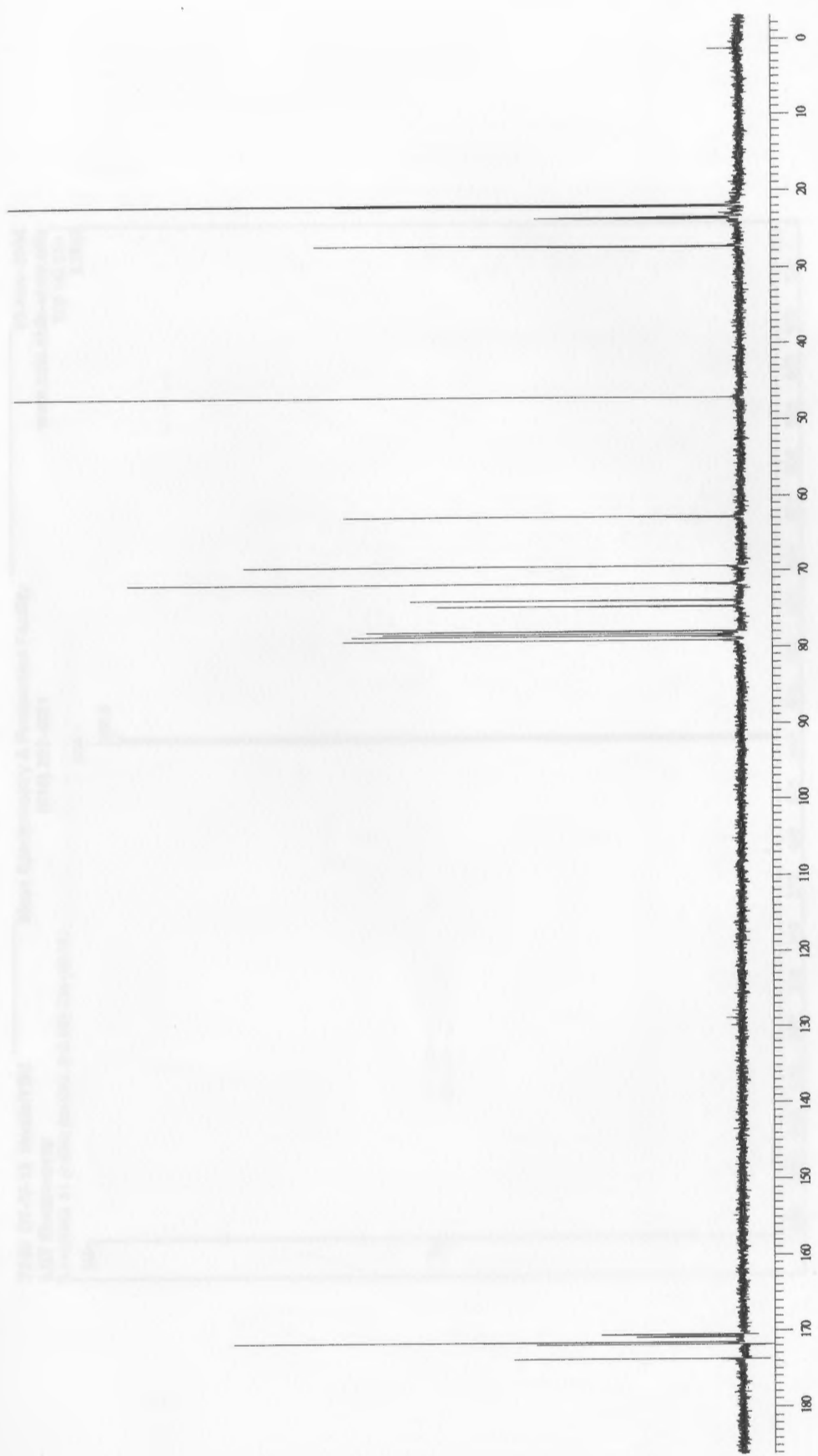
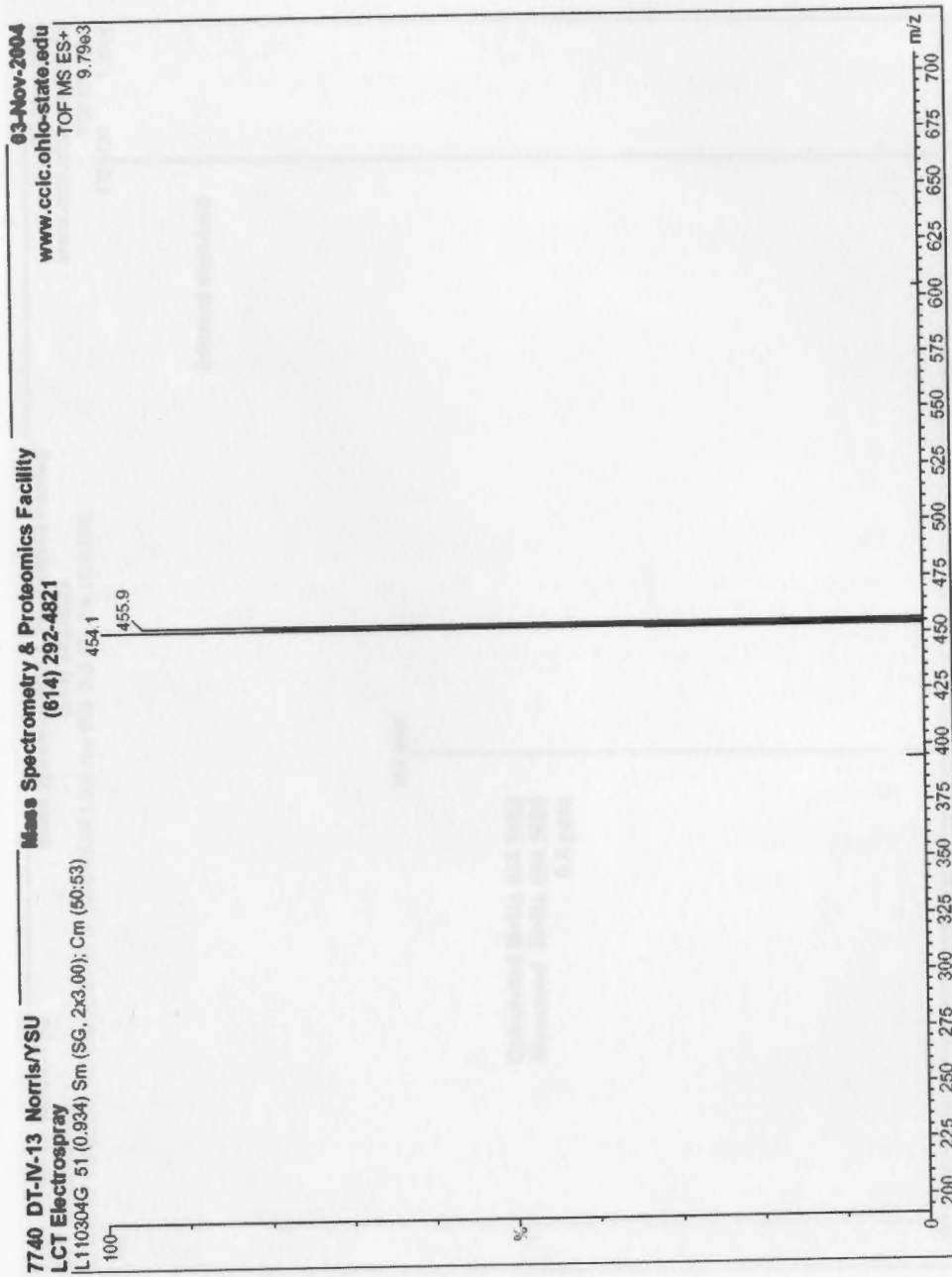


Figure 65: 100 MHz  $^{13}\text{C}$  NMR spectrum of amide 15



**Figure 66:** Low resolution mass spectrum of amide 15

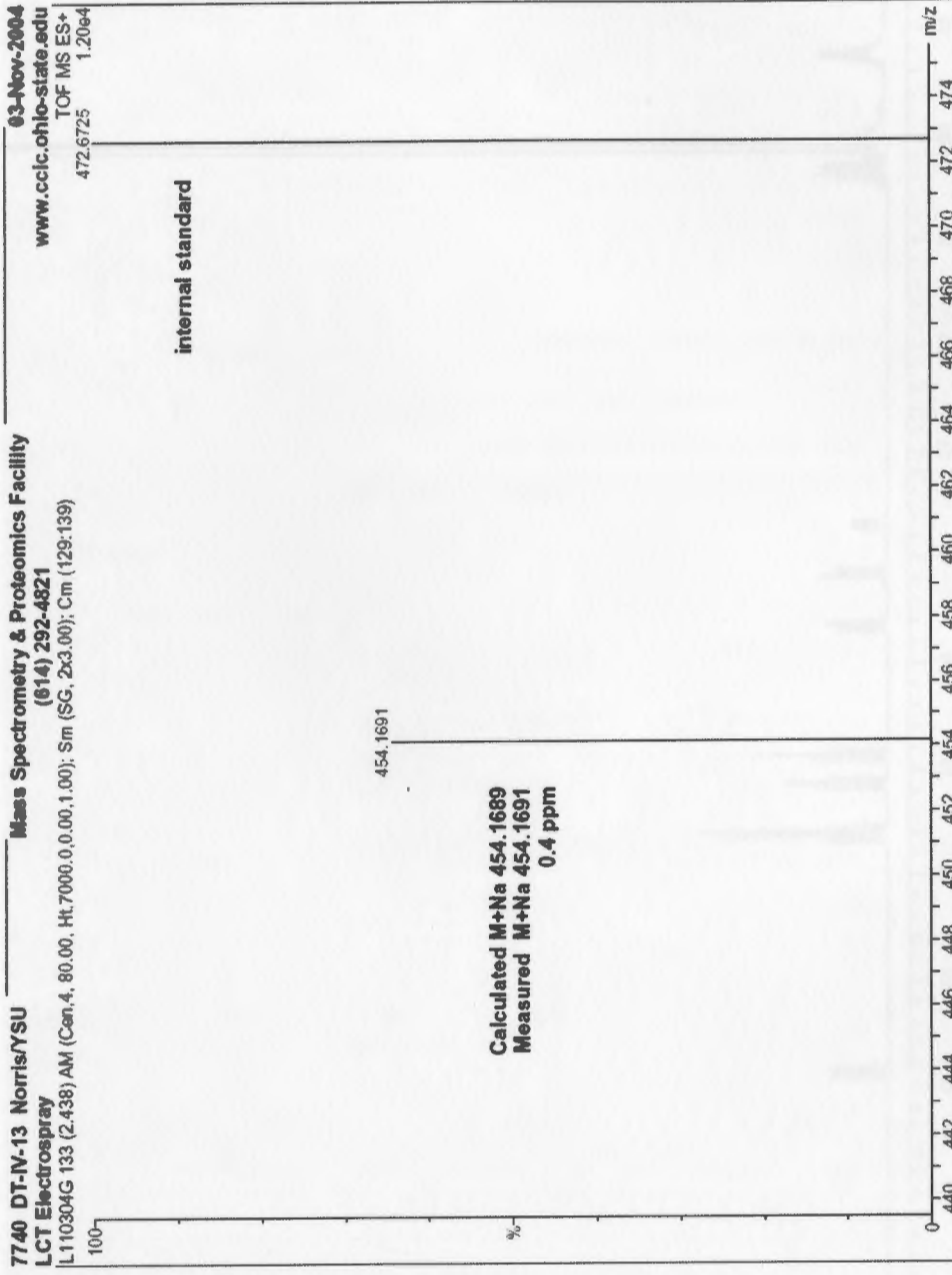
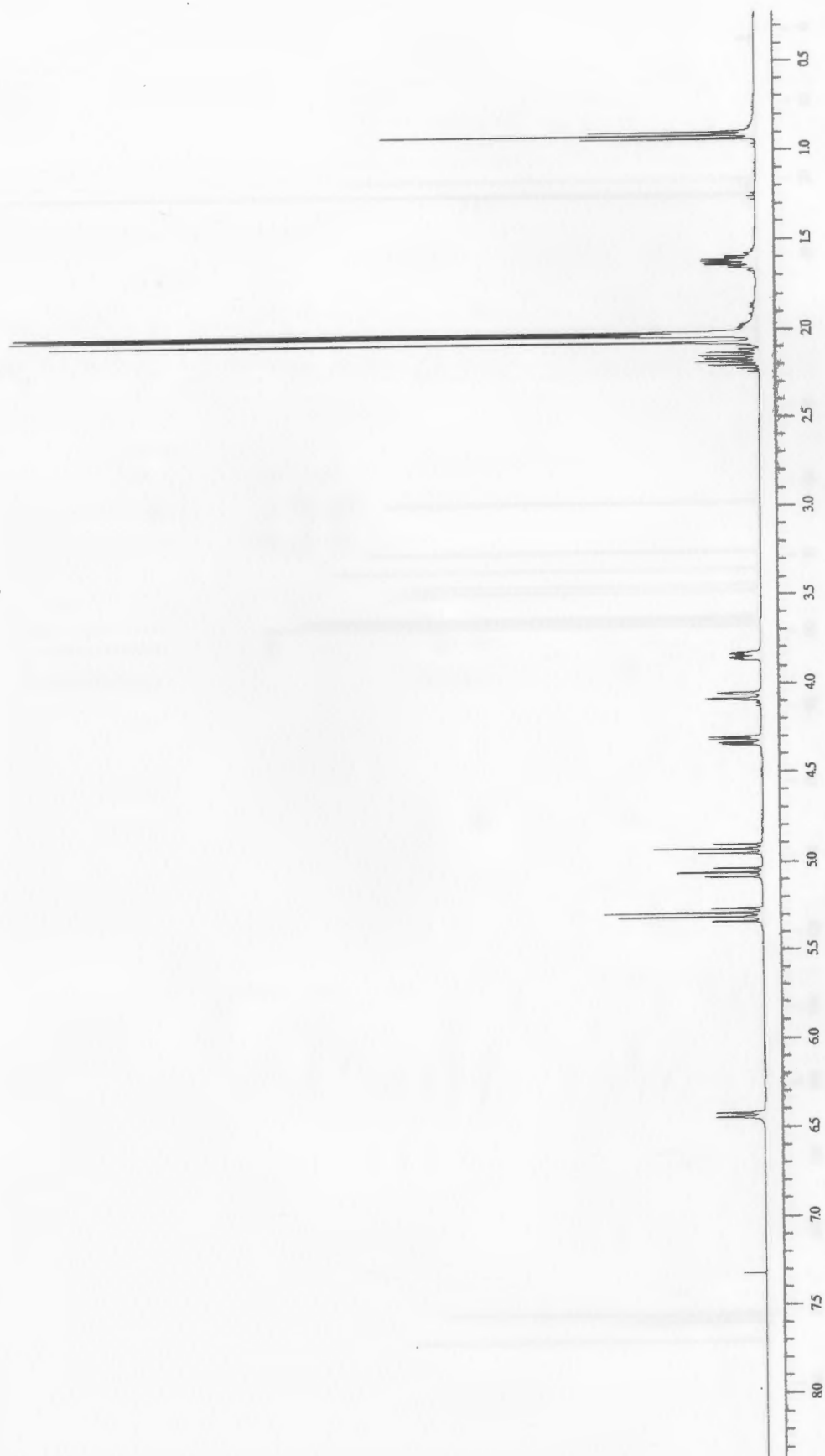
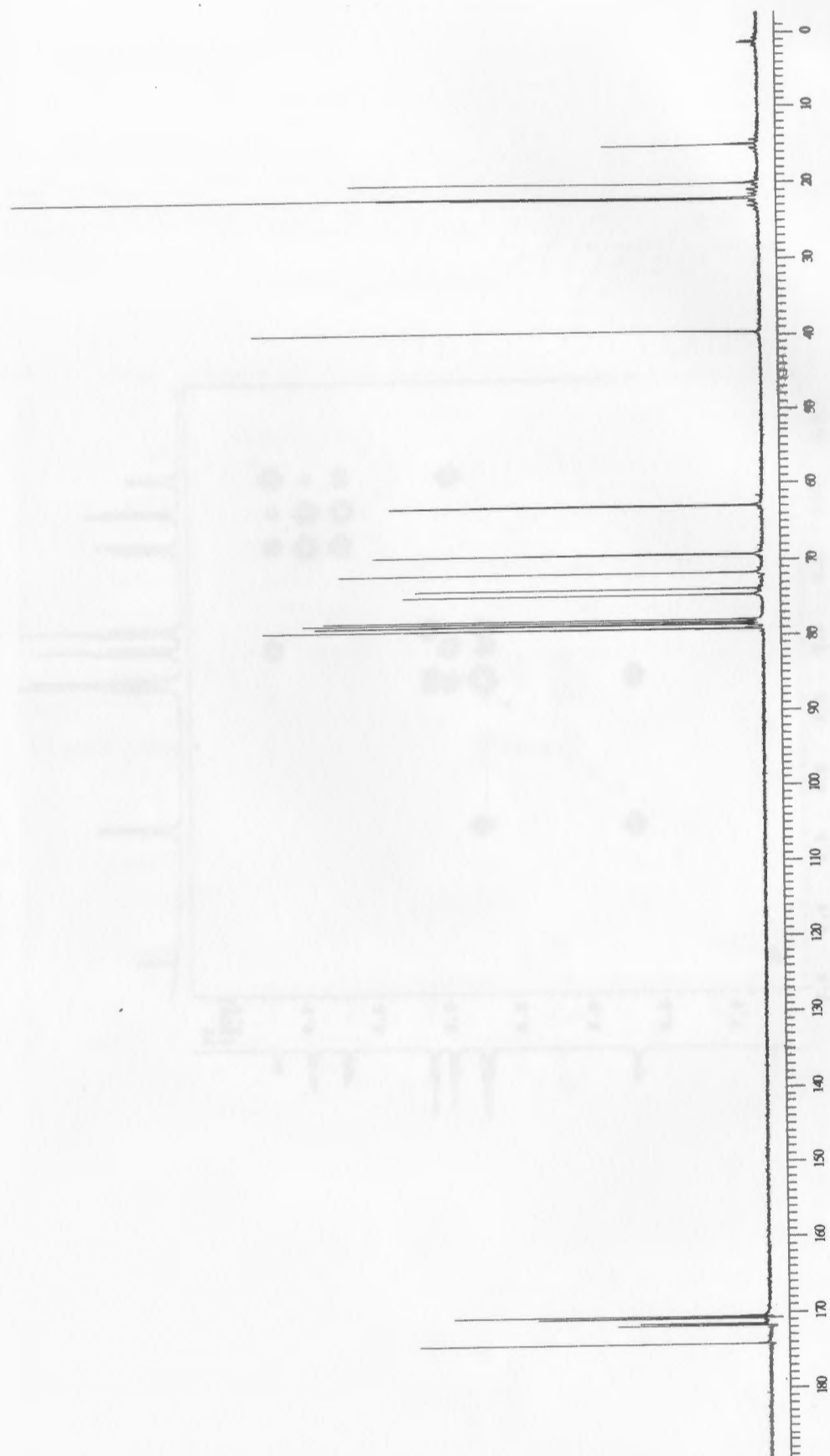


Figure 67: High resolution mass spectrum of amide 15



**Figure 68:** 400 MHz  $^1\text{H}$  NMR spectrum of amide 16



**Figure 69:** 100 MHz  $^{13}\text{C}$  NMR spectrum of amide 16

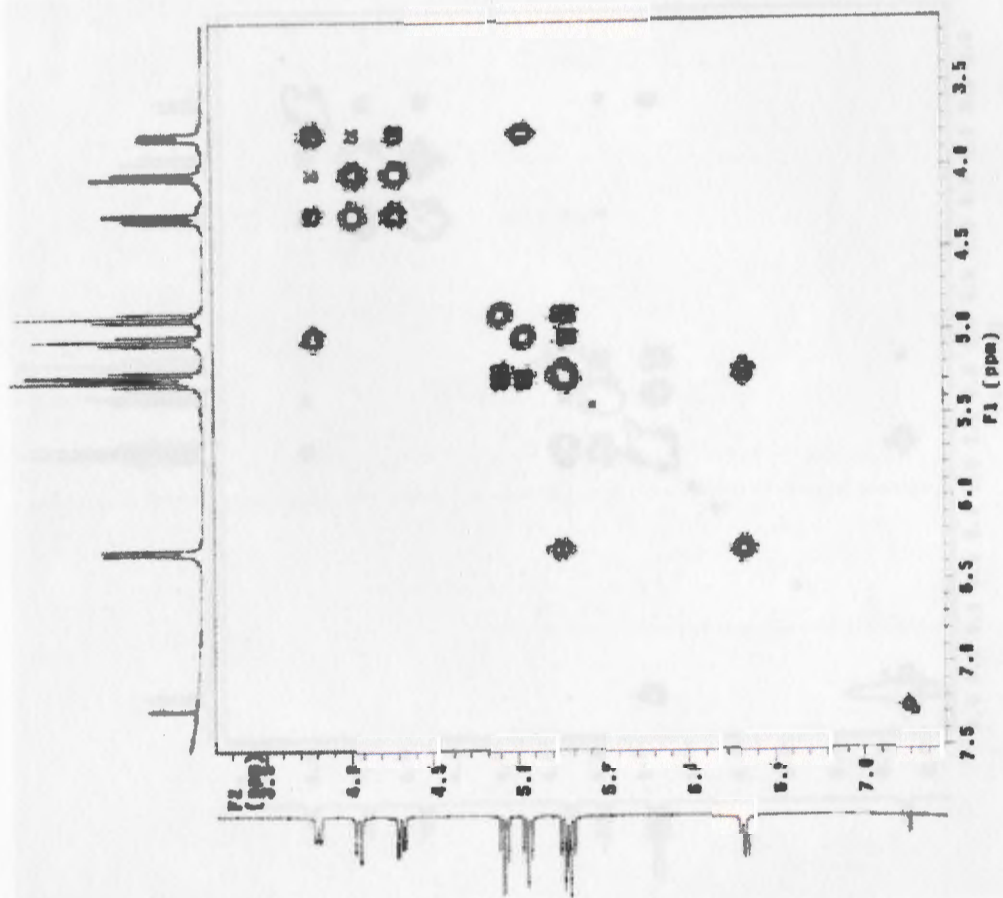
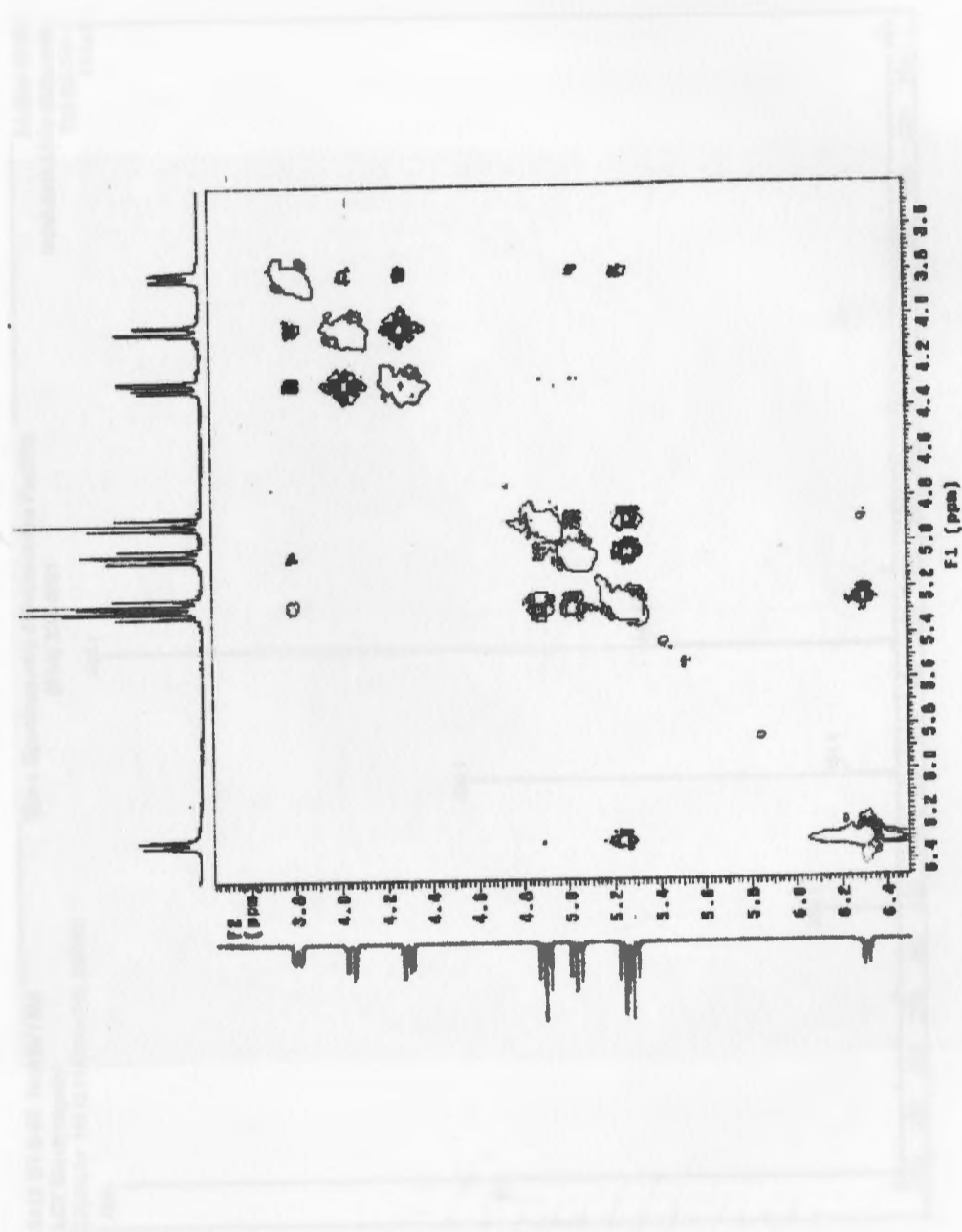


Figure 70: COSY spectrum of amide 16

Figure 71:  $n\text{Oe}$  spectrum of amide 16



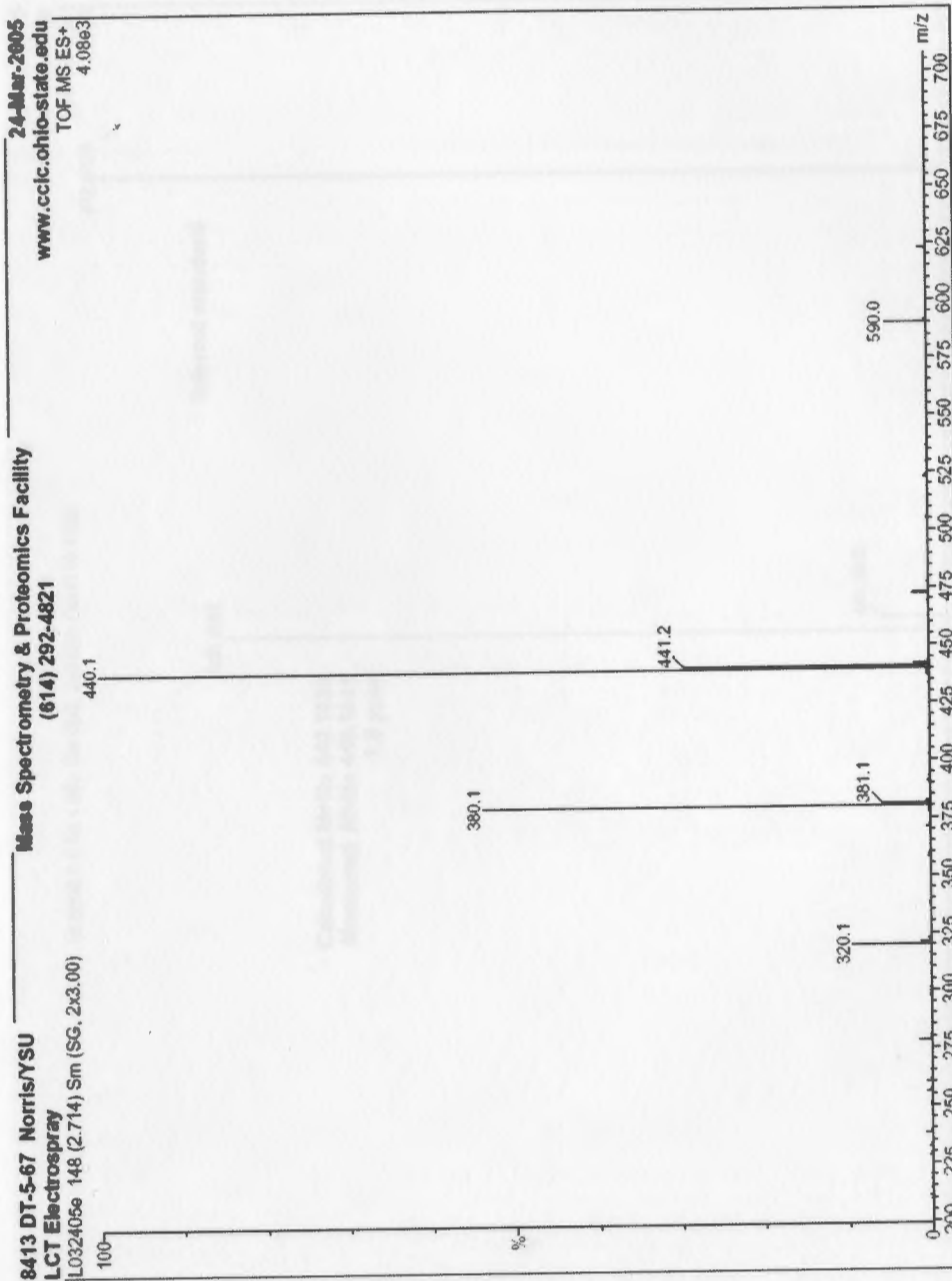
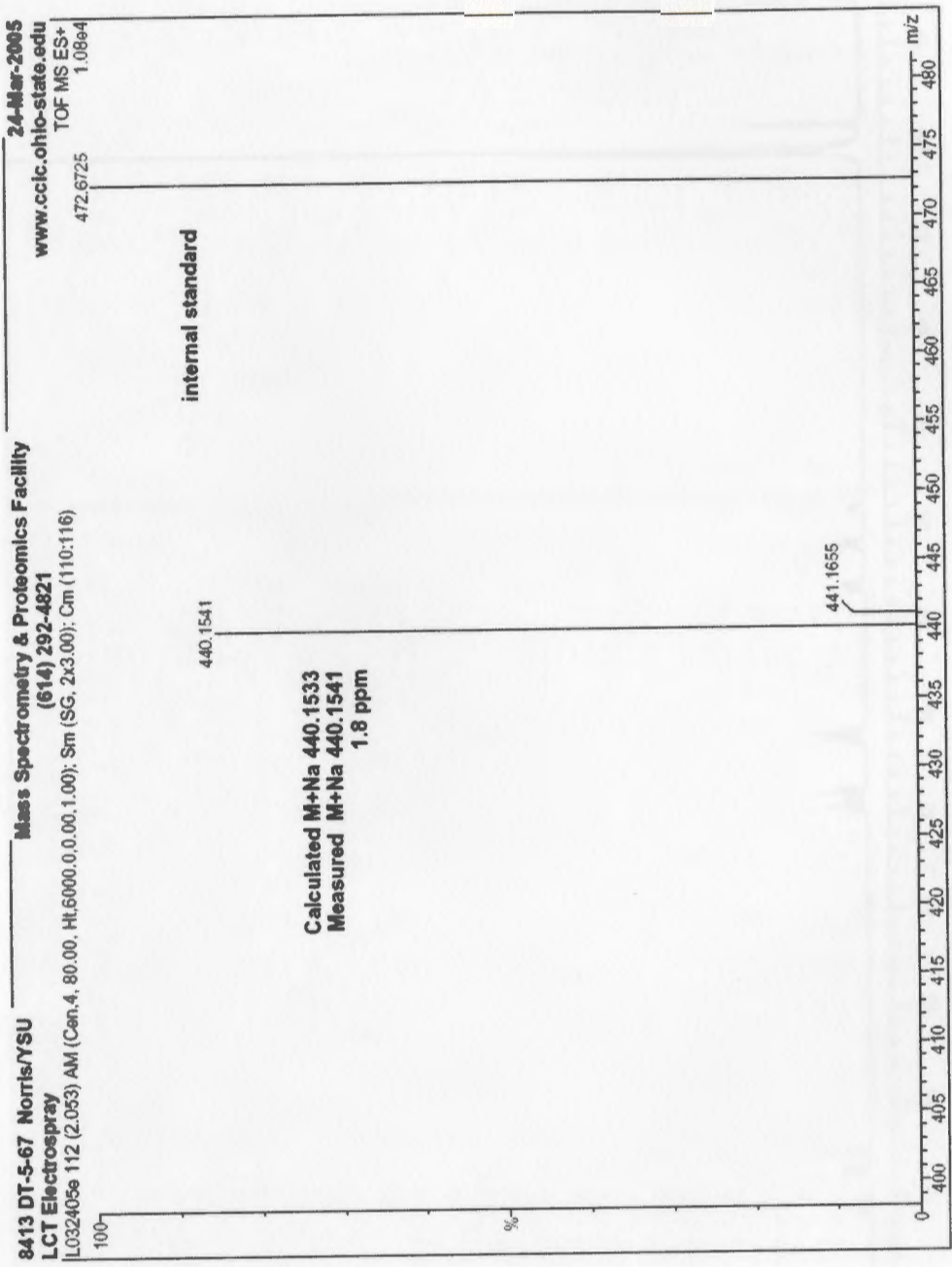
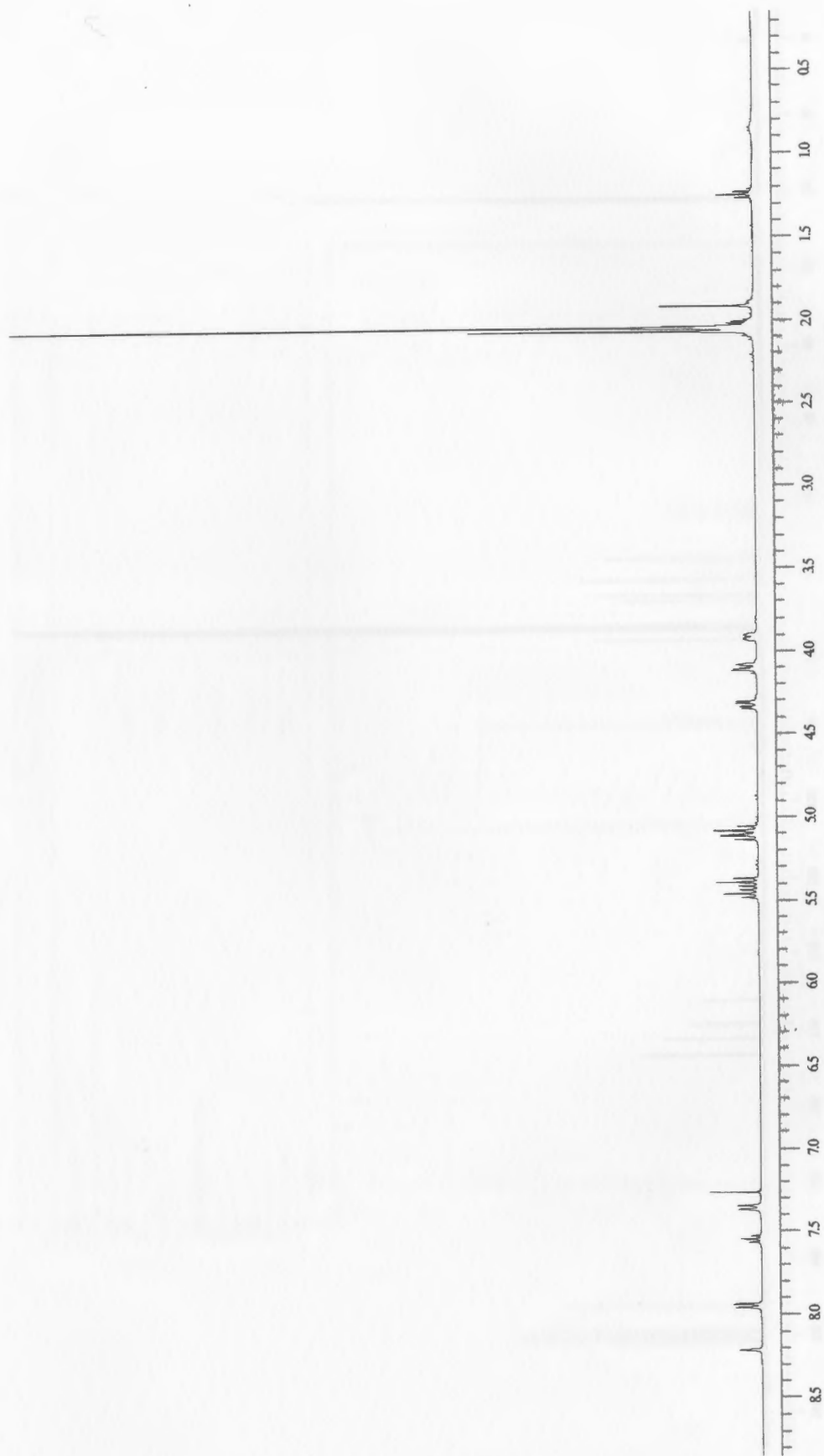


Figure 72: Low resolution mass spectrum of amide 16



**Figure 73: High resolution mass spectrum of amide 16**



**Figure 74:** 400 MHz  $^1\text{H}$  NMR spectrum of amide 17

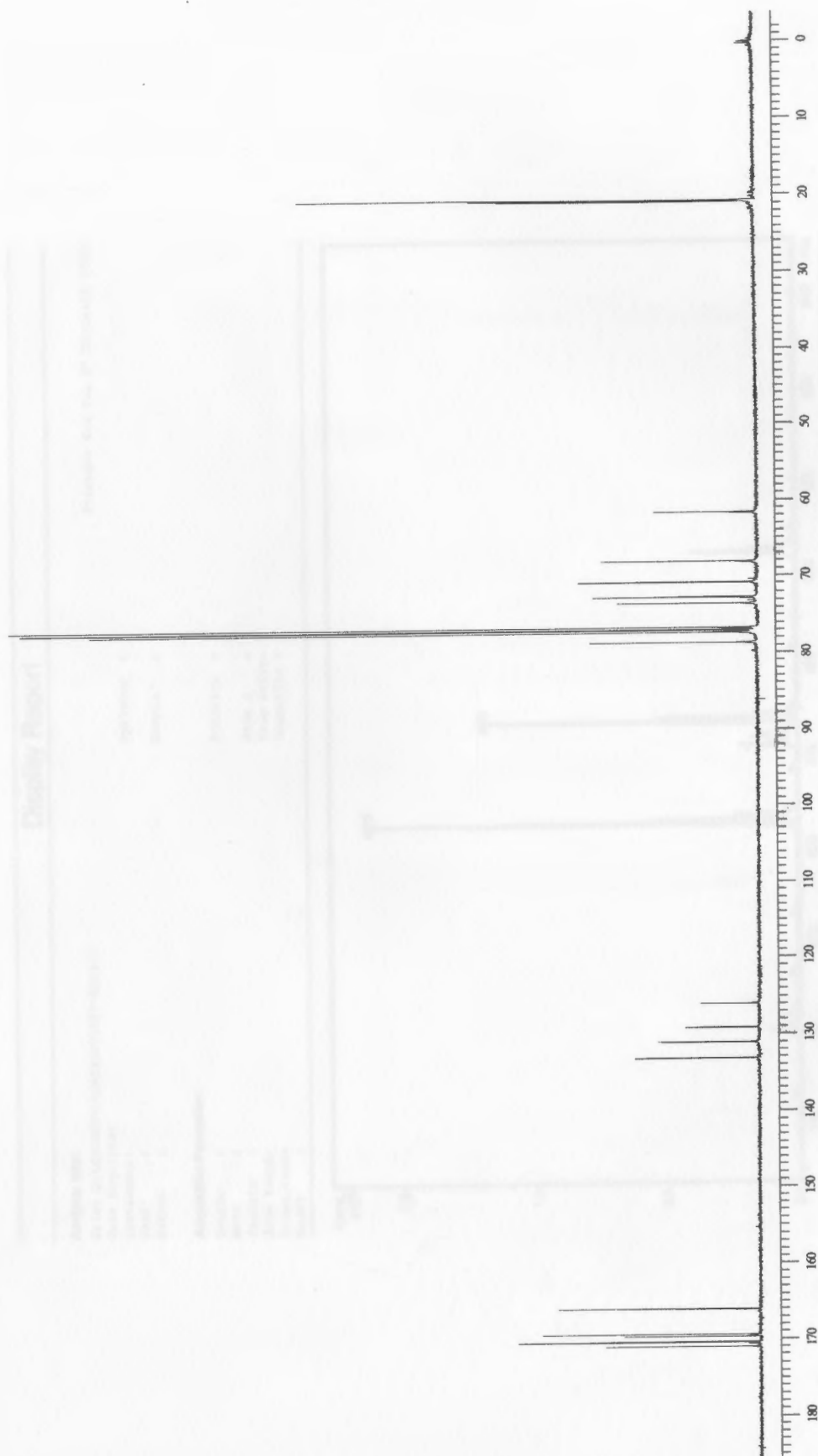
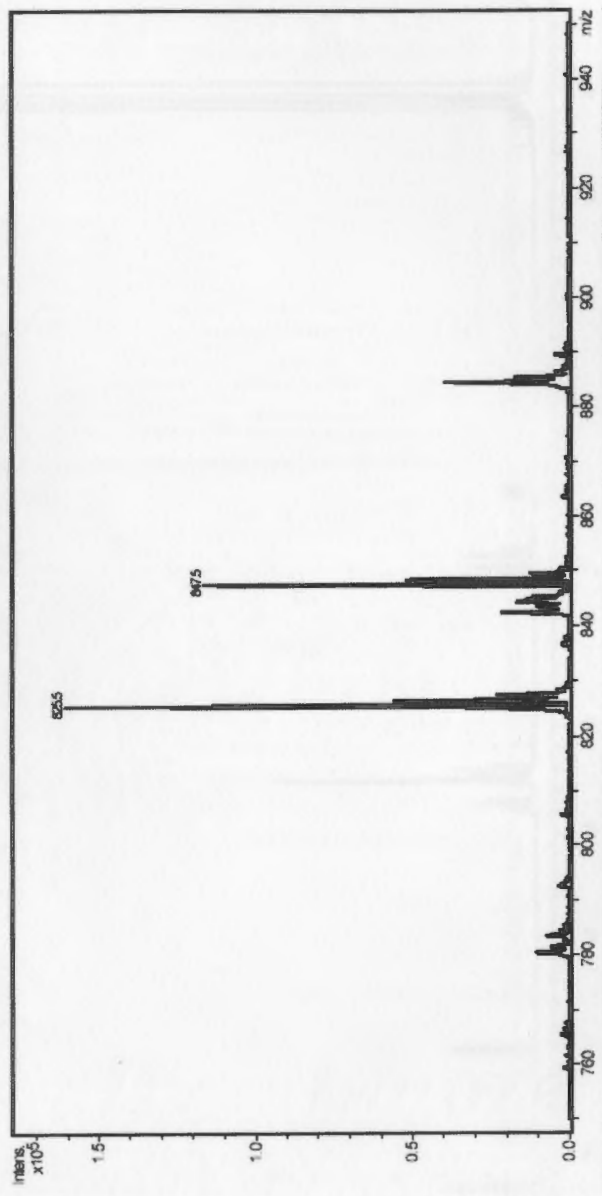


**Figure 75:** 100 MHz  $^{13}\text{C}$  NMR spectrum of amide 17

# Display Report

**Analysis Info:**  
File: D:\HPCHEM\1\DATA\DT\DT7-6302.D  
Date acquired: Wed Jul 27 18:24:04 2005  
Instrument:  
Task :  
Method :  
Operator :  
Sample :  
Polarity :  
Skim 1 :  
Trap Drive:  
Summation :  
**Acquisition Parameter:**  
Source :  
Mode :  
CapExit :  
Scan Range:  
Accum.time:  
MS/MS :



Brucker DataAnalysis Esquire-AC 1.6m, © Bruker Daltonik GmbH  
Licensed to EQ\_135, Uni. of Ohio  
- 1 -

Figure 76: Low resolution mass spectrum of amide 17

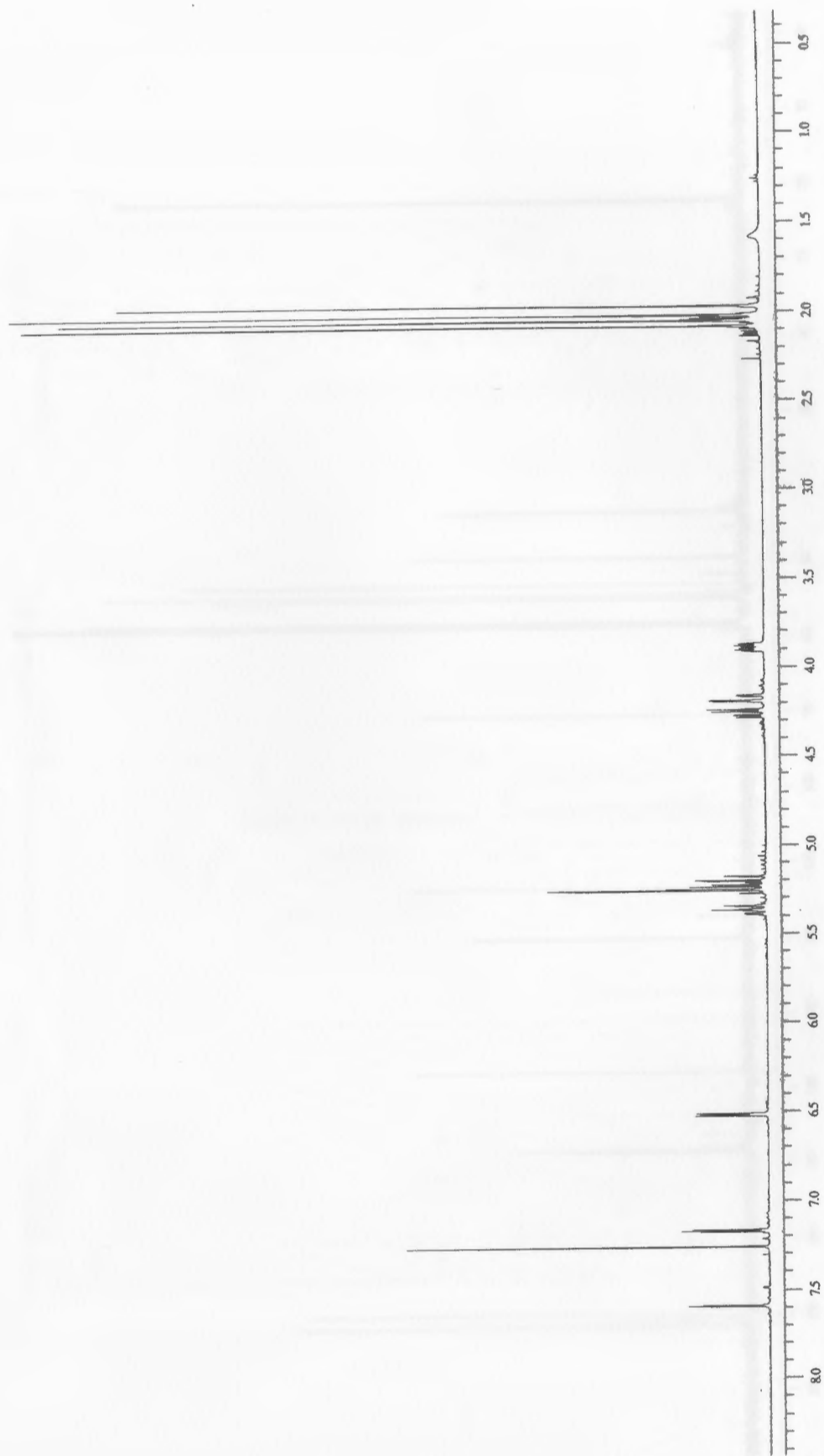


**Figure 77:** 400 MHz <sup>1</sup>H NMR spectrum of imidoyl chloride 18

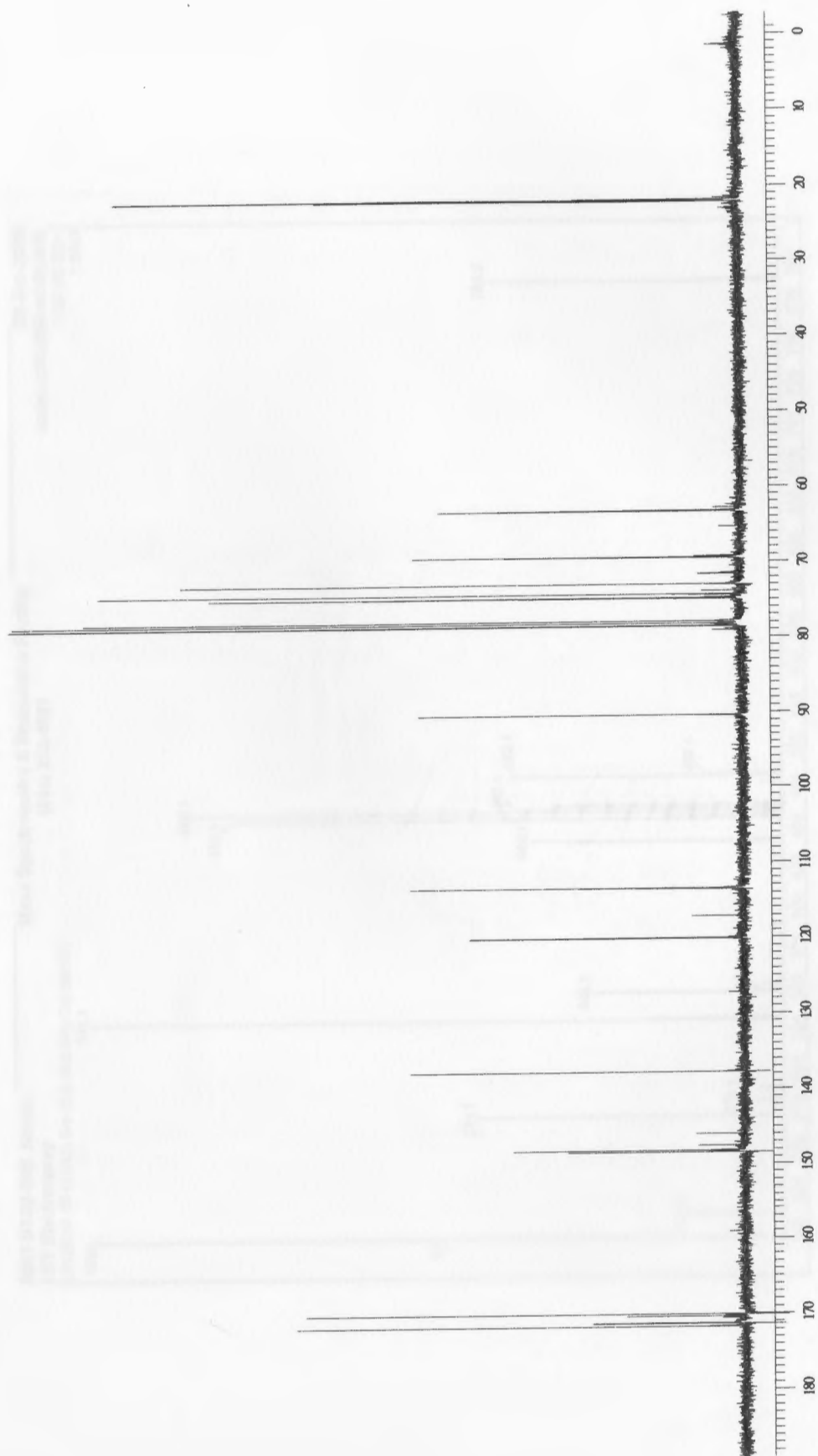


Figure 78: 100 MHz  $^{13}\text{C}$  NMR spectrum of imidoyl chloride 18

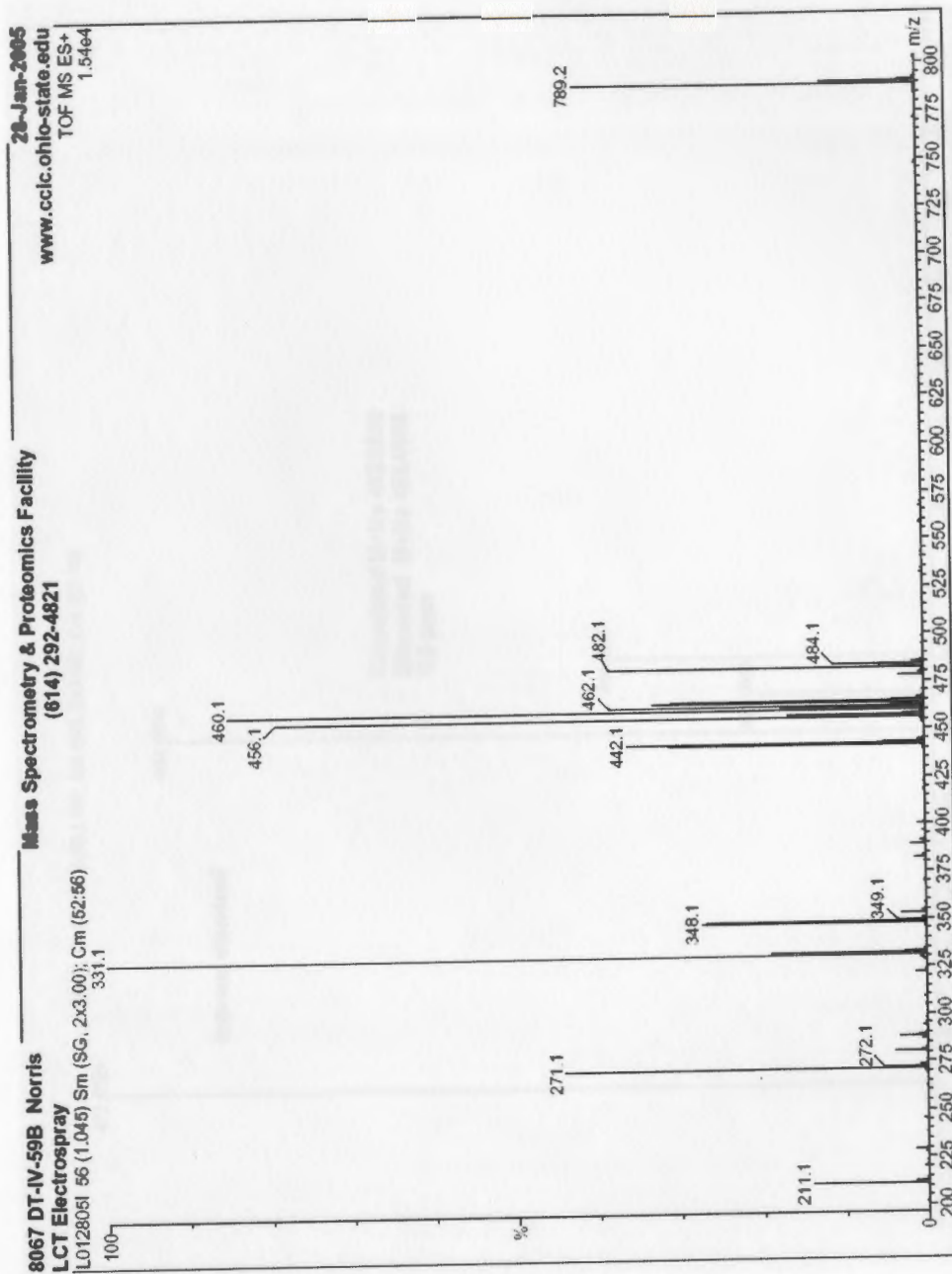


Figure 79: Low resolution mass spectrum of imidoyl chloride 18



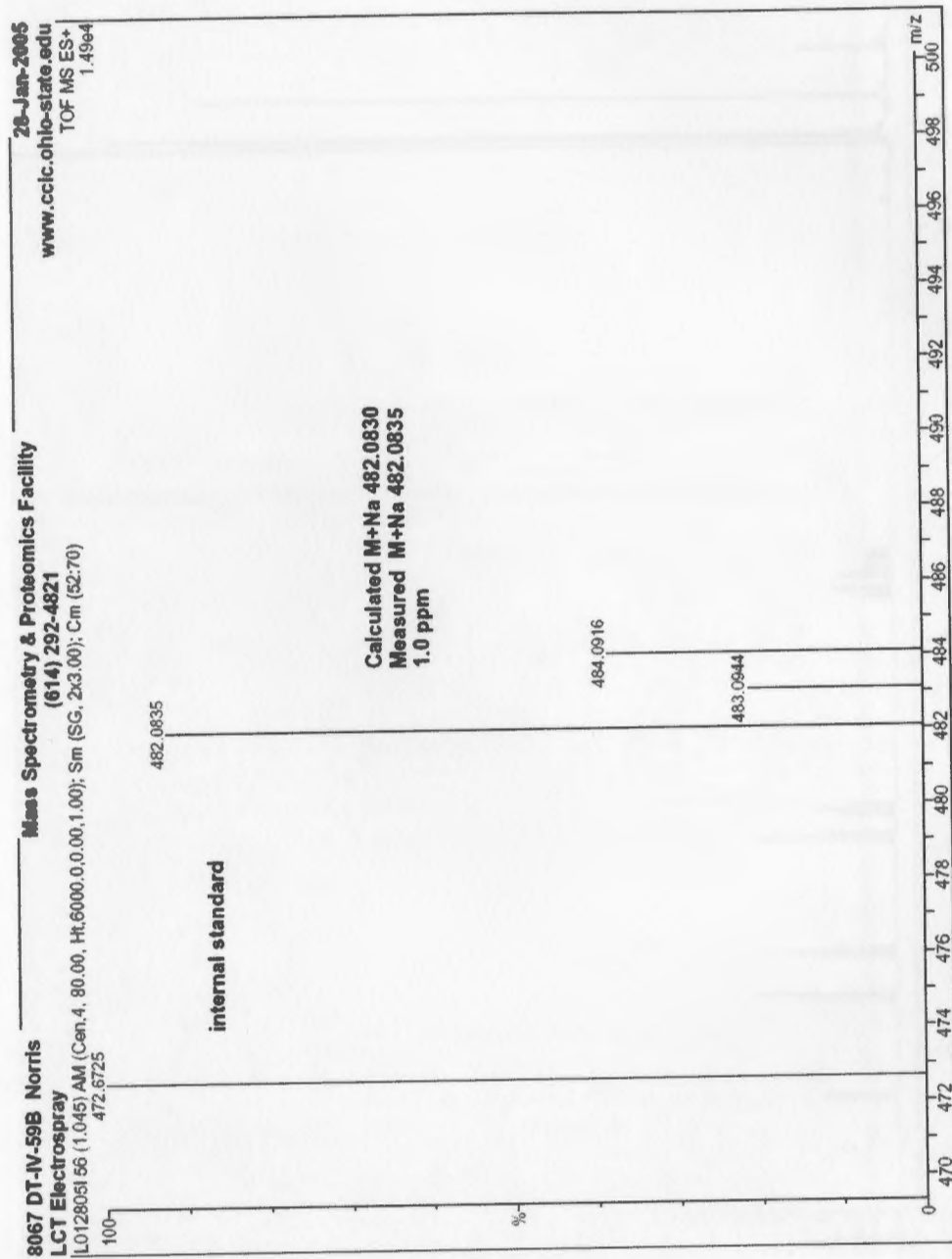
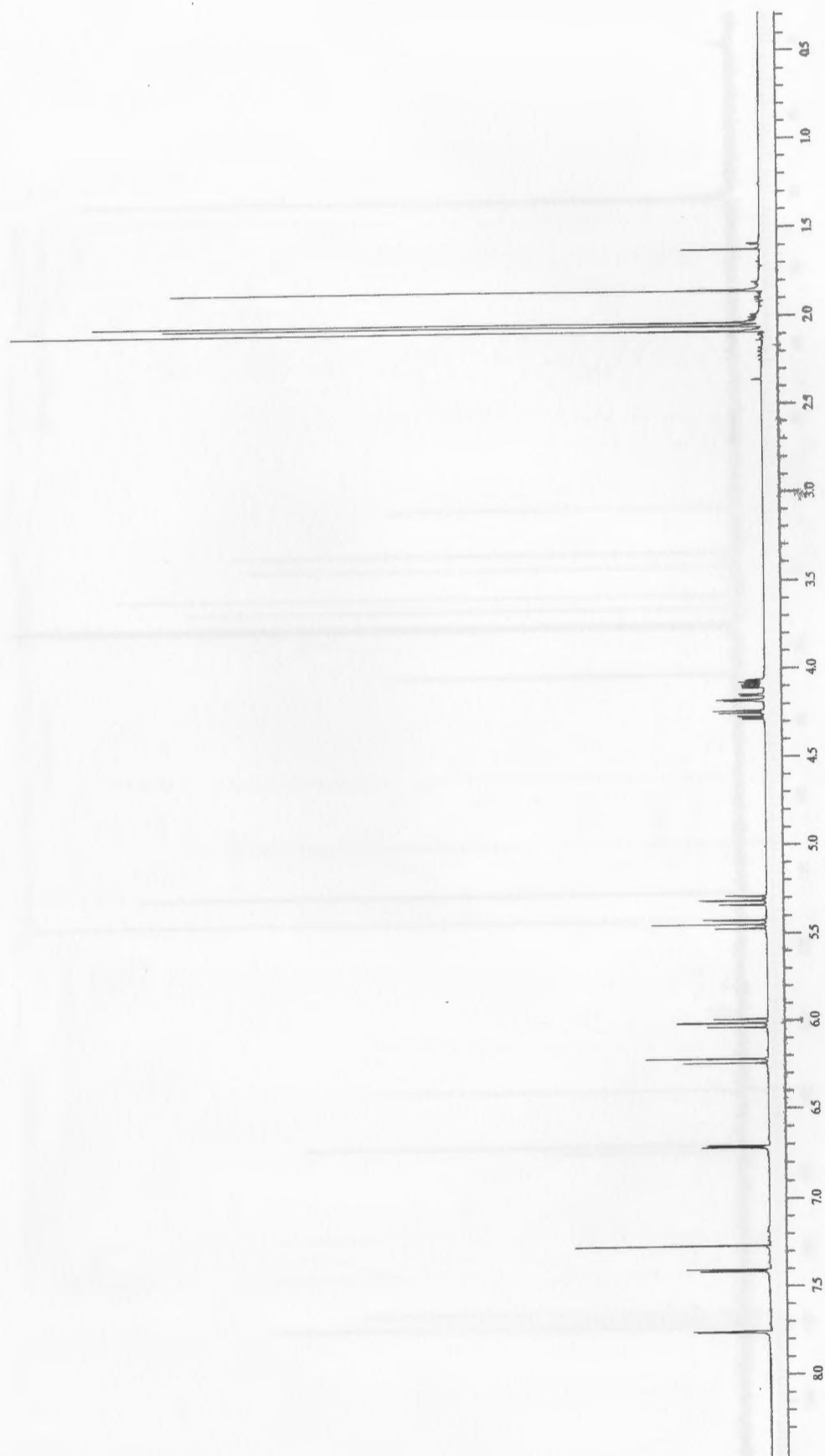
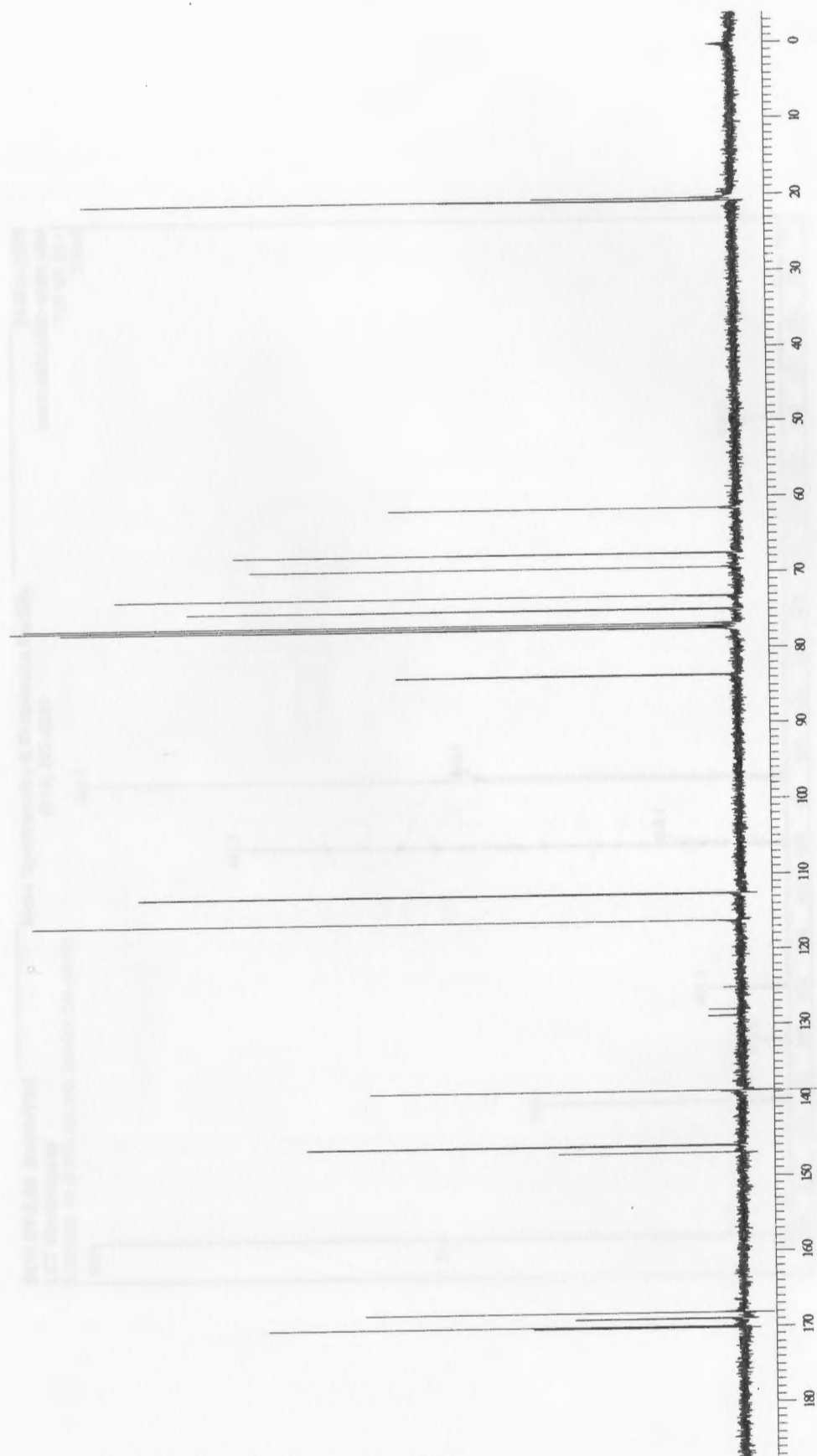


Figure 80: High resolution mass spectrum of imidoyl chloride 18



**Figure 81:** 400 MHz  $^1\text{H}$  NMR spectrum of 1,5-disubstituted tetrazole 19



**Figure 82:** 100 MHz  $^{13}\text{C}$  NMR spectrum of 1,5-disubstituted tetrazole 19

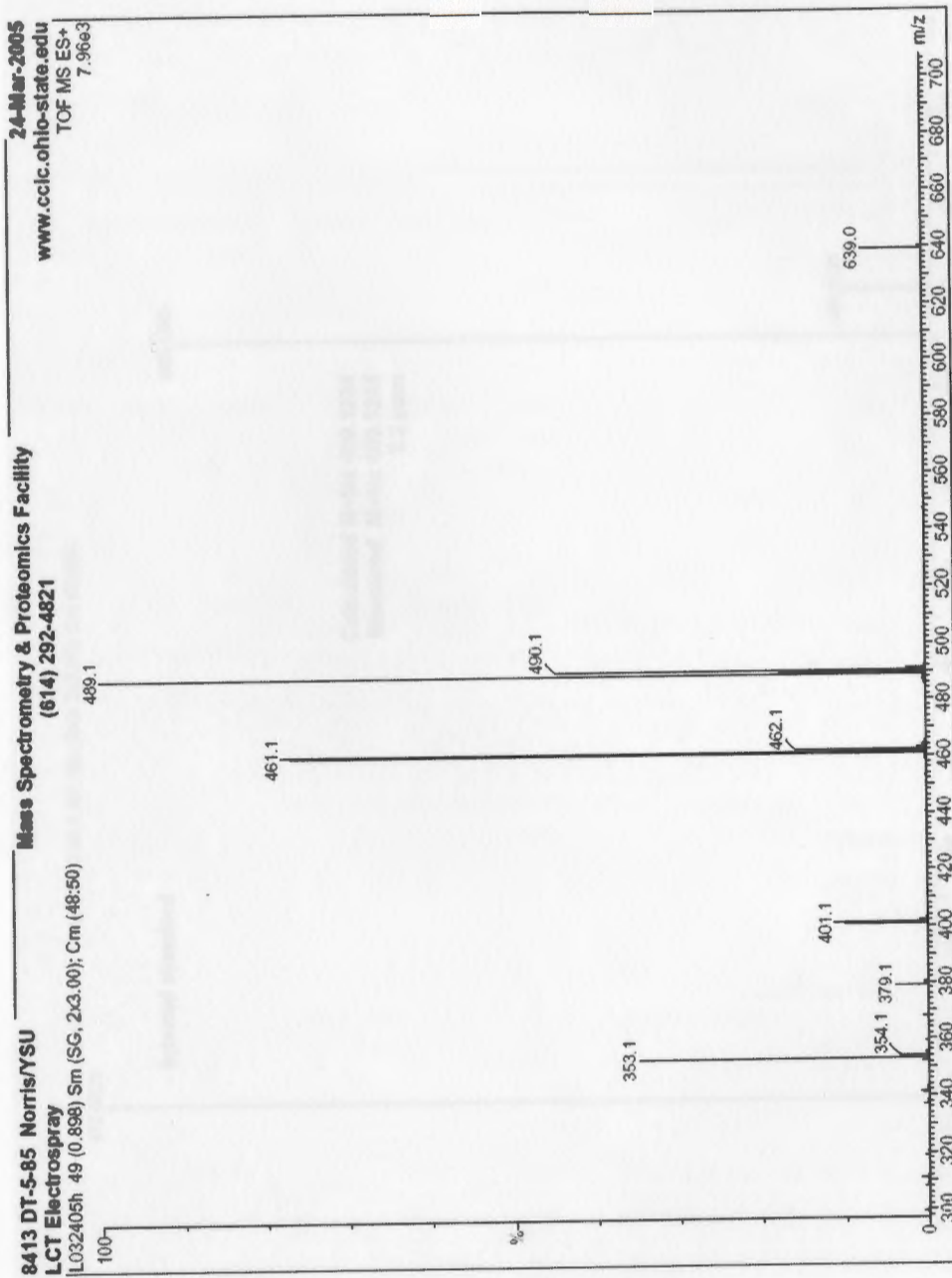


Figure 83: Low resolution mass spectrum of 1,5-disubstituted tetrazole 19

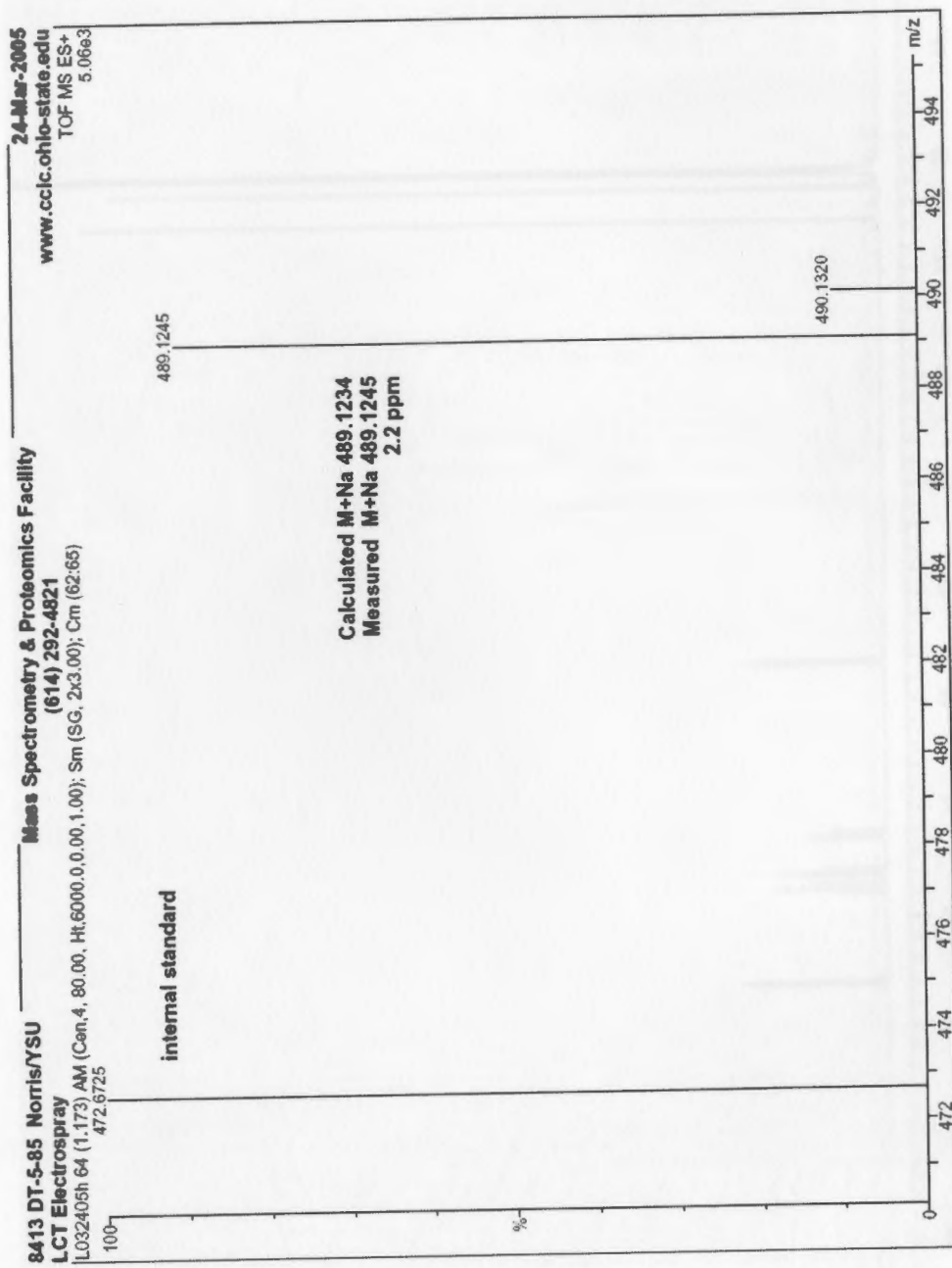
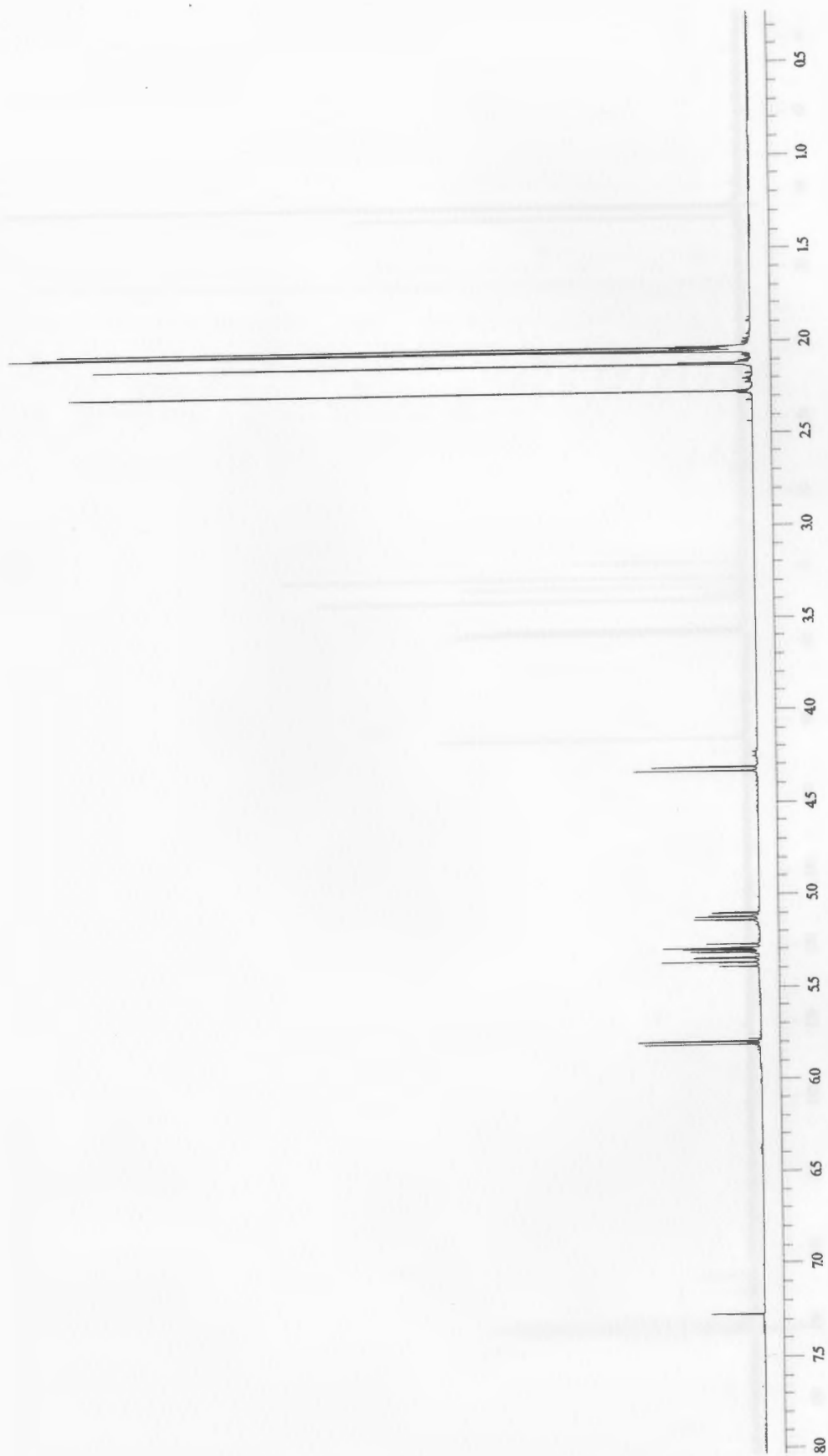


Figure 84: High resolution mass spectrum of 1,5-disubstituted tetrazole 19



**Figure 85:** 400 MHz  $^1\text{H}$  NMR spectrum of anhydride 21

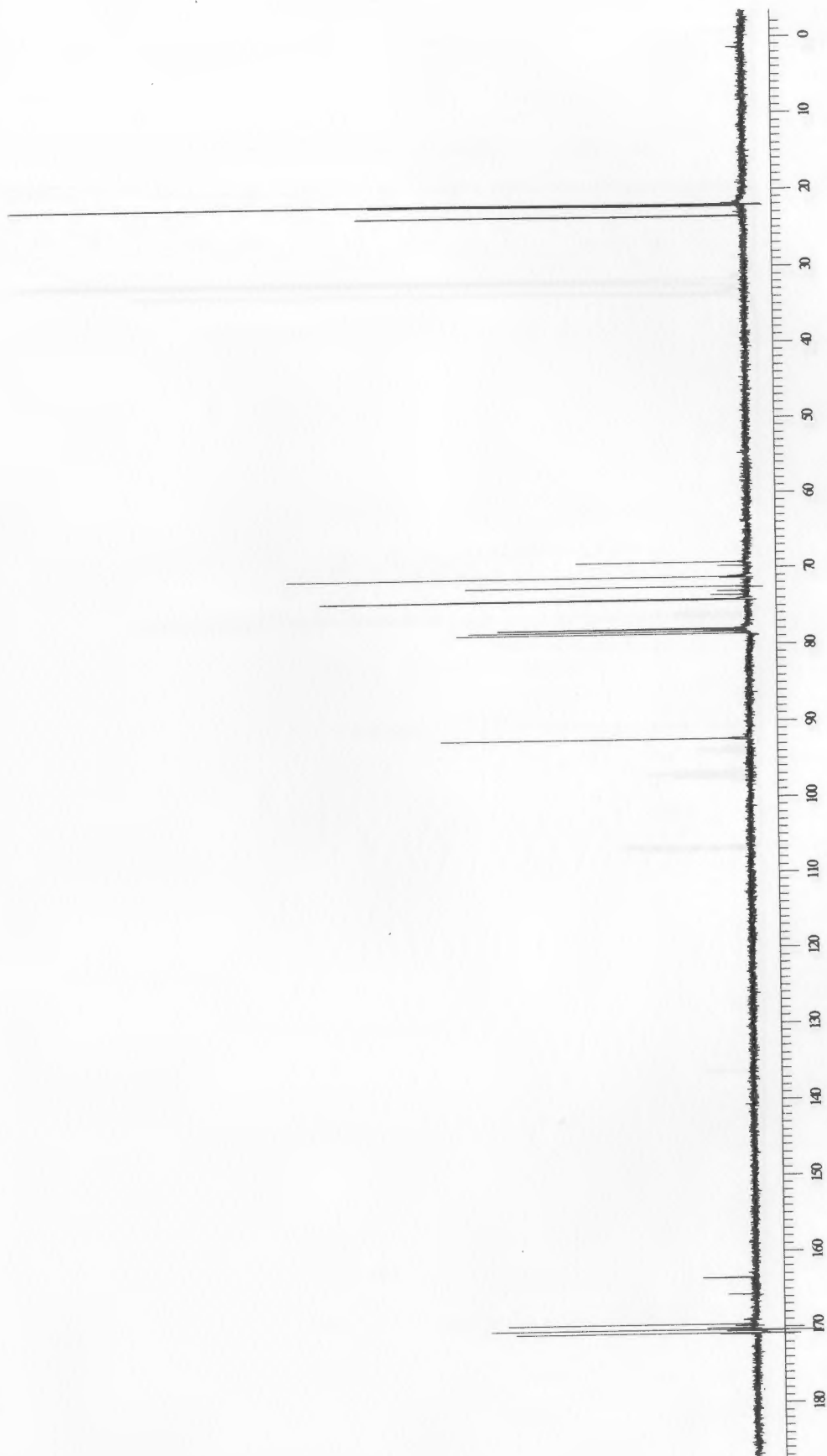
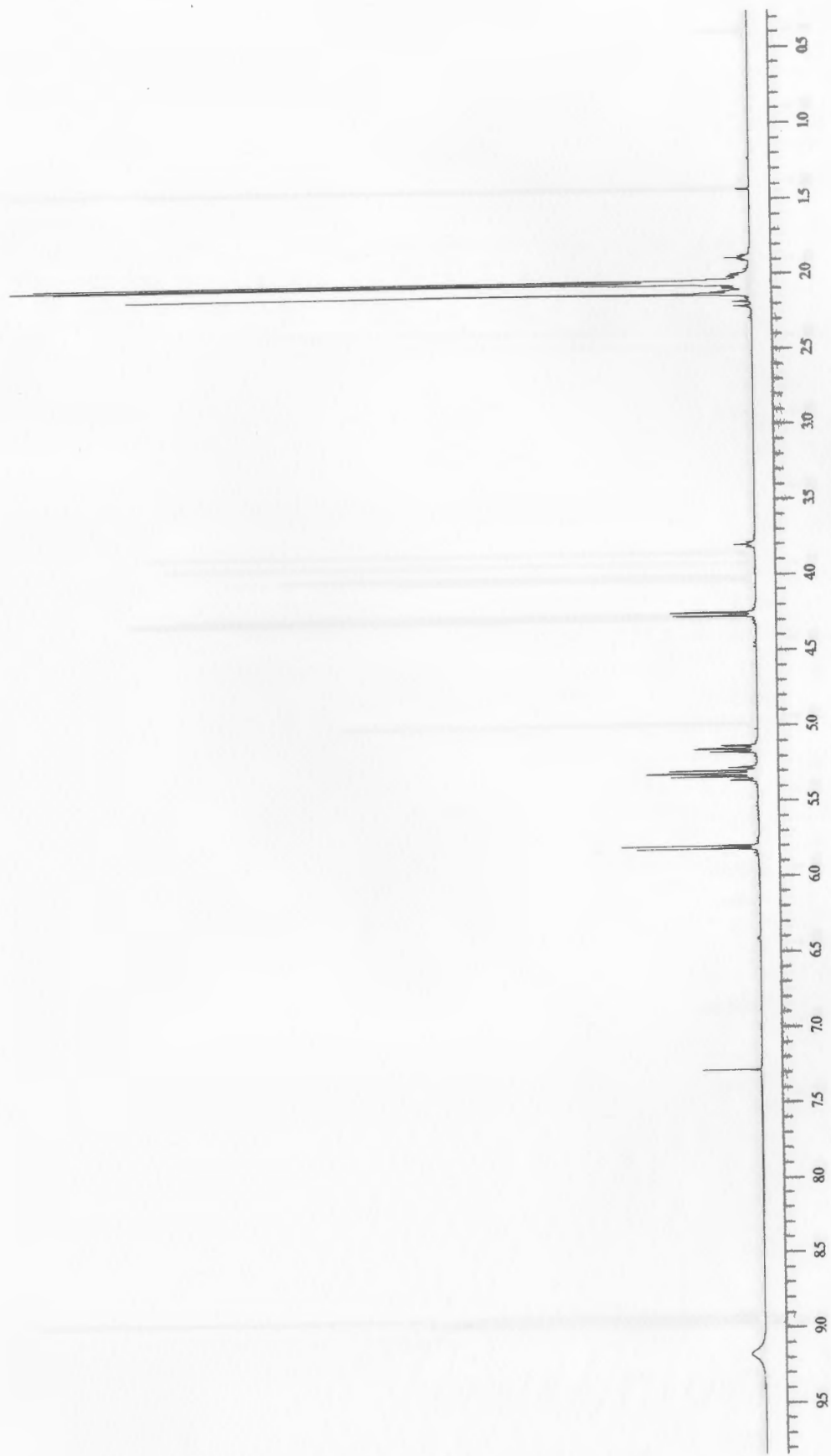


Figure 86: 100 MHz  $^{13}\text{C}$  NMR spectrum of anhydride 21



**Figure 87:** 400 MHz  $^1\text{H}$  NMR spectrum of carboxylic acid 22





**Figure 88:** 100 MHz  $^{13}\text{C}$  NMR spectrum of carboxylic acid 22

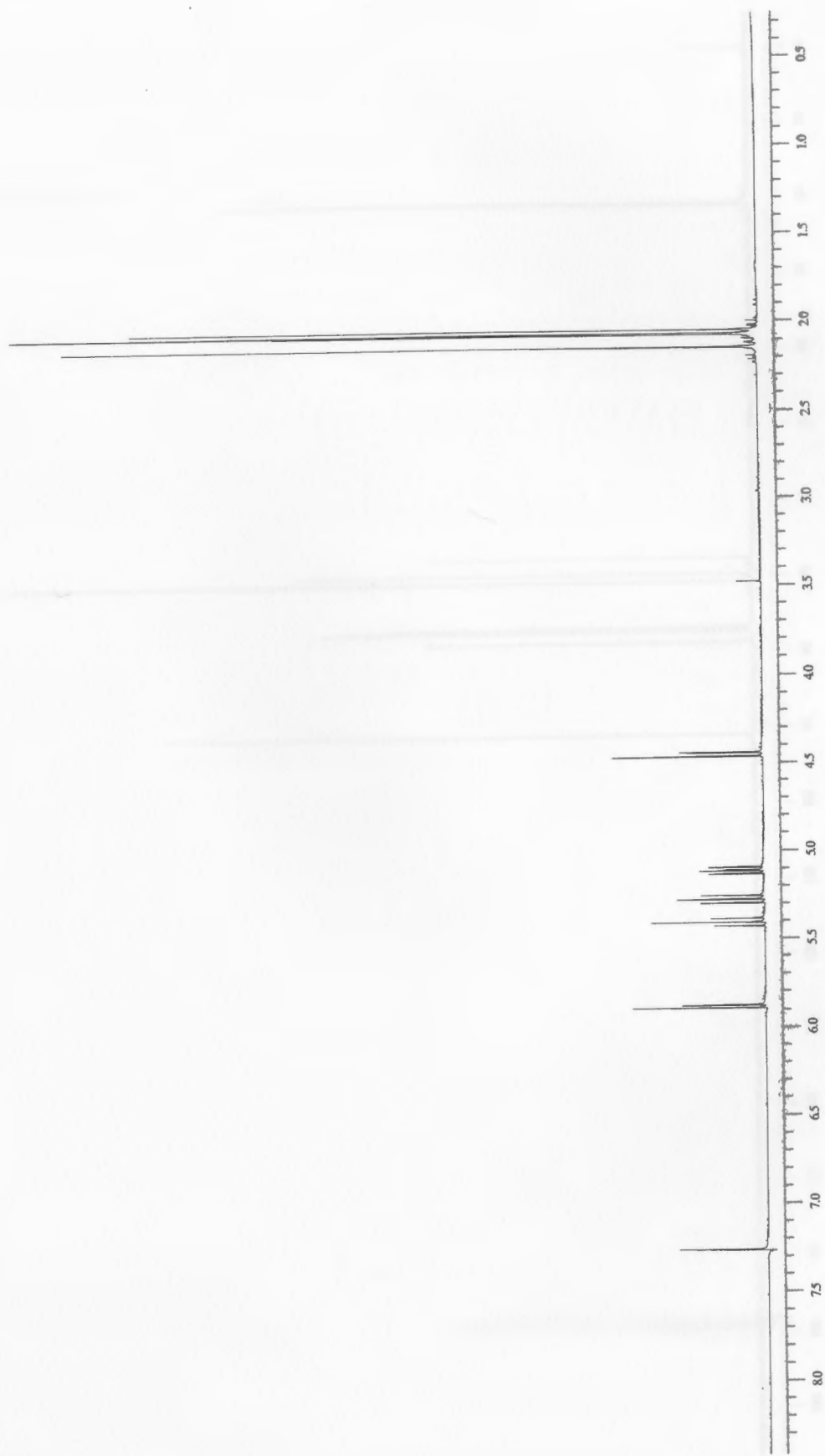


**Figure 89:** 400 MHz  $^1\text{H}$  NMR spectrum of acid chloride 23

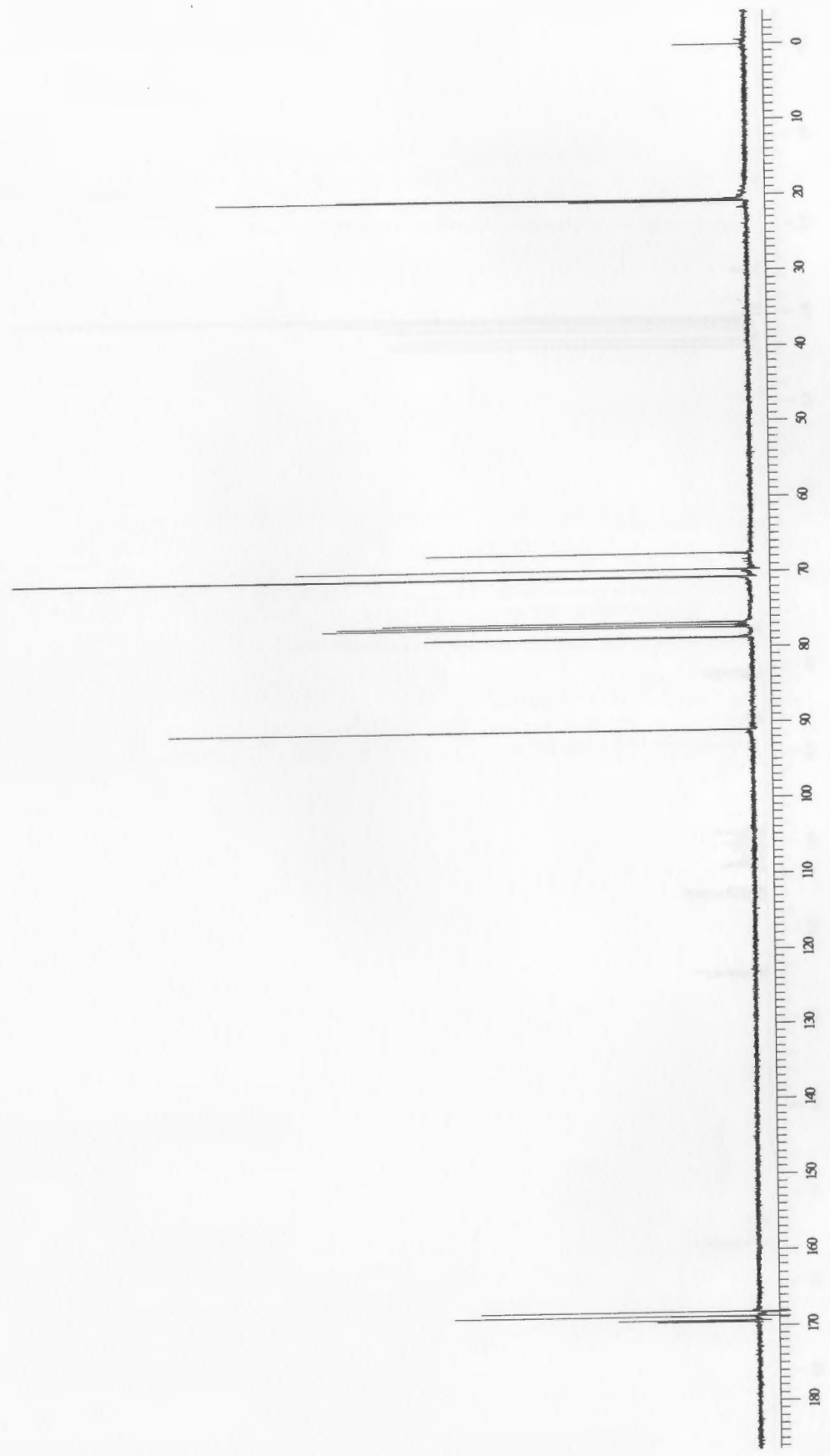
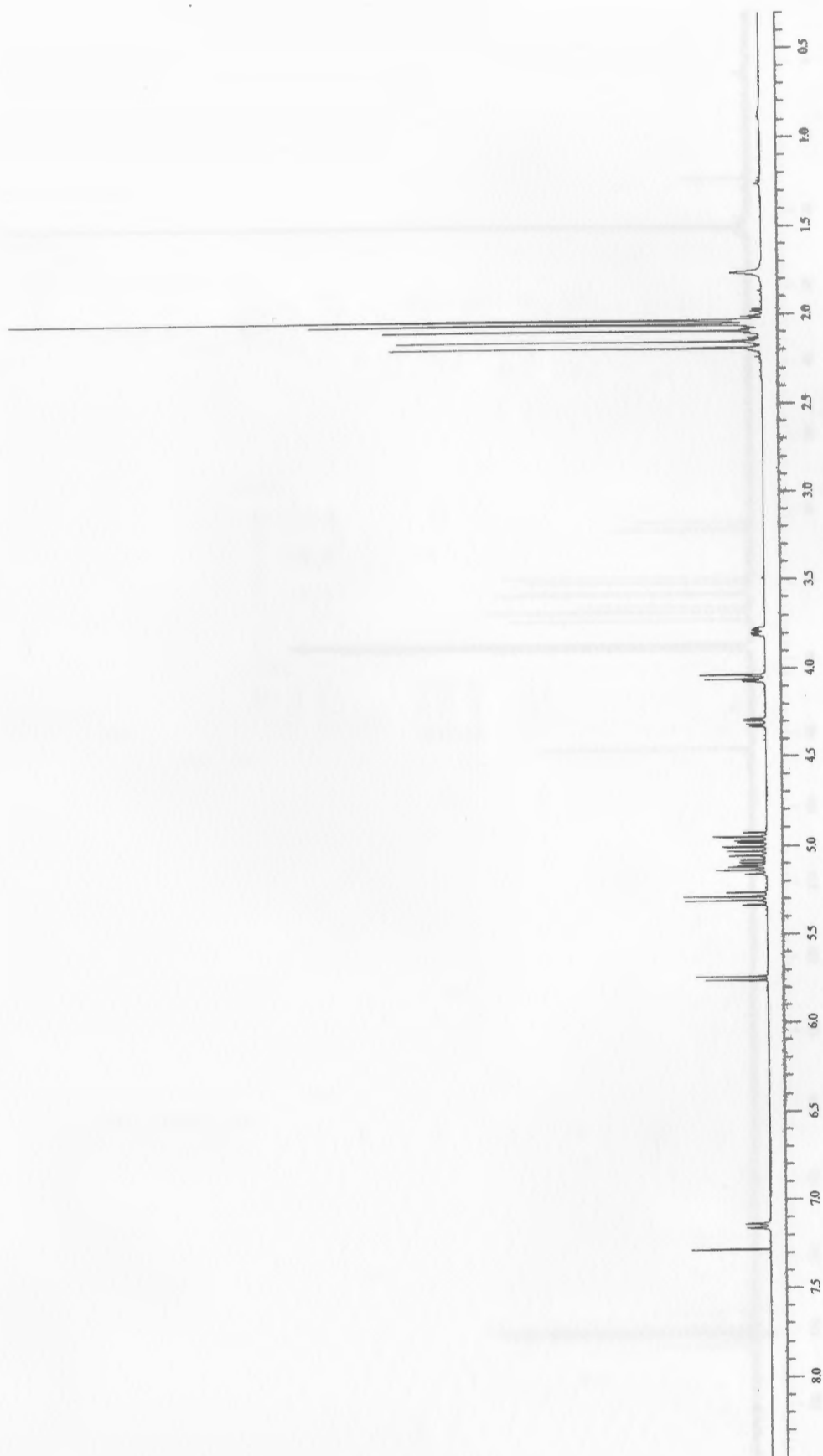
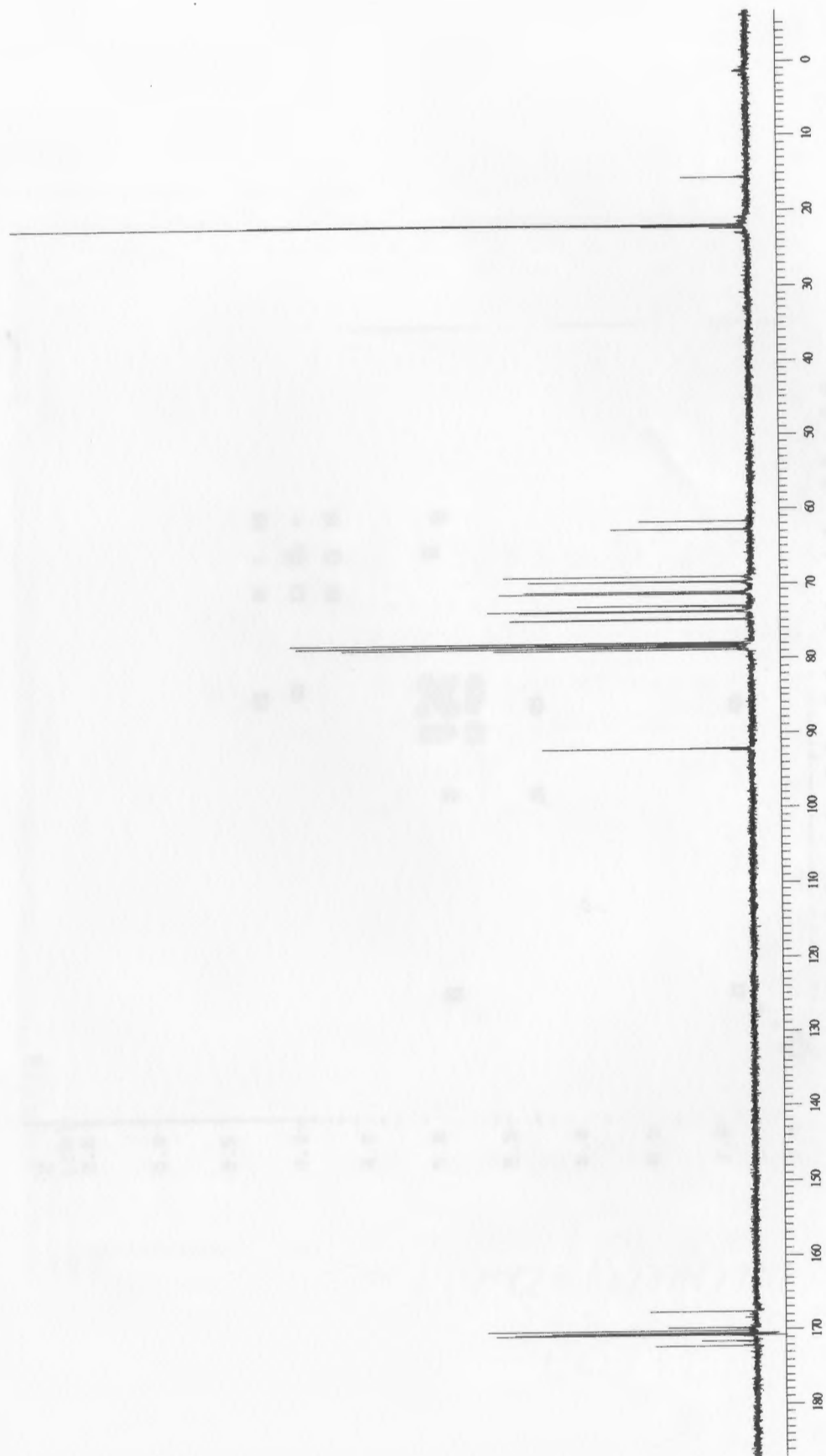


Figure 90: 100 MHz  $^{13}\text{C}$  NMR spectrum of acid chloride 23



**Figure 91:** 400 MHz  $^1\text{H}$  NMR spectrum of amide-linked carbohydrate dimer 24



**Figure 92:** 100 MHz  $^{13}\text{C}$  NMR spectrum of amide-linked carbohydrate dimer 24

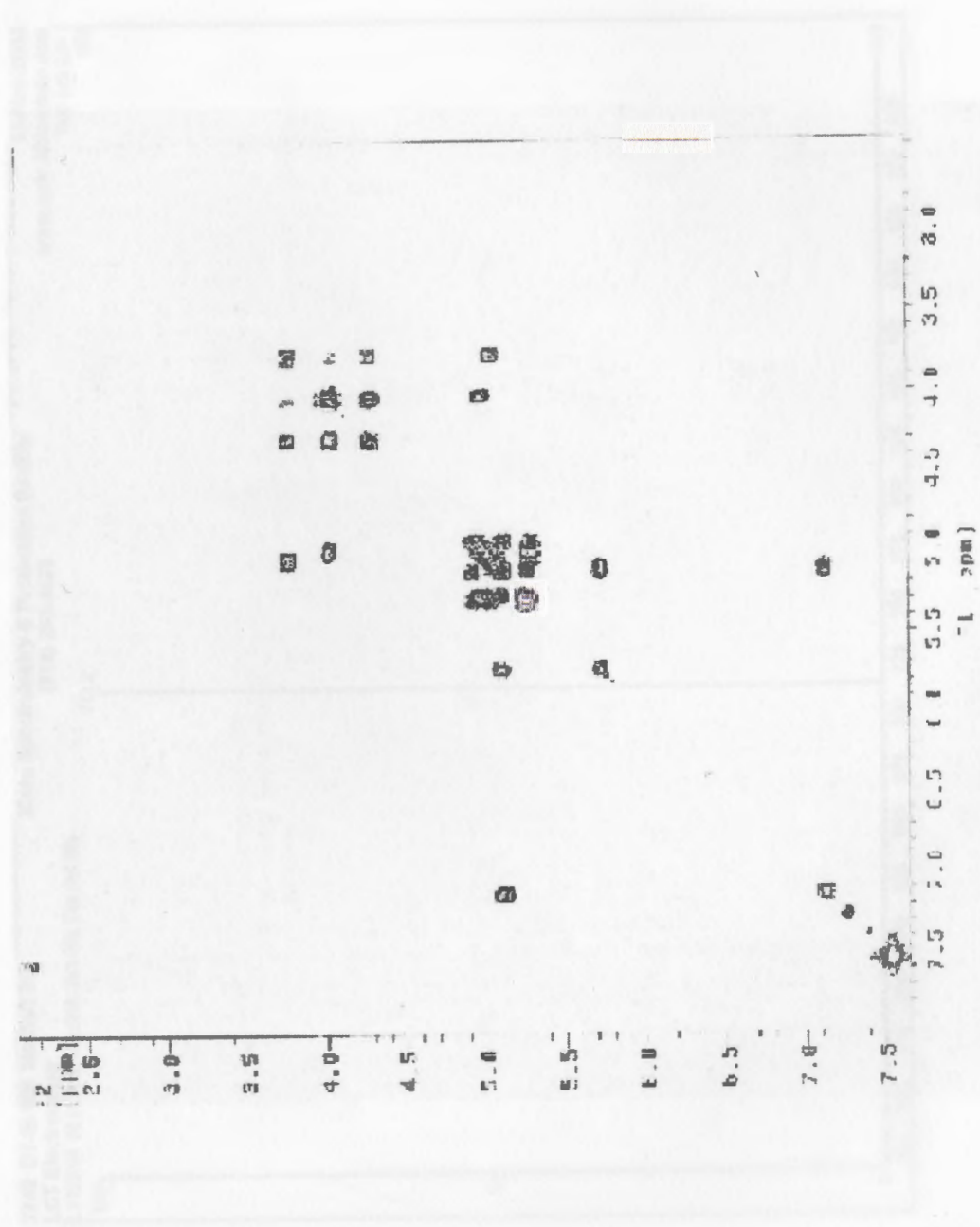


Figure 93: Cosy spectrum of dimer 24

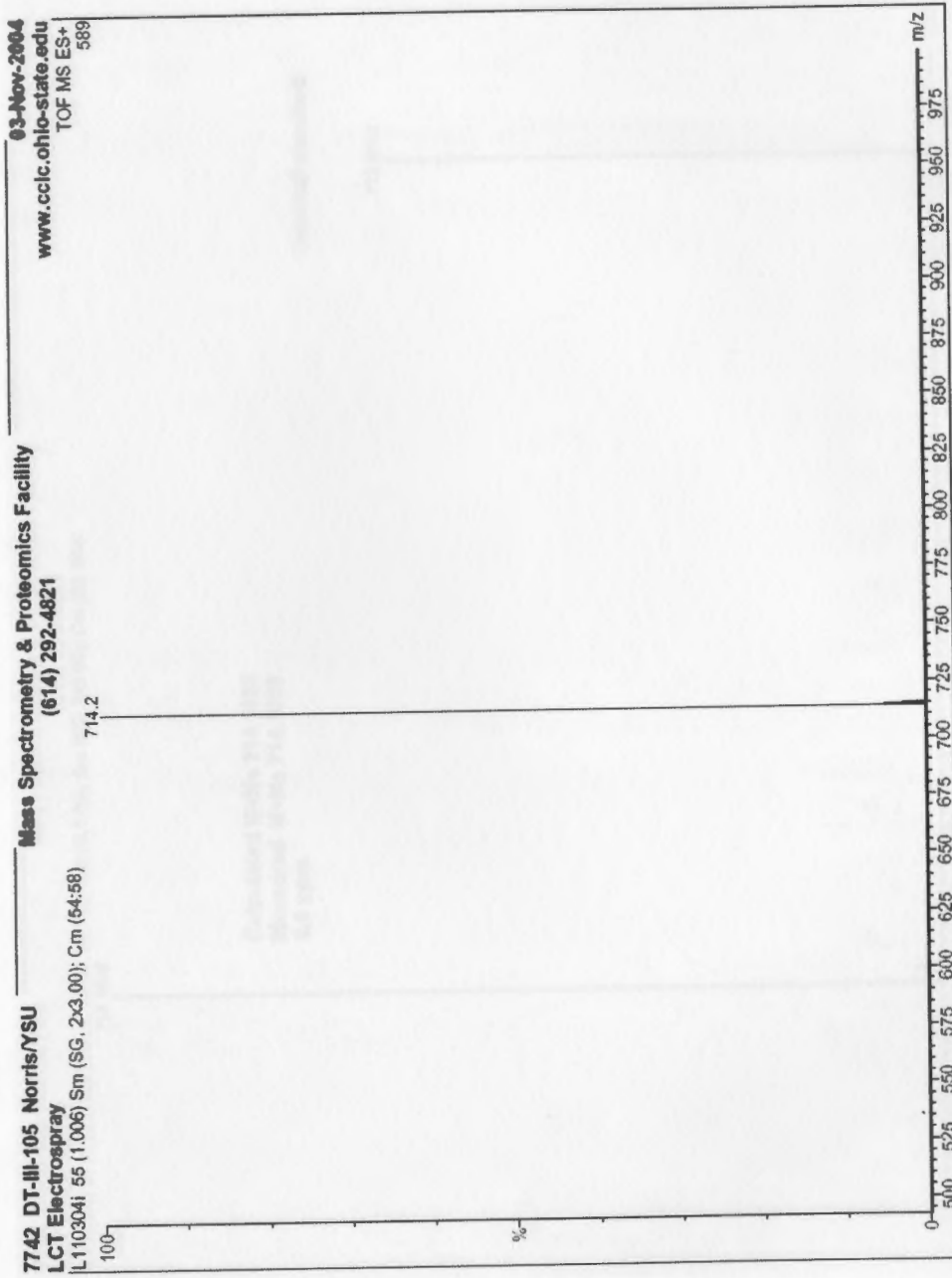


Figure 94: Low resolution mass spectrum of dimer 24

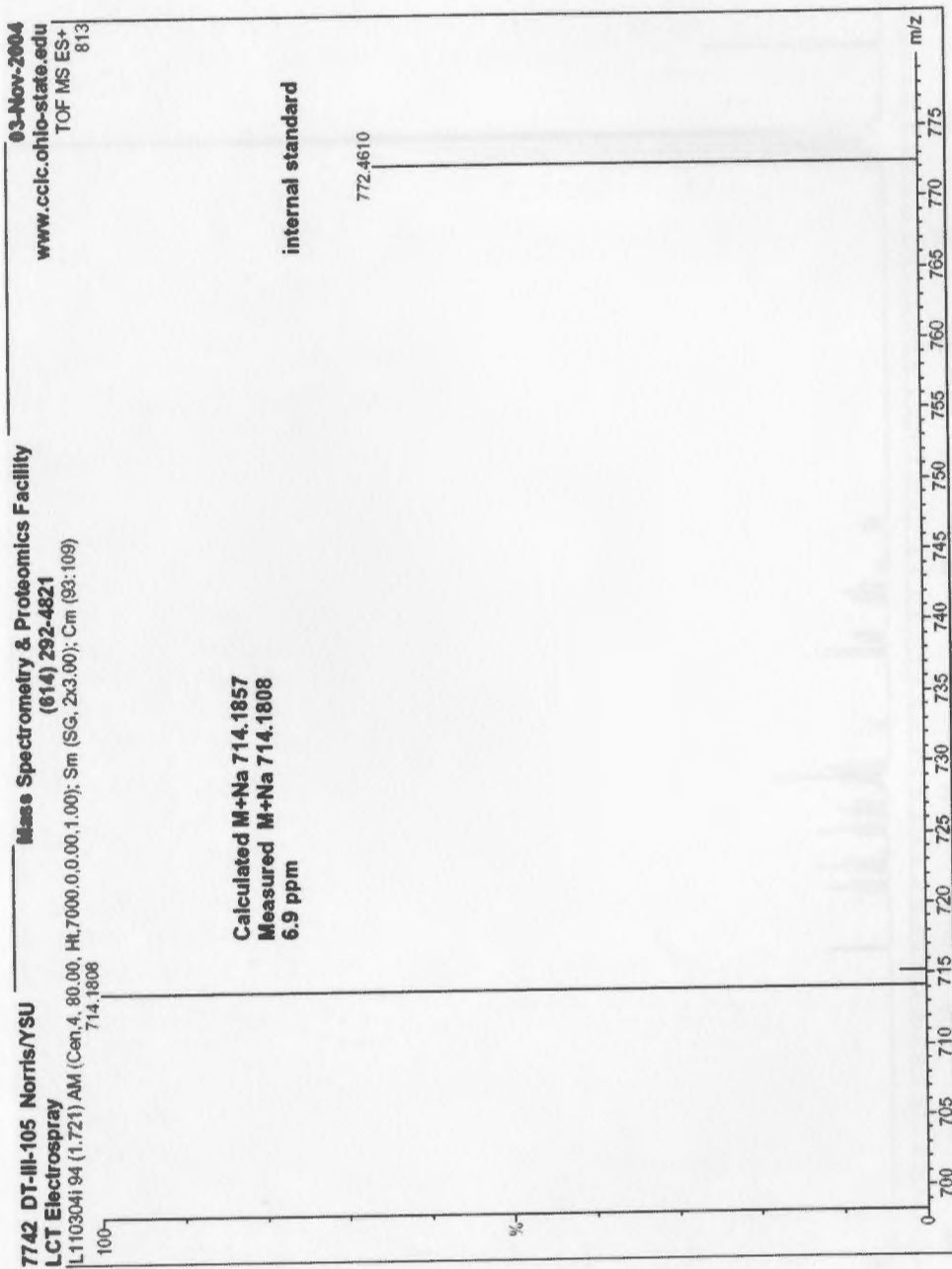
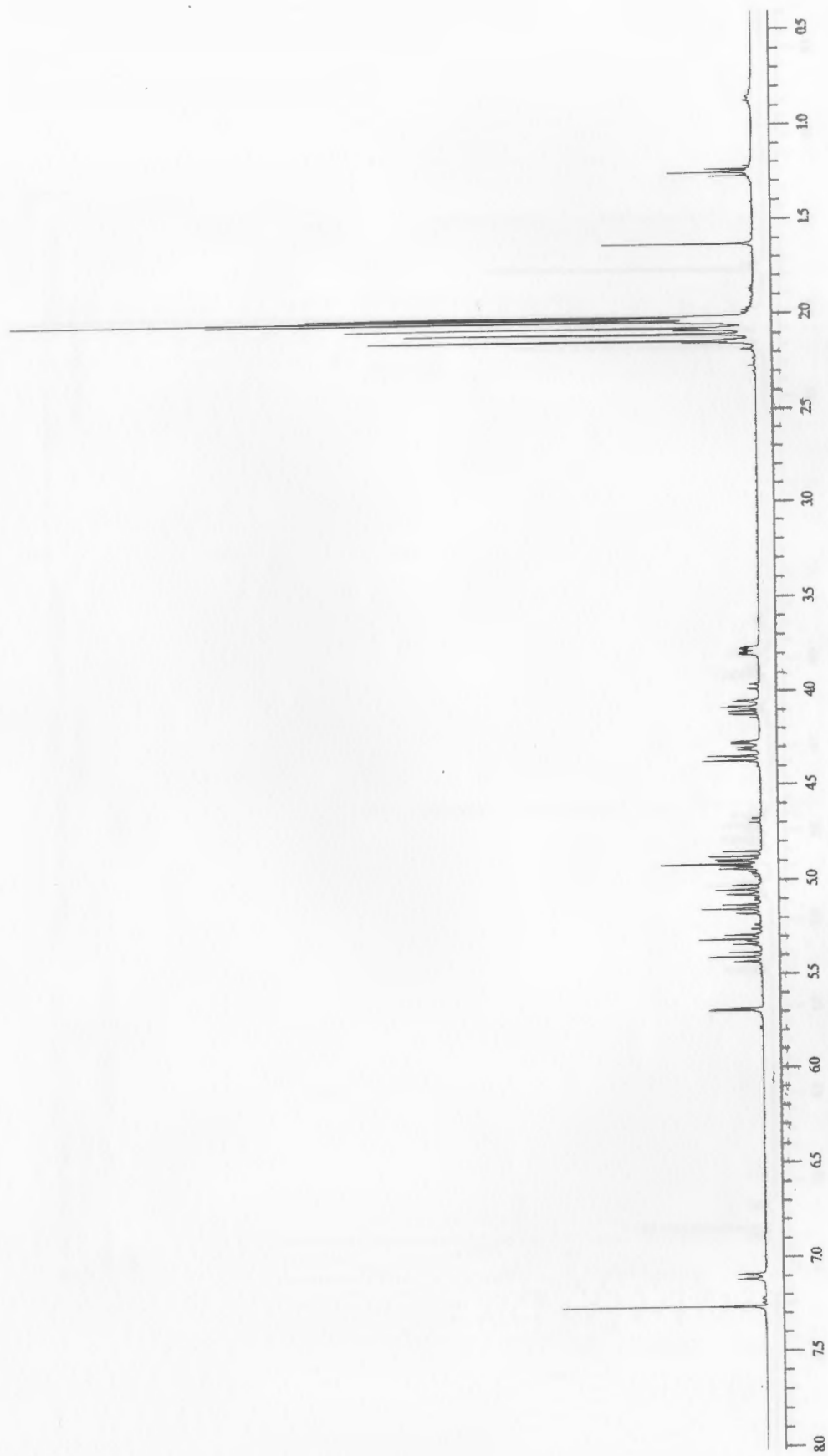


Figure 95: High resolution mass spectrum of dimer 24





**Figure 96:** 400 MHz  $^1\text{H}$  NMR spectrum of azide 25



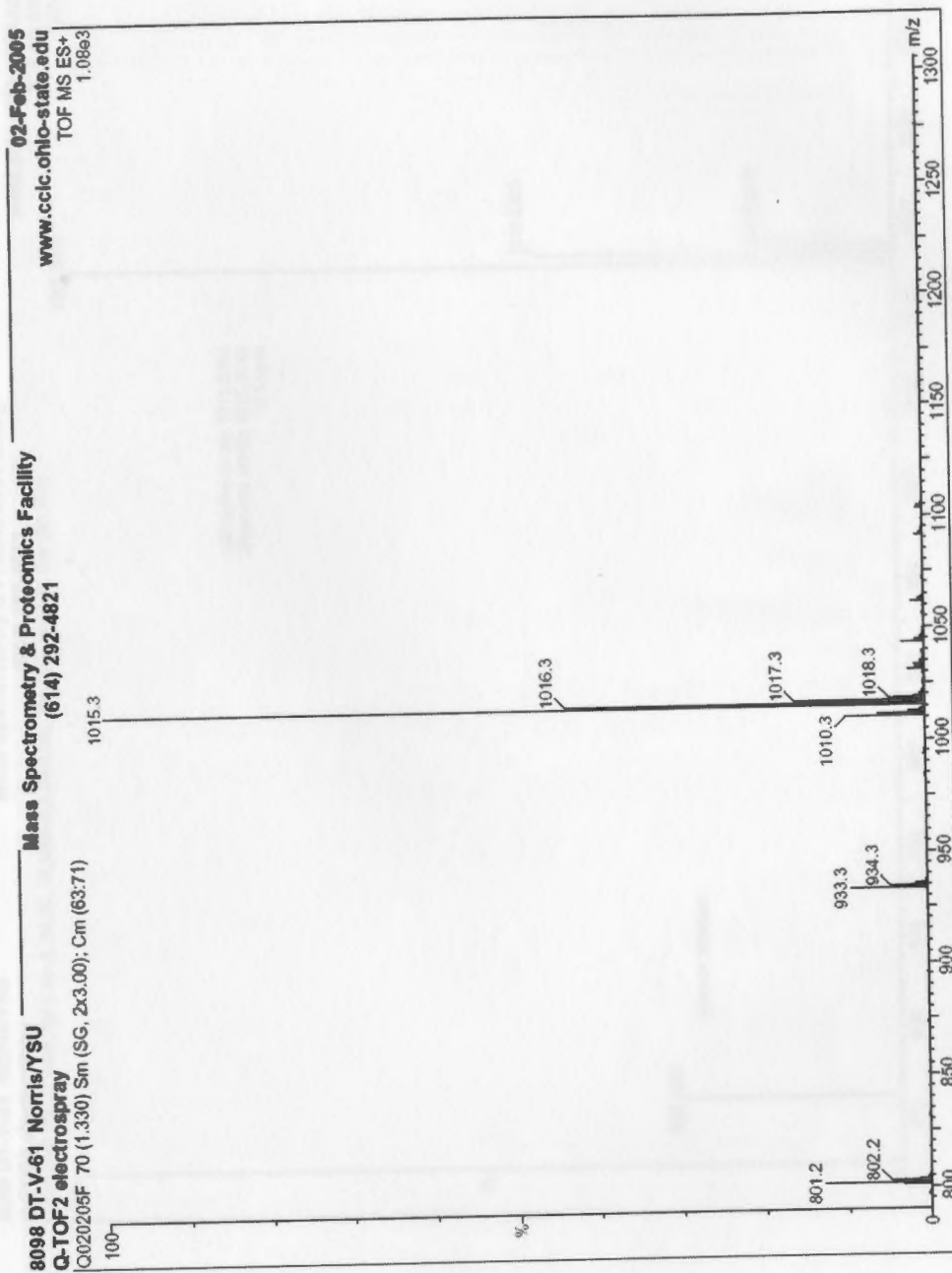


Figure 98: Low resolution mass spectrum of amide linked trimer 26

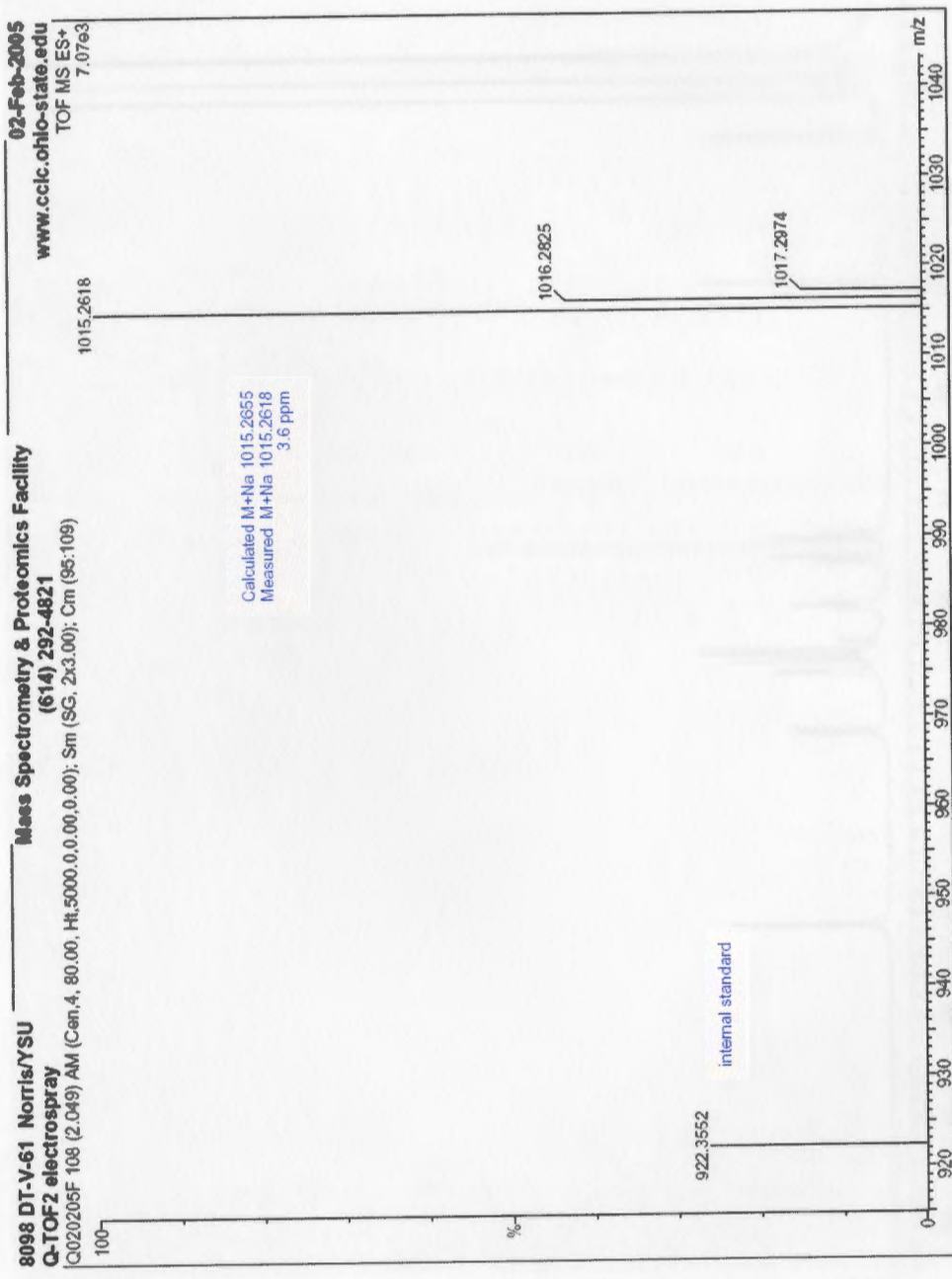
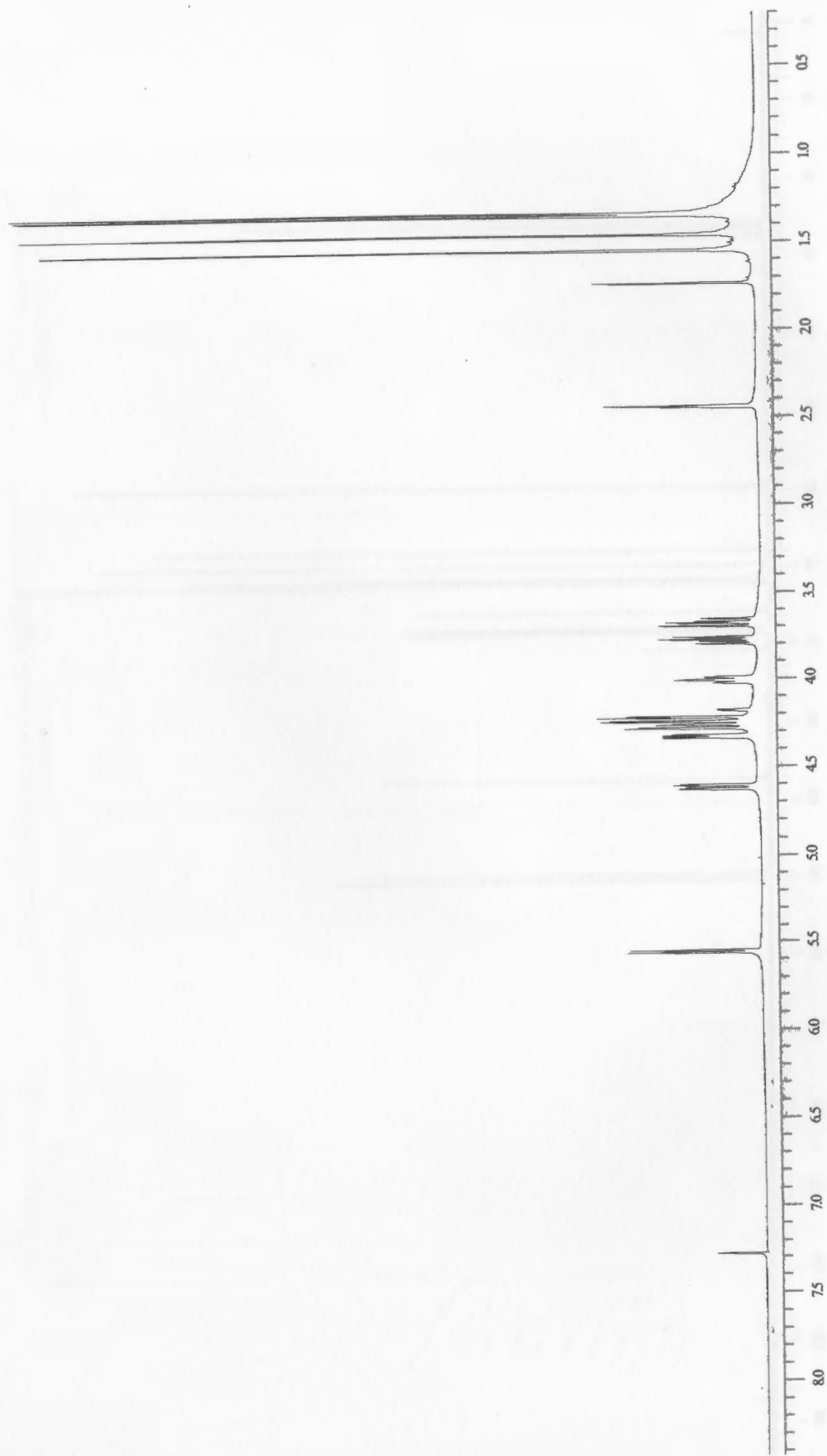


Figure 99: High resolution mass spectrum of amide linked trimer 26



**Figure 100:** 400 MHz  $^1\text{H}$  NMR spectrum of alkyne 28

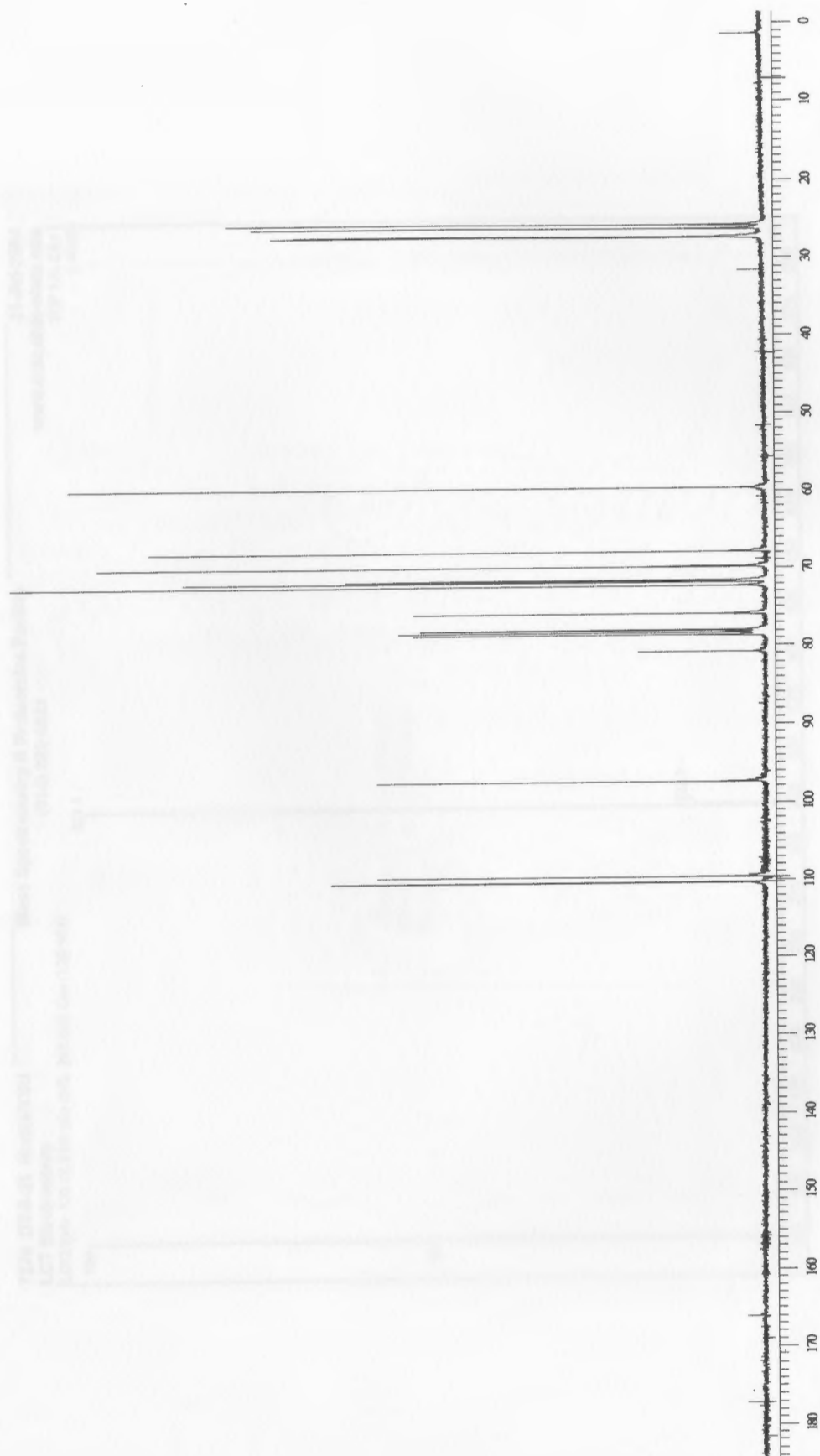


Figure 101: 100 MHz  $^{13}\text{C}$  NMR spectrum of alkyne 28

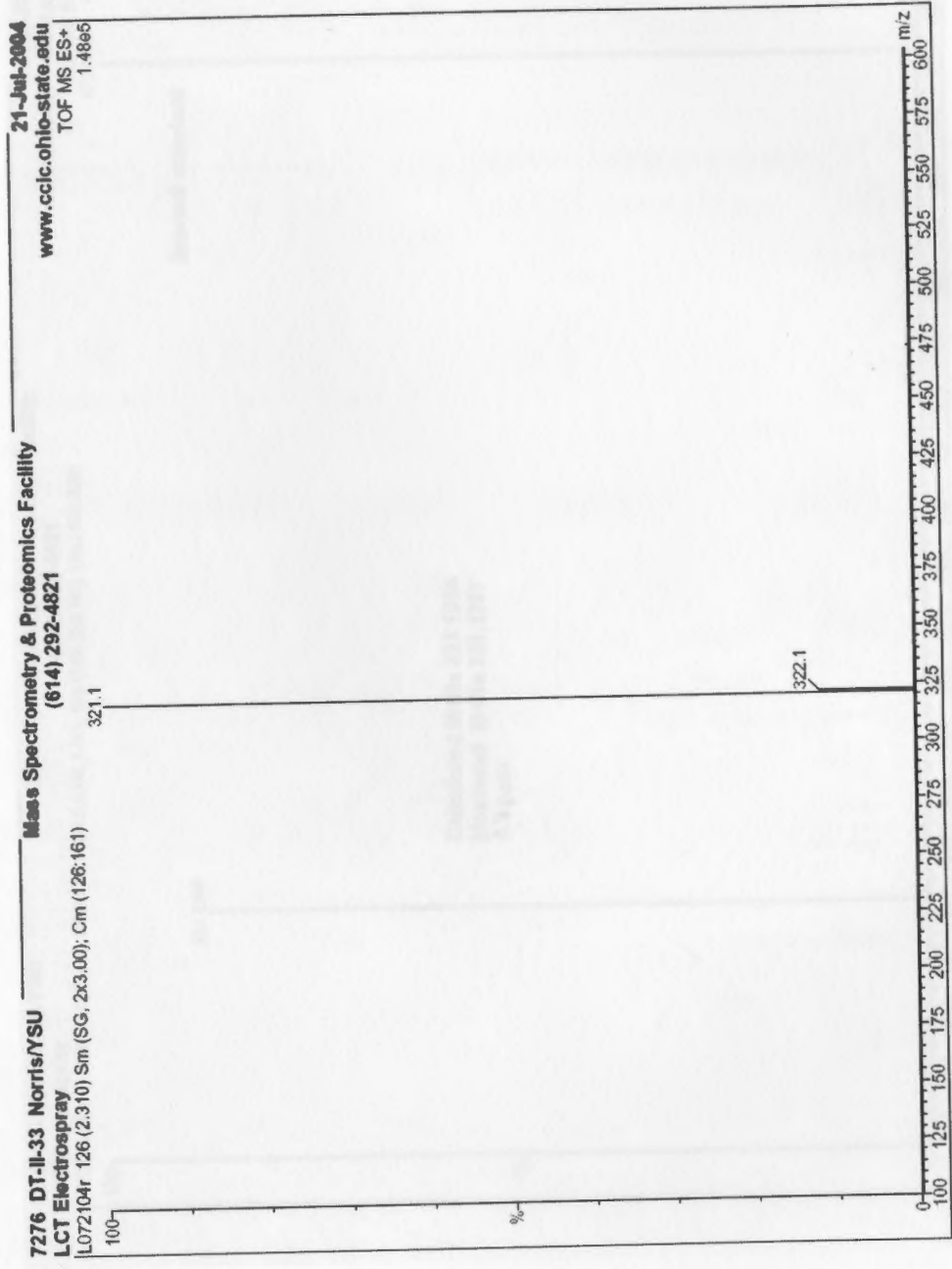


Figure 102: Low resolution mass spectrum alkyne 28

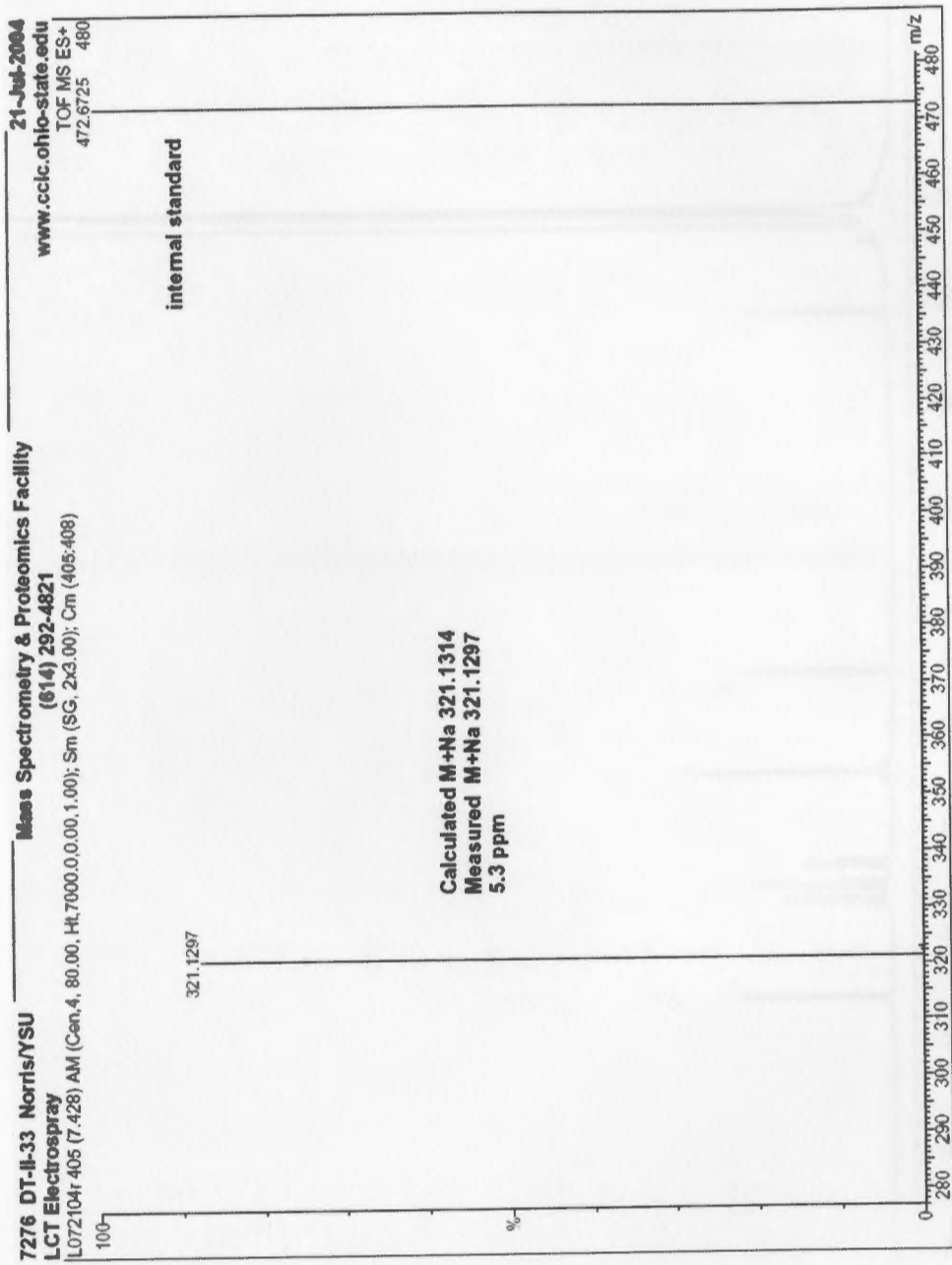
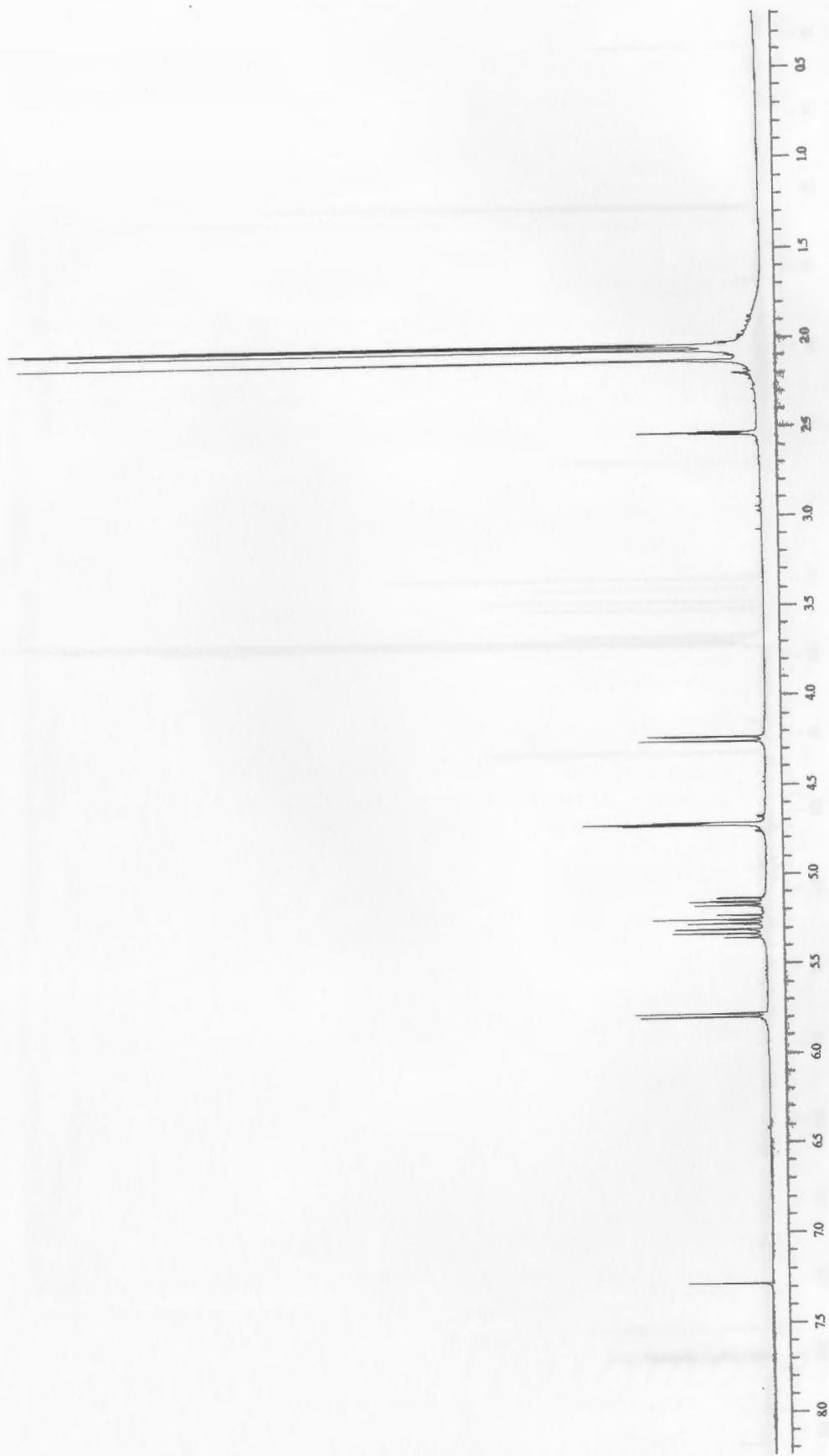
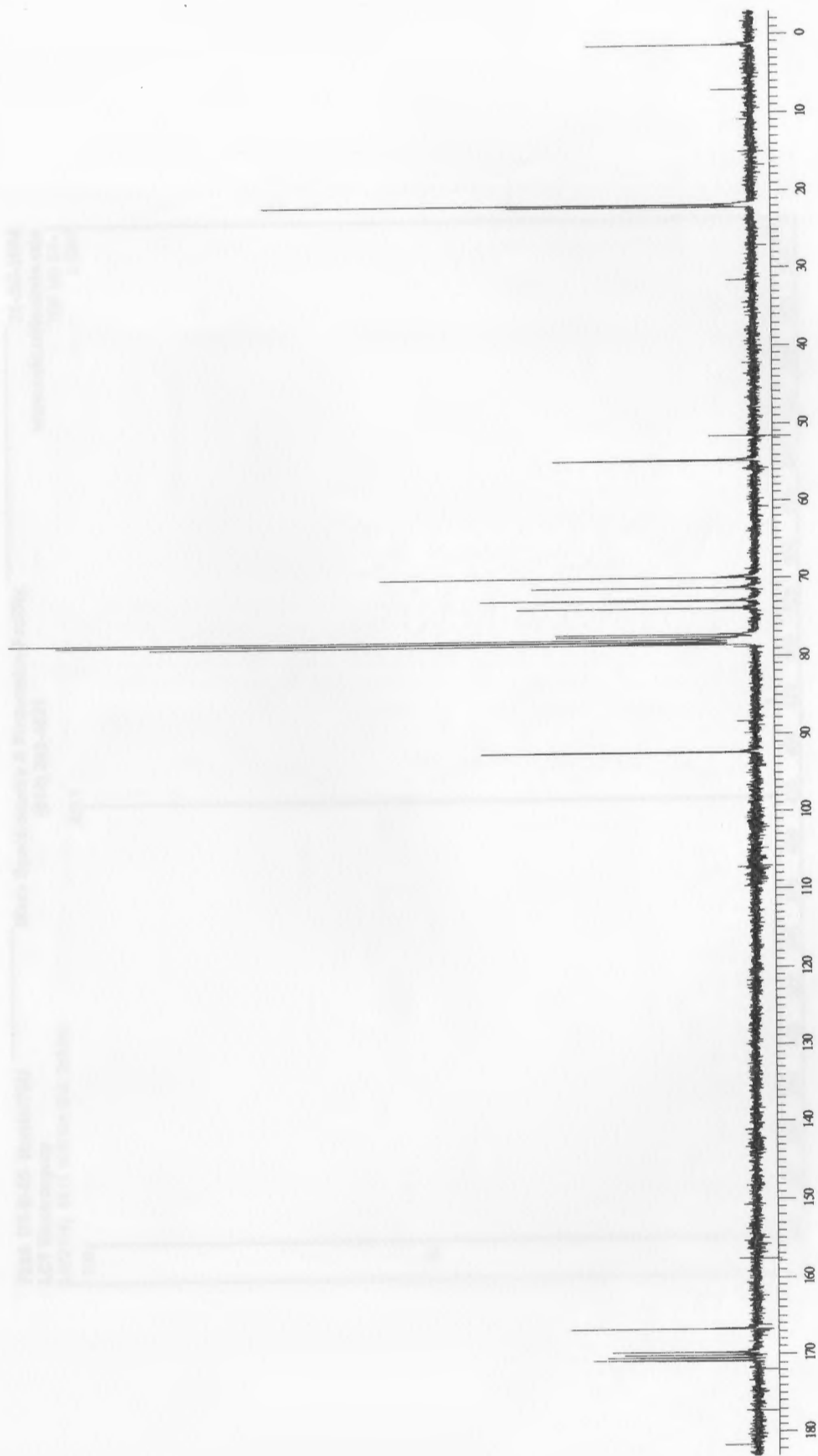


Figure 103: High resolution mass spectrum alkyne 28





**Figure 104:** 400 MHz  $^1\text{H}$  NMR spectrum of alkyne 29



**Figure 105:** 100 MHz  $^{13}\text{C}$  NMR spectrum of alkyne 29

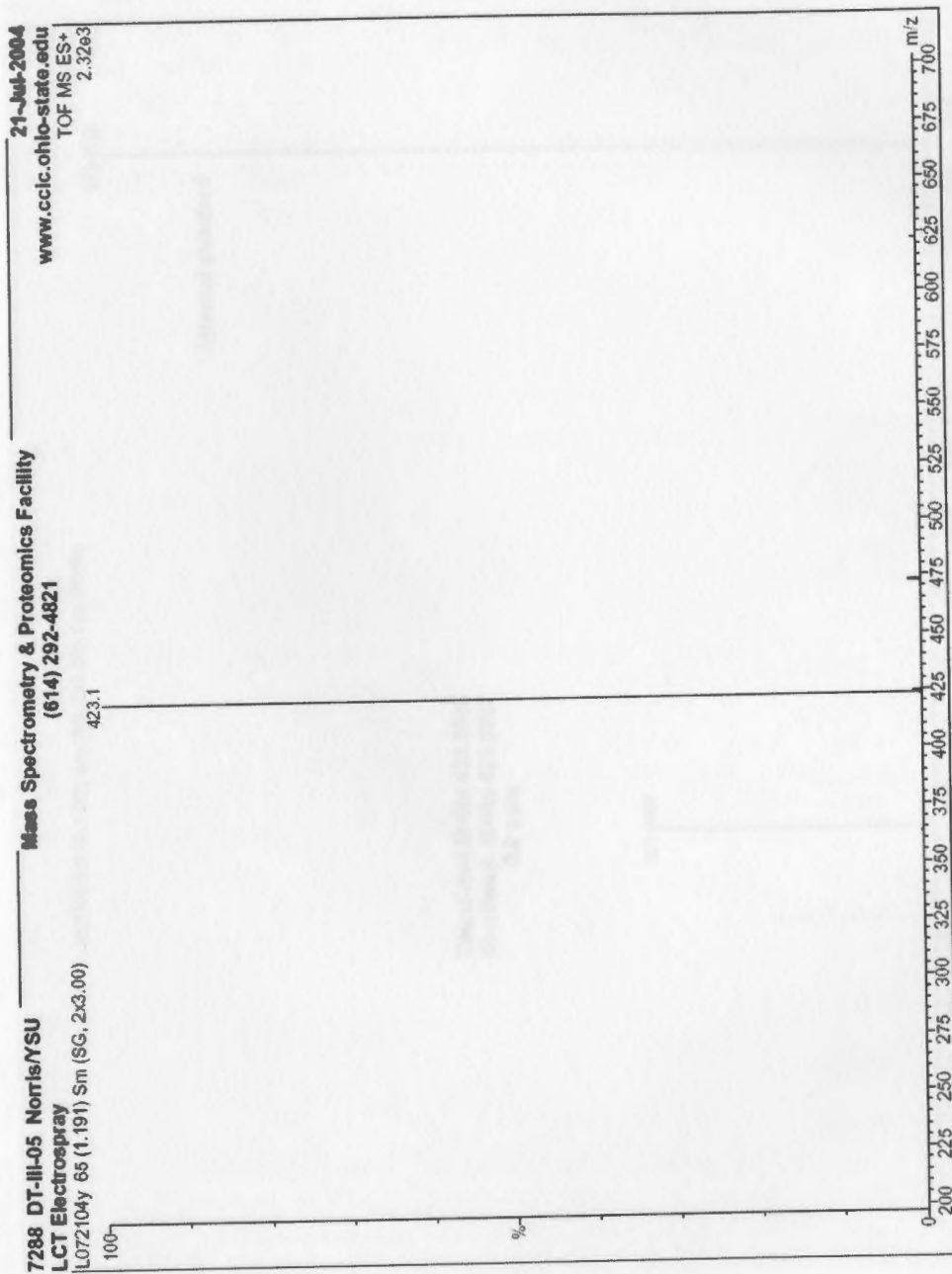


Figure 106: Low resolution mass spectrum alkyne 29

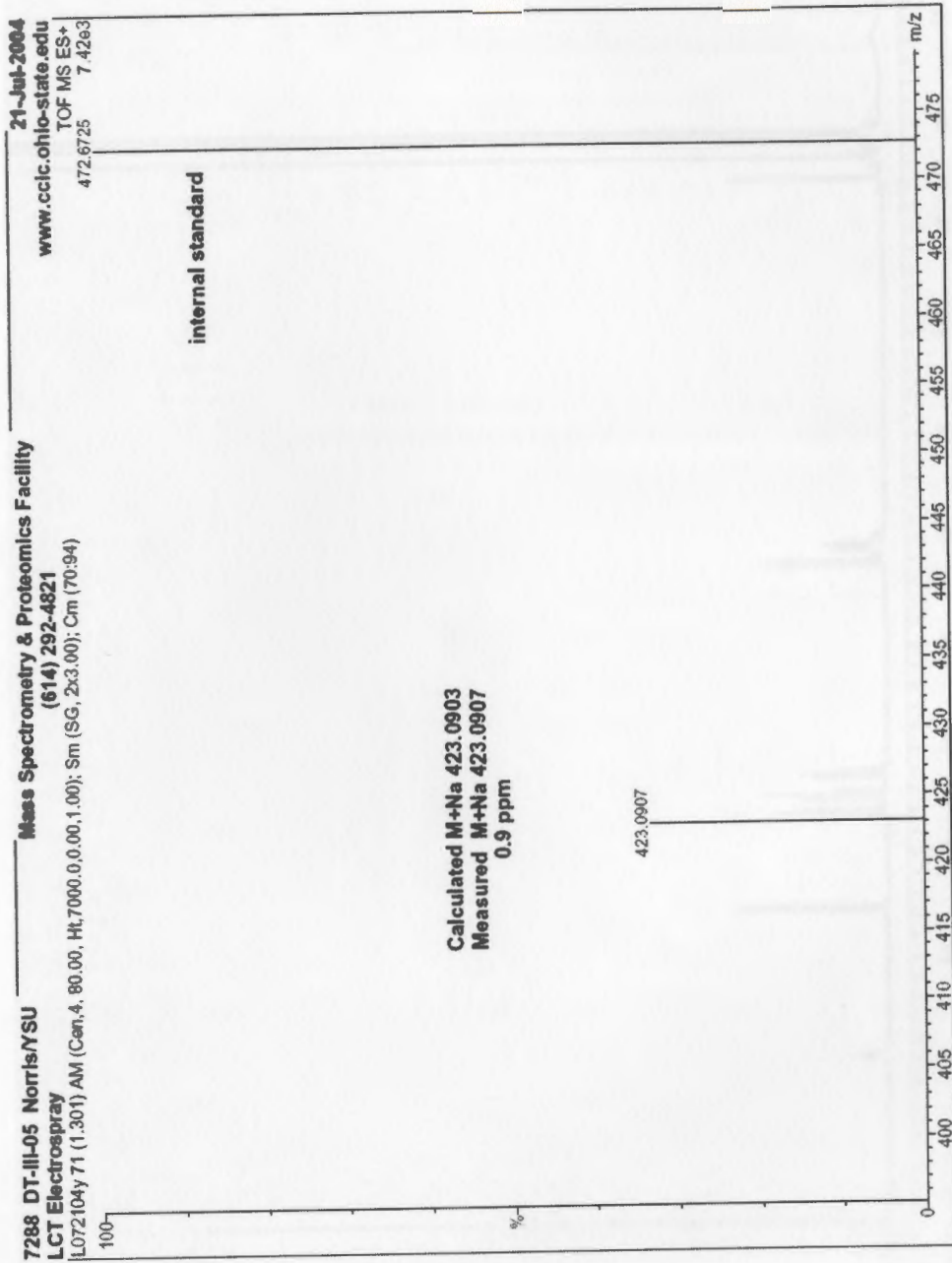
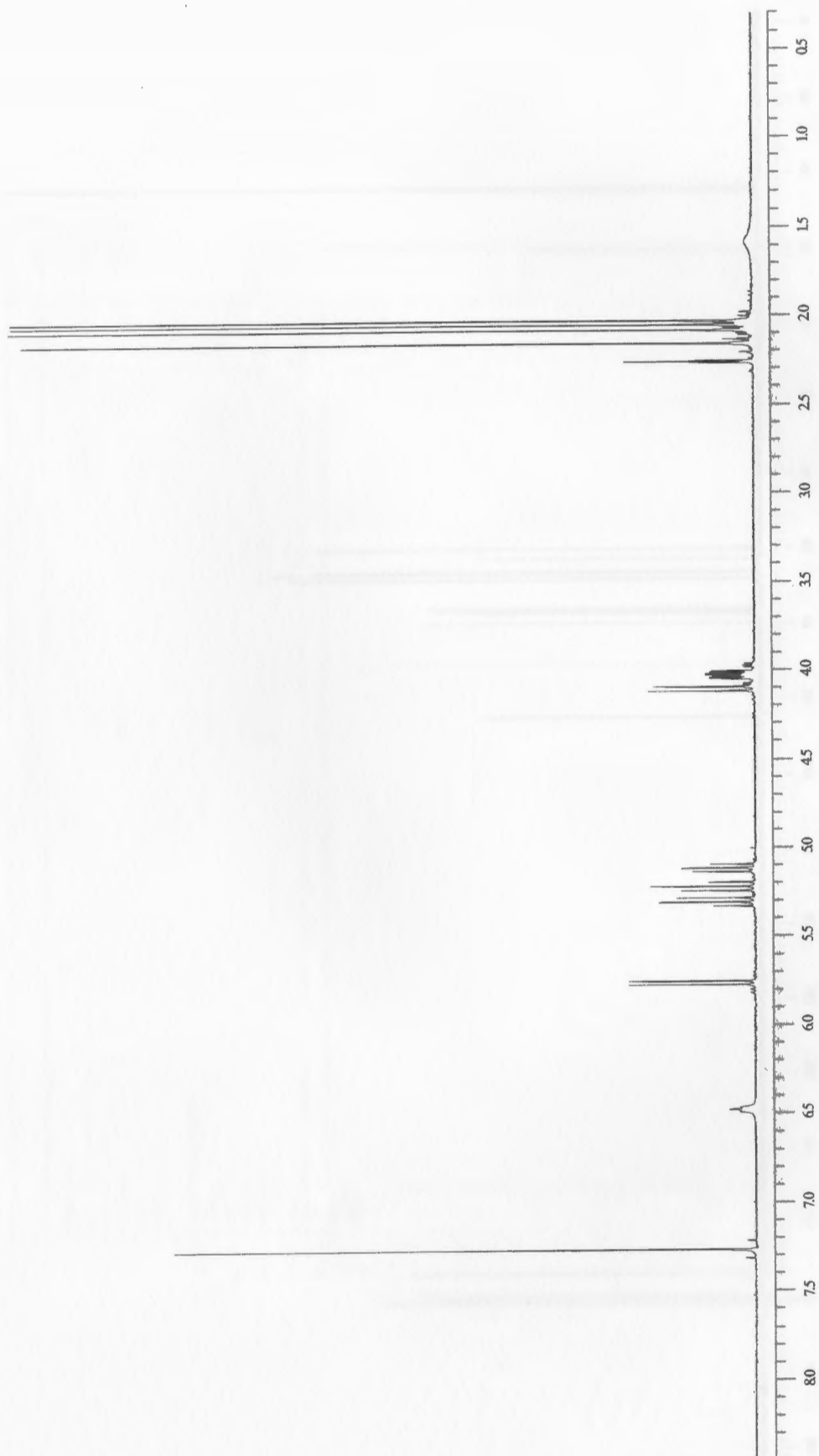


Figure 107: High resolution mass spectrum alkyne 29



**Figure 108:** 400 MHz  $^1\text{H}$  NMR spectrum of alkyne 30

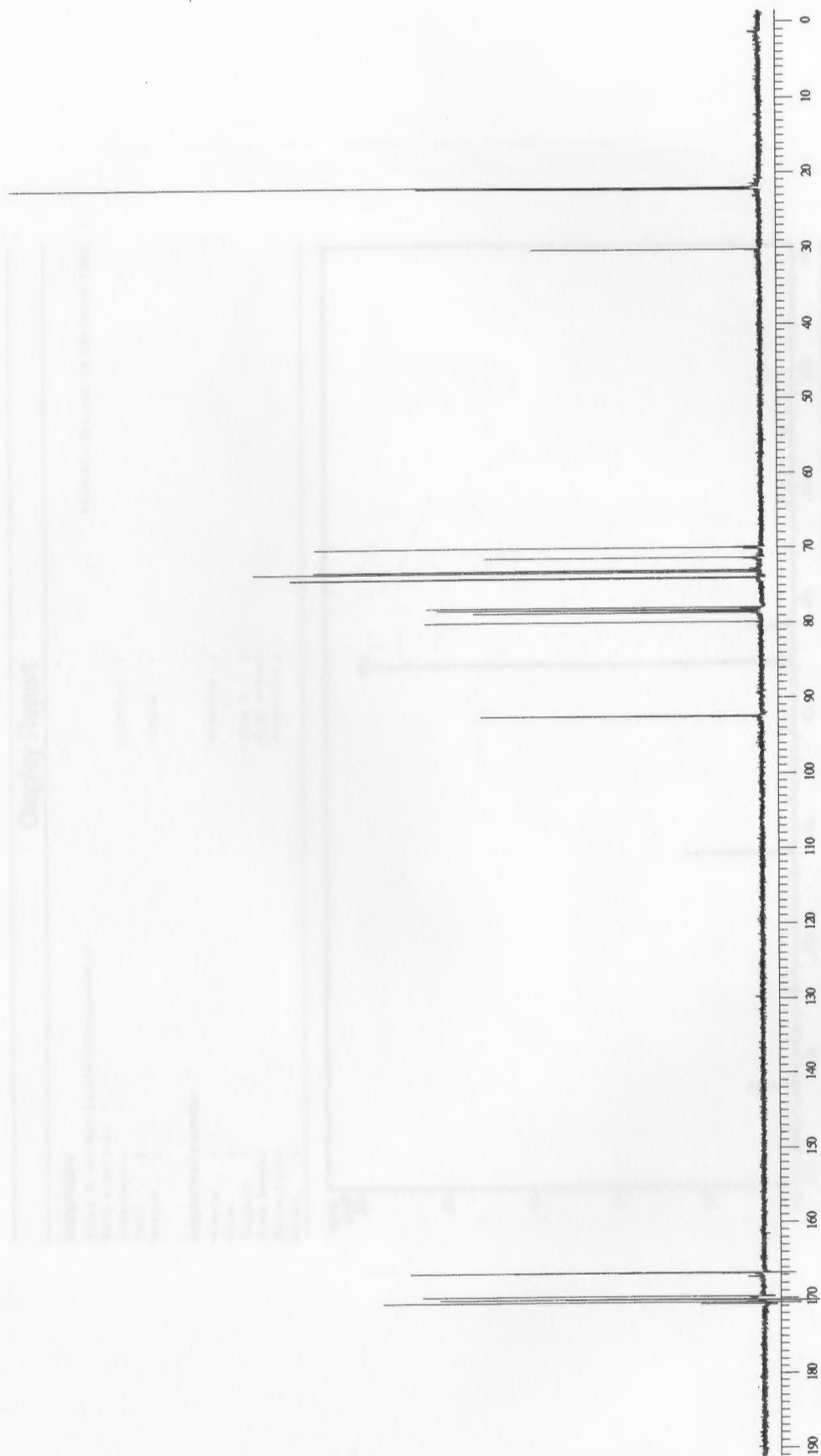


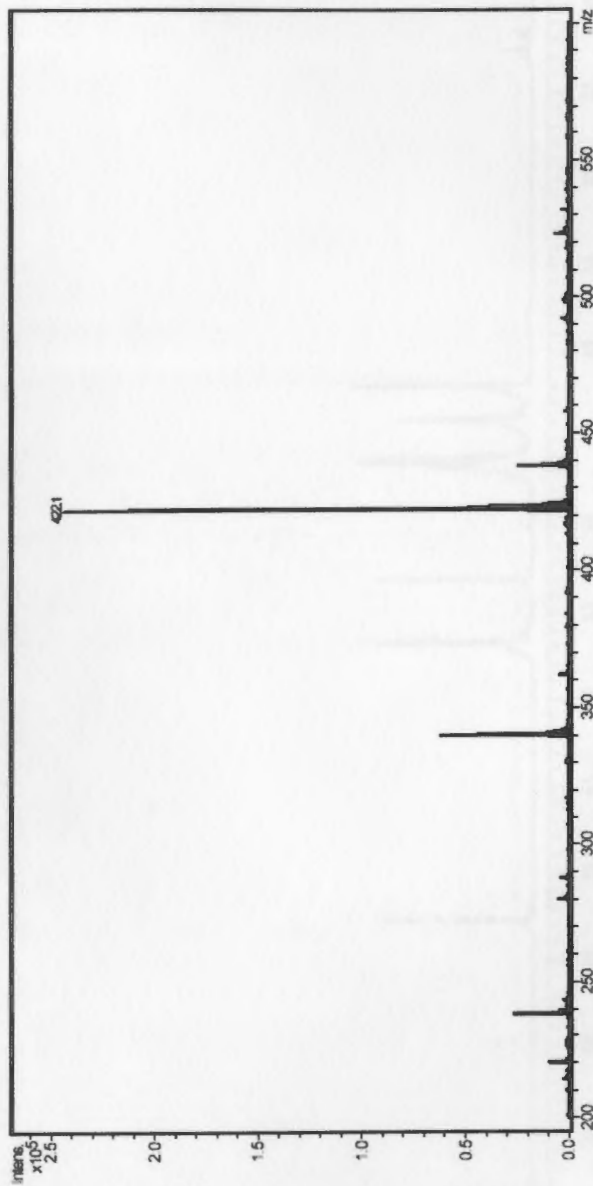
Figure 109: 100 MHz  $^{13}\text{C}$  NMR spectrum of alkyne 30

## Display Report

**Analysis Info:**

File: D:\HPCHEM\1\DATA\DT\MAL000.D  
 Date acquired: Printed: Fri Jul 29 08:06:04 2005  
 Instrument:  
 Task :  
 Method :  
 Operator :  
 Sample :  
 Acquisition Parameter:  
 Source :  
 Mode :  
 CapExit :  
 Scan Range:  
 Accum.time:  
 MS/MS :

Polarity :  
 Skim 1 :  
 Trap Drive:  
 Summation :



Bruker DataAnalysis Esquire-IC 1.6m, © Bruker Daltonik GmbH  
 Licensed to EQ\_135, Uni. of Ohio

- 1 -

**Figure 110: Low resolution mass spectrum alkyne 30**

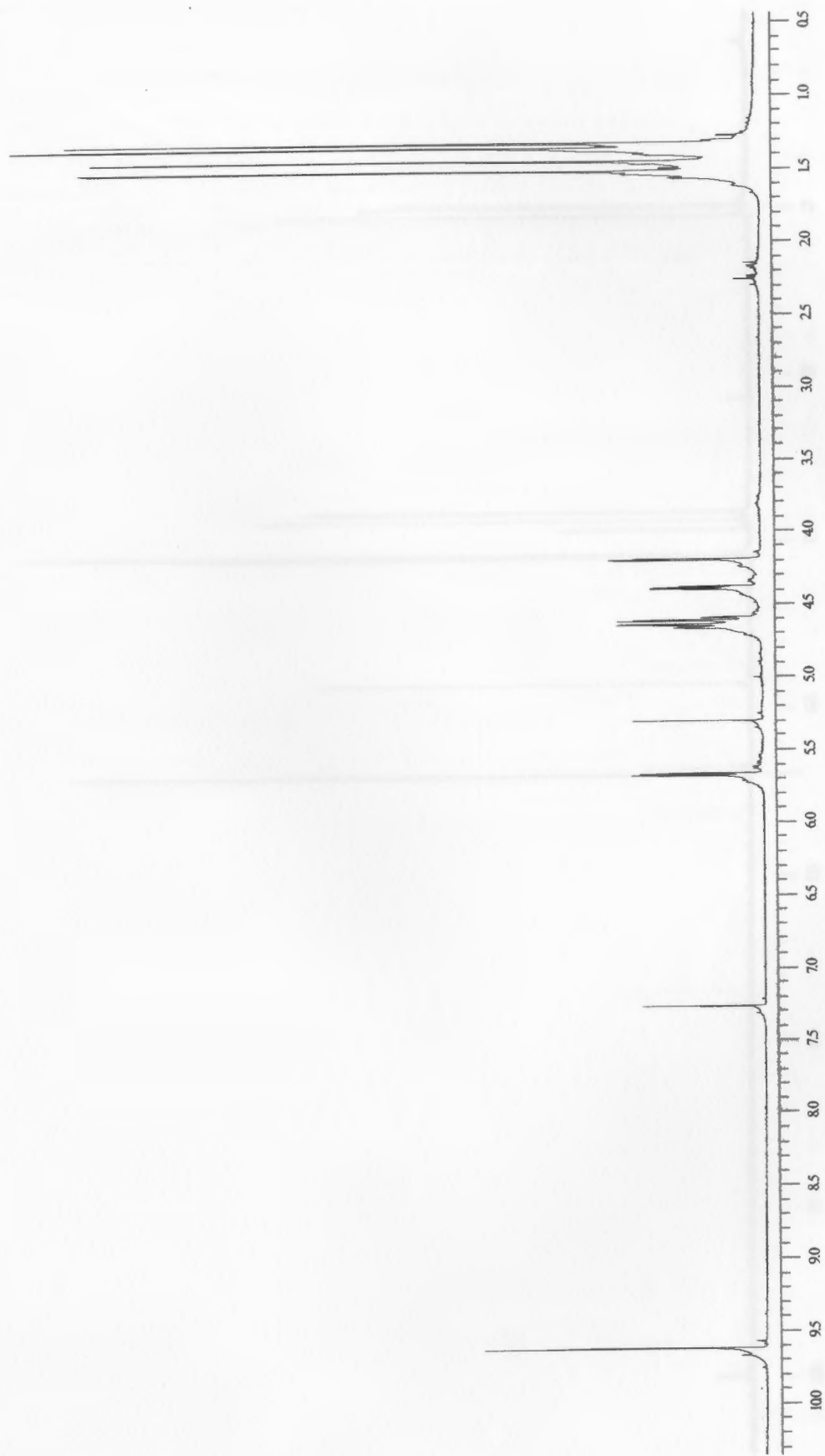
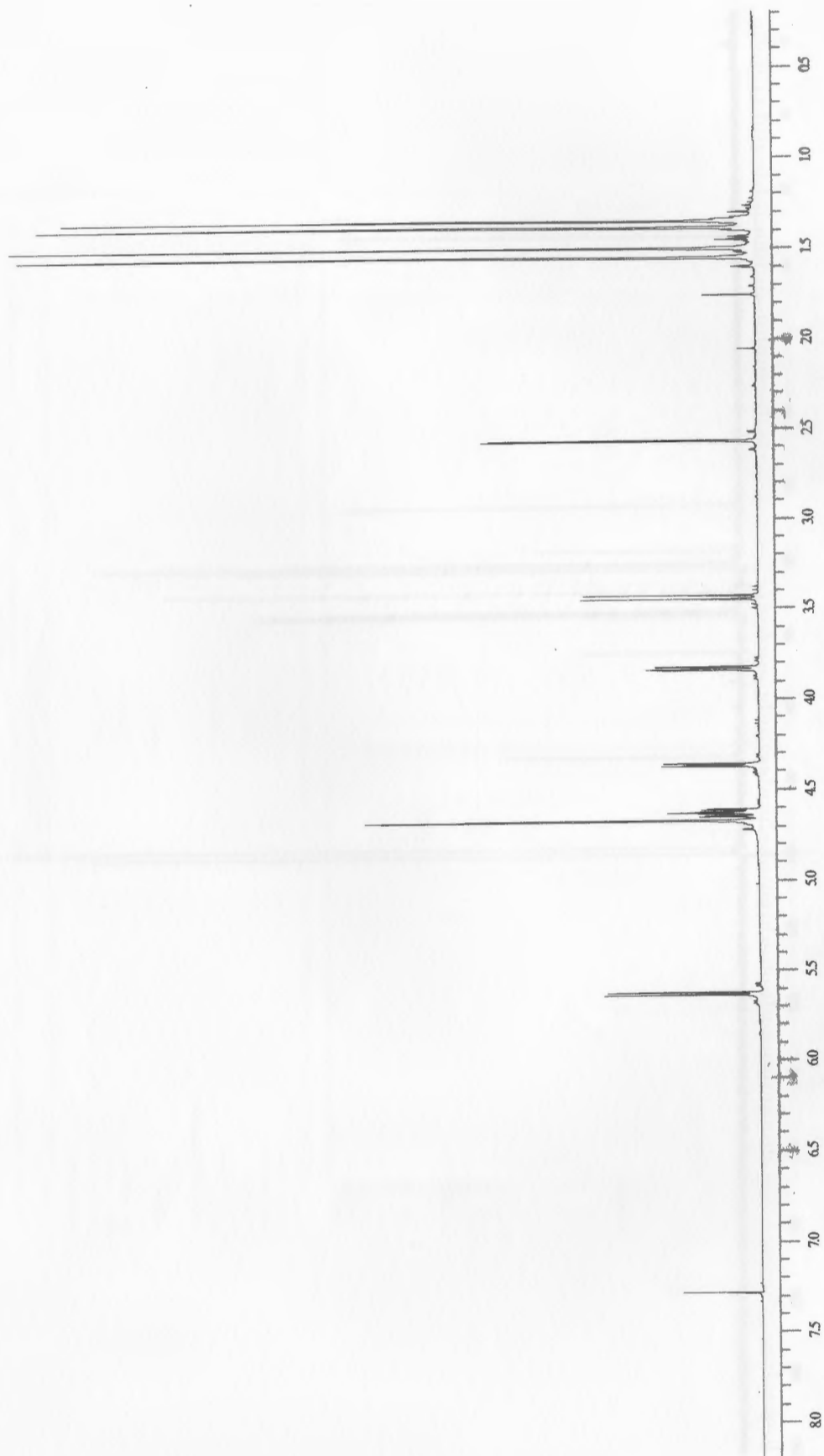


**Figure 111:** 400 MHz  $^1\text{H}$  NMR spectrum of aldehyde 31

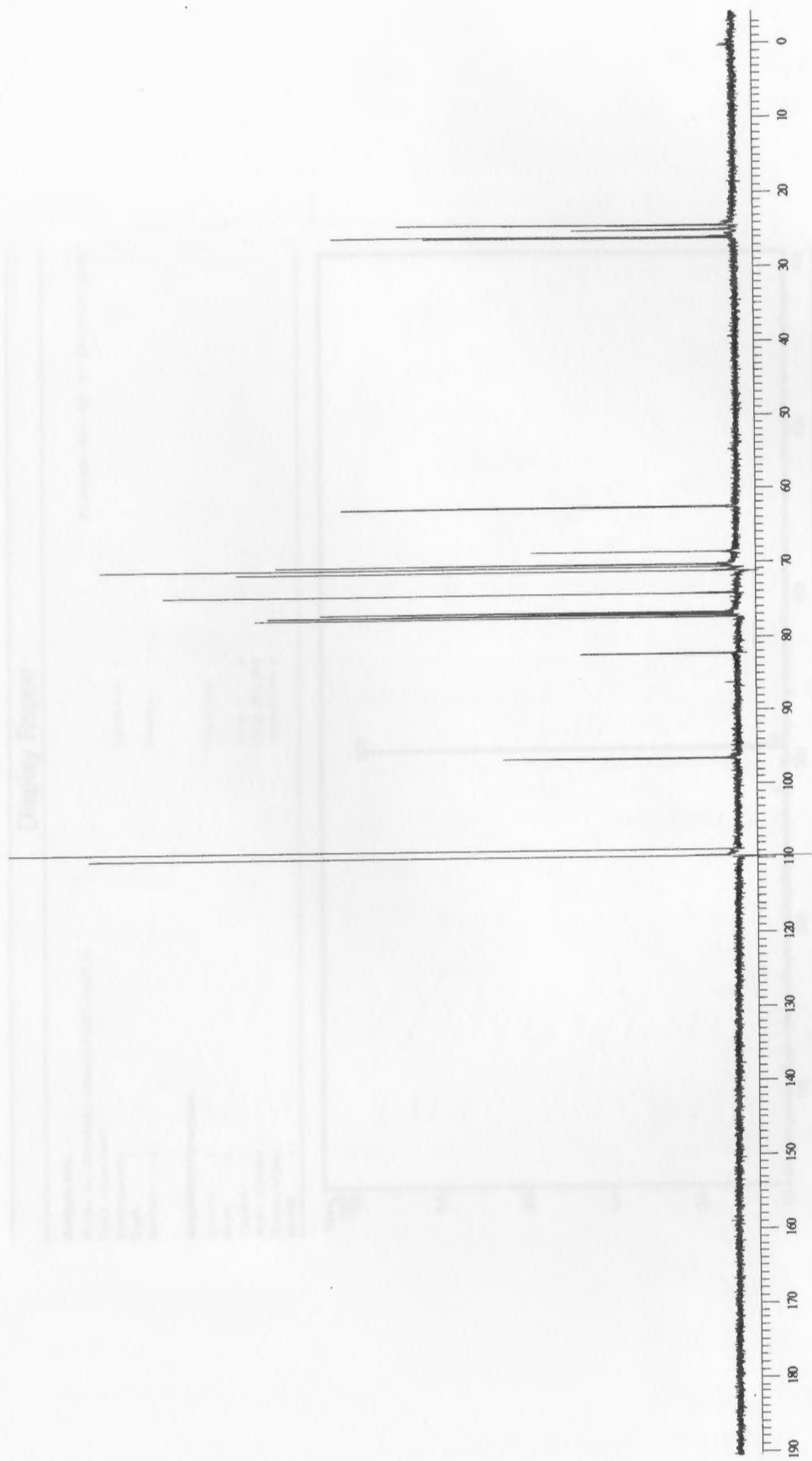




Figure 112: 100 MHz  $^{13}\text{C}$  NMR spectrum of aldehyde 31



**Figure 113:** 400 MHz  $^1\text{H}$  NMR spectrum of propargyl alcohol 32



**Figure 114:** 100 MHz  $^{13}\text{C}$  NMR spectrum of propargyl alcohol 32

## Display Report

## Analysis Info:

File: D:\HPCHEM\1\DATA\DT\DT7-3902.D

Date acquired:

Instrument:

Task :

Method :

Operator :

Sample :

Printed: Wed Jul 27 16:23:17 2005

## Acquisition Parameter:

Source :

Mode :

CapExit :

Scan Range:

Accum.time:

MS/MS :

Polarity :

Skim 1 :

Trap Drive:

Summation :



Brucker DataAnalysis Esquire-LC 1.6m, © Brucker Daltonik GmbH  
Licensed to EQ 135, Uni. of Ohio

- 1 -

Figure 115: Low resolution mass spectrum propargyl alcohol 32

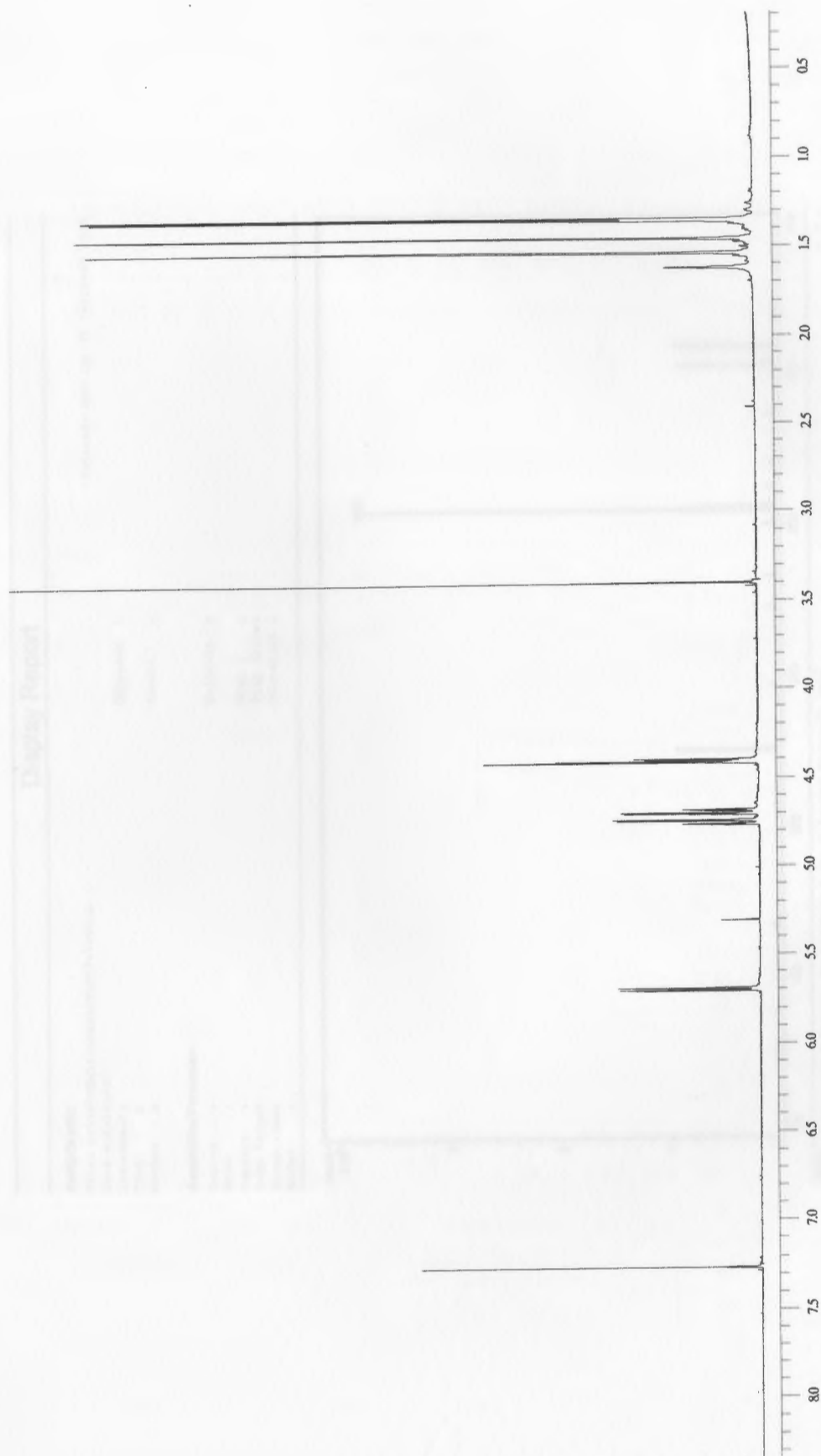
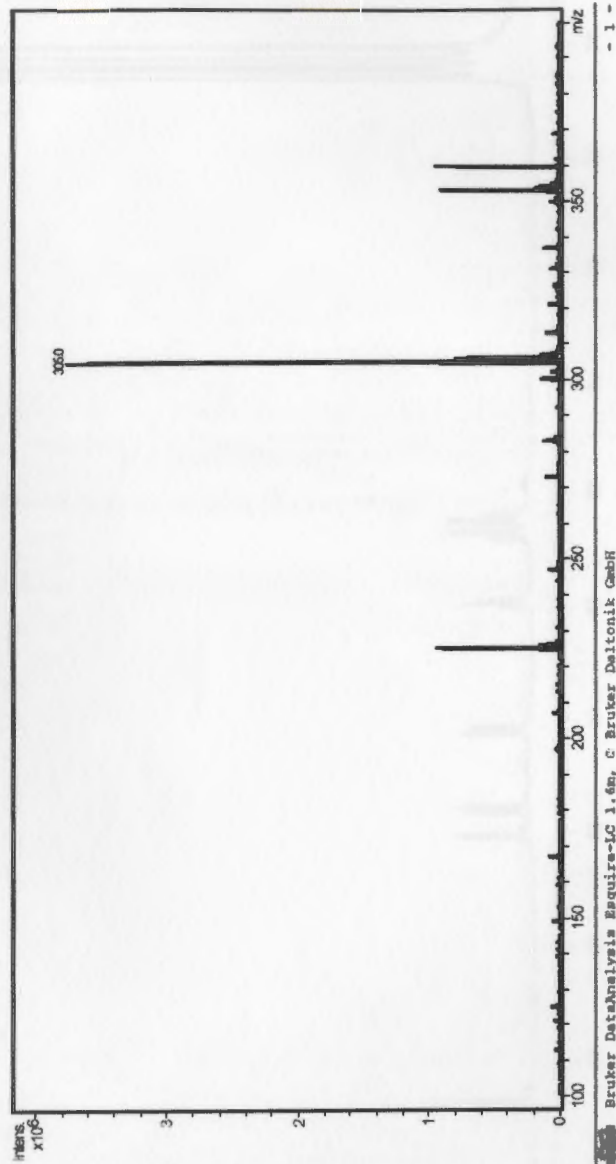


**Figure 116:** 400 MHz  $^1\text{H}$  NMR spectrum of alkynyl ketone 33

## Display Report

**Analysis Info:**  
File: D:\HPCHEM1\DATA\DATA7-7902.D  
Date acquired: Wed Jul 27 18:25:47 2005  
Instrument:  
Task :  
Method :  
Operator :  
Sample :  
Polarity :  
Skim 1 :  
Trap Drive:  
Summation :  
**Acquisition Parameter:**  
Source :  
Mode :  
CapExit :  
Scan Range:  
Accum.time:  
MS/MS :



Brucker DataAnalysis Esquire-IC 1.6m, © Bruker Daltonik GmbH  
Licensed to EQ\_133, Uni. of Ohio

Figure 117: Low resolution mass spectrum alkynyl ketone 33

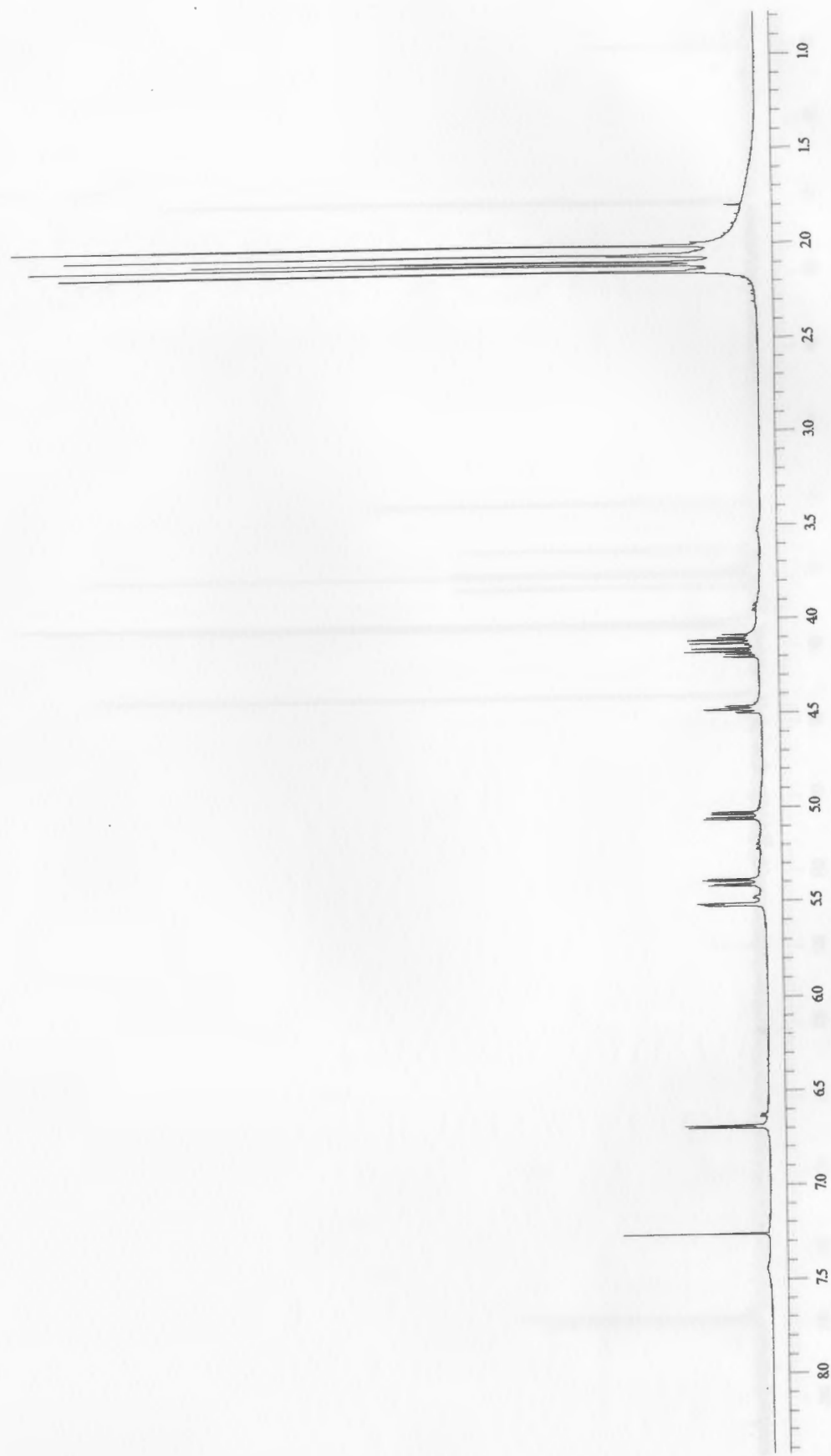


**Figure 118:** 400 MHz  $^1\text{H}$  NMR spectrum of galactosyl bromide 35

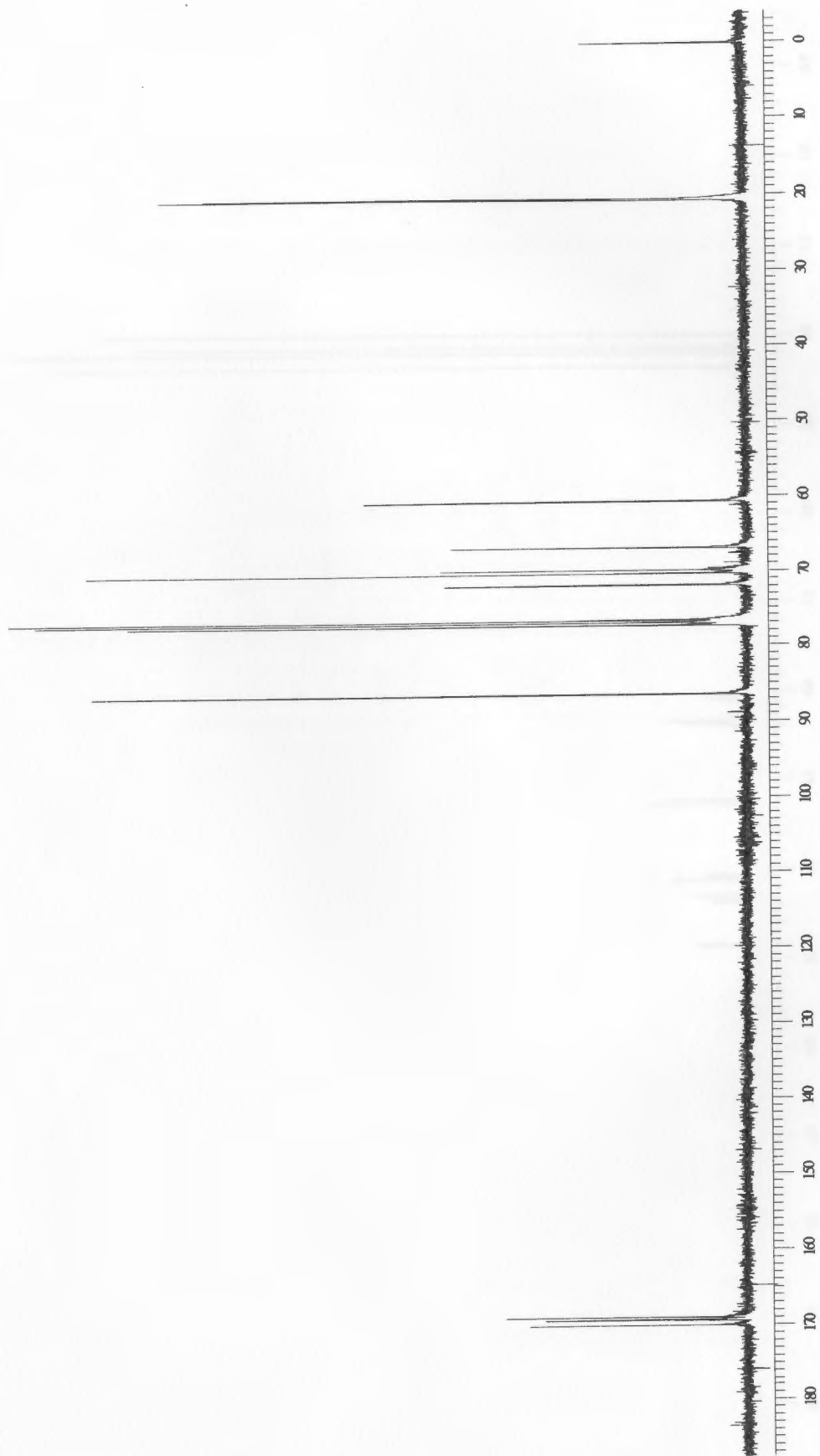


**Figure 119:** 100 MHz  $^{13}\text{C}$  NMR spectrum of galactosyl bromide 35



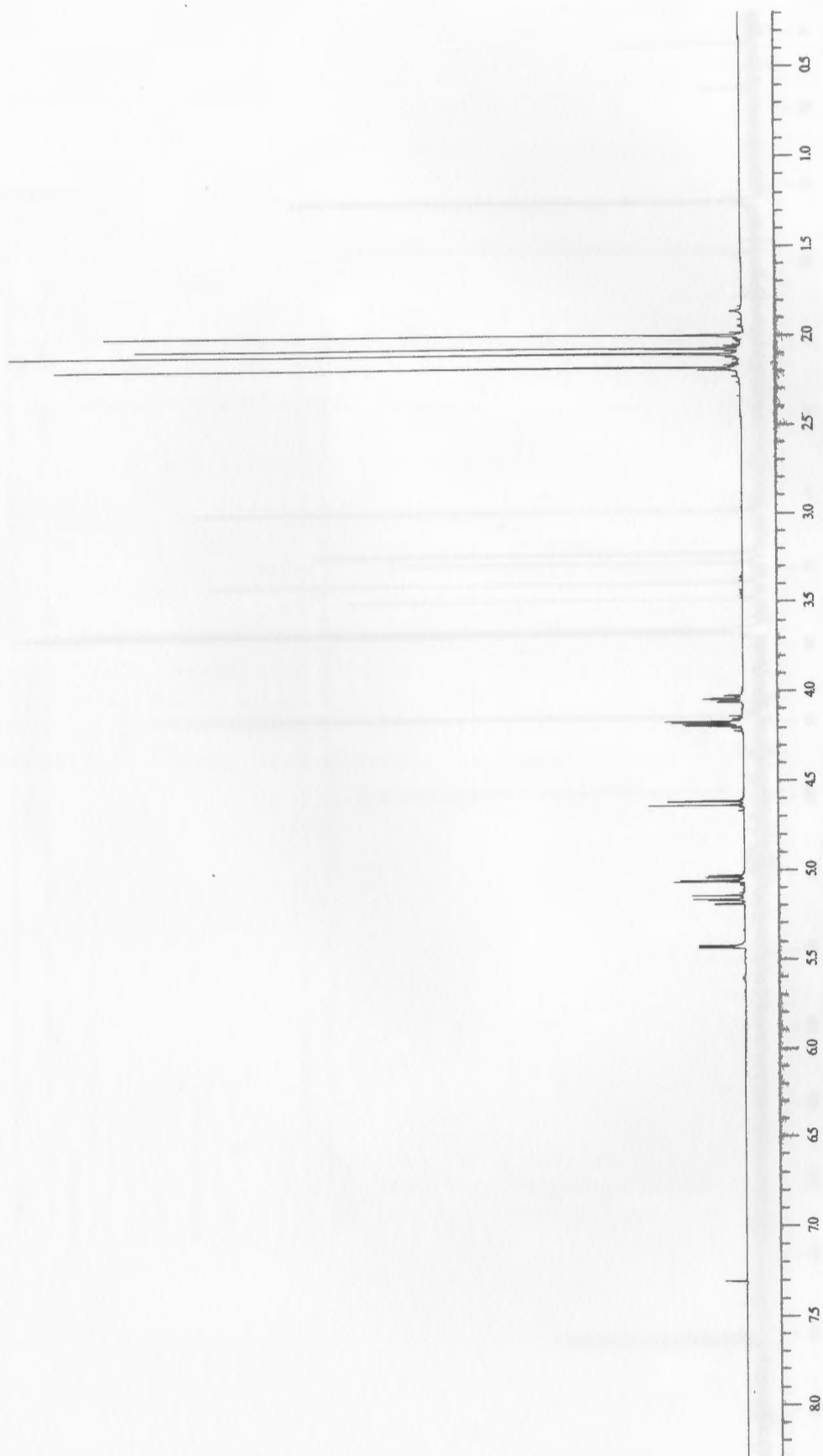


**Figure 120:** 400 MHz  $^1\text{H}$  NMR spectrum of galactosyl azide 36

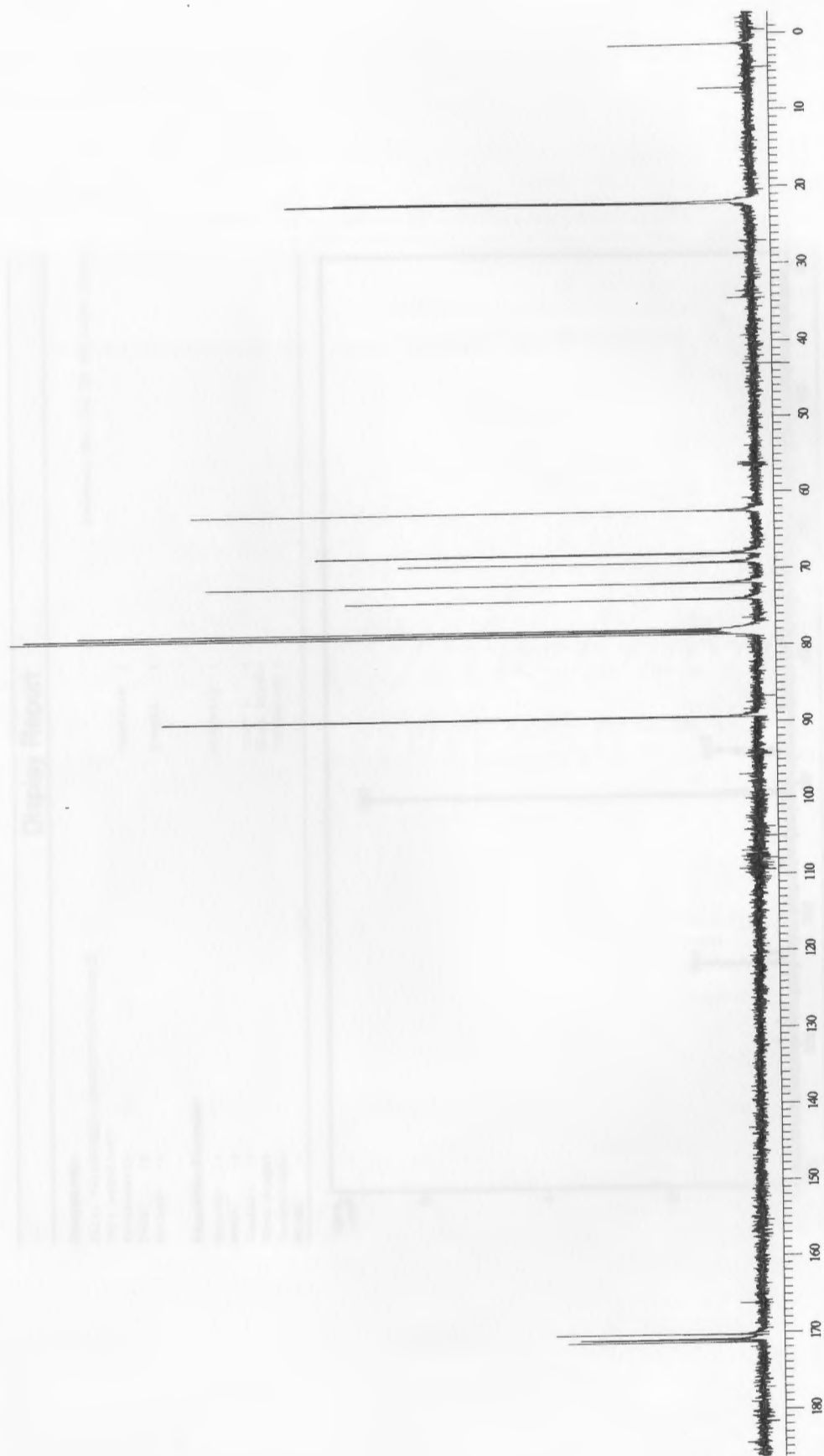


Figure 121: 100 MHz  $^{13}\text{C}$  NMR spectrum of galactosyl azide 36

## Display Report

**Analysis Info:**

File: D:\EPCHEM\1\DATA\DT\DT7-1093.D

Date acquired:

Instrument:

Task :

Method :

Operator :

Sample :

Printed: Wed Jul 27 18:26:30 2005

**Acquisition Parameter:**

Source :

Mode :

CapExit :

Scan Range:

Accum.time:

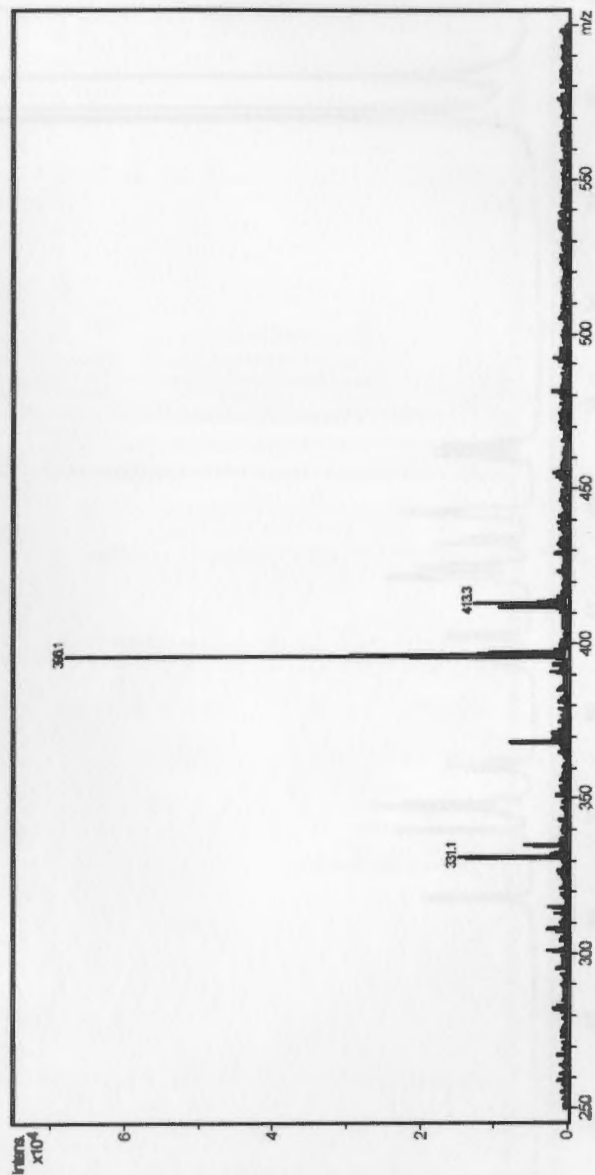
MS/MS :

Polarity :

Skim 1 :

Trap Drive:

Summation :


 Bruker DataAnalysis Esquire-IC 1.6m, © Bruker Daltonik GmbH  
 Licensed to EQ\_135, Uni. of Ohio

- 1 -

**Figure 122:** Low resolution mass spectrum galactosyl azide 36

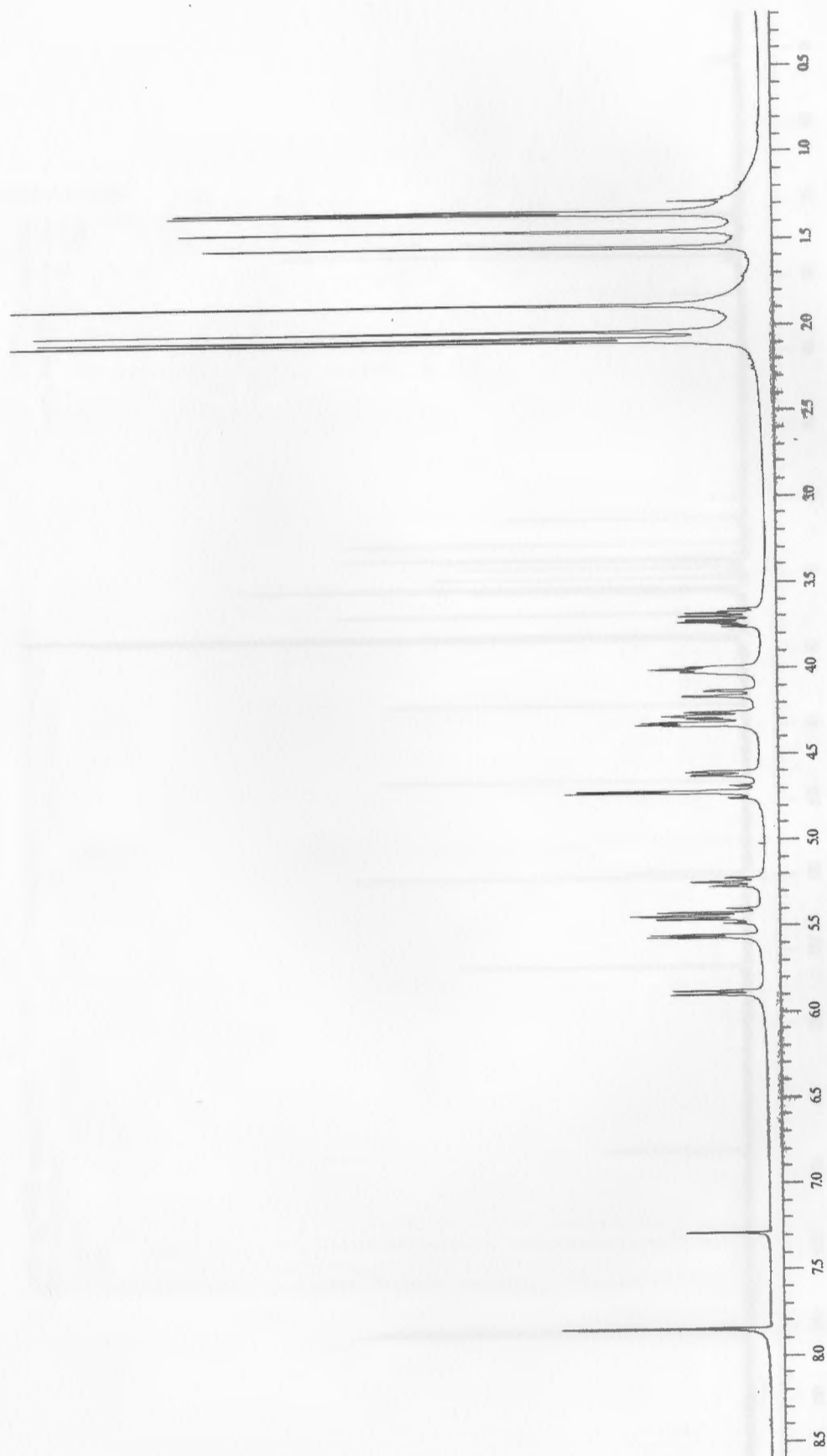


**Figure 123:** 400 MHz  $^1\text{H}$  NMR spectrum of triazole 37

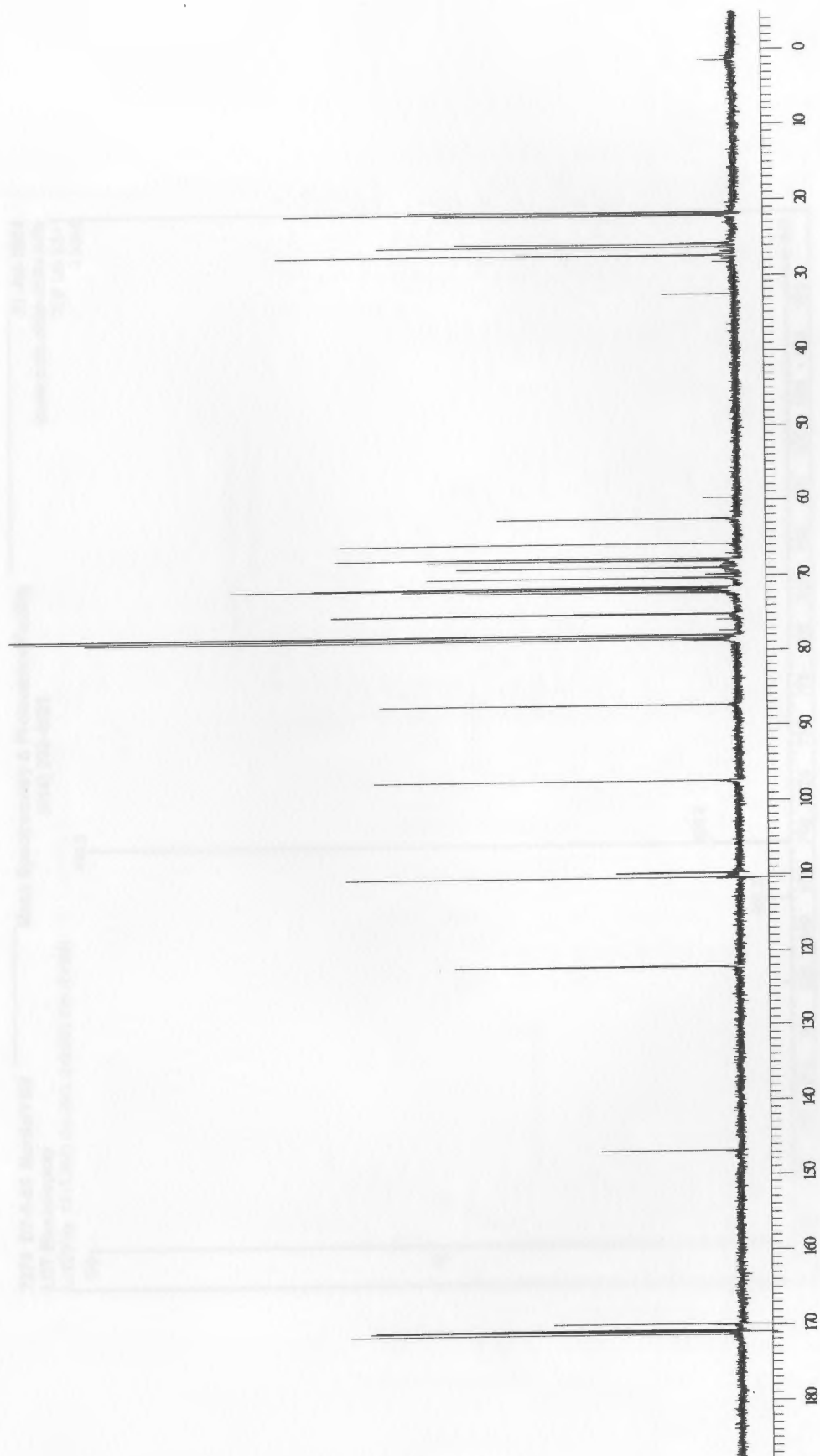


Figure 124: 100 MHz  $^{13}\text{C}$  NMR spectrum of triazole 37

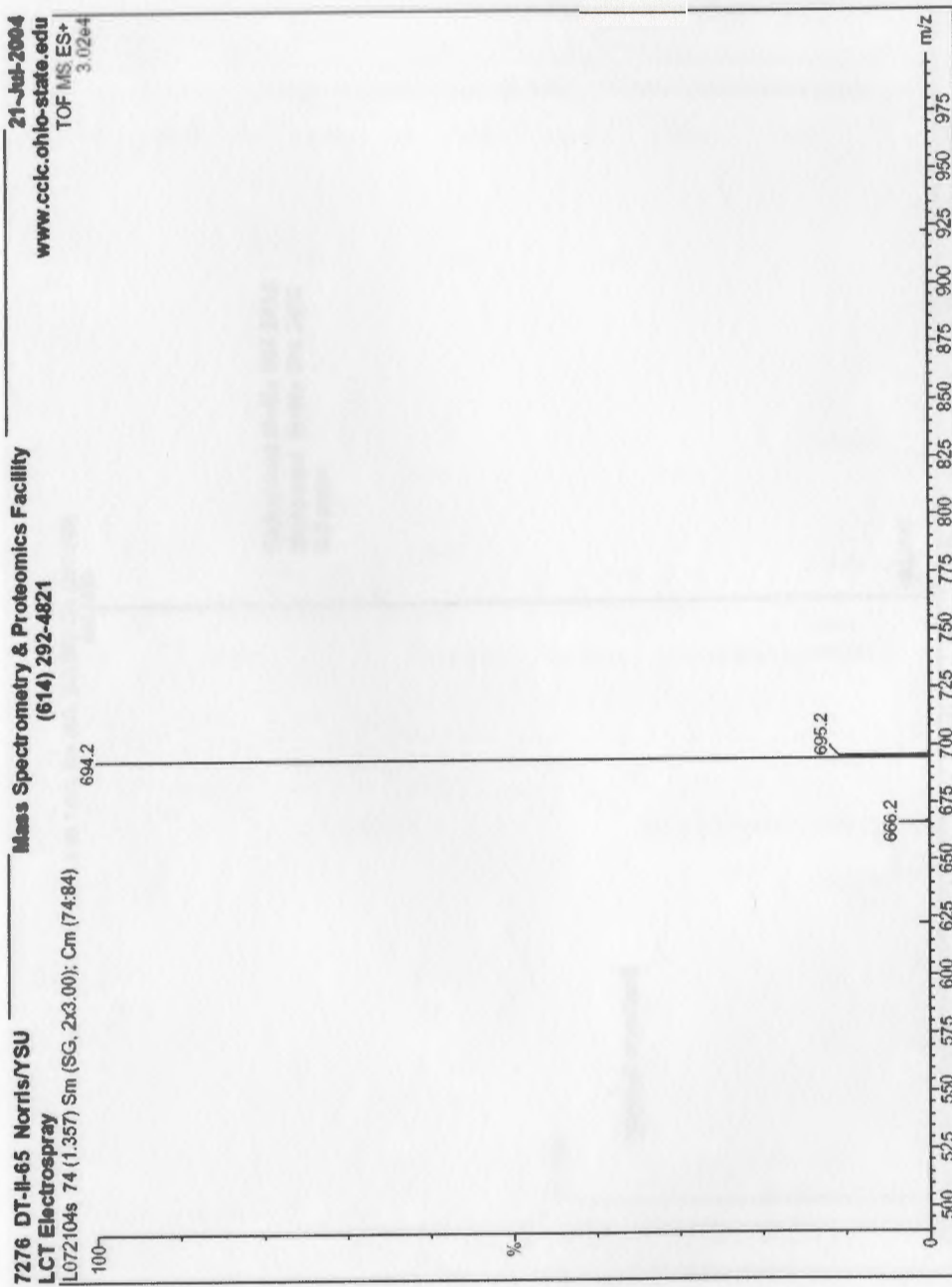


Figure 125: Low resolution mass spectrum of triazole 37

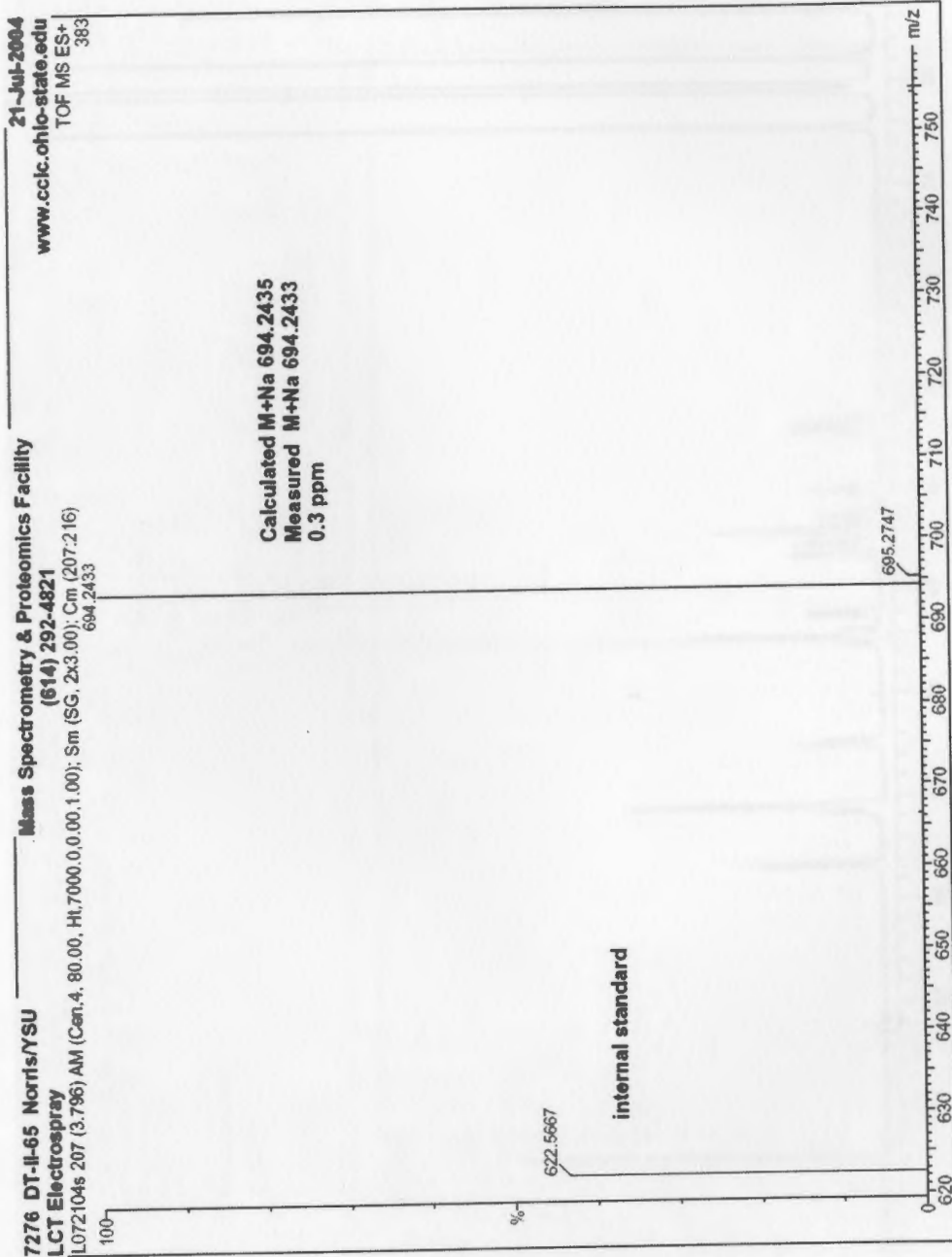
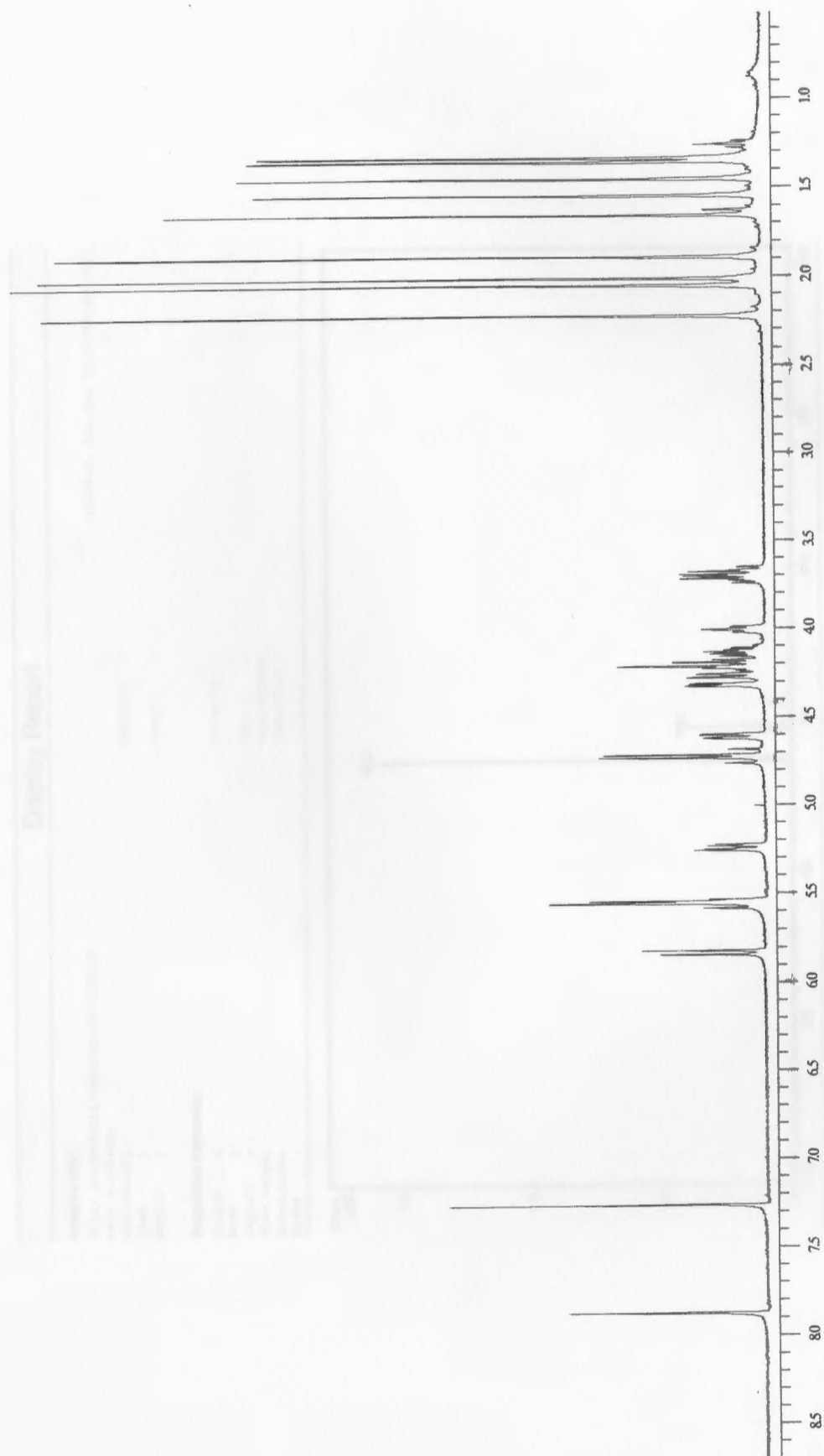


Figure 126: High resolution mass spectrum of triazole 37

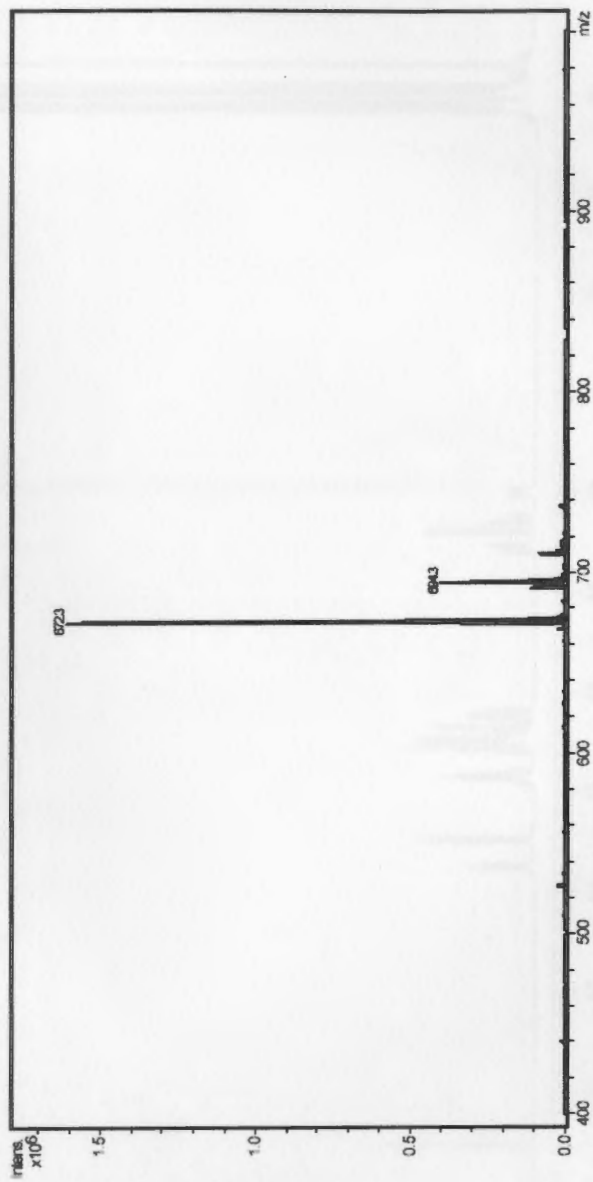


**Figure 127:** 400 MHz  $^1\text{H}$  NMR spectrum of triazole 38



## Display Report

**Analysis Info:**  
File: D:\HPCHEM\1\DATA\DF\DF7-1072.D  
Date acquired: Printed: Fri Jul 29 07:58:44 2005  
Instrument:  
Task :  
Method :  
Operator :  
Sample :  
Acquisition Parameter:  
Source :  
Mode :  
CapExit :  
Scan Range:  
Accun.time:  
MS/MS :  
Polarity :  
Skim 1 :  
Trap Drive:  
Summation :



Brucker DataAnalysis Esquire-LC 1.6m, © Brucker Daltonik GmbH  
Licensed to EQ 135, Uni. of Ohio

- 1 -

Figure 128: Low resolution mass spectrum of triazole 38

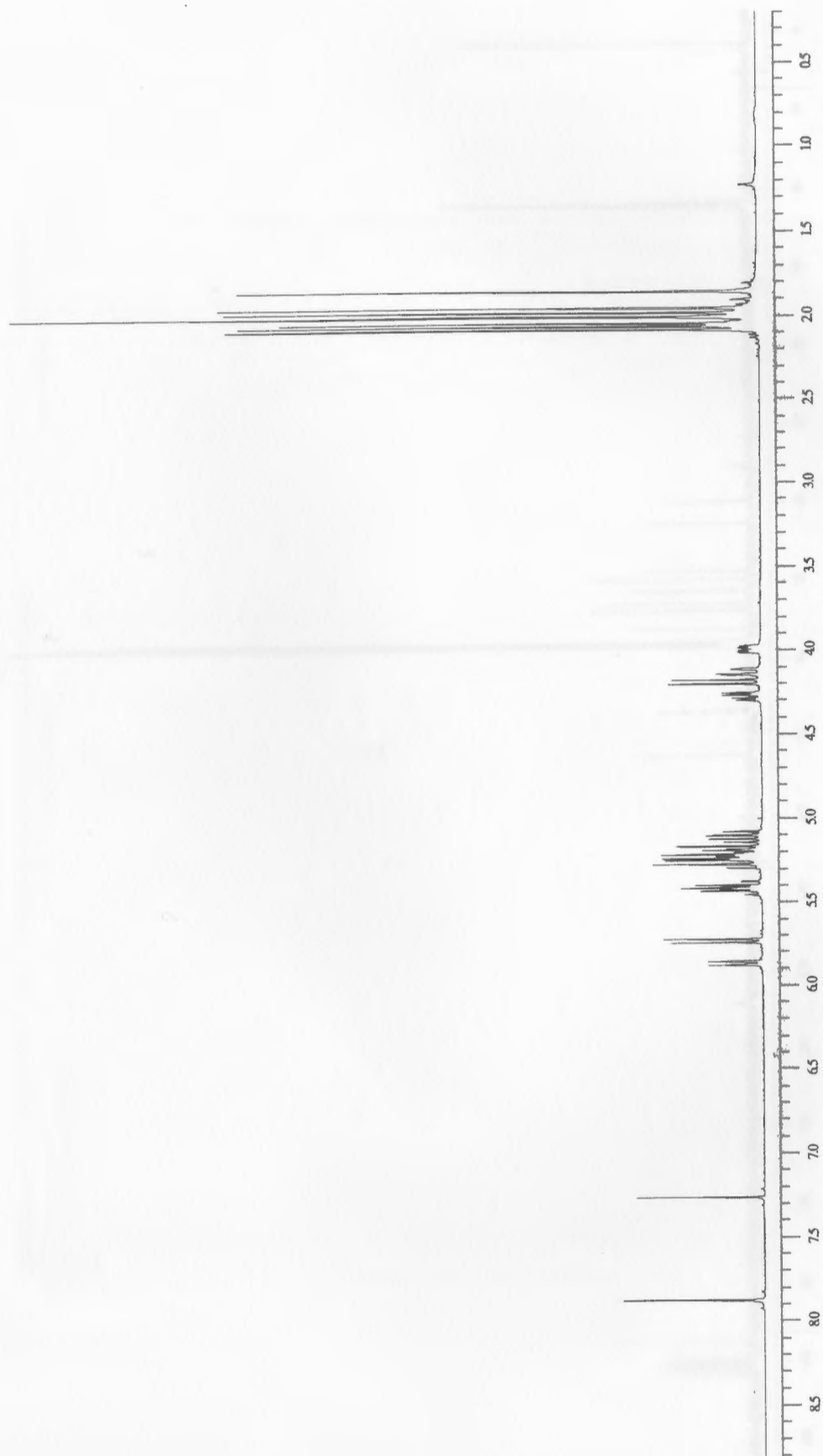


**Figure 129:** 400 MHz  $^1\text{H}$  NMR spectrum of triazole 39

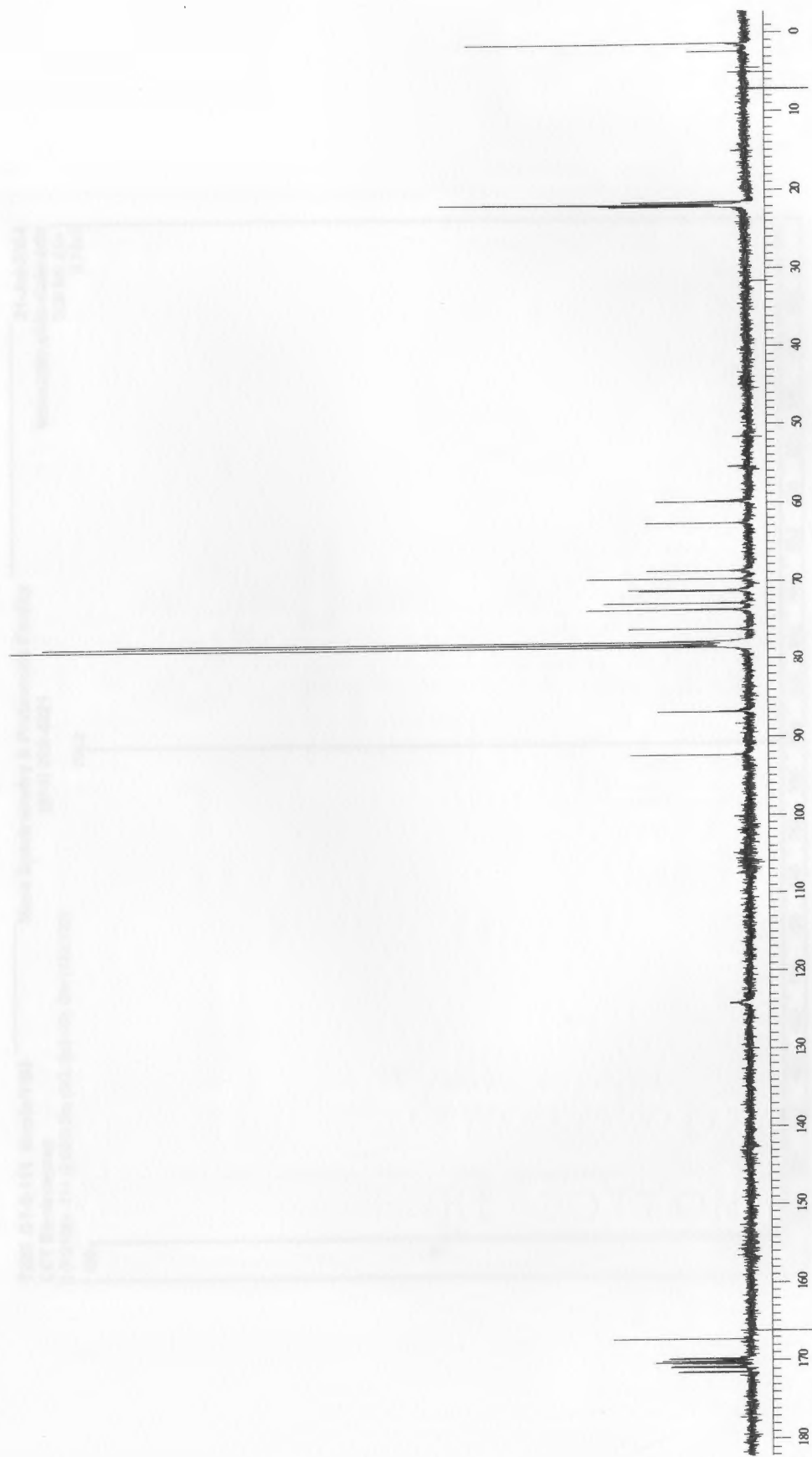


**Figure 130:** 100 MHz  $^{13}\text{C}$  NMR spectrum of triazole 39

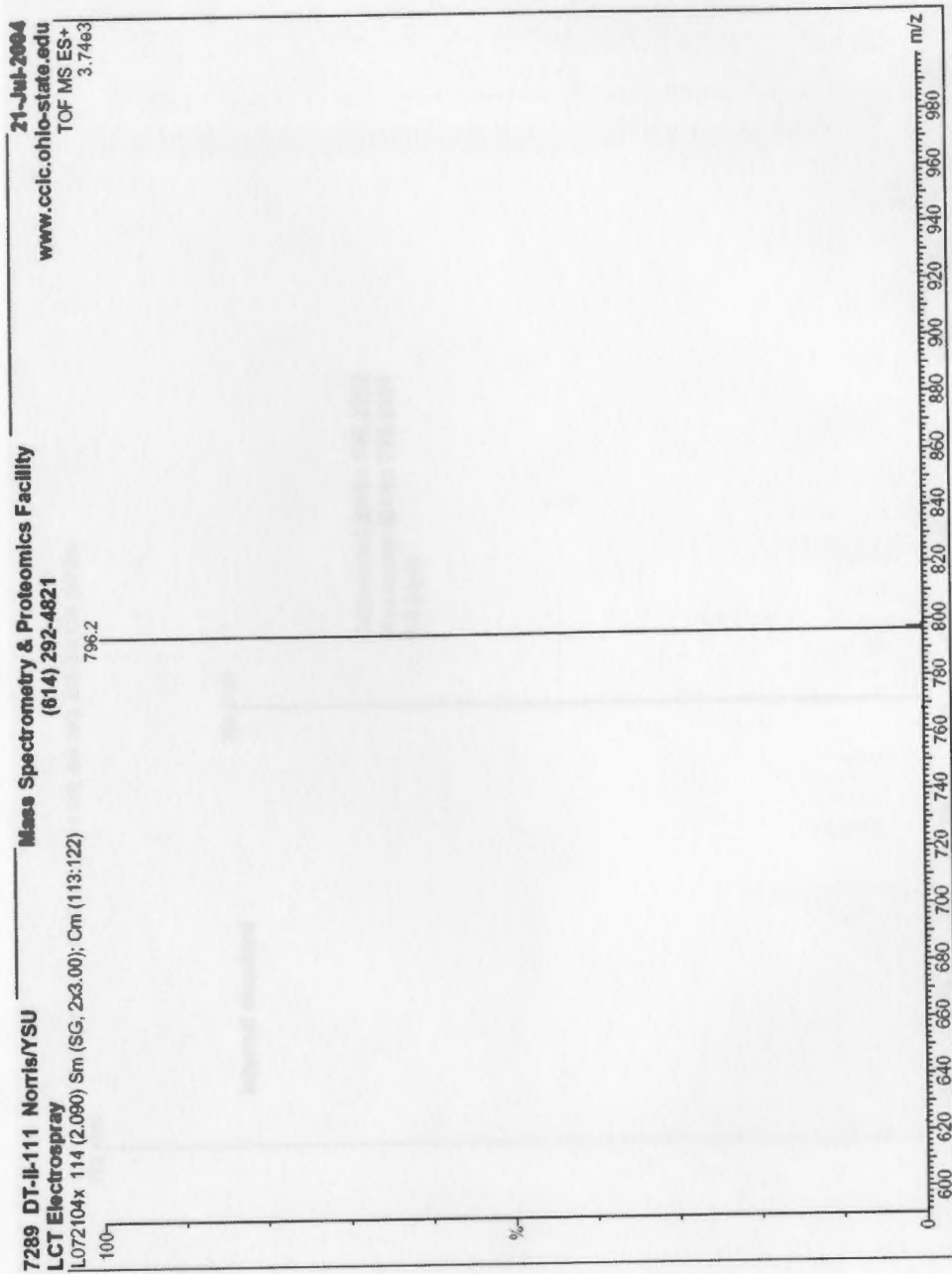


Figure 131: Low resolution mass spectrum of triazole 39

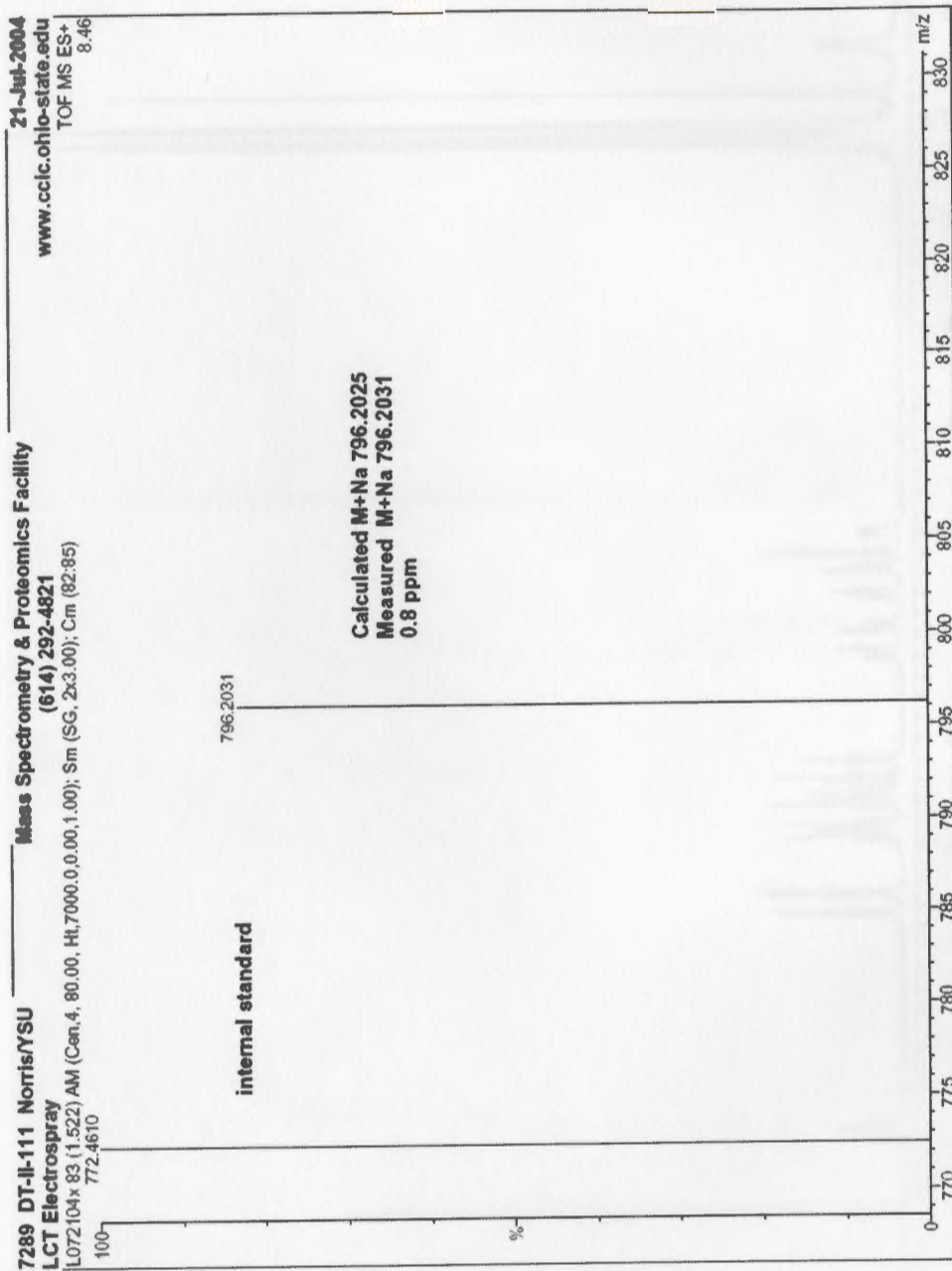
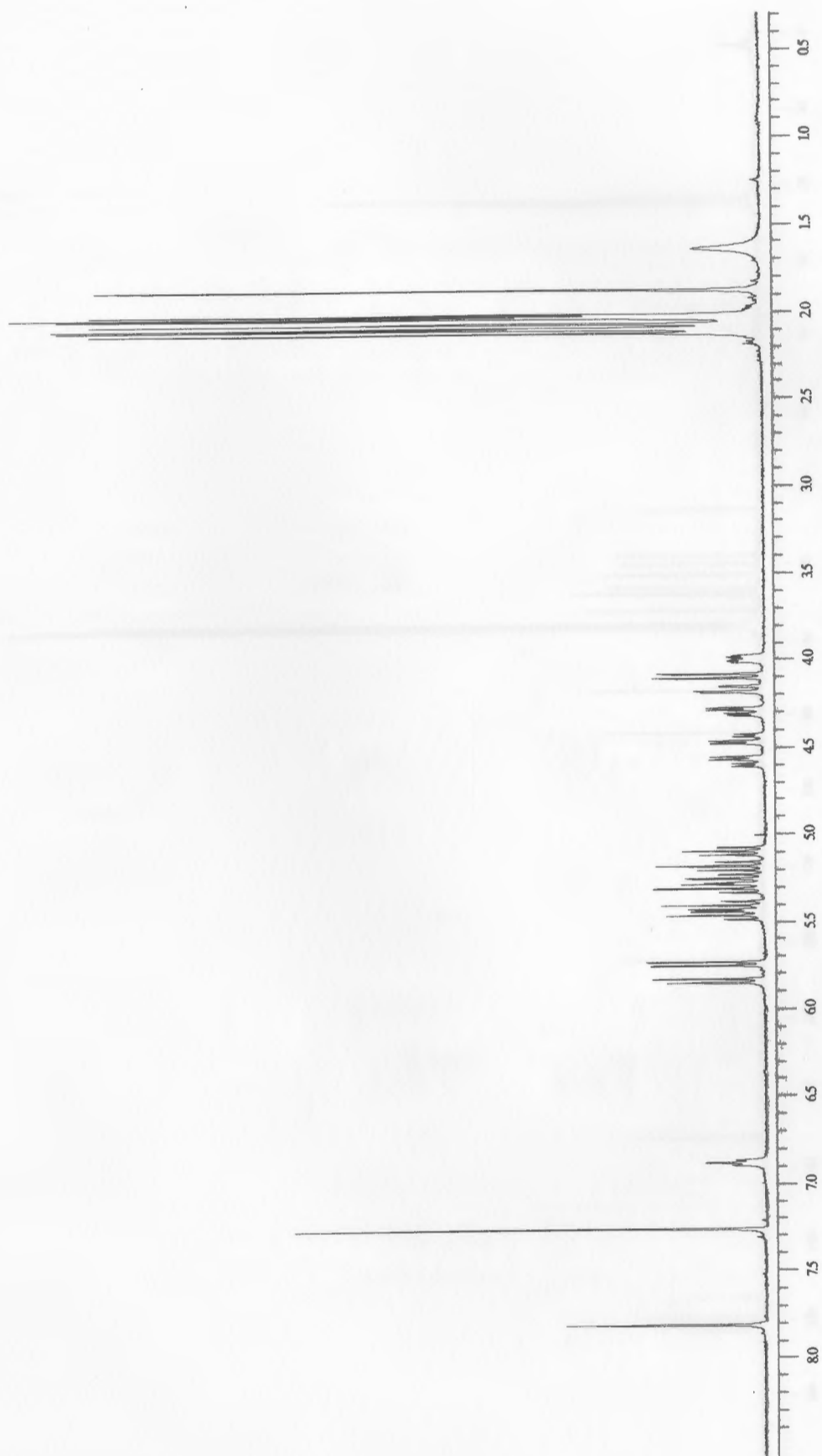
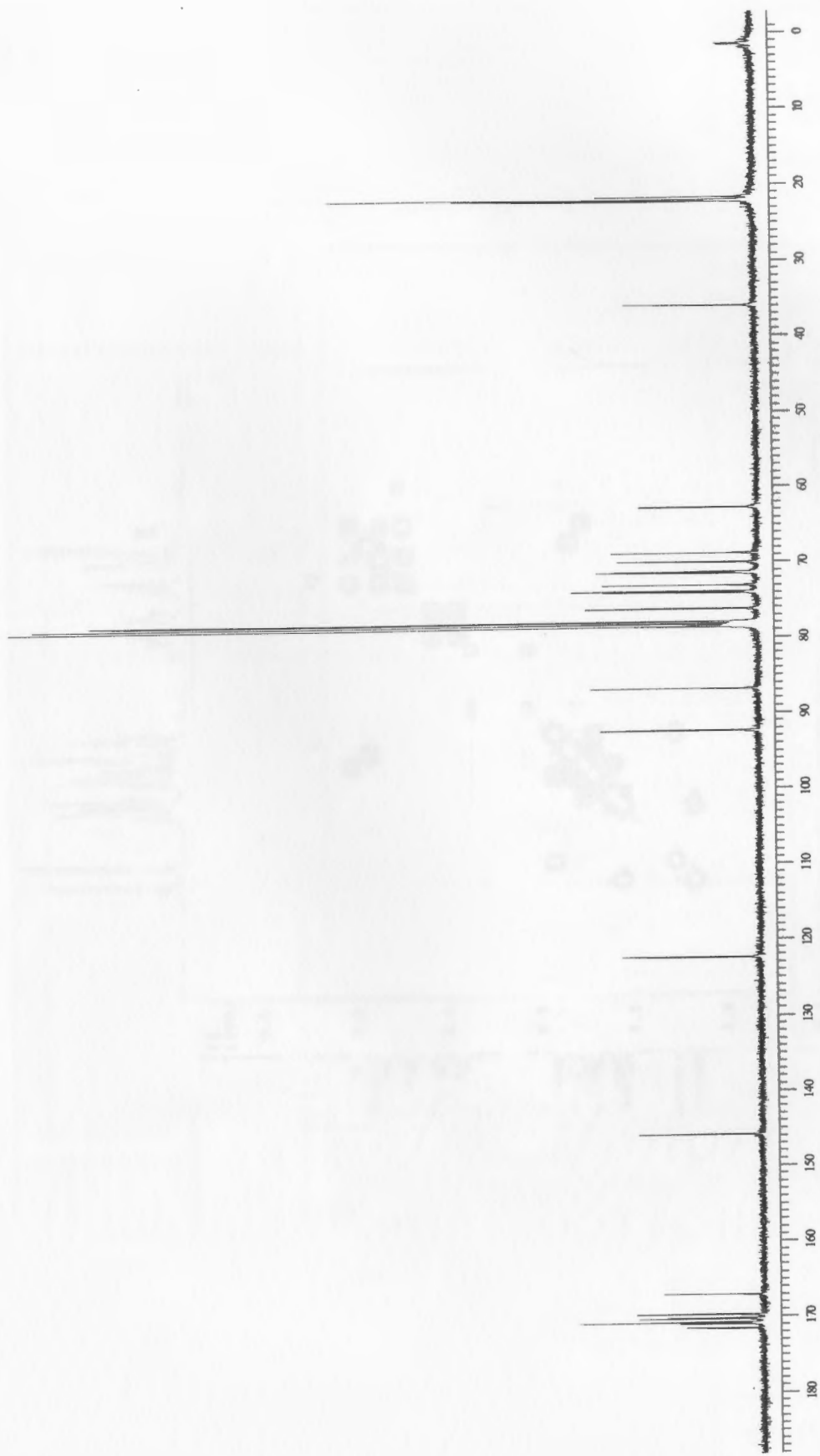


Figure 132: High resolution mass spectrum of triazole 39



**Figure 133:** 400 MHz  $^1\text{H}$  NMR spectrum of triazole 40



**Figure 134:** 100 MHz  $^{13}\text{C}$  NMR spectrum of triazole 40

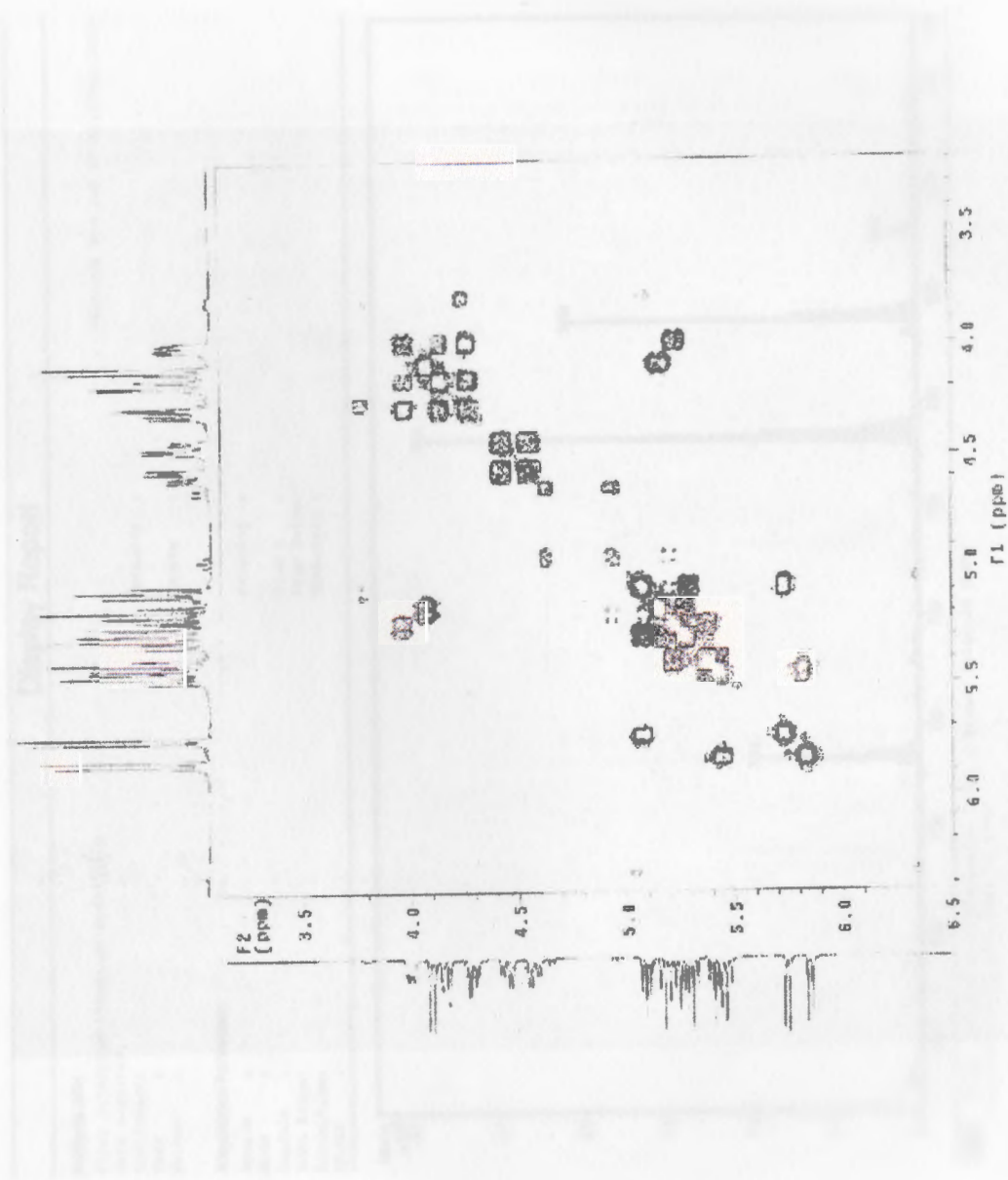


**Figure 135:** Cosy spectrum of triazole 40



## Display Report

**Analysis Info:**

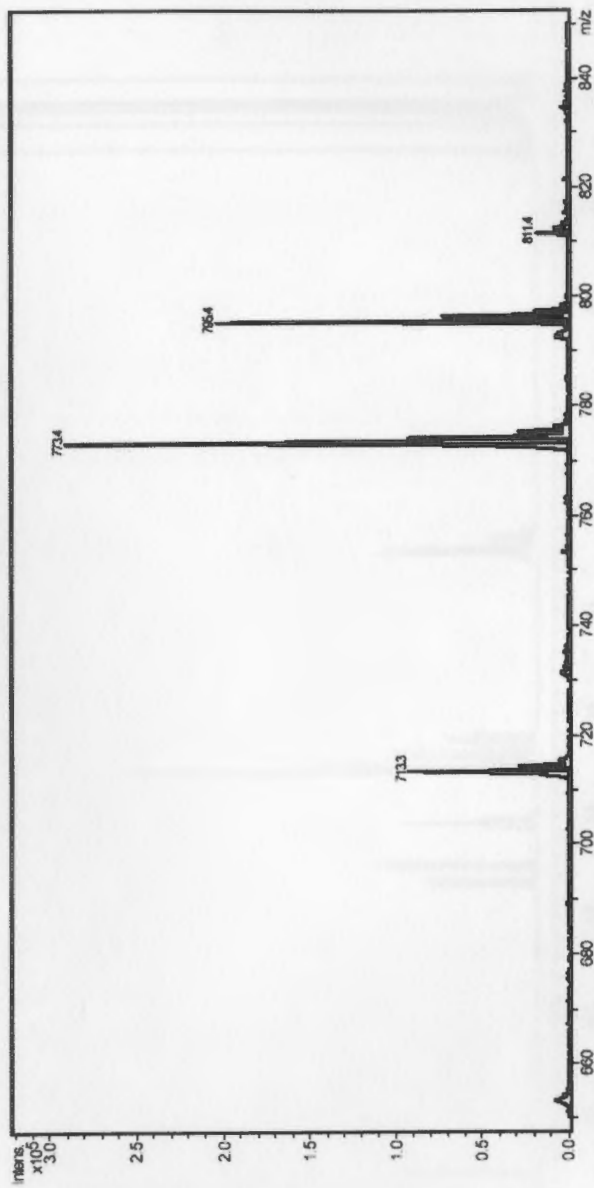
File: D:\HPCHEM\1\DATA\DT\DT6-7301.D  
 Date acquired:  
 Instrument:  
 Task :  
 Method :

Printed: Wed Jul 27 18:27:42 2005

Operator :  
 Sample :

**Acquisition Parameter:**

Source :  
 Mode :  
 CapExit :  
 Scan Range:  
 Accum.time:  
 MS/MS :  
 Polarity :  
 Skim 1 :  
 Trap Drive:  
 Summation :



Braker Dataanalysis Esquire-IC 1.6m, © Bruker Daltonik GmbH  
 Licensed to EQ\_135, Uni. of Ohio

**Figure 136:** Low resolution mass spectrum of triazole 40

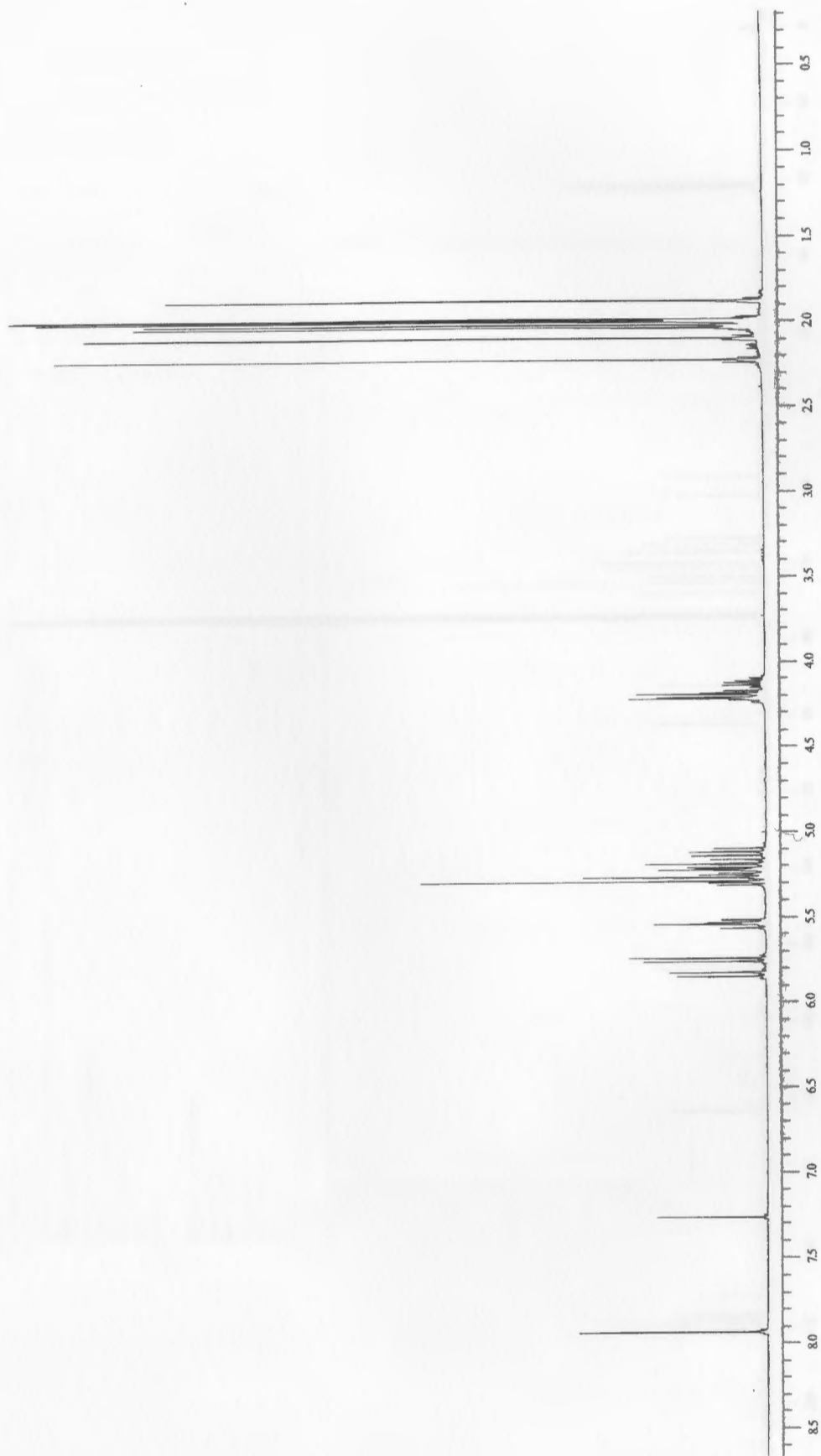


**Figure 137:** 400 MHz <sup>1</sup>H NMR spectrum of triazole 41

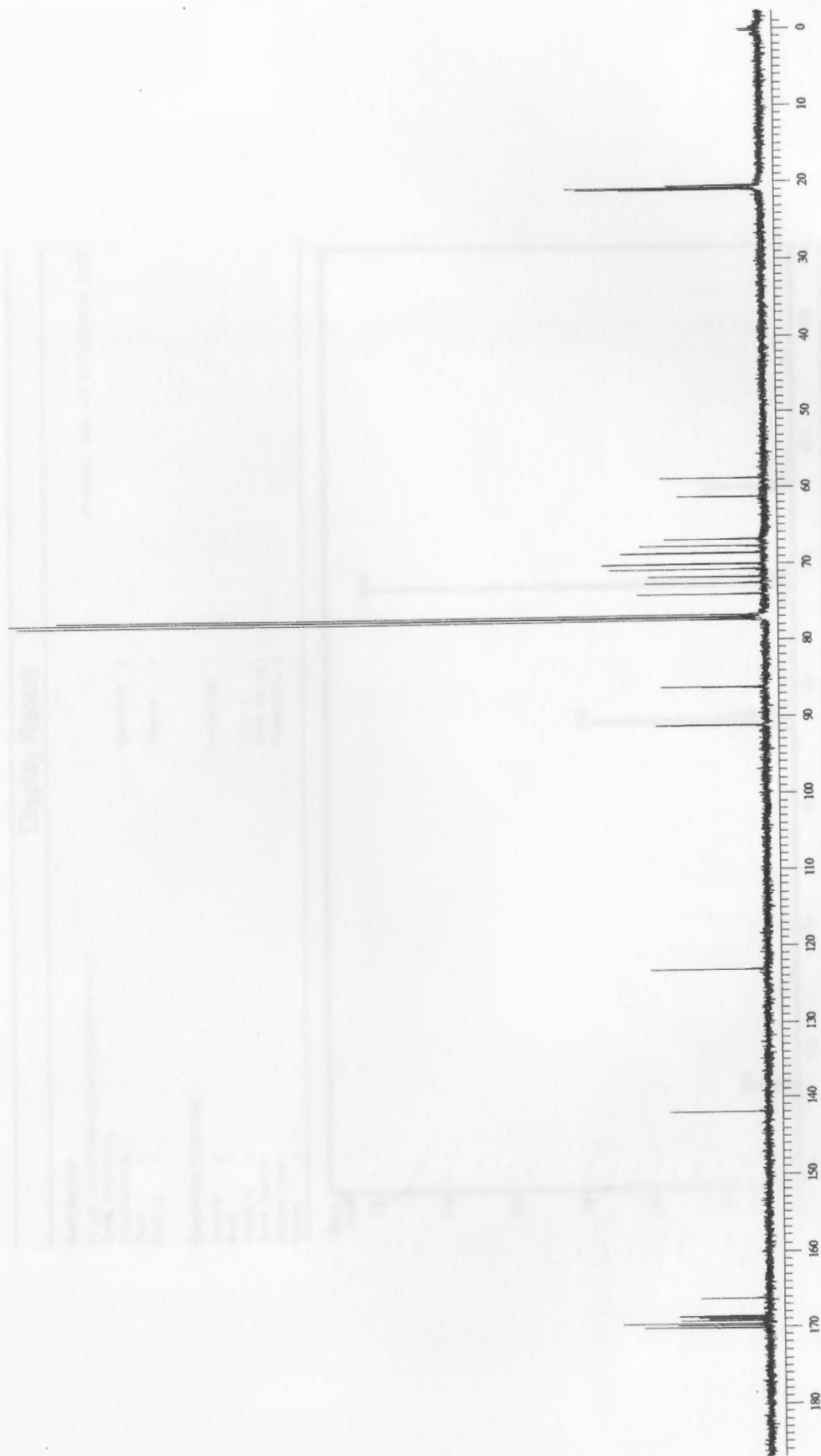


**Figure 138:** 100 MHz  $^{13}\text{C}$  NMR spectrum of triazole 41

## Display Report

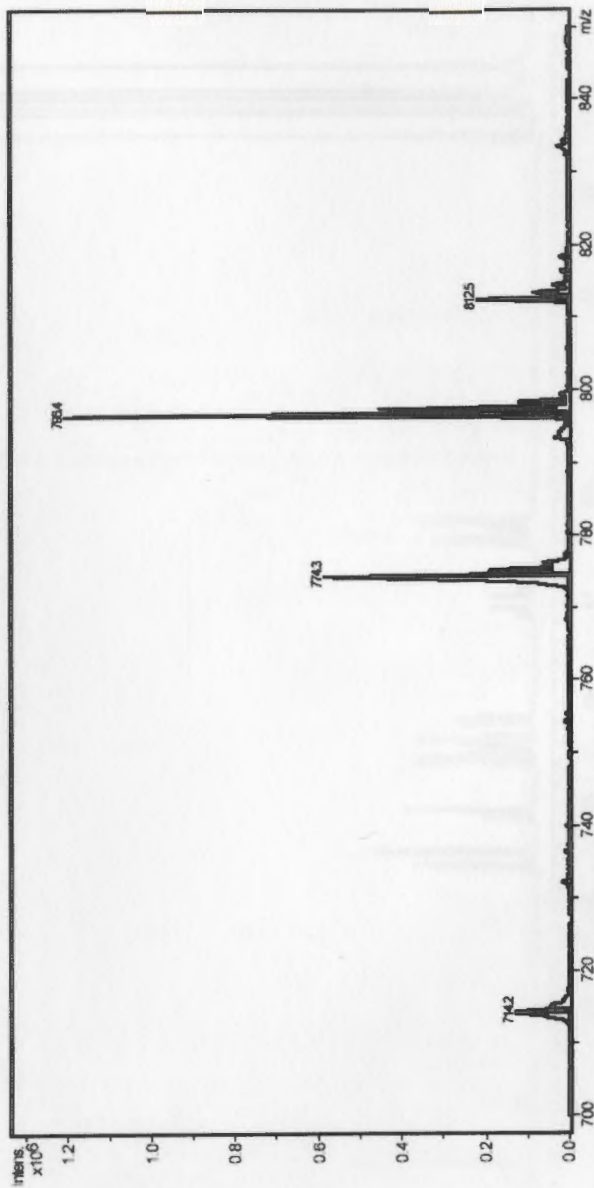
**Analysis Info:**

File: D:\HPCHEM\1\DATA\DT\DT7-59031.D  
 Date acquired:  
 Instrument:  
 Task :  
 Metho :  
 Operator :  
 Sample :

Printed: Wed Jul 27 18:29:14 2005

**Acquisition Parameter:**

Source :  
 Mode :  
 CapExit :  
 Scan Range:  
 Accum.time:  
 MS/MS :  
 Polarity :  
 Skim 1 :  
 Trap Drive:  
 Summation :



Brucker DataAnalysis Esquire-LC 1.6m, © Bruker Daltonik GmbH  
 Licensed to EQ\_139, Dnl. of Ohio

- 1 -

**Figure 139:** Low resolution mass spectrum of triazole 41

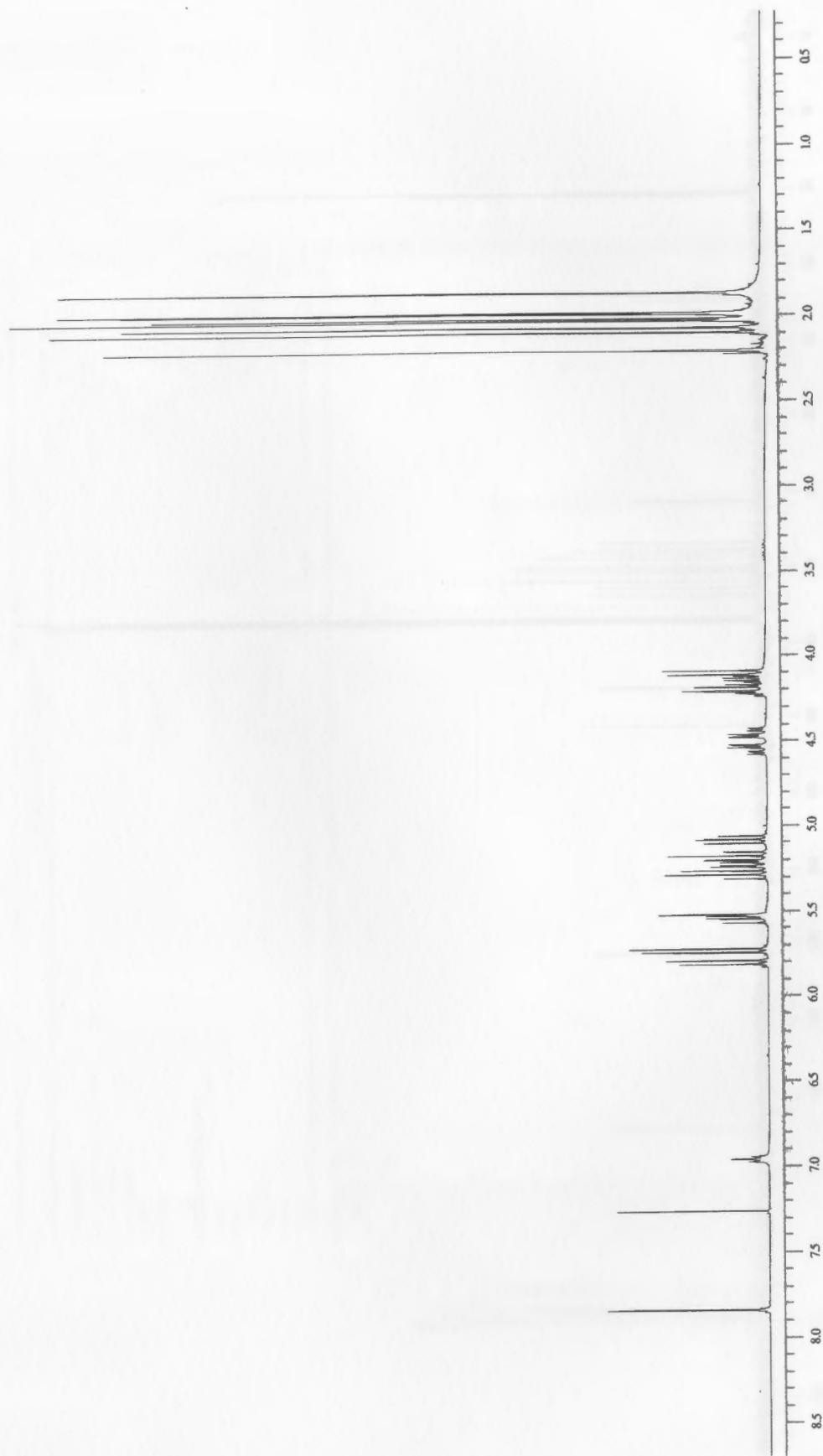


**Figure 140:** 400 MHz  $^1\text{H}$  NMR spectrum of triazole 42

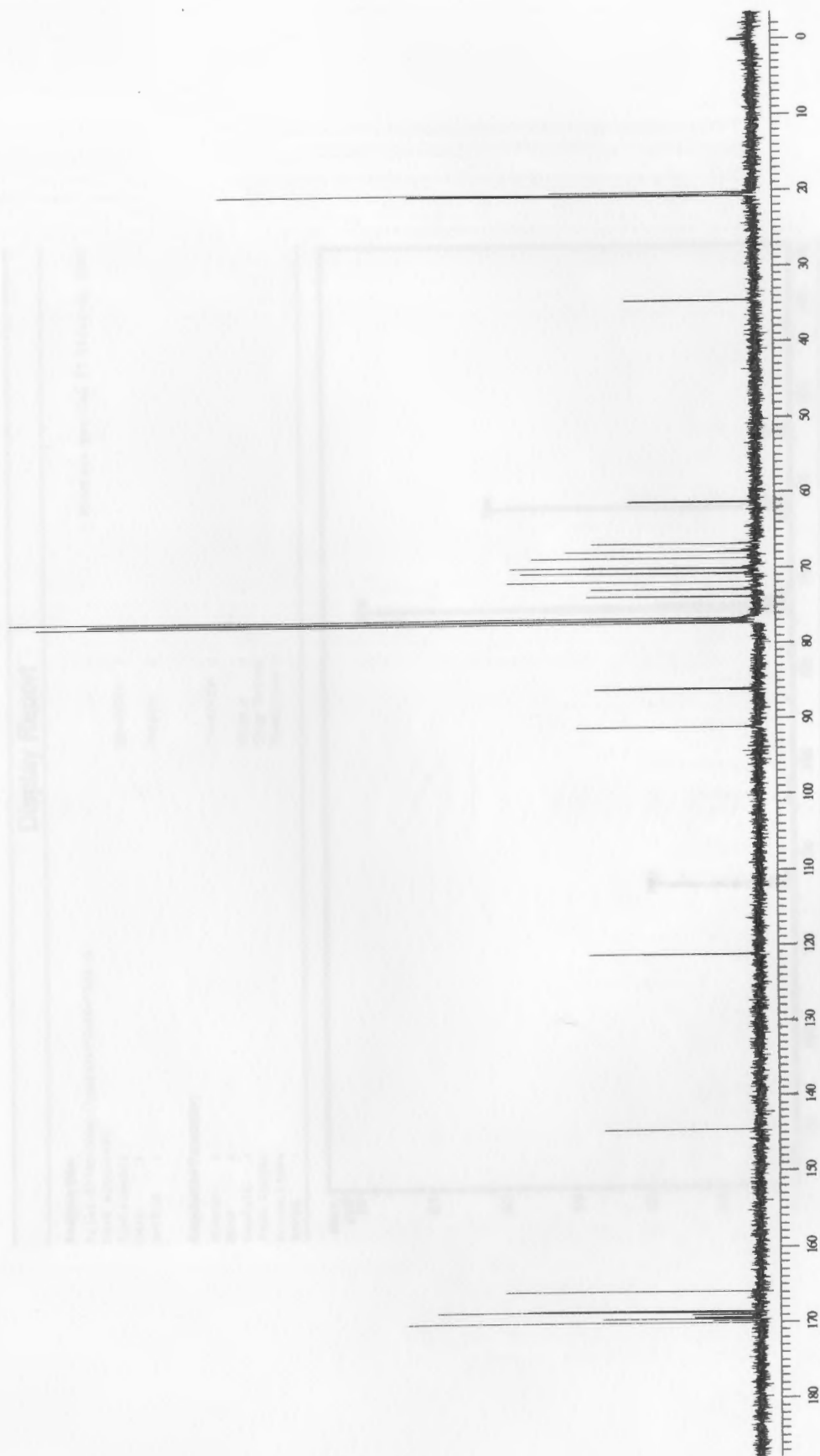


**Figure 141:** 100 MHz  $^{13}\text{C}$  NMR spectrum of triazole 42

## Display Report

**Analysis Info:**

File: D:\HPCHEM\1\DATA\DTADTG-7301.D  
 Date acquired:  
 Instrument:  
 Task :  
 Method :

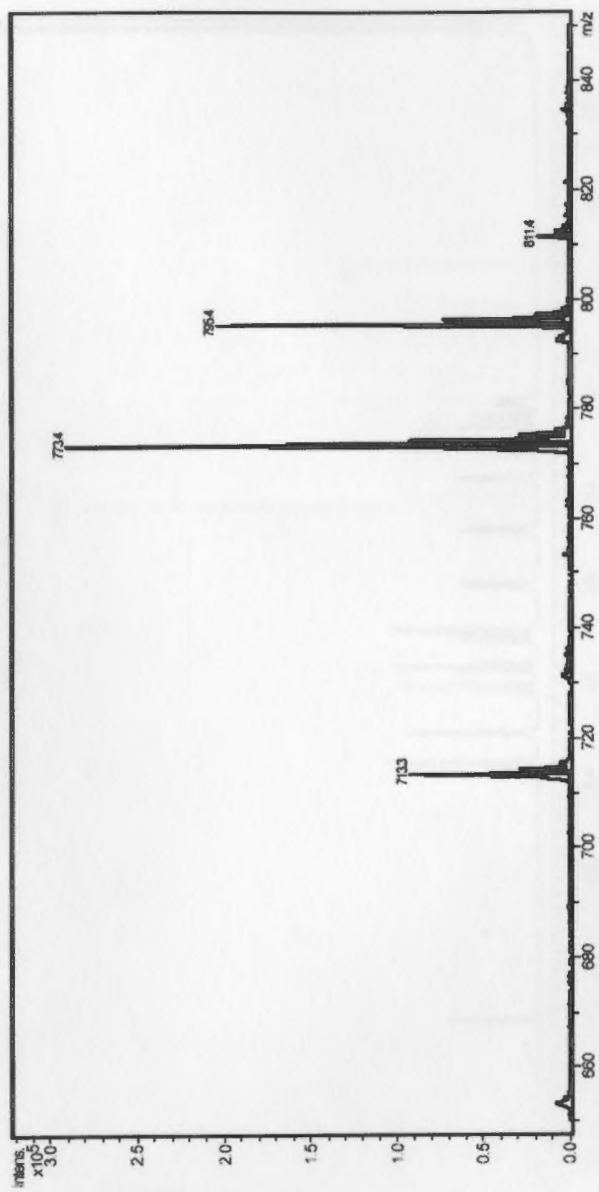
Printed: Wed Jul 27 18:27:42 2005

Operator :  
 Sample :

**Acquisition Parameter:**

Source :  
 Mode :  
 CapExit :  
 Scan Range:  
 Accum.time:  
 MS/MS :

Polarity :  
 Skim 1 :  
 Trap Drive:  
 Summation :



Brucker DataAnalysis Esquire-IC 1.6m, © Bruker Daltonik GmbH  
 Licensed to EO 135, Uni. of Ohio

- 1 -

**Figure 142: Low resolution mass spectrum of triazole 42**

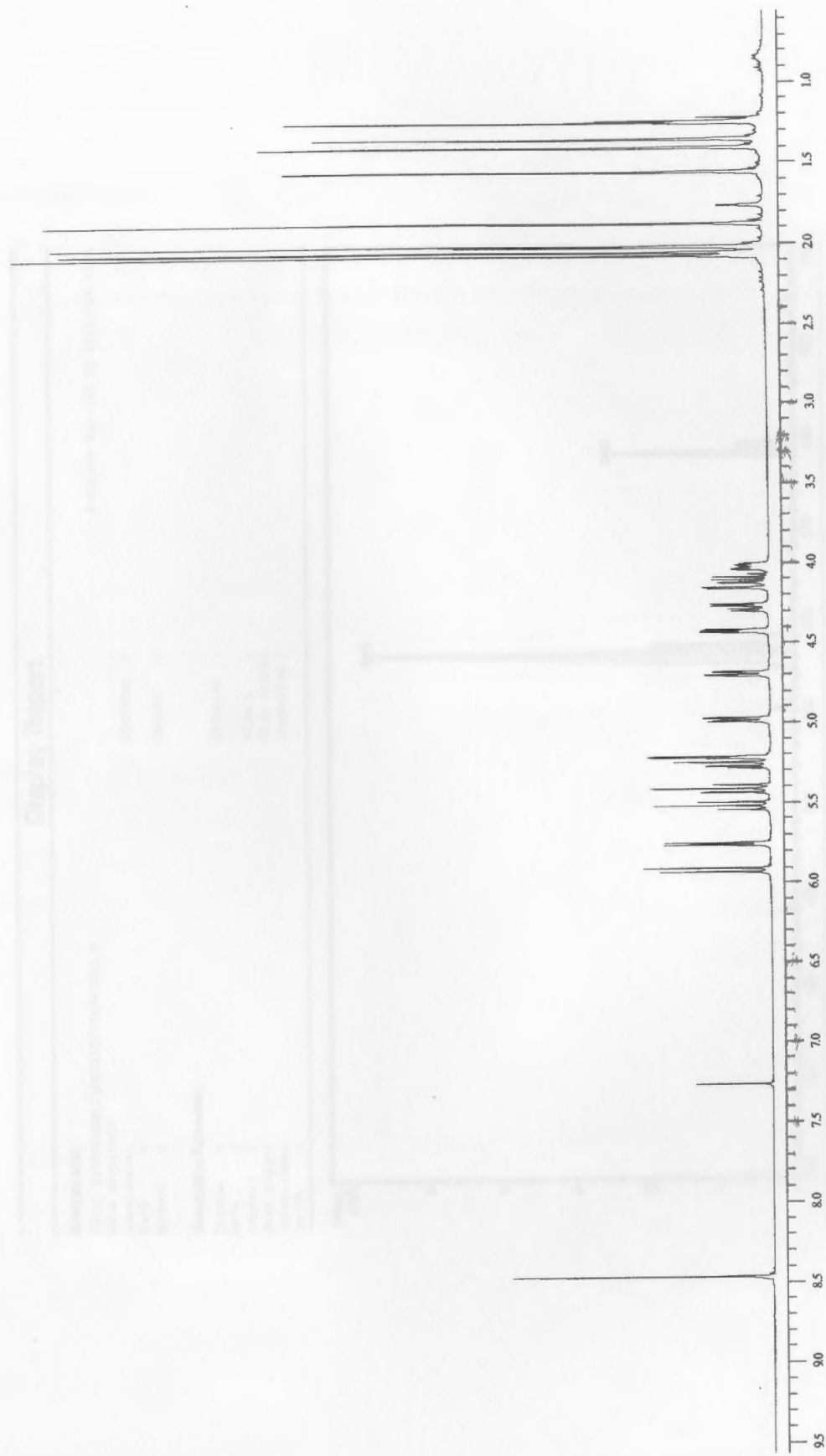


Figure 143: 400 MHz  $^1\text{H}$  NMR spectrum of triazole 43



## Display Report

**Analysis Info:**  
 File: D:\VPCHEM\1\DATA\DT\DT7-1033.D  
 Date acquired:   
 Instrument:   
 Task:   
 Method:   
 Operator:   
 Sample:   
 Polarity:   
 Skim 1:   
 Trap Drive:   
 Summation:

**Acquisition Parameter:**  
 Source:   
 Mode:   
 CapExit:   
 Scan Range:   
 Accum.time:   
 MS/MS:

Printed: Wed Jul 27 18:29:56 2005

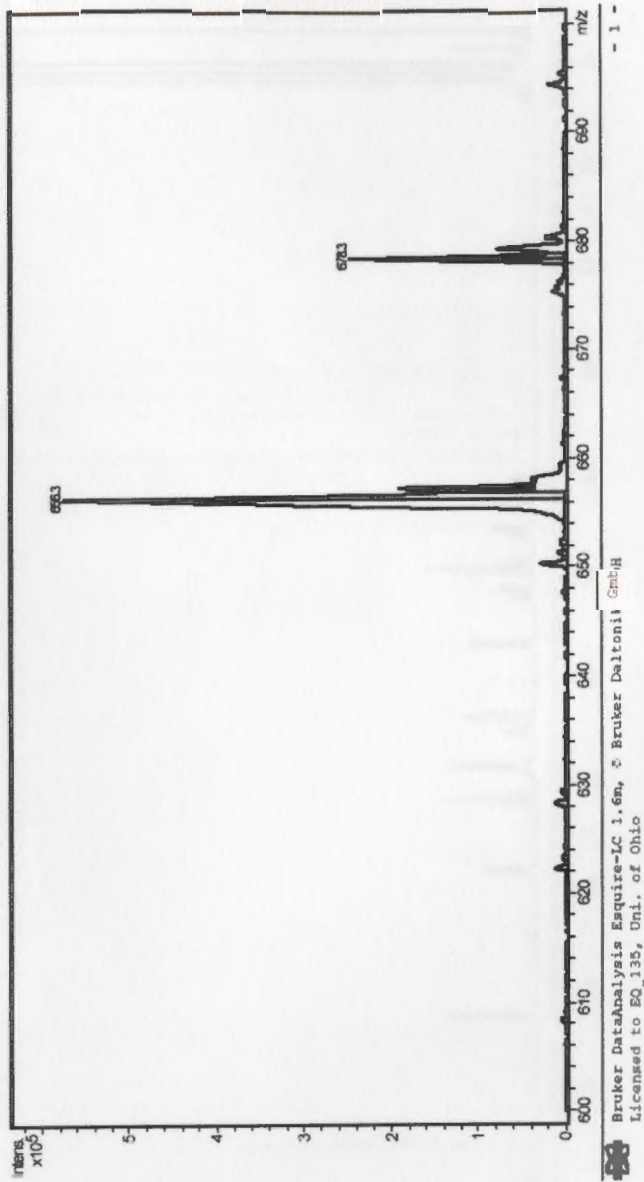


**Figure 144:** Low resolution mass spectrum of triazole 43

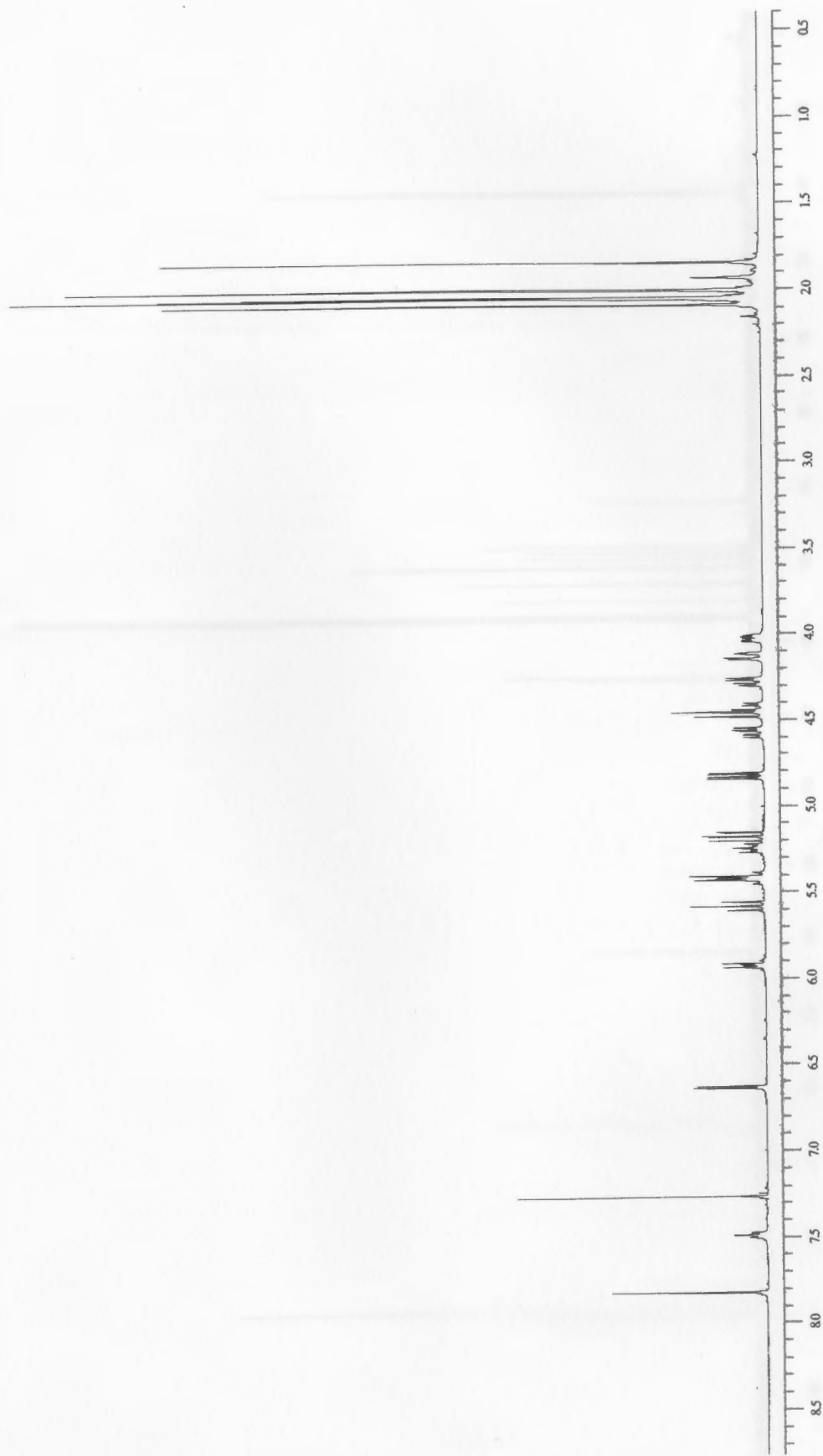


**Figure 145:** 400 MHz  $^1\text{H}$  NMR spectrum of bromide 44

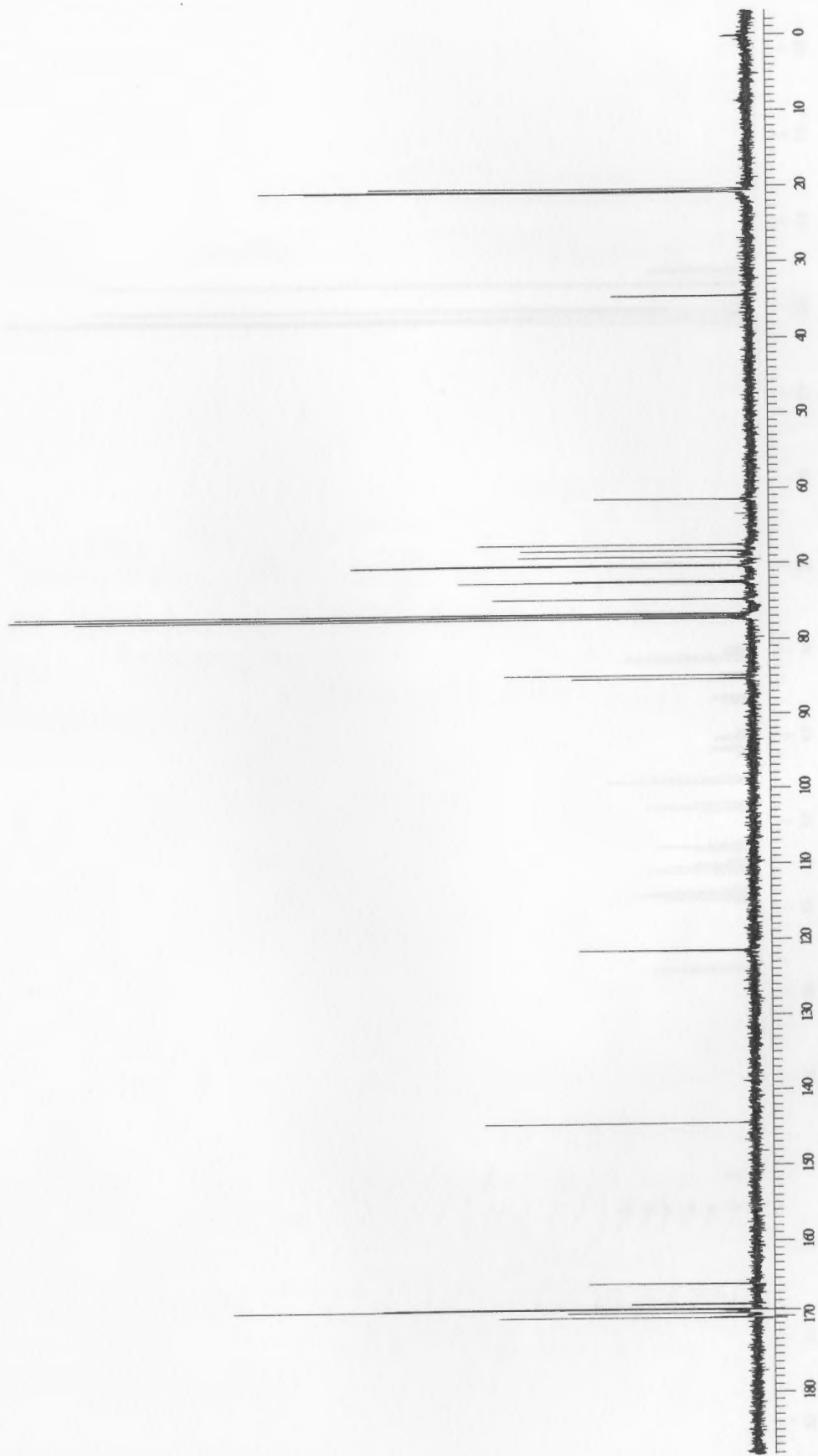
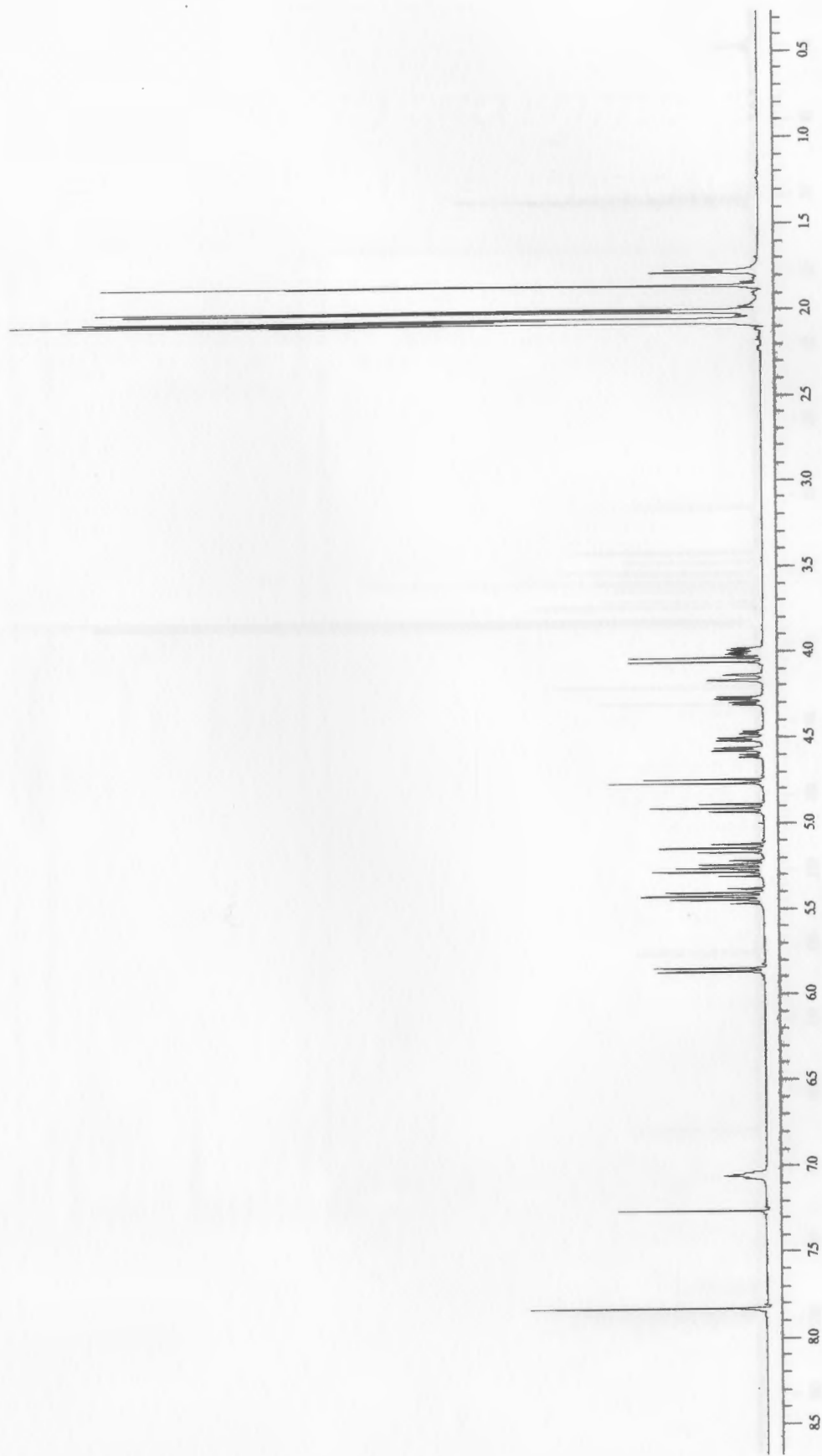


Figure 146: 100 MHz  $^{13}\text{C}$  NMR spectrum of bromide 44

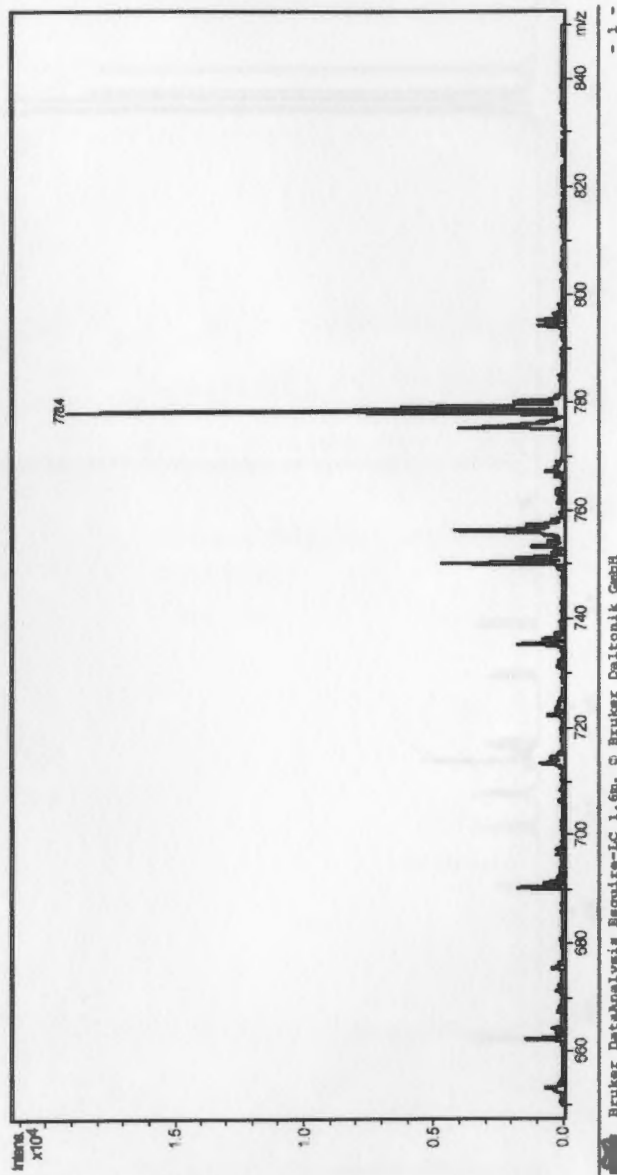


**Figure 147:** 400 MHz  $^1\text{H}$  NMR spectrum of azide 45



## Display Report

**Analysis Info:**  
File: D:\HECHEM\1\DATA\DF\DT7-9902.D  
Date acquired: Wed Jul 27 18:31:04 2005  
Instrument:  
Task :  
Method :  
Operator :  
Sample :  
Polarity :  
Skim 1 :  
Trap Drive:  
Summation :  
**Acquisition Parameter:**  
Source :  
Mode :  
CapExit :  
Scan Range:  
Accun.time:  
MS/MS :



Braker DataAnalysis Esquire-LC 1.6m, © Bruker Daltonik GmbH  
Licensed to EQ 135, Uni. of Ohio

Figure 149: Low resolution mass spectrum of azide 45

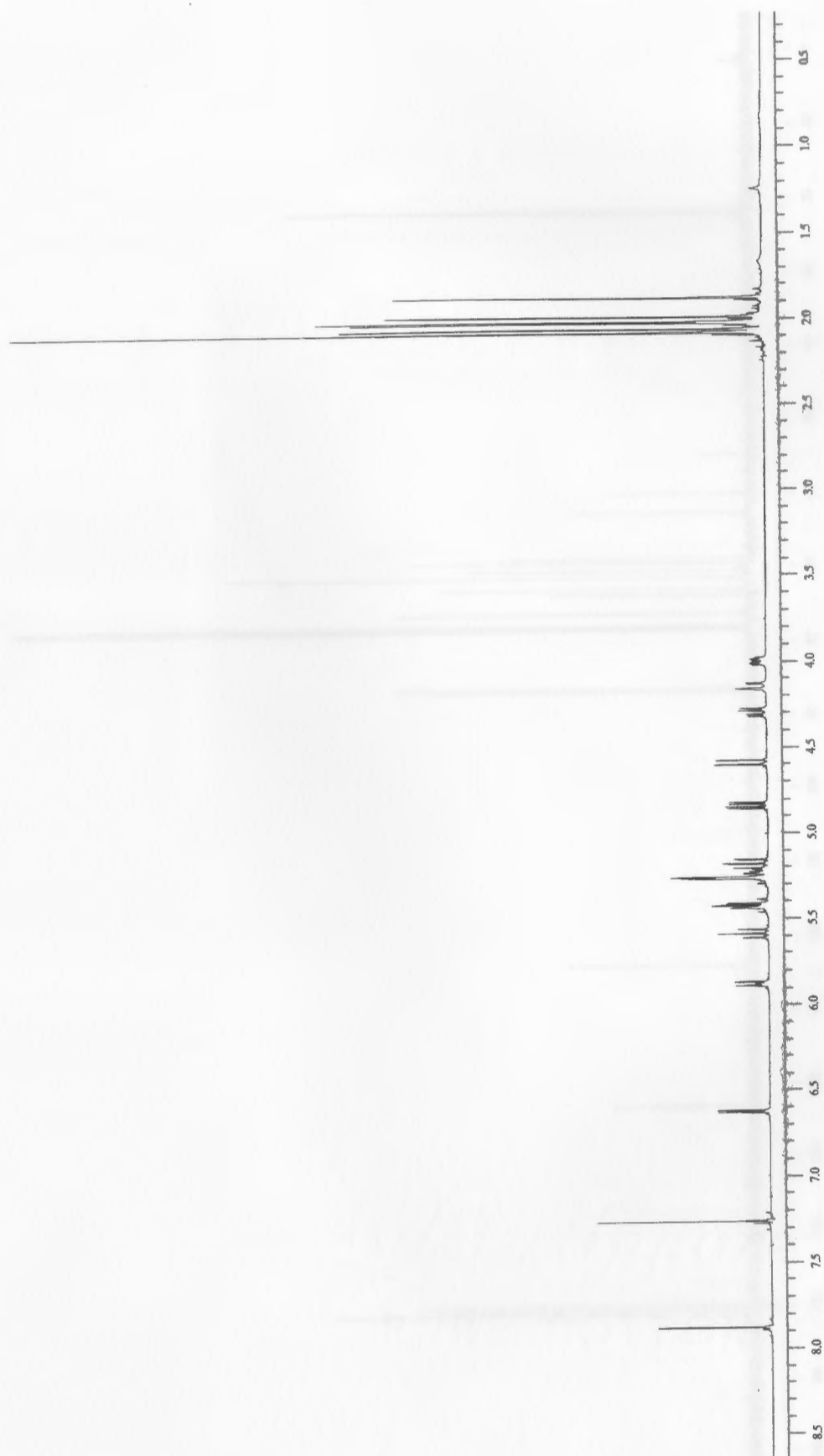


**Figure 150:** 400 MHz  $^1\text{H}$  NMR spectrum of bromide 46

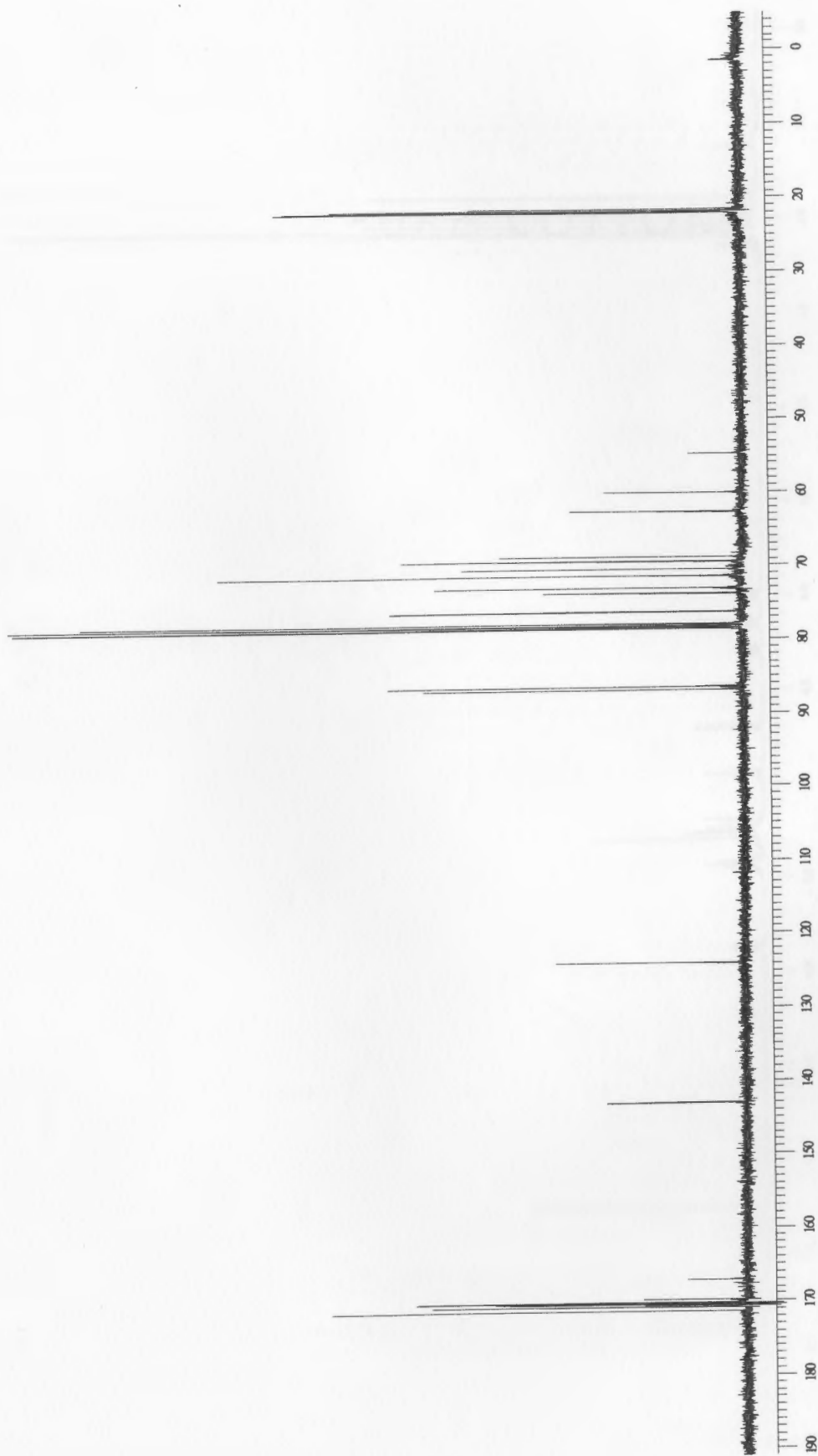
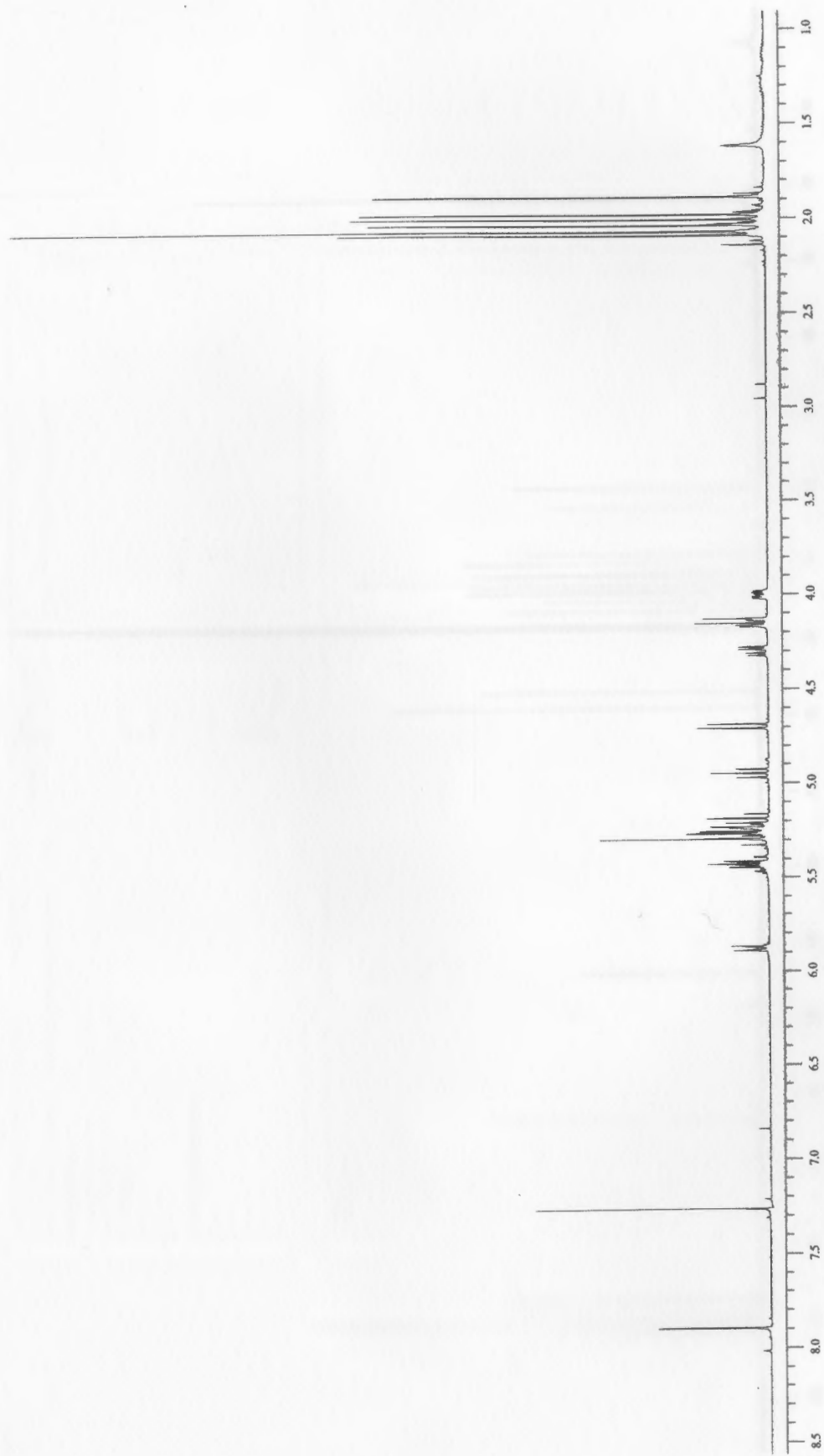


Figure 151: 100 MHz  $^{13}\text{C}$  NMR spectrum of bromide 46





**Figure 152:** 400 MHz  $^1\text{H}$  NMR spectrum of azide 47

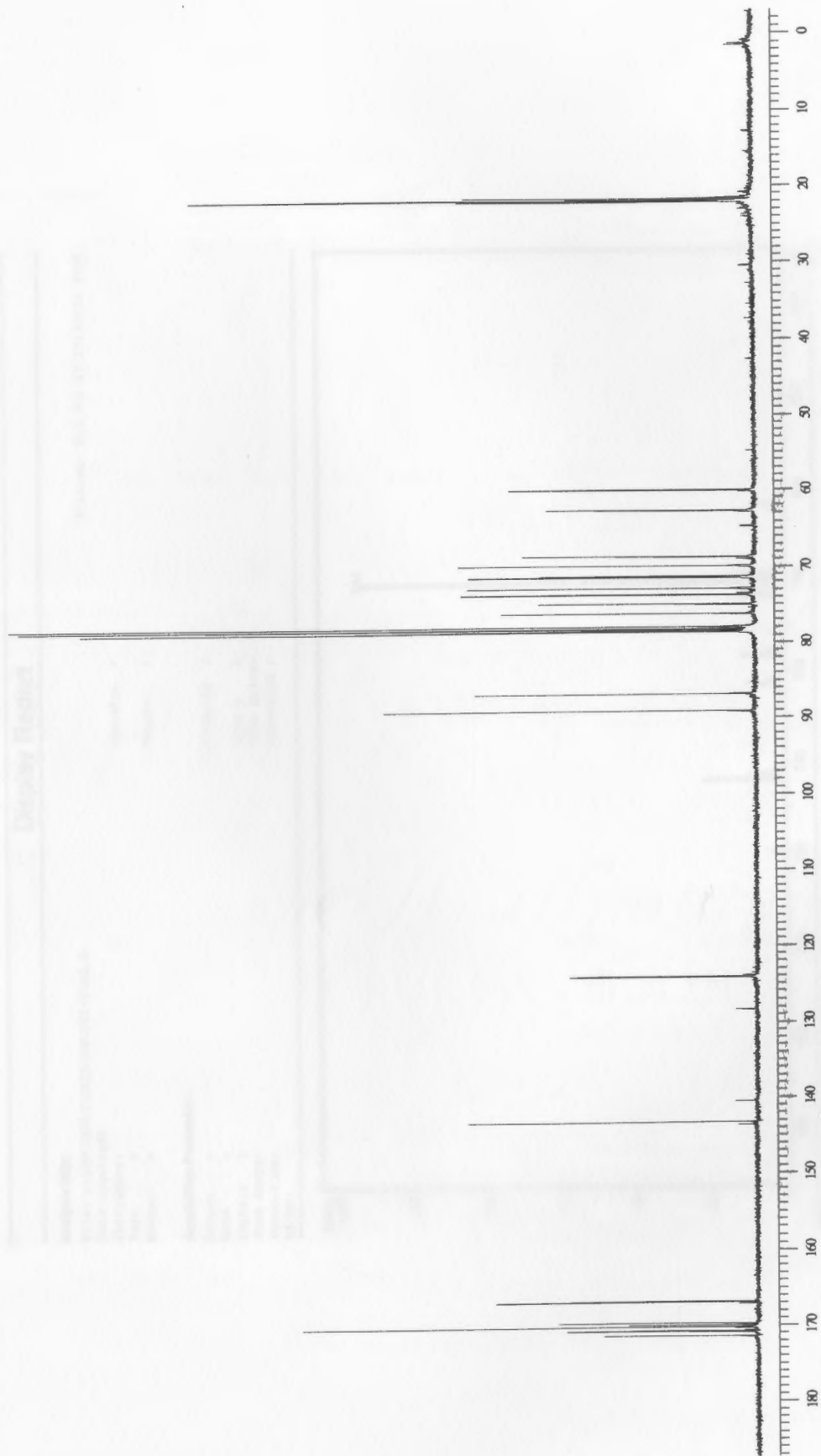


Figure 153: 100 MHz <sup>13</sup>C NMR spectrum of azide 47

## Display Report

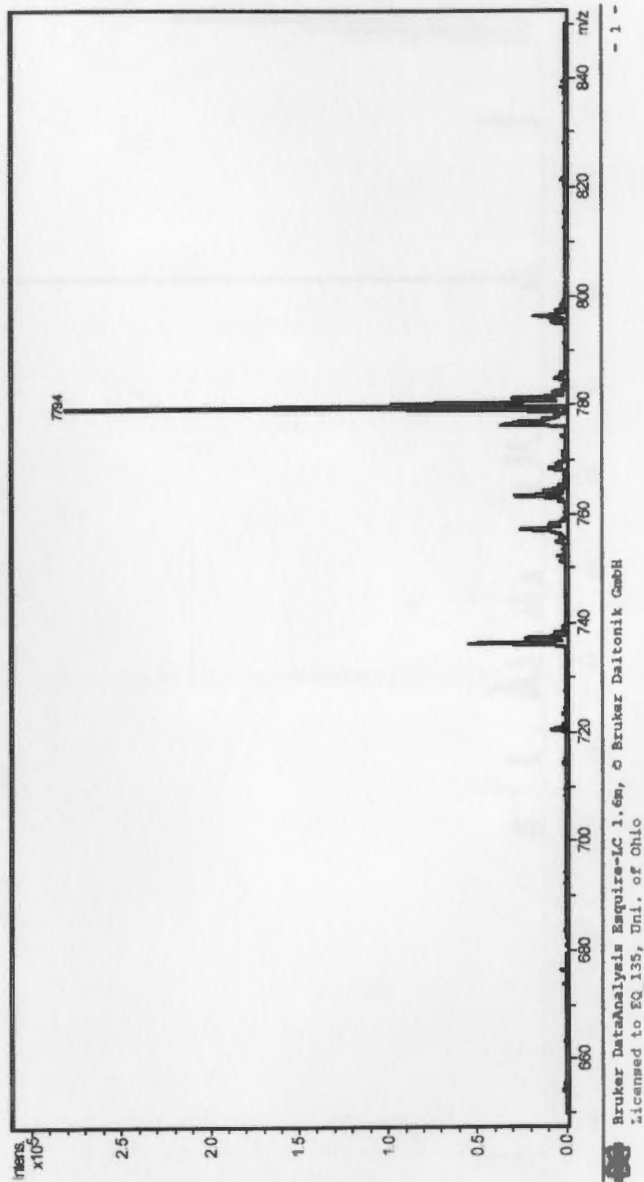
**Analysis info:**

File: D:\MPCHEM\1\DATA\DT\DT7-9702.D  
 Date acquired: Wed Jul 27 18:30:34 2005  
 Instrument:  
 Task :  
 Method :

Operator :  
 Sample :

**Acquisition Parameter:**

Source :  
 Mode :  
 Capexit :  
 Scan Range:  
 Accum.time:  
 MS/MS :  
 Polarity :  
 Skim 1 :  
 Trap Drive:  
 Summation :



Brucker DataAnalysis Esquire-IC 1.6m, © Bruker Daltonik GmbH  
 licensed to EQ\_135, Uni. of Ohio

**Figure 154:** Low resolution mass spectrum of azide 47

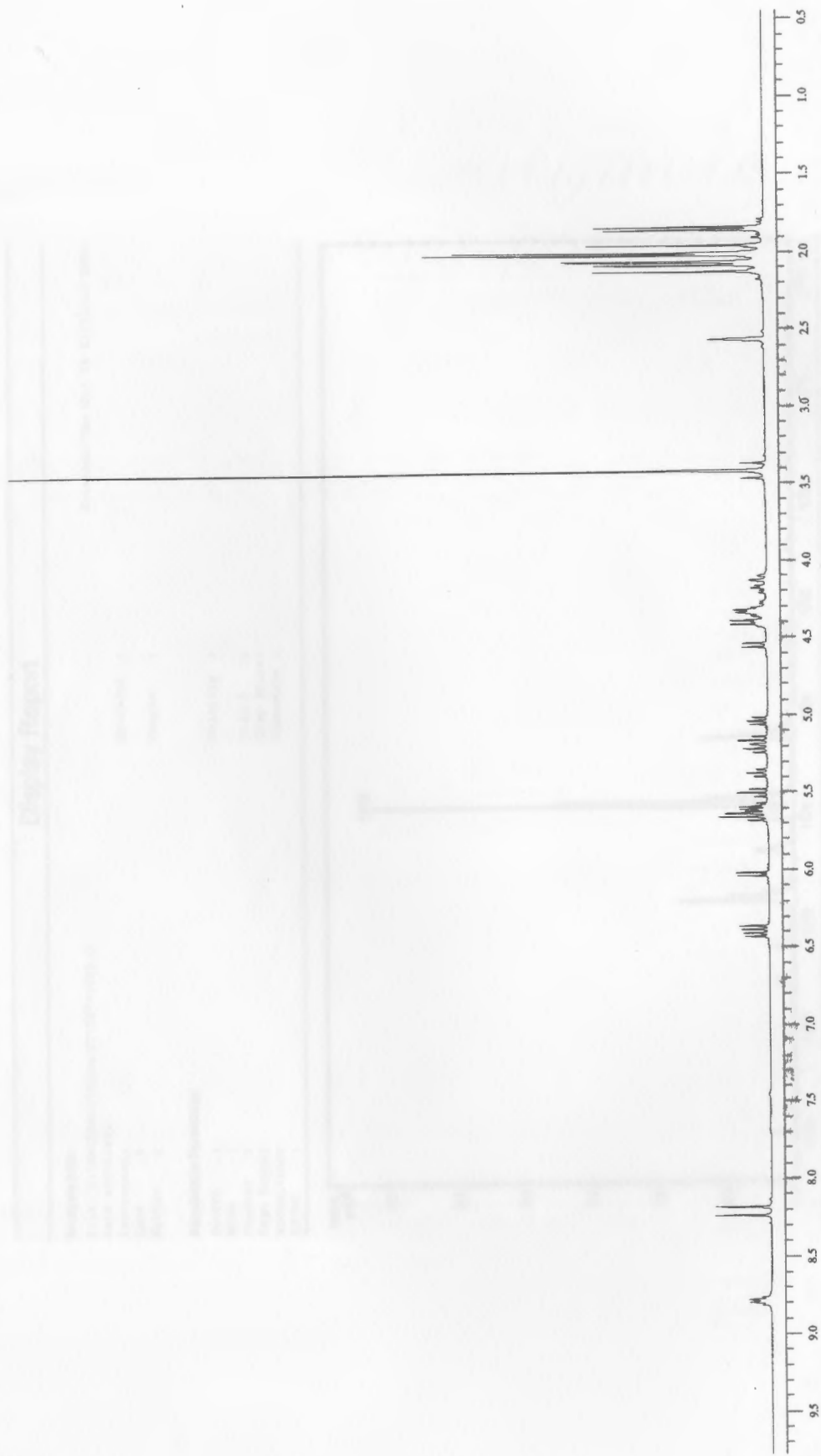


**Figure 155:** 400 MHz  $^1\text{H}$  NMR spectrum of triazole-linked trimer 48

## Display Report

**Analysis Info:**

File: D:\HCHEM1\DATA\DT\DT7-1903.D  
 Date acquired:  
 Instrument:  
 Task :  
 Method :

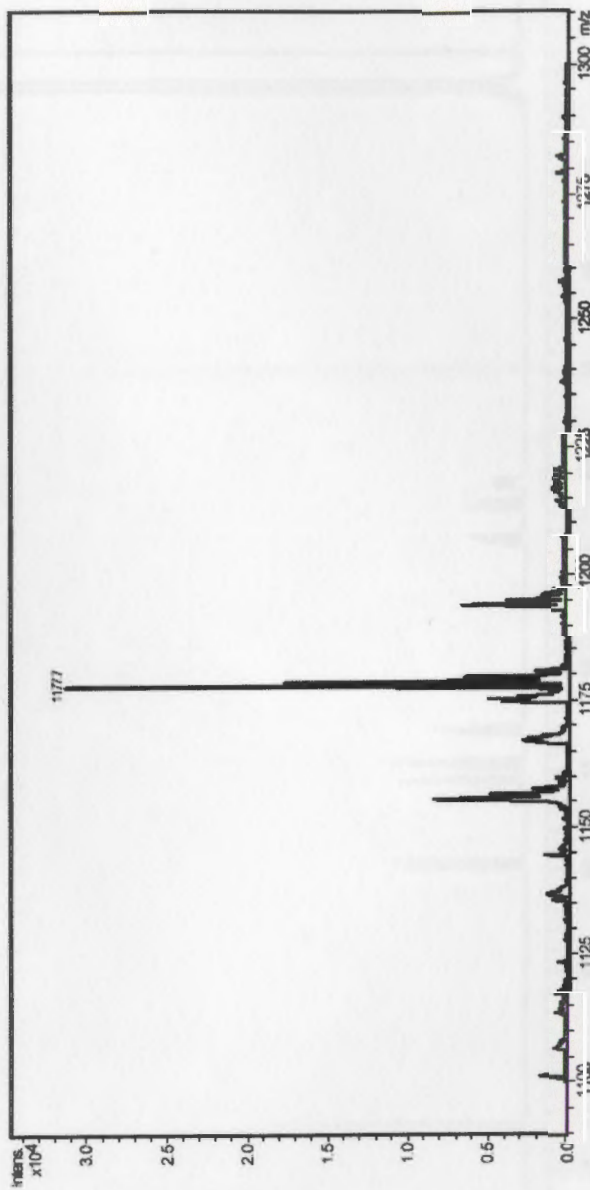
Printed: Thu Jul 28 12:31:23 2005

Operator :  
 Sample :

**Acquisition Parameter:**

Source :  
 Mode :  
 CapExit :  
 Scan Range:  
 Accum.time:  
 MS/MS :

Polarity :  
 Skim 1 :  
 Trap Drive:  
 Summation :



Bruker DataAnalysis Esquire-IC 1.6m, © Bruker Daltonik GmbH  
 Licensed to EO\_135, Uni. of Ohio

Figure 156: Low resolution mass spectrum of triazole-linked trimer 48

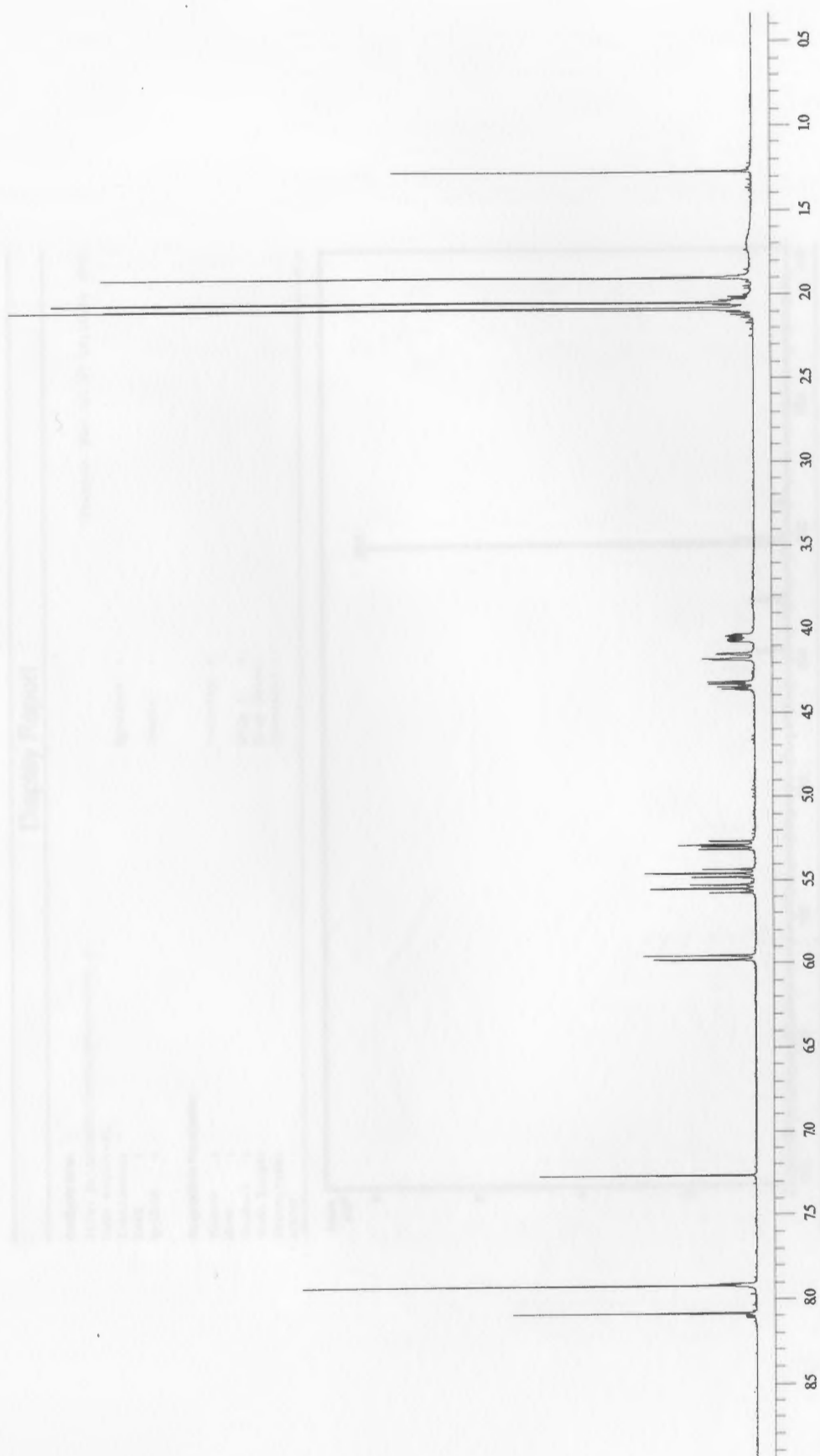
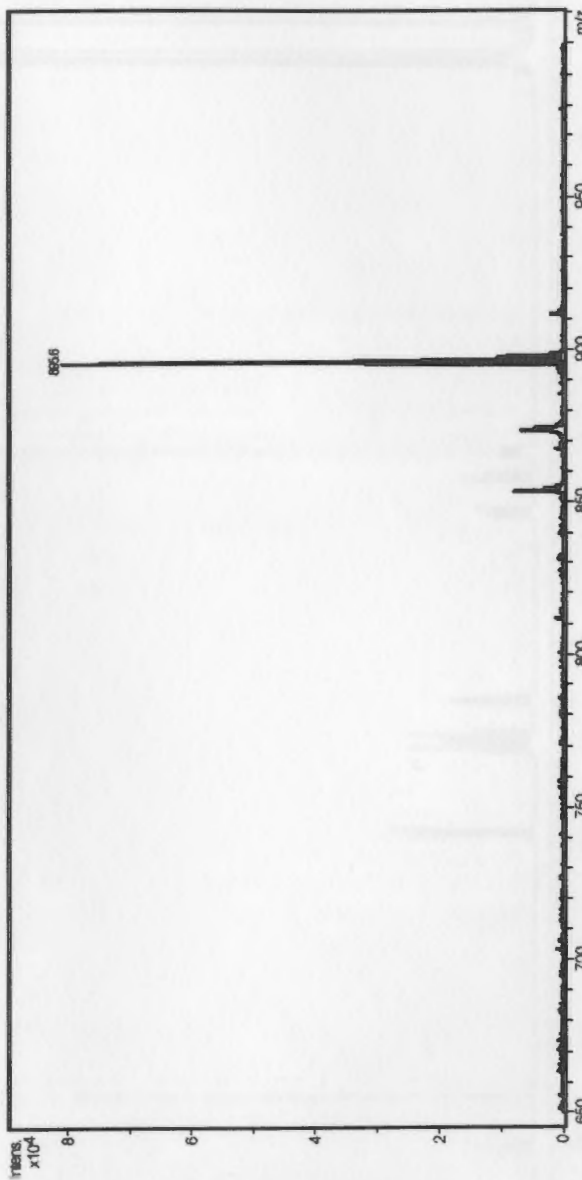


**Figure 157:** 400 MHz  $^1\text{H}$  NMR spectrum of divalent triazole 49

## Display Report

**Analysis Info:**  
 File: D:\BPCHEM\1\DATA\DT\DT5-3701.D  
 Date acquired: Printed: Wed Jul 27 18:31:51 2005  
 Instrument:  
 Task:  
 Method :  
 Operator :  
 Sample :  
 Polarity :  
 Source :  
 Mode :  
 CapExit :  
 Scan Range:  
 Accum.time:  
 MS/MS :  
 Skim 1 :  
 Trap Drive:  
 Summation :

**Acquisition Parameter:**



Bruker DataAnalysis Esquire-LC 1.6m, © Bruker Daltonik GmbH  
 Licensed to EQ\_135, Uni. of Ohio

**Figure 158:** Low resolution mass spectrum of divalent triazole 49

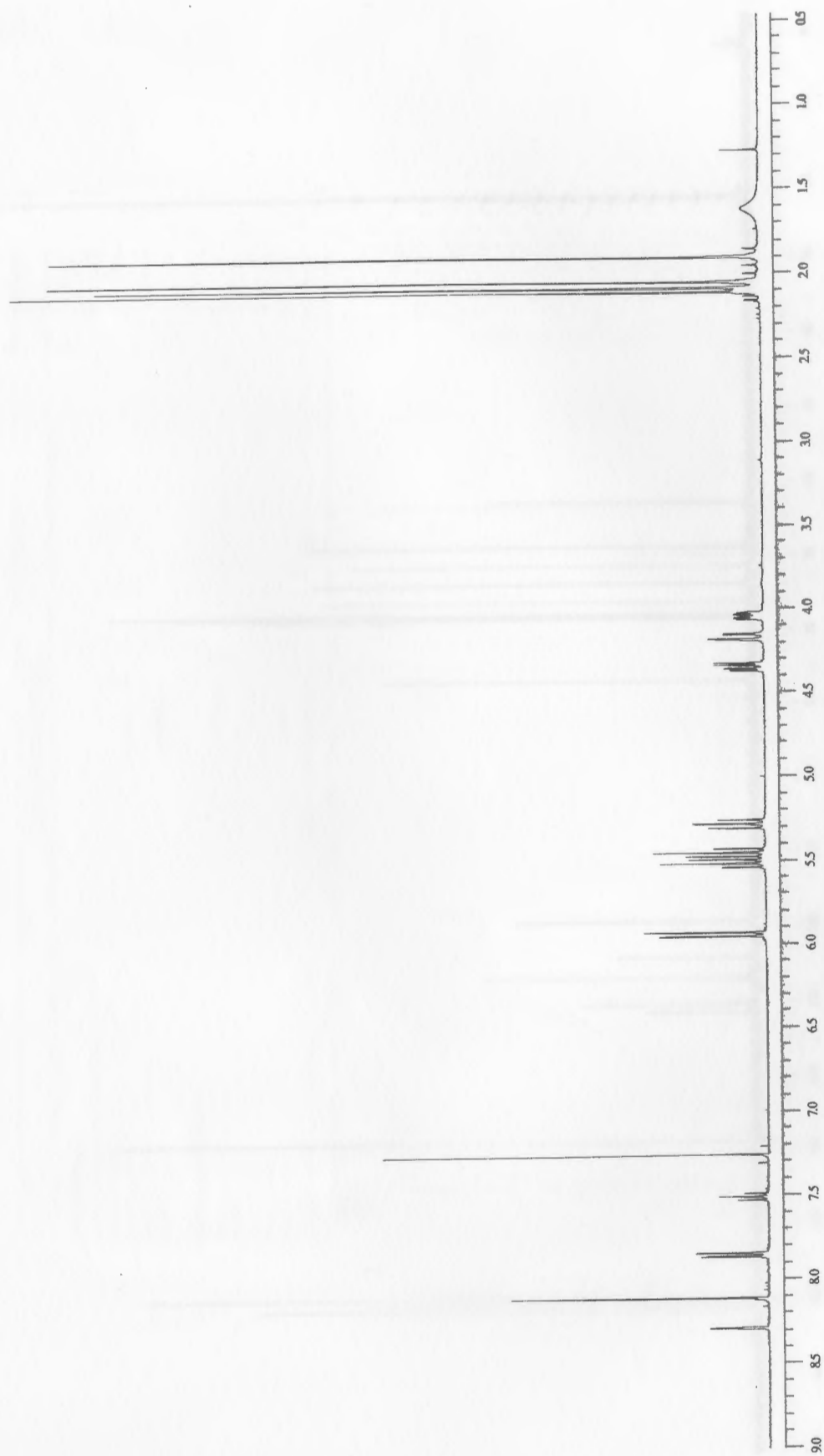


**Figure 159:** 400 MHz  $^1\text{H}$  NMR spectrum of divalent triazole 50



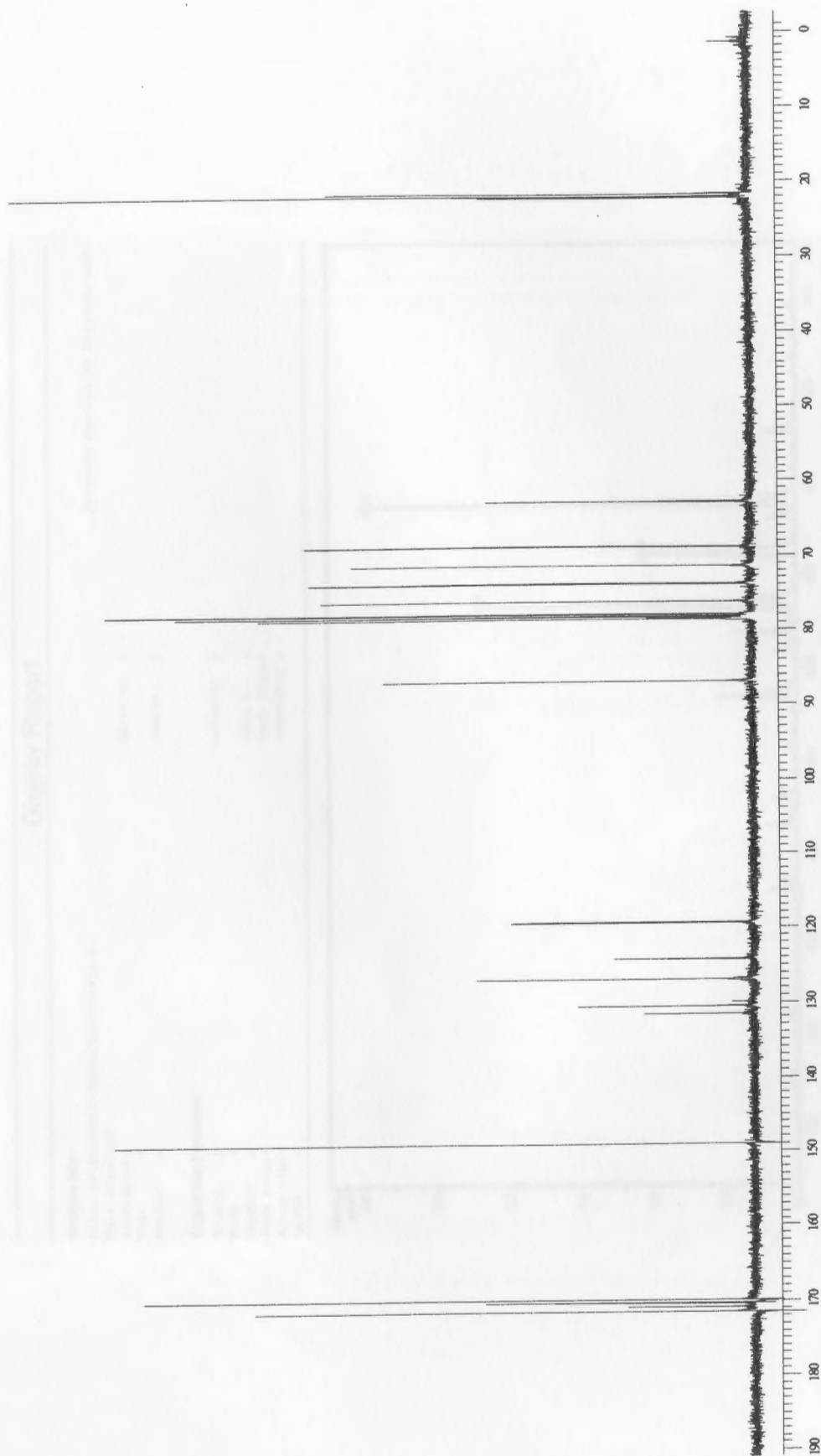


Figure 160: 100 MHz  $^{13}\text{C}$  NMR spectrum of divalent triazole 50

## Display Report

## Analysis Info:

File: D:\HFCHEN\1\DATA\DT\DT-5-972.D

Printed: Wed Jul 27 18:32:26 2005

Date acquired:

Instrument:

Task:

Method:

Operator:

Sample:

## Acquisition Parameter:

Source:

Node:

CapExit:

Scan Range:

Accum.time:

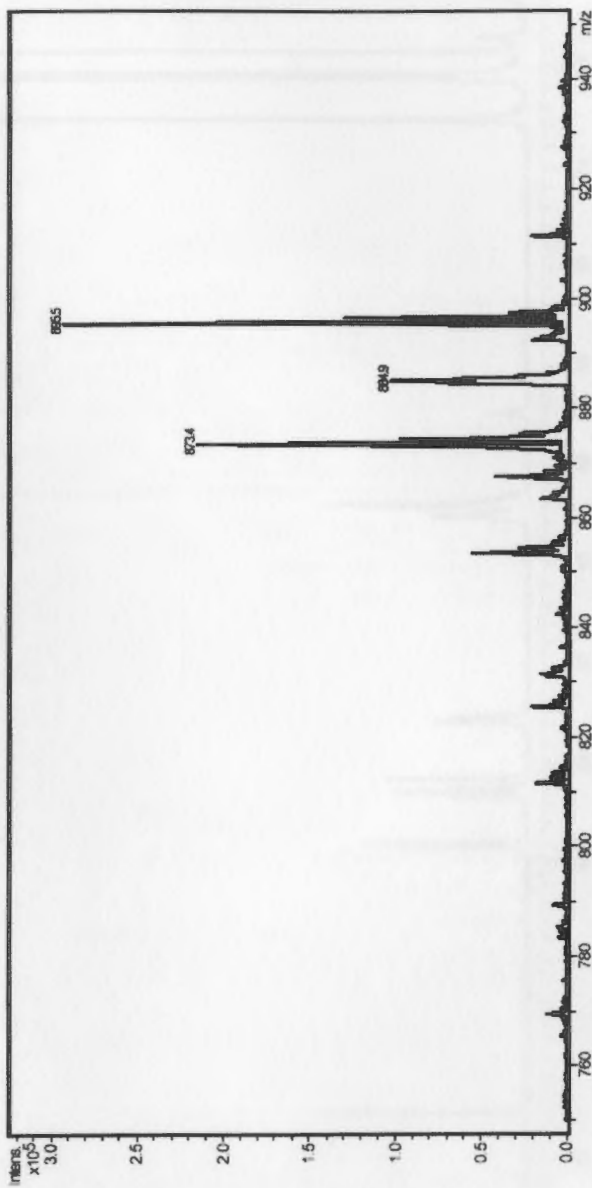
MS/MS:

Polarity:

Skim 1:

Trap Drive:

Summation:

Bruker DataAnalysis Esquire-LC 1.6m, © Bruker Daltonik GmbH  
Licensed to EQ\_135, Uni. of Ohio

- 1 -

Figure 161: Low resolution mass spectrum of divalent triazole 50

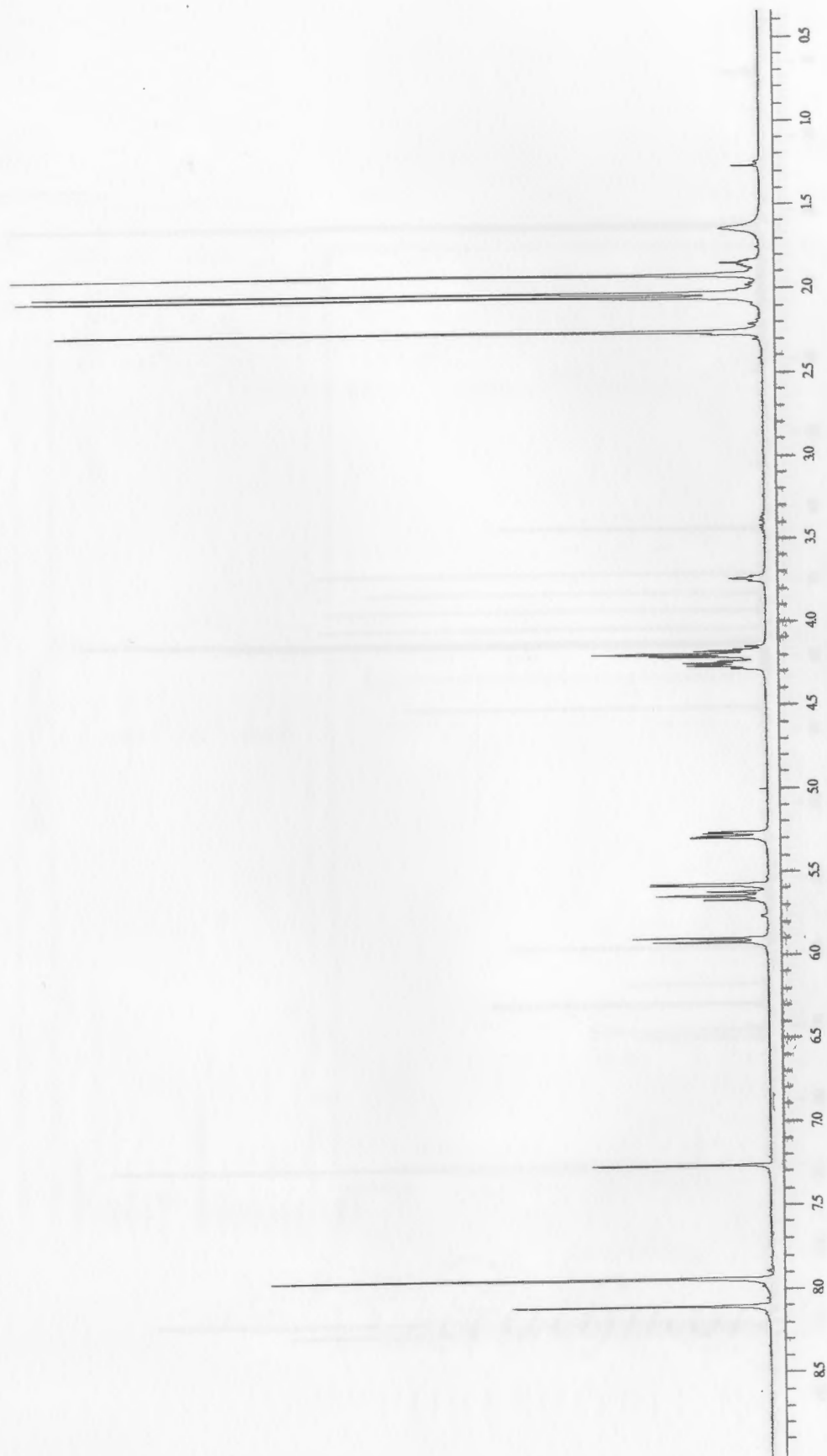


**Figure 162:** 400 MHz  $^1\text{H}$  NMR spectrum of divalent triazole 51

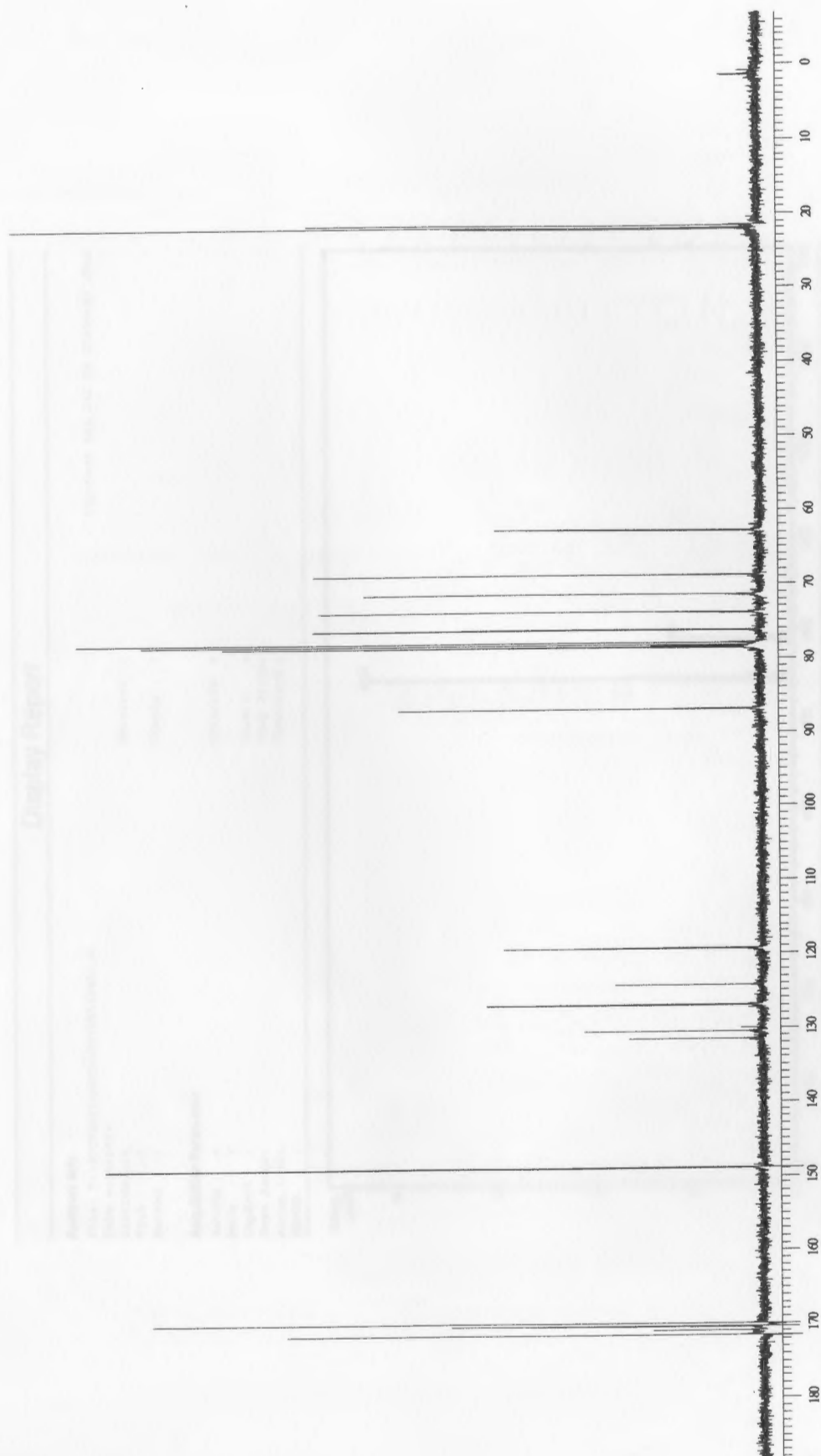


Figure 163: 100 MHz  $^{13}\text{C}$  NMR spectrum of divalent triazole 51

## Display Report

**Analysis Info:**

File: D:\HPCHEM\1\DATA\DF\DF5-9902.D  
 Date acquired:  
 Instrument:  
 Task :  
 Method :

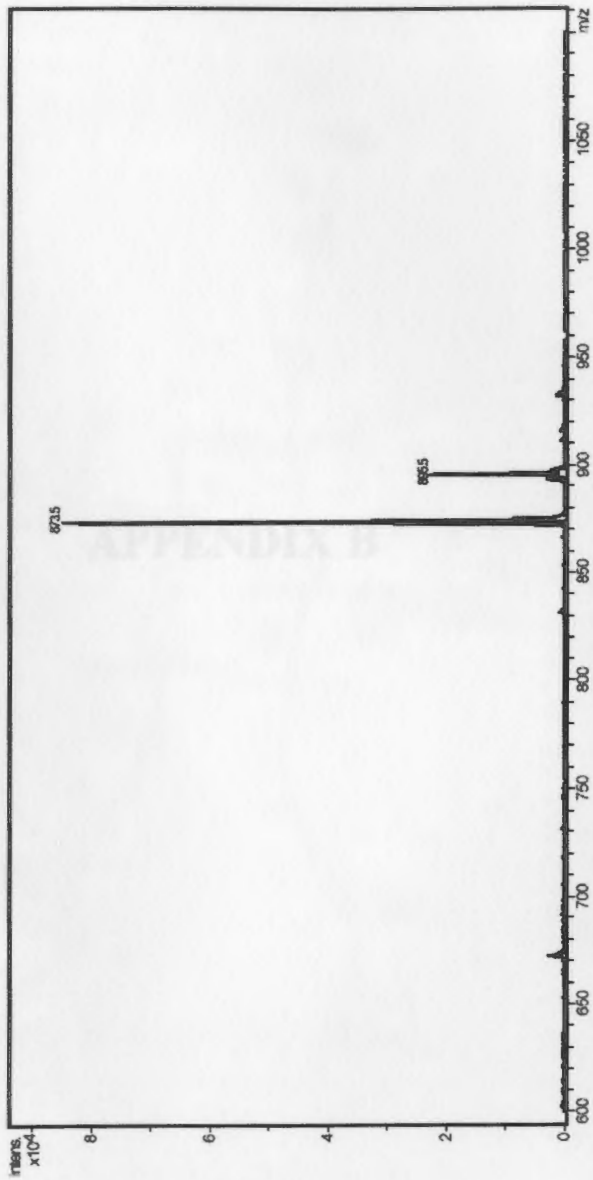
Printed: Fri Jul 29 07:59:43 2005

Operator :  
 Sample :

**Acquisition Parameter:**

Source :  
 Mode :  
 CapExit :  
 Scan Range:  
 Accum.time:  
 MS/MS :

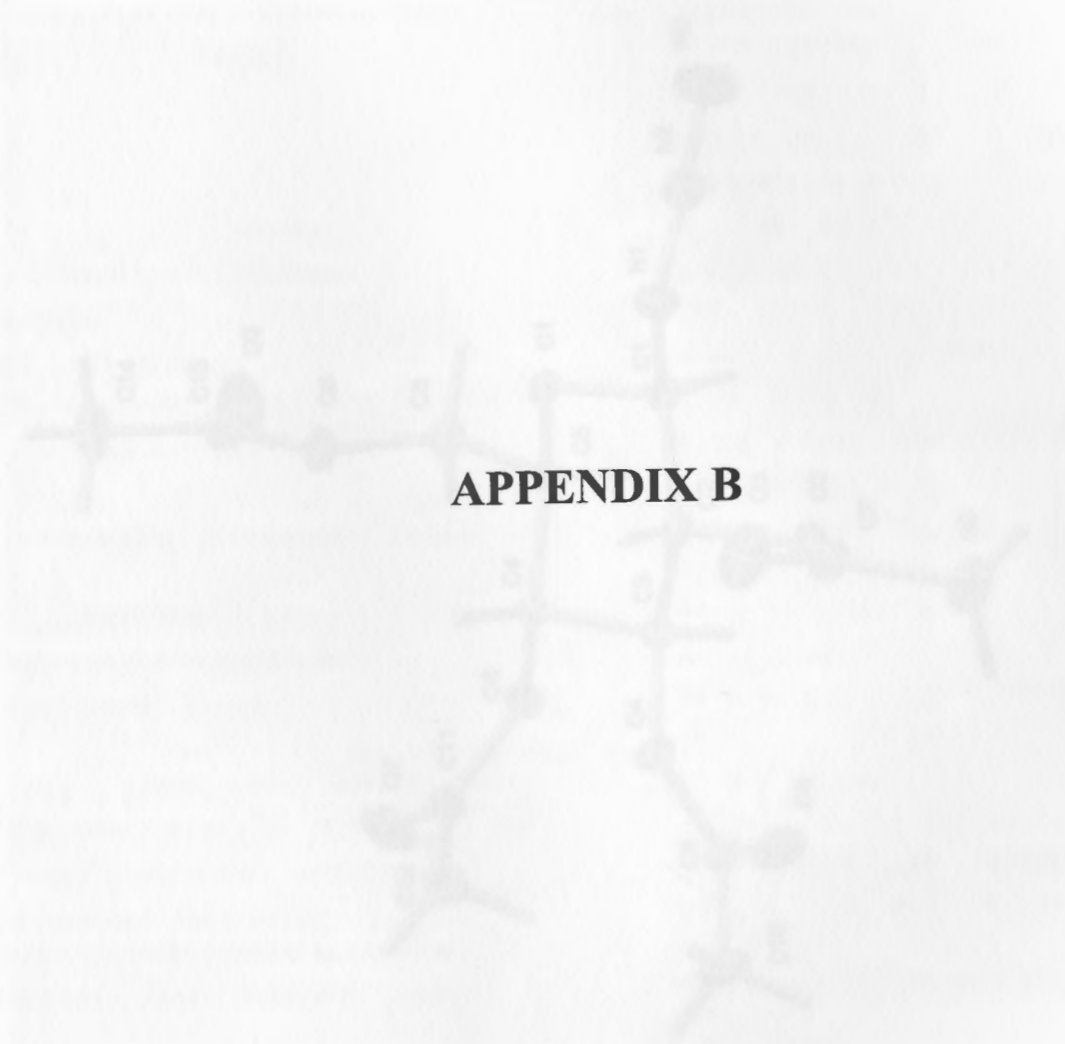
Polarity :  
 Skim 1 :  
 Trap Drive:  
 Summation :



Broker DataAnalysis Esquire-LC 1.6m, © Bruker Daltonik GmbH  
 Licensed to EQ\_135, Uni. of Ohio

- 1 -

**Figure 164:** Low resolution mass spectrum of divalent triazole 51



## APPENDIX B

Figure 16b: X-ray crystal structure of acetic acid



Table 5. Critical data and structure refinement for azide 3.

Identification code	3
Empirical formula	$C_{14}H_{12}N_3O_9$
Formula weight	333.26
Temperature	100(2) K
Wavelength	0.71073 Å
Crystal system, space group	Trigonal, $R\bar{3}m$
Unit cell dimensions	$a = b = c = 10.101(1)$ Å, $\alpha = \beta = \gamma = 120^\circ$
Volume	1010.0(1) Å <sup>3</sup>
Z, Calculated density	1.457 g cm <sup>-3</sup>
Absorption coefficient ( $\mu$ )	0.100 mm <sup>-1</sup>
Reflections collected / unique	1000 / 1000
Completeness to theta =	100%
Absorption correction	None
Refinement method	Full-matrix least-squares on $F^2$
Data / restraints / parameters	1000 / 0 / 14
Goodness-of-fit on $F^2$	1.000
Final $S$ indices (I > 3 $\sigma$ )	0.000
$S$ indices (all data)	0.000
Absolute structure parameter	0.000
Largest diff. peak and hole	0.000 / 0.000 e <sup>-</sup> Å <sup>-3</sup>

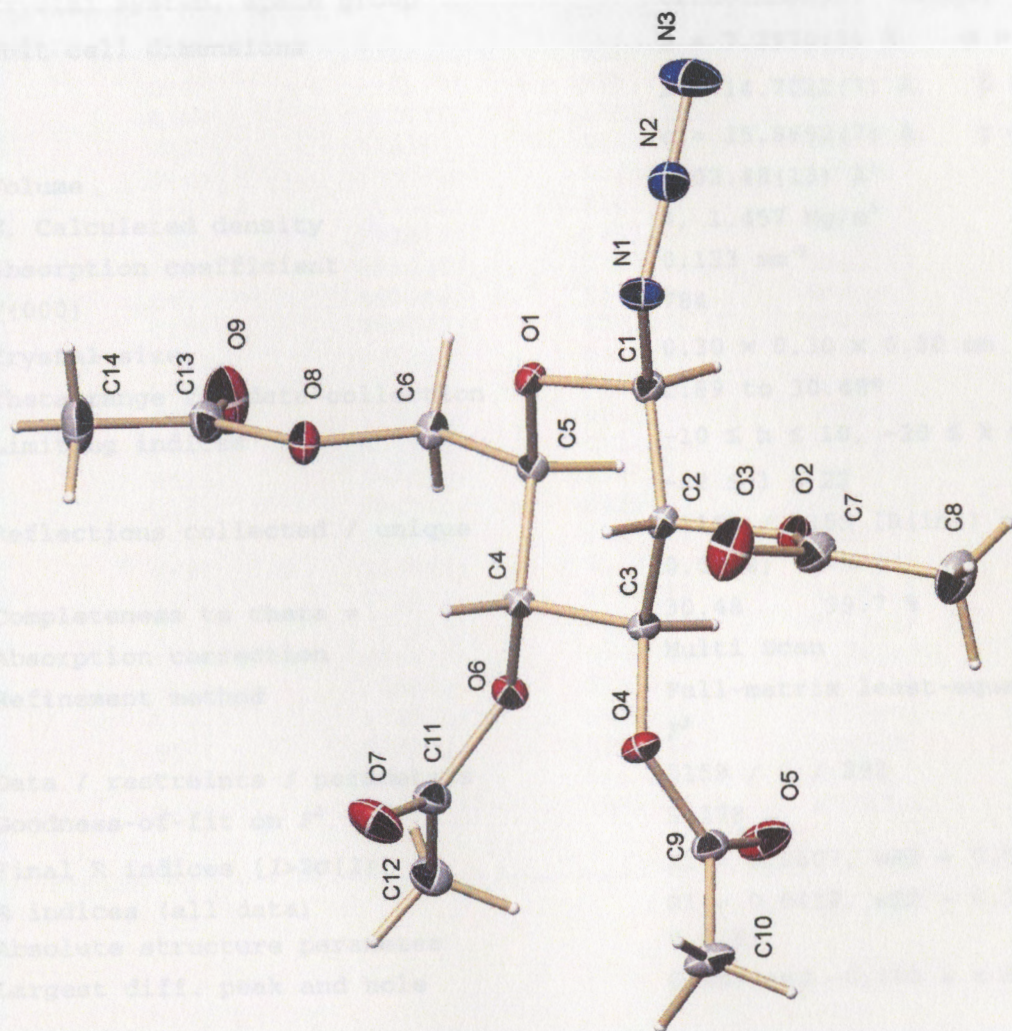


Figure 165: X-ray crystal structure of azide 3

Table 1. Crystal data and structure refinement for 04mz36am.

Identification code	04mz36am
Empirical formula	C14 H19 N3 O9
Formula weight	373.32
Temperature	100(2) K
Wavelength	0.71073 Å
Crystal system, space group	Orthorhombic, $P2_12_12_1$
Unit cell dimensions	$a = 7.2970(3)$ Å, $\alpha = 90^\circ$ $b = 14.7022(7)$ Å, $\beta = 90^\circ$ $c = 15.8692(7)$ Å, $\gamma = 90^\circ$
Volume	1702.48(13) Å <sup>3</sup>
Z, Calculated density	4, 1.457 Mg/m <sup>3</sup>
Absorption coefficient	0.123 mm <sup>-1</sup>
F(000)	784
Crystal size	0.30 × 0.30 × 0.30 mm
Theta range for data collection	1.89 to 30.48°
Limiting indices	$-10 \leq h \leq 10$ , $-20 \leq k \leq 20$ , $-22 \leq l \leq 22$
Reflections collected / unique	21165 / 5159 [R(int) = 0.0208]
Completeness to theta =	30.48 99.7 %
Absorption correction	Multi Scan
Refinement method	Full-matrix least-squares on $F^2$
Data / restraints / parameters	5159 / 0 / 292
Goodness-of-fit on $F^2$	1.178
Final R indices [ $I > 2\sigma(I)$ ]	R1 = 0.0407, wR2 = 0.0999
R indices (all data)	R1 = 0.0412, wR2 = 0.1002
Absolute structure parameter	0.0(6)
Largest diff. peak and hole	0.469 and -0.188 e × Å <sup>-3</sup>



Table 2. Atomic coordinates [ $\times 10^4$ ] and equivalent isotropic displacement parameters [ $\text{\AA}^2 \times 10^3$ ] for 04mz36am.  $U(\text{eq})$  is defined as one third of the trace of the orthogonalized  $U_{ij}$  tensor.

	x	y	z	$U(\text{eq})$
O(8)	4766(1)	3627(1)	10312(1)	15(1)
O(6)	2902(1)	5707(1)	10372(1)	13(1)
O(1)	6527(1)	4762(1)	9084(1)	12(1)
O(2)	5723(1)	6819(1)	7862(1)	15(1)
O(4)	2350(1)	6575(1)	8697(1)	14(1)
O(7)	173(2)	5222(1)	9878(1)	26(1)
N(1)	7798(2)	5102(1)	7778(1)	16(1)
O(5)	2330(2)	7720(1)	9642(1)	23(1)
O(3)	4614(2)	6361(1)	6602(1)	29(1)
C(3)	4062(2)	6242(1)	9027(1)	12(1)
C(4)	3801(2)	5428(1)	9609(1)	11(1)
C(2)	5213(2)	5981(1)	8264(1)	12(1)
N(2)	9457(2)	4930(1)	7856(1)	18(1)
N(3)	10938(2)	4738(1)	7827(1)	30(1)
C(13)	4660(2)	2995(1)	10930(1)	19(1)
C(6)	5847(2)	4412(1)	10532(1)	13(1)
O(9)	5337(2)	3105(1)	11609(1)	32(1)
C(9)	1665(2)	7346(1)	9040(1)	15(1)
C(5)	5732(2)	5110(1)	9843(1)	11(1)
C(10)	2(2)	7660(1)	8575(1)	20(1)
C(1)	6966(2)	5492(1)	8534(1)	13(1)
C(12)	394(2)	5855(1)	11275(1)	19(1)
C(11)	1068(2)	5550(1)	10433(1)	16(1)
C(7)	5297(2)	6938(1)	7032(1)	18(1)
C(14)	3679(3)	2161(1)	10635(1)	29(1)
C(8)	5783(2)	7883(1)	6764(1)	24(1)

Table 3. Bond lengths [Å] and angles [deg] for 04mz36am.

---

O(8)-C(13)	1.3529(15)
O(8)-C(6)	1.4401(15)
O(6)-C(11)	1.3612(15)
O(6)-C(4)	1.4359(14)
O(1)-C(1)	1.4199(14)
O(1)-C(5)	1.4325(14)
O(2)-C(7)	1.3638(15)
O(2)-C(2)	1.4370(14)
O(4)-C(9)	1.3532(15)
O(4)-C(3)	1.4396(15)
O(7)-C(11)	1.1979(17)
N(1)-N(2)	1.2433(16)
N(1)-C(1)	1.4607(15)
O(5)-C(9)	1.2044(17)
O(3)-C(7)	1.1974(18)
C(3)-C(2)	1.5224(16)
C(3)-C(4)	1.5242(16)
C(3)-H(3)	0.934(19)
C(4)-C(5)	1.5308(16)
C(4)-H(4)	0.902(19)
C(2)-C(1)	1.5295(17)
C(2)-H(2)	0.893(19)
N(2)-N(3)	1.1176(19)
C(13)-O(9)	1.1963(19)
C(13)-C(14)	1.496(2)
C(6)-C(5)	1.5006(16)
C(6)-H(6A)	0.996(19)
C(6)-H(6B)	0.927(19)
C(9)-C(10)	1.4933(19)
C(5)-H(5)	0.979(19)
C(10)-H(10A)	0.96(2)
C(10)-H(10B)	0.89(2)
C(10)-H(10C)	0.91(2)
C(1)-H(1)	0.914(19)
C(12)-C(11)	1.4917(19)
C(12)-H(12A)	0.92(2)
C(12)-H(12B)	0.94(2)
C(12)-H(12C)	0.90(2)
C(7)-C(8)	1.496(2)
C(14)-H(14A)	0.87(3)
C(14)-H(14B)	0.98(3)
C(14)-H(14C)	0.95(3)
C(8)-H(8A)	0.94(2)
C(8)-H(8B)	0.94(3)
C(8)-H(8C)	0.95(2)
C(13)-O(8)-C(6)	113.94(10)
C(11)-O(6)-C(4)	117.44(10)
C(1)-O(1)-C(5)	109.83(9)
C(7)-O(2)-C(2)	118.64(10)
C(9)-O(4)-C(3)	117.33(10)

N(2)-N(1)-C(1)	113.72(11)
O(4)-C(3)-C(2)	106.00(9)
O(4)-C(3)-C(4)	112.22(10)
C(2)-C(3)-C(4)	110.68(9)
O(4)-C(3)-H(3)	109.9(12)
C(2)-C(3)-H(3)	110.1(11)
C(4)-C(3)-H(3)	108.0(11)
O(6)-C(4)-C(3)	110.15(9)
O(6)-C(4)-C(5)	107.65(9)
C(3)-C(4)-C(5)	105.82(9)
O(6)-C(4)-H(4)	108.0(12)
C(3)-C(4)-H(4)	113.1(11)
C(5)-C(4)-H(4)	112.0(11)
O(2)-C(2)-C(3)	106.27(9)
O(2)-C(2)-C(1)	108.11(10)
C(3)-C(2)-C(1)	110.98(9)
O(2)-C(2)-H(2)	109.9(12)
C(3)-C(2)-H(2)	111.6(12)
C(1)-C(2)-H(2)	109.8(12)
N(3)-N(2)-N(1)	171.38(15)
O(9)-C(13)-O(8)	122.46(13)
O(9)-C(13)-C(14)	126.18(14)
O(8)-C(13)-C(14)	111.32(12)
O(8)-C(6)-C(5)	109.91(10)
O(8)-C(6)-H(6A)	110.3(11)
C(5)-C(6)-H(6A)	108.8(11)
O(8)-C(6)-H(6B)	108.2(12)
C(5)-C(6)-H(6B)	108.3(12)
H(6A)-C(6)-H(6B)	111.3(16)
O(5)-C(9)-O(4)	123.53(12)
O(5)-C(9)-C(10)	125.34(12)
O(4)-C(9)-C(10)	111.13(11)
O(1)-C(5)-C(6)	110.24(10)
O(1)-C(5)-C(4)	106.15(9)
C(6)-C(5)-C(4)	115.93(10)
O(1)-C(5)-H(5)	110.5(11)
C(6)-C(5)-H(5)	109.0(10)
C(4)-C(5)-H(5)	104.8(11)
C(9)-C(10)-H(10A)	106.7(13)
C(9)-C(10)-H(10B)	113.2(15)
H(10A)-C(10)-H(10B)	112(2)
C(9)-C(10)-H(10C)	109.0(14)
H(10A)-C(10)-H(10C)	104.0(19)
H(10B)-C(10)-H(10C)	111(2)
O(1)-C(1)-N(1)	107.60(10)
O(1)-C(1)-C(2)	109.80(10)
N(1)-C(1)-C(2)	107.61(10)
O(1)-C(1)-H(1)	108.5(12)
N(1)-C(1)-H(1)	111.3(12)
C(2)-C(1)-H(1)	112.0(12)
C(11)-C(12)-H(12A)	108.8(13)
C(11)-C(12)-H(12B)	114.8(13)
H(12A)-C(12)-H(12B)	103.5(19)
C(11)-C(12)-H(12C)	109.4(14)
H(12A)-C(12)-H(12C)	110(2)
H(12B)-C(12)-H(12C)	109.9(19)
O(7)-C(11)-O(6)	123.47(12)

O(7)-C(11)-C(12)	126.79(12)
O(6)-C(11)-C(12)	109.73(11)
O(3)-C(7)-O(2)	123.69(13)
O(3)-C(7)-C(8)	126.50(13)
O(2)-C(7)-C(8)	109.80(12)
C(13)-C(14)-H(14A)	107.8(18)
C(13)-C(14)-H(14B)	110.5(16)
H(14A)-C(14)-H(14B)	112(2)
C(13)-C(14)-H(14C)	110.6(16)
H(14A)-C(14)-H(14C)	109(2)
H(14B)-C(14)-H(14C)	106(2)
C(7)-C(8)-H(8A)	106.9(15)
C(7)-C(8)-H(8B)	110.7(15)
H(8A)-C(8)-H(8B)	115(2)
C(7)-C(8)-H(8C)	108.7(15)
H(8A)-C(8)-H(8C)	109(2)
H(8B)-C(8)-H(8C)	107(2)

Symmetry transformations used to generate equivalent atoms:

1(1)	14(1)	13(1)	15(1)	-2(1)	-2(1)
2(1)	15(1)	14(1)	16(1)	-7(1)	-2(1)
3(1)	16(1)	15(1)	17(1)	-2(1)	2(1)
4(1)	17(1)	16(1)	18(1)	-15(1)	-5(1)
5(1)	18(1)	17(1)	19(1)	5(1)	-4(1)
6(1)	19(1)	18(1)	20(1)	-5(1)	5(1)
7(1)	20(1)	19(1)	21(1)	0(1)	0(1)
8(1)	21(1)	20(1)	22(1)	-5(1)	5(1)
9(1)	22(1)	21(1)	23(1)	0(1)	0(1)
10(1)	23(1)	22(1)	24(1)	-5(1)	5(1)
11(1)	24(1)	23(1)	25(1)	0(1)	0(1)
12(1)	25(1)	24(1)	26(1)	-5(1)	5(1)
13(1)	26(1)	25(1)	27(1)	0(1)	0(1)
14(1)	27(1)	26(1)	28(1)	-5(1)	5(1)
15(1)	28(1)	27(1)	29(1)	0(1)	0(1)
16(1)	29(1)	28(1)	30(1)	-5(1)	5(1)
17(1)	30(1)	29(1)	31(1)	0(1)	0(1)
18(1)	31(1)	30(1)	32(1)	-5(1)	5(1)
19(1)	32(1)	31(1)	33(1)	0(1)	0(1)
20(1)	33(1)	32(1)	34(1)	-5(1)	5(1)
21(1)	34(1)	33(1)	35(1)	0(1)	0(1)
22(1)	35(1)	34(1)	36(1)	-5(1)	5(1)
23(1)	36(1)	35(1)	37(1)	0(1)	0(1)
24(1)	37(1)	36(1)	38(1)	-5(1)	5(1)
25(1)	38(1)	37(1)	39(1)	0(1)	0(1)
26(1)	39(1)	38(1)	40(1)	-5(1)	5(1)
27(1)	40(1)	39(1)	41(1)	0(1)	0(1)
28(1)	41(1)	40(1)	42(1)	-5(1)	5(1)
29(1)	42(1)	41(1)	43(1)	0(1)	0(1)
30(1)	43(1)	42(1)	44(1)	-5(1)	5(1)
31(1)	44(1)	43(1)	45(1)	0(1)	0(1)
32(1)	45(1)	44(1)	46(1)	-5(1)	5(1)
33(1)	46(1)	45(1)	47(1)	0(1)	0(1)
34(1)	47(1)	46(1)	48(1)	-5(1)	5(1)
35(1)	48(1)	47(1)	49(1)	0(1)	0(1)
36(1)	49(1)	48(1)	50(1)	-5(1)	5(1)
37(1)	50(1)	49(1)	51(1)	0(1)	0(1)
38(1)	51(1)	50(1)	52(1)	-5(1)	5(1)
39(1)	52(1)	51(1)	53(1)	0(1)	0(1)
40(1)	53(1)	52(1)	54(1)	-5(1)	5(1)
41(1)	54(1)	53(1)	55(1)	0(1)	0(1)
42(1)	55(1)	54(1)	56(1)	-5(1)	5(1)
43(1)	56(1)	55(1)	57(1)	0(1)	0(1)
44(1)	57(1)	56(1)	58(1)	-5(1)	5(1)
45(1)	58(1)	57(1)	59(1)	0(1)	0(1)
46(1)	59(1)	58(1)	60(1)	-5(1)	5(1)
47(1)	60(1)	59(1)	61(1)	0(1)	0(1)
48(1)	61(1)	60(1)	62(1)	-5(1)	5(1)
49(1)	62(1)	61(1)	63(1)	0(1)	0(1)
50(1)	63(1)	62(1)	64(1)	-5(1)	5(1)
51(1)	64(1)	63(1)	65(1)	0(1)	0(1)
52(1)	65(1)	64(1)	66(1)	-5(1)	5(1)
53(1)	66(1)	65(1)	67(1)	0(1)	0(1)
54(1)	67(1)	66(1)	68(1)	-5(1)	5(1)
55(1)	68(1)	67(1)	69(1)	0(1)	0(1)
56(1)	69(1)	68(1)	70(1)	-5(1)	5(1)
57(1)	70(1)	69(1)	71(1)	0(1)	0(1)
58(1)	71(1)	70(1)	72(1)	-5(1)	5(1)
59(1)	72(1)	71(1)	73(1)	0(1)	0(1)
60(1)	73(1)	72(1)	74(1)	-5(1)	5(1)
61(1)	74(1)	73(1)	75(1)	0(1)	0(1)
62(1)	75(1)	74(1)	76(1)	-5(1)	5(1)
63(1)	76(1)	75(1)	77(1)	0(1)	0(1)
64(1)	77(1)	76(1)	78(1)	-5(1)	5(1)
65(1)	78(1)	77(1)	79(1)	0(1)	0(1)
66(1)	79(1)	78(1)	80(1)	-5(1)	5(1)
67(1)	80(1)	79(1)	81(1)	0(1)	0(1)
68(1)	81(1)	80(1)	82(1)	-5(1)	5(1)
69(1)	82(1)	81(1)	83(1)	0(1)	0(1)
70(1)	83(1)	82(1)	84(1)	-5(1)	5(1)
71(1)	84(1)	83(1)	85(1)	0(1)	0(1)
72(1)	85(1)	84(1)	86(1)	-5(1)	5(1)
73(1)	86(1)	85(1)	87(1)	0(1)	0(1)
74(1)	87(1)	86(1)	88(1)	-5(1)	5(1)
75(1)	88(1)	87(1)	89(1)	0(1)	0(1)
76(1)	89(1)	88(1)	90(1)	-5(1)	5(1)
77(1)	90(1)	89(1)	91(1)	0(1)	0(1)
78(1)	91(1)	90(1)	92(1)	-5(1)	5(1)
79(1)	92(1)	91(1)	93(1)	0(1)	0(1)
80(1)	93(1)	92(1)	94(1)	-5(1)	5(1)
81(1)	94(1)	93(1)	95(1)	0(1)	0(1)
82(1)	95(1)	94(1)	96(1)	-5(1)	5(1)
83(1)	96(1)	95(1)	97(1)	0(1)	0(1)
84(1)	97(1)	96(1)	98(1)	-5(1)	5(1)
85(1)	98(1)	97(1)	99(1)	0(1)	0(1)
86(1)	99(1)	98(1)	100(1)	-5(1)	5(1)

Table 4. Anisotropic displacement parameters [ $\text{\AA}^2 \times 10^3$ ] for 04mz36am.  
The anisotropic displacement factor exponent takes the form:

$$-2 \pi^2 [(h a^*)^2 U_{11} + \dots + 2 h k a^* b^* U_{12}]$$

	U11	U22	U33	U23	U13	
U12						
O(8)	19(1)	13(1)	14(1)	2(1)	-3(1)	-
4(1)						
O(6)	13(1)	16(1)	12(1)	-2(1)	1(1)	-
1(1)						
O(1)	15(1)	9(1)	12(1)	0(1)	1(1)	
1(1)						
O(2)	19(1)	13(1)	12(1)	3(1)	-1(1)	-
1(1)						
O(4)	14(1)	13(1)	15(1)	-2(1)	-2(1)	
4(1)						
O(7)	15(1)	40(1)	21(1)	-7(1)	-2(1)	-
4(1)						
N(1)	15(1)	21(1)	13(1)	-2(1)	2(1)	
4(1)						
O(5)	26(1)	22(1)	23(1)	-10(1)	-5(1)	
8(1)						
O(3)	48(1)	22(1)	17(1)	0(1)	-8(1)	-
3(1)						
C(3)	11(1)	12(1)	12(1)	-1(1)	0(1)	
2(1)						
C(4)	11(1)	11(1)	10(1)	0(1)	0(1)	
0(1)						
C(2)	15(1)	10(1)	10(1)	0(1)	0(1)	
1(1)						
N(2)	20(1)	18(1)	16(1)	-3(1)	1(1)	
0(1)						
N(3)	19(1)	40(1)	30(1)	-14(1)	1(1)	
7(1)						
C(13)	18(1)	18(1)	20(1)	6(1)	1(1)	-
2(1)						
C(6)	16(1)	12(1)	11(1)	0(1)	-3(1)	-
2(1)						
O(9)	41(1)	32(1)	23(1)	14(1)	-9(1)	-
11(1)						
C(9)	16(1)	14(1)	15(1)	0(1)	3(1)	
3(1)						
C(5)	11(1)	12(1)	11(1)	0(1)	-1(1)	
0(1)						
C(10)	20(1)	21(1)	19(1)	-2(1)	-3(1)	
9(1)						
C(1)	14(1)	11(1)	13(1)	0(1)	1(1)	
0(1)						

0(1)	C(12)	18(1)	22(1)	17(1)	1(1)	4(1)	
1(1)	C(11)	14(1)	17(1)	16(1)	1(1)	2(1)	
4(1)	C(7)	24(1)	16(1)	14(1)	2(1)	0(1)	
11(1)	C(14)	33(1)	19(1)	35(1)	7(1)	-3(1)	-
0(1)	C(8)	37(1)	18(1)	16(1)	5(1)	-1(1)	

---

B(1)	4654(30)	5781(33)	4324(25)	18
B(2)	3130(30)	4978(32)	3275(23)	17
B(3)	4080(30)	5433(32)	7400(31)	16
B(4)	7150(30)	4294(32)	10511(31)	15
B(5)	5340(30)	4443(32)	11019(32)	14
B(6)	6270(30)	5461(32)	10004(32)	13
B(7)	-1040(30)	7504(32)	8940(32)	12
B(8)	-170(30)	7370(32)	4080(32)	11
B(9)	0(30)	8272(32)	8487(32)	10
B(10)	7760(30)	5472(32)	5804(32)	9
B(11)	120(30)	4475(32)	11733(32)	8
B(12)	2040(30)	5434(32)	11734(32)	7
B(13)	-304(30)	5435(32)	11039(32)	6
B(14)	240(30)	1024(32)	11074(32)	5
B(15)	300(30)	1030(32)	10214(32)	4
B(16)	300(30)	7118(32)	10764(32)	3
B(17)	1070(30)	1442(32)	4275(32)	2
B(18)	40(30)	1045(32)	7087(32)	1
B(19)	4074(30)	4236(32)	4379(32)	0

---



Table 5. Hydrogen coordinates ( $\times 10^4$ ) and isotropic displacement parameters ( $\text{\AA}^2 \times 10^3$ ) for 04mz36am.

	x	y	z	U(eq)
H(3)	4650(30)	6701(13)	9333(11)	14
H(4)	3130(30)	4979(12)	9375(11)	13
H(2)	4580(30)	5633(13)	7905(11)	14
H(6A)	7150(30)	4236(13)	10611(12)	16
H(6B)	5360(30)	4663(13)	11019(12)	16
H(5)	6370(30)	5661(12)	10024(11)	13
H(10A)	-1010(30)	7586(15)	8949(14)	30
H(10B)	-170(30)	7370(16)	8086(14)	30
H(10C)	80(30)	8272(16)	8497(14)	30
H(1)	7760(30)	5872(13)	8804(12)	15
H(12A)	520(30)	6475(16)	11311(13)	29
H(12B)	1080(30)	5639(15)	11734(13)	29
H(12C)	-800(30)	5695(15)	11334(13)	29
H(14A)	3440(40)	1826(19)	11076(17)	43
H(14B)	4410(40)	1839(19)	10214(16)	43
H(14C)	2570(40)	2318(18)	10364(16)	43
H(8A)	5750(30)	7892(16)	6170(15)	36
H(8B)	6910(30)	8065(18)	7007(14)	36
H(8C)	4870(30)	8290(17)	6973(14)	36

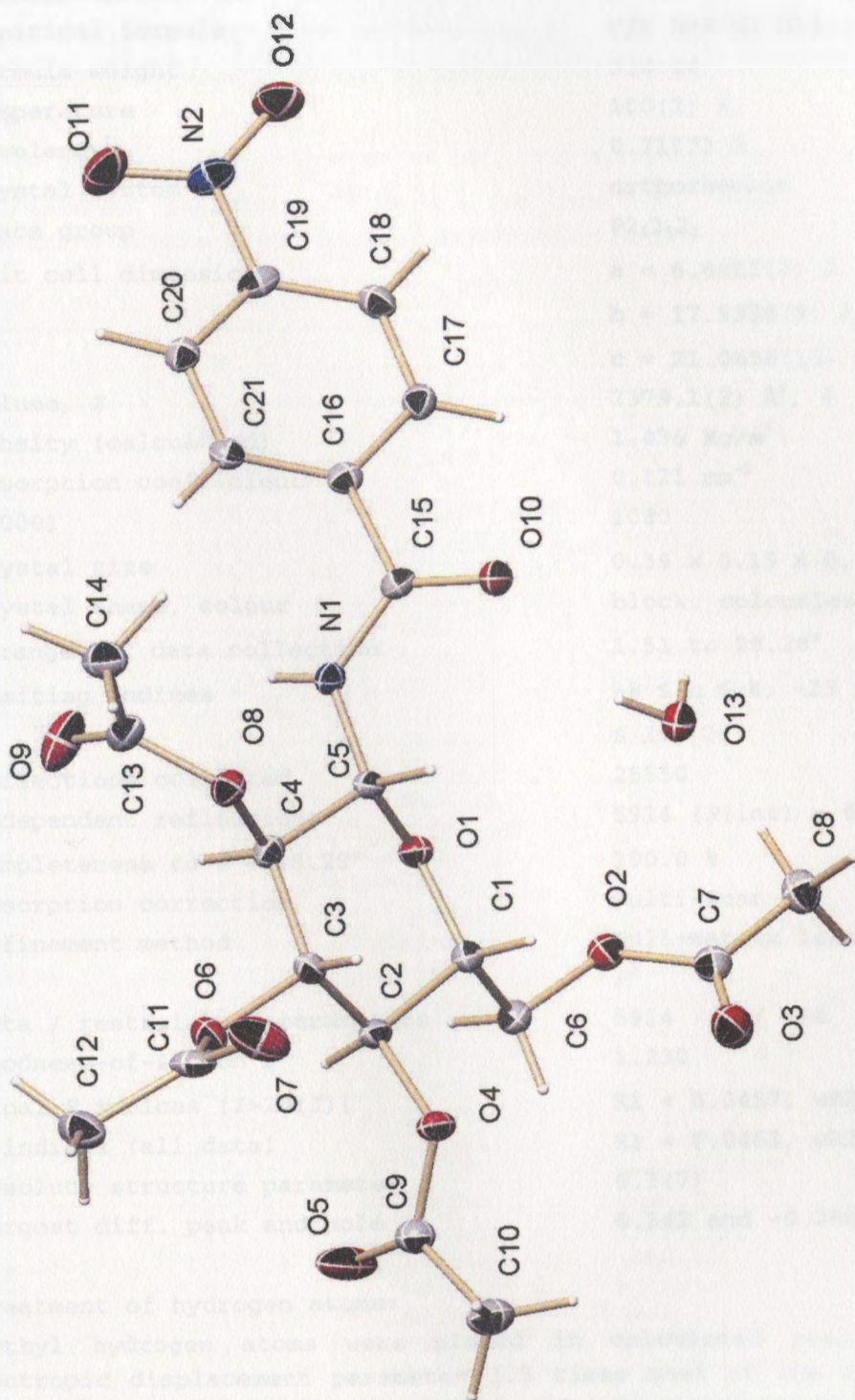


Figure 166: X-ray crystal structure of amide 4



Table 1. Crystal data and structure refinement for 04mz57am:

Identification code	04mz57am
Empirical formula	C <sub>21</sub> H <sub>26</sub> N <sub>2</sub> O <sub>13</sub>
Formula weight	514.44
Temperature	100(2) K
Wavelength	0.71073 Å
Crystal system	orthorhombic
Space group	P2 <sub>1</sub> 2 <sub>1</sub> 2 <sub>1</sub>
Unit cell dimensions	a = 6.4411(3) Å, α = 90° b = 17.5338(9) Å, β = 90° c = 21.0656(10) Å, γ = 90°
Volume, Z	2379.1(2) Å <sup>3</sup> , 4
Density (calculated)	1.436 Mg/m <sup>3</sup>
Absorption coefficient	0.121 mm <sup>-1</sup>
F(000)	1080
Crystal size	0.39 × 0.15 × 0.15 mm
Crystal shape, colour	block, colourless
θ range for data collection	1.51 to 28.28°
Limiting indices	-8 ≤ h ≤ 8, -23 ≤ k ≤ 23, -27 ≤ l ≤ 28
Reflections collected	25550
Independent reflections	5914 (R(int) = 0.0296)
Completeness to θ = 28.28°	100.0 %
Absorption correction	multi-scan
Refinement method	Full-matrix least-squares on F <sup>2</sup>
Data / restraints / parameters	5914 / 0 / 374
Goodness-of-fit on F <sup>2</sup>	1.230
Final R indices [I > 2σ(I)]	R1 = 0.0457, wR2 = 0.1077
R indices (all data)	R1 = 0.0463, wR2 = 0.1081
Absolute structure parameter	0.3(7)
Largest diff. peak and hole	0.342 and -0.286 e Å <sup>-3</sup>

## Treatment of hydrogen atoms:

Methyl hydrogen atoms were placed in calculated positions with an isotropic displacement parameter 1.5 times that of the adjacent carbon atom. The positions of the amide and the water hydrogen atoms were isotropically refined. The positions of all other hydrogen atoms were refined were restraint to have an isotropic displacement parameter 1.2 times that of the adjacent carbon atom.

Refinement of  $F^2$  against ALL reflections. The weighted R-factor  $wR$  and goodness of fit are based on  $F^2$ , conventional R-factors  $R$  are based on  $F$ , with  $F$  set to zero for negative  $F^2$ . The threshold expression of  $F^2 > 2\sigma(F^2)$  is used only for calculating R-factors.

Table 2. Atomic coordinates [ $\times 10^4$ ] and equivalent isotropic displacement parameters [ $\text{\AA}^2 \times 10^3$ ] for 04mz57am.  $U(\text{eq})$  is defined as one third of the trace of the orthogonalized  $U_{ij}$  tensor.

	x	y	z	U(eq)
C(19)	-406(3)	8168(1)	731(1)	18(1)
O(1)	3390(2)	4714(1)	1889(1)	16(1)
O(6)	837(2)	2768(1)	1165(1)	21(1)
O(2)	6354(2)	4705(1)	2898(1)	19(1)
O(4)	4648(2)	2681(1)	1920(1)	19(1)
C(21)	-350(3)	6815(1)	659(1)	16(1)
C(5)	2863(3)	4765(1)	1230(1)	15(1)
C(1)	4559(3)	4042(1)	2033(1)	16(1)
O(8)	990(2)	4134(1)	398(1)	18(1)
O(3)	9124(2)	4011(1)	2607(1)	29(1)
C(18)	1650(3)	8197(1)	928(1)	19(1)
C(16)	1702(3)	6828(1)	869(1)	16(1)
O(12)	-591(3)	9485(1)	674(1)	32(1)
N(2)	-1564(3)	8888(1)	666(1)	23(1)
O(10)	4813(2)	6105(1)	817(1)	20(1)
O(7)	2440(3)	2223(1)	332(1)	35(1)
C(3)	2407(3)	3353(1)	1214(1)	17(1)
C(2)	3257(3)	3329(1)	1886(1)	16(1)
C(4)	1387(3)	4116(1)	1071(1)	16(1)
C(15)	2954(3)	6104(1)	938(1)	16(1)
C(9)	4275(3)	2129(1)	2349(1)	21(1)
C(20)	-1434(3)	7492(1)	592(1)	17(1)
N(1)	1877(2)	5486(1)	1132(1)	15(1)
C(6)	5038(3)	4069(1)	2737(1)	19(1)
O(11)	-3455(3)	8848(1)	609(1)	33(1)
C(17)	2694(3)	7513(1)	1002(1)	18(1)
O(5)	2826(3)	2131(1)	2707(1)	39(1)
O(9)	-2297(2)	4518(1)	555(1)	35(1)
C(7)	8411(3)	4600(1)	2798(1)	20(1)
C(11)	1022(3)	2246(1)	692(1)	22(1)
C(14)	-939(4)	4452(1)	-506(1)	27(1)
C(8)	9638(3)	5293(1)	2971(1)	24(1)
C(10)	5937(4)	1531(1)	2319(1)	27(1)
C(13)	-907(3)	4376(1)	203(1)	21(1)
C(12)	-791(4)	1709(1)	709(1)	30(1)
O(13)	7908(2)	5662(1)	1670(1)	19(1)

All esds (except the esd in the dihedral angle between two l.s. planes) are estimated using the full covariance matrix. The cell esds are taken into account individually in the estimation of esds in distances, angles and torsion angles; correlations between esds in cell parameters are only used when they are defined by crystal symmetry. An approximate (isotropic) treatment of cell esds is used for estimating esds involving l.s. planes.

Table 3. Bond lengths [Å] and angles [deg] for 04mz57am.

C(19)-C(20)	1.388(3)	C(4)-H(4)	0.97(2)
C(19)-C(18)	1.389(3)	C(15)-N(1)	1.351(2)
C(19)-N(2)	1.472(2)	C(9)-O(5)	1.200(3)
O(1)-C(1)	1.430(2)	C(9)-C(10)	1.499(3)
O(1)-C(5)	1.433(2)	C(20)-H(20)	0.96(2)
O(6)-C(11)	1.359(2)	N(1)-H(1B)	0.78(2)
O(6)-C(3)	1.444(2)	C(6)-H(6A)	0.95(3)
O(2)-C(7)	1.354(2)	C(6)-H(6B)	0.94(2)
O(2)-C(6)	1.441(2)	C(17)-H(17)	0.93(3)
O(4)-C(9)	1.346(2)	O(9)-C(13)	1.188(3)
O(4)-C(2)	1.449(2)	C(7)-C(8)	1.496(3)
C(21)-C(20)	1.385(3)	C(11)-C(12)	1.500(3)
C(21)-C(16)	1.394(3)	C(14)-C(13)	1.500(3)
C(21)-H(21)	0.92(2)	C(14)-H(14A)	0.9800
C(5)-N(1)	1.430(2)	C(14)-H(14B)	0.9800
C(5)-C(4)	1.520(2)	C(14)-H(14C)	0.9800
C(5)-H(5)	0.98(2)	C(8)-H(8A)	0.9800
C(1)-C(6)	1.516(3)	C(8)-H(8B)	0.9800
C(1)-C(2)	1.537(2)	C(8)-H(8C)	0.9800
C(1)-H(1A)	0.96(2)	C(10)-H(10A)	0.9800
O(8)-C(13)	1.357(2)	C(10)-H(10B)	0.9800
O(8)-C(4)	1.440(2)	C(10)-H(10C)	0.9800
O(3)-C(7)	1.198(2)	C(12)-H(12A)	0.9800
C(18)-C(17)	1.384(3)	C(12)-H(12B)	0.9800
C(18)-H(18)	0.93(2)	C(12)-H(12C)	0.9800
C(16)-C(17)	1.389(3)	O(13)-H(13A)	0.79(3)
C(16)-C(15)	1.510(2)	O(13)-H(13B)	0.81(4)
O(12)-N(2)	1.221(2)		
N(2)-O(11)	1.226(2)	C(20)-C(19)-C(18)	123.27(18)
O(10)-C(15)	1.224(2)	C(20)-C(19)-N(2)	118.07(16)
O(7)-C(11)	1.187(3)	C(18)-C(19)-N(2)	118.65(17)
C(3)-C(2)	1.518(2)	C(1)-O(1)-C(5)	112.43(13)
C(3)-C(4)	1.521(2)	C(11)-O(6)-C(3)	117.92(15)
C(3)-H(3)	0.94(2)	C(7)-O(2)-C(6)	115.67(15)
C(2)-H(2)	0.92(2)	C(9)-O(4)-C(2)	119.18(14)



C(20)-C(21)-C(16)	119.76(17)	C(21)-C(20)-C(19)	118.04(16)
C(20)-C(21)-H(21)	118.3(16)	C(21)-C(20)-H(20)	121.9(14)
C(16)-C(21)-H(21)	121.9(16)	C(19)-C(20)-H(20)	120.0(14)
N(1)-C(5)-O(1)	107.45(14)	C(15)-N(1)-C(5)	121.67(15)
N(1)-C(5)-C(4)	110.63(14)	C(15)-N(1)-H(1B)	118.7(17)
O(1)-C(5)-C(4)	108.36(13)	C(5)-N(1)-H(1B)	118.6(17)
N(1)-C(5)-H(5)	110.1(14)	O(2)-C(6)-C(1)	111.96(15)
O(1)-C(5)-H(5)	108.5(14)	O(2)-C(6)-H(6A)	106.7(14)
C(4)-C(5)-H(5)	111.7(13)	C(1)-C(6)-H(6A)	107.7(15)
O(1)-C(1)-C(6)	106.79(14)	O(2)-C(6)-H(6B)	109.7(15)
O(1)-C(1)-C(2)	109.83(13)	C(1)-C(6)-H(6B)	108.9(15)
C(6)-C(1)-C(2)	109.48(14)	H(6A)-C(6)-H(6B)	112(2)
O(1)-C(1)-H(1A)	110.4(14)	C(18)-C(17)-C(16)	120.19(17)
C(6)-C(1)-H(1A)	108.8(14)	C(18)-C(17)-H(17)	119.5(14)
C(2)-C(1)-H(1A)	111.4(14)	C(16)-C(17)-H(17)	120.3(14)
C(13)-O(8)-C(4)	117.67(14)	O(3)-C(7)-O(2)	123.01(18)
C(17)-C(18)-C(19)	117.76(18)	O(3)-C(7)-C(8)	125.39(18)
C(17)-C(18)-H(18)	121.1(16)	O(2)-C(7)-C(8)	111.58(16)
C(19)-C(18)-H(18)	121.1(16)	O(7)-C(11)-O(6)	123.96(19)
C(17)-C(16)-C(21)	120.96(17)	O(7)-C(11)-C(12)	126.39(19)
C(17)-C(16)-C(15)	117.47(16)	O(6)-C(11)-C(12)	109.63(18)
C(21)-C(16)-C(15)	121.53(17)	C(13)-C(14)-H(14A)	109.5
O(12)-N(2)-O(11)	124.05(17)	C(13)-C(14)-H(14B)	109.5
O(12)-N(2)-C(19)	118.33(17)	H(14A)-C(14)-H(14B)	109.5
O(11)-N(2)-C(19)	117.62(17)	C(13)-C(14)-H(14C)	109.5
O(6)-C(3)-C(2)	107.41(14)	H(14A)-C(14)-H(14C)	109.5
O(6)-C(3)-C(4)	107.96(14)	H(14B)-C(14)-H(14C)	109.5
C(2)-C(3)-C(4)	111.34(15)	C(7)-C(8)-H(8A)	109.5
O(6)-C(3)-H(3)	109.5(15)	C(7)-C(8)-H(8B)	109.5
C(2)-C(3)-H(3)	109.9(15)	H(8A)-C(8)-H(8B)	109.5
C(4)-C(3)-H(3)	110.6(14)	C(7)-C(8)-H(8C)	109.5
O(4)-C(2)-C(3)	106.88(14)	H(8A)-C(8)-H(8C)	109.5
O(4)-C(2)-C(1)	106.90(14)	H(8B)-C(8)-H(8C)	109.5
C(3)-C(2)-C(1)	111.29(14)	C(9)-C(10)-H(10A)	109.5
O(4)-C(2)-H(2)	109.7(14)	C(9)-C(10)-H(10B)	109.5
C(3)-C(2)-H(2)	111.9(15)	H(10A)-C(10)-H(10B)	109.5
C(1)-C(2)-H(2)	110.0(15)	C(9)-C(10)-H(10C)	109.5
O(8)-C(4)-C(5)	108.11(14)	H(10A)-C(10)-H(10C)	109.5
O(8)-C(4)-C(3)	106.95(14)	H(10B)-C(10)-H(10C)	109.5
C(5)-C(4)-C(3)	110.17(14)	O(9)-C(13)-O(8)	123.75(18)
O(8)-C(4)-H(4)	107.7(14)	O(9)-C(13)-C(14)	126.28(19)
C(5)-C(4)-H(4)	111.7(14)	O(8)-C(13)-C(14)	109.96(17)
C(3)-C(4)-H(4)	111.9(14)	C(11)-C(12)-H(12A)	109.5
O(10)-C(15)-N(1)	124.51(17)	C(11)-C(12)-H(12B)	109.5
O(10)-C(15)-C(16)	120.09(17)	H(12A)-C(12)-H(12B)	109.5
N(1)-C(15)-C(16)	115.40(15)	C(11)-C(12)-H(12C)	109.5
O(5)-C(9)-O(4)	123.98(18)	H(12A)-C(12)-H(12C)	109.5
O(5)-C(9)-C(10)	125.74(18)	H(12B)-C(12)-H(12C)	109.5
O(4)-C(9)-C(10)	110.27(16)	H(13A)-O(13)-H(13B)	100(3)

---

Symmetry transformations used to generate equivalent atoms:

Table 4. Anisotropic displacement parameters [ $\text{\AA}^2 \times 10^3$ ] for 04mz57am. The anisotropic displacement factor exponent takes the form:  $-2 \pi^2 [(h a^*)^2 U_{11} + \dots + 2 h k a^* b^* U_{12}]$

	U11	U22	U33	U23	U13	U12
C(19)	23(1)	18(1)	14(1)	1(1)	0(1)	6(1)
O(1)	17(1)	15(1)	17(1)	1(1)	-1(1)	1(1)
O(6)	21(1)	19(1)	22(1)	0(1)	-1(1)	-5(1)
O(2)	20(1)	19(1)	17(1)	0(1)	-1(1)	1(1)
O(4)	19(1)	16(1)	23(1)	6(1)	3(1)	4(1)
C(21)	18(1)	15(1)	15(1)	2(1)	1(1)	-2(1)
C(5)	14(1)	14(1)	17(1)	3(1)	1(1)	0(1)
C(1)	14(1)	16(1)	18(1)	2(1)	0(1)	0(1)
O(8)	17(1)	21(1)	16(1)	1(1)	-1(1)	2(1)
O(3)	22(1)	23(1)	40(1)	-1(1)	5(1)	2(1)
C(18)	24(1)	16(1)	18(1)	1(1)	-2(1)	-4(1)
C(16)	17(1)	17(1)	13(1)	3(1)	3(1)	1(1)
O(12)	40(1)	15(1)	40(1)	-2(1)	-7(1)	4(1)
N(2)	31(1)	17(1)	21(1)	-3(1)	-3(1)	7(1)
O(10)	14(1)	20(1)	27(1)	5(1)	2(1)	1(1)
O(7)	52(1)	20(1)	34(1)	-5(1)	14(1)	-3(1)
C(3)	16(1)	14(1)	20(1)	1(1)	1(1)	-1(1)
C(2)	15(1)	14(1)	20(1)	3(1)	1(1)	2(1)
C(4)	14(1)	18(1)	16(1)	2(1)	0(1)	2(1)
C(15)	17(1)	16(1)	14(1)	1(1)	-2(1)	3(1)
C(9)	24(1)	17(1)	22(1)	2(1)	-2(1)	0(1)
C(20)	17(1)	21(1)	14(1)	2(1)	0(1)	1(1)
N(1)	12(1)	17(1)	18(1)	3(1)	3(1)	3(1)
C(6)	17(1)	19(1)	20(1)	3(1)	-2(1)	-1(1)
O(11)	28(1)	25(1)	47(1)	-4(1)	-8(1)	10(1)
C(17)	17(1)	20(1)	17(1)	0(1)	-1(1)	0(1)
O(5)	43(1)	27(1)	47(1)	19(1)	23(1)	13(1)
O(9)	24(1)	50(1)	31(1)	-12(1)	-6(1)	15(1)
C(7)	21(1)	23(1)	16(1)	3(1)	0(1)	-2(1)
C(11)	34(1)	13(1)	20(1)	5(1)	-5(1)	-1(1)
C(14)	34(1)	22(1)	26(1)	3(1)	-9(1)	-3(1)
C(8)	23(1)	27(1)	20(1)	-2(1)	-2(1)	-4(1)
C(10)	30(1)	23(1)	29(1)	6(1)	3(1)	6(1)
C(13)	23(1)	14(1)	26(1)	-4(1)	-8(1)	2(1)
C(12)	39(1)	20(1)	30(1)	3(1)	-10(1)	-10(1)
O(13)	16(1)	21(1)	21(1)	-2(1)	-1(1)	1(1)

Table 5. Hydrogen coordinates ( $\times 10^4$ ) and isotropic displacement parameters ( $\text{\AA}^2 \times 10^3$ ) for 04mz57am.

	x	y	z	U(eq)
H(21)	-1010(40)	6368(14)	552(11)	20
H(5)	4140(40)	4736(13)	981(11)	18
H(1A)	5850(40)	4041(13)	1800(11)	19
H(18)	2290(40)	8657(14)	1019(11)	23
H(3)	3480(40)	3252(13)	922(11)	20
H(2)	2210(40)	3276(13)	2183(11)	19
H(4)	60(40)	4171(13)	1287(11)	19
H(20)	-2830(40)	7505(13)	433(11)	21
H(6A)	3770(40)	4143(13)	2955(11)	22
H(6B)	5690(40)	3611(14)	2855(11)	22
H(17)	4070(40)	7515(13)	1138(11)	22
H(14A)	-2353	4570	-647	41
H(14B)	-484	3972	-699	41
H(14C)	-1	4864	-635	41
H(8A)	10262	5222	3391	35
H(8B)	8720	5739	2979	35
H(8C)	10737	5374	2656	35
H(10A)	5620	1124	2622	41
H(10B)	7279	1761	2425	41
H(10C)	5997	1319	1889	41
H(12A)	-640	1328	372	45
H(12B)	-2079	1996	643	45
H(12C)	-840	1453	1122	45
H(1B)	740(40)	5542(13)	1257(11)	13(5)
H(13A)	6950(50)	5657(16)	1438(13)	31(7)
H(13B)	7760(50)	6080(20)	1831(16)	49(9)

Table 6. Hydrogen bond distances [ $\text{\AA}$ ] and angles [deg] for 04mz57am

D-H	H...A	D...A	$\angle$ (DHA)	
0.81(4)	2.12(4)	2.928(2)	175(3)	O13-H13B...O5_\$2
0.79(3)	2.06(3)	2.793(2)	156(3)	O13-H13A...O10
0.78(2)	2.03(2)	2.813(2)	174(2)	N1-H1B...O13_\$1

Symmetry transformations used to generate equivalent atoms:

\$1: x-1, y, z; \$2: -x+1, y+0.5, -z+0.5



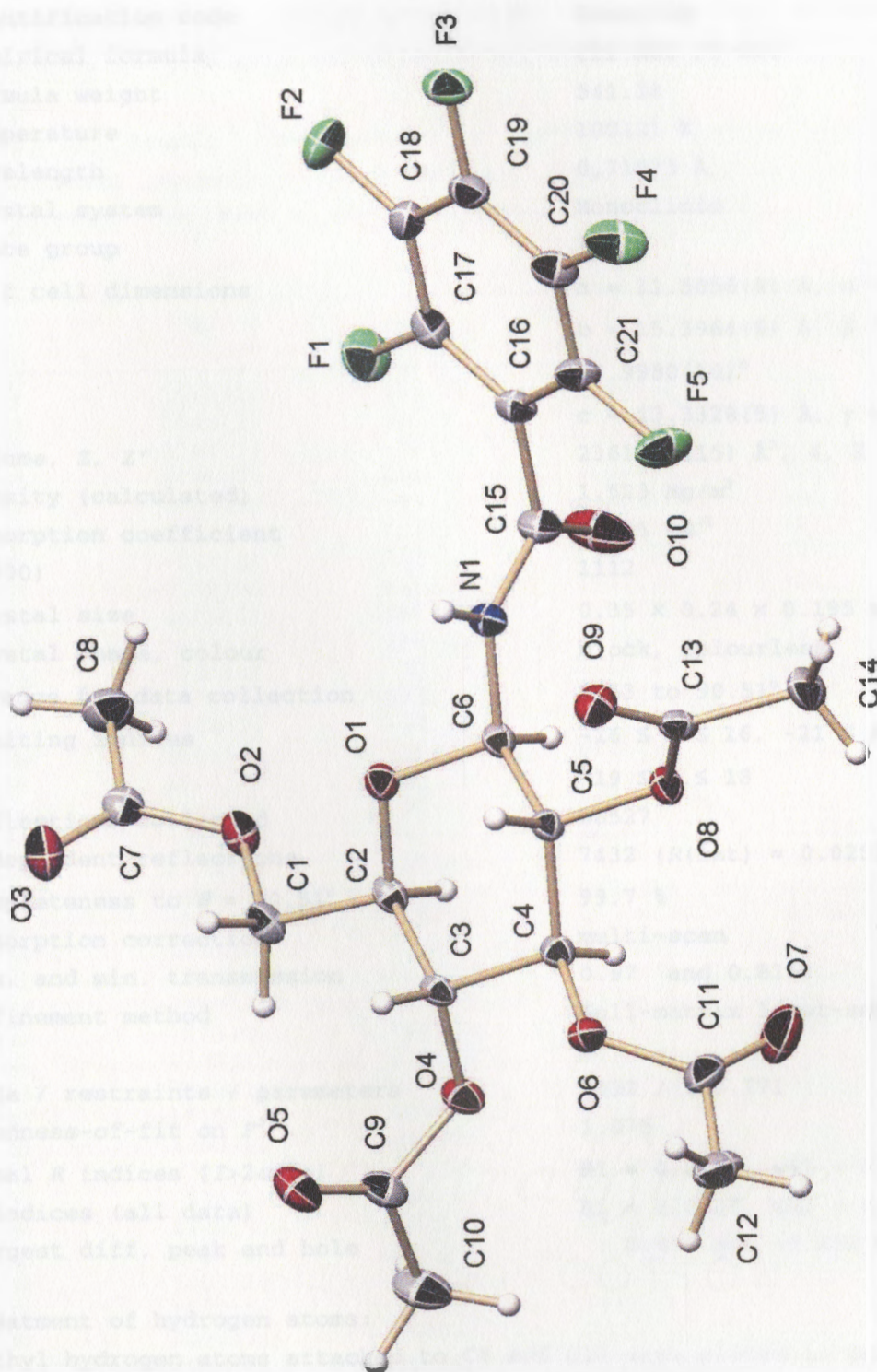


Figure 167: X-ray crystal structure of amide 6

Table 1. Crystal data and structure refinement for 04mz155m:

Identification code	04mz155m
Empirical formula	C <sub>21</sub> H <sub>20</sub> F <sub>5</sub> O <sub>10</sub>
Formula weight	541.38
Temperature	100(2) K
Wavelength	0.71073 Å
Crystal system	Monoclinic
Space group	P2 <sub>1</sub>
Unit cell dimensions	a = 11.5056(4) Å, $\alpha$ = 90° b = 15.3964(6) Å, $\beta$ = 90.9980(10)° c = 13.3328(5) Å, $\gamma$ = 90°
Volume, Z, Z'	2361.48(15) Å <sup>3</sup> , 4, 2
Density (calculated)	1.523 Mg/m <sup>3</sup>
Absorption coefficient	0.145 mm <sup>-1</sup>
F(000)	1112
Crystal size	0.35 × 0.24 × 0.195 mm
Crystal shape, colour	block, colourless
$\theta$ range for data collection	1.53 to 30.51°
Limiting indices	-16 ≤ h ≤ 16, -21 ≤ k ≤ 21, -19 ≤ l ≤ 18
Reflections collected	28527
Independent reflections	7432 (R(int) = 0.0252)
Completeness to $\theta$ = 30.51°	99.7 %
Absorption correction	multi-scan
Max. and min. transmission	0.97 and 0.8153
Refinement method	Full-matrix least-squares on F <sup>2</sup>
Data / restraints / parameters	7432 / 1 / 771
Goodness-of-fit on F <sup>2</sup>	1.075
Final R indices [I > 2 $\sigma$ (I)]	R1 = 0.0420, wR2 = 0.1020
R indices (all data)	R1 = 0.0438, wR2 = 0.1034
Largest diff. peak and hole	0.416 and -0.232 e × Å <sup>-3</sup>

## Treatment of hydrogen atoms:

Methyl hydrogen atoms attached to C8 and C10 were placed in calculated positions. All other hydrogen atoms were located in the difference density Fourier map. Methyl hydrogen atoms were refined with an isotropic displacement parameter 1.5 times, all others with one 1.2 times that of the adjacent carbon or nitrogen atom.



Refinement of  $F^2$  against ALL reflections. The weighted R-factor  $wR$  and goodness of fit are based on  $F^2$ , conventional R-factors  $R$  are based on  $F$ , with  $F$  set to zero for negative  $F^2$ . The threshold expression of  $F^2 > 2\sigma(F^2)$  is used only for calculating R-factors.

Table 2. Atomic coordinates [ $\times 10^4$ ] and equivalent isotropic displacement parameters [ $\text{\AA}^2 \times 10^3$ ] for 04mz155m.  $U(\text{eq})$  is defined as one third of the trace of the orthogonalized  $U_{ij}$  tensor.

	x	y	z	U(eq)
C(1)	1743(2)	116(1)	1752(2)	20(1)
C(2)	2549(2)	398(1)	2598(1)	17(1)
C(3)	3745(2)	-32(1)	2560(1)	16(1)
C(4)	4469(2)	211(1)	3482(1)	16(1)
C(5)	3782(2)	55(1)	4432(1)	15(1)
C(6)	2615(2)	527(1)	4348(1)	16(1)
C(7)	-278(2)	306(1)	1467(1)	21(1)
C(8)	-1279(2)	918(2)	1583(2)	31(1)
C(9)	4432(2)	-191(2)	888(2)	23(1)
C(10)	5037(3)	298(2)	70(2)	34(1)
C(11)	6523(2)	77(2)	3716(2)	25(1)
C(12)	7516(2)	-534(2)	3576(2)	30(1)
C(13)	4478(2)	-53(1)	6117(1)	17(1)
C(14)	5163(2)	425(2)	6901(2)	25(1)
C(15)	1506(2)	1082(1)	5743(2)	21(1)
C(16)	809(2)	798(1)	6644(1)	18(1)
C(17)	-386(2)	804(1)	6616(2)	22(1)
C(18)	-1022(2)	523(2)	7427(2)	23(1)
C(19)	-456(2)	230(1)	8286(2)	22(1)
C(20)	741(2)	218(1)	8330(2)	22(1)
C(21)	1353(2)	513(1)	7515(2)	21(1)
F(1)	-961(1)	1063(1)	5788(1)	34(1)
F(2)	-2185(1)	536(1)	7396(1)	36(1)
F(3)	-1072(1)	-19(1)	9069(1)	30(1)
F(4)	1302(1)	-57(1)	9155(1)	34(1)
F(5)	2522(1)	511(1)	7581(1)	32(1)
N(1)	1935(1)	403(1)	5224(1)	17(1)
O(1)	1988(1)	179(1)	3507(1)	17(1)
O(2)	725(1)	659(1)	1809(1)	21(1)
O(3)	-326(2)	-416(1)	1129(1)	29(1)
O(4)	4342(1)	321(1)	1710(1)	21(1)
O(5)	4058(2)	-916(1)	838(1)	29(1)
O(6)	5487(1)	-322(1)	3484(1)	19(1)
O(7)	6582(2)	819(1)	3969(2)	38(1)
O(8)	4432(1)	419(1)	5255(1)	18(1)
O(9)	4021(1)	-746(1)	6210(1)	22(1)
O(10)	1642(2)	1843(1)	5543(2)	40(1)
C(31)	956(2)	3122(1)	3435(2)	18(1)
C(32)	1620(2)	2807(1)	2540(1)	16(1)
C(33)	2880(2)	3130(1)	2559(1)	15(1)

C(34)	3501(2)	2888(1)	1596(1)	16(1)
C(35)	2770(2)	3142(1)	681(1)	16(1)
C(36)	1549(2)	2775(1)	779(1)	16(1)
C(37)	-1076(2)	3110(1)	3705(1)	19(1)
C(38)	-2131(2)	2546(2)	3734(2)	24(1)
C(39)	3760(2)	3203(1)	4197(1)	18(1)
C(40)	4470(2)	2691(2)	4945(2)	25(1)
C(41)	5584(2)	2875(2)	1544(2)	26(1)
C(42)	6621(2)	3455(2)	1477(2)	25(1)
C(43)	3421(2)	3252(1)	-1007(1)	20(1)
C(44)	3949(2)	2733(2)	-1831(2)	29(1)
C(45)	185(2)	2349(1)	-522(1)	18(1)
C(46)	-486(2)	2615(1)	-1458(1)	19(1)
C(47)	52(2)	2914(1)	-2306(1)	19(1)
C(48)	-552(2)	3095(1)	-3188(2)	23(1)
C(49)	-1738(2)	2960(2)	-3222(2)	25(1)
C(50)	-2302(2)	2650(2)	-2392(2)	25(1)
C(51)	-1686(2)	2483(1)	-1512(2)	22(1)
F(6)	1210(1)	3017(1)	-2295(1)	26(1)
F(7)	-10(1)	3396(1)	-3992(1)	33(1)
F(8)	-2344(1)	3124(1)	-4062(1)	35(1)
F(9)	-3449(1)	2511(1)	-2449(1)	37(1)
F(10)	-2254(1)	2188(1)	-722(1)	32(1)
N(2)	824(2)	2984(1)	-74(1)	18(1)
O(11)	1044(1)	3133(1)	1657(1)	17(1)
O(12)	-139(1)	2662(1)	3433(1)	20(1)
O(13)	-1042(1)	3871(1)	3910(1)	28(1)
O(14)	3517(1)	2708(1)	3363(1)	17(1)
O(15)	3406(1)	3927(1)	4299(1)	23(1)
O(16)	4581(1)	3355(1)	1565(1)	18(1)
O(17)	5599(2)	2107(1)	1575(3)	59(1)
O(18)	3305(1)	2747(1)	-174(1)	20(1)
O(19)	3129(1)	3994(1)	-1050(1)	26(1)
O(20)	138(2)	1603(1)	-232(1)	26(1)

---

All esds (except the esd in the dihedral angle between two l.s. planes) are estimated using the full covariance matrix. The cell esds are taken into account individually in the estimation of esds in distances, angles and torsion angles; correlations between esds in cell parameters are only used when they are defined by crystal symmetry. An approximate (isotropic) treatment of cell esds is used for estimating esds involving l.s. planes.

Table 3. Bond lengths [Å] and angles [deg] for 04mz155m.

C(1)-O(2)	1.442(2)	C(18)-C(19)	1.383(3)
C(1)-C(2)	1.512(3)	C(19)-F(3)	1.328(2)
C(1)-H(1A)	1.02(3)	C(19)-C(20)	1.378(3)
C(1)-H(1B)	0.94(3)	C(20)-F(4)	1.335(2)
C(2)-O(1)	1.424(2)	C(20)-C(21)	1.381(3)
C(2)-C(3)	1.529(3)	C(21)-F(5)	1.347(2)
C(2)-H(2)	0.95(3)	N(1)-H(1)	0.86(3)
C(3)-O(4)	1.440(2)	C(31)-O(12)	1.445(2)
C(3)-C(4)	1.520(3)	C(31)-C(32)	1.507(3)
C(3)-H(3)	0.91(3)	C(31)-H(31A)	0.95(3)
C(4)-O(6)	1.430(2)	C(31)-H(31B)	0.93(3)
C(4)-C(5)	1.523(2)	C(32)-O(11)	1.432(2)
C(4)-H(4)	0.90(3)	C(32)-C(33)	1.534(3)
C(5)-O(8)	1.432(2)	C(32)-H(32)	0.86(3)
C(5)-C(6)	1.530(3)	C(33)-O(14)	1.442(2)
C(5)-H(5)	0.92(3)	C(33)-C(34)	1.526(2)
C(6)-O(1)	1.426(2)	C(33)-H(33)	0.96(3)
C(6)-N(1)	1.430(2)	C(34)-O(16)	1.436(2)
C(6)-H(6)	0.91(3)	C(34)-C(35)	1.522(3)
C(7)-O(3)	1.200(3)	C(34)-H(34)	0.96(3)
C(7)-O(2)	1.348(3)	C(35)-O(18)	1.440(2)
C(7)-C(8)	1.498(3)	C(35)-C(36)	1.522(3)
C(8)-H(8A)	0.9800	C(35)-H(35)	0.96(3)
C(8)-H(8B)	0.9800	C(36)-O(11)	1.426(2)
C(8)-H(8C)	0.9800	C(36)-N(2)	1.435(2)
C(9)-O(5)	1.198(3)	C(36)-H(36)	0.93(3)
C(9)-O(4)	1.356(2)	C(37)-O(13)	1.203(3)
C(9)-C(10)	1.506(3)	C(37)-O(12)	1.336(2)
C(10)-H(10A)	0.9800	C(37)-C(38)	1.494(3)
C(10)-H(10B)	0.9800	C(38)-H(38A)	0.97(3)
C(10)-H(10C)	0.9800	C(38)-H(38B)	0.91(4)
C(11)-O(7)	1.193(3)	C(38)-H(38C)	0.93(4)
C(11)-O(6)	1.371(2)	C(39)-O(15)	1.196(3)
C(11)-C(12)	1.494(3)	C(39)-O(14)	1.372(2)
C(12)-H(12A)	0.90(4)	C(39)-C(40)	1.502(3)
C(12)-H(12B)	0.93(4)	C(40)-H(40A)	0.90(4)
C(12)-H(12C)	0.95(4)	C(40)-H(40B)	0.93(4)
C(13)-O(9)	1.197(3)	C(40)-H(40C)	0.85(4)
C(13)-O(8)	1.361(2)	C(41)-O(17)	1.184(3)
C(13)-C(14)	1.493(3)	C(41)-O(16)	1.371(3)
C(14)-H(14A)	0.97(4)	C(41)-C(42)	1.494(3)
C(14)-H(14B)	0.91(4)	C(42)-H(42A)	0.97(4)
C(14)-H(14C)	0.94(4)	C(42)-H(42B)	0.90(4)
C(15)-O(10)	1.212(3)	C(42)-H(42C)	0.92(4)
C(15)-N(1)	1.351(3)	C(43)-O(19)	1.192(3)
C(15)-C(16)	1.520(3)	C(43)-O(18)	1.364(2)
C(16)-C(17)	1.375(3)	C(43)-C(44)	1.496(3)
C(16)-C(21)	1.381(3)	C(44)-H(44A)	0.91(4)
C(17)-F(1)	1.338(2)	C(44)-H(44B)	0.89(4)
C(17)-C(18)	1.386(3)	C(44)-H(44C)	0.96(4)
C(18)-F(2)	1.338(2)	C(45)-O(20)	1.213(3)



C(45)-N(2)	1.355(3)	C(7)-C(8)-H(8A)	109.5
C(45)-C(46)	1.512(3)	C(7)-C(8)-H(8B)	109.5
C(46)-C(47)	1.377(3)	H(8A)-C(8)-H(8B)	109.5
C(46)-C(51)	1.396(3)	C(7)-C(8)-H(8C)	109.5
C(47)-F(6)	1.342(2)	H(8A)-C(8)-H(8C)	109.5
C(47)-C(48)	1.384(3)	H(8B)-C(8)-H(8C)	109.5
C(48)-F(7)	1.333(3)	O(5)-C(9)-O(4)	123.67(19)
C(48)-C(49)	1.381(3)	O(5)-C(9)-C(10)	126.6(2)
C(49)-F(8)	1.334(2)	O(4)-C(9)-C(10)	109.75(19)
C(49)-C(50)	1.377(3)	C(9)-C(10)-H(10A)	109.5
C(50)-F(9)	1.338(2)	C(9)-C(10)-H(10B)	109.5
C(50)-C(51)	1.384(3)	H(10A)-C(10)-H(10B)	109.5
C(51)-F(10)	1.330(3)	C(9)-C(10)-H(10C)	109.5
N(2)-H(2A)	0.78(3)	H(10A)-C(10)-H(10C)	109.5
		H(10B)-C(10)-H(10C)	109.5
O(2)-C(1)-C(2)	106.37(15)	O(7)-C(11)-O(6)	122.5(2)
O(2)-C(1)-H(1A)	109.3(17)	O(7)-C(11)-C(12)	126.7(2)
C(2)-C(1)-H(1A)	110.6(17)	O(6)-C(11)-C(12)	110.7(2)
O(2)-C(1)-H(1B)	112.4(18)	C(11)-C(12)-H(12A)	111(2)
C(2)-C(1)-H(1B)	110.7(18)	C(11)-C(12)-H(12B)	109(2)
H(1A)-C(1)-H(1B)	107(3)	H(12A)-C(12)-H(12B)	109(3)
O(1)-C(2)-C(1)	106.64(16)	C(11)-C(12)-H(12C)	112(2)
O(1)-C(2)-C(3)	110.32(14)	H(12A)-C(12)-H(12C)	104(3)
C(1)-C(2)-C(3)	113.05(16)	H(12B)-C(12)-H(12C)	111(3)
O(1)-C(2)-H(2)	110.9(18)	O(9)-C(13)-O(8)	123.57(17)
C(1)-C(2)-H(2)	109.5(17)	O(9)-C(13)-C(14)	126.52(19)
C(3)-C(2)-H(2)	106.4(17)	O(8)-C(13)-C(14)	109.90(17)
O(4)-C(3)-C(4)	106.35(15)	C(13)-C(14)-H(14A)	110(2)
O(4)-C(3)-C(2)	107.75(15)	C(13)-C(14)-H(14B)	111(2)
C(4)-C(3)-C(2)	110.33(15)	H(14A)-C(14)-H(14B)	108(3)
O(4)-C(3)-H(3)	113.2(18)	C(13)-C(14)-H(14C)	114(2)
C(4)-C(3)-H(3)	110.7(18)	H(14A)-C(14)-H(14C)	105(3)
C(2)-C(3)-H(3)	108.4(18)	H(14B)-C(14)-H(14C)	109(3)
O(6)-C(4)-C(3)	107.35(15)	O(10)-C(15)-N(1)	125.82(19)
O(6)-C(4)-C(5)	110.16(15)	O(10)-C(15)-C(16)	121.57(19)
C(3)-C(4)-C(5)	110.41(15)	N(1)-C(15)-C(16)	112.61(17)
O(6)-C(4)-H(4)	109.5(18)	C(17)-C(16)-C(21)	117.61(18)
C(3)-C(4)-H(4)	108.2(18)	C(17)-C(16)-C(15)	121.20(18)
C(5)-C(4)-H(4)	111.1(18)	C(21)-C(16)-C(15)	121.19(18)
O(8)-C(5)-C(4)	107.65(14)	F(1)-C(17)-C(16)	120.31(19)
O(8)-C(5)-C(6)	108.43(14)	F(1)-C(17)-C(18)	118.51(19)
C(4)-C(5)-C(6)	109.40(14)	C(16)-C(17)-C(18)	121.16(19)
O(8)-C(5)-H(5)	111.4(17)	F(2)-C(18)-C(19)	119.12(19)
C(4)-C(5)-H(5)	114.4(17)	F(2)-C(18)-C(17)	120.8(2)
C(6)-C(5)-H(5)	105.4(17)	C(19)-C(18)-C(17)	120.10(18)
O(1)-C(6)-N(1)	108.41(15)	F(3)-C(19)-C(20)	120.7(2)
O(1)-C(6)-C(5)	108.02(15)	F(3)-C(19)-C(18)	119.65(19)
N(1)-C(6)-C(5)	111.63(15)	C(20)-C(19)-C(18)	119.66(19)
O(1)-C(6)-H(6)	112.1(18)	F(4)-C(20)-C(19)	120.46(19)
N(1)-C(6)-H(6)	107.1(18)	F(4)-C(20)-C(21)	120.50(19)
C(5)-C(6)-H(6)	109.6(18)	C(19)-C(20)-C(21)	119.02(19)
O(3)-C(7)-O(2)	122.3(2)	F(5)-C(21)-C(16)	119.57(18)
O(3)-C(7)-C(8)	126.2(2)	F(5)-C(21)-C(20)	118.00(18)
O(2)-C(7)-C(8)	111.46(19)	C(16)-C(21)-C(20)	122.43(19)

C(15)-N(1)-C(6)	121.64(17)	O(15)-C(39)-C(40)	126.62(18)
C(15)-N(1)-H(1)	122.6(19)	O(14)-C(39)-C(40)	110.30(17)
C(6)-N(1)-H(1)	115.7(19)	C(39)-C(40)-H(40A)	109(2)
C(2)-O(1)-C(6)	110.45(14)	C(39)-C(40)-H(40B)	111(2)
C(7)-O(2)-C(1)	116.03(16)	H(40A)-C(40)-H(40B)	110(3)
C(9)-O(4)-C(3)	117.43(16)	C(39)-C(40)-H(40C)	107(2)
C(11)-O(6)-C(4)	116.87(16)	H(40A)-C(40)-H(40C)	108(3)
C(13)-O(8)-C(5)	116.75(14)	H(40B)-C(40)-H(40C)	112(3)
O(12)-C(31)-C(32)	107.14(15)	O(17)-C(41)-O(16)	123.3(2)
O(12)-C(31)-H(31A)	108.4(17)	O(17)-C(41)-C(42)	126.0(2)
C(32)-C(31)-H(31A)	110.6(17)	O(16)-C(41)-C(42)	110.6(2)
O(12)-C(31)-H(31B)	108.5(17)	C(41)-C(42)-H(42A)	107(2)
C(32)-C(31)-H(31B)	110.3(18)	C(41)-C(42)-H(42B)	112(2)
H(31A)-C(31)-H(31B)	112(3)	H(42A)-C(42)-H(42B)	105(3)
O(11)-C(32)-C(31)	107.73(15)	C(41)-C(42)-H(42C)	113(2)
O(11)-C(32)-C(33)	108.82(14)	H(42A)-C(42)-H(42C)	114(3)
C(31)-C(32)-C(33)	111.99(15)	H(42B)-C(42)-H(42C)	106(3)
O(11)-C(32)-H(32)	109.1(19)	O(19)-C(43)-O(18)	123.63(18)
C(31)-C(32)-H(32)	116.0(18)	O(19)-C(43)-C(44)	126.5(2)
C(33)-C(32)-H(32)	102.9(19)	O(18)-C(43)-C(44)	109.89(19)
O(14)-C(33)-C(34)	106.04(14)	C(43)-C(44)-H(44A)	104(2)
O(14)-C(33)-C(32)	109.52(14)	C(43)-C(44)-H(44B)	110(2)
C(34)-C(33)-C(32)	111.32(14)	H(44A)-C(44)-H(44B)	104(3)
O(14)-C(33)-H(33)	109.8(17)	C(43)-C(44)-H(44C)	113(2)
C(34)-C(33)-H(33)	109.2(16)	H(44A)-C(44)-H(44C)	114(3)
C(32)-C(33)-H(33)	110.9(17)	H(44B)-C(44)-H(44C)	112(3)
O(16)-C(34)-C(35)	108.34(15)	O(20)-C(45)-N(2)	124.70(19)
O(16)-C(34)-C(33)	108.64(15)	O(20)-C(45)-C(46)	119.60(18)
C(35)-C(34)-C(33)	110.60(15)	N(2)-C(45)-C(46)	115.70(17)
O(16)-C(34)-H(34)	109.2(17)	C(47)-C(46)-C(51)	117.64(18)
C(35)-C(34)-H(34)	109.2(16)	C(47)-C(46)-C(45)	122.52(17)
C(33)-C(34)-H(34)	110.8(16)	C(51)-C(46)-C(45)	119.58(18)
O(18)-C(35)-C(34)	106.75(15)	F(6)-C(47)-C(46)	119.42(17)
O(18)-C(35)-C(36)	108.62(15)	F(6)-C(47)-C(48)	117.94(18)
C(34)-C(35)-C(36)	109.50(15)	C(46)-C(47)-C(48)	122.62(19)
O(18)-C(35)-H(35)	109.9(17)	F(7)-C(48)-C(49)	120.16(18)
C(34)-C(35)-H(35)	109.2(17)	F(7)-C(48)-C(47)	121.24(19)
C(36)-C(35)-H(35)	112.7(16)	C(49)-C(48)-C(47)	118.6(2)
O(11)-C(36)-N(2)	108.92(15)	F(8)-C(49)-C(50)	119.6(2)
O(11)-C(36)-C(35)	108.46(14)	F(8)-C(49)-C(48)	120.1(2)
N(2)-C(36)-C(35)	111.93(15)	C(50)-C(49)-C(48)	120.33(19)
O(11)-C(36)-H(36)	111.7(18)	F(9)-C(50)-C(49)	119.2(2)
N(2)-C(36)-H(36)	107.5(17)	F(9)-C(50)-C(51)	120.6(2)
C(35)-C(36)-H(36)	108.3(18)	C(49)-C(50)-C(51)	120.25(19)
O(13)-C(37)-O(12)	122.81(19)	F(10)-C(51)-C(50)	118.90(19)
O(13)-C(37)-C(38)	125.69(19)	F(10)-C(51)-C(46)	120.54(19)
O(12)-C(37)-C(38)	111.49(17)	C(50)-C(51)-C(46)	120.6(2)
C(37)-C(38)-H(38A)	107(2)	C(45)-N(2)-C(36)	119.39(17)
C(37)-C(38)-H(38B)	111(2)	C(45)-N(2)-H(2A)	120(2)
H(38A)-C(38)-H(38B)	111(3)	C(36)-N(2)-H(2A)	120(2)
C(37)-C(38)-H(38C)	111(2)	C(36)-O(11)-C(32)	110.52(13)
H(38A)-C(38)-H(38C)	109(3)	C(37)-O(12)-C(31)	117.01(16)
H(38B)-C(38)-H(38C)	108(3)	C(39)-O(14)-C(33)	116.47(15)
O(15)-C(39)-O(14)	123.03(18)	C(41)-O(16)-C(34)	117.35(16)
		C(43)-O(18)-C(35)	116.90(15)

Table 4. Anisotropic displacement parameters [ $\text{\AA}^2 \times 10^3$ ] for 04mz155m. The anisotropic displacement factor exponent takes the form:  $-2 \pi^2 [(h a^*)^2 U_{11} + \dots + 2 h k a^* b^* U_{12}]$

	U11	U22	U33	U23	U13	U12
C(1)	24(1)	19(1)	17(1)	-2(1)	-6(1)	6(1)
C(2)	23(1)	15(1)	13(1)	0(1)	-2(1)	1(1)
C(3)	21(1)	15(1)	11(1)	1(1)	3(1)	-1(1)
C(4)	18(1)	15(1)	14(1)	0(1)	1(1)	-1(1)
C(5)	17(1)	16(1)	12(1)	0(1)	1(1)	-1(1)
C(6)	19(1)	16(1)	13(1)	1(1)	-1(1)	-1(1)
C(7)	24(1)	24(1)	16(1)	4(1)	0(1)	-1(1)
C(8)	25(1)	35(1)	34(1)	-3(1)	3(1)	6(1)
C(9)	29(1)	27(1)	13(1)	-1(1)	1(1)	5(1)
C(10)	50(1)	35(1)	18(1)	4(1)	10(1)	3(1)
C(11)	20(1)	32(1)	22(1)	2(1)	4(1)	-6(1)
C(12)	19(1)	47(1)	24(1)	1(1)	4(1)	3(1)
C(13)	15(1)	24(1)	13(1)	-1(1)	1(1)	5(1)
C(14)	23(1)	34(1)	19(1)	-5(1)	-6(1)	1(1)
C(15)	24(1)	22(1)	17(1)	1(1)	4(1)	2(1)
C(16)	22(1)	16(1)	17(1)	-1(1)	5(1)	3(1)
C(17)	25(1)	21(1)	19(1)	-3(1)	-3(1)	2(1)
C(18)	17(1)	24(1)	27(1)	-7(1)	1(1)	-2(1)
C(19)	26(1)	19(1)	22(1)	-4(1)	7(1)	-3(1)
C(20)	25(1)	24(1)	18(1)	2(1)	2(1)	6(1)
C(21)	19(1)	25(1)	20(1)	0(1)	4(1)	6(1)
F(1)	33(1)	43(1)	24(1)	0(1)	-10(1)	4(1)
F(2)	17(1)	50(1)	42(1)	-7(1)	-1(1)	-7(1)
F(3)	37(1)	26(1)	27(1)	-3(1)	15(1)	-7(1)
F(4)	38(1)	45(1)	19(1)	9(1)	2(1)	14(1)
F(5)	18(1)	50(1)	29(1)	5(1)	4(1)	10(1)
N(1)	20(1)	14(1)	16(1)	1(1)	3(1)	1(1)
O(1)	18(1)	19(1)	13(1)	0(1)	-2(1)	-2(1)
O(2)	25(1)	17(1)	22(1)	-2(1)	-7(1)	3(1)
O(3)	31(1)	24(1)	33(1)	-3(1)	-8(1)	-4(1)
O(4)	30(1)	20(1)	14(1)	1(1)	5(1)	-2(1)
O(5)	41(1)	27(1)	20(1)	-5(1)	1(1)	1(1)
O(6)	17(1)	21(1)	18(1)	-1(1)	2(1)	1(1)
O(7)	27(1)	32(1)	54(1)	-2(1)	-1(1)	-11(1)
O(8)	21(1)	17(1)	14(1)	0(1)	-1(1)	-3(1)
O(9)	23(1)	25(1)	18(1)	6(1)	-1(1)	-2(1)
O(10)	67(1)	18(1)	35(1)	2(1)	24(1)	5(1)
C(31)	18(1)	17(1)	20(1)	-1(1)	4(1)	0(1)
C(32)	17(1)	14(1)	16(1)	1(1)	1(1)	2(1)
C(33)	18(1)	14(1)	13(1)	1(1)	0(1)	1(1)
C(34)	15(1)	17(1)	14(1)	1(1)	0(1)	0(1)
C(35)	17(1)	18(1)	14(1)	-1(1)	1(1)	1(1)
C(36)	18(1)	15(1)	15(1)	1(1)	-1(1)	1(1)
C(37)	19(1)	21(1)	16(1)	1(1)	3(1)	2(1)
C(38)	22(1)	24(1)	26(1)	-2(1)	4(1)	-2(1)
C(39)	18(1)	23(1)	12(1)	1(1)	0(1)	-7(1)
C(40)	29(1)	26(1)	18(1)	3(1)	-7(1)	-4(1)
C(41)	18(1)	32(1)	29(1)	-3(1)	0(1)	1(1)
C(42)	16(1)	39(1)	19(1)	3(1)	-1(1)	-5(1)



C(43)	16(1)	29(1)	15(1)	-2(1)	2(1)	-2(1)
C(44)	26(1)	40(1)	20(1)	-5(1)	8(1)	3(1)
C(45)	19(1)	21(1)	14(1)	-2(1)	0(1)	-2(1)
C(46)	18(1)	21(1)	18(1)	-2(1)	-3(1)	-1(1)
C(47)	19(1)	22(1)	18(1)	-2(1)	-3(1)	-1(1)
C(48)	26(1)	24(1)	18(1)	-2(1)	-3(1)	3(1)
C(49)	25(1)	23(1)	26(1)	-8(1)	-11(1)	7(1)
C(50)	17(1)	25(1)	33(1)	-9(1)	-7(1)	3(1)
C(51)	19(1)	21(1)	25(1)	-4(1)	-1(1)	0(1)
F(6)	17(1)	39(1)	22(1)	3(1)	-1(1)	-4(1)
F(7)	38(1)	43(1)	17(1)	5(1)	-1(1)	4(1)
F(8)	38(1)	37(1)	28(1)	-7(1)	-18(1)	12(1)
F(9)	17(1)	44(1)	50(1)	-9(1)	-8(1)	1(1)
F(10)	23(1)	41(1)	34(1)	3(1)	6(1)	-6(1)
N(2)	21(1)	16(1)	19(1)	1(1)	-5(1)	-1(1)
O(11)	16(1)	18(1)	15(1)	1(1)	0(1)	3(1)
O(12)	17(1)	17(1)	28(1)	-2(1)	6(1)	-1(1)
O(13)	25(1)	20(1)	39(1)	-3(1)	10(1)	1(1)
O(14)	20(1)	17(1)	14(1)	0(1)	-3(1)	0(1)
O(15)	27(1)	21(1)	20(1)	-4(1)	1(1)	-2(1)
O(16)	15(1)	20(1)	19(1)	1(1)	1(1)	-2(1)
O(17)	23(1)	25(1)	129(2)	-4(1)	2(1)	5(1)
O(18)	22(1)	21(1)	15(1)	-2(1)	3(1)	2(1)
O(19)	28(1)	29(1)	21(1)	5(1)	4(1)	0(1)
O(20)	37(1)	20(1)	22(1)	2(1)	-6(1)	-8(1)

Table 5. Hydrogen coordinates ( $\times 10^4$ ) and isotropic displacement parameters ( $\text{\AA}^2 \times 10^3$ ) for 04mz155m.

	x	y	z	U(eq)
H(1A)	2130(30)	210(20)	1070(20)	24
H(1B)	1560(30)	-480(20)	1810(20)	24
H(2)	2680(20)	1000(20)	2560(20)	20
H(3)	3640(20)	-620(20)	2520(20)	19
H(4)	4670(20)	770(19)	3430(20)	19
H(5)	3600(20)	-521(19)	4550(20)	18
H(6)	2740(20)	1110(20)	4290(20)	19
H(8A)	-1956	696	1207	47
H(8B)	-1067	1491	1324	47
H(8C)	-1469	966	2295	47
H(10A)	5246	-105	-466	51
H(10B)	5742	572	345	51
H(10C)	4516	747	-203	51
H(12A)	7680(30)	-600(30)	2920(30)	45
H(12B)	7330(30)	-1070(30)	3840(30)	45
H(12C)	8220(30)	-320(30)	3860(30)	45
H(14A)	4750(30)	940(20)	7100(30)	38
H(14B)	5870(30)	590(20)	6670(30)	38

H(14C)	5280(30)	110(20)	7500(30)	38
H(1)	1790(20)	-130(20)	5380(20)	20
H(31A)	1370(20)	2990(20)	4040(20)	22
H(31B)	800(20)	3720(20)	3380(20)	22
H(32)	1700(20)	2250(20)	2490(20)	19
H(33)	2910(20)	3750(19)	2650(20)	18
H(34)	3660(20)	2274(19)	1570(20)	19
H(35)	2780(20)	3765(19)	610(20)	20
H(36)	1600(20)	2170(20)	810(20)	19
H(38A)	-2790(30)	2920(20)	3890(20)	36
H(38B)	-2040(30)	2120(20)	4200(30)	36
H(38C)	-2260(30)	2280(20)	3110(30)	36
H(40A)	4760(30)	3060(20)	5410(30)	37
H(40B)	5070(30)	2400(20)	4630(30)	37
H(40C)	4010(30)	2340(30)	5230(30)	37
H(42A)	7310(30)	3090(20)	1480(30)	37
H(42B)	6700(30)	3800(20)	2020(30)	37
H(42C)	6580(30)	3830(20)	940(30)	37
H(44A)	3390(30)	2340(30)	-2010(30)	43
H(44B)	4520(30)	2410(30)	-1590(30)	43
H(44C)	4200(30)	3090(20)	-2380(30)	43
H(2A)	780(20)	3460(20)	-270(20)	22

Table 6. Hydrogen bonds for 04mz155m [ $\text{\AA}$  and deg].

D-H...A	d(D-H)	d(H...A)	d(D...A)	$\angle$ (DHA)
N(2)-H(2A)...O(3)#1	0.78(3)	2.13(3)	2.889(2)	162(3)
N(1)-H(1)...O(13)#2	0.86(3)	2.01(3)	2.827(2)	158(3)

Symmetry transformations used to generate equivalent atoms:

#1  $-x, y+1/2, -z$     #2  $-x, y-1/2, -z+1$





Table 1. Crystal data and structure refinement for 04mz145m:

Identification code	04mz145m
Empirical formula	C <sub>19</sub> H <sub>23</sub> N <sub>1</sub> O <sub>10</sub> S <sub>1</sub>
Formula weight	457.44
Temperature	100(2) K
Wavelength	0.71073 Å
Crystal system	Monoclinic
Space group	C2
Unit cell dimensions	a = 16.247(3) Å, α = 90° b = 14.105(3) Å, β = 124.950(3)° c = 11.182(2) Å, γ = 90°
Volume, Z	2100.4(7) Å <sup>3</sup> , 4
Density (calculated)	1.447 Mg/m <sup>3</sup>
Absorption coefficient	0.211 mm <sup>-1</sup>
F(000)	960
Crystal size	0.44 × 0.39 × 0.36 mm
Crystal shape, colour	block, colourless
θ range for data collection	2.10 to 30.50°
Limiting indices	-22 ≤ h ≤ 23, -20 ≤ k ≤ 20, -15 ≤ l ≤ 15
Reflections collected	12648
Independent reflections	6292 (R(int) = 0.0157)
Completeness to θ = 30.50°	99.9 %
Absorption correction	multi-scan
Max. and min. transmission	0.93 and 0.7448
Refinement method	Full-matrix least-squares on F <sup>2</sup>
Data / restraints / parameters	6292 / 1 / 284
Goodness-of-fit on F <sup>2</sup>	1.034
Final R indices [I > 2σ(I)]	R1 = 0.0322, wR2 = 0.0848
R indices (all data)	R1 = 0.0326, wR2 = 0.0852
Absolute structure parameter	-0.01(4)
Number of Friedel Pairs	2964
Largest diff. peak and hole	0.413 and -0.292 e × Å <sup>-3</sup>

## Treatment of hydrogen atoms:

All hydrogen atoms were placed in calculated positions and were refined with an isotropic displacement parameter 1.5 (methyl) or 1.2 times (all others) that of the adjacent non hydrogen atom.

Refinement of  $F^2$  against ALL reflections. The weighted R-factor  $wR$  and goodness of fit are based on  $F^2$ , conventional R-factors  $R$  are based on  $F$ , with  $F$  set to zero for negative  $F^2$ . The threshold expression of  $F^2 > 2\sigma(F^2)$  is used only for calculating R-factors.

Table 2. Atomic coordinates [ $\times 10^4$ ] and equivalent isotropic displacement parameters [ $\text{\AA}^2 \times 10^3$ ] for 04mz145m.  $U(\text{eq})$  is defined as one third of the trace of the orthogonalized  $U_{ij}$  tensor.

	x	y	z	U(eq)
S(1)	8545(1)	5203(1)	4047(1)	21(1)
O(1)	10175(1)	1713(1)	6882(1)	15(1)
O(7)	10535(1)	-537(1)	8697(1)	16(1)
O(3)	7658(1)	780(1)	4378(1)	15(1)
N(1)	8884(1)	2432(1)	4739(1)	15(1)
O(9)	11599(1)	2241(1)	9820(1)	18(1)
O(5)	8944(1)	-861(1)	5432(1)	15(1)
O(2)	8642(1)	3644(1)	5849(1)	20(1)
O(6)	8682(1)	-1760(1)	6858(1)	22(1)
C(1)	9102(1)	1758(1)	5842(1)	13(1)
C(3)	9130(1)	-25(1)	6286(1)	14(1)
C(4)	10249(1)	82(1)	7489(1)	14(1)
C(8)	8692(1)	4027(1)	3833(1)	15(1)
O(10)	11365(1)	1720(1)	11512(1)	26(1)
O(8)	11053(1)	-1661(1)	7828(1)	26(1)
O(4)	7458(1)	570(1)	2228(1)	30(1)
C(7)	8732(1)	3367(1)	4891(1)	14(1)
C(5)	10432(1)	1094(1)	8069(1)	14(1)
C(6)	11511(1)	1283(1)	9308(1)	18(1)
C(18)	11479(1)	2367(1)	10914(1)	18(1)
C(10)	8752(1)	4753(1)	2013(1)	19(1)
C(16)	10940(1)	-1389(1)	8744(1)	18(1)
C(12)	7105(1)	684(1)	2914(1)	17(1)
C(9)	8798(1)	3883(1)	2707(1)	18(1)
C(14)	8743(1)	-1683(1)	5840(1)	17(1)
C(2)	8734(1)	777(1)	5167(1)	13(1)
C(11)	8628(1)	5520(1)	2651(1)	21(1)
C(19)	11507(1)	3395(1)	11254(2)	25(1)
C(15)	8645(1)	-2477(1)	4872(1)	23(1)
C(13)	6008(1)	738(1)	2285(1)	23(1)
C(17)	11212(1)	-1937(1)	10071(1)	25(1)

All esds (except the esd in the dihedral angle between two l.s. planes) are estimated using the full covariance matrix. The cell esds are taken into account individually in the estimation of esds in distances, angles and torsion angles; correlations between esds in cell parameters are only used when they are defined by crystal symmetry. An

approximate (isotropic) treatment of cell esds is used for estimating esds involving l.s. planes.

Table 3. Bond lengths [Å] and angles [deg] for 04mz145m.

S(1)-C(11)	1.7025(13)	C(2)-H(2)	1.0000
S(1)-C(8)	1.7119(12)	C(11)-H(11)	0.9500
O(1)-C(5)	1.4366(13)	C(19)-H(19A)	0.9800
O(1)-C(1)	1.4403(12)	C(19)-H(19B)	0.9800
O(7)-C(16)	1.3565(14)	C(19)-H(19C)	0.9800
O(7)-C(4)	1.4437(13)	C(15)-H(15A)	0.9800
O(3)-C(12)	1.3492(14)	C(15)-H(15B)	0.9800
O(3)-C(2)	1.4381(12)	C(15)-H(15C)	0.9800
N(1)-C(7)	1.3705(14)	C(13)-H(13A)	0.9800
N(1)-C(1)	1.4322(14)	C(13)-H(13B)	0.9800
N(1)-H(1B)	0.8800	C(13)-H(13C)	0.9800
O(9)-C(18)	1.3559(14)	C(17)-H(17A)	0.9800
O(9)-C(6)	1.4430(14)	C(17)-H(17B)	0.9800
O(5)-C(14)	1.3509(13)	C(17)-H(17C)	0.9800
O(5)-C(3)	1.4364(13)		
O(2)-C(7)	1.2256(14)	C(11)-S(1)-C(8)	92.06(6)
O(6)-C(14)	1.2035(15)	C(5)-O(1)-C(1)	110.43(8)
C(1)-C(2)	1.5236(15)	C(16)-O(7)-C(4)	117.49(9)
C(1)-H(1)	1.0000	C(12)-O(3)-C(2)	118.36(8)
C(3)-C(2)	1.5286(15)	C(7)-N(1)-C(1)	120.29(9)
C(3)-C(4)	1.5288(15)	C(7)-N(1)-H(1B)	119.9
C(3)-H(3)	1.0000	C(1)-N(1)-H(1B)	119.9
C(4)-C(5)	1.5248(15)	C(18)-O(9)-C(6)	116.58(9)
C(4)-H(4)	1.0000	C(14)-O(5)-C(3)	118.67(9)
C(8)-C(9)	1.3809(16)	N(1)-C(1)-O(1)	108.14(8)
C(8)-C(7)	1.4776(15)	N(1)-C(1)-C(2)	110.04(9)
O(10)-C(18)	1.2056(16)	O(1)-C(1)-C(2)	108.05(8)
O(8)-C(16)	1.2015(16)	N(1)-C(1)-H(1)	110.2
O(4)-C(12)	1.2040(15)	O(1)-C(1)-H(1)	110.2
C(5)-C(6)	1.5102(15)	C(2)-C(1)-H(1)	110.2
C(5)-H(5)	1.0000	O(5)-C(3)-C(2)	103.55(8)
C(6)-H(6A)	0.9900	O(5)-C(3)-C(4)	110.94(8)
C(6)-H(6B)	0.9900	C(2)-C(3)-C(4)	112.16(8)
C(18)-C(19)	1.4945(18)	O(5)-C(3)-H(3)	110.0
C(10)-C(11)	1.3731(17)	C(2)-C(3)-H(3)	110.0
C(10)-C(9)	1.4297(16)	C(4)-C(3)-H(3)	110.0
		O(7)-C(4)-C(5)	106.76(8)
C(10)-H(10)	0.9500	O(7)-C(4)-C(3)	110.28(8)
C(16)-C(17)	1.4969(16)	C(5)-C(4)-C(3)	108.10(8)
C(12)-C(13)	1.4965(16)	O(7)-C(4)-H(4)	110.5
C(9)-H(9)	0.9500	C(5)-C(4)-H(4)	110.5
C(14)-C(15)	1.5005(17)	C(3)-C(4)-H(4)	110.5



C(9)-C(8)-C(7)	131.84(10)	O(6)-C(14)-C(15)	125.54(11)
C(9)-C(8)-S(1)	111.69(8)	O(5)-C(14)-C(15)	110.12(10)
C(7)-C(8)-S(1)	116.40(8)	O(3)-C(2)-C(1)	107.16(9)
O(2)-C(7)-N(1)	122.50(10)	O(3)-C(2)-C(3)	107.30(8)
O(2)-C(7)-C(8)	121.72(10)	C(1)-C(2)-C(3)	113.88(9)
N(1)-C(7)-C(8)	115.78(9)	O(3)-C(2)-H(2)	109.5
O(1)-C(5)-C(6)	108.09(9)	C(1)-C(2)-H(2)	109.5
O(1)-C(5)-C(4)	107.01(8)	C(3)-C(2)-H(2)	109.5
C(6)-C(5)-C(4)	113.33(9)	C(10)-C(11)-S(1)	112.43(9)
O(1)-C(5)-H(5)	109.4	C(10)-C(11)-H(11)	123.8
C(6)-C(5)-H(5)	109.4	S(1)-C(11)-H(11)	123.8
C(4)-C(5)-H(5)	109.4	C(18)-C(19)-H(19A)	109.5
O(9)-C(6)-C(5)	109.12(9)	C(18)-C(19)-H(19B)	109.5
O(9)-C(6)-H(6A)	109.9	H(19A)-C(19)-H(19B)	109.5
C(5)-C(6)-H(6A)	109.9	C(18)-C(19)-H(19C)	109.5
O(9)-C(6)-H(6B)	109.9	H(19A)-C(19)-H(19C)	109.5
C(5)-C(6)-H(6B)	109.9	H(19B)-C(19)-H(19C)	109.5
H(6A)-C(6)-H(6B)	108.3	C(14)-C(15)-H(15A)	109.5
O(10)-C(18)-O(9)	123.29(12)	C(14)-C(15)-H(15B)	109.5
O(10)-C(18)-C(19)	125.80(11)	H(15A)-C(15)-H(15B)	109.5
O(9)-C(18)-C(19)	110.92(11)	C(14)-C(15)-H(15C)	109.5
C(11)-C(10)-C(9)	111.82(10)	H(15A)-C(15)-H(15C)	109.5
C(11)-C(10)-H(10)	124.1	H(15B)-C(15)-H(15C)	109.5
C(9)-C(10)-H(10)	124.1	C(12)-C(13)-H(13A)	109.5
O(8)-C(16)-O(7)	123.86(11)	C(12)-C(13)-H(13B)	109.5
O(8)-C(16)-C(17)	125.22(12)	H(13A)-C(13)-H(13B)	109.5
O(7)-C(16)-C(17)	110.91(10)	C(12)-C(13)-H(13C)	109.5
O(4)-C(12)-O(3)	123.84(11)	H(13A)-C(13)-H(13C)	109.5
O(4)-C(12)-C(13)	125.58(11)	H(13B)-C(13)-H(13C)	109.5
O(3)-C(12)-C(13)	110.59(10)	C(16)-C(17)-H(17A)	109.5
C(8)-C(9)-C(10)	111.99(10)	C(16)-C(17)-H(17B)	109.5
C(8)-C(9)-H(9)	124.0	H(17A)-C(17)-H(17B)	109.5
C(10)-C(9)-H(9)	124.0	C(16)-C(17)-H(17C)	109.5
O(6)-C(14)-O(5)	124.31(11)	H(17A)-C(17)-H(17C)	109.5

Table 4. Anisotropic displacement parameters [ $\text{\AA}^2 \times 10^3$ ] for 04mz145m. The anisotropic displacement factor exponent takes the form:  $-2 \pi^2 [(h a^*)^2 U_{11} + \dots + 2 h k a^* b^* U_{12}]$

	U11	U22	U33	U23	U13	U12
S(1)	32(1)	14(1)	23(1)	1(1)	19(1)	3(1)
O(1)	14(1)	14(1)	15(1)	1(1)	8(1)	-2(1)
O(7)	18(1)	16(1)	14(1)	3(1)	10(1)	2(1)
O(3)	13(1)	18(1)	13(1)	0(1)	7(1)	0(1)
N(1)	20(1)	12(1)	15(1)	0(1)	12(1)	1(1)
O(9)	22(1)	18(1)	16(1)	-5(1)	12(1)	-5(1)
O(5)	21(1)	11(1)	15(1)	-2(1)	11(1)	-3(1)
O(2)	29(1)	17(1)	21(1)	0(1)	18(1)	2(1)
O(6)	27(1)	18(1)	22(1)	1(1)	16(1)	-3(1)
C(1)	14(1)	12(1)	14(1)	0(1)	8(1)	0(1)
C(3)	16(1)	12(1)	14(1)	-1(1)	10(1)	-2(1)
C(4)	15(1)	14(1)	13(1)	1(1)	8(1)	0(1)
C(8)	17(1)	11(1)	16(1)	1(1)	10(1)	1(1)

O(10)	36(1)	24(1)	28(1)	-2(1)	24(1)	-6(1)
O(8)	32(1)	25(1)	25(1)	5(1)	19(1)	10(1)
O(4)	27(1)	47(1)	17(1)	-5(1)	14(1)	-9(1)
C(7)	14(1)	13(1)	15(1)	0(1)	8(1)	1(1)
C(5)	15(1)	14(1)	13(1)	-1(1)	8(1)	-1(1)
C(6)	16(1)	19(1)	16(1)	-5(1)	7(1)	-2(1)
C(18)	17(1)	21(1)	16(1)	-4(1)	10(1)	-3(1)
C(10)	22(1)	18(1)	19(1)	3(1)	13(1)	3(1)
C(16)	16(1)	18(1)	17(1)	4(1)	9(1)	2(1)
C(12)	20(1)	17(1)	14(1)	-1(1)	9(1)	-4(1)
C(9)	22(1)	15(1)	19(1)	2(1)	13(1)	3(1)
C(14)	16(1)	13(1)	18(1)	-1(1)	8(1)	-2(1)
C(2)	13(1)	13(1)	13(1)	0(1)	8(1)	-1(1)
C(11)	24(1)	17(1)	20(1)	4(1)	12(1)	2(1)
C(19)	34(1)	20(1)	27(1)	-5(1)	21(1)	-2(1)
C(15)	30(1)	14(1)	24(1)	-5(1)	15(1)	-4(1)
C(13)	16(1)	29(1)	16(1)	0(1)	5(1)	-1(1)
C(17)	27(1)	25(1)	23(1)	11(1)	14(1)	7(1)

Table 5. Hydrogen coordinates ( $\times 10^4$ ) and isotropic displacement parameters ( $\text{\AA}^2 \times 10^3$ ) for 04mz144m.

	x	y	z	U(eq)
H(1B)	8849	2245	3960	18
H(1)	8776	1955	6337	16
H(3)	8739	-53	6723	16
H(4)	10659	-55	7101	17
H(5)	9987	1232	8398	17
H(6A)	11726	830	10113	21
H(6B)	11950	1196	8968	21
H(10)	8800	4794	1207	23
H(9)	8891	3279	2426	22
H(2)	8925	654	4475	15
H(11)	8593	6157	2347	25
H(19A)	11478	3466	12101	37
H(19B)	10931	3718	10412	37
H(19C)	12131	3677	11473	37
H(15A)	8030	-2836	4527	34
H(15B)	9227	-2898	5424	34
H(15C)	8612	-2215	4034	34
H(13A)	5617	569	1248	34
H(13B)	5838	1384	2392	34
H(13C)	5850	295	2803	34
H(17A)	11823	-2305	10429	38
H(17B)	10662	-2367	9820	38
H(17C)	11330	-1496	10832	38

Table 6. Hydrogen bonds for 04mz144m [ $\text{\AA}$  and deg].

D-H...A	d(D-H)	d(H...A)	d(D...A)	$\angle(\text{DHA})$
N(1)-H(1B)...O(1)#1	0.88	2.38	3.1344(16)	143.6

Symmetry transformations used to generate equivalent atoms:

#1  $-x+2, y, -z+1$



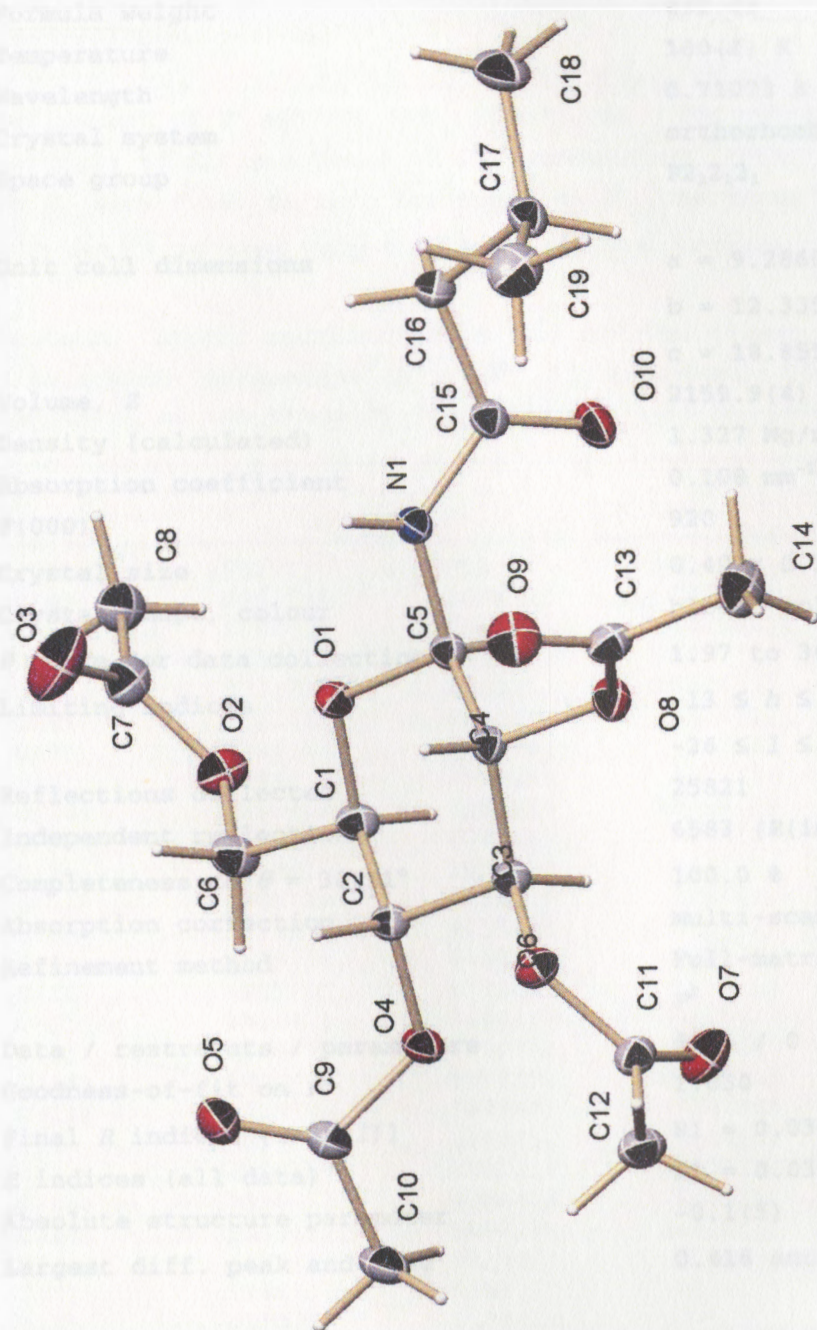


**Figure 169:** X-ray crystal structure of amide 16



Table 1. Crystal data and structure refinement for 04mz72am:

Identification code	04mz72am
Empirical formula	C <sub>19</sub> H <sub>29</sub> N <sub>1</sub> O <sub>10</sub>
Formula weight	431.43
Temperature	100(2) K
Wavelength	0.71073 Å
Crystal system	orthorhombic
Space group	P2 <sub>1</sub> 2 <sub>1</sub> 2 <sub>1</sub>
Unit cell dimensions	a = 9.2860(9) Å, α = 90° b = 12.3357(12) Å, β = 90° c = 18.8553(18) Å, γ = 90°
Volume, Z	2159.9(4) Å <sup>3</sup> , 4
Density (calculated)	1.327 Mg/m <sup>3</sup>
Absorption coefficient	0.108 mm <sup>-1</sup>
F(000)	920
Crystal size	0.40 × 0.38 × 0.35 mm
Crystal shape, colour	block, colourless
θ range for data collection	1.97 to 30.51°
Limiting indices	-13 ≤ h ≤ 13, -17 ≤ k ≤ 17, -26 ≤ l ≤ 26
Reflections collected	25821
Independent reflections	6583 (R(int) = 0.0303)
Completeness to θ = 30.51°	100.0 %
Absorption correction	multi-scan
Refinement method	Full-matrix least-squares on F <sup>2</sup>
Data / restraints / parameters	6583 / 0 / 369
Goodness-of-fit on F <sup>2</sup>	1.030
Final R indices [I > 2σ(I)]	R1 = 0.0365, wR2 = 0.0930
R indices (all data)	R1 = 0.0387, wR2 = 0.0949
Absolute structure parameter	-0.1(5)
Largest diff. peak and hole	0.416 and -0.182 e × Å <sup>-3</sup>

The assignment of the absolute structure is based on known chiral centers retained during the synthesis of the compound.

Treatment of hydrogen atoms:

All hydrogen atoms were located in the density Fourier map. Methyl hydrogen atoms were refined with an isotropic displacement parameter 1.5 times that of the adjacent carbon atom, all others were isotropically refined.

Refinement of  $F^2$  against ALL reflections. The weighted R-factor  $wR$  and goodness of fit are based on  $F^2$ , conventional R-factors  $R$  are based on  $F$ , with  $F$  set to zero for negative  $F^2$ . The threshold expression of  $F^2 > 2\sigma(F^2)$  is used only for calculating R-factors.

Table 2. Atomic coordinates [ $\times 10^4$ ] and equivalent isotropic displacement parameters [ $\text{\AA}^2 \times 10^3$ ] for 04mz99am.  $U(\text{eq})$  is defined as one third of the trace of the orthogonalized  $U_{ij}$  tensor.

	x	y	z	U(eq)
O(1)	4258(1)	5002(1)	9813(1)	17(1)
O(4)	3453(1)	3094(1)	8372(1)	19(1)
C(3)	3098(1)	4985(1)	8419(1)	16(1)
O(6)	3365(1)	5089(1)	7672(1)	18(1)
O(2)	4271(1)	2962(1)	10574(1)	23(1)
O(8)	2523(1)	6854(1)	8571(1)	19(1)
O(9)	4329(1)	8021(1)	8333(1)	29(1)
O(5)	5691(1)	2391(1)	8317(1)	28(1)
O(10)	1690(1)	7369(1)	10309(1)	24(1)
O(7)	1206(1)	4340(1)	7421(1)	29(1)
C(1)	3796(1)	3996(1)	9512(1)	18(1)
N(1)	3904(1)	6824(1)	9966(1)	16(1)
C(2)	3994(1)	4055(1)	8708(1)	16(1)
C(4)	3529(1)	6031(1)	8782(1)	15(1)
C(12)	2825(1)	4799(1)	6471(1)	24(1)
C(15)	3002(1)	7484(1)	10326(1)	17(1)
C(5)	3396(1)	5894(1)	9587(1)	15(1)
C(16)	3691(1)	8358(1)	10772(1)	20(1)
C(13)	3071(1)	7840(1)	8381(1)	21(1)
C(6)	4696(1)	3108(1)	9846(1)	23(1)
C(8)	4658(1)	3022(1)	11805(1)	27(1)
C(11)	2336(1)	4704(1)	7224(1)	20(1)
C(17)	3159(1)	9497(1)	10575(1)	23(1)
C(9)	4437(1)	2334(1)	8169(1)	20(1)
C(7)	5196(1)	3302(1)	11078(1)	25(1)
O(3)	6310(1)	3755(1)	10954(1)	44(1)
C(10)	3710(1)	1458(1)	7758(1)	26(1)
C(18)	3340(2)	10277(1)	11198(1)	34(1)
C(14)	1877(2)	8630(1)	8252(1)	33(1)
C(19)	3943(2)	9915(1)	9919(1)	33(1)

All esds (except the esd in the dihedral angle between two l.s. planes) are estimated using the full covariance matrix. The cell esds are taken into account individually in the estimation of esds in distances, angles and torsion angles; correlations between esds in cell parameters are only used when they are defined by crystal symmetry. An approximate (isotropic) treatment of cell esds is used for estimating esds involving l.s. planes.

Table 3. Bond lengths [Å] and angles [deg] for 04mz99am.

O(1)-C(5)	1.4257(11)	C(8)-C(7)	1.4987(17)
O(1)-C(1)	1.4296(12)	C(8)-H(8A)	0.98(2)
O(4)-C(9)	1.3634(12)	C(8)-H(8B)	0.96(2)
O(4)-C(2)	1.4354(12)	C(8)-H(8C)	0.95(2)
C(3)-O(6)	1.4363(11)	C(17)-C(19)	1.5255(19)
C(3)-C(4)	1.5143(13)	C(17)-C(18)	1.5274(18)
C(3)-C(2)	1.5188(14)	C(17)-H(17)	0.950(19)
C(3)-H(3)	0.993(15)	C(9)-C(10)	1.4919(15)
O(6)-C(11)	1.3607(13)	C(7)-O(3)	1.1988(16)
O(2)-C(7)	1.3475(14)	C(10)-H(10A)	0.93(2)
O(2)-C(6)	1.4397(13)	C(10)-H(10B)	0.96(2)
O(8)-C(13)	1.3664(12)	C(10)-H(10C)	0.96(2)
O(8)-C(4)	1.4359(12)	C(18)-H(18A)	0.96(2)
O(9)-C(13)	1.1929(15)	C(18)-H(18B)	0.93(2)
O(5)-C(9)	1.1989(14)	C(18)-H(18C)	1.00(2)
O(10)-C(15)	1.2270(13)	C(14)-H(14A)	0.90(2)
O(7)-C(11)	1.1998(14)	C(14)-H(14B)	0.97(2)
C(1)-C(6)	1.5145(15)	C(14)-H(14C)	0.96(2)
C(1)-C(2)	1.5296(14)	C(19)-H(19A)	1.03(2)
C(1)-H(1)	0.968(14)	C(19)-H(19B)	0.98(2)
N(1)-C(15)	1.3505(13)	C(19)-H(19C)	0.93(2)
N(1)-C(5)	1.4314(12)		
N(1)-H(1A)	0.871(16)	C(5)-O(1)-C(1)	112.53(7)
C(2)-H(2)	0.950(14)	C(9)-O(4)-C(2)	117.19(8)
C(4)-C(5)	1.5318(14)	O(6)-C(3)-C(4)	108.76(8)
C(4)-H(4)	0.896(15)	O(6)-C(3)-C(2)	108.94(8)
C(12)-C(11)	1.4959(15)	C(4)-C(3)-C(2)	109.68(8)
C(12)-H(12A)	0.968(19)	O(6)-C(3)-H(3)	109.4(8)
C(12)-H(12B)	0.95(2)	C(4)-C(3)-H(3)	113.7(9)
C(12)-H(12C)	0.945(19)	C(2)-C(3)-H(3)	106.3(9)
C(15)-C(16)	1.5108(14)	C(11)-O(6)-C(3)	117.11(8)
C(5)-H(5)	0.981(14)	C(7)-O(2)-C(6)	117.29(8)
C(16)-C(17)	1.5349(15)	C(13)-O(8)-C(4)	117.37(8)
C(16)-H(16A)	0.949(15)	O(1)-C(1)-C(6)	107.29(8)
C(16)-H(16B)	0.936(19)	O(1)-C(1)-C(2)	108.39(8)
C(13)-C(14)	1.4957(17)	C(6)-C(1)-C(2)	112.34(8)
C(6)-H(6A)	0.994(18)	O(1)-C(1)-H(1)	110.1(9)
C(6)-H(6B)	0.966(15)	C(6)-C(1)-H(1)	109.7(9)

C(2)-C(1)-H(1)	109.0(8)	C(7)-C(8)-H(8A)	108.1(12)
C(15)-N(1)-C(5)	122.00(9)	C(7)-C(8)-H(8B)	108.3(11)
C(15)-N(1)-H(1A)	121.3(10)	H(8A)-C(8)-H(8B)	111.7(16)
C(5)-N(1)-H(1A)	116.3(10)	C(7)-C(8)-H(8C)	112.8(11)
O(4)-C(2)-C(3)	105.91(8)	H(8A)-C(8)-H(8C)	109.5(16)
O(4)-C(2)-C(1)	110.89(8)	H(8B)-C(8)-H(8C)	106.5(16)
C(3)-C(2)-C(1)	109.00(8)	O(7)-C(11)-O(6)	123.57(10)
O(4)-C(2)-H(2)	108.6(9)	O(7)-C(11)-C(12)	126.08(10)
C(3)-C(2)-H(2)	111.9(9)	O(6)-C(11)-C(12)	110.36(9)
C(1)-C(2)-H(2)	110.5(8)	C(19)-C(17)-C(18)	111.01(11)
O(8)-C(4)-C(3)	107.78(8)	C(19)-C(17)-C(16)	110.59(10)
O(8)-C(4)-C(5)	107.44(8)	C(18)-C(17)-C(16)	110.76(10)
C(3)-C(4)-C(5)	109.41(8)	C(19)-C(17)-H(17)	106.7(11)
O(8)-C(4)-H(4)	112.8(10)	C(18)-C(17)-H(17)	109.1(11)
C(3)-C(4)-H(4)	109.6(10)	C(16)-C(17)-H(17)	108.5(11)
C(5)-C(4)-H(4)	109.7(10)	O(5)-C(9)-O(4)	123.03(10)
C(11)-C(12)-H(12A)	108.5(11)	O(5)-C(9)-C(10)	127.08(10)
C(11)-C(12)-H(12B)	111.2(11)	O(4)-C(9)-C(10)	109.89(9)
H(12A)-C(12)-H(12B)	111.5(16)	O(3)-C(7)-O(2)	123.85(12)
C(11)-C(12)-H(12C)	112.0(11)	O(3)-C(7)-C(8)	125.01(12)
H(12A)-C(12)-H(12C)	105.4(16)	O(2)-C(7)-C(8)	111.13(10)
H(12B)-C(12)-H(12C)	108.1(16)	C(9)-C(10)-H(10A)	111.9(12)
O(10)-C(15)-N(1)	122.18(10)	C(9)-C(10)-H(10B)	107.7(12)
O(10)-C(15)-C(16)	121.18(9)	H(10A)-C(10)-H(10B)	108.5(16)
N(1)-C(15)-C(16)	116.61(9)	C(9)-C(10)-H(10C)	111.8(12)
O(1)-C(5)-N(1)	106.54(8)	H(10A)-C(10)-H(10C)	110.7(17)
O(1)-C(5)-C(4)	109.63(8)	H(10B)-C(10)-H(10C)	106.0(16)
N(1)-C(5)-C(4)	112.30(8)	C(17)-C(18)-H(18A)	111.9(13)
O(1)-C(5)-H(5)	112.2(8)	C(17)-C(18)-H(18B)	110.7(14)
N(1)-C(5)-H(5)	108.0(8)	H(18A)-C(18)-H(18B)	109(2)
C(4)-C(5)-H(5)	108.2(8)	C(17)-C(18)-H(18C)	112.0(13)
C(15)-C(16)-C(17)	112.47(9)	H(18A)-C(18)-H(18C)	107.6(19)
C(15)-C(16)-H(16A)	110.4(9)	H(18B)-C(18)-H(18C)	105.6(18)
C(17)-C(16)-H(16A)	111.0(9)	C(13)-C(14)-H(14A)	106.5(14)
C(15)-C(16)-H(16B)	103.2(12)	C(13)-C(14)-H(14B)	106.4(13)
C(17)-C(16)-H(16B)	112.5(12)	H(14A)-C(14)-H(14B)	104.3(19)
H(16A)-C(16)-H(16B)	106.8(14)	C(13)-C(14)-H(14C)	115.3(14)
O(9)-C(13)-O(8)	123.42(10)	H(14A)-C(14)-H(14C)	109.2(18)
O(9)-C(13)-C(14)	126.33(11)	H(14B)-C(14)-H(14C)	114.4(18)
O(8)-C(13)-C(14)	110.25(10)	C(17)-C(19)-H(19A)	108.3(12)
O(2)-C(6)-C(1)	109.66(9)	C(17)-C(19)-H(19B)	113.4(13)
O(2)-C(6)-H(6A)	108.6(10)	H(19A)-C(19)-H(19B)	112.3(18)
C(1)-C(6)-H(6A)	109.9(10)	C(17)-C(19)-H(19C)	109.9(13)
O(2)-C(6)-H(6B)	110.2(8)	H(19A)-C(19)-H(19C)	107.5(18)
C(1)-C(6)-H(6B)	111.3(9)	H(19B)-C(19)-H(19C)	105.3(17)
H(6A)-C(6)-H(6B)	107.1(14)		

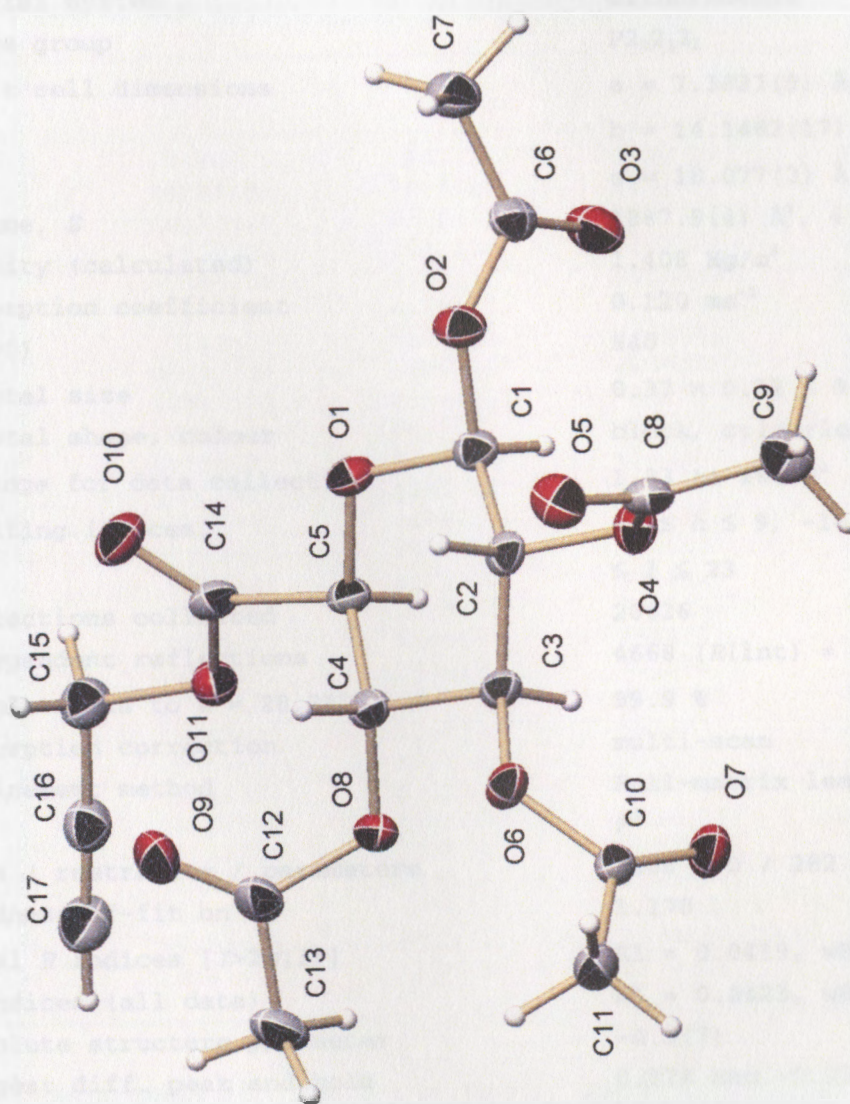


Table 4. Anisotropic displacement parameters [ $\text{\AA}^2 \times 10^3$ ] for 04mz99am. The anisotropic displacement factor exponent takes the form:  $-2 \pi^2 [(h a^*)^2 U_{11} + \dots + 2 h k a^* b^* U_{12}]$

	U11	U22	U33	U23	U13	U12
O(1)	20(1)	12(1)	20(1)	0(1)	-3(1)	1(1)
O(4)	19(1)	14(1)	24(1)	-4(1)	1(1)	0(1)
C(3)	17(1)	14(1)	16(1)	0(1)	0(1)	-1(1)
O(6)	20(1)	19(1)	17(1)	0(1)	-1(1)	-4(1)
O(2)	31(1)	20(1)	20(1)	3(1)	-1(1)	-4(1)
O(8)	19(1)	13(1)	26(1)	3(1)	-3(1)	0(1)
O(9)	30(1)	20(1)	38(1)	5(1)	1(1)	-6(1)
O(5)	22(1)	25(1)	36(1)	-6(1)	-1(1)	5(1)
O(10)	15(1)	19(1)	38(1)	-4(1)	2(1)	1(1)
O(7)	25(1)	34(1)	29(1)	2(1)	-6(1)	-10(1)
C(1)	22(1)	12(1)	19(1)	0(1)	0(1)	-1(1)
N(1)	13(1)	15(1)	21(1)	-3(1)	1(1)	-1(1)
C(2)	18(1)	13(1)	19(1)	0(1)	0(1)	-1(1)
C(4)	14(1)	14(1)	18(1)	1(1)	-1(1)	0(1)
C(12)	31(1)	23(1)	20(1)	-3(1)	-4(1)	2(1)
C(15)	18(1)	13(1)	21(1)	1(1)	-1(1)	1(1)
C(5)	15(1)	12(1)	18(1)	0(1)	0(1)	0(1)
C(16)	20(1)	17(1)	22(1)	-3(1)	-2(1)	1(1)
C(13)	29(1)	14(1)	20(1)	1(1)	-5(1)	-2(1)
C(6)	32(1)	16(1)	20(1)	3(1)	0(1)	4(1)
C(8)	33(1)	25(1)	22(1)	4(1)	-2(1)	3(1)
C(11)	23(1)	16(1)	21(1)	-1(1)	-5(1)	0(1)
C(17)	18(1)	16(1)	36(1)	-5(1)	-3(1)	2(1)
C(9)	22(1)	16(1)	22(1)	-2(1)	4(1)	1(1)
C(7)	29(1)	20(1)	25(1)	5(1)	-4(1)	1(1)
O(3)	36(1)	58(1)	36(1)	13(1)	-9(1)	-17(1)
C(10)	23(1)	21(1)	35(1)	-11(1)	5(1)	-1(1)
C(18)	35(1)	22(1)	45(1)	-14(1)	1(1)	1(1)
C(14)	36(1)	17(1)	47(1)	5(1)	-16(1)	3(1)
C(19)	40(1)	23(1)	35(1)	4(1)	-6(1)	0(1)

Table 5. Hydrogen coordinates ( $\times 10^4$ ) and isotropic displacement parameters ( $\text{\AA}^2 \times 10^3$ ) for 04mz99am.

	x	y	z	U(eq)
H(3)	2075(15)	4782(13)	8497(7)	17(3)
H(1)	2789(15)	3874(12)	9617(7)	14(3)
H(2)	4984(15)	4131(12)	8592(7)	12(3)
H(4)	4440(16)	6196(12)	8669(8)	18(3)
H(12A)	1990(20)	4740(16)	6164(10)	36
H(12B)	3530(20)	4267(16)	6361(10)	36
H(12C)	3220(20)	5488(16)	6373(10)	36
H(5)	2375(15)	5793(12)	9703(7)	12(3)
H(16A)	4709(16)	8315(12)	10743(7)	18(3)
H(16B)	3440(19)	8161(16)	11235(10)	36(4)
H(6A)	4543(19)	2415(15)	9589(9)	31(4)
H(6B)	5711(16)	3273(12)	9818(8)	15(3)
H(8A)	4940(20)	3608(17)	12129(11)	40
H(8B)	5070(20)	2344(17)	11941(10)	40
H(8C)	3640(20)	2929(15)	11821(9)	40
H(17)	2170(20)	9452(14)	10454(9)	32(4)
H(10A)	4310(20)	862(16)	7691(11)	39
H(10B)	3463(19)	1750(16)	7299(10)	39
H(10C)	2820(20)	1243(16)	7972(10)	39
H(18A)	2980(20)	10990(19)	11089(11)	51
H(18B)	4300(20)	10333(19)	11327(12)	51
H(18C)	2830(20)	10015(18)	11634(11)	51
H(14A)	2100(20)	8986(18)	7853(11)	50
H(14B)	1950(20)	9176(19)	8623(12)	50
H(14C)	930(20)	8315(19)	8204(11)	50
H(19A)	5010(20)	10035(18)	10049(11)	49
H(19B)	3500(20)	10564(18)	9714(11)	49
H(19C)	3910(20)	9398(17)	9563(11)	49
H(1A)	4809(17)	6986(13)	9911(8)	21(3)



**Figure 170:** X-ray crystal structure of alkyne 29

Table 1. Crystal data and structure refinement for 04mz55am:

Identification code	04mz55am
Empirical formula	C <sub>17</sub> H <sub>20</sub> O <sub>11</sub>
Formula weight	400.33
Temperature	100(2) K
Wavelength	0.71073 Å
Crystal system	orthorhombic
Space group	P2 <sub>1</sub> 2 <sub>1</sub> 2 <sub>1</sub>
Unit cell dimensions	a = 7.3827(9) Å, α = 90° b = 14.1462(17) Å, β = 90° c = 18.077(2) Å, γ = 90°
Volume, Z	1887.9(4) Å <sup>3</sup> , 4
Density (calculated)	1.408 Mg/m <sup>3</sup>
Absorption coefficient	0.120 mm <sup>-1</sup>
F(000)	840
Crystal size	0.37 × 0.22 × 0.22 mm
Crystal shape, colour	block, colourless
θ range for data collection	1.83 to 28.28°
Limiting indices	-9 ≤ h ≤ 9, -18 ≤ k ≤ 18, -23 ≤ l ≤ 23
Reflections collected	20026
Independent reflections	4668 (R(int) = 0.0194)
Completeness to θ = 28.28°	99.9 %
Absorption correction	multi-scan
Refinement method	Full-matrix least-squares on F <sup>2</sup>
Data / restraints / parameters	4668 / 0 / 282
Goodness-of-fit on F <sup>2</sup>	1.170
Final R indices [I > 2σ(I)]	R1 = 0.0419, wR2 = 0.1017
R indices (all data)	R1 = 0.0423, wR2 = 0.1020
Absolute structure parameter	-0.3(7)
Largest diff. peak and hole	0.378 and -0.224 e Å <sup>-3</sup>

## Treatment of hydrogen atoms:

Methyl hydrogen atoms were placed in calculated positions. The positions of all other hydrogen atoms were refined and all but the acetylenic hydrogen atom were restraint to have an isotropic displacement parameter 1.2 or 1.5 times of the adjacent carbon atom.

Refinement of F<sup>2</sup> against ALL reflections. The weighted R-factor wR and



goodness of fit are based on  $F^2$ , conventional R-factors R are based on  $F$ , with  $F$  set to zero for negative  $F^2$ . The threshold expression of  $F^2 > 2\sigma(F^2)$  is used only for calculating R-factors.

Table 2. Atomic coordinates [ $\times 10^4$ ] and equivalent isotropic displacement parameters [ $\text{\AA}^2 \times 10^3$ ] for 04mz55am.  $U(\text{eq})$  is defined as one third of the trace of the orthogonalized  $U_{ij}$  tensor.

	x	y	z	U(eq)
O(6)	7394(2)	7967(1)	8795(1)	23(1)
O(8)	10820(2)	7599(1)	8191(1)	23(1)
O(11)	14190(2)	8674(1)	7753(1)	24(1)
O(2)	9510(2)	11043(1)	9437(1)	26(1)
O(4)	7465(2)	9443(1)	9933(1)	24(1)
O(1)	11083(2)	10111(1)	8681(1)	22(1)
O(7)	7619(2)	7004(1)	9789(1)	29(1)
C(4)	10197(2)	8539(1)	8334(1)	20(1)
O(10)	12850(2)	10039(1)	7421(1)	32(1)
O(5)	4942(2)	10075(1)	9430(1)	30(1)
C(5)	11796(2)	9206(1)	8502(1)	20(1)
O(3)	11332(2)	11198(1)	10427(1)	34(1)
C(2)	8389(2)	9482(1)	9237(1)	21(1)
C(14)	12987(2)	9377(1)	7826(1)	22(1)
C(3)	8972(2)	8492(1)	9011(1)	19(1)
C(10)	6893(2)	7215(1)	9218(1)	21(1)
C(8)	5750(2)	9806(1)	9964(1)	23(1)
C(7)	10171(3)	12596(1)	9835(1)	31(1)
C(1)	10063(2)	10096(1)	9343(1)	22(1)
C(6)	10433(2)	11561(1)	9955(1)	24(1)
C(9)	5095(3)	9824(1)	10748(1)	30(1)
C(11)	5344(3)	6712(1)	8860(1)	27(1)
O(9)	10941(2)	7945(1)	6974(1)	34(1)
C(12)	11132(3)	7385(1)	7462(1)	27(1)
C(16)	16024(3)	7802(1)	6926(1)	29(1)
C(13)	11709(3)	6376(1)	7384(1)	34(1)
C(15)	15268(3)	8732(1)	7082(1)	31(1)
C(17)	16641(3)	7059(2)	6777(1)	35(1)

All esds (except the esd in the dihedral angle between two l.s. planes) are estimated using the full covariance matrix. The cell esds are taken into account individually in the estimation of esds in distances, angles and torsion angles; correlations between esds in cell parameters are only used when they are defined by crystal symmetry. An approximate (isotropic) treatment of cell esds is used for estimating esds involving l.s. planes.

Table 3. Bond lengths [Å] and angles [deg] for 04mz55am.

O(6)-C(10)	1.3604(19)	C(14)-O(11)-C(15)	113.76(14)
O(6)-C(3)	1.436(2)	C(6)-O(2)-C(1)	116.51(14)
O(8)-C(12)	1.373(2)	C(8)-O(4)-C(2)	117.48(13)
O(8)-C(4)	1.432(2)	C(1)-O(1)-C(5)	112.20(12)
O(11)-C(14)	1.340(2)	O(8)-C(4)-C(3)	107.16(13)
O(11)-C(15)	1.454(2)	O(8)-C(4)-C(5)	110.98(13)
O(2)-C(6)	1.370(2)	C(3)-C(4)-C(5)	108.92(13)
O(2)-C(1)	1.411(2)	O(8)-C(4)-H(4)	110.5(13)
O(4)-C(8)	1.368(2)	C(3)-C(4)-H(4)	108.2(13)
O(4)-C(2)	1.433(2)	C(5)-C(4)-H(4)	111.0(14)
O(1)-C(1)	1.413(2)	O(1)-C(5)-C(14)	104.72(13)
O(1)-C(5)	1.4209(19)	O(1)-C(5)-C(4)	108.16(13)
O(7)-C(10)	1.200(2)	C(14)-C(5)-C(4)	112.45(13)
C(4)-C(3)	1.523(2)	O(1)-C(5)-H(5)	110.6(13)
C(4)-C(5)	1.542(2)	C(14)-C(5)-H(5)	112.5(13)
C(4)-H(4)	0.95(2)	C(4)-C(5)-H(5)	108.3(13)
O(10)-C(14)	1.194(2)	O(4)-C(2)-C(3)	109.61(13)
O(5)-C(8)	1.195(2)	O(4)-C(2)-C(1)	107.34(13)
C(5)-C(14)	1.523(2)	C(3)-C(2)-C(1)	109.26(13)
C(5)-H(5)	0.95(2)	O(4)-C(2)-H(2)	110.6(13)
O(3)-C(6)	1.196(2)	C(3)-C(2)-H(2)	110.7(13)
C(2)-C(3)	1.521(2)	C(1)-C(2)-H(2)	109.3(13)
C(2)-C(1)	1.523(2)	O(10)-C(14)-O(11)	125.28(17)
C(2)-H(2)	0.96(2)	O(10)-C(14)-C(5)	124.61(16)
C(3)-H(3)	0.94(2)	O(11)-C(14)-C(5)	110.11(13)
C(10)-C(11)	1.495(2)	O(6)-C(3)-C(2)	108.64(13)
C(8)-C(9)	1.498(3)	O(6)-C(3)-C(4)	106.64(12)
C(7)-C(6)	1.493(3)	C(2)-C(3)-C(4)	110.07(13)
C(7)-H(7A)	0.9800	O(6)-C(3)-H(3)	109.4(13)
C(7)-H(7B)	0.9800	C(2)-C(3)-H(3)	111.6(13)
C(7)-H(7C)	0.9800	C(4)-C(3)-H(3)	110.4(13)
C(1)-H(1)	0.96(2)	O(7)-C(10)-O(6)	123.78(15)
C(9)-H(9A)	0.9800	O(7)-C(10)-C(11)	126.58(16)
C(9)-H(9B)	0.9800	O(6)-C(10)-C(11)	109.64(14)
C(9)-H(9C)	0.9800	O(5)-C(8)-O(4)	123.29(16)
C(11)-H(11A)	0.9800	O(5)-C(8)-C(9)	126.67(16)
C(11)-H(11B)	0.9800	O(4)-C(8)-C(9)	110.03(15)
C(11)-H(11C)	0.9800	C(6)-C(7)-H(7A)	109.5
O(9)-C(12)	1.193(2)	C(6)-C(7)-H(7B)	109.5
C(12)-C(13)	1.496(3)	H(7A)-C(7)-H(7B)	109.5
C(16)-C(17)	1.176(3)	C(6)-C(7)-H(7C)	109.5
C(16)-C(15)	1.457(3)	H(7A)-C(7)-H(7C)	109.5
C(13)-H(13A)	0.9800	H(7B)-C(7)-H(7C)	109.5
C(13)-H(13B)	0.9800	O(2)-C(1)-O(1)	104.09(13)
C(13)-H(13C)	0.9800	O(2)-C(1)-C(2)	108.81(13)
C(15)-H(15A)	0.94(3)	O(1)-C(1)-C(2)	109.53(13)
C(15)-H(15B)	0.92(3)	O(2)-C(1)-H(1)	110.8(14)
C(17)-H(17)	0.94(3)	O(1)-C(1)-H(1)	111.6(13)
		C(2)-C(1)-H(1)	111.8(14)
C(10)-O(6)-C(3)	118.17(13)	O(3)-C(6)-O(2)	122.24(17)
C(12)-O(8)-C(4)	115.61(13)	O(3)-C(6)-C(7)	126.65(18)
O(2)-C(6)-C(7)	111.11(16)	C(17)-C(16)-C(15)	177.8(2)

C(8)-C(9)-H(9A)	109.5	C(12)-C(13)-H(13A)	109.5
C(8)-C(9)-H(9B)	109.5	C(12)-C(13)-H(13B)	109.5
H(9A)-C(9)-H(9B)	109.5	H(13A)-C(13)-H(13B)	109.5
C(8)-C(9)-H(9C)	109.5	C(12)-C(13)-H(13C)	109.5
H(9A)-C(9)-H(9C)	109.5	H(13A)-C(13)-H(13C)	109.5
H(9B)-C(9)-H(9C)	109.5	H(13B)-C(13)-H(13C)	109.5
C(10)-C(11)-H(11A)	109.5	O(11)-C(15)-C(16)	108.62(15)
C(10)-C(11)-H(11B)	109.5	O(11)-C(15)-H(15A)	109.4(16)
H(11A)-C(11)-H(11B)	109.5	C(16)-C(15)-H(15A)	110.5(16)
C(10)-C(11)-H(11C)	109.5	O(11)-C(15)-H(15B)	107.8(15)
H(11A)-C(11)-H(11C)	109.5	C(16)-C(15)-H(15B)	111.0(16)
H(11B)-C(11)-H(11C)	109.5	H(15A)-C(15)-H(15B)	109(2)
O(9)-C(12)-O(8)	122.90(17)	C(16)-C(17)-H(17)	175.5(18)
O(9)-C(12)-C(13)	126.74(17)	H(13B)-C(130)-H(13C)	109.5
O(8)-C(12)-C(13)	110.35(15)		

Symmetry transformations used to generate equivalent atoms:

Table 4. Anisotropic displacement parameters [ $\text{\AA}^2 \times 10^3$ ] for 04mz55am. The anisotropic displacement factor exponent takes the form:  $-2 \pi^2 [(h a^*)^2 U_{11} + \dots + 2 h k a^* b^* U_{12}]$

	U11	U22	U33	U23	U13	U12
O(6)	23(1)	24(1)	21(1)	5(1)	-5(1)	-7(1)
O(8)	29(1)	18(1)	21(1)	-2(1)	-2(1)	-4(1)
O(11)	26(1)	23(1)	23(1)	0(1)	1(1)	2(1)
O(2)	28(1)	19(1)	30(1)	-2(1)	-5(1)	3(1)
O(4)	22(1)	28(1)	23(1)	5(1)	-1(1)	3(1)
O(1)	22(1)	15(1)	27(1)	2(1)	-1(1)	1(1)
O(7)	35(1)	30(1)	22(1)	7(1)	-2(1)	-5(1)
C(4)	23(1)	19(1)	19(1)	2(1)	-4(1)	-3(1)
O(10)	38(1)	23(1)	36(1)	8(1)	10(1)	3(1)
O(5)	26(1)	34(1)	31(1)	-1(1)	-7(1)	5(1)
C(5)	23(1)	15(1)	21(1)	0(1)	-2(1)	-1(1)
O(3)	43(1)	29(1)	31(1)	-6(1)	-9(1)	4(1)
C(2)	23(1)	20(1)	19(1)	4(1)	-4(1)	1(1)
C(14)	21(1)	19(1)	27(1)	1(1)	-2(1)	-5(1)
C(3)	22(1)	18(1)	19(1)	2(1)	-4(1)	-4(1)
C(10)	24(1)	19(1)	20(1)	-1(1)	5(1)	-1(1)
C(8)	22(1)	17(1)	30(1)	-3(1)	-2(1)	-2(1)
C(7)	36(1)	24(1)	34(1)	-5(1)	4(1)	2(1)
C(1)	24(1)	18(1)	23(1)	1(1)	-4(1)	1(1)
C(6)	23(1)	24(1)	26(1)	-4(1)	6(1)	-1(1)
C(9)	28(1)	32(1)	32(1)	-2(1)	2(1)	3(1)
C(11)	29(1)	27(1)	24(1)	0(1)	3(1)	-8(1)
O(9)	44(1)	38(1)	20(1)	-3(1)	-2(1)	-11(1)
C(12)	29(1)	30(1)	24(1)	-5(1)	-2(1)	-11(1)
C(16)	29(1)	32(1)	27(1)	2(1)	4(1)	0(1)
C(13)	40(1)	30(1)	32(1)	-13(1)	-1(1)	-8(1)

C(15)	33(1)	27(1)	32(1)	2(1)	9(1)	1(1)
C(17)	37(1)	31(1)	37(1)	4(1)	10(1)	7(1)

Table 5. Hydrogen coordinates ( $\times 10^4$ ) and isotropic displacement parameters ( $\text{\AA}^2 \times 10^3$ ) for 04mz55am.

	x	y	z	U(eq)
H(4)	9500(30)	8766(15)	7932(11)	24
H(5)	12460(30)	8953(15)	8910(11)	24
H(2)	7630(30)	9759(15)	8865(11)	25
H(3)	9560(30)	8176(15)	9400(12)	23
H(7A)	11105	12831	9496	47
H(7B)	10266	12928	10309	47
H(7C)	8971	12708	9620	47
H(1)	10780(30)	9890(16)	9754(12)	26
H(9A)	3811	9999	10758	46
H(9B)	5798	10287	11031	46
H(9C)	5247	9196	10968	46
H(11A)	5006	6162	9159	40
H(11B)	5703	6503	8364	40
H(11C)	4307	7142	8821	40
H(13A)	12375	6295	6919	51
H(13B)	10637	5967	7382	51
H(13C)	12493	6203	7800	51
H(15A)	14530(40)	8934(18)	6689(14)	37
H(15B)	16170(40)	9170(18)	7161(13)	37
H(17)	17170(40)	6470(20)	6696(15)	53(8)



Table 1. Crystal data and structure determination for compound 30

Identification code	30
Empirical formula	$C_{17}H_{17}NO$
Formula weight	251.32
Temperature	100 K
Wavelength	0.71073 Å
Crystal system	Trigonal
Space group	$R\bar{3}c$
Unit cell dimensions	$a = 10.101(1)$ Å, $b = 10.101(1)$ Å, $c = 13.372(2)$ Å

Volume, Å<sup>3</sup>

Density (calculated)

Z

Crystal size (mm)

Crystal color

Crystal habit

Diffractometer

Scan range (° 2 $\theta$ )

Limiting indices

Reflections collected

Independent reflections

Completeness to  $\theta =$ 

Absorption correction

Max. and min. transmission

Refinement method

Data / restraints / parameters

Goodness-of-fit on  $F^2$ Final  $R$  indices [I > 2 $\sigma$ (I)]

R indices (all data)

Largest diff. peak and hole

Treatment of hydrogen atoms

All hydrogen atoms were placed in calculated positions and refined with an isotropic displacement parameter fixed at the value of the adjacent carbon

R indices (all data)

Largest diff. peak and hole

Treatment of hydrogen atoms

All hydrogen atoms were placed in calculated positions and refined with an isotropic displacement parameter fixed at the value of the adjacent carbon

R indices (all data)

Largest diff. peak and hole

Treatment of hydrogen atoms

All hydrogen atoms were placed in calculated positions and refined with an isotropic displacement parameter fixed at the value of the adjacent carbon

R indices (all data)

Largest diff. peak and hole

Treatment of hydrogen atoms

All hydrogen atoms were placed in calculated positions and refined with an isotropic displacement parameter fixed at the value of the adjacent carbon

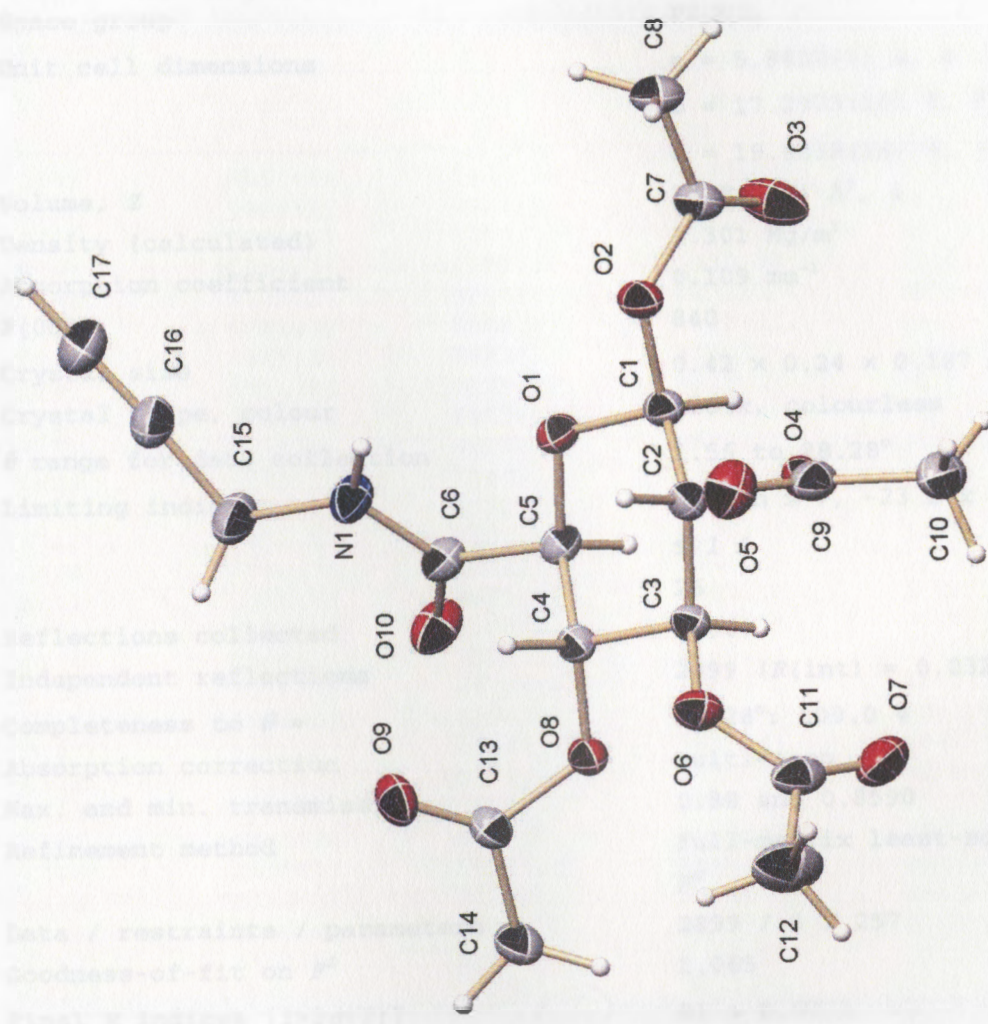


Figure 171: X-ray crystal structure of alkyne 30

Table 1. Crystal data and structure refinement for 05mz051m:

Identification code	05mz051m
Empirical formula	C17 H21 N1 O10
Formula weight	399.35
Temperature	100(2) K
Wavelength	0.71073 Å
Crystal system	Orthorhombic
Space group	P2 <sub>1</sub> 2 <sub>1</sub> 2 <sub>1</sub>
Unit cell dimensions	a = 5.9422(5) Å, α = 90° b = 17.2973(16) Å, β = 90° c = 19.8338(18) Å, γ = 90°
Volume, Z	2038.6(3) Å <sup>3</sup> , 4
Density (calculated)	1.301 Mg/m <sup>3</sup>
Absorption coefficient	0.109 mm <sup>-1</sup>
F(000)	840
Crystal size	0.42 × 0.24 × 0.187 mm
Crystal shape, colour	block, colourless
θ range for data collection	1.56 to 28.28°
Limiting indices	-7 ≤ h ≤ 7, -23 ≤ k ≤ 23, -26 ≤ l ≤ 26
Reflections collected	21061
Independent reflections	2899 (R(int) = 0.0324)
Completeness to θ =	28.28°: 100.0 %
Absorption correction	multi-scan
Max. and min. transmission	0.98 and 0.8590
Refinement method	Full-matrix least-squares on F <sup>2</sup>
Data / restraints / parameters	2899 / 0 / 257
Goodness-of-fit on F <sup>2</sup>	1.065
Final R indices [I > 2σ(I)]	R1 = 0.0335, wR2 = 0.0894
R indices (all data)	R1 = 0.0347, wR2 = 0.0906
Largest diff. peak and hole	0.273 and -0.192 e × Å <sup>-3</sup>

## Treatment of hydrogen atoms:

All hydrogen atoms were placed in calculated positions and were refined with an isotropic displacement parameter 1.5 (methyl) or 1.2 times (all others) that of the adjacent carbon atom.

Refinement of  $F^2$  against ALL reflections. The weighted R-factor  $wR$  and goodness of fit are based on  $F^2$ , conventional R-factors  $R$  are based on  $F$ , with  $F$  set to zero for negative  $F^2$ . The threshold expression of  $F^2 > 2\sigma(F^2)$  is used only for calculating R-factors.

Table 2. Atomic coordinates [ $\times 10^4$ ] and equivalent isotropic displacement parameters [ $\text{\AA}^2 \times 10^3$ ] for 05mz051m.  $U(\text{eq})$  is defined as one third of the trace of the orthogonalized  $U_{ij}$  tensor.

	x	y	z	U(eq)
O(8)	9267(2)	10435(1)	8178(1)	23(1)
O(2)	5480(2)	7574(1)	8373(1)	27(1)
O(1)	7220(2)	8485(1)	7767(1)	25(1)
O(9)	12926(2)	10198(1)	7958(1)	33(1)
O(6)	8373(2)	9816(1)	9452(1)	28(1)
C(1)	5665(3)	8384(1)	8302(1)	23(1)
O(4)	4863(2)	8672(1)	9450(1)	27(1)
O(7)	5511(3)	10625(1)	9695(1)	40(1)
O(10)	9534(2)	9902(1)	6704(1)	36(1)
C(5)	7750(3)	9277(1)	7636(1)	23(1)
O(3)	1883(2)	7584(1)	8017(1)	43(1)
C(3)	7239(2)	9551(1)	8855(1)	22(1)
C(4)	8858(2)	9624(1)	8270(1)	22(1)
C(14)	11592(3)	11514(1)	7990(1)	34(1)
N(1)	10568(3)	8671(1)	6929(1)	31(1)
O(5)	7191(2)	8100(1)	10199(1)	39(1)
C(7)	3500(3)	7231(1)	8196(1)	28(1)
C(8)	3676(3)	6372(1)	8262(1)	35(1)
C(9)	5411(3)	8390(1)	10071(1)	30(1)
C(2)	6614(2)	8706(1)	8955(1)	23(1)
C(11)	7339(3)	10371(1)	9819(1)	32(1)
C(13)	11415(3)	10650(1)	8036(1)	25(1)
C(6)	9360(3)	9310(1)	7039(1)	26(1)
C(10)	3518(3)	8519(1)	10554(1)	39(1)
C(16)	12966(3)	7915(1)	6190(1)	36(1)
C(15)	12319(4)	8688(1)	6416(1)	40(1)
C(12)	8836(5)	10608(1)	10394(1)	51(1)
C(17)	13562(4)	7309(1)	5992(1)	48(1)

All esds (except the esd in the dihedral angle between two l.s. planes) are estimated using the full covariance matrix. The cell esds are taken into account individually in the estimation of esds in distances, angles and torsion angles; correlations between esds in cell parameters are only used when they are defined by crystal symmetry. An approximate (isotropic) treatment of cell esds is used for estimating esds involving l.s. planes.

Table 3. Bond lengths [Å] and angles [deg] for 05mz051m.

O(8)-C(13)	1.3589(18)	C(15)-H(15B)	0.9900
O(8)-C(4)	1.4356(16)	C(12)-H(12A)	0.9800
O(2)-C(7)	1.3643(19)	C(12)-H(12B)	0.9800
O(2)-C(1)	1.4130(16)	C(12)-H(12C)	0.9800
O(1)-C(1)	1.4178(17)	C(17)-H(17)	0.9500
O(1)-C(5)	1.4294(16)		
O(9)-C(13)	1.2005(19)	C(13)-O(8)-C(4)	116.91(11)
O(6)-C(11)	1.353(2)	C(7)-O(2)-C(1)	118.21(12)
O(6)-C(3)	1.4373(16)	C(1)-O(1)-C(5)	113.39(10)
C(1)-C(2)	1.5177(19)	C(11)-O(6)-C(3)	117.16(13)
C(1)-H(1)	1.0000	O(2)-C(1)-O(1)	104.33(11)
O(4)-C(9)	1.364(2)	O(2)-C(1)-C(2)	107.89(12)
O(4)-C(2)	1.4321(17)	O(1)-C(1)-C(2)	110.58(11)
O(7)-C(11)	1.197(2)	O(2)-C(1)-H(1)	111.3
O(10)-C(6)	1.2251(18)	O(1)-C(1)-H(1)	111.3
C(5)-C(6)	1.524(2)	C(2)-C(1)-H(1)	111.3
C(5)-C(4)	1.5406(19)	C(9)-O(4)-C(2)	117.41(12)
C(5)-H(5)	1.0000	O(1)-C(5)-C(6)	108.36(11)
O(3)-C(7)	1.192(2)	O(1)-C(5)-C(4)	108.64(11)
C(3)-C(4)	1.5119(19)	C(6)-C(5)-C(4)	110.57(12)
C(3)-C(2)	1.5211(19)	O(1)-C(5)-H(5)	109.7
C(3)-H(3)	1.0000	C(6)-C(5)-H(5)	109.7
C(4)-H(4)	1.0000	C(4)-C(5)-H(5)	109.7
C(14)-C(13)	1.501(2)	O(6)-C(3)-C(4)	107.87(11)
C(14)-H(14A)	0.9800	O(6)-C(3)-C(2)	108.25(11)
C(14)-H(14B)	0.9800	C(4)-C(3)-C(2)	109.64(11)
C(14)-H(14C)	0.9800	O(6)-C(3)-H(3)	110.3
N(1)-C(6)	1.3363(19)	C(4)-C(3)-H(3)	110.3
N(1)-C(15)	1.455(2)	C(2)-C(3)-H(3)	110.3
N(1)-H(1A)	0.8800	O(8)-C(4)-C(3)	106.67(11)
O(5)-C(9)	1.197(2)	O(8)-C(4)-C(5)	110.47(11)
C(7)-C(8)	1.495(2)	C(3)-C(4)-C(5)	108.74(12)
C(8)-H(8A)	0.9800	O(8)-C(4)-H(4)	110.3
C(8)-H(8B)	0.9800	C(3)-C(4)-H(4)	110.3
C(8)-H(8C)	0.9800	C(5)-C(4)-H(4)	110.3
C(9)-C(10)	1.495(2)	C(13)-C(14)-H(14A)	109.5
C(2)-H(2)	1.0000	C(13)-C(14)-H(14B)	109.5
C(11)-C(12)	1.503(3)	H(14A)-C(14)-H(14B)	109.5
C(10)-H(10A)	0.9800	C(13)-C(14)-H(14C)	109.5
C(10)-H(10B)	0.9800	H(14A)-C(14)-H(14C)	109.5
C(10)-H(10C)	0.9800	H(14B)-C(14)-H(14C)	109.5
C(16)-C(17)	1.174(3)	C(6)-N(1)-C(15)	118.73(13)
C(16)-C(15)	1.462(2)	C(6)-N(1)-H(1A)	120.6
C(15)-H(15A)	0.9900	C(15)-N(1)-H(1A)	120.6



O(3)-C(7)-O(2)	123.32(13)	O(10)-C(6)-N(1)	123.91(15)
O(3)-C(7)-C(8)	126.24(15)	O(10)-C(6)-C(5)	120.42(13)
O(2)-C(7)-C(8)	110.44(14)	N(1)-C(6)-C(5)	115.65(13)
C(7)-C(8)-H(8A)	109.5	C(9)-C(10)-H(10A)	109.5
C(7)-C(8)-H(8B)	109.5	C(9)-C(10)-H(10B)	109.5
H(8A)-C(8)-H(8B)	109.5	H(10A)-C(10)-H(10B)	109.5
C(7)-C(8)-H(8C)	109.5	C(9)-C(10)-H(10C)	109.5
H(8A)-C(8)-H(8C)	109.5	H(10A)-C(10)-H(10C)	109.5
H(8B)-C(8)-H(8C)	109.5	H(10B)-C(10)-H(10C)	109.5
O(5)-C(9)-O(4)	123.49(15)	C(17)-C(16)-C(15)	177.0(2)
O(5)-C(9)-C(10)	126.26(16)	N(1)-C(15)-C(16)	112.58(14)
O(4)-C(9)-C(10)	110.23(15)	N(1)-C(15)-H(15A)	109.1
O(4)-C(2)-C(1)	107.47(12)	C(16)-C(15)-H(15A)	109.1
O(4)-C(2)-C(3)	107.87(11)	N(1)-C(15)-H(15B)	109.1
C(1)-C(2)-C(3)	109.37(11)	C(16)-C(15)-H(15B)	109.1
O(4)-C(2)-H(2)	110.7	H(15A)-C(15)-H(15B)	107.8
C(1)-C(2)-H(2)	110.7	C(11)-C(12)-H(12A)	109.5
C(3)-C(2)-H(2)	110.7	C(11)-C(12)-H(12B)	109.5
O(7)-C(11)-O(6)	124.28(16)	H(12A)-C(12)-H(12B)	109.5
O(7)-C(11)-C(12)	126.27(17)	C(11)-C(12)-H(12C)	109.5
O(6)-C(11)-C(12)	109.45(17)	H(12A)-C(12)-H(12C)	109.5
O(9)-C(13)-O(8)	123.47(13)	H(12B)-C(12)-H(12C)	109.5
O(9)-C(13)-C(14)	126.02(15)	C(16)-C(17)-H(17)	180.0
O(8)-C(13)-C(14)	110.51(13)		

Table 4. Anisotropic displacement parameters [ $\text{\AA}^2 \times 10^3$ ] for 05mz051m. The anisotropic displacement factor exponent takes the form:  $-2 \pi^2 [(h a^*)^2 U_{11} + \dots + 2 h k a^* b^* U_{12}]$

	U11	U22	U33	U23	U13	U12
O(8)	21(1)	19(1)	29(1)	1(1)	1(1)	0(1)
O(2)	24(1)	18(1)	40(1)	0(1)	-3(1)	-1(1)
O(1)	28(1)	19(1)	28(1)	-2(1)	3(1)	1(1)
O(9)	22(1)	32(1)	44(1)	9(1)	3(1)	3(1)
O(6)	30(1)	28(1)	25(1)	-2(1)	-4(1)	-6(1)
C(1)	22(1)	18(1)	30(1)	-1(1)	-2(1)	0(1)
O(4)	24(1)	26(1)	32(1)	1(1)	6(1)	-2(1)
O(7)	50(1)	30(1)	40(1)	-9(1)	7(1)	3(1)
O(10)	52(1)	25(1)	30(1)	6(1)	7(1)	10(1)
C(5)	25(1)	19(1)	25(1)	0(1)	0(1)	3(1)
O(3)	37(1)	34(1)	59(1)	12(1)	-22(1)	-9(1)
C(3)	20(1)	21(1)	24(1)	-2(1)	-2(1)	-1(1)
C(4)	21(1)	18(1)	26(1)	1(1)	0(1)	1(1)
C(14)	30(1)	25(1)	46(1)	3(1)	4(1)	-5(1)
N(1)	38(1)	22(1)	34(1)	3(1)	12(1)	5(1)
O(5)	45(1)	42(1)	30(1)	4(1)	2(1)	6(1)
C(7)	31(1)	25(1)	27(1)	0(1)	-3(1)	-6(1)
C(8)	38(1)	23(1)	43(1)	-3(1)	0(1)	-6(1)
C(9)	37(1)	23(1)	30(1)	-2(1)	7(1)	-6(1)
C(2)	21(1)	22(1)	26(1)	0(1)	1(1)	-1(1)
C(11)	45(1)	25(1)	26(1)	-1(1)	5(1)	-11(1)
C(13)	22(1)	26(1)	26(1)	4(1)	-1(1)	-2(1)
C(6)	32(1)	23(1)	23(1)	0(1)	1(1)	4(1)
C(10)	44(1)	35(1)	37(1)	-5(1)	14(1)	-9(1)
C(16)	35(1)	34(1)	39(1)	-3(1)	10(1)	3(1)
C(15)	47(1)	28(1)	44(1)	-2(1)	21(1)	2(1)
C(12)	70(1)	53(1)	32(1)	-12(1)	-4(1)	-18(1)
C(17)	45(1)	38(1)	62(1)	-13(1)	12(1)	5(1)

Table 5. Hydrogen coordinates ( $\times 10^4$ ) and isotropic displacement parameters ( $\text{\AA}^2 \times 10^3$ ) for 05mz051m.

	x	y	z	U(eq)
H(1)	4177	8623	8192	28
H(5)	6342	9568	7527	28
H(3)	5860	9868	8770	26
H(4)	10297	9349	8373	26
H(14A)	11134	11683	7538	51
H(14B)	13151	11672	8073	51
H(14C)	10606	11751	8327	51
H(1A)	10309	8247	7163	38
H(8A)	4588	6166	7891	52
H(8B)	2168	6144	8245	52
H(8C)	4388	6243	8693	52
H(2)	7952	8400	9104	27
H(10A)	3574	9051	10722	58
H(10B)	3659	8159	10934	58
H(10C)	2081	8431	10324	58
H(15A)	13659	8954	6601	48
H(15B)	11777	8990	6025	48
H(12A)	8655	10242	10767	77
H(12B)	8420	11128	10545	77
H(12C)	10407	10607	10244	77
H(17)	14045	6819	5831	58

Table 6. Hydrogen bonds for 05mz051m [ $\text{\AA}$  and deg]

D-H...A	d(D-H)	d(H...A)	d(D...A)	$\angle$ (DHA)
N(1)-H(1A)...O(3)#1	0.88	2.25	2.9670(19)	138.4

Symmetry transformations used to generate equivalent atoms: #1  $x+1, y, z$

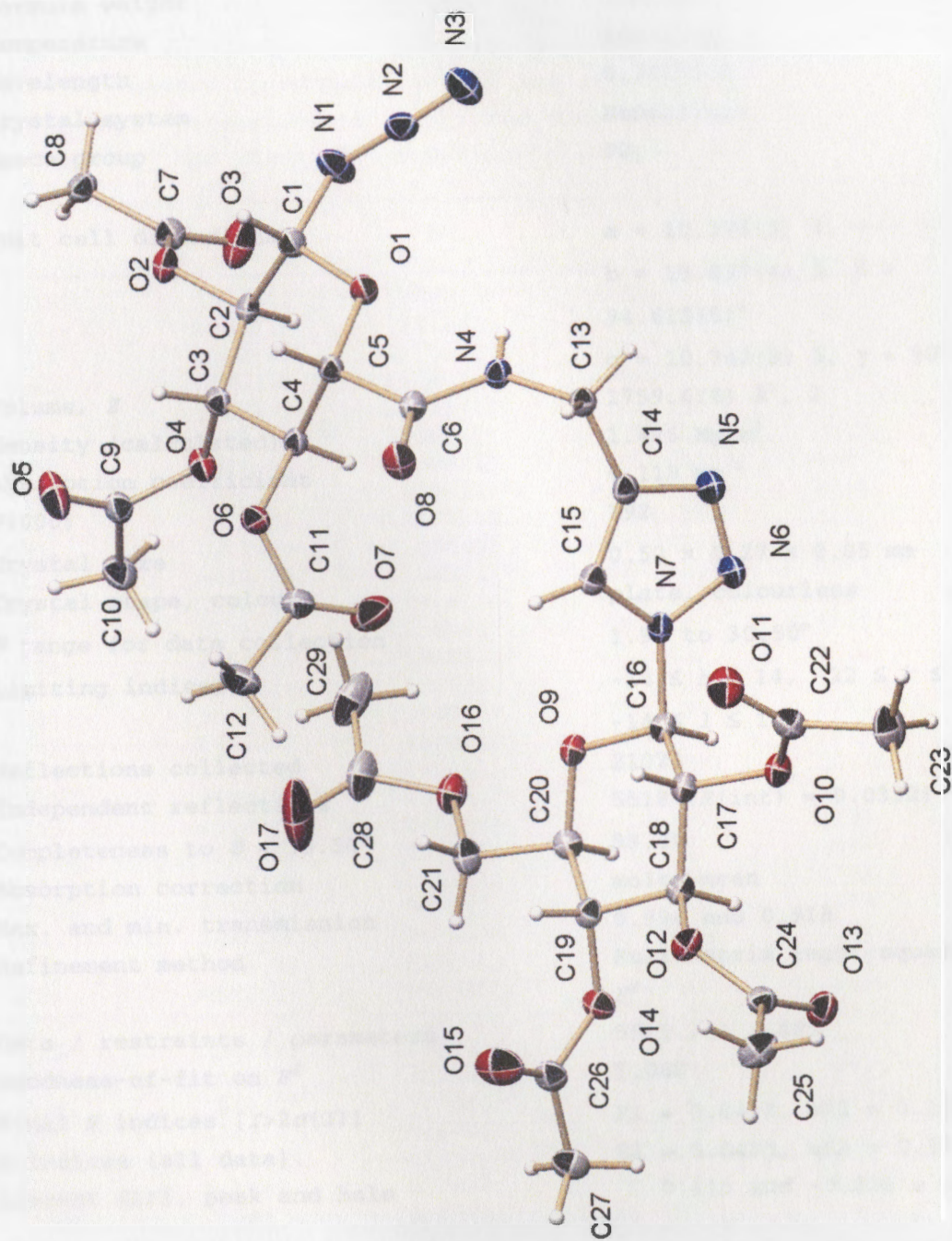


Figure 172: X-ray crystal structure of azide 45



Table 1. Crystal data and structure refinement for 05mz097m:

Identification code	05mz097m
Empirical formula	C <sub>29</sub> H <sub>37</sub> N <sub>7</sub> O <sub>17</sub>
Formula weight	755.66
Temperature	100(2) K
Wavelength	0.71073 Å
Crystal system	Monoclinic
Space group	P2 <sub>1</sub>
Unit cell dimensions	a = 10.376(3) Å, α = 90° b = 15.837(4) Å, β = 94.613(5)° c = 10.742(3) Å, γ = 90°
Volume, Z	1759.6(8) Å <sup>3</sup> , 2
Density (calculated)	1.426 Mg/m <sup>3</sup>
Absorption coefficient	0.119 mm <sup>-1</sup>
F(000)	792
Crystal size	0.52 × 0.27 × 0.05 mm
Crystal shape, colour	plate, colourless
θ range for data collection	1.90 to 30.50°
Limiting indices	-14 ≤ h ≤ 14, -22 ≤ k ≤ 22, -14 ≤ l ≤ 15
Reflections collected	21023
Independent reflections	5518 (R(int) = 0.0332)
Completeness to θ = 30.50°	99.3%
Absorption correction	multi-scan
Max. and min. transmission	0.994 and 0.918
Refinement method	Full-matrix least-squares on F <sup>2</sup>
Data / restraints / parameters	5518 / 1 / 485
Goodness-of-fit on F <sup>2</sup>	1.082
Final R indices [I > 2σ(I)]	R1 = 0.0430, wR2 = 0.1053
R indices (all data)	R1 = 0.0455, wR2 = 0.1070
Largest diff. peak and hole	0.415 and -0.222 e × Å <sup>-3</sup>

Refinement of F<sup>2</sup> against ALL reflections. The weighted R-factor wR and goodness of fit are based on F<sup>2</sup>, conventional R-factors R are based on F, with F set to zero for negative F<sup>2</sup>. The threshold expression of F<sup>2</sup> > 2σ(F<sup>2</sup>) is used only for calculating R-factors

## Treatment of hydrogen atoms:

All hydrogen atoms were placed in calculated positions and were refined with an isotropic displacement parameter 1.5 times (methyl) or 1.2 times (all others) that of the adjacent carbon or nitrogen atom.

Table 2. Atomic coordinates [ $\times 10^4$ ] and equivalent isotropic displacement parameters [ $\text{\AA}^2 \times 10^3$ ] for 05mz097m.  $U(\text{eq})$  is defined as one third of the trace of the orthogonalized  $U_{ij}$  tensor.

	x	y	z	U(eq)
O(1)	1900(1)	11049(1)	-3911(1)	19(1)
O(2)	2863(1)	13218(1)	-3173(1)	20(1)
O(3)	1002(2)	13756(1)	-2581(2)	33(1)
O(4)	3446(1)	12288(1)	-866(1)	21(1)
O(5)	5518(2)	12713(1)	-759(2)	36(1)
O(6)	4400(1)	10652(1)	-1379(1)	20(1)
O(7)	3234(2)	10006(1)	17(2)	40(1)
O(8)	3535(1)	9166(1)	-3009(2)	27(1)
N(1)	909(2)	12277(1)	-4699(2)	29(1)
N(2)	277(2)	11804(1)	-5424(2)	22(1)
N(3)	-412(2)	11441(1)	-6079(2)	32(1)
C(1)	2122(2)	11916(1)	-4142(2)	19(1)
C(2)	2431(2)	12380(1)	-2918(2)	17(1)
C(3)	3498(2)	11949(1)	-2102(2)	17(1)
C(4)	3255(2)	11003(1)	-2014(2)	16(1)
C(5)	3002(2)	10624(1)	-3318(2)	17(1)
C(6)	2676(2)	9683(1)	-3255(2)	18(1)
C(7)	2039(2)	13864(1)	-2968(2)	20(1)
C(8)	2576(2)	14699(1)	-3305(2)	21(1)
C(9)	4514(2)	12650(1)	-296(2)	21(1)
C(10)	4241(2)	12937(2)	981(2)	29(1)
C(11)	4260(2)	10194(1)	-335(2)	22(1)
C(12)	5550(2)	9973(2)	300(2)	31(1)
N(4)	1420(2)	9493(1)	-3475(2)	17(1)
N(5)	-596(2)	8156(1)	-1958(2)	25(1)
N(6)	-618(2)	7923(1)	-788(2)	25(1)
N(7)	616(2)	7950(1)	-283(2)	17(1)
C(13)	962(2)	8628(1)	-3459(2)	18(1)
C(14)	647(2)	8333(1)	-2195(2)	18(1)
C(15)	1433(2)	8203(1)	-1123(2)	18(1)
O(9)	1749(1)	8363(1)	1523(1)	18(1)
O(10)	645(1)	6225(1)	776(1)	20(1)
O(11)	1680(2)	6020(1)	-956(2)	30(1)
O(12)	2650(1)	5963(1)	2684(1)	20(1)
O(13)	1157(1)	5290(1)	3722(2)	25(1)
O(14)	2699(1)	7329(1)	4495(1)	20(1)
O(15)	4809(2)	6993(2)	4597(2)	41(1)
O(16)	2296(2)	9778(1)	2950(2)	25(1)
O(17)	4204(2)	10432(2)	3109(3)	66(1)
C(16)	897(2)	7736(1)	1017(2)	17(1)
C(17)	1544(2)	6873(1)	1185(2)	17(1)

C(18)	1875(2)	6718(1)	2565(2)	17(1)
C(19)	2662(2)	7438(1)	3160(2)	18(1)
C(20)	2021(2)	8288(1)	2845(2)	19(1)
C(21)	2958(2)	8996(1)	3215(2)	23(1)
C(22)	871(2)	5805(1)	-292(2)	21(1)
C(23)	14(2)	5047(2)	-452(3)	33(1)
C(24)	2174(2)	5289(1)	3268(2)	19(1)
C(25)	3089(2)	4553(1)	3279(2)	28(1)
C(26)	3842(2)	7093(1)	5107(2)	22(1)
C(27)	3698(2)	6994(1)	6465(2)	24(1)
C(28)	3058(3)	10454(2)	2874(3)	35(1)
C(29)	2310(3)	11219(2)	2421(3)	40(1)

All esds (except the esd in the dihedral angle between two l.s. planes) are estimated using the full covariance matrix. The cell esds are taken into account individually in the estimation of esds in distances, angles and torsion angles; correlations between esds in cell parameters are only used when they are defined by crystal symmetry. An approximate (isotropic) treatment of cell esds is used for estimating esds involving l.s. planes.

Table 3. Bond lengths [Å] and angles [deg] for 05mz097m.

O(1)-C(1)	1.417(2)	O(9)-C(20)	1.430(2)
O(1)-C(5)	1.432(2)	O(10)-C(22)	1.362(2)
O(2)-C(7)	1.363(2)	O(10)-C(17)	1.432(2)
O(2)-C(2)	1.434(2)	O(11)-C(22)	1.194(3)
O(3)-C(7)	1.197(3)	O(12)-C(24)	1.353(2)
O(4)-C(9)	1.350(2)	O(12)-C(18)	1.440(2)
O(4)-C(3)	1.438(2)	O(13)-C(24)	1.197(2)
O(5)-C(9)	1.194(3)	O(14)-C(26)	1.361(2)
O(6)-C(11)	1.353(2)	O(14)-C(19)	1.442(2)
O(6)-C(4)	1.434(2)	O(15)-C(26)	1.191(3)
O(7)-C(11)	1.195(3)	O(16)-C(28)	1.337(3)
O(8)-C(6)	1.225(2)	O(16)-C(21)	1.433(3)
N(1)-N(2)	1.231(3)	O(17)-C(28)	1.196(3)
N(1)-C(1)	1.465(2)	C(16)-C(17)	1.527(3)
N(2)-N(3)	1.121(3)	C(16)-H(16)	1.0000
C(1)-C(2)	1.518(3)	C(17)-C(18)	1.514(3)
C(1)-H(1)	1.0000	C(17)-H(17)	1.0000
C(2)-C(3)	1.517(3)	C(18)-C(19)	1.514(3)
C(2)-H(2)	1.0000	C(18)-H(18)	1.0000
C(3)-C(4)	1.523(3)	C(19)-C(20)	1.528(3)
C(3)-H(3)	1.0000	C(19)-H(19)	1.0000
C(4)-C(5)	1.526(3)	C(20)-C(21)	1.515(3)
C(4)-H(4)	1.0000	C(20)-H(20)	1.0000
C(5)-C(6)	1.531(3)	C(21)-H(21A)	0.9900
C(5)-H(5)	1.0000	C(21)-H(21B)	0.9900
C(6)-N(4)	1.339(2)	C(22)-C(23)	1.496(3)
C(7)-C(8)	1.490(3)	C(23)-H(23A)	0.9800
C(8)-H(8A)	0.9800	C(23)-H(23B)	0.9800
C(8)-H(8B)	0.9800	C(23)-H(23C)	0.9800
C(8)-H(8C)	0.9800	C(24)-C(25)	1.502(3)
C(9)-C(10)	1.495(3)	C(25)-H(25A)	0.9800
C(10)-H(10A)	0.9800	C(25)-H(25B)	0.9800
C(10)-H(10B)	0.9800	C(25)-H(25C)	0.9800
C(10)-H(10C)	0.9800	C(26)-C(27)	1.487(3)
C(11)-C(12)	1.494(3)	C(27)-H(27A)	0.9800
C(12)-H(12A)	0.9800	C(27)-H(27B)	0.9800
C(12)-H(12B)	0.9800	C(27)-H(27C)	0.9800
C(12)-H(12C)	0.9800	C(28)-C(29)	1.499(4)
N(4)-C(13)	1.451(2)	C(29)-H(29A)	0.9800
N(4)-H(4A)	0.8800	C(29)-H(29B)	0.9800
N(5)-N(6)	1.311(3)	C(29)-H(29C)	0.9800
N(5)-C(14)	1.364(2)		
N(6)-N(7)	1.351(2)	C(1)-O(1)-C(5)	113.41(14)
N(7)-C(15)	1.347(2)	C(7)-O(2)-C(2)	117.08(14)
N(7)-C(16)	1.444(2)	C(9)-O(4)-C(3)	119.14(15)
C(13)-C(14)	1.496(3)	C(11)-O(6)-C(4)	117.53(15)
C(13)-H(13A)	0.9900	N(2)-N(1)-C(1)	114.66(18)
C(13)-H(13B)	0.9900	N(3)-N(2)-N(1)	171.9(2)
C(14)-C(15)	1.373(3)	O(1)-C(1)-N(1)	107.61(15)
C(15)-H(15)	0.9500	O(1)-C(1)-C(2)	110.06(15)
O(9)-C(16)	1.410(2)	N(1)-C(1)-C(2)	106.21(16)



O(1)-C(1)-H(1)	110.9	C(11)-C(12)-H(12C)	109.5
N(1)-C(1)-H(1)	110.9	H(12A)-C(12)-H(12C)	109.5
C(2)-C(1)-H(1)	110.9	H(12B)-C(12)-H(12C)	109.5
O(2)-C(2)-C(3)	107.61(14)	C(6)-N(4)-C(13)	121.68(16)
O(2)-C(2)-C(1)	109.25(15)	C(6)-N(4)-H(4A)	119.2
C(3)-C(2)-C(1)	112.08(15)	C(13)-N(4)-H(4A)	119.2
O(2)-C(2)-H(2)	109.3	N(6)-N(5)-C(14)	109.09(17)
C(3)-C(2)-H(2)	109.3	N(5)-N(6)-N(7)	106.67(16)
C(1)-C(2)-H(2)	109.3	C(15)-N(7)-N(6)	111.55(16)
O(4)-C(3)-C(2)	106.60(14)	C(15)-N(7)-C(16)	128.94(16)
O(4)-C(3)-C(4)	106.97(15)	N(6)-N(7)-C(16)	119.49(15)
C(2)-C(3)-C(4)	111.22(14)	N(4)-C(13)-C(14)	113.71(16)
O(4)-C(3)-H(3)	110.6	N(4)-C(13)-H(13A)	108.8
C(2)-C(3)-H(3)	110.6	C(14)-C(13)-H(13A)	108.8
C(4)-C(3)-H(3)	110.6	N(4)-C(13)-H(13B)	108.8
O(6)-C(4)-C(3)	106.06(14)	C(14)-C(13)-H(13B)	108.8
O(6)-C(4)-C(5)	111.06(15)	H(13A)-C(13)-H(13B)	107.7
C(3)-C(4)-C(5)	110.27(15)	N(5)-C(14)-C(15)	108.59(17)
O(6)-C(4)-H(4)	109.8	N(5)-C(14)-C(13)	120.89(17)
C(3)-C(4)-H(4)	109.8	C(15)-C(14)-C(13)	130.52(17)
C(5)-C(4)-H(4)	109.8	N(7)-C(15)-C(14)	104.09(16)
O(1)-C(5)-C(4)	107.25(15)	N(7)-C(15)-H(15)	128.0
O(1)-C(5)-C(6)	107.78(14)	C(14)-C(15)-H(15)	128.0
C(4)-C(5)-C(6)	111.38(15)	C(16)-O(9)-C(20)	113.11(14)
O(1)-C(5)-H(5)	110.1	C(22)-O(10)-C(17)	117.15(15)
C(4)-C(5)-H(5)	110.1	C(24)-O(12)-C(18)	118.32(14)
C(6)-C(5)-H(5)	110.1	C(26)-O(14)-C(19)	117.80(15)
O(8)-C(6)-N(4)	124.66(18)	C(28)-O(16)-C(21)	115.33(18)
O(8)-C(6)-C(5)	120.09(17)	O(9)-C(16)-N(7)	106.22(15)
N(4)-C(6)-C(5)	115.25(16)	O(9)-C(16)-C(17)	109.24(14)
O(3)-C(7)-O(2)	122.82(19)	N(7)-C(16)-C(17)	112.12(15)
O(3)-C(7)-C(8)	125.10(19)	O(9)-C(16)-H(16)	109.7
O(2)-C(7)-C(8)	112.08(16)	N(7)-C(16)-H(16)	109.7
C(7)-C(8)-H(8A)	109.5	C(17)-C(16)-H(16)	109.7
C(7)-C(8)-H(8B)	109.5	O(10)-C(17)-C(18)	105.97(14)
H(8A)-C(8)-H(8B)	109.5	O(10)-C(17)-C(16)	109.61(14)
C(7)-C(8)-H(8C)	109.5	C(18)-C(17)-C(16)	108.87(15)
H(8A)-C(8)-H(8C)	109.5	O(10)-C(17)-H(17)	110.8
H(8B)-C(8)-H(8C)	109.5	C(18)-C(17)-H(17)	110.8
O(5)-C(9)-O(4)	124.01(19)	C(16)-C(17)-H(17)	110.8
O(5)-C(9)-C(10)	126.38(19)	O(12)-C(18)-C(19)	108.00(15)
O(4)-C(9)-C(10)	109.61(17)	O(12)-C(18)-C(17)	107.61(15)
C(9)-C(10)-H(10A)	109.5	C(19)-C(18)-C(17)	111.31(15)
C(9)-C(10)-H(10B)	109.5	O(12)-C(18)-H(18)	110.0
H(10A)-C(10)-H(10B)	109.5	C(19)-C(18)-H(18)	110.0
C(9)-C(10)-H(10C)	109.5	C(17)-C(18)-H(18)	110.0
H(10A)-C(10)-H(10C)	109.5	O(14)-C(19)-C(18)	107.49(15)
H(10B)-C(10)-H(10C)	109.5	O(14)-C(19)-C(20)	107.61(15)
O(7)-C(11)-O(6)	123.62(19)	C(18)-C(19)-C(20)	111.13(15)
O(7)-C(11)-C(12)	125.8(2)	O(14)-C(19)-H(19)	110.2
O(6)-C(11)-C(12)	110.59(18)	C(18)-C(19)-H(19)	110.2
C(11)-C(12)-H(12A)	109.5	C(20)-C(19)-H(19)	110.2
C(11)-C(12)-H(12B)	109.5	O(9)-C(20)-C(21)	105.71(16)
H(12A)-C(12)-H(12B)	109.5	O(9)-C(20)-C(19)	109.94(15)

C(21)-C(20)-C(19)	109.62(16)	C(24)-C(25)-H(25B)	109.5
O(9)-C(20)-H(20)	110.5	H(25A)-C(25)-H(25B)	109.5
C(21)-C(20)-H(20)	110.5	C(24)-C(25)-H(25C)	109.5
C(19)-C(20)-H(20)	110.5	H(25A)-C(25)-H(25C)	109.5
O(16)-C(21)-C(20)	107.46(16)	H(25B)-C(25)-H(25C)	109.5
O(16)-C(21)-H(21A)	110.2	O(15)-C(26)-O(14)	123.2(2)
C(20)-C(21)-H(21A)	110.2	O(15)-C(26)-C(27)	126.31(19)
O(16)-C(21)-H(21B)	110.2	O(14)-C(26)-C(27)	110.51(16)
C(20)-C(21)-H(21B)	110.2	C(26)-C(27)-H(27A)	109.5
H(21A)-C(21)-H(21B)	108.5	C(26)-C(27)-H(27B)	109.5
O(11)-C(22)-O(10)	122.76(19)	H(27A)-C(27)-H(27B)	109.5
O(11)-C(22)-C(23)	126.9(2)	C(26)-C(27)-H(27C)	109.5
O(10)-C(22)-C(23)	110.34(18)	H(27A)-C(27)-H(27C)	109.5
C(22)-C(23)-H(23A)	109.5	H(27B)-C(27)-H(27C)	109.5
C(22)-C(23)-H(23B)	109.5	O(17)-C(28)-O(16)	123.1(3)
H(23A)-C(23)-H(23B)	109.5	O(17)-C(28)-C(29)	124.9(2)
C(22)-C(23)-H(23C)	109.5	O(16)-C(28)-C(29)	112.0(2)
H(23A)-C(23)-H(23C)	109.5	C(28)-C(29)-H(29A)	109.5
H(23B)-C(23)-H(23C)	109.5	C(28)-C(29)-H(29B)	109.5
O(13)-C(24)-O(12)	123.63(18)	H(29A)-C(29)-H(29B)	109.5
O(13)-C(24)-C(25)	125.16(19)	C(28)-C(29)-H(29C)	109.5
O(12)-C(24)-C(25)	111.21(16)	H(29A)-C(29)-H(29C)	109.5
C(24)-C(25)-H(25A)	109.5	H(29B)-C(29)-H(29C)	109.5

Table 4. Anisotropic displacement parameters [ $\text{\AA}^2 \times 10^3$ ] for 05mz097m. The anisotropic displacement factor exponent takes the form:  $-2 \pi^2 [(h a^*)^2 U_{11} + \dots + 2 h k a^* b^* U_{12}]$

	U11	U22	U33	U23	U13	U12
O(1)	17(1)	13(1)	26(1)	2(1)	-3(1)	1(1)
O(2)	17(1)	15(1)	27(1)	-1(1)	5(1)	-2(1)
O(3)	25(1)	21(1)	57(1)	-1(1)	18(1)	2(1)
O(4)	17(1)	26(1)	20(1)	-6(1)	3(1)	-4(1)
O(5)	21(1)	50(1)	37(1)	-16(1)	6(1)	-12(1)
O(6)	14(1)	25(1)	21(1)	3(1)	0(1)	1(1)
O(7)	28(1)	52(1)	40(1)	22(1)	7(1)	2(1)
O(8)	21(1)	18(1)	40(1)	1(1)	-2(1)	4(1)
N(1)	31(1)	17(1)	37(1)	-2(1)	-14(1)	5(1)
N(2)	21(1)	21(1)	23(1)	5(1)	0(1)	4(1)
N(3)	26(1)	32(1)	36(1)	-3(1)	-7(1)	0(1)
C(1)	18(1)	15(1)	24(1)	1(1)	-2(1)	0(1)
C(2)	15(1)	15(1)	21(1)	0(1)	3(1)	-3(1)
C(3)	14(1)	19(1)	17(1)	-2(1)	2(1)	-1(1)
C(4)	13(1)	16(1)	20(1)	2(1)	1(1)	-1(1)
C(5)	14(1)	16(1)	20(1)	1(1)	0(1)	0(1)
C(6)	17(1)	16(1)	20(1)	-1(1)	3(1)	-1(1)
C(7)	20(1)	18(1)	22(1)	-2(1)	1(1)	1(1)
C(8)	26(1)	16(1)	21(1)	2(1)	2(1)	-2(1)
C(9)	20(1)	19(1)	23(1)	-1(1)	-1(1)	-2(1)
C(10)	30(1)	37(1)	20(1)	-5(1)	-1(1)	-7(1)
C(11)	23(1)	23(1)	21(1)	2(1)	0(1)	1(1)
C(12)	28(1)	35(1)	28(1)	3(1)	-9(1)	5(1)
N(4)	16(1)	13(1)	22(1)	1(1)	1(1)	0(1)
N(5)	19(1)	29(1)	28(1)	5(1)	0(1)	-4(1)
N(6)	15(1)	31(1)	28(1)	5(1)	-1(1)	-5(1)
N(7)	14(1)	15(1)	22(1)	1(1)	2(1)	-1(1)
C(13)	21(1)	14(1)	19(1)	-1(1)	1(1)	-2(1)
C(14)	18(1)	13(1)	22(1)	-1(1)	1(1)	-1(1)
C(15)	15(1)	17(1)	22(1)	0(1)	4(1)	1(1)
O(9)	19(1)	15(1)	20(1)	-1(1)	4(1)	-3(1)
O(10)	21(1)	16(1)	24(1)	-2(1)	4(1)	-4(1)
O(11)	33(1)	33(1)	26(1)	-9(1)	8(1)	-4(1)
O(12)	20(1)	16(1)	26(1)	2(1)	7(1)	4(1)
O(13)	20(1)	23(1)	31(1)	5(1)	5(1)	0(1)
O(14)	16(1)	26(1)	18(1)	-1(1)	2(1)	4(1)
O(15)	21(1)	67(1)	37(1)	12(1)	6(1)	14(1)
O(16)	26(1)	18(1)	32(1)	-4(1)	8(1)	-3(1)
O(17)	36(1)	32(1)	128(2)	-13(1)	3(1)	-15(1)
C(16)	17(1)	16(1)	19(1)	0(1)	4(1)	-2(1)
C(17)	17(1)	16(1)	19(1)	-1(1)	3(1)	-1(1)
C(18)	16(1)	15(1)	21(1)	1(1)	5(1)	2(1)
C(19)	15(1)	19(1)	19(1)	0(1)	4(1)	0(1)
C(20)	18(1)	18(1)	20(1)	-2(1)	3(1)	1(1)
C(21)	21(1)	21(1)	28(1)	-5(1)	2(1)	-3(1)
C(22)	22(1)	18(1)	24(1)	-3(1)	-1(1)	5(1)
C(23)	31(1)	20(1)	47(1)	-9(1)	2(1)	-5(1)

C(24)	22(1)	17(1)	18(1)	0(1)	-1(1)	-1(1)
C(25)	31(1)	20(1)	33(1)	3(1)	9(1)	9(1)
C(26)	20(1)	20(1)	26(1)	2(1)	-1(1)	4(1)
C(27)	25(1)	23(1)	24(1)	-1(1)	-1(1)	7(1)
C(28)	36(1)	22(1)	50(2)	-8(1)	13(1)	-10(1)
C(29)	51(2)	18(1)	56(2)	-3(1)	26(1)	-2(1)

Table 5. Hydrogen coordinates ( $\times 10^4$ ) and isotropic displacement parameters ( $\text{\AA}^2 \times 10^3$ ) for 05mz097m.

	x	y	z	U(eq)
H(1)	2833	11989	-4710	23
H(2)	1634	12412	-2455	20
H(3)	4360	12061	-2423	20
H(4)	2497	10897	-1518	20
H(5)	3771	10710	-3808	20
H(8A)	2480	15101	-2626	32
H(8B)	2107	14907	-4072	32
H(8C)	3494	14636	-3440	32
H(10A)	4893	13352	1286	43
H(10B)	4269	12451	1548	43
H(10C)	3381	13196	948	43
H(12A)	5450	9510	890	47
H(12B)	5912	10467	752	47
H(12C)	6133	9797	-326	47
H(4A)	859	9903	-3633	20
H(13A)	1633	8253	-3762	22
H(13B)	179	8577	-4044	22
H(15)	2343	8275	-1000	21
H(16)	81	7744	1453	21
H(17)	2338	6843	716	21
H(18)	1064	6640	2996	21
H(19)	3558	7428	2881	21
H(20)	1211	8350	3281	22
H(21A)	3241	8958	4115	28
H(21B)	3730	8957	2734	28
H(23A)	386	4583	62	49
H(23B)	-61	4876	-1332	49
H(23C)	-845	5186	-192	49
H(25A)	2631	4057	2924	42
H(25B)	3422	4432	4140	42
H(25C)	3810	4691	2779	42
H(27A)	3756	7549	6870	36
H(27B)	4387	6628	6836	36
H(27C)	2856	6740	6585	36
H(29A)	2430	11311	1536	61
H(29B)	2622	11713	2905	61
H(29C)	1390	11133	2526	61

Table 6. Hydrogen bonds for 05mz097m [ $\text{\AA}$  and deg].

D-H...A	d(D-H)	d(H...A)	d(D...A)	$\angle$ (DHA)
N(4)-H(4A)...O(13)#1	0.88	2.17	2.950(2)	146.7

Symmetry transformations used to generate equivalent atoms: #1 -  
 $x, y+1/2, -z$